U.PORTO

DOUTORAMENTO

CIÊNCIAS BIOMÉDICAS

Development of a Resveratrol Drug Delivery System Presenting Enhanced Bioavailability

Teófilo Vasconcelos

D

2021

U.PORTO

Teófilo Vasconcelos: Development of a Resveratrol Drug Delivery System Presenting Enhanced Bioavailability

D.ICBAS **2021**

Development of a Resveratrol Drug Delivery System Presenting Enhanced Bioavailability
Teófilo Vasconcelos

INSTITUTO DE CIÊNCIAS BIOMÉDICAS ABEL SALAZAR

TEÓFILO CARDOSO VASCONCELOS

Development of a Resveratrol Drug Delivery System Presenting Enhanced Bioavailability

Tese de Candidatura ao grau de Doutor em Ciências Biomédicas submetida ao Instituto de Ciências Biomédicas Abel Salazar da Universidade do Porto.

Orientador:

Doutor Bruno Filipe Carmelino Cardoso Sarmento

Categoria - Investigador Principal/ Professor Associado Convidado
Afiliação – i3S – Instituto de Investigação e Inovação em Saúde, INEB – Instituto de Engenharia Biomédica, Universidade do Porto & IUCS - Instituto Universitário de Ciências da Saúde

Co-orientadora:

Doutora Sara Andreia de Barros Costa Marques

Categoria – Investigadora/Professora Auxiliar Convidada
Afiliação – CIBIO-InBIO/UP - Centro de Investigação em Biodiversidade e Recursos Genéticos da Universidade do Porto & ICBAS-UP – Instituto de Ciências Biomédicas de Abel Salazar, Universidade do Porto

The work presented in this thesis was developed at:

Nanomedicines & Translational Drug Delivery Laboratory
I3S – instituto de Investigação e Inovação em Saúde
INEB – Instituto Nacional de Engenharia Biomédica
University of Porto, Porto, Portugal
Address: Rua Alfredo Allen, 208
4200-135 Porto, Portugal
www.i3s.up.pt | www.ineb.up.pt

And

Pharmaceutical Sciences Laboratory
R & D Area - Research Department
Bial - Portela & Cª, S.A.
Address: À Av. da Siderurgia Nacional
4745-457 S. Mamede do Coronado
Portugal
www.bial.com

Eu, Teófilo Cardoso de Vasconcelos, declaro que a presente tese é da minha autoria e não foi utilizada previamente noutro curso ou unidade curricular, desta ou de outra instituição. As referências a outros autores (afirmações, ideias, pensamentos) respeitam escrupulosamente as regas da atribuição, e encontram-se devidamente indicadas no texto e nas referências bibliográficas, de acordo com as normas de referenciação. Tenho consciência de que a prática de plágio e auto-plágio constitui um ilícito académico. Declaro também que nenhum dos artigos apresentados nesta tese se encontram publicados em qualquer outra tese ou dissertação.

Porto, 21 de Fevereiro de 2021

Financial Support

Teófilo Vasconcelos PhD fees were partially supported by Bial - Portela & Cª, S.A.
This dissertation was partially financed by Bial - Portela & Cª, S.A and by the project NORTE-01-0145-FEDER-000012, supported by Norte Portugal Regional Operational Programme (NORTE 2020), under the PORTUGAL 2020 Partnership Agreement, through the European Regional Development Fund (ERDF). This work was financed by FEDER - Fundo Europeu de Desenvolvimento Regional funds through the COMPETE 2020 - Operational Programme for Competitiveness and Internationalisation (POCI), Portugal 2020, and by Portuguese funds through FCT - Fundação para a Ciência e a Tecnologia/ Ministério da Ciência, Tecnologia e Ensino Superior in the framework of the project "Institute for Research and Innovation in Health Sciences" (POCI-01-0145-FEDER-007274) and NETDIAMOND (POCI-01-0145-FEDER-016385).

PUBLICATIONS

Ao abrigo do dispositivo do nº2, alínea a) do decreto-Lei nº 115/2013 de Agosto, fazem parte integrante desta tese de doutoramento os seguintes trabalhos já publicados:

- **Teófilo Vasconcelos**, Sara Marques, Bruno Sarmento. The biopharmaceutical classification system of excipients. Therapeutic Delivery 8: 65-78, 2017

- **Teófilo Vasconcelos,** Sara Marques, José das-Neves, Bruno Sarmento. Amorphous solid dispersions: rational selection of a manufacturing process. Advanced Drug Delivery Reviews 100: 85-101, 2016

- **Teófilo Vasconcelos**, Fabíola Prezotti, Francisca Araújo, Carlos Lopes, Ana Loureiro, Sara Marques, Bruno Sarmento. Third-generation solid dispersion combining Soluplus and poloxamer 407 enhances the oral bioavailability of Resveratrol. International Journal of Pharmaceutics Volume 595, 2021, 120245

- **Teófilo Vasconcelos**, Sara Marques, Bruno Sarmento. Measuring the emulsification dynamics and stability of self-emulsifying drug delivery systems. European Journal of Pharmaceutics and Biopharmaceutics 123: 1-8, 2018

- **Teófilo Vasconcelos**, Francisca Araújo, Carlos Lopes, Ana Loureiro, José das Neves, Sara Marques, Bruno Sarmento. Multicomponent self-nano emulsifying delivery systems of Resveratrol with enhanced pharmacokinetics profile. European Journal of Pharmaceutical Sciences 137: 105011, 2019

O candidato, Teófilo Vasconcelos foi responsável pelo planeamento, execução laboratorial (superior a 80% do conteúdo) e redação dos artigos acima referidos.

ACKNOWLEDGMENTS

Embora esta tese esteja na sua totalidade escrita em inglês, decidi escrever os meus agradecimentos na nossa língua para melhor me poder expressar. Durante este longo percurso, a minha vida mudou bastante, tanto pessoal com profissionalmente. Pessoalmente, em 2015 nasceu o Tiago e em 2019 a Mafalda, fazendo-me crescer muito enquanto pessoa, preenchendo cada minuto da nossa existência e obrigando-me a ser melhor todos os dias. Perdi os 2 avós que ainda tinha e dos quais sinto saudades. Mudei de casa, estando agora mais perto do mar. Profissionalmente, quando inicie esta tese era um cientista sénior, em 2015 fui promovido a responsável do serviço de tecnologia farmacêutica e biodisponibilidade gerindo uma equipa de 5 pessoas e em 2019 passei a chefe do laboratório de ciências farmacêuticas, tendo 3 serviços sobre minha responsabilidade e uma equipa de 18 pessoas. De igual modo durante este período estive envolvidos em mutos projetos profissionalmente, mas de salientar as aprovações relativas ao projeto do Zebinix® / Aptiom ™ pela FDA (2014) e Coreia do Sul (2020) e de uma formulação pediátrica (suspensão oral) na Europa (EMA, 2016). De igual modo a aprovação do Ongentys® na Europa (2016), Estados Unidos (2020), Japão (2020) e Austrália (2020) foram marcos importantes do meu percurso. Deste modo, o já não muito miúdo que iniciou este projeto de Doutoramento, definitivamente é muito diferente hoje em dia.

Por tudo o acima referido, inúmeras pessoas se cruzaram comigo contribuindo significativamente para a minha evolução, aprendizagem e consequentemente para o trabalho realizado durante este período. Deste modo gostaria de agradecer:

Aos meus orientadores, Professor Doutor Bruno Sarmento e Professora Doutora Sara Marques pela sua orientação, rigor, incentivo, oportunidades proporcionadas, conhecimento, amizade e pela liberdade controlada que me concederam. Um muito obrigado por me terem permitido realizar este objetivo, sem o vosso apoio tudo seria diferente para pior.

Ao Bial pelo apoio financeiro e pessoal, pelo incentivo e facilidades prestadas na conciliação entre trabalho e estudo. Gostaria de salientar a minha equipa, na realidade, os amigos, que no dia-a-dia me apoiam, sendo excecionais pessoal e profissionalmente. Sem o seu apoio não teria tido disponibilidade para terminar esta etapa. Um muito obrigado também por todas as discussões científicas e sabedoria partilhada. Um muito obrigado (por ordem alfabética), Alvaro Sousa, Amelia Vieira, Andreia Moreira, Carlos Cunha, Cristina Mesquita, Filipe Correia, Hugo Almeida, Jaison Machado, João Teixeira, Luisa Sousa, Maria João Gomes, Maria João Santos, Pedro Barrocas, Pedro Pala,

Professor Sousa Lobo, Raquel Figueiredo, Rita Pires, Vera Soares. Ao Professor Doutor Patrício Soares-da-Silva, um muito obrigado pelas discussões cruciais para o desenrolar desta Tese e pela promoção da realização deste projeto. Ao Ricardo Lima, muito obrigado pelo companheirismo e incentivo para abraçar deste desafio, sem a sua motivação e facilitação não teria conseguido embarcar nesta cruzada, um muito obrigado. A Eric Chevalier, un grand merci pour toute l'aide et tous les enseignements qui m'aident dans ma vie professionnelle. Ana Loureiro, Carlos Lopes e Francisca Araújo um muito obrigado pelo vosso apoio na realização dos estudos de farmacocinética em rato.

Ao INEB/ I3S e ao ICBAS-UP, por me acolherem e por todo o apoio institucional. Em particular, gostaria de agradecer ao grupo “Nanomedicines & Translational Drug Delivery”, por todo o apoio e pelas discussões cientificas e aprendizagem partilhada. À Francisca Araújo e à Fabíola Prezotti (que esteve temporariamente no I3S) um muito obrigado pelo apoio na realização dos estudos de permeabilidade celular.

À Sara, um muito obrigado pela ajuda, paciência, motivação, carinho e compreensão e orgulho, sem os quais não conseguiria terminar esta etapa. Ao Tiago e à Mafalda, por todos os mimos e cabelos brancos ou falta de cabelo que me provaram durantes estes anos.

Aos meus pais (onde quer que estejas pai) e irmã, pela ajuda, por incutirem o amor ao estudo e à realização profissional, entre outros valores que regem a minha vida e pelo orgulho que sentem por mim.

A todos os meus amigos e familiares, que de alguma forma partilharam experiências comigo e que contribuíram para eu fosse quem sou hoje.

A todos um profundo e sincero, MUITO OBRIGADO.

“O homem é do tamanho do seu sonho”

Fernando Pessoa

Contents

A. Abbreviations and Symbol List

ANOVA	One-way analysis of variance
ASES	Aerosol solvent extraction system
ATCC	American Type Culture Collection
ATP	Adenosine triphosphate
ATR	Attenuated total reflection
AUC	Area under curve
BCRP	Breast cancer resistance protein
BCS	Biopharmaceutical classification system
BCSE	Biopharmaceutical classification system of excipients
CMC	Critical micellar concentration
COP	Copovidone
CTAB	Cetyltrimethylammonium bromide
CYP	Cytochrome P450
DMEM	Dulbecco's Modified Eagle medium
DMSO	Dimethyl sulfoxide
DSC	Differential scanning calorimetry
EDTA	Ethylenediaminetetraacetic acid
EMA	European Medicines Agency
EU	European Union
FBS	Foetal bovine serum
FDA	Food and Drug Administration
FTIR	Fourier transform infrared
GAS	Gaseous antisolvent
GI	Gastrointestinal
GMP	Good manufacturing practices
HBBS	Hank's balanced salt solution
HLB	Hydrophilic-lipophilic balance
HME	Hot melt extrusion
HPC	Hydroxypropylcellulose
HPLC	High-performance liquid chromatography

HPMC	Hydroxypropyl methylcellulose
HPMCAS	Hydroxypropyl methylcellulose acetate succinate
ICH	International Conference Harmonisation
LC-MS/MS	Liquid chromatography with tandem mass spectrometry
mRNA	Messenger RNA
MRP1	Multidrug resistance protein 1
MRP2	Multidrug resistance protein 2
N.A.	Not available
NCE	New chemical entities
NEAA	Non-essential amino acids
O/W	Oil−in−water
OATP	Organic anion-transporting polypeptide
P_{app}	Apparent permeability
PBS	Phosphate buffered saline
PC	Phosphocholine
PCA	Particles by compressed antisolvent
PEG	Polyethyleneglycol
PEO	Polyethylene oxide
PGC-1α	Peroxisome proliferator-activated receptor gamma coactivator 1-alpha
P-gp	P-glycoprotein
PGSS	Particles from gas saturated solutions
PVOH	Polyvinyl alcohol
PVP	Povidone
PVP-VA	Povidone-vinyl acetate
RES	Resveratrol
RESS	Rapid expansion of a supercritical solution
SAS	Supercritical antisolvent
SCFs	Supercritical fluids
SEDDS	Self-Emulsifying Drug Delivery Systems
SEDS	Solution enhanced dispersion by supercritical fluids
SEM	Scanning Electron Microscopy
SLS	Sodium Lauryl Sulphate

SSA	Specific surface area
T80	Tween® 80
TEER	Transepithelial Electrical Resistance
TPGS	d-alpha Tocopheryl Polyethylene Glycol 1000 Succinate
USA	United States of America
UV	Ultraviolet
XRPD	X-ray Powder Diffraction

B. List of Tables

C. List of Figures

D. Abstract

In last two decades, pharmaceutical industry has faced a paradigm change in the drug development, moving from compounds without major pharmacokinetic challenges to very potent compounds with poor pharmacokinetic properties. This led to an adaptation of development strategy, making formulation and drug delivery as key elements for the success of a discovery project.

Resveratrol is a good example of a very promising compound with proved *in vitro* efficacy in multiple therapeutic areas and indications, from antioxidant to anti-cancer, passing through antimicrobial, anti-aging, anti-diabetic or cardiovascular protective among others. However, it failed in clinical practice due to its poor pharmacokinetic properties. Resveratrol presents very poor water solubility (< 0.01 mg/mL), is subtract of efflux mechanisms and highly metabolised in the gastrointestinal tract. Therefore, it is one the most complex but at same time interesting compounds to use as model drug.

In the present thesis two different approaches were used to improve Resveratrol pharmacokinetic properties. A third-generation solid dispersion and a self-emulsifying drug delivery system were explored, in parallel, targeting to improve Resveratrol water solubility and reducing its intestinal metabolism and efflux mechanisms. Both approaches started by a high-throughput screening of carriers and formulation optimisation, followed by an *in vitro* technological and performance evaluation, Caco-2 permeability studies and finally, an *in vivo* rat pharmacokinetic profile.

Third-generation solid dispersion approach was able to identify several carriers able to enhance Resveratrol solubility above 2000 folds, such as Soluplus®. Additionally, second generation solid dispersions (binary composition) were prepared with several carriers, such as Soluplus®; poloxamers, HPMCAS, PEG6000, Povidone and copovidone at different ratios. FTIR and solubility data were able to confirm interactions between Resveratrol and carriers with potential to improve Resveratrol aqueous solubility. Based on the previous data, Soluplus® at a ratio of 1:2 (Resveratrol: Soluplus®) was selected as carrier. This ratio ensured a fully amorphous solid dispersion confirmed by DSC. Gelucire and Poloxamer 407 were included in previous composition at 5 and 15% each without affecting the amorphous state of Resveratrol (DSC data). Particularly, poloxamer 407 at 15% significantly improved Resveratrol drug release, at pH 1.2 but also at pH 6.8. The inclusion of both surfactants, at 15%, significantly improved Resveratrol permeability in Caco-2 cells over solid dispersion only composed by Resveratrol: Soluplus®. This data suggests that both surfactants were able to reduce intestinal metabolism and/ or efflux mechanisms of Resveratrol. Formulation containing poloxamer 407 presented a higher amount of Resveratrol recovered and was

less affected by apical to basal and basal to apical ratios being selected for rat pharmacokinetic studies. In rat pharmacokinetics studies a significant improvement in C_{max} and AUC_{0-t} was observed in third generation solid dispersion containing poloxamer 407 over the second generation solid dispersion without this surfactant.

In the self-emulsifying drug delivery system approach, a high-throughput screening of Resveratrol solubility revealed that all excipients significantly improved Resveratrol solubility. From this, two sets of three excipients were used for the formulation of SEDDS. One excipient with HLB above ten and another below six were selected for each set. The third component was selected from co-solvents and/or excipients with HLB in the range of 6-10. Therefore, set 1 was compose of Lauroglycol®90/ Labrasol®/ Capryol® and set 2 by Tween 80/ Transcutol®/ Imwitor® 742. Phase diagrams were built regarding solubility, dispersibility and robustness to dilution. Droplet size and specific surface area were also characterised, allowing the selection of 1 formulation from each set of compositions. The Lauroglycol®90/ Labrasol®/ Capryol® composed of 12.5/75/12.5 and Tween 80/ Transcutol®/ Imwitor® composed of 33/33/33 were selected for further studies. A significant improvement in permeability was observed for both formulations compared to pure Resveratrol. Moreover, a fast permeability process was observed which could be related to small droplet size of both formulations, but more evident for Tween 80/ Transcutol®/ Imwitor® formulation. In rat pharmacokinetic profile formulation Lauroglycol®90/ Labrasol®/ Capryol® presented a significant improvement in C_{max} over pure Resveratrol but not in AUC. These data indicate that a fast and intense *in vivo* oral absorption was observed for formulation composed of Lauroglycol®90/ Labrasol®/ Capryol®. The increase in C_{max} may have been associated to the reduction in metabolisation and/or efflux mechanisms as suggested by Caco-2 cell permeability data.

Alltogether, data indicate that is possible to improve Resveratrol bioavailability by increasing it solubility, but mostly by reducing its metabolism and efflux mechanisms. In this thesis, SEDDS presented higher bioavailability than third generation solid dispersion and therefore are suggested as a better strategy to improve Resveratrol bioavailability.

Resumo

A indústria farmacêutica durante as ultimas duas décadas tem sofrido uma mudança de paradigma no desenvolvimento de produtos, passando de compostos sem desafios sob o ponto de vista farmacocinético, para compostos muito potentes com inadequadas propriedades farmacocinéticas. Tal facto, tem levado a uma adaptação da estratégia de desenvolvimento por parte desta industria, transformando as áreas de formulação e de administração de fármacos em elementos cruciais para o sucesso do desenvolvimento de novos medicamentos.

O Resveratrol é um excelente exemplo de um fármaco com muito potencial, que demonstrou, *in vitro,* ser eficaz em múltiplas áreas terapêuticas e em diversas indicações, que variam desde antioxidante a anticancerígeno, passando por antimicrobiano, antienvelhecimento, antidiabético ou protetor cardiovascular entre outras, que falhou na prática clínica devido às suas inadequadas propriedades farmacocinéticas. O Resveratrol apresenta uma solubilidade em meio aquoso muito baixa (< 0.01 mg/mL), é substrato para mecanismos de efluxo intestinal e é altamente metabolizado no trato gastrointestinal. Consequentemente, é um dos fármacos mais complexos, mas simultaneamente dos mais interessantes para ser usado como fármaco modelo de formulação.

Na presente tese usaram-se duas abordagens para melhorar as propriedades farmacocinéticas do Resveratrol. Uma dispersão sólida de terceira geração e uma formulação auto-emulsificante foram desenvolvidas em paralelo com o objetivo de melhorar a solubilidade aquosa do Resveratrol e reduzir o seu metabolismo intestinal e propensão para ser substrato para mecanismos de efluxo. As duas abordagens iniciaram-se através de uma atividade de “screening” de excipientes e otimização de formulações. Seguida de uma avaliação *in vitro* das propriedades tecnologias e de desempenho das formulações, realização de estudos de permeabilidade em células Caco-2 e finalmente, pela realização de estudos de farmacocinética *in vivo* em modelo de rato.

Durante o desenvolvimento da dispersão sólida de terceira geração identificaram-se vários excipientes capazes de aumentar a solubilidade do Resveratrol, alguns, como o Soluplus®, 2000 vezes superior. De seguida prepararam-se várias dispersões sólidas binárias, ou de segunda geração, com excipientes, tais como, Soluplus®; poloxameros, HPMCAS, PEG6000, Povidona e copovidona, utilizados a várias concentrações. Os dados de FTIR e de solubilidade aquosa permitiram confirmar a existência de interações moleculares entre os excipientes e o Resveratrol, com potencial para aumentar a

solubilidade aquosa deste fármaco. Com base nestes dados, o Soluplus® a um rácio de 1:2 (Resveratrol: Soluplus®) foi selecionado como excipiente transportador. O uso deste rácio garante que o Resveratrol se encontra totalmente amorfizado de acordo com os dados obtidos por DSC. O Gelucire e o poloxamero 407 foram incluídos na composição anterior, nas concentrações de 5 e 15%, sem afetar o estado amorfo do Resveratrol (dados de DSC). Especialmente, o poloxamero 407 a 15% foi capaz de aumentar significativamente a libertação do Resveratrol tanto a pH 1.2 como a pH 6.8. A inclusão de ambos os surfactantes (Gelucire e poloxamero 407) aumentou significativamente a permeabilidade do Resveratrol através de células Caco-2, comparativamente com a permeabilidade da dispersão sólida apenas composta por Resveratrol:Soluplus® (1:2). Estes dados sugerem que os dois surfactantes são capazes de reduzir os mecanismos de efluxo e/ou de metabolização aos quais o Resveratrol está sujeito. A formulação contendo poloxamero 407, demostrou uma maior recuperação de Resveratrol total, no estudo de permeabilidade em Caco-2 e foi menos influenciada pelo modo de aplicação do Resveratrol (apical vs basal) e consequentemente foi selecionada para o estudo farmacocinético em rato. Esta formulação, contendo poloxamero 407, demostrou um aumento de cerca de 3 vezes no C_{max} e um aumento significativo no AUC_{0-t}, relativamente à dispersão solida sem este excipiente.

Durante o desenvolvimento da formulação auto-emusificante todos os excipientes aumentaram significativamente a solubilidade do Resveratrol. A partir dos excipientes testados foram criados dois grupos de formulações, compostos por 3 excipientes cada. Em cada um dos grupos, um excipiente possuía HLB superior a 10, outro abaixo de 6, o terceiro componente foi selecionado do grupo de co-solventes e/ou excipientes com HLB entre 6 e 10. Os dois grupos foram compostos pelos seguintes excipientes: Lauroglycol®90/ Labrasol®/ Capryol® e por Tween 80/ Transcutol®/ Imwitor® 742. Com cada um destes grupos de componentes foram criados diagramas de fase relativamente à solubilidade, dispersibilidade e estabilidade sob o efeito de diluição. O tamanho de gotícula e a área de superfície destas, também foram usados para caracterizar estas formulações, permitindo a seleção de uma formulação proveniente de cada grupo. Do grupo, Lauroglycol®90/ Labrasol®/ Capryol® a composição selecionada é constituída pelo rácio 12.5/75/12.5, por seu lado, no grupo Tween 80/ Transcutol®/ Imwitor® a formulação é composta pelo rácio 33/33/33. As formulações selecionadas, de cada um dos grupos anteriormente referidos, demostraram um aumento significativo na permeabilidade do Resveratrol em Caco-2. A formulação composta por Tween 80/ Transcutol®/ Imwitor apresentou adicionalmente um perfil de permeabilidade extremamente rápido que poderá ser relacionado com o tamanho de gotícula extremamente pequeno nesta formulação. No estudo de farmacocinética em

rato, a formulação Lauroglycol®90/ Labrasol®/ Capryol® apresentou um aumento significativo no valor C_{max} relativamente ao Resveratrol em estado cristalino, mas tal não foi observado para o AUC. Estes dados indicam uma absorção rápida e intensa após administração oral da formulação Lauroglycol®90/ Labrasol®/ Capryol®. O aumento no valor de C_{max} poderá estar associado a uma redução do metabolismo intestinal e/ ou dos mecanismos de efluxo intestinal, tal como sugerido pelo estudo de permeabilidade em células Caco-2.

Os dados obtidos nesta tese permitem concluir que é possível aumentar a biodisponibilidade do Resveratrol através do aumento da sua solubilidade aquosa, mas principalmente através da redução do seu metabolismo intestinal e bloqueio dos mecanismos de efluxo. Nesta tese, a formulação auto-emulsificante apresentou uma maior biodisponibilidade do que a formulação de dispersão sólida de terceira geração, pelo que se apresenta como a melhor estratégia para aumentar a biodisponibilidade do Resveratrol.

E. Introduction

This chapter was based on the following publications:

Teófilo Vasconcelos, Sara Marques, Bruno Sarmento. The biopharmaceutical classification system of excipients. Therapeutic Delivery 8: 65-78, 2017

Teófilo Vasconcelos, Sara Marques, José das Neves, Bruno Sarmento. Amorphous solid dispersions: rational selection of a manufacturing process. Advanced Drug Delivery Reviews 100: 85-101, 2016

1. Introduction

Oral delivery is the simplest and easiest way to administer drugs [1, 2]. Solid oral dosage forms have many advantages over other non-solid oral dosage forms due to the great stability, small bulk volume, accurate dosage, and easy production. Therefore, most of the new chemical entities (NCE) under development in our days are intended to be used as solid dosage forms that originate an effective and reproducible *in vivo* plasma concentration after oral administration [3, 4]. However, despite more potent, most of NCE are low water soluble drugs and/or poorly absorbed after oral administration [4, 5], for which the use can be inhibited due to these drawbacks [6-8]. Moreover, most of this promising NCE, despite their high permeability, are only absorbed in the upper small intestine, presenting, therefore, a small absorption window [9]. Consequently, if these drugs are not completely released in this gastrointestinal (GI) area, they will present reduced oral bioavailability or at least high inter and intra-individual variability in bioavailability [9, 10].

Resveratrol (RES) is one the most thrilling research areas with more than 15000 manuscripts published, among those more than 11000 in last 10 years and more than 7000 in last 5 years, according to PubMed data (Figure 1.1).

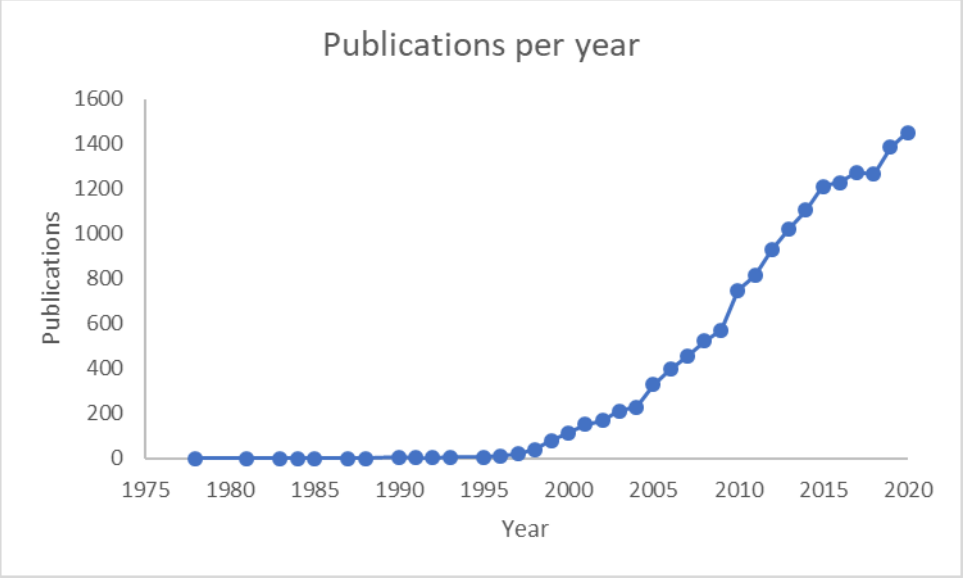

Figure 1-1 Resveratrol publications per year (Pubmed Search results assessed on 21 February 2021, using keyword Resveratrol).

Most of the manuscripts related to Resveratrol (Figure 1.2) discuss its effects as antioxidant (75%) [11, 12], cancer (27%) [13, 14], anti-inflammatory (18%) [15, 16], cardiovascular (13%) [12, 17], antimicrobial (9%) [18, 19], aging (9%) [20, 21], diabetes

(8%) [22, 23], obesity (5%) [22, 24], Alzheimer and Parkinson (both represent 5%) [25, 26] and drug delivery systems (4%) [27, 28] among others.

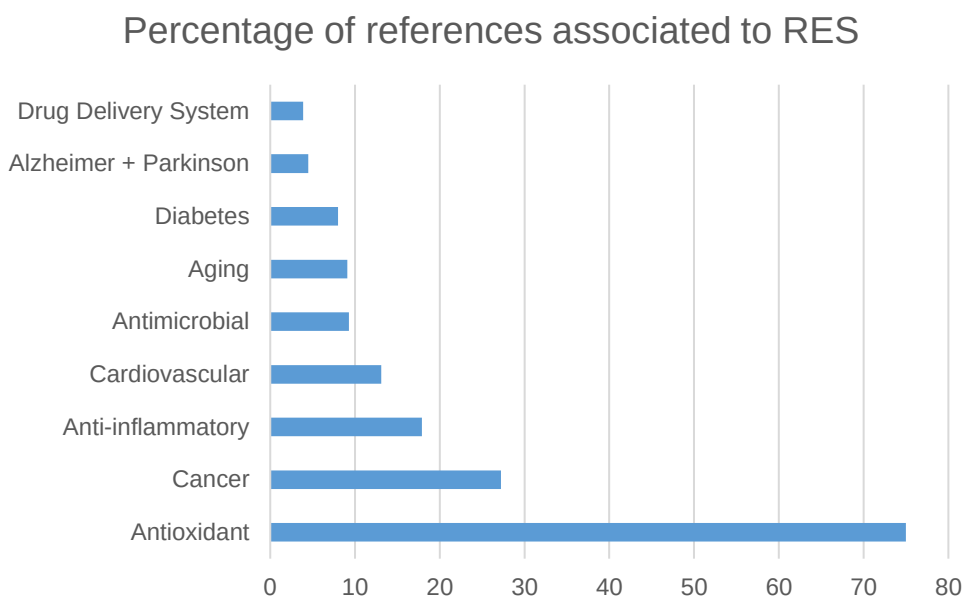

Figure 1-2 References associated to Resveratrol publications (Pubmed Search results assessed on 13 June 2020, using keyword Resveratrol + each of the above keywords was used to generate the data).

Among Resveratrol multiple activities, it is speculated that it can activate Sirtuin 1, an enzyme that deacetylates proteins in cell nuclei that contribute to cellular regulation (reaction to stressors, longevity) [29]. Moreover, it also activates peroxisome proliferator-activated receptor gamma coactivator 1-alpha (PGC-1α) and improves the functioning of the mitochondria [30]. The activation of Sirtuin 1 may further activate superoxide dismutase that reduces the free radicals in circulation which can be an explanation for the speculated longevity activity and anticancer activity of Resveratrol [31]. It also possesses antioxidant and anti-angiogenic properties [32] and can directly inhibit the cardiac fibroblasts [33]. Resveratrol interacts with several others enzymes, such as aromatase [34] and gamma-glutamylcysteine ligase [35] which both contribute to the large number of activities currently being explored for this product.

Among cancer therapy indication, Resveratrol has been used/tested in breast, prostate, colon or skin cancers among others. Regarding cardiovascular applications, Resveratrol was mainly linked to a reduction of high blood pressure, anti-platelet aggregation and inhibition for cardiac fibrosis. In neurology, Resveratrol has been explored in Huntington's disease, Alzheimer, Parkinson, and also as antidepressant as examples. Resveratrol has also been explored due to its effect in metabolism, being extensively

studied in lowering glucose blood levels, obesity, increasing lifespan and due to its estrogenic and antioxidant effect. Resveratrol anti-inflammatory [36] and antimicrobial [18] properties are also being extensively studied.

Despite, such a potential variety of activities and data provided by animal models, the human clinical use of Resveratrol is very limited and most of the clinical trials showed doubtful results [37, 38]. This is mainly attributed to the high therapeutic doses required (> 500 mg) and poor pharmacokinetic properties of Resveratrol, since it presents very limited oral bioavailability (less than 5% of the oral dose reaches plasma), mainly due to its poor water solubility and high intestinal metabolisation [39, 40]. For this later a drug delivery system strategy can be explored, but, despite such a seething field, the publications related to Resveratrol drug delivery systems only represent 4% of total publications and more than 90% and 70% of those were published in last 10 years and 5 years, respectively. Therefore, the improvement of oral bioavailability of Resveratrol is a current demand in the pharmaceutical field to allow the exploration of this multifaceted drug.

A drug delivery system for Resveratrol should address its three major challenges:

- Very poor water solubility (< 0.01 mg/mL)
- Highly metabolized by intestinal and hepatic cytochromes (CYPs)
- Substrate of efflux mechanisms

The Resveratrol poor solubility is aligned with one of the major challenges of the pharmaceutical industry nowadays, that is related with strategies that improve the water solubility of drugs [6, 41, 42]. Improving the bioavailability of poor water-soluble drugs allow dose reduction and not only improve efficacy but also increases financial turnover from companies. Generally, after oral administration, the drug must be released in the GI tract and, only after, absorbed through the GI endothelium to the blood stream. Bearing this in mind, it is obvious that drug release is a crucial and a limiting step for oral bioavailability, particularly for drugs with low water solubility in the GI conditions. By enhancing the drug release and increasing solubility, it is possible to improve its bioavailability, reduce variability and, ultimately, reduce its side effects [9, 41, 43-45]. Drugs that do not dissolve properly in the GI fluid can never be largely and reproducible absorbed because their biopharmaceutical properties are compromised and, consequently, are not available for absorption [4, 7, 9].

Physical-chemical approaches to improve drug water solubility include salt formation, polymorphic change or chemical modification. All these physical-chemical approaches are not recommended as priority for Resveratrol since may represent a new

chemical entity requiring new set of clinical trials and the impact in its metabolisation and efflux is not known.

Generally, solubility enhancement strategies based on formulation can be divided in particle size reduction techniques, liquid formulations and formulations using carriers.

The particle size reduction techniques such as milling or micronisation are commonly used as approaches to improve solubility based on the increase of surface area [7, 46]. These approaches present limited efficacy for compounds with a solubility below 0.1 mg/mL such as Resveratrol, since the particle size reduction limit is around 2 to 5 microns which frequently is not enough to improve considerably the drug solubility or drug release in small intestine [7, 47, 48], and consequently to improve the bioavailability of these compounds [47, 49, 50]. Moreover, the products obtained from these techniques generally present poor mechanical properties, such as low flow and high adhesion, and are extremely difficult to handle [47, 48] particularly in drug products with high dose, such as Resveratrol. Finally, these techniques do not impact intestinal metabolism and/ or efflux and therefore have limited application in Resveratrol.

Regarding liquid formulations, these can be divided in oil formulations, water formulation and Self-Emulsifying Drug Delivery Systems (SEDDS). The latter, which are isotropic mixtures of oils, surfactants, solvents and co-solvents/surfactants, can be used for the design of formulations in order to improve the oral absorption of highly lipophilic drug compounds. SEDDS can be orally administered in soft or hard gelatine capsules and form fine relatively stable oil−in−water (o/w) emulsions upon aqueous dilution owing to the gentle agitation of the GI fluids [51]. These drug delivery systems may also modulate the efflux mechanisms and be absorbed by the Peyer's patches avoiding the first passage metabolism [52]. Therefore, these drug delivery systems represent an interesting approach, particularly because Resveratrol presents a LogP of 3.14 (*in silico* data retrieved from Gastroplus® software version 9.6) meaning that has potential solubility in some lipids.

In the case of formulations using carriers based on the structure of the carrier, these can be divided in liposomes, micro/ nanoparticles (capsules of spheres) and solid dispersions. Liposomes are not orally stable and therefore should not be explored in Resveratrol. Micro/ nanoparticles present some potential to overcome Resveratrol poor solubility issues, however their manufacturing processes are not scalable, resulting in poor yield and consequently very expensive products, therefore are not recommended as promising approach for Resveratrol. From this group, solid dispersions are the most promising approach [53]. Solid dispersions can be defined as molecular mixtures of poor water soluble drugs in hydrophilic carriers, which present a drug release profile that is driven

by the polymer properties [5, 54]. In solid dispersion, drug is in its supersaturated state due to forced solubilisation in the carrier [38, 55, 56]. It is characterized by the reduction of drug particle size to nearly a molecular level, by solubilizing or co-dissolving the drug in the water soluble carrier, by providing better wettability and dispersibility and by forming amorphous products [29, 57]. This approach can be explored to overcome Resveratrol poor water solubility, particularly because exist technologies able to allow an industrialisation to large scale. This topic was subject of a review paper entitled; *"Amorphous Solid Dispersions: Rational selection of a manufacturing process"*, that is presented below.

Overcoming the intestinal metabolism (Figure 1.3) of Resveratrol can be achieved by changing the administration route, targeting drug release in specific GI regions, modulating metabolism and/or efflux mechanisms or by chemical modification.

Possible Resveratrol administration routes, other than oral, include intravenous and subcutaneous that due to the invasiveness and long-term therapy of Resveratrol are generally discouraged. Other include pulmonary, topical, rectal or vaginal that are less acceptable than oral and/or may not be feasible due to the high Resveratrol doses needed even with a potential dose reduction due to metabolism reduction.

As alternative, the chemical modification by inclusion of protective groups, results in a new chemical entity that is no longer Resveratrol and requires full set of clinical trials and therefore is not a recommended approach.

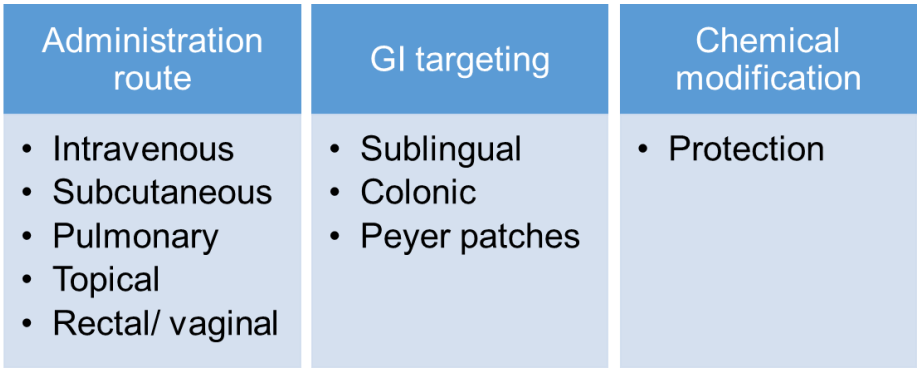

Figure 1-3 Strategies to overcome Resveratrol intestinal metabolism and efflux.

Targeting specific GI regions can be explored to overcome metabolism and or efflux mechanics. Sublingual administration is a possible approach since it prevents first passage effect, however Resveratrol dose is extremely high making unfeasible the development of a dosage form with acceptable size, moreover sublingual absorption is not adequate for a dose such as 500 mg. Colon presents lower efflux and metabolism mechanisms and could be explored has a target for Resveratrol, however the liquid volume in colon is very low,

limiting the amount of Resveratrol able to solubilize and consequently to be absorbed, associated to the high dose, this approach is not the most adequate. Another GI tract target approach could be the investigation of Peyer patches to absorb Resveratrol directly to the lymphatic system avoiding therefore the first passage effect. For this purpose, lipid formulations, particularly SEDDS with certain excipients, such has medium chain triglycerides, can promote absorption trough Peyer patches and can be explored to improve Resveratrol bioavailability.

The use of excipients able to modulate intestinal metabolism and efflux mechanisms can be explored to improve the bioavailability of Resveratrol. This topic was a subject of a deeper review entitled “The biopharmaceutical classification system of excipients” that is presented below.

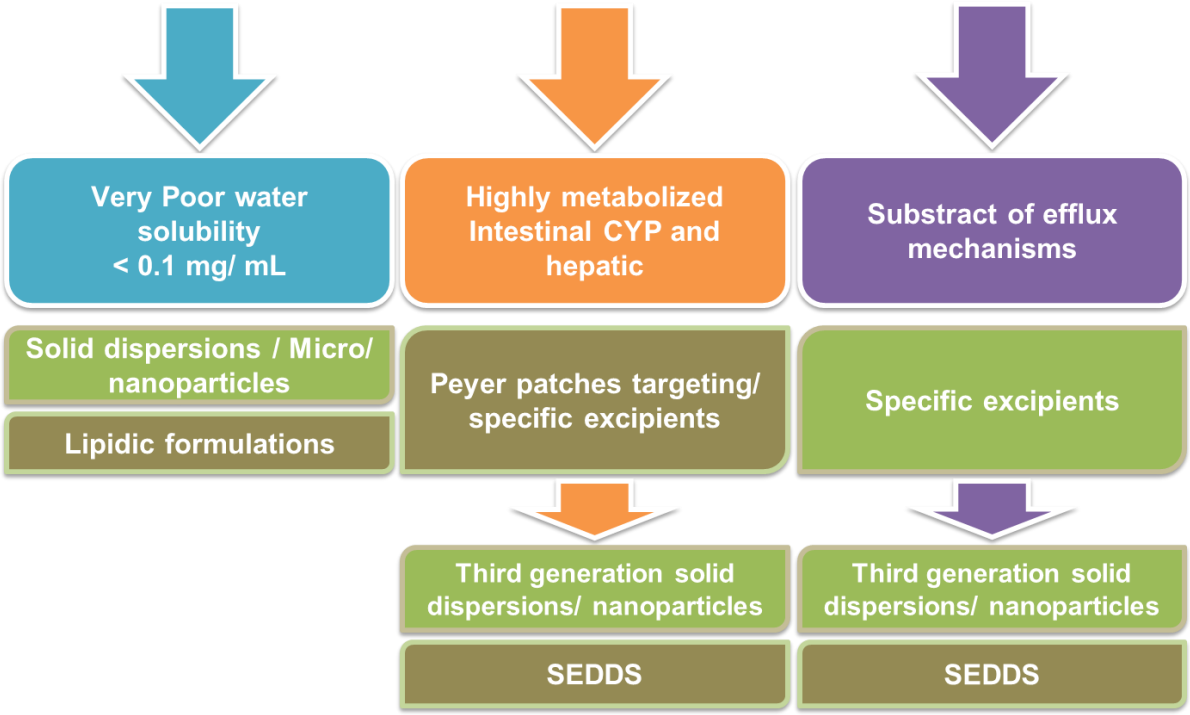

Figure 1-4 Formulation strategies to overcome Resveratrol challenges.

In summary, the poor water solubility of Resveratrol can be overcome by using lipidic formulations, micro/ nanoparticles or solid dispersions (Figure 1.4). High intestinal metabolism of Resveratrol can be surpassed by targeting Peyer patches absorption and/or by using excipients able to interact with intestinal metabolism. These strategies are translated into the use of SEDDS, nanoparticles or third generation solid dispersions. The intestinal high efflux mechanisms effect in Resveratrol absorption can be mitigated or limited

by using specific excipients that generally are used in SEDDS. Nevertheless, these can also be incorporated in micro/ nanoparticles or in third generation solid dispersions.

Therefore, Resveratrol as a form of Trans-Resveratrol has been selected as candidate for this project. From this, an attempt to develop a third-generation solid dispersion formulation and a SEDDS in parallel in order to explore a reduction of the GI metabolism of Resveratrol will be conducted.

2. The biopharmaceutical classification system of excipients

2.1. Introduction

Pharmaceutical excipients were traditionally defined has inert components used in medicines, crucial to guarantee an adequate quality, safety and efficacy of a medicine [58-60]. They are substances other than the active drug which are included during the manufacturing process or are contained in a finished pharmaceutical dosage form [61]. Despite regarded as therapeutically inert they are essential to transport the active drug to the location in the body where the drug is intended to exert its action [61, 62]. In addition, pharmaceutical excipients are key elements to ensure an adequate processability or stabilisation of the drug substance [58, 59, 62]. Considering this, a professional expert in pharmaceutical formulation could convert the most amazing drug substance in an ineffective medicine by altering and conjugating the pharmaceutical excipients present in the final dosage form. On the other hand, a drug substance with poor pharmacokinetic profile can be improved by an adequate selection of excipients. For example, a drug that undergoes degradation by oxidation or hydrolysis can have its stability improved by selecting excipients with reduction properties such as lactose [63], or moisture protection such as moisture sensitive film-coating [64-66], respectively; a drug that causes stomach irritation and therefore originating a high incidence of side effects can be improved by using a gastro-resistant coating system [67, 68] or by being incorporated in a gastro-resistant matrix (e.g. containing Hypromellose acetate succinate – HPMCAS [69, 70]). Thus, the role of excipients in the final dosage form is undeniable.

2.2. Excipients properties

Despite their widely pharmaceutical functions, chemical moiety or reactivity, physical state or source, pharmaceutical excipients were recognized as safe and without biological activity or interaction. Several excipients are able to modulate the drug performance by controlling the drug release, such has metacrylates, carbopol® or HPMC [59, 71]. Others may improve the drug solubility resulting in higher bioavailability such has povidone or polyethylene glycol (PEG). However, in any case, excipients are recognized as being able to interact with our biological systems [61, 71]. In the last decade, new therapeutical challenges were overcome by using drugs that are outside the conventional drugable space

driven by the Lipinski rule [72]. These valuable drugs are extremely challenging from the pharmaceutical perspective. Particularly because associated to their poor physical chemical properties for the oral route, such has high melting point and /or molecular weight and/ or high logP are associated to poor intrinsic permeability or poor permeability due to efflux mechanisms or intestinal metabolisation [72-74]. The combination of these factors result in an increased number of drugs belonging to class III and IV accordingly to the biopharmaceutical classification system (BCS) proposed by Amidon [61, 74, 75].

The pharmaceutical industry, in particular the industries associated to the development of new excipients, provided an assertive response to these new challenges developing new products able to support the establishment of new drugs products. However, this effort led to the development of excipients that no longer can be considered as inert because they interfere and interact with our biological systems [75].

2.3. Biological mechanisms targeted by new excipients

The two major biological mechanisms used to protect our organism from external xenobiotics are biotransformation and efflux pumps [61]. Among the metabolizing enzymes present in the small intestinal mucosa, the cytochrome P450 (CYPs) are of particular importance, being responsible for the majority of phase I drug metabolism reactions [76-78]. From these, CYP3A and CYP2C are the most representative in the intestinal mucosa, in which, CYP3A4, CYP3A5 and CYP2C9 are the most representative in this order of relevance. Additionally, CYP2J2 and CYP1A1 are also present in intestinal mucosa and are associated to inter-individual variability. The distribution of most CYP enzymes is not uniform along the human gastrointestinal tract. For instance, CYP3A shows a slightly lower level of expression at the duodenum followed by an increase at the jejunum, then finally decreasing toward the ileum [79, 80].

Efflux transporters are present in all human biological barriers, being the most important in intestine, liver, kidney and blood-brain barrier. This manuscript will only focus in the intestinal barrier where the most relevant efflux transporters include P-glycoprotein (P-gp), multidrug resistance proteins (MRP2), organic anion-transporting polypeptide (OATP) and breast cancer resistance protein (BCRP) [81, 82]. These proteins located in the luminal side of the intestine walls use ATP to actively pump drugs or xenobiotics back to the intestine. This mechanism is extremely important in drug resistance, resulting in poor bioavailability and drug – drug interaction. The efflux transporters distribution along the gastro-intestinal (GI) tract is not uniform. Both OATP and MRP2 have higher expression in the jejunum, but in the case of MRP2 jejunum predominance is followed by the duodenum and ileum, with very little expression in the colon [83, 84]. The P-gp efflux pump expression

increases from proximal to distal regions of the small intestine being higher at the jejunum and ileum. The BCRP maximum expression exists in the duodenum and decreases continuously down to the rectum, in which, the BCRP expression in the duodenum is comparable to P-gp [84].

Some excipients have shown the ability to interfere and inhibit these protective mechanisms [61]. This ability has been explored for enhancing the drug oral bioavailability in the delivery field [85, 86]. The current state of the excipients able to influence these mechanisms is presented in next sections.

2.4. Excipients able to interact with metabolic mechanisms

The excipients interaction with the metabolic mechanism in the intestine can occur by three different processes, namely direct inhibition (chemical) [87], regulation of mRNA expression (reduced or increased) [88] or regulation of protein expression (reduced or increased) [78, 89]. Surfactants are the excipients that mostly interact with intestinal metabolism, as summarized in Table 2.1.

Table 2-1. Properties of surfactants with interaction on intestinal metabolism.

Surfactant	Common name	Hydrophilic component	Lipid component	HLB
Kolliphor® HS15	Macrogol-15-hydroxystearate	15 molecules of ethylene oxide	hydroxy stearate (mono and di esters)	14-16
Kolliphor® EL	Peg-35 castor oil	35 molecules of ethylene oxide	Glycerol triricinoleate	12-14
Kolliphor® RH40	Peg-40 hydrogenated castor oil	40 – 45 molecules of ethylene oxide	Hydrogenated Glycerol triricinoleate	14-16
Myrj® 52	Peg-40 stearate	40 molecules of ethylene oxide	stearate	17
Brij® 30	Polyoxyl 4 lauryl ether	4 molecules of ethylene oxide	lauryl (dodecyl)	10
Brij® 35	Polyoxyl 23 lauryl ether	23 molecules of ethylene oxide	lauryl (dodecyl)	17
Tween® 20	Polyoxyethylene (20) sorbitan monolaurate	20 molecules of ethylene oxide	sorbitan monolaurate	17
Tween® 80	Polyoxyethylene (20) sorbitan monooleate	20 molecules of ethylene oxide	sorbitan monooleate	15
P181	Poloxamer 181	10% polyoxyethylene content	polyoxypropylene molecular mass of 1800 g/mol	3
P188	Poloxamer 188	10% polyoxyethylene content	polyoxypropylene molecular mass of 1800 g/mol	>24
P235	Poloxamer 235	50% polyoxyethylene content	polyoxypropylene molecular mass of 2300 g/mol	Not available
P333	Poloxamer 333	30% polyoxyethylene content	polyoxypropylene molecular mass of 3300 g/mol	7-12
P403	Poloxamer 403	30% polyoxyethylene content	polyoxypropylene molecular mass of 4000 g/mol	7-12
P407	Poloxamer 407	70% polyoxyethylene content	polyoxypropylene molecular mass of 4000 g/mol	18-23
Vitamin E TPGS	Vitamin E polyethylene glycol succinate	Polyethylene glycol 1000 succinate	Vitamin E	13
Labrasol®	Caprylocaproyl macrogol-8 glycerides	8 molecules of ethylene oxide	Caprylic/Capric Glycerides	12
Gelucire ® 44/12	Lauroyl macrogol-32 glycerides	32 molecules of ethylene oxide	Lauroyl glycerides	11

2.4.1. CYP3A inhibition

The Kolliphor® HS15 [90], Kolliphor® EL [89, 90] Tween® 20 [89], Tween® 80 [90, 91], PEG400 [92, 93], Myrj® 52 [89] poloxamer 188 [89] and poloxamer 235 [92] showed *in vitro* ability to inhibit CYP3A, which was generally dose dependent [61]. This inhibition was

further confirmed *in vivo* by an increase in bioavailability of midazolam, which is a CYP3A substrate in the presence of Kolliphor® EL [90] and Tween® 20 [89]. In opposite, Myrj® 52 and poloxamer 188 induced an *in vivo* reduction of midazolam area under the curve (AUC) [89]. These excipients interact with CYP due to subtract competition [87], reduction in CYP3A protein expression as observed for Kolliphor® RH40 [91] or via enzymatic conformation change. In other studies, poloxamers P403 and P407 [94], Kolliphor® EL [93] and Vitamin E TPGS [92, 93] had little or no effect on intestinal cytochrome P4503A activity [94] in opposition to the previously stated. This data suggest that dose can be a relevant factor in the CYP inhibition.

2.4.2. CYP3A4 inhibition

The inhibition of specific CYP3A4 was observed *in vitro* for Kolliphor® EL [95], Kolliphor® RH40 [78, 89, 95, 96] Vitamin E TPGS [95], Tween® 80 [95-97], poloxamer 188 [97, 98], Myrj® 52 [99, 100], Brij® 35 [100], thiomers [100], modified cyclodextrins [101] and sucrose laurate [95], in a dose dependent manner below the critical micellar concentration (CMC) [95]. From these, Tween® 80 reduced the mRNA and protein expression of this metabolic mechanism [88]. Other excipients such as binders, fillers, solvents, or co-solvents may also affect CYP3A activity as well. Thompkins *et al* studied nineteen common excipients and concluded that the polymers HPMC and croscarmellose sodium caused a moderate but statistically significant 1.8-fold and 2.4-fold increase in CYP3A4 mRNA expression, respectively [88]. Nevertheless, this was not translated into protein expression increase and the mRNA increase was marginal when compared to the positive control [88]. In the same study the authors concluded that HPMC, pre-gelatinized starch and Tween® 80 showed statistically significant effects over CYP3A4 in multiple cell lines studied. Silicon dioxide. magnesium stearate and pre-gelatinized starch decreased CYP3A4 mRNA expression by more than 40%, 70%, and 65%, respectively [88]. However, di-calcium phosphate, HPMC, crospovidone, PEG3350, propylene glycol, citric acid and malic acid decreased the protein expression. The remaining excipients (lactose, cellulose microcrystalline, povidone, sodium starch glycolate, sodium lauryl sulfate and sucrose) showed no effect over this metabolism mechanism [88]. In another study, eight plasticizers were studied, acetyl tributyl citrate, tributyl citrate, acetyl triethyl citrate, and triethyl citrate, diethyl phthalate and dibutyl phthalate, dibutyl sebacate, and triacetin, in which all showed induction of CYP3A4. From these acetyl tributyl citrate was the most potent *in vitro* with also *in vivo* confirmation. The demonstrated data suggested that this induction only occurred in the intestine and not in the liver [102].

2.4.3. CYP3A5 inhibition

The CYP3A5 has been *in vitro* inhibited by the following excipients PEG1000, Tween® 20, cetyltrimethylammonium bromide (CTAB), Tween® 80 and poloxamer 188, through decreasing potency [97].

2.4.4. CYP2C9 inhibition

Christiansen *et al* studied the *in vitro* inhibition of CYP2C9 caused by several excipients [95]. Results obtained by other researchers indicate that Kolliphor® EL [95], Kolliphor® RH40 [95], Myrj® 52 [99] and Tween® 80 [95] were the most powerful inhibitors followed by sucrose laurate [95]. Vitamin ET PGS was 10-fold weaker than the most potent. In another study using a screening kit, PEG1000 and poloxamer 188 showed moderate inhibiting of CYP2C9 [97]. On the other hand, modified cyclodextrins enhanced CYP2C9 activity [101].

2.4.5. Glucuronidation

Excipients do not only limit their interaction with Phase I metabolization but can also interference in the Phase II path. This impact was recently assessed for glucuronidation. The reported data indicate that parabens (methyl and propyl) were able to almost completely inhibit glucuronidation. Surfactants also presented potential to inhibit this mechanism, with decreasing order Tween® 20 > Kolliphor® EL > Kolliphor® RH > PEG400 > Tween® 80 > Kolliphor® H15 [103]. Table 2.2 presents a summary of the excipients interaction with the metabolization systems.

Table 2-2. Excipients effect in cytochrome P-450.

Excipient	CYP3A	CYP3A4	CYP3A5	CYP2C9	Glucuronidation
Kolliphor® HS15	+				+
Kolliphor® EL	+	+		+	+
Kolliphor® RH40		+		+	+
Tween® 20	+		+		+
Tween® 80	+	+	+	+	+
PEG400	+				+
PEG1000			+	+	
PEG3350	+				
Myrj® 52	±	+		+	
Brij® 35		+			
Poloxamer 188	±	+	+	+	
Poloxamer 235	+				
Poloxamer 403	-				
Poloxamer 407	-				
Vit. E TPGS	-	+			
Thiomers		+			
Modified Cyclodextrins		+		↑	
Sucrose Laurate		+		+	
HPMC	+				
Croscarmelose Sodium	+				
Sodium starch glycolate	+				
Silicon dioxide	+				
Magnesium stearate	+				
Di-calcium phosphate	+				
Crospovidone	+				
Propylene glycol	+				
Acetic acid	+				
Malic Acid	+				
Triacetin	↑				
Phtalates	↑				
Lactose	-				
Cellulose microcrystalline	-				
Povidone	-				
Sodium starch glycolate	-				
Sodium lauryl sulfate	-				
Sucrose	-				
Cetyltrimethylammonium bromide	+				

(+) inhibition; (-) no inhibition; (±) variable information (↑) enzymatic induction

2.5. Transporters interaction

As commonly accepted, drug transport mechanisms, in particular the efflux transport to the intestinal lumen, conditions poor drug bioavailability [104]. In the last years, several reports suggest that some excipients are able to module and interact with this efflux mechanism [61, 85, 86, 105, 106]. Nevertheless, their mechanisms and specific transporters interaction is not yet clear.

Chelation of crucial micronutrients for an adequate enzymatic activity can be a possible mechanism to reduce the efflux transport mechanisms. Bromberg *et al* demonstrated that polymers based on polymetacrylates were able to strongly bind bivalent cations such as zinc and calcium preventing their association to certain transporters, thereby inactivating them and enhancing doxorubicin permeability [84, 107].

A transformation in the cell membrane implying an inactivation of the efflux pumps can be another mechanism of interaction between excipients and transporters mechanisms [81, 85]. This type of interaction has been associated with surfactants that due to their amphiphilic structure are able to interact with lipids in the cell membrane and change both its physical and functional properties. Indeed, surfactants are able to alter the membrane fluidity, which can modify the orientation of the efflux pumps on its surface, preventing the substrate binding, and/or activation of pump by co-factors [81, 85]. In addition, surfactants have been found to enhance the absorption of compounds by both transcellular and paracellular routes through reduction of the membrane viscosity and increasing its elasticity [84, 93, 108, 109].

Competitive inhibition of substrate binding and inhibition of efflux pump ATPase have also been proposed as possible mechanisms [92, 110], as well as down-regulation of the transporter, as observed for P-gp expression [111].

Among the pharmaceutical surfactants, polymers and lipid compounds are the most frequently associated to inhibition of intestinal efflux transporters [84, 112]. However, due to their unclear mechanism of action, most of the excipients are not specific of a single transporter [113].

2.5.1. P-gp inhibition

P-gp, also known has multidrug resistance protein (MRP1) or ATP-binding cassette sub-family B member 1 (ABCB1), is the most studied efflux mechanism in the gastrointestinal tract [61]. This transporter is also widely presented in liver, kidney and blood-brain barrier [84]. P-gp is a 170 kDa transmembrane glycoprotein, which includes 10-15 kDa of N-terminal glycosylation. At intestinal level P-gp is presented in the luminal side of the cell [114]. Substrate enters P-gp either from an opening within the membrane or from the cytoplasm. ATP binds at the cytoplasmic side of the protein. ATP hydrolysis moves the substrate into a position to be excreted from the cell [114].

Kolliphor® RH [113, 115], Kolliphor® EL [85, 93, 116-119], Labrasol® [120], Tween® 20 [117], Tween® 80 [85, 119, 121-123], sucrose laurate [119] Span® 20 [113], poloxamer 235 (P85) [84, 124, 125], poloxamer 181 [117, 126], poloxamer 188 [98, 120],

poloxamer 333 [119] poloxamer 403 [94], poloxamer 407 [94], Brij® 35 [127], Myrj® 52 [61, 99], Softigen® 767 (PEG-6 Caprylic/ Capric Glycerides) [128], PEG-15 Stearyl Ether (acconon E) [128] and Gelucire® 44/14 [129] were demonstrated to *in vitro* inhibit P-gp below or at their CMC concertation [113]. Generally, above the CMC concentration surfactants tend to decrease their impact in P-gp due to drug entrapment into the formed micelles [96, 124]. In a human study, Kolliphor® EL was only effective below its CMC, suggesting that above CMC the drug may be entrapped into the micelles and was not able to be absorbed [118]. On contrary, vitamin E TPGS is able to inhibit P-gp efflux above and below its CMC [93, 113, 119, 130, 131] enhancing the permeability of doxorubicin [131], vinblastine [131], paclitaxel [131], etoposide [130] and colchicine [131]. In an *in vivo* human study, it showed inhibition of P-gp at a concentration of 0.04% (w/v), resulting in an enhancement of talinolol AUC (0-infinity) and C_{max} at 40% and 100%, respectively [132].

The polymers PEG400 and PEG300 inhibit P-gp in a dose dependent manner, being PEG400 more potent [133].

The exact mechanism of action for the P-gp inhibition is unclear. An alteration in membrane fluidity was observed for Vitamin E TPGS [110, 121, 134] which increased the membrane rigidity. On the other way, Tween® 80 [121], Kolliphor® EL [121] poloxamer 235 [125] fluidized the membrane. Both changes resulted in a decrease in ATPase activity and in a P-gp inhibition. An interaction with one or both of the P-gp ATP nucleotide binding domains inhibition of ATPase activity of drug efflux proteins and intracellular ATP depletion was described for Vitamin E TPGS [134], Myrj® 52 [99] and poloxamer 235 [125]. Poloxamer 181 on the other way, which is a cationic surfactant was able to interfere with ionic flux in the plasma membrane and cause compensatory ATP consumption by Na^+, K^+-ATPase, thus decreasing the intracellular ATP concentration and inhibiting P-gp [126].

The surfactants effect on efflux mechanisms is structure and interaction dependent since the excipients from the same family of the ones presenting P-gp inhibition properties do not present the same capacity. For instance, Span® 40, Span® 80, Propylene glycol, triacetin and Ethyl oleate do not affect P-gp activity at levels below or at their CMC concentration [113]. Also, PEG200 [133] and PEG400 [130] at 5, 0.1 and 0.5% w/v also did not have P-gp effect. In other cases, excipients reported has P-gp inhibitors, such as Tween® 80 [116], poloxamer 188 (0.8%) [132] and Kolliphor® RH40 [119] were shown to have negative results in some studies.

Phospholipids are another group of known P-gp inhibitors. The 1,2-dioctanoyl-sn-glycero-3-phosphocholine (8:0 PC) [85, 135], 1,2-didecanoyl-sn-glycero-3-phosphocholine (10:0 PC) [85, 135] and unsaturated docosahexaeonic acid residues (cis-22:6 PC) showed

to be strong inhibitors. Their effects on membrane fluidity were not consistent with their P-gp inhibiting effects, and, therefore, suggested a more complex mode of action [85], such as direct P-gp inhibitors interacting with the transporter probably in their monomeric state, whereas a different, as yet unknown mechanism of action applied for cis-22:6 PC [135].

The monoglycerides 1-monoolein and 1-monostearin were not P-gp inhibitors at non cytotoxic concentrations but at higher concentrations P-gp inhibition was observed [136]. Caprylic/Capric Glycerides (Imwitor® 742) and Miglyol® which are triglycerides showed P-gp inhibition, which was potent for Imwitor® 742 [128].

2.5.2. MRP2 inhibition

Multidrug resistance-associated protein 2 (MRP2), also known as ATP-binding cassette sub-family C member 2 (ABCC2) is a transporter mainly expressed in the liver, kidney and intestine [61, 137]. Surfactants and polymers, similarly for P-gp, have also demonstrated to influence MRP2 transport. Kolliphor® EL [104, 119, 137, 138], vitamin E TPGS [119], Tween® 80 [119], sodium lauryl sulfate (0.2 mg/mL) [139], Labrasol® [138], poloxamer 235 [125], poloxamer 407 [137, 138], PEG2000 [137, 138], PEG400 [137, 138], Trascutol® [137] and Kolliphor ® RH 40 [119, 137, 138] had previously demonstrated *in vitro* MRP2 inhibition. Other excipients as lipids have also been studied. Maisine® 35-1 (Glycerol monolinoleate) [137], Caprylic/Capric triglyceride (Labrafac Lipophile® WL 1349) [138], Glyceryl Caprylate (Capmul MCM) [138] and β-cyclodextrin [137] have some effect in MRP2.

Kolliphor ® RH 40 was more potent in inhibiting MRPP2 than P-gp [119]. Tween® 80 [119] and poloxamer 235 [125] presented a lower potency in inhibiting MRP2 than P-gp. In the particular case of the poloxamer 235, this was attributed to a considerably greater effect on the P-gp ATPase activity interaction when compared to the MRP2 ATPases [125]. On the other hand, poloxamer 333 [119], poloxamer 188 [137, 139] and sucrose laurate [119] which are P-gp inhibitors have no effect in MRP2 efflux mechanism. Other excipients showed variable results in inhibiting MRP2, for instance Kolliphor® EL (0.2 mg/mL) [139], poloxamer 407 [139] and Labrasol® [137] also provided negative results.

Hanke *et al*, concluded that surfactants caused an alteration in ABCC2 mRNA or protein expression [119]. These findings indicate that the observed interactions are caused by specific inhibition of the transporter activity [119]. Conformational changes of the transporter due to membrane fluidisation and/or nonspecific steric interaction of the drug-binding sites was also speculated [125]. The effect of sodium lauryl sulfate on the active secretion of amoxicillin was mainly attributed to the reversible cellular ATP depletion [139].

Li *et al* observed positive and negative interactions between excipients that alone are MRP2 inhibitors suggesting that an adequate selection and combination of these is crucial for an acceptable performance of the drug product [137].

2.5.3. BCRP inhibition

BCRP also known as ATP-binding cassette sub-family G member 2 (ABCG2) is present at the apical membrane of the intestine, in the blood brain barrier among other tissues [61]. Surfactants, such has Kolliphor® EL [104, 113], Tween® 20 [113] poloxamer 235 [113], Span® 20 [113] and Brij® 30[113] were found to inhibit the BCRP efflux mechanism. Some other compounds that are P-gp and MRP2 inhibitors and are not BCRP inhibitors including Kolliphor® RH40 [113], Tween® 80 [113], vitamin E TPGS [113], Myrj® 52 [113] and Gelucire® 44/14 [113] which is a further evidence that structure specificity plays an important role in surfactant mediated inhibition. Excipients such as Span® 40, Span® 80, propylene glycol, triacetin and ethyl oleate are not inhibitors of BCRP [113].

Excipients that are BCRP inhibitors have no significant effects on intracellular ATP levels of these transporters showing that ATP depletion is not their mechanism of action. In addition was demonstrated that the same excipient may have different mechanisms of action in different transporters such as BCRP and P-gp [113].

2.5.4. OATP inhibition

OATP is a membrane transport protein that mediates the transport of mainly organic anions across the cell membrane. Since these are uptake transporters and not efflux transporters, their inhibition may reduce the absorption of their substrate drugs [61]. The OATPs present in the intestine are OATP1A2, OATP1B3, OATP12B1.

Very little information is available related to the inhibition of this transporter by excipients. Engel *et al*, studied the effect of regular excipients in the inhibition of OATPs showing that Kolliphor® HS15 and Kolliphor® EL were the most potent inhibitors of all OATP transporters with the strongest effect on intestinal proteins [77]. PEG400 was a selective and potent modulator of only OATP1A2 [77]. Table 2.3 summaries the effect of excipients on most relevant transporter mechanisms.

Table 2-3. Excipients effect in transporters.

Excipient	P-gp	MRP2	BCRP	OATP
Kolliphor® HS15				+
Kolliphor® EL	+	±	+	+
Kolliphor® RH40	±	+	-	
Tween® 20	+			
Tween® 80	±	+	+	
PEG400	+	+	-	+
PEG300	+			
PEG2000		+		
Myrj® 52	+		-	
Brij® 35	+			
Brij® 30			+	
Span® 20	+		+	
Span® 40	-		-	
Span® 80	-		-	
Poloxamer 181	+			
Poloxamer 188	±	-		
Poloxamer 235	+	+	+	
Poloxamer 333	+	-		
Poloxamer 403	+			
Poloxamer 407	+	±		
Vit. E TPGS	+	+	-	
Sodium lauryl sulfate		+		
Transcutol®		+		
Sucrose Laurate	+	-		
Labrasol®	+	±		
Gelucire® 44/14	+		-	
Stearyl ether	+			
Softigen® 767	+			
8:0 phosphocholine	+			
10:0 phosphocholine	+			
cis-22:6 phosphocholin	+			
Propylene glycol	-		-	
Ethyl oleate	-		-	
Triacetin	-		-	
Imwitor 742®	+			
Miglyol®	+			

(+) inhibition; (-) no inhibition; (±) variable information

2.6. Data limitations on the interaction of excipients with transporters and metabolism mechanisms

The currently available information is rare and present some limitations. One of the most important is the scarce number of *in vivo* studies and, from these, almost none are from human. In fact, despite talinolol case with TPGS [132], which has more than 10 years, no other relevant human studies are available. This lack prevents an adequate translation of the *in vitro* data into clinical application.

Most of the studies used *in vitro* systems, particularly Caco-2 and modified Caco-2 monolayers. These models can be reliable but caution on the data interpretation should be made. Particularly, because excipients and formulation toxicities can artificially increase drug permeation by damaging and disrupting cell monolayers or killing the cells, consequently providing misleading results [140]. These effect has been demonstrated for some surfactants, which generally demonstrated concentration-dependent effects on reducing cell viability and consequently improved the drug permeability through the monolayer [140-142].

A large number of *in vitro* studies are currently available. However, some of these *in vitro* data are not translated into *in vivo* results, showing that some excipients that *in vitro* demonstrate positive results reveal negative results *in vivo* [89, 128]. This fact suggests that additional physiological factors, such as intestinal liquid volume or endogenous content of surfactants can impact the interaction of excipients with biological barriers.

Another current limitation on the accessible data is the study design of some *in vivo* studies. Some of these studies, use ineffective doses [118] or/ and high doses of surfactants [103, 118]. These may result in both false positive and negative results, which in any case, will not be translational into a daily use.

Despite these limitations, the potential of excipients to interact with our biological barriers is unquestionable and should be subject of a deeply scrutiny.

2.7. Regulatory perspective and biopharmaceutical classification system of excipients

More and more regulators have a huge concern about the risk associated to drug properties and its impact in safety efficacy and quality of the drug product. The BCS classification was an important tool in this work [143]. In fact, its translation into regulatory guidelines, such as “Waiver of *in vivo* bioavailability and bioequivalence studies for immediate-release solid oral dosage forms based on a biopharmaceutics classification system - FDA” [144] and “Guideline on the investigation of bioequivalence - EMA” [145] is nothing more than the risk analysis of the drug substance properties. The concept of the BCS classification, despite its 20 years, is extremely up-to-date based on recent ICH guidelines Q8/ Q9/ Q10 [58] which reinforce that the risk analysis and risk management of pharmaceutical products should start on its conception phase.

The risk associated to the drug substance regarding safety, quality and efficacy is well established and tightly controlled. However, for excipient, limited and scarce information and control is required. Nonetheless, based on the new classes of excipients

and the recent studies [61, 86, 104, 108], it is possible to conclude that the dogma related to the inertness of the excipients is a myth. As any myth it is true until is proven the opposite and at this stage it is possible to assume that this myth was busted. Current knowledge, particularly for drugs belonging to the BCS class III and IV and in some extension for drugs of BCS class II, excipients risk analysis and management is crucial and should be enforced. Guidelines refer that excipients are equivalent based on their action in the dosage form, however this should be extended for it *in vivo* interaction. For instance, the replacement of the surfactant Tween® 80 for a similar excipient, even from chemical similar excipients, for example Tween® 20 may have a dramatic *in vivo* impact in a drug suffering of efflux by BCRP [113].

In here, it is proposed for the first time a new classification of excipients in four classes like drugs substances are. This would be the BCSE. The excipients are classified in their capacity to impact metabolisation and efflux mechanisms. First class would include excipients with low risk of interference with intestinal metabolisation and efflux mechanisms. Second class would include excipients that are able to interfere with intestinal metabolisation without impact in the efflux mechanisms. Third class would include excipients with influence in the efflux mechanism and no impact in metabolism. The last and forth class would include the riskiest excipients, which have impact in both metabolisation and efflux mechanisms. Figure 2.1, shows diagram of the BCSE.

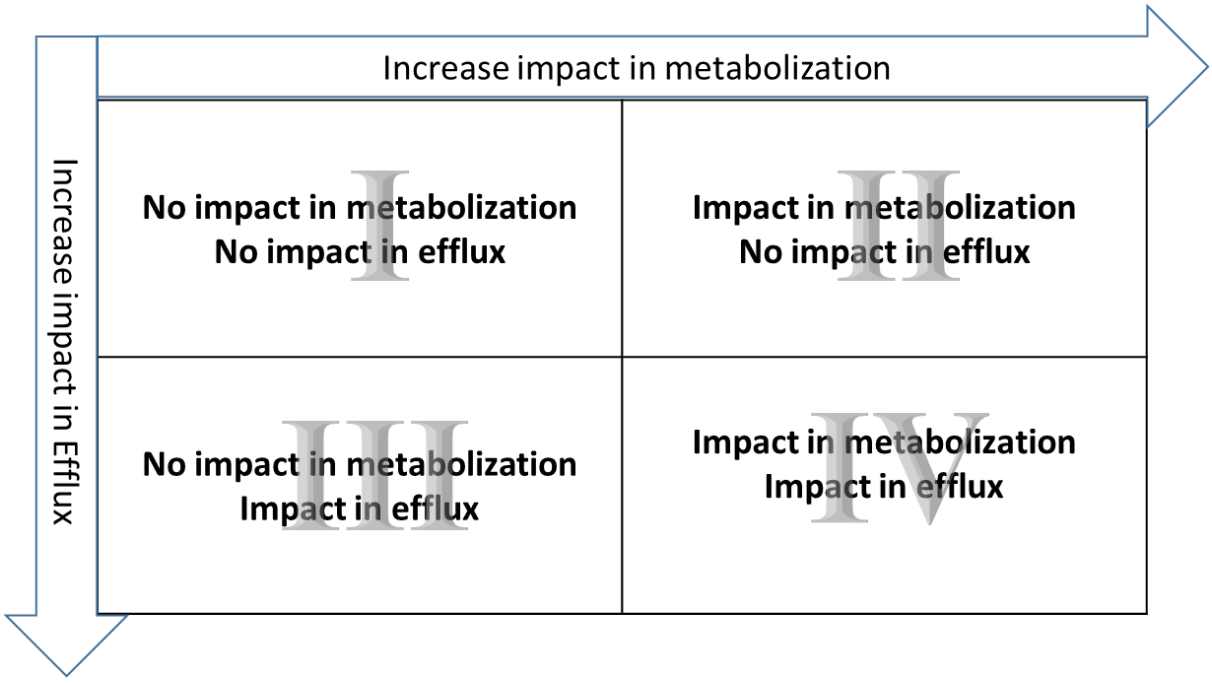

Figure 2-1 Biopharmaceutical classification system of Excipients.

BCSE class I present low risk of impact in drug safety and efficacy and include excipients such as microcrystalline cellulose or lactose. The excipients included in this class can be replaced within technologically equivalent ones without major concerns.

BCSE class II and III excipients present a high risk, particularly when used with drugs that undergo intestinal metabolisation or are efflux subtracts, respectively. Excipients known to belong to these classes are present in Table 2.2 and Table 2.3. These excipients should not be replaced by technological similar ones without further studies. Any quali-quantitative change of these excipients in a formulation should consider using excipients from the same BCSE class. However, even within these ones a large-scale bioequivalence study would be recommend in order to accommodate the inter-individual variability existent in the expression of metabolisation and efflux mechanisms.

Like BCSE class II and III, the excipients belonging to the BCSE class IV are very critical because even a small change can have a dramatic impact in drug exposure and consequently efficacy and/ or safety.

Up to date there are no bio-inequivalence reports due to the use of excipients. However, this can be because, unfortunately, negative results tend to not be published, but not only. It is also very difficult to *in vitro* demonstrate or confirm the *in vivo* data. The later occurs because models are not specific and robust, being difficult to assure that a specific target was inhibited or interfered. Additionally, most of the reference drugs, stated as specific inhibitors are, in fact, acting in multiple mechanisms in simultaneous.

Excipients from BCSE classes II to IV are frequently key elements for the drug product performance due to their biopharmaceutical interaction and should not be avoided. However, waivers of products containing excipients form these classes and drug substances belonging to BCS class II to IV should be avoided.

At this stage there is very limited information regarding the biopharmaceutical activity of excipients and it is highly probable that excipients can move from one to other class with the gathering of knowledge about them. Moreover, currently available data must be validated and translated into *in vivo* and clinical data. This is particularly important because negative results are generally not published, which would help to increase the number of excipients belonging to BCSE class I. Figure 2.2 presents a summary of the classification of the current state of the art and knowledge about the excipients.

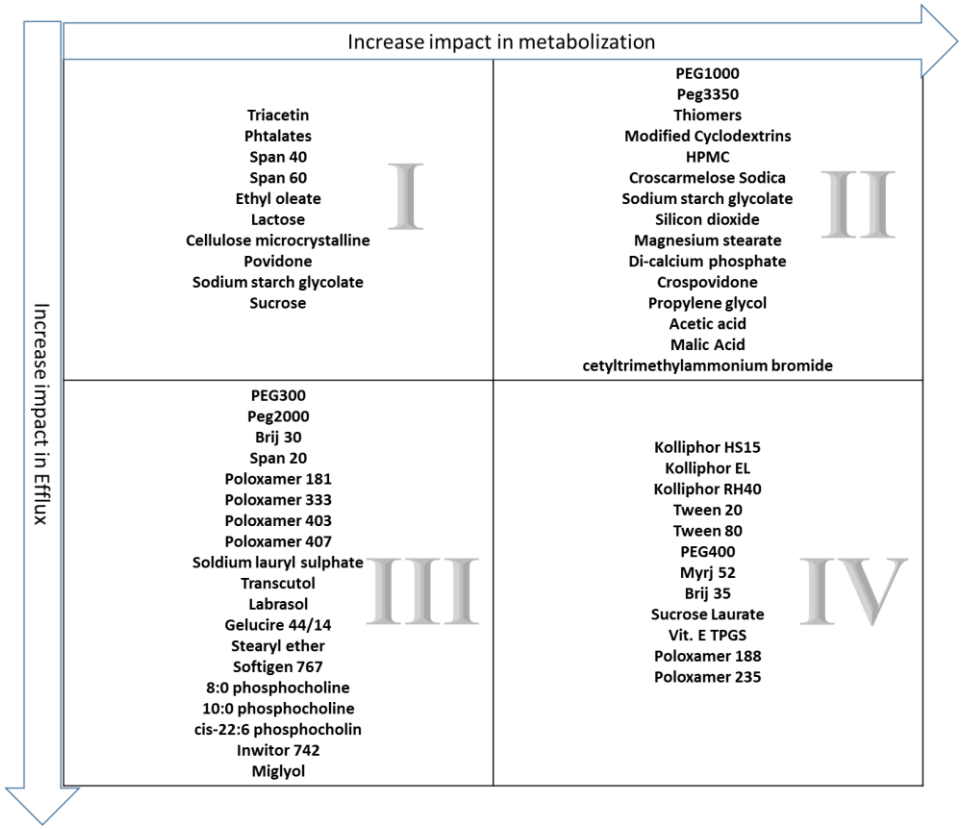

Figure 2-2 List of example excipients in each BCSE class.

2.8. Future perspective

The use of excipients as oral bioavailability enhancers through inhibition of efflux mechanism and/or intestinal metabolisation enhancers is currently one of the hot topics in the pharmaceutical field. However, very limited information is available at this time related to these properties of the excipients. Moreover, the currently *in vitro* methods are not robust, and it is difficult to make sure that a specific target was inhibited or interfered. Most of the reference drugs, stated as specific inhibitors are, in fact, acting in multiple mechanisms in simultaneous.

In the next years, new excipients specifically designed to inhibit precise targets such as P-gp's, BCRP or CYP3A4 will be developed by the excipients industry increasing the number of compounds in BCSE classes II to IV. More and more information will be gathered related to the currently available excipients increasing particularly the number of excipients in BCSE class I.

Moreover, new, reliable and robust *in vitro* methods will be developed or optimized for specific transporters or metabolizers. A dramatic increase in *in vivo* data, including data gathered from human studies, will be generated in the next years. These will allow us to

have a much better picture of the excipients ability to interfere with biological barriers. Finally, regulatory authorities will increase its control and implement specific controls over excipients from BCSE classes II to IV.

The BCSE classification will be an important tool in the pharmaceutical development field. However, a risk analysis based on BCSE classification and its association to specific drugs or drug classes must be done to strengthen the application of this classification.

3. Amorphous solid dispersions: rational selection of a manufacturing process

3.1. Introduction

The majority of drugs molecules developed by the pharmaceutical industry during the last decades of the 20th century were classified according to the biopharmaceutical classification system (BCS) as class I drugs [146, 147]. This means that most of the drugs presented high permeability and high solubility. If a molecule failed to meet these criteria, it would most probably be discarded from the industry development pipeline due to concerns about low bioavailability and/or troublesome formulation process [146].

In the 1990's, with the advent of Computer Science and its application to the pharmaceutical field, a new paradigm was raised in the Pharmaceutical Industry regarding drug candidate selection, introducing target-modulation candidate selection [148-150]. This new tool provided the Pharmaceutical Industry with the ability to produce more potent and specific drugs. However, these more potent drugs generally present poor water solubility, and consequently, fit BCS classes II or IV [43, 53]. This change in drug candidate properties brought new challenges since most of the new molecules resulted in poor *in vivo* dissolution and consequently poor and/or highly variable bioavailability [151]. Additionally, most of them present small absorption windows, generally located in the upper small intestine [9, 53]. In addition, and emphasizing the current challenges faced by the Pharmaceutical Industry, several of these drugs present poor permeability or are substrates of efflux transporters [152, 153].

The presented challenges forced the Pharmaceutical Industry to pursuit approaches to improve dug solubility, exploring chemical, physical or formulation approaches [53]. Chemical approaches comprise molecular modification of drug structure, such as the inclusion of polar groups, resulting in the formation of new chemical entities that may present different potency and pharmacokinetics [154]. Other examples of chemical approaches include the formation of salts [154-160] and co-crystals [161], but their application is very restricted. Salts are only feasible for weak acid or basic drugs and co-crystals generally do not sufficiently enhance *in vivo* drug solubility. Additionally, both salts and co-crystals tend to precipitate *in vivo* [162, 163]. The basic principle behind all physical approaches is that increasing the contact surface area enhances solubility [157]. This is accomplished by particle size reduction, resulting in crystals in the micro- or nano-size range [164, 165]. The feasibility and simplicity of this approach is adequate in some cases.

However, tends to be inadequate for drugs presenting water solubility below 50 µm/mL [164]. Formulation approaches consist in the production of liquid systems based on lipid vehicles and/or surfactants [7, 45, 166], or solid formulations that generally resembles in using carrier(s) [157]. From the later, amorphous solid dispersions depict one of the most interesting approaches, since drug presents a reduced particle size, improved wettability, high porosity and enhanced solubility [53]. A wide range of manufacturing processes to obtain amorphous products are currently available and will be further explored in this review, as well as, a rational approach for the selection of the manufacturing process.

3.1.1. Amorphous products

Amorphous products are pharmaceutical materials characterized by its solid-state nature and lack of distinct intermolecular arrangement, without crystalline structure and, consequently, with poor thermodynamically stability [43, 53]. In a standard crystalline structure, the solubility/ dissolution process firstly needs to break the crystal structure in order to occur molecular dissolution. In the case of amorphous products, the first step is abbreviated and lower energy is required to promote dissolution [43, 167]. Amorphous materials also present broad background signal patterns in X-ray Powder Diffraction (XRPD) analysis, absence of enthalpy energy related to melting processes, and irregular surface structures, among other typical thermal, microscopic and spectroscopic properties, such as dynamic mechanical properties, particle porosity or Infra-red spectrum, respectively [168].

Amorphous products may be classified in two types: (i) molecularly pure, and (ii) solid dispersions. Main features of different amorphous products are presented in Table 3.1.

Table 3-1. Classification and characteristics of amorphous products.

Amorphous products/materials	Characteristics	Production	Advantages	Disadvantages
Molecularly pure	Chemically composed by the pure drug alone	Laboratorial scale (mainly)	Enhanced solubility	Difficult to scale up and solid state instability
Solid dispersions	Formulated products	Laboratorial and industrial scales	Solid state stability and enhanced solubility	Drug substance loading in the final formulation

3.1.1.1. Molecularly pure amorphous products

Molecularly pure amorphous products are only composed by the pure drug, which due to the specific manufacturing process results in amorphous products. Generally, processes to obtain molecularly pure amorphous products require a fast solvent evaporation process. It can be achieved by using rotary evaporator evaporation, spray-drying or freeze-drying. Fast removal of the solvent prevents the formation of crystal structures and, thus, random amorphous materials are formed [169]. Traditionally, pure amorphous products are obtained in a laboratorial scale and are undesirable because they are difficult to scale up due to their high instability, a consequence of their high-energy state [169]. Hence, pure amorphous products are rapidly converted into crystalline structures [169, 170]. Zafirlukast (Accolate®, Astra Zeneca) is one of the very few commercially available molecularly pure amorphous drugs. This amorphous neutral drug is known to convert to a monohydrate form in the presence of water, with decreased bioavailability compared to the amorphous form [171, 172]. Another example is cefuroxime axetil (Ceftin®, GlaxoSmithKline) [173, 174], an amorphous drug that crystallizes in the presence of water [170].

Quinapril hydrochloride (Accupril®, Pfizer) is a salt present at an amorphous state that in the presence of moisture dissociates and crystalizes into the free drug, which is less soluble [175, 176].

3.1.1.2. Amorphous solid dispersions

Amorphous solid dispersions can be defined as molecular mixtures of poor water-soluble drugs with hydrophilic carriers, responsible for modulate drug release profile, and characterized by the reduction of drug particle size to a molecular level solubilizing or co-dissolving the drug in the soluble carriers. Overall, they provide better wettability and dispersibility as the drug is in its supersaturated state due to forced solubilisation in the hydrophilic carriers [53, 177-182]. Solid dispersions can be classified as first, second or third generation [53]. Briefly, first generation originates crystalline solid dispersions where a molecule of a crystalline carrier replaces one drug molecule in its crystalline structure. Second generation originates amorphous solid dispersions and uses polymeric carriers. The third generation comprises amorphous solid dispersion composed by a combination of amorphous carriers and most preferably a combination of amorphous carriers and surfactants, presenting enhanced drug release, long term stability and higher bioavailability [53].

Amorphous solid dispersions use specific carriers that amorphise the drug substance and stabilize it in the solid state [167, 183, 184]. These formulated amorphous products with adequate stability drawn increased interest, particularly over the last decade, resulting in an increase of marketed products using this technology as documented in Table 3.2.

Solid dispersions currently represent the most exciting research and development field related to pharmaceutical amorphous products. The increasing number of medicines under development and reaching the market [185, 186] justifies that the remaining review will be focused on this topic.

Table 3-2. Examples of commercially available medicines using solid dispersion technologies.

Product name	Drug substance	Polymer	Preparation method	Year of approval
Cesamet™ (US) / Canemes®(Austria)	Nabilone	PVP	N.A.	1985 (FDA)
Sporanox®	Itraconazole	HPMC	Spray drying on sugar beads	1992
Prograf™	Tacrolimus	HPMC	Spray drying	1994 (FDA/MHRA)
Gris-PEG™	Griseofluvin	PEG	Melt extrusion	2000 (FDA)
Crestor®	Rosuvastatin	HPMC	Spray drying	2004 (EMA) 2002 (FDA)
Cymbalta®	Duloxetine	HPMCAS	N/A	2004 (EMA/FDA)
Kaletra®	Lopinavir/ritonavir	PVP-VA	Melt extrusion	2005 (FDA) 2001(EMA)
Eucreas® Galvumet™	Vildagliptin/Metformin HCL	HPC	Melt extrusion (metformin)	2007 (EMA)
Intelence®	Etravirine	HPMC	Spray drying	2008 (EMA/FDA)
Modigraf®	Tacrolimus	HPMC	Spray drying	2009 (EMA)
Samsca®	Tolvaptan	N/A	Granulation	2009 (EMA/FDA)
Zotress™ (US) Certican®/ Votubia® (EU)	Everolimus	HPMC	Spray drying	2010 (EMA/FDA)
Onmel™	Itraconazole	HPMC	Melt extrusion	2010 (FDA)
Fenoglide™	Fenofibrate	PEG/ Poloxamer 188	Spray melt	2010 (FDA)
Novir®	Ritonavir	PVP-VA	Melt extrusion	2010 (FDA) 2009 (EMA)
Incivek™ (US) / Incivo ® (EU)	Telaprevir	HPMCAS	Spray drying	2011 (EMA/FDA)
Zelboraf®	Vemurafenib	HPMCAS	Co-precipitation	2012 (EMA) 2011 (FDA)
Kalydeco®	Ivacaftor	HPMCAS	Spray drying	2012 (EMA/FDA)
Noxafil®	Posaconazole	HPMCAS	Melt-Extrusion	2014 (EMA) 2013 (FDA)
Viekira™ (US)/ Viekirax® (EU)	Ombitasvir / Paritaprevir / Ritonavir	PVP-VA/ TPGS	Melt Extrusion	2014 (EMA/FDA)
Orkambi®	Lumacaftor / Ivacaftor	HPMCAS /SLS	Spray Drying	2015 (EMA/FDA)

HPMC – hydroxypropyl methylcellulose; HPC – hydroxypropylcellulose; HPMCAS – hydroxypropyl methylcellulose acetate succinate; PEG – polyethylene glycol; PVP – povidone; PVP-VA – povidone-vinyl acetate (copovidone); SLS – Sodium Lauryl sulfate; TPGS - d-alpha Tocopheryl Polyethylene Glycol 1000 Succinate. N.A. – not available; US – United States of America; EU – European Union; EMA – European Medicines Agency; FDA – Food and Drug Administration; MHRA - Medicines and Health Products Regulatory Agency.

3.2. Manufacturing of amorphous products

Two major distinct processes are used to manufacture amorphous materials: solvent evaporation and melting. Both have been shown useful at the laboratorial and industrial scales (production accordingly to the good manufacturing practices – GMP). Some mechanical processes, such as ball milling or grinding, are also able to induce some amorphisation [187]. However, degree and robustness of amorphisation are very low and, thus, of limited usefulness [53, 187].

Solvent evaporation processes consist in solubilizing both drug substance and carrier(s) in common solvents or solvent mixture followed by solvent removal. Non-covalent molecular interactions between drug and carrier(s) during solvent removal are responsible for the formation of an amorphous product [53, 188, 189].

As for melting processes, these generally comprise solubilizing a drug in a molten of amorphous polymer(s). The molten product is further solidified by cooling originating an amorphous solid dispersion [53].

3.2.1. General advantages Vs disadvantages

Both solvent evaporation and melting processes have their own advantages and drawbacks that should be considered in order to select the most suitable manufacturing process. Noteworthy, different manufacturing processes may originate products with different properties [190, 191]. Therefore, an adequate selection of the manufacturing process is crucial for the success of the product.

In solvent evaporation processes the thermal decomposition of drugs and/or carriers is preventable in most cases since organic solvent evaporation can be performed at low temperature [192]. Additionally, the wide availability of organic solvents allows to select a solvent or mixture of solvents able to solubilize both drug and carrier(s) [192]. However, organic solvents may be difficult to remove from the final product, which can be especially concerning when highly toxic solvents are required to be employed [7, 193]. Moreover, it is also possible that slight alterations in the conditions used for solvent evaporation may lead to large changes in product performance [194].

Avoidance of organic solvent use is a major advantage of melting methods as it better assures product safety and compliance with quality control and environmental requirements [195]. High temperatures can induce drug degradation, being this the major drawback of melting processes. Furthermore, some drugs may decompose under melting,

thus limiting application [196]. Melting processes also require drug solubility/miscibility, which can be very difficult to achieve for some molecules [53, 186, 197].

3.2.2. Laboratorial scale

Laboratorial processes by either melting or solvent-evaporation are expected to be fast, cheap and require low material resources, especially drug substance. Laboratorial processes can be divided in micro-scale and mini-scale. Micro-scale processes are intended to produce a few micrograms of product and can generally be used for preliminary screening. These processes have limited robustness and poor reproducibility. Mini-scale processes can already generate a few to several hundred grams of product and are characterized for being more robust and reproducible.

3.2.2.1. Solvent evaporation

Laboratorial solvent evaporation processes can be divided in four major groups depending on solvent removal conditions: (i) high temperature and normal pressure, (ii) high temperature and negative pressure, (iii) freeze-drying, or (iv) supercritical fluids (SCFs). Table 3.3 presents some of the most recent applications of laboratorial solvent evaporation methods to prepare amorphous solid dispersions.

Table 3-3. List and description of some recent studies employing solvent evaporation methods.

Drug	Carrier	Drug: Carier(s) ratio	Technique	Solvent	Solid content in solution	Solvent evaporation temperature	Comment	Ref
Atorvastatin	Soluplus®	2:8	Spray Drying (Sd 1000)	Methanol	1%	Inlet temp. 65-80ºC; Outlet temp 50-60ºC	FR: 2–3 mL/min AAP: 10 kPa DAFR: 0.60–0.70 m3/min	[198]
Celecoxib	PVP: HPMC	N/A	Rotavapor	Methanol:DCM (1:1 V/V)	N/A	N/A	N/A	[199]
Celecoxib	PVP: HPMCAS	N/A	Rotavapor	Methanol:DCM (1:1 V/V)	N/A	N/A	N/A	[199]
Celecoxib	Phospholipoid E80 (PL): trehalose	1:10:16	Spray Drying (Büchi B-90 Nano Spray Dryer)	Ethanol:Water (8:2, W/W)	N/A	Inlet temp. 80 °C	FR: 12.5 mL/min DAFR: 140 L/min	[200]
Celecoxib	Phospholipoid E80 (PL): trehalose	1:10:16	Freeze Drying (Christ Gamma 2-16 Lsc)	TBA:Water (6:4 V/V)	N/A	0.1 mbar @ 25 °C/ 24 h; FB 0.01 mbar @ 25 °C/ 4 h	Frozen at −80 °C for 24 h / freeze dryer at −60 °C.	[200]
Cilostazol	Eudragit(®) L100: Eudragit(®) S100 (1:1)	1:5	Spray Drying (B-290, Buchi)	Methanol	N/A	Inlet temp. 75º C	FR: 1.5 mL/min DAFR: 538 L/h	[201]
Clopidogrel	Tween 80 / HPMC	10 : 2.5 : 2.5	Spray Drying (Buchi Mini Spray-Dryer B290)	Water	20 mg / mL	Inlet temp. 150ºC Outlet temp 75-85ºC	FR: 5 mL/min Aspirator 100%	[202]
Diazepam	PVP	N/A	Freeze-Drying (Christ Lyophilizer, Type Alpha 2-4)	TBA:Water (4:6 V/V)	N/A	0.220 mbar @ −35°C /1 day FB 0.05 mbar@ 20°C/1 day	Condenser temp. 53ºC	[5]
Dimenhydrinate	Ethyl cellulose	1:1; 1:3;1:5	Solvent Cast	Ethanol	N/A	60ºC	N/A	[10]
Docetaxel	Soluplus®	1:10	Freeze-Drying	N/A	N/A	N/A	N/A	[203]
Felodipine	PVP	1:9	Solvent Cast	Ethanol	N/A	40ºC	N/A	[47]
Fenofibrate	Silica	1:3	SCF	CO2	N/A	Temp. 50°C Pressure: 2550 PSI	N/A	[204]
Fenofibrate	Gelucire1 50/13	22:88	SCF-PGSS (Separex®)	CO2	Not applicable	Temp. 78ºC Pressure:80 bar	Fenofibrate was melted in Gelucire® 50/13	[205]
Flurbiprofen	PVP	N/A	Solvent Cast	Ethanol	N/A	40ºC	N/A	[206]
Glibenclamide	Magnesium aluminometasilicate (Neusilin® UFL2)	1:2.5	Rotavapor	DCM	2%	35ºC	N/A	[207]

Drug	Carrier	Drug: Carrier(s) ratio	Technique	Solvent	Solid content in solution	Solvent evaporation temperature	Comment	Ref
Glibenclamide	Eudragit® S100	1:1	Spray Drying	Methanol:DCM (1:1 V/V)	50 mg/mL	Inlet temp 90°C	SFR: 4 g/mL AAP: 0.05 MPa	[208]
Glibenclamide	PMC (50%-60%): PEG (34-40%): Poloxamer (6-10%)	1:10	SCF-SAS	Methylene Chloride-Ethanol (1:1) FB CO2	0.10%	Pressure: 1500 to 3000 PSI	FR CO2: 2 mL/min FR sol. 0.2 mL/min	[209]
Glycyrrhizic acid	Silica	N/A	SCF-SAS	Ethanol FB CO2	10-40 mg/mL	Temp. 35-65ºC Pressure: 200-250 bar	FR CO2: 10-20mL/min FR sol. 4-10 mL/min	[210]
Itraconazole	HPMC	1:1	Solvent Cast	Methanol:DCM (1:1 V/V)	1%	N/A	N/A	[211]
Itraconazole	HPMC	N/A	Rotavapor	Methanol:DCM	N/A	45 °C	N/A	[211]
Itraconazole	Eudragit® E	N/A	Spray Drying (Pro-Cep-T 4m8-Trix Spray Dryer)	Methanol:DCM (1:4 V/V)	2.40%	Inlet temp 70ºC	SFR: 150 mL/g DARF: 0.3 m3/min	[188]
Itaconazole	HPMC/ Poloxamer 407/L-Ascorbic Acid	4:4.5:0.5:1	SCF-SAS	Methanol/DCM (1:3 V/V) FB CO2	7.50%	Temp. 50°C Pressure :95 bars	FR CO2: 20 mL/min FR sol. 0.4 mL/min	[212]
Megestrol acetate	HPMC	1:2	SCF-SAS (Thar SAS200 equipment)	Methylene Chloride: Ethanol (45:55 W/W) FB CO2	5%	Temp. 40°C Pressure: 15 MPa	FR CO2: 11 g/min FR sol. 1 mL/min	[213]
Megestrol acetate	HPMC/TPGS	1:2:0.5	SCF - SAS (Thar SAS200 equipment)	Methylene Chloride: Ethanol (45:55 W/W) FB CO2	5%	Temp. 40°C Pressure: 15 MPa	FR CO2: 11 g/min FR sol. 1 mL/min	[213]
Miconazole	PVP-VA	2:8-4:6	Spray Drying (Buchi Mini Spray-Dryer B191)	DCM	5%	Inlet temp 60°C, Outlet temp 40°C	FR:6.8 mL/min DARF: 0.56 m3/min	[214]
Nifedipine	Soluplus®	3:7	Freeze-Drying (FD- 80)	TBA:Methanol	10%	0°C for 4 days	Quenched by liquid nitrogen	[215]
Phenytoin	Eudragit® S100	15:85	Spray Drying	Acetone:Methanol (50:50 W/W)	50 mg/mL	Inlet temp 90°C	SFR: 4 g/mL AAP: 0.05 MPa	[208]
Progesterone	Gelucire 44/14	1:10	SCF-PGSS	CO2	Not applicable	Temp. 60ºC Pressure:186 bar	Progesterone was melted in Gelucire® 44/14	[216]

Drug	Carrier	Drug: Carrier(s) ratio	Technique	Solvent	Solid content in solution	Solvent evaporation temperature	Comment	Ref
Puerarin	Phospholipids PC70	1:1.2	SCF-GAS	Ethanol FB CO2	20%	Temp. 38ºC Pressure:10 MPa	N/A	[217]
Puerarin	Phospholipids PC70	1:1.2	SCF-SEDS	Ethanol FB CO2	100 mg/mL	Temp. 35ºC Pressure:10 MPa	FR CO2: 45 mL/min FR sol. 0.45 mL/min	[217]
Resveratrol	Soluplus®	1:1	Solvent Cast	Ethanol	10%	60ºC	N/A	[218]
Rofecoxib	PVP	1:1; 1:3; 1:9	Solvent Cast	Methanol:Chloroform (2:1 V/V)	N/A	45ºC	N/A	[219]
Simvastatin–lysine (1:1 molar)	SLS	1:0.5	Spray Drying (Buchi Mini Spray-Dryer B191)	Water	N/A	Inlet temp 100°C Outlet temp 45°C	FR: 3.9 mL/min DARF: 600 L/h	[220]
Sirolimus	Eudragit® E:TPGS	1:8:1	Spray Drying (Buchi Mini Spray-Dryer B191)	Ethanol:Methylene Chloride (55:45, W/W)	3%	Inlet temp 65-80 °C Outlet temp 45-55 °C	FR: 3–6 mL/min	[221]
Tadalafil	PVP-VA	1:9-2:8	Spray Drying (Buchi Mini Spray-Dryer B290)	Acetone:Water (9:1, V/V)	1%	Inlet temp 65 C Outlet temp 52ºC	FR: 7 mL/min aspirator 100%	[222]
Tadalafil	PVP-VA	1:1	Freeze-Drying	Water:ACN (55:45)	0.40%	0.2 mbar @ 50 C / 72h	N/A	[223]
Tolbutamide	PVP	N/A	Solvent Cast	Ethanol	N/A	40ºC	N/A	[206]
Valsartan	HPMC:Poloxamer 407	2:7:1	SCF - SAS (Thar SAS200 equipment)	DCM:Ethanol (45:55 W/W) FB CO2	50 mg/mL	Temp. 40°C Pressure: 15 MPa	FR CO2: 11 g/min FR sol. 1 mL/min	[224]
Zidovudine	Poly(L-Lactic Acid)	1:2	SCF-SAS	Ethanol: DCM (5:95) FB CO2	15%	Temp. 45ºC Pressure:85 bar	FR CO2: 3 mL/min FR sol. 0.75 mL/min	[225]
Zoplicone	PVP	1:1	Rotavapor FB Freeze-Drying	Methanol	0.5%	N/A / -72ºC / 12h	N/A	[226]

FR – Fed Rate; AAP – Atomisation Air Pressure; DAFR – Drying Air Flow Rate; DCM - Dichloromethane ; N/A – Not available; temp. – temperature; FB – Followed By; TBA – tert-butyl Alcohol; SFR – Solution Feed Rate; Sol. – Solution; SCF-PGSS – super critical fluid - particles from gas-saturated suspension; SCF-SAS - super critical fluid - supercritical antisolvent; ACN - Acetonitrile

Solvent casting [218] is a basic laboratorial process of preparing solid dispersions and consists in dissolving the drug and the polymeric carrier(s) in the same solvent(s). The solution is then spread into a petri dish and allowed to evaporate under normal pressure at room temperature [227], in a hot plate [10] or in an low temperature oven followed by cooling in a desiccator [218] which have successfully been employed in the development of solid dispersions of paracetamol, dimenhydrinate and Resveratrol respectively. Typically, the resulting films are pulverized and milled [218]. As an alternative, miniaturisation can be achieved by replacing petri dishes with low volume glass vials [228, 229]. This type of approaches presents the possibility of producing very small amounts of product and was used for preliminary screening of itraconazole and JNJ-25894934 (a new chemical entity from ALZA corporation) [228, 229]. However, it can only be used for solvents with very low boiling temperature such as ethanol [47, 48, 206, 218], chloroform [44, 219] or a mixture of ethanol and dichloromethane [178]. Additionally, it may be difficult to ensure that the solvent is completely removed, which may affect data generated for solubility, permeability or bioavailability. An alternative involves the use of scalable laboratorial spray driers [70, 188, 198, 201]. The solution of drug and polymer(s) is sprayed into a hot air stream that induces fast solvent evaporation and, consequently, the production of small homogenous solid particles composed by drug and carrier(s) in an amorphous state (see section 3.2.1).

One of the most practical laboratorial processes used to produce solids dispersion involves the use of a rotary evaporator [182, 230, 231] which has recently used in the development of Celecoxib [199, 200], Glibenclamide [207-209], Itraconazole [188, 211, 212], Nifedipine [215], Zoplicone [226] (see Table 3.3 for details). This is used to remove the solvent(s) under vacuum, allowing a faster sample processing and/or the use of solvents with higher boiling point such as tetrahydrofuran, dimethyl formamide or dimethyl sulfoxide (DMSO) that could not be used in a solvent casting process. The final product is removed from the volumetric flask and can be further milled if desirable. An alternative approach involves solvent casting in a petri dish or vial followed by evaporation in a low-pressure chamber or oven.

Freeze-drying or lyophilisation, recently employed in the development of Celecoxib [199, 200], Diazepam [5], Docetaxel [203], Nifedipine [215], Tadalafil [222, 223] and Zoplicone [226] (see Table 3.3 for details), comprises freezing a solution/suspension of drug and carrier(s) followed by reducing the surrounding pressure to allow water and solvents in the sample to undergo solid-gas transition [5, 232]. In a freeze-drying process, drug and carrier(s) maintain their molecular dispersion structure observed upon dissolution [203, 215, 226]. Laboratorial freeze-driers are able to produce from a few milligrams up to some grams of lyophilised products. The use of organic solvents in freeze-drying is very limited, but

possible for instance with 2-methyl-2-propanol [233], tert-butanol [233], methanol, acetonitrile or water/DMSO mixtures [193].

The use of supercritical fluids (SCFs) is also possible in order to produce solid dispersions. Recent applications of SCFs in the manufacture of solid dispersions are depicted in Table 3.3. SCFs are gases that under certain pressure and temperature present simultaneously gaseous and liquid state properties [234, 235]. Liquid properties are advantageous for solubilisation, while gaseous features favour drug and carrier(s) diffusion and solvent removal [234]. Almost all gases present SCFs properties under adequate conditions. However, only few can be used in the pharmaceutical field due to their adequate critical temperature. More than 98% of all applications have been developed using carbon dioxide [235]. Carbon dioxide presents low critical temperature (31.18 °C) and pressure (7.4 MPa), and is inexpensive, non-flammable, non-toxic, recyclable and environmentally friendly [209, 212, 234]. Another example of SCF used in the pharmaceutical field is trifluoromethane [236] which was recently used in the development of simvastatin nanoparticles. SCFs major disadvantages are the difficulty to completely remove organic solvents (when used) and to scale-up, as well as the price of the equipment [235].

Processes using SCFs can be divided in two main groups [234]. The first includes processes that use SCFs as solvents, such as rapid expansion of a supercritical solution (RESS). RESS consists of dissolving the drug and carrier(s) in a SCF that is then rapidly expanded by sudden decompression, typically by passing through an orifice at low pressure [237]. The product properties produced by this process depend on the pre-expansion conditions like temperature and pressure of the vessel and post-expansion conditions such as the nozzle temperature, geometry, size, distance and angle of impact against the surface of the jet stream [234]. RESS process is adequate for laboratory scale since it can be easily implemented, but very difficult to scale up. Another limitation is the required solubility of drug and carriers in the SCFs that for most of drugs is not feasible, thus limiting the application of this process [234, 237]. Solid dispersions of fenofibrate have been produced by RESS and deposited over silica particles [204]. Solid dispersions of alpha lipoic acid [238] and spironolactone [239] have also recently been produced by RESS process.

A second group of processes encompasses the use of SCFs as antisolvent. Drug and carrier(s) are dissolved in an organic solvent that is removed by a SCF antisolvent. There are different techniques based on such principle, differing in the mixing procedure between the drug/carrier(s) solution and the SCF [234, 237]. The organic solvent can be sprayed into a SCF in supercritical antisolvent (SAS) (Figure 3.1) or particles by compressed antisolvent (PCA). Atorvastatin [240], megestrol acetate [213] and valsartan [224] amorphous nanoparticles have been produced by a SAS approach, and shown to

present enhanced solubility and bioavailability. Indomethacin [241], cefdinir [242] and glycyrrhizic acid [210] solid dispersions have also been produced by this process and obtained particles shown to have homogenous particle size and improved solubility. Zidovudine-poly(L-lactic acid) particles were further shown to possess improved permeability using an *ex vivo* everted rat intestinal sac model [225]. A recent study demonstrated that glibenclamide solid dispersions prepared by SAS presented higher solubility than products obtained by equivalent solvent evaporation processes [209]. This was attributed to the effects of the solution and the supercritical carbon dioxide on enhanced plasticisation of polymers, thus increasing diffusion of the drug into the polymer matrix.

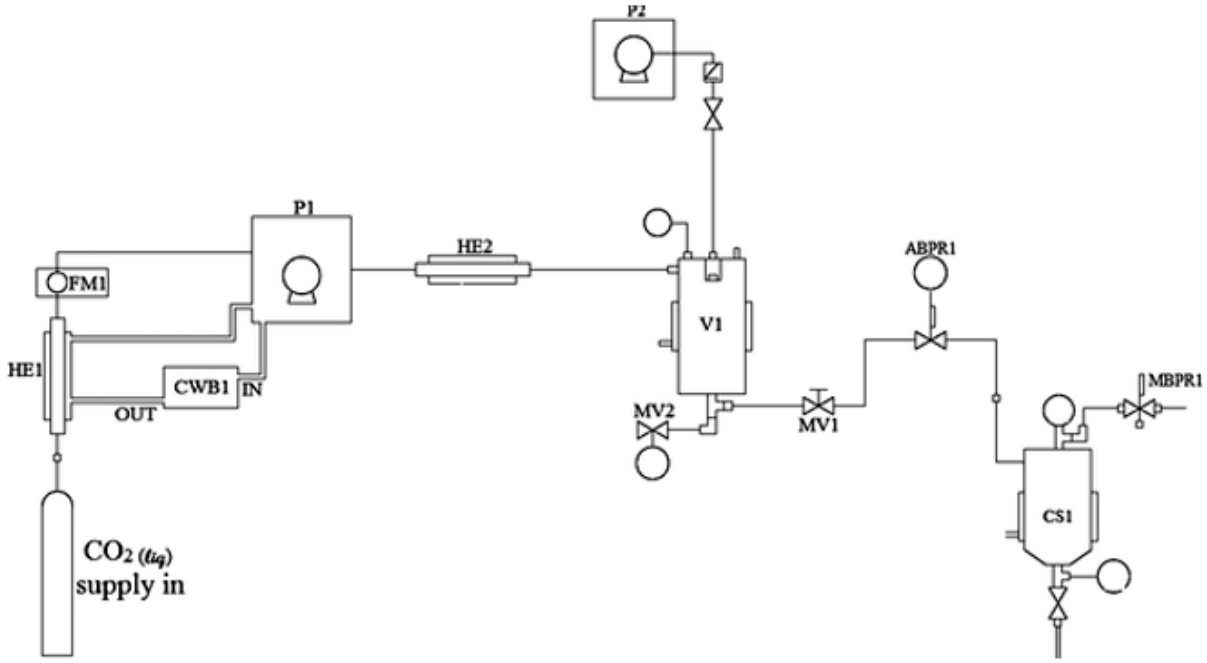

Figure 3-1 Schematic representation of the SAS process. Republished with permission of John Wiley and Son, from [225], Copyright 2015; permission conveyed through Copyright Clearance Center, Inc.

In aerosol solvent extraction system (ASES), both organic solvent and SCF are sprayed at the same time by different nozzles into the chamber [243]. Itraconazole solid dispersions have been produced by ASES using HPMC–as carrier [243]. Obtained amorphous nanoparticles (100-500 nm) showed enhanced solubility and bioavailability [243]. Solid dispersions of atenolol have also been produced using ASES [244]. Alternatively, the SCF can be added into the organic solvent, being gaseous antisolvent (GAS) technique one example of this approach [234]. Phenytoin solid dispersions have been produced GAS associated to PCA using PVP) as carrier [48].

Recently, solid dispersions of fenofibrate and Gelucire® 50/13 have been manufactured by particles from gas saturated solutions (PGSS) [205]. In this process, the SCF saturates the organic solution that is then sprayed to form particles [205, 216]. In another study, PGSS was employed to produce solid dispersions of progesterone [216]. Optimized conditions included high pressure and temperature, and longer processing, as well as a lower drug: carrier ratio.

A technique termed solution enhanced dispersion by supercritical fluids (SEDS) which uses a special nozzle was patented by Hanna and York and proposed to produce particulate products [245]. This nozzle allows the organic solvent and SCF to be atomized simultaneously. Puerarin microparticles were produced by SEDS using phospholipids as carriers [217].These were shown to possess a higher degree of amorphisation when compared to particles produced by GAS.

3.2.2.2. Melting

Melting processes comprise heating a formulated sample followed by its cooling. The techniques employed to heat and cool are important variables of melting processes. Table 3.4 presents some of the most recent solid dispersions prepared by melting processes.

Table 3-4. List of recent solid dispersions prepared by melting processes.

Drug	Carrier	Drug:Carrier Ratio	Technique	Temperature (ºC)	Processing parameters	ref
Bicalutamide	PVP-VA	5:95	HME (TSE - Minilab II)	170	Screw speed: 150 rpm	[246]
Caffeine	PVP or PVP-VA	2:8	HME (TSE - Minilab II)	155	Screw speed: 100 rpm Residence time: 5 min	[247]
Carbamazepine	AFFINISOL™ HPMC	15:85/ 30:70	HME (TSE - Leistritz Nano-16)	120 - 180	Screw speed: 150 - 200 rpm Feed rate: 5 g/min Kneading elements: 2 (30° and 60°) Strand die: 3-mm Screw diameter: 16 mm	[248]
Carbamazepine	PVP-VA or Soluplus® or Eudragit® EPO	15:85/ 30:70	HME (TSE - Leistritz Nano-16)	120 - 180	Screw speed: 150 - 200 rpm Feed rate: 5 g/min Kneading elements: 2 (30° and 60°) Strand die: 3-mm Screw diameter: 16 mm	[248]
Celecoxib	PVOH:sorbitol (6:4)	15:85	HME (TSE - Prism Eurolab 16 Thermo)	140	Screw speed: 100 rpm Kneading elements: 3 Strand die: 3-mm Screw diameter: 16 mm	[249]
Disulfiram	Kolliphor® P 188 or Kolliphor® P 237	4:6	Melt Quenching	80	Cooling at room temperature	[250]
Efavirenz	(PVP or PEG8000):Tween 80	1:10:1.1	Melt Quenching	80	Cooling at ice bath followed by 2 days in the freezer	[251]
Felodipine	PEG:PEO:Tween 80	10:36:27:27	HME (TSE - Minilab II)	65	Screw speed: 150 - 200 rpm Residence time: 5 min	[252]
Fenofibrate	Ethyl cellulose or hydroxypropyl cellulose or PEG	1:10	HME (TSE - Process 11 Thermo)	125, 140, 75	Screw speed: 100 rpm Feed rate: 10 g/min Screw diameter: 11 mm	[253]
Hydrochlorothiazide	PVOH:sorbitol (6:4)	15:85	HME (TSE - Prism Eurolab 16 Thermo)	140	Screw speed: 100 rpm Kneading elements: 3 Strand die: 3-mm Screw diameter: 16 mm	[249]
Indomethacin	Magnesium aluminometasilicate (MAS-Neusilin® US2)	2:8/ 4:6	HME (TSE)	180	Screw speed: 100 rpm Feed rate: 1 Kg/h Screw L/D ratio: 40:1	[254]
Indomethacin	PVP or PVP-VA	9:1 - 1:1	Cryomilling Followed By *In Situ* Melt Quenching	170	**Cryomilled** at 10 Hz, five cycles (2 min of milling and 2 min of cooling) Melt quenching: 170 °C / 10 min Spinning at 4 khz Rapidly cooled to room temperature	[255]
Miconazole	PVP-VA	2:8	HME (TSE - MP19PC)	Zone 1: 25-40 Zone 2 and 3: 125	Screw speed: 300 rpm Kneading elements: Zone 1 (5 FP 30°, 4 FP 60°, 6 AP 90°) Zone 2 (3 RP 60°) Screw L/D ratio of 25/1	[214]
Paracetamol	PVP or PVP-VA	4:6	HME (TSE - Minilab II)	120	Screw speed: 100 rpm Residence time: 5 min	[247]
Valsartan	Soluplus®:TPGS	3:6:1	HME (TSE - STS-25HS)	80-100 (zone 1-6)	Screw speed: 150 rpm Feed rate: 28–30 g/min Extrusion pressure: 100 bars	[256]

HME – Hot Melt Extrusion; TSE – Twin Screw Extruder; rpm – rotations per minute; min – minute; PVOH – Polyvinyl alcohol; PEO – Polyethylene Oxide; N.A. – Not Available; FPW – Forwarding Paddles; AP – Alternating Paddles; RP – Reversing Paddles; L/D – length/ diameter

Laboratorial melting processes can be extremely simple. For example, a solid dispersion can be obtained by combining the formulation ingredients in a differential scanning calorimetry (DSC) pan and heating the sample until melting of all components, followed by natural or forced cooling [257]. Generally, less than 10 mg of product are obtained.

Moving up in scale, when both components present a low melting points, or when the drug substance has high solubility in the carrier(s), a melt- quenching approach can be used. Briefly, a water bath [258] or a hot plate [250] can be used to melt both components. Then the homogenous molten mass can be rapidly solidified by (i) placing it in a freezer [258], (ii) using an ice bath [259, 260], (iii) placing it over a stainless steel surface as thin layer spreading followed by a cool air draft [261], (iv) spreading it on plates placed over dry ice [262], (v) immersing in liquid nitrogen or grinding the material in liquid nitrogen (cryo-grinding) [183, 187, 263], or (vi) pouring it into petri dishes placed at room temperature inside a desiccator [264, 265]. After solidification, the mixture needs to be pulverized in order to facilitate handling [258]. These techniques can be used to produce up to several grams that then can be used to further physicochemical and technological characterisation.

Hot melt extrusion (HME) has been explored as a scale-up procedure to produce solid dispersions by melting process. It consists in the extrusion at high rotation speed of the drug and carrier(s), previously mixed, at melting temperature for a small period. The resulting product is then collected after cooling at room temperature and milled into a powder or granule form [197, 249, 256, 266]. A significant advance of HME has been the introduction of twin-screw melt extrusion as illustrated in Figure 3.2 [256, 267]. It consists in the use of a special twin screw extruder and the presence of two independent hoppers in which the temperature can vary over a broad range [268]. Currently several laboratory-scale equipment are available from different manufactures, such as Thermo Fisher Scientific, Brabender Technologies, Coperion GmbH or Leistritz Advanced Technologies Corp., which use this technology and can be used to produce from few grams of product to several Kilograms [195, 197].

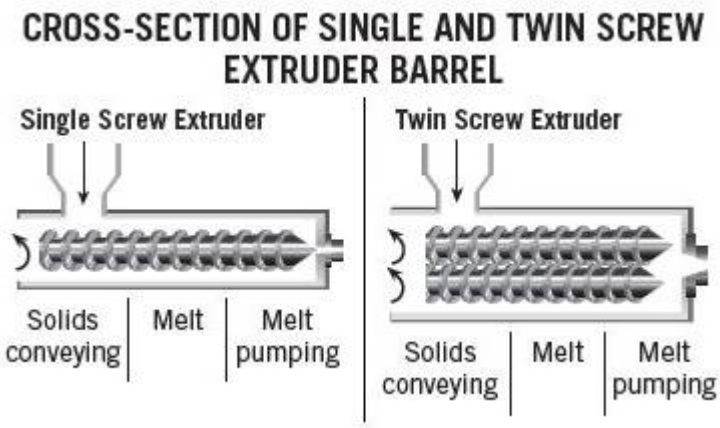

Figure 3-2 Schematic of a single screw and twin-screw extruder. Reprinted from [269], with kind permission from Springer Science+Business Media (Copyright American Association of Pharmaceutical Scientists 2013).

Advantages and description of hot melt extrusion will be further detailed below when industrial scale processes are discussed. Examples of laboratorial melt extrusion solid dispersion developments are depicted in Table 3.4.

Table 3-5. Impact of laboratorial method in product properties. Subsequent operations such as milling were not considered.

Method	Particle size reduction	Particle porosity	Wettability*	Yield	Scalability
Solvent cast (different variations)	Poor (coarse product)	Poor	Poor	Poor	Poor
Rotavapor	Poor	Poor	Poor	Poor	Poor
Spray drying	High	Medium	High	Medium	Medium
Freeze Drying	High	High	High	High	Medium
SCF	High	High	High	Medium	Poor
Melt-Quenching (freeze/ ice bath/ room temp.)	Poor (coarse product)	Poor	Poor	Medium	Poor
Cryo-grinding	Poor	Poor	Poor	Medium	Poor
HME	Poor	Poor	Medium	High	High

* Wettability is more linked with composition of carriers than with manufacturing process

Variations in preparation methods affect final product properties. Table 3.5 summarizes the differentiation among laboratorial methods regarding particle size reduction, particle porosity, wettability and process parameters such as yield and scalability.

3.2.3. Industrial scale

Industrial and, consequently, good manufacturing practices (GMP) compliant processes to manufacture solid dispersions are scarce. Mostly because the majority of the simple and easy laboratorial processes and equipment are difficult to scale up and fulfil GMP requirements, such as contact materials, reproducibility (automatisation), and sanitation in addition to the most evident, such as the impossibility to perform installation/ operational and performance qualification of these equipment. Additionally, processes need to be robust and reproducible, which again is hard to ensure for processes such as solvent cast evaporation or water bath melting process. At industrial scales, the production outputs vary from 1 Kg batch size to several hundred kilograms.

3.2.3.1. Solvent evaporation

From an industrial point of view, the manufacture of solid dispersions by solvent evaporation is usually limited to a few specific cases. [53]. The types of solvent, drying conditions and therefore the rate of evaporation vary drastically among different processes. Overall, spray-drying and frezee-drying are the most representative of the solvent evaporation methods used in the industry for manufacturing solid dispersions.

The spray drying process is relatively easy to scale up from a laboratorial spray dryer to an industrial one (Figure 3.3) [270, 271]. Industrial spray dryers have a nominal drying gas rate ranging from 50 to 5000 Kg/h which may result in a water evaporation capacity up to 400 Kg/h. Product properties and performance depend on process parameters and formulation aspects [196]. Relevant process parameters include inlet temperature, feed rate humidity and flow rate of drying gas and atomisation conditions [196, 272, 273]. The type and size of the spray nozzles highly contributes to the amorphous solid dispersion's particles, in particularly to the particle size, but also texture and smoothness [270, 271]. Additionally, the solid content may also affect the solution viscosity and consequently the drying process and the final product [271]. Formulation variables such as composition (drug, carrier, solvent) and solid content in the feed, solvent type, viscosity and surface tension of the drying solution are significant for product properties [196, 273]. Table 3.6 presents the impact of spray drying parameters in final product properties, such as particle size, porosity or smoothness.

Table 3-6. Impact of spray drying parameters in product properties [274, 275].

Parameter (Increase)	Particle Size	Particle Porosity	Product Moisture	Particle Smoothness	Assay	Powder Yield
Inlet Temperature	Increase	Decrease	Decrease	Decrease	Increase	Increase
Drying Flow Rate	Decrease	Increase	Decrease	Increase	Increase	Increase
Feed Rate	Decrease	Decrease	Increase	Increase	Decrease	Decrease
Humidity	Increase	Increase	Increase	Decrease	Decrease	Increase
Spray Nozzles (Increase In Droplet Size)	Increase	Increase	Increase	Decrease	Decrease	Increase
Solid Content In Solution	Increase	Decrease	Decrease	Decrease	Increase	Increase
Solution Viscosity or Surface Tension	Increase	Decrease	Increase	Decrease	Decrease	Increase

The first challenge in developing an amorphous solid dispersion is finding an adequate solvent system. It must be able to solubilize drug and carrier(s) to a large extension (ideally over 50 mg/mL) and produce a low viscosity solution [196]. Additionally, from a GMP and industrial perspective solvent(s) should present low toxicity and high volatility, which is critical because residual solvents in final products must be within the acceptable values of the International Conference Harmonisation (ICH) Q3C(R5) guideline [70, 276]. This guideline defines three different classes of solvents, being Class 3 solvents preferable while the use of those in Classes 1 and 2 should be avoided or limited, respectively. Unfortunately, most of the times it is not possible to achieve an effective solvent system for the components of solid dispersions with solvents from Class 3, or these solvents do not present adequate properties for spray-drying. In these cases, Class II solvents may be justified. Typical examples of solvent used in pharmaceutical spray-drying processes are presented in Table 3.7 [277].

Table 3-7. Organic solvents commonly employed in spray drying.

Solvents	Boiling point (°C)	Dielectric constant	Solubility in water (g/100 g)	Density (g/mL)	ICH limit (ppm)
Acetone [278, 279]	56.2	20.7	Miscible	1.049	Class 3
Chloroform [279]	61.7	4.81	0.795	1.498	60
Methanol [280, 281]	64.6	32.6	Miscible	0.791	3000
Methylene chloride [282]	39.8	9.08	1.32	1.326	600
Isopropanol [283, 284]	82.6	18.2	Miscible	0.786	Class 3
Ethanol [285]	78.5	24.6	Miscible	0.789	Class 3
Dichloromethane [279, 286]	39.6	9.08	175	1.326	600
Dimethyl formamide [287]	153	36.7	Miscible	0.944	880
DMSO [287]	189	47	25.3	1.092	Class 3
Glycerin [277]	290	42.5	Miscible	1.261	–
Ethyl acetate [288]	77	6	8.7	0.895	Class 3
Butyl acetate [281]	126.1	5.07	0.68	0.882	Class 3
Water [280]	100	78.5	–	0.998	–
Tetrahydrofuran [284]	66	7.52	Miscible	0.889	720

The carrier selection influences the final product properties, particularly amorphisation degree, physical and chemical stability and wettability. For instance, the inclusion of a surfactant as carriers, such as tween 80 [289, 290], sodium lauryl sulfate [289, 290], Poloxamer [289], Myrj® [289], sodium taurocholate [290] or Triton X100 [290], forming a third generation solid dispersion originates products with enhanced solubility, which may improve bioavailability [182]. Carriers used in the preparation of solid dispersions by spray drying are generally the same described in the melting methods (section 3.2.1). In these particular cases, polymers with high melting point or glass transition can be employed and are even preferred. Carriers such as Metacrilates [231, 290, 291], povidone and derivatives

[292], PEG [293], HPMC [285, 293], HPMCAS[273] and Soluplus® [190], which was originally developed for melt-extrusion, are frequently employed in the preparation of solid dispersions by spray drying. The interplay of formulation and process parameters is, thus, crucial to obtain a stable amorphous process and a smooth process [70, 196, 273]. A list of spray drying solid dispersions currently available in the market can be found in Table 3.3, and Table 3.8 illustrates the details on processing parameters of some of the most recent products produced by this process.

Table 3-8. Process parameters of some commercial spray drying solid dispersions.

Product	**Orkambi®**	**Incivek^{tm} (USA) / Incivo ® (EU)**	**Intelence®**
Drug	Ivacaftor	Telaprevir	Etravirine
Carrier	HPMCAS: SLS	HPMCAS	HPMC
Drug: Carrier(s) Ratio	5:4.5:0.5	5:1	1:3
Technique	Spray Drying	Spray Drying	Spray Drying
Solvent	Methanol	DCM	DCM:Ethanol (9:1)
Equipment	N/A	Niro Size 4	SD12.5
Solid Content in Solution	10%	30%	5%
Inlet Temperature (ºc)	145	75	115
Outlet Temperature (ºc)	75	43	49
Aspiration	100%	N/A	N/A
Flow Rate	35%	30%	1250 Kg/h
Liquid Flow Rate	200 mL/h	150 Kg/h	202 Kg/h
Reference	US2015141459 [294]	WO2008080167 [295]	WO2007141308 [296]
Company	Vertex Pharma	Vertex Pharma	Tibotec

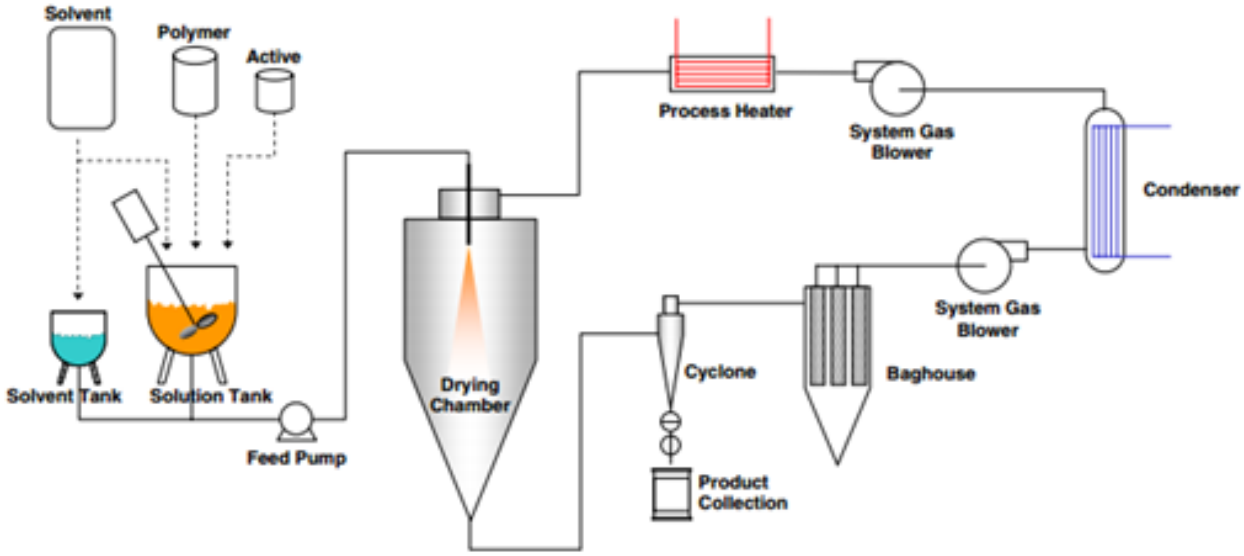

Figure 3-3 Scheme of a spray drying process. Reprinted from [271], with kind permission from Springer Science+Business Media.

Another industrial manufacturing process to obtain amorphous solid dispersions is freeze-drying, previously described in section 3.1.2. Freeze-drying at industrial scale uses larger equipment capable to control both phases of the process (freeze and lyophilisation). This advantage over laboratorial equipment provides a higher robustness and reliability of the industrial scale. Additionally, freeze-drying has the advantage of promoting minimal stress (thermal) to the drug and presents minimal risk of phase separation [193]. The manufacture of solid dispersion by freeze-drying is limited to drugs with some water solubility or inorganic solvents miscible water [203, 215, 226, 297]. Amorphous solid dispersions have been prepared using the carriers already presented for another processes [203, 215, 223, 226, 228, 233]. At industrial scale, in order to obtain an adequate solid material after lyophilisation, a cryoprotective material may be required. Cryoprotective are generally sugars such as: mannitol, glucose, sucrose, sorbitol, fructose, dextran, maltose or trehalose, among others [298]. The use of organic solvents at industrial scale s is more limited and it is recommended to be less than 10% [233].

3.2.3.2. Melting

Only two types of melting processes are available at an industrial scale. These are melt agglomeration and melt extrusion.

Melt agglomeration process use standard granulation equipment, like high shear mixers [179, 299] as used for diazepam [299] or fluid bed driers [189, 300] as used for paracetamol [300]. However, instead of a granulation liquid, a melted mass of drug and

carrier(s) is added to the remaining excipients of the formulation [301]. This molten material acts as a granulation liquid, ensuring an adequate homogeneity and adsorption of the drug and carrier(s) on the remaining excipients that can then be further processed. This process allows a production from few Kg to around 500 Kg batch size. Carriers used in melt-agglomeration can be liquids, namely polyethylene glycol (PEG) 300 and caprylocaproyl macrogol-8 glycerides (Labrasol®), or solids presenting low melting/glass transition temperature, such as PEG 3000 [179], PEG 6000 [189], poloxamer 188 [179, 302] or stearoyl polyoxyl-32 glycerides (Gelucire® 50/13) [299, 303].

The avoidance of organic solvents and drying procedures are advantages of melt-agglomeration. Additionally, it can be helpful for water sensitive drugs [301, 304]. The use of high temperatures, however, prevents its application to thermolabile drugs. The limited availability of suitable carriers for this process can also be seen as a limitation [301].

Hot melt extrusion (HME), and particularly the twin-screw melt extrusion with its highest representative being Meltrex™ from Soliqs, is one of the most employed industrial solid dispersion manufacturing process. In fact, the development and application of twin-screw melt extrusion should be considered one of the major driving forces for the wide dissemination of the solid dispersion concept (Figure 3.4) [53, 195, 197] particularly after Kaletra® development [305]. Twin-screw presents several advantages over single screw versions and represent the current state of the art for melting processes. [53]. The use of two screws contributes to a reduced residence time of the drug in the extruder, allowing for continuous mass flow with enhanced mixing. Moreover, twin-screw extruders avoid drug and excipients thermal stress and feature self-cleaning of the screws [197, 306]. The application of twin-screw technology to drugs susceptible to oxidation and hydrolysis is also possible by eliminating oxygen and moisture from the mixture [197, 307, 308]. It further presents easier material feeding and less tendency to over-heat [307]. The success is such that currently, almost all products developed by HME are in fact by HME using twin-screw extruders.

Figure 3-4 Hot melt twin screw extruder (Image courtesy of Thermo Fisher Scientific Inc.).

HME allows continuous processing, solvent-free and is easily scaled-up, since the same principle and design can be transposed to different scales [195]. The major difference between laboratorial and industrial equipment is the diameter of the screws. Screws, from laboratorial extruders can vary from 11 to 16 mm in diameter, while values for the industrial ones range from 16 to 50 mm [195, 197]. The possibility of having continuous processing is highly advantageous in the pharmaceutical field because it allows huge versatility in manufacturing capability even with small extruders [309]. This process allows the industrial/ GMP production of batch sizes ranging from few Kg to tons.

The successful development of a solid dispersion by HME depends on composition and process parameters. Adequate selection of carriers and plasticizers is crucial. Apart from screw design, which is the most important variable, other parameters such as feed rate, temperature and rotation speed are crucial for defining the final product properties [197]. In a recent study, it was shown that the degassing process also enhanced the cross-sectional uniformity of the extruded material [310].The design of the equipment is highly versatile which allows the adaptation of processes to the desired results and to very different starting materials.

The reason for this versatility is the modular design comprising the screws and barrels [308]. Barrels can be flanged together or linked by internal tie rods. Screws are the most important part of the extruder. Their design distinguishes between processes that the extruder can or cannot fulfil and, therefore, define the quality and quantity of the extruded material [308, 311]. The kneading paddle elements of the screws play an important role in changing the crystallinity and dissolution properties of solid dispersions (Figure 3.5).

Nakamichi *et al* [267] showed that the physicochemical properties of the extruded material were significantly influenced by the operating conditions of the machine, namely by the revolution rate of screws and the amount of water added to the feed materials. The screw speed and feeding rate are related to shear stress, shear rate and mean residence time, which can affect the dissolution rate and stability of the final products [195]. Certain minimum temperatures are required in HME in order to reduce the torque needed to rotate the screw(s) and allow an efficient process [195]. Composition and process parameters of the most recent solid dispersions developed using melting extrusion processes are depicted in Table 3.4.

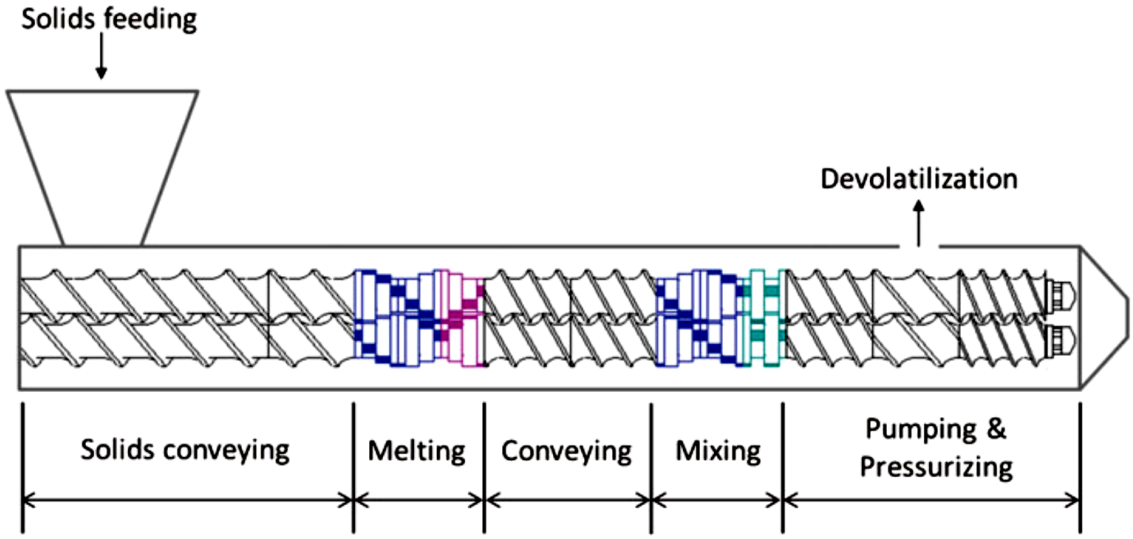

Figure 3-5 Schematic representation of a twin-screw extruder and elementary steps. Reprinted from [312], with kind permission from Springer Science+Business Media (Copyright Controlled Release Society 2014).

Carriers used in HME are generally polymers or waxes with low melting point or glass transition temperature that are used as solubilisers of the drug substance [307, 311]. Commonly used carriers include PVP [293, 311], povidone-vinyl acetate (PVP-VA) [293], copovidone [313-315], various grades of PEG [292, 293], cellulose esters [311, 316, 317], cellulose acrylates [293], and poly-methacrylate derivatives [313, 315, 318]. Due to the specificities of this technology, the polymer industry has recently developed several polymers specifically for the HME, such as HPMC acetate succinate (HPMCAS) [191, 314, 319, 320] and Soluplus® [313, 316, 321], as well as specific grades of HPMC (Affinisol®) [248]. Due to their individual properties, these carriers are 5frequently used in combination

in order to achieve enhanced amorphisation, stability, dissolution or bioavailability [292, 317].

HME processes are characterized by high shear stress. Therefore, a plasticizer is frequently required to allow more efficient processing [197]. Additionally, the inclusion of these components can be explored in order to tailor drug release of final products. Vitamin E (tocopherol), D-alpha tocopheryl PEG 1000 succinate [256, 320], poloxamers [321-323], Tween® [289, 324], Myrj® [289] and low molecular weight PEGs [197, 321] are examples of plasticizers that were shown able to improve product performance, namely concerning s dissolution and/or bioavailability. In a different approach, pressurized carbon dioxide injected during HME has been shown useful in reducing the temperature of various polymer melts in addition to acting as a foaming agent [325, 326].

HME requires high energy input mainly due to the observed shear forces and temperatures used. This is an important drawback alongside the poor ability to process thermolabile compounds [195]. However, changes in the design of the equipment as well as the addition of plasticizers may contribute to reduce the processing temperatures and residence time and, thereby, avoid thermal degradation of drug substances during processing [197].

Table 3-9. Process parameters of some commercial spray drying solid dispersions.

Product	Eucreas ®	Kaletra®	Noxafil®	Viekira™ (US)/ Viekirax® (EU)
Drug	Vildagliptin/Metformin HCL (SD only Metformin)	Lopinavir/Ritonavir	Posaconazole	Ombitasvir / Paritaprevir / Ritonavir
Carrier	HPC	PVP-VA: Span20	HPMCAS	HPMCAS/ TPGS/ Propylene Glycol Monolaurate
Drug:Carrier Ratio	10:1	1:3.5:0.5	1:3	13:79:4:4
Equipment	Prism 16 Thermo	Leistritz Micro 18 Twin-Screw Extruder	Leistritz Micro 18 Twin-Screw Extruder	N/A
Temperature (ºC)	180	120	120-135	160
Screw Speed (rpm)	150	N/A	150	N/A
Feed Rate	30-45 g/min	2.1 Kg/h	4 Kg/h	N/A
Reference	US2011/0045062 [327]	US20050084529 [305]	US20150150990 [328]	WO2015103490 [329]
Company	Novartis	Abbot	Merck	Abbvie

Currently there are several amorphous solid dispersions available in the market manufactured by this manufacturing process, such as Kaletra®; Novir®, Onmel™, Noxafil®,

Gris-PEG™ and the recent Viekirax® (Europe)/ Viekira™ (USA). Table 3.9 presents the composition and process parameters of some of these products.

3.3. Selection of a manufacturing process for amorphous products

Amorphous solid dispersions advantages over other solubility enhancement approaches are the presence of particles with reduced particle size, improved wettability, high porosity and the amorphous state. This later represents the major advantage of solid dispersions but also their major disadvantage. Amorphous products are thermodynamically instable and tend to crystallize during stability studies, storage, shipping or *in vivo* drug release. Therefore, an adequate solid dispersion should maintain its amorphous state from the manufacture moment until drug absorption [53, 330, 331]. Several factors contribute to drug crystallisation, but most of them are related to drug mobility increase, induced by temperature, moisture or organic solvents presence. Consequently, an adequate manufacturing process and composition selection is crucial to meet the desired goals, namely obtaining a stable amorphous product with enhanced bioavailability [53, 330-332]. A rational selection of the manufacturing process based on the physicochemical properties of the drug being formulated is possible and represents a key element in the product development.

3.3.1. Laboratorial scale

At the laboratorial scale, the primary criteria for selecting the manufacturing process are based on drug properties such as thermal stability and melting point. Another important issue relates to equipment availability and the purpose of the study, for instance, if the work is still at a screening or optimisation stage. When considering melting methods, the intention or not to scale up the process and the viscosity of the molten mass should be taken into account.

The properties of the organic solvents required to solubilize the drug and carrier(s) are the main factors to consider if selecting a solvent evaporation manufacturing process. Boiling point, solubility capacity and solvent toxicity (classification) are of particular relevance. For instance, It is proposed that the drug/ carrier solubility must be higher when ICH class 1 are required to be employed, due to its toxicity. Figure 3.6 depicts a decision tree that can be used to select the most adequate manufacturing process at laboratorial scale.

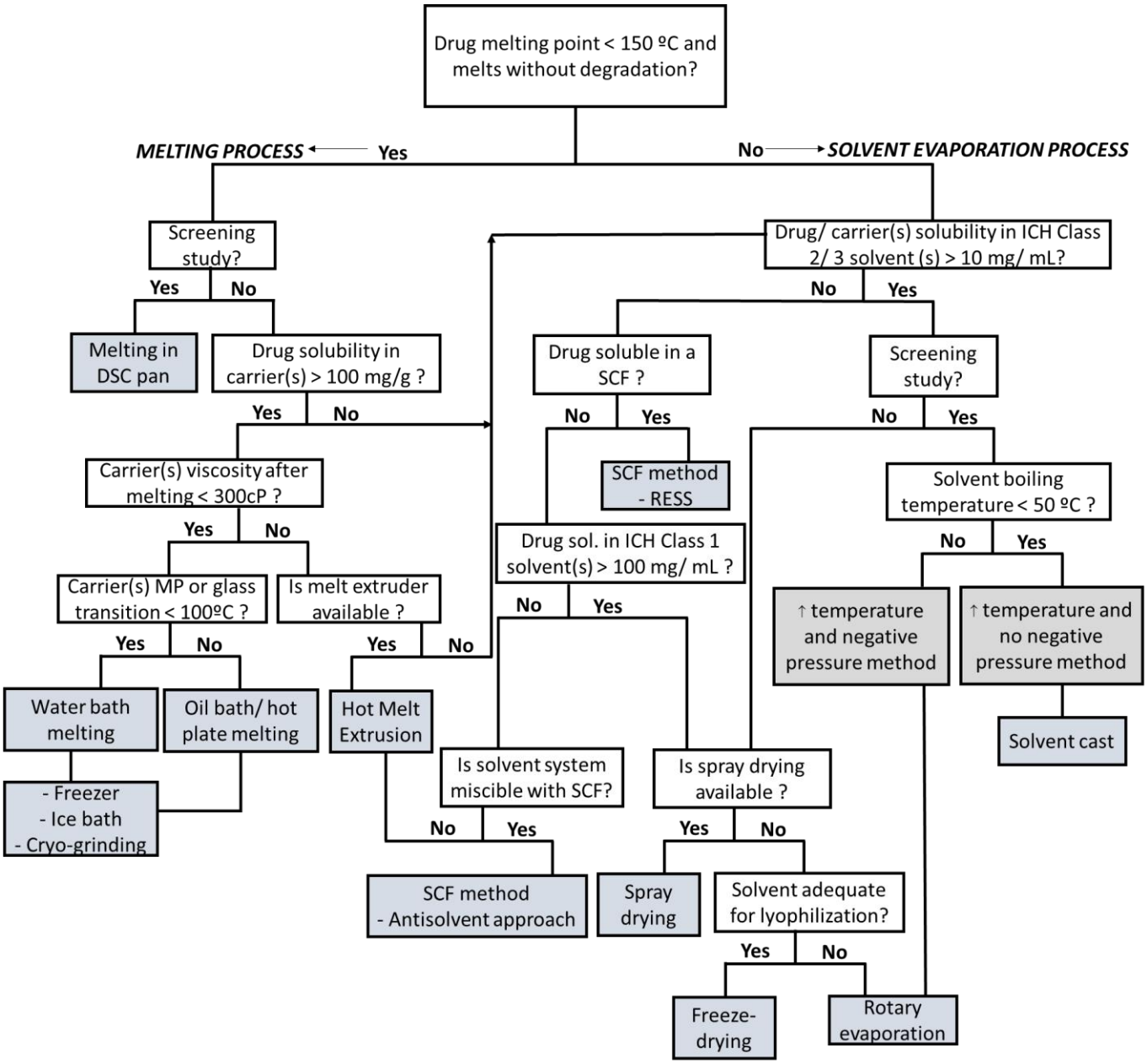

Figure 3-6 Decision tree for selection of manufacturing process at the laboratorial scale. DSC – Differential scanning calorimetry; cP – CentiPoise; SCF – Super critical fluid; MP – Melting point; Sol. – Solubility; ICH – International Conference Harmonisation.

3.3.2. Industrial scale

The industrial production of amorphous solid dispersions has limited options and is restricted to only a few manufacturing processes. At this scale, the main limitations will be equipment availability, as well as drug carrier solubility and thermal stability of the drug. HME is preferable among all melting processes. Alternatively, melt agglomeration can be used if the molten drug carrier mass presents low viscosity.

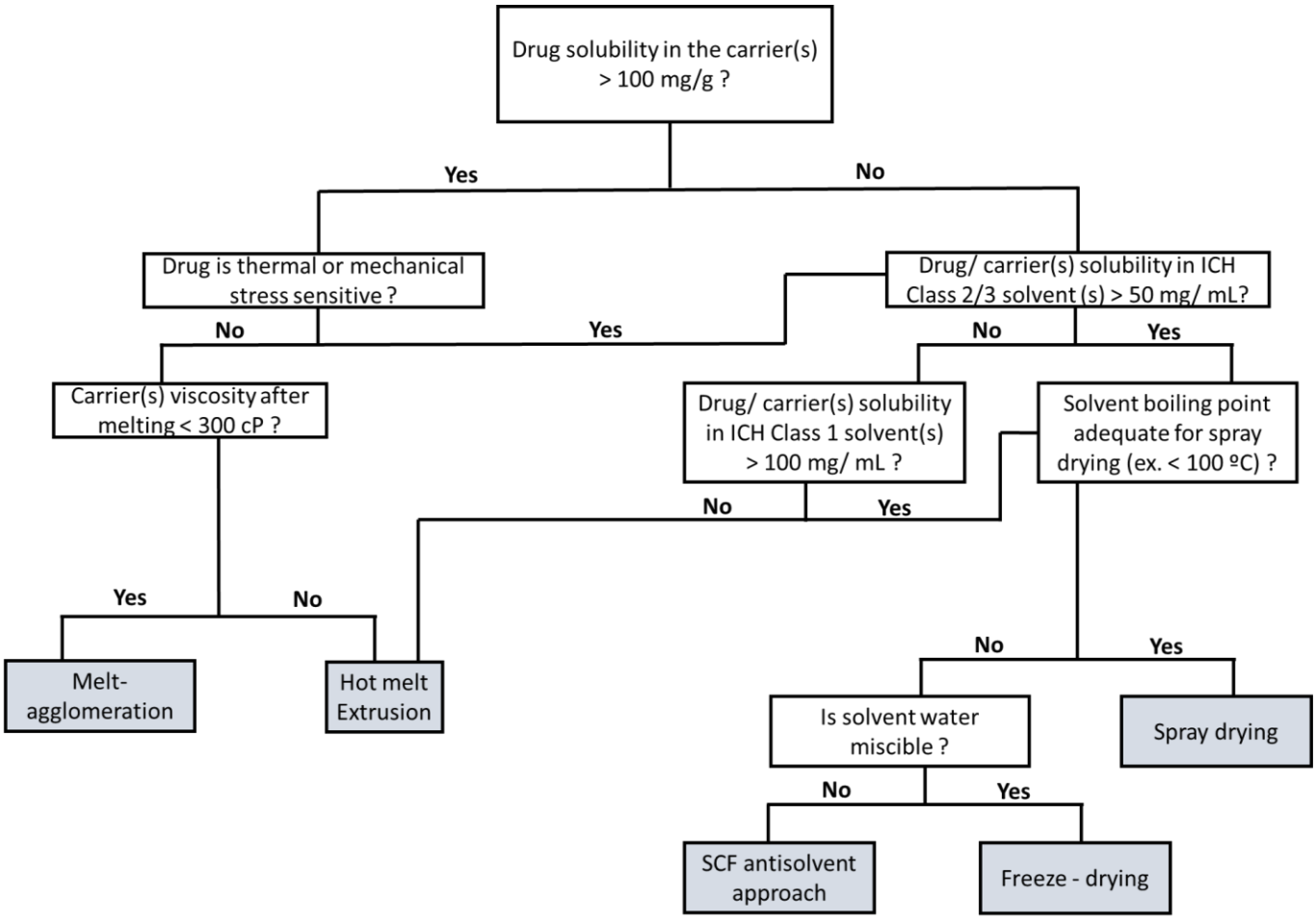

Figure 3-7 Decision tree for selection of manufacturing process at the industrial scale. cP – CentiPoise; SCF – Super critical fluid; ICH – International Conference Harmonisation.

The selection rationale for solvent evaporation processes is based on solvent toxicity and solvent loading capacity that if very low will prevent an industrial effective process. Figure 3.7 provides a decision tree for selecting the most adequate manufacturing process at the industrial scale. At this scale, additional considerations should be taken, such has process yield, batch size and particle properties. For instance, solvent evaporation processes generate smaller, rounder and porous particles than melting processes. However, increased porosity or presence of some residual solvents in the final product may induce drug crystallisation by adsorbing environmental moisture and/ or increasing drug mobility. In opposition, melting processes provide higher yields, and allow larger batch size than solvent evaporation processes.

3.4. Conclusions

Amorphous products, namely amorphous solid dispersions, are one of the most seething areas in the pharmaceutical field and, in particular, in the pharmaceutical industry. There is a current need to develop production processes at the laboratorial scale and scale these up to the industrial level in a reliable manner. In this review, the current state of the art of manufacturing processes used at laboratorial scale for development was presented. There is a wide range of different manufacturing processes, allowing the fitting of a suitable solution for all types of drugs. Industrial manufacturing processes were also described, particularly bearing in mind scalability of laboratorial methods previously used during development. Two decision trees for selecting available laboratorial and industrial scale manufacturing processes are also proposed. These tools could be used as guidance for an adequate development and industrialisation of amorphous solid dispersions.

F. Overview and aims of the thesis

4. Overview

Resveratrol is a multifaceted drug with high therapeutically potential however, despite such a potential, the human clinical use of Resveratrol is very limited and most of the clinical trials exhibited doubtful results. This is mainly attributed to the poor pharmacokinetic properties of Resveratrol, primarily due to its poor water solubility and extensive metabolisation [333]. Therefore, the improvement of oral bioavailability of Resveratrol is crucial for its success.

Most of the drug deliveries systems being explored are associated to nanotechnology and/ or to vectoring Resveratrol for specific organs or pathologies and not necessarily focus in improving the Resveratrol pharmacokinetic profile. In order to improve Resveratrol pharmacokinetic profile, an enhancement in its water solubility together with reducing its intestinal metabolism should be attempted. Therefore, the drug delivery system to be developed should be able to improve these two properties. Thus, as third generation amorphous solid dispersion and self-emulsifying drug delivery systems were considered as the most promising approaches with higher potential to improve Resveratrol pharmacokinetic profile.

Third generation solid dispersions are able to improve water solubility by transforming and sustaining drug in its amorphous state. Furthermore, the inclusion of a surfactant, in a low concentration, can reduce or inhibit the intestinal metabolism as well as efflux mechanism. Therefore, the selection of the surfactant in the third-generation solid dispersion is crucial for its performance regarding efflux pumps and metabolism mechanisms.

Generally, self-emulsifying drug delivery systems, are liquid formulations that contain the drug solubilized and therefore dissolution step is overcome. Additionally, depending on the lipid and surfactant selection, intestinal metabolism as well as efflux mechanism can be reduced or even blocked. Furthermore, lymphatic absorption can be achieved through Peyer patches skipping first passage metabolism.

Based on the above rationale, both third generation solid dispersion and self-emulsifying drug delivery systems were explored in parallel. Research activities were carried out at Pharmaceutical Sciences Laboratory (LCF), from Research Department of BIAL – Portela and Company and at Nanomedicines & Translational Drug Delivery Laboratoty from i3S – Instituto de Investigação e Inovação em Saúde – Universidade do Porto.

5. Aims

The main objective of this thesis was the development of a Resveratrol drug delivery system with enhanced and reproducible oral bioavailability.

Two different approaches were explored in parallel, solid dispersion and self-emulsifying drug delivery system, consequently different intermediate goals were defined.

The second intermediate goal within the solid dispersion approach was to develop a Resveratrol solid dispersion completely amorphous which should be physical, and chemical characterized. It was expected that the final formulation prototype presented an improved and sustained solubility and dissolution. Later, a surfactant must be included to generate a third generation solid dispersion. Lastly, *in vitro* and *in vivo* improved bioavailability should be achieved. Briefly, in order to achieve these goals, the following tasks were carried out:

- High-throughput screening of carriers
- Selection of hydrophilic carrier and its content optimisation
- Optimisation of formulations (selection and content optimisation of surfactant)
- *In vitro* studies – Permeability studies
- *In vivo* studies – Animal pharmacokinetic profile

The data generated during the development of this approach is further described in chapter G.

Regarding the self-emulsifying drug delivery system approach the second goal was to develop a lipid formulation able to self-emulsify in stable micro or nanoemulsion. The final formulation prototypes were expected to present an improved and sustained solubility and dispersibility. Lastly, *in vitro* and *in vivo* improved bioavailability should be achieved. In order to achieve these goals, the following tasks were carried out:

- High-throughput screening of lipids, surfactants and co-solvents
- Phase diagram development
- Evaluation of self-emulsification process and its stability
- *In vitro* studies – Permeability studies
- *In vivo* studies – Animal pharmacokinetic profile

The data generated during the development of this approach is described in chapter H.

G. Third generation Solid Dispersion Approach

This chapter was based on:

Teófilo Vasconcelos, Fabíola Prezotti, Francisca Araújo, Carlos Lopes, Ana Loureiro, Sara Marques, Bruno Sarmento. Third-generation solid dispersion combining Soluplus and poloxamer 407 enhances the oral bioavailability of Resveratrol. International Journal of Pharmaceutics, Volume 595,2021,120245.

6. Third-generation solid dispersion combining Soluplus and poloxamer 407 enhances the oral bioavailability of Resveratrol

6.1. Introduction

Oral delivery is the simplest and easiest way to administer drugs [1, 2]. Therefore, most of the new chemical entities (NCE) under development are intended to be used as solid dosage forms that originate an effective and reproducible *in vivo* plasma concentration after oral administration [3, 4]. However, despite more potent, most of NCE are low water soluble drugs and/or poorly absorbed after oral administration [4, 5] for which the use can be inhibited due to these drawbacks [6-8]. Moreover, most of this promising NCE, despite their high permeability, are only absorbed in the upper small intestine, presenting, therefore, a small absorption window [9]. Consequently, if these drugs are not completely released in this gastrointestinal area, they will present reduced oral bioavailability or at least high inter and intra-individual variability in bioavailability [9, 10].

Despite, a large variety of potential activities and data provided by animal models, the human clinical use of Resveratrol is very limited and most of the clinical trials showed doubtful results [37, 38]. This is mainly attributed to the high doses required (> 500 mg) and poor pharmacokinetic properties of Resveratrol, since it presents very limited oral bioavailability (less than 5% of the oral dose reaches plasma), due to its poor water solubility and high metabolisation [39, 40].

Generally, solubility enhancement strategies based on formulation can be divided in particle size reduction techniques, liquid formulations or formulations using carriers.

The particle size reduction techniques such as milling or micronisation are commonly used as approaches to improve solubility based on the increase of surface area [7, 46]. These approaches present limited efficacy for compounds with a solubility below 0.1 mg/mL such as Resveratrol, since the particle size reduction limit is around 2 to 5 microns which frequently is not enough to improve considerably the drug solubility or drug release in small intestine [7, 47, 48], and consequently to improve the bioavailability of these compounds [47, 49, 50]. Moreover, the products obtained from these techniques generally present poor mechanical properties, such as low flow and high adhesion, and are extremely difficult to handle [47, 48] particularly in drug products with high dose, such as Resveratrol.

Finally, these techniques do not impact intestinal metabolism and/ or efflux and therefore have limited application in Resveratrol.

In solid dispersion, drug is in its supersaturated state due to forced solubilisation in the carrier [38, 55, 56]. It is characterized by the reduction of drug particle size to nearly a molecular level, by solubilizing or co-dissolving the drug in the water-soluble carrier, by providing better wettability and dispersibility and by forming amorphous products [29, 57]. The use of excipients able to modulate intestinal metabolism and efflux mechanisms can be explored to improve the bioavailability of Resveratrol [52]. In the present work a third-generation solid dispersion was intended to be developed to improve Resveratrol bioavailability over an equivalent second-generation solid dispersion.

6.2. Materials and methods

6.2.1. Reagents

Povidone, crospovidone, copovidone (COP) and sodium laurilsulfate were purchased from BASF (BTC-Europe), Spain. Soluplus®, PEG 6000, Kolliphor® P188 (poloxamer 188), Kolliphor® P 338 (poloxamer P338), Kolliphor® P 407 (poloxamer P407), were a gift from BASF (BTC-Europe), Spain. Hypromellose Acetate Succinate, low grade (HPMCAS-LG), Hypromellose Acetate Succinate, Medium grade (HPMCAS-MG) were a gift from Ashland, Spain. Copolymer of ethyl acrylate, methyl methacrylate and a low content of methacrylic acid ester with quaternary ammonium groups (Eudragit® RLPO) was acquired from Evonik, Germany. Polyoxyethylene (100) Stearate (Myrj 59P), Tween® 80 (T80) were acquired from Croda, Spain. Resveratrol was acquired to Abatra technology, China. Acetonitrile was obtained from Sigma Aldrich, Germany.

Culture flasks and Transwell® plates were purchased from Corning Inc., USA. Dulbecco's Modified Eagle medium (DMEM), L-glutamine, non-essential amino acids (NEAA), Penicillin (10000 IU/mL), Streptomycin (10 mg/mL) and trypsine-EDTA were purchased from HyClone, USA. Hank's balanced salt solution (HBBS) and heat inactivated *foetal* bovine serum (FBS) were purchased from Life Technologies Gibco, USA. Purified water was obtained by a milliQ purification system. All other materials were of analytical grade or equivalent.

6.2.2. High-throughput screening of Resveratrol solubility

Resveratrol solubility was accessed in fourteen excipients (carriers), which were polymers selected from the major groups of hydrophilic carriers with potential to amorphize Resveratrol. From Polyvinil derivates: povidone, crospovidone and COP were used.

PEG6000, Soluplus® and Polyoxyethylene (100) Stearate (Myrj 59P) were selected from Polyethyleneglynol and derivates. From poloxamers, P 188, P 338 and P 407 were used. Hypromellose Acetate Succinate (low and medium grade) and copolymer of ethyl acrylate, methyl methacrylate and a low content of methacrylic acid ester with quaternary ammonium groups (Eudragit® RLPO) were evaluated. Finally, two surfactants were also tested, namely Tween 80 and sodium laurilsulfate.

Water solutions at 5% of each of the above excipients were prepared. In the particular case of HPMCAS that is not soluble in water pH (pH around 5.5), a phosphate buffer solution at pH 6.9 was prepared.

The Resveratrol solubility was accessed in each of the above solutions. Briefly, an excess amount of Resveratrol (15-25 mg) was added to a 2 mL HPLC vial. One millilitre of each of the above solutions was added to the vial and the preparations were magnet stirred for 2 hours at room temperature 15-25 ºC. Each preparation was prepared in triplicate. As a control, the solubility in purified water was accessed. After 2h, the solutions were filtrated through a 0.45 µm filter and assayed by HPLC.

6.2.3. Preparation of Resveratrol solid dispersions

The solid dispersions were prepared by the solvent cast method for the screening phase, selection of carrier and its content optimisation. Briefly, approximately 0.6 - 1g of Resveratrol was dissolved in approximately 15 mL of ethanol under stirring at 40ºC. After Resveratrol complete dissolution, the respective amount of polymer was dissolved in the previous solution under the same conditions. Then, after complete solubilisation, the obtained solution was spread into a Petri dish and dried at 65ºC during at least 18h and until achieving a constant mass, meaning that no further ethanol was present in the formulation. The obtained films were removed from the Petri dish and pulverized in a mortar. For solubility, permeability and pharmacokinetic studies, solid dispersions were prepared by the same principle but using a rotavapor instead of a solvent cast process.

6.2.4. Selection of hydrophilic carrier and its content optimisation

From the high throughput screening, several hydrophilic carriers were selected for further studies. Several solid dispersions with different Resveratrol to polymer ratios were prepared for each selected polymer and accordingly to the following ratios: Resveratrol:Polymer (5:1) - (83% Resveratrol), Resveratrol:Polymer (2:1) - (67% Resveratrol), Resveratrol:Polymer (1:1) - (50% Resveratrol), Resveratrol:Polymer (1:2) - (33% Resveratrol) and Resveratrol:Polymer (1:5) - (17% Resveratrol).

6.2.5. Solid dispersions characterisation

6.2.5.1. Fourier transform infrared

Attenuated total reflection ATR-FTIR spectra were obtained using a Bruker spectrophotometer (Tensor 27, Bruker, USA) equipped with a crystal diamond universal ATR sampling accessory. Before each measurement, the ATR crystal was carefully cleaned with ethanol. During the measurement, the sample was in contact with the universal diamond ATR top-plate. For each sample, the spectrum represented an average of 100 scans was recorded in the range of 4000-400 cm^{-1} with a 4 cm^{-1} resolution. Appearance, broadening or disappearance of absorption band(s) on the spectra of the solid dispersions in comparison with the individual spectrum of drug and polymeric carriers were used to determine possible interactions between pure Resveratrol and polymers.

6.2.5.2. Water solubility

The solid dispersions solubility was accessed for each product after 24 hours stirring. The 24h timepoint was selected because it allowed the measurement of the thermodynamic solubility that also considers recrystallisation events. Briefly, an excess amount of solid dispersion, corresponding to approximately 15 -25 mg of Resveratrol was added to a 2 mL HPLC vial. One milliliter of each polymer solution was added to the vial and the preparations were magnet stirred during 24 hours at room temperature 15-25 ºC. Each set of experiments was prepared in triplicate (one from each solid dispersion batch with the same formula). As a control, the solubility of Resveratrol in purified water was accessed.

6.2.5.3. Scanning Electron Microscopy

Optimized formulations were analysed by SEM. A Phenom Pro-X Electron microscope (PhenomWorld, Thermo Fisher Scientific, USA) equipped with a CeB6 electron source and backscatter electron detector was used to determine the morphology and particle size of the samples.

The powder was placed on the conductive adhesive tape. The holder for non-conductive samples was used. The excess of sample (loosely bound to the tape) was removed using compressed air.

6.2.5.4. X-Ray Powder Diffraction

Optimized formulations were analysed by XRPD. XRPD determinations were performed using a table-top diffractometer MiniFlex 600 (Rigaku, Japan) with a D/teX Ultra detector. In all measurements Cu Kα radiation (40 kV, 15 mA) was used.

6.2.5.5. Particle size measurement

Optimized formulations were analysed for particle size measurement. These were assessed as cumulative percentile of 10, 50 and 90% of particles (D10, D50 and D90) of solid dispersions containing Resveratrol and measured using the SEM equipment described above. Particle morphology was assessed by Automated Image Mapping software and particle size determination was made by Particlemetric software.

6.2.5.6. Differential Scanning Calorimetry

A QA T2000 DSC was used for all the DSC studies performed on the drug, polymer and solid dispersions. Samples ranging from 5 to 10mg were used and the results were normalized to the Resveratrol content. The samples were placed in a 100µL pan. The pans were covered with a lid and the lid is crimped into place. Thermograms were generated under inert atmosphere using a heating rate of 10g/min from 0 to 300ºC.

6.2.5.7. Drug release profiles

Third-generation solid dispersions composed by Resveratrol: carrier: surfactant were evaluated for drug release by micro-method. Briefly, an amount equivalent to 2 mg of Resveratrol was added to a flask containing 4 mL of dissolution medium (pH 1.2 buffer or phosphate buffer pH 6.8). Drug release at pH 1.2 and 6.8 was evaluated and analysed by HPLC at different timepoints. In order to explain the drug release mechanism, three models were used, zero-order, Higuchi, and Korsmeyer-Peppas were explored as described by Costa and Sousa Lobo [334]. The *in-vitro* release data up to 60 minutes were, fitted to them, and the best model that describes the drug release was selected based on the best fit expressed by the higher value of the determination coefficient (R^2).

6.2.6. Permeability studies

Permeability experiments were performed on a Caco-2 cell monolayer model [335]. The Caco-2 (C2BBe1) cell line (passages 64–66) was obtained from the American Type

Culture Collection (ATCC, Manassas, VA, USA). Cells grew in culture flasks in a complete medium consisting of DMEM supplemented with 10% (v/v) FBS, 1% (v/v) L-glutamine, 1% (v/v) NEAA, and 1% (v/v) antibiotic mixture (final concentration of 100 U/mL Penicillin and 100 U/mL Streptomycin). Cells were sub-cultured once a week using 0.25% Trypsin-EDTA (1x) to detach the cells from the flasks and seeded at a density of 0.5 x 10^6 cells per 75 cm^2 flasks. The culture medium was replaced every other day. Cells were maintained at 37 °C, 5% CO_2 and 95% relative humidity.

For the permeability experiments, 1 x 10^5 cells/cm^2 of Caco-2 were seeded in 12-Transwell® cell culture inserts and were allowed to grow and differentiate for 21 days with medium replacement every other day. After that time, medium was carefully removed from the apical and basolateral compartments and the inserts were gently washed twice with phosphate buffered saline (PBS) (pH 7.4, 37 ºC). Then, 1.5 and 2.5 mL of HBSS was added to the apical and basolateral part of the Transwell®, respectively, and allowed to equilibrate for 30 min inside the incubator. Afterwards, the media from the apical compartment was removed and 1.5 mL of free Resveratrol at 50 µg/mL in HBSS was added. The formulations were placed directly in the apical compartment without removing the media. Plates were placed inside an orbital shaking incubator (IKA®KS 4000 IC, IKA, Staufen, Germany) at 100 rpm and 37 ºC. Aliquots (200 µL) were withdrawn from the basolateral chamber at pre-determined times (5, 15, 30, 45, 60, 90, 120, and 180 min) and immediately replaced with HBSS. At the end, an aliquot from the apical compartment was collected [335]. Tests were performed in triplicate and an insert without the addition of sample was used as a control. Before, during, and at the end of the permeability experiments, the Transepithelial Electrical Resistance (TEER) was measured using an EVOM2® epithelial voltammeter with chopstick electrodes (World Precision Instruments, Sarasota, FL, USA) in order to monitor the formation, confluence, and integrity of the cell monolayers. Experiments were performed in triplicate. The concentration of Resveratrol in the samples was determined by HPLC-UV analysis. The drug apparent permeability (P_{app}) was calculated from the following Equation (X):

$$P_{app} = [(dQ/dt) \times V]/(A \times C0) \quad (X)$$

Where P_{app} is the apparent permeability (cm/s); dQ/dt (µM/s) is the flux across the monolayer obtained from the angular coefficient of the curve of the amount of drug transported versus time; V(cm^3) is the acceptor chamber volume, which in this case corresponds to 2.5 cm^3 (basolateral chamber); A(cm^2) is the insert membrane growth area (equal to 4.67 cm^2 for a 6 well plate); and C0 (µM) is the initial concentration in the apical compartment [335].

6.2.7. Pharmacokinetic studies

For the pharmacokinetic studies, male, 7-weeks old Wistar rats, weighing 150–250 grams, purchased from Charles River Laboratories (France), were housed in cages on wood litter with free access to pellet chow diet (2014 Harlan) and tap water. The animal houses were maintained in a 12-hour light/dark cycle (07.00 to 19.00 hours) in a controlled ambient temperature of 22 ± 2ºC and relative humidity of 50 ± 20%. Rats were randomly divided into 2 groups, with 5 animals per group.

Administrations were performed by single intragastric bolus at a volume of 4 mL/kg. Hydroxypropyl Methylcellulose solution (0.25%, w/v) was used as vehicle. All animal procedures followed the guidelines from Directive 2010/63/EU of the European Parliament on the protection of animals used for scientific purposes and the Portuguese law on animal welfare (Decreto-Lei 113/2013). Resveratrol was orally administered at a dose of 100 mg/kg by gavage.

Approximately 150 µL of blood were collected at each time point from the tail vein. Samples were collected at pre-dose, 0.5, 1, 2, 4 and 7 h after administration and were assayed for Resveratrol by Liquid Chromatography with tandem mass spectrometry (LC-MS/MS). The C_{max}, T_{max} and AUC_{0-t} over 7 h were calculated for each group using GraphPad Prism, (GraphPad software Inc., CA, USA).

6.2.8. Chromatographic conditions

6.2.8.1. HPLC – UV

Resveratrol quantifications used in solubility assay and permeability studies were conducted using a Waters HPLC system and data was processed with Empower3®Software (Waters Corporation, Milford, MA, USA). The stationary phase consisted of a C18 reversed-phase column Waters Symmetry Shield RP18 (3.5µm, 100×4.6 mm) at 30ºC. The mobile phase consisted of (A) water and (B) acetonitrile (65:35, v/v) in isocratic mode and a flow rate of 1 mL/min. The run time was set at 10 min, the injection volume used was 10 µL for assay and solubility determinations and 50 µL for permeability studies. Detection by UV was fixed at 307 nm. Analytical method was validated according the ICH guidelines.

6.2.8.2. LC – MS/MS

Resveratrol quantification used for exposure assessment were conducted in a LC-MS/MS TQ G6470A from Agilent, data was acquired with MassHunter workstation data acquisition version B.08.00 and analysed with MassHunter workstation software for quantitative analysis version B.07.01. The stationary phase consisted of a Waters CORTECS T3 column (2.7µm, 100×2.1 mm) at 40°C. The mobile phases consisted of (A) water 0.1% formic acid and (B) acetonitrile 0.1% formic acid using the following gradient: 0 min 80% of A and 20% of B; 0.5 min 80% of A and 20% of B; 4.0 min 50% of A and 50% of B; 4.1 min 80% of A and 20% of B at a flow rate of 0.3 mL/min. The run time was set at 6 min, the injection volume used was 2 µL and the autosampler was kept at 4°C. The samples were injected into detector using the Agilent Jetstream electrospray ionisation in negative mode polarity. The multiple reaction monitoring pair was m/z 227.3→143.1 for Resveratrol with a collision energy of 26 V; and m/z 271.3→119.1 for Naringenin (ISTD) with a collision energy of 25 V. The fragmentation used was 140 V. The analytical method was validated according the ICH guidelines.

6.2.9. Statistical analysis

For solubility determinations, triplicates of formulations were statistically analysed in Microsoft® Excel® 2016 MSO. Student's t-test was used within pairs of experiments using a two-tail test with two-sample equal variance. Pairs were considered statically different with p values below 0.05. For Pharmacokinetics, Student's t-test for pairs of samples and one-way analysis of variance for all tests (ANOVA) with unpaired and Bonferroni post-hoc test (GraphPadPrism, GraphPad software Inc., CA, USA) were used to analyse the data, respectively. The level of significance was set at probabilities of $p < 0.05$.

6.3. Results

6.3.1. High-throughput screening of Resveratrol solubility

Resveratrol solubility was assessed in water base solution containing 5% of carrier after two hours of stirring at room temperature. Fourteen carriers were screen and solubility data are depicted on Figure 6.1. Pure Resveratrol showed a solubility of 2 µg/mL in water after 2h of stirring. Most of the tested carriers significantly enhanced the solubility of Resveratrol. Particularly Soluplus® and T80, which showed an enhancement higher than 2000 folds. Then, poloxamer P407, Myrj 59P and Povidone increased solubility more than

500-fold. Eudragit RLPO and both HPMCASs were the only carriers that did not significantly improved Resveratrol solubility under the tested conditions.

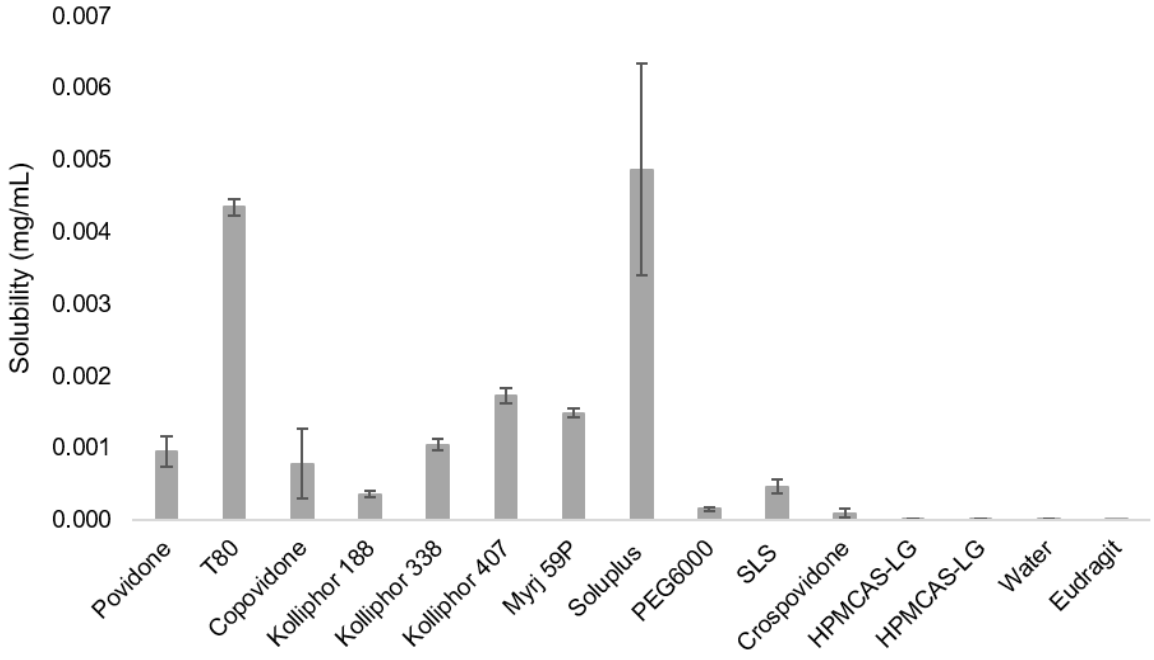

Figure 6-1 Solubility of Resveratrol in solutions containing five percent of each of the described carriers. (*) carriers that were significantly different from control (purified water).

6.3.2. Solid dispersions characterisation - FTIR data

FTIR spectrums were generated with the solid dispersions manufactured by solvent cast and using single carriers in different ratios in relation to Resveratrol.

6.3.2.1. HPMCAS

Generally, the number of Resveratrol characteristic bands (Figure 6.2.A and 6.2.B) decreased or presented slight shifts with the increase of the carrier content. Most of these changes were related to alcohol and aromatic functions of Resveratrol, which may indicate some hydrogen bonds between Resveratrol and HPMCAS through the alcohol function and some pi interactions between Resveratrol aromatic rings, probably with the saccharide ring of HPMCAS. Additionally, is also observed a decrease in the intensity of Resveratrol characteristic peaks over the expected by the dilution factor, which is more evident for formulations with a content of polymer of at least 50%. No major differences were observed between grades of HPMCAS.

6.3.2.2. PEG and derivates

Due to its chemical structure PEG6000 presented (Figure 6.2.C) as most relevant bands the bands related to C-H and –CH at wave lengths 2882 cm^{-1} and around 1400 cm^{-1}, respectively, and the band related to the ether C-O stretching at wavelength 1096 cm^{-1}. The alcohol functional group was almost neglected in the PEG600 spectra determined. The evaluation of the solid dispersion preparations suggested some interactions between PEG6000 ether group and Resveratrol alcohol group.

Generally, from Figure 6.2.D, the number of Resveratrol characteristic bands decreased or presented slight shifts with the increase of the carrier content. Most of these alterations were related to Resveratrol alcohol and aromatic functions, which may indicate some hydrogen bonds between Resveratrol and Soluplus® through Resveratrol alcohol function and Soluplus® alcohol or ketone groups. Additionally, some pi interactions between Resveratrol aromatic rings, probably with the oxygen of Soluplus® ester groups may have occurred. Also, generally it was observed a decrease in the intensity of characteristic Resveratrol peaks in the solid dispersion over the expected dilution factor, which was more evident for formulations with a content of polymer higher than 50%.

6.3.2.3. Polyvinil derivates

The COP is a vinylpyrrolidone and vinyl acetate copolymer and therefore presented a strong band at wavelength 1655 cm^{-1} from the amide group and other at 1730 cm^{-1} and 1237 cm^{-1} from the acetate group (Figure 6.2.E). The intensity of Resveratrol bands decreased or disappeared with the polymer increase in the solid dispersions. This was above the expected by the dilution factor, which may indicate some interactions between Resveratrol and COP that is corroborated by the same effect in the COP specific bands.

The Povidone is a vinylpyrrolidone polymer and therefore presented a strong band at around wavelength 1650 cm^{-1} from the amide group (Figure 6.2.F. The Resveratrol bands disappeared with the polymer increase in the solid dispersions. This was over the expected by the dilution factor, which may indicate some interactions between Resveratrol and Povidone that is corroborated by the same effect in the Povidone specific bands.

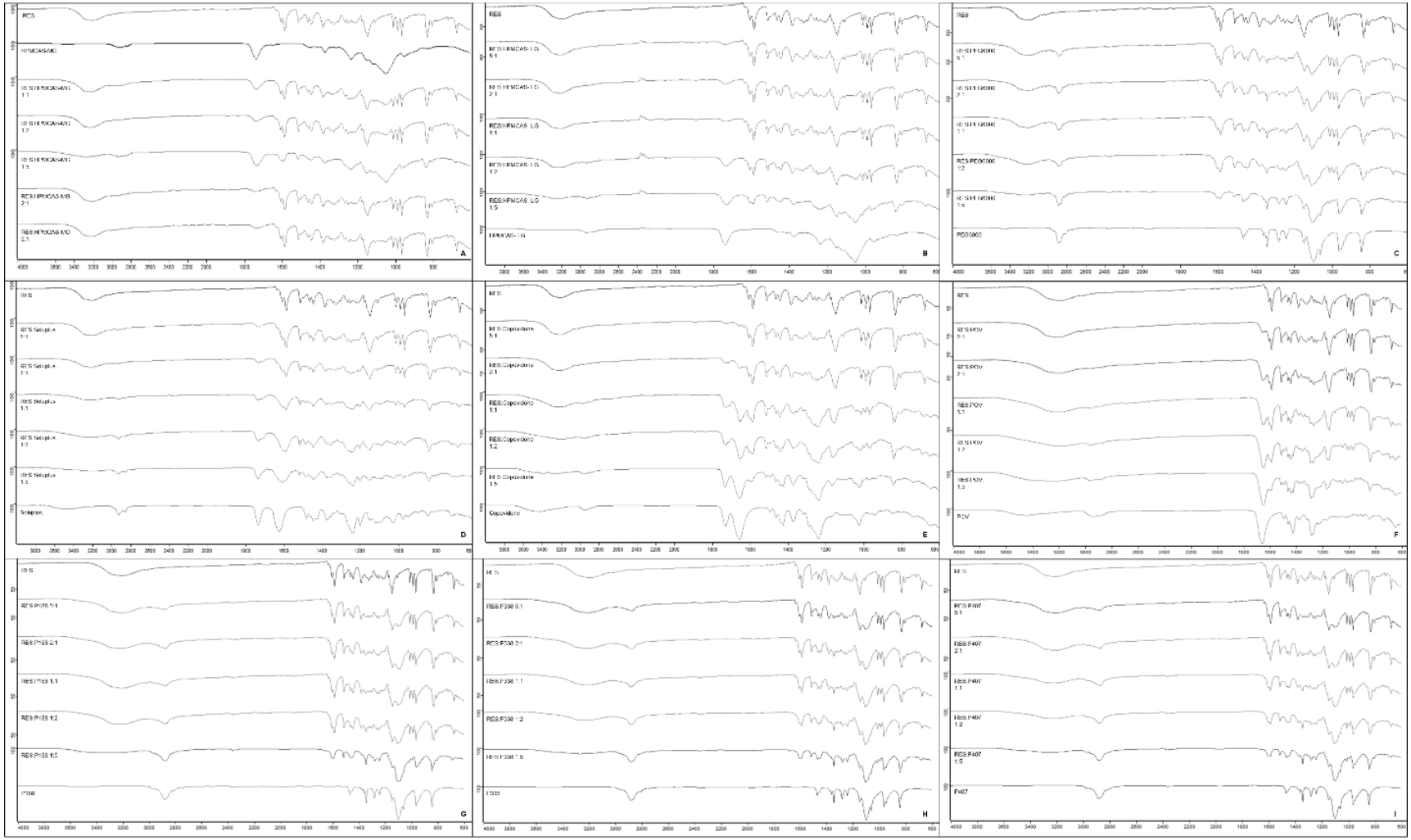

Figure 6-2 Spectra of solid dispersions prepared with HPMCAS-MG (2.A), HPMCAS-LG (2.B), PEG6000 (2.C), Soluplus® (2.D), Copovidone (COP) (2.E), Povidone (2.F), Kolliphor® P 188 (2.G), Kolliphor® P 338 (2.H), Kolliphor® P 407 (2.I).

6.3.2.4. Poloxamers

Poloxamers are non-ionic triblock copolymers composed of a central hydrophobic chain of polyoxypropylene (poly(propylene oxide)) flanked by two hydrophilic chains of polyoxyethylene (poly(ethylene oxide)). Thus, FTIR spectra was composed mainly by ether and alkane functional groups, which can be observed C-H and –CH bands at wavelengths 2881 cm^{-1} and around 1342 cm^{-1}, respectively and the band related to the ether C-O stretching at wavelength 1097 cm^{-1}. The alcohol functional group was almost neglected in the obtained spectra (Figure 6.2.G, H, I). The evaluation of the solid dispersions suggested some interactions between poloxamers ether group and Resveratrol alcohol or aromatic groups.

The poloxamers FTIR spectra were compared based on the poloxamer type (data not shown). Thus, generally the obtained spectra were very similar. Nevertheless, some considerations should be taken, in the cases that Resveratrol was at a ratio of 1:1 and 2:1 to poloxamers, the Resveratrol bands were more evident when poloxamer 188 was used, which may suggest a lower amorphisation capacity of this polymer at these ratios.

6.3.3. Solubility data

Solubility data were generated with the solid dispersions manufactured by solvent cast method and using single carriers in different ratios in relation to Resveratrol.

Resveratrol presented a water solubility of around 5.6 µg/ mL after 24 hours of stirring at room temperature.

6.3.3.1. HPMCAS

Generally, the Resveratrol preparation in solid dispersions using povidone derivates as carriers improved the Resveratrol solubility in all the drug: carrier ratios tested (Figure 6.3.A).

The observed improvements were generally at least 10-fold going up to 30 fold. No significant differences were observed between the two grades of HPMCAS tested within the same drug: carrier ratio. Nevertheless, HPMCAS-LG presented higher solubility values in almost all ratios which may be explained by the higher viscosity of MG grade that may slowdown the drug release. HPMCAS-MG generally presented lower standard deviations than HPMCAS-LG.

In the case of HPMCAS-MG the increase in carrier content did not presented an increase in the solubility as theoretically expected. In fact, the solubility was very similar within all ratios tested, which can be explained by the high incorporation capacity of this grade, showing that a small amount is required to obtain the optimum improvement. It may also indicate that a lower content is required for a complete Resveratrol amorphisation. In the case of HPMCAS-LG was observed that the formulation containing the highest drug content presented a lower solubility than all the other ratios. This may corroborate the data obtained with the HPMCAS-MG, since, this LG grade theoretically presents lower carrier capacity, it may require a higher amount to generate the fully amorphisations and consequently maximum increase in solubility. Additionally, this (83% Resveratrol) was the only ratio where the MG present a higher solubility than the LG.

As conclusion, the HPMCAS appeared to be good carriers for Resveratrol, which may require a small amount of carrier to achieve a complete amorphisation. Despite, independently of the grade, the medium grade presented a higher amorphisation capacity for very low ratios. After achieving a complete amorphisation, the viscosity of the grade appeared to have an important role in the solubility obtained, lower viscosity (LG) resulted in higher solubility probably due to a faster release.

6.3.3.2. PEG and derivate

The Resveratrol preparation in solid dispersions using Soluplus® and PEG6000 as carriers improved Resveratrol solubility in drug: carrier ratios when the carrier was at least 50% (Figure 6.3.B). The observed improvement was generally small, between 2 to 5 folds. Only one formulation (ratio) of each carrier was significantly higher than pure Resveratrol, this was mainly due to high variability between replicates (High RSD).

As conclusion, PEG and the tested derivate, Soluplus®, despite presenting very good solubility improvement in the screening study, did not present such a good solubility when formulated as solid dispersions. This may indicate that the solid structure formed by these compounds presented lower release capacity that can be attribute to its high internal cohesiveness. Suggesting that these compounds may require the inclusion of a surfactant to promote the rupture of the internal structure.

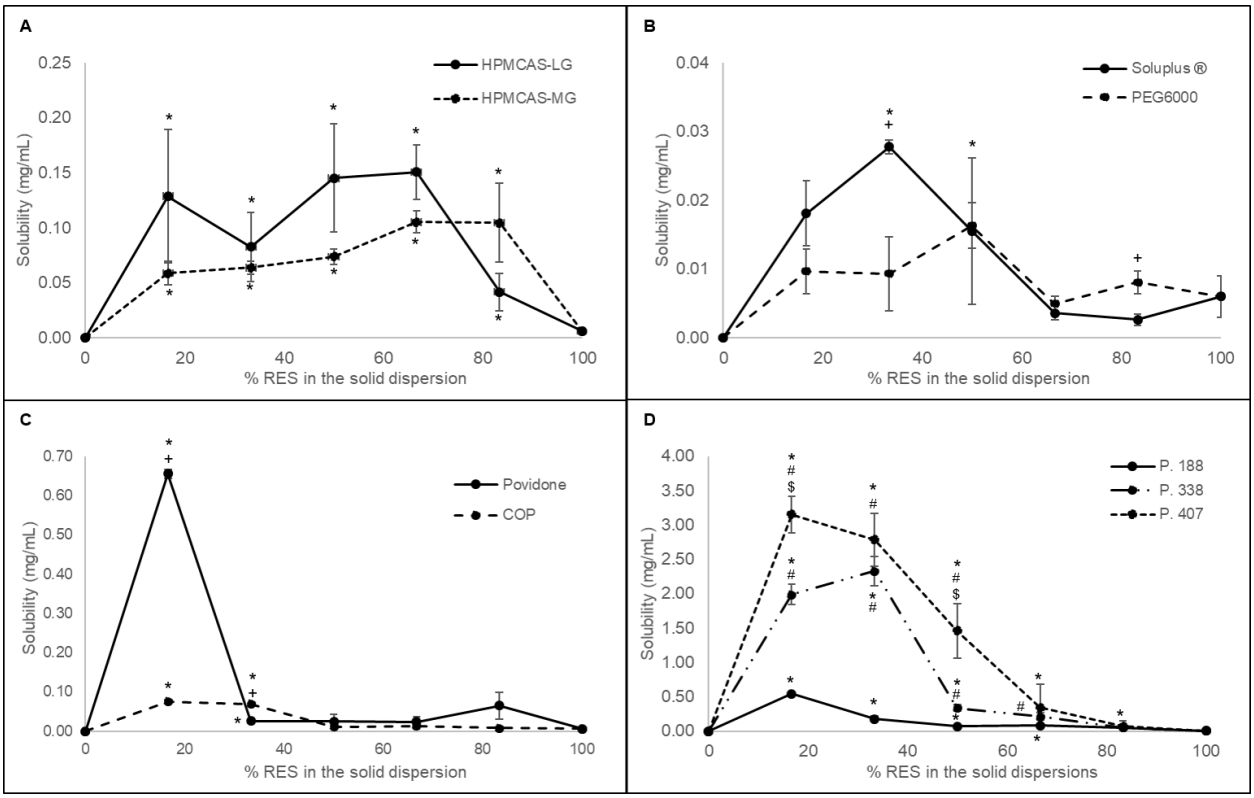

Figure 6-3 Solubility, after 24h of Resveratrol solid dispersions prepared at different drug: carrier ratios – RES:HPMCAS (A); RES: PEG / Soluplus® (B); RES: Povidone (C); RES: Poloxamer (D).

(*) significantly different from control (pure Resveratrol – 100%), (+) significantly different from the solid dispersion at the same drug: carrier ratio with the different carriers, (#) significantly different from the solid dispersion at the same drug: carrier ratio of P188, ($) significantly different from the solid dispersion at the same drug: carrier ratio of P338.

6.3.3.3. Polyvinyl derivates

Generally, the Resveratrol preparation in solid dispersions using povidone derivates as carriers improved the Resveratrol solubility in all the drug: carrier ratios tested (Figure 6.3.C). The observed improvement ranged from 2 to 10 folds with COP and between 4 to 100 folds with povidone. The improvements were statistically significant when both carriers were at a level of at least 67%. Moreover, from this value it was also possible to observe a significant difference between both polymers. Resveratrol solubility in povidone formulations was significantly higher than COP when carrier was at 83% and in COP was significantly higher than in povidone when the carrier content was 67%.

In the particular case of povidone, only when carrier was 67% of formulation a significant increase in Resveratrol solubility was observed and was only around 5-fold

increase, but, when the carrier was 83%, Resveratrol solubility increased massively (more than 100 folds).

Regarding COP, when the solid dispersions contained less than 50% of carrier, none or minimal (2 folds) improvements in the solubility was observed. When the carrier was above this level a tenfold increase was observed, suggesting that only under these conditions a full amorphisation was achieved. Resveratrol solubility increased with the increase in carrier content. This was common to both carriers (Povidone and COP), particularly when povidone was used at a level of 83%, with up to 100-fold solubility increase.

6.3.3.4. Poloxamers

Generally, Resveratrol preparations in solid dispersions using poloxamers as carriers highly improved Resveratrol solubility (Figure 6.3.D). The observed improvement ranged from 10 to 600 folds. Generally, the solubility increased with the polyoxypropylene molecular mass of the carrier and with the carrier content in the solid dispersion.

Poloxamer 188 was the carrier that presented the lower solubility increase, which ranged from 10 to around 200 folds increasing with the increase in polymer content. When poloxamer was in the solid dispersion at least at a level of 33% the solubility was significantly higher than pure Resveratrol.

Poloxamer 338 was able to increase Resveratrol solubility with the increment of carrier content in the solid dispersion ranging from 40 to around 500 folds. Formulations containing poloxamer 338 presented the highest solubility when its content in the solid dispersion was 67%. When poloxamer 338 was in the solid dispersion at least at a level of 33% the solubility was significantly higher than pure Resveratrol and when it was equal or higher than 50% it was significantly higher than the solubility obtained with poloxamer 188.

The poloxamer 407, was the poloxamer that presented the highest solubility enhancement, which was observed in all drug: carrier ratios. The solubility increased with the increase of carrier content in the solid dispersion ranging from 60 to more than 600 folds presenting the highest solubility when its content in the solid dispersion was 83%. When poloxamer 407 was in the solid dispersion at least at a level of 17%, the solubility was significantly higher than pure Resveratrol and when it was equal or higher than 50% it was significantly higher than the solubility obtained with poloxamer 188. Moreover, at the ratios where carrier was at 83% and 50% the solubility was also significantly higher than when poloxamer 338 was used.

Thus, poloxamers used as carriers promoted a solubility increase with the increase in carries content, this may be explained by the amorphisation of Resveratrol in combination

with the surfactant properties of poloxamers. Poloxamer 407 presented the highest improvements. Unfortunately, all solid dispersions with poloxamers presented poor technological properties, such as lack of complete solidification, they look like a grass material. Nevertheless, these data suggest that the use of poloxamers in the Resveratrol solid dispersions may be extremely beneficial, however their content must be at a low level.

6.3.4. Carrier Selection

Generally, it was considered that from the screening data several carriers showed promising solubility data. Miscibility between carriers and Resveratrol was demonstrated by FTIR for solid dispersions prepared by solvent cast. Here, solubility results lower than expected were observed. Therefore, Soluplus®, which presented the highest Resveratrol solubility improvement during screening, demonstrated molecular interaction observed by FTIR and a significant but small improvement in solubility when solid dispersions were prepared by solvent cast. Thus, this carrier was selected as carrier for further studies, because of its potential observed on the screening solubility and FTIR data, which can be potentiated by the inclusion of a surfactant that was expected to improve solubility and dissolution data in addition to the potential to reduce intestinal metabolism and efflux mechanisms of Resveratrol.

6.3.4.1. Differential Scanning Calorimetry

Thermograms of Resveratrol: Soluplus® at different ratios, were obtained. Resveratrol thermogram present a sharp endothermic peak at 266.8ºC corresponding to its melting with an energy of 252.2 J/g. In DSC data (Figure 6.4 and Table 6.1), when Resveratrol is present at a level higher or equal than 50% an endothermic peak related to Resveratrol melting point was observed around 260ºC. However, a decreased in intensity and shifted to an earlier melting point was observed with the increase of Soluplus®. When Resveratrol was below 50% in the formulation no endothermic peak related to Resveratrol was observed. This data corroborates solubility data previously described, meaning that a ratio above 1:1 between Resveratrol and Soluplus® is required to achieve a fully amorphous solid dispersion. Based on solubility, FTIR and DSC data a ratio of Resveratrol:Soluplus® (1:2) was selected for further studies.

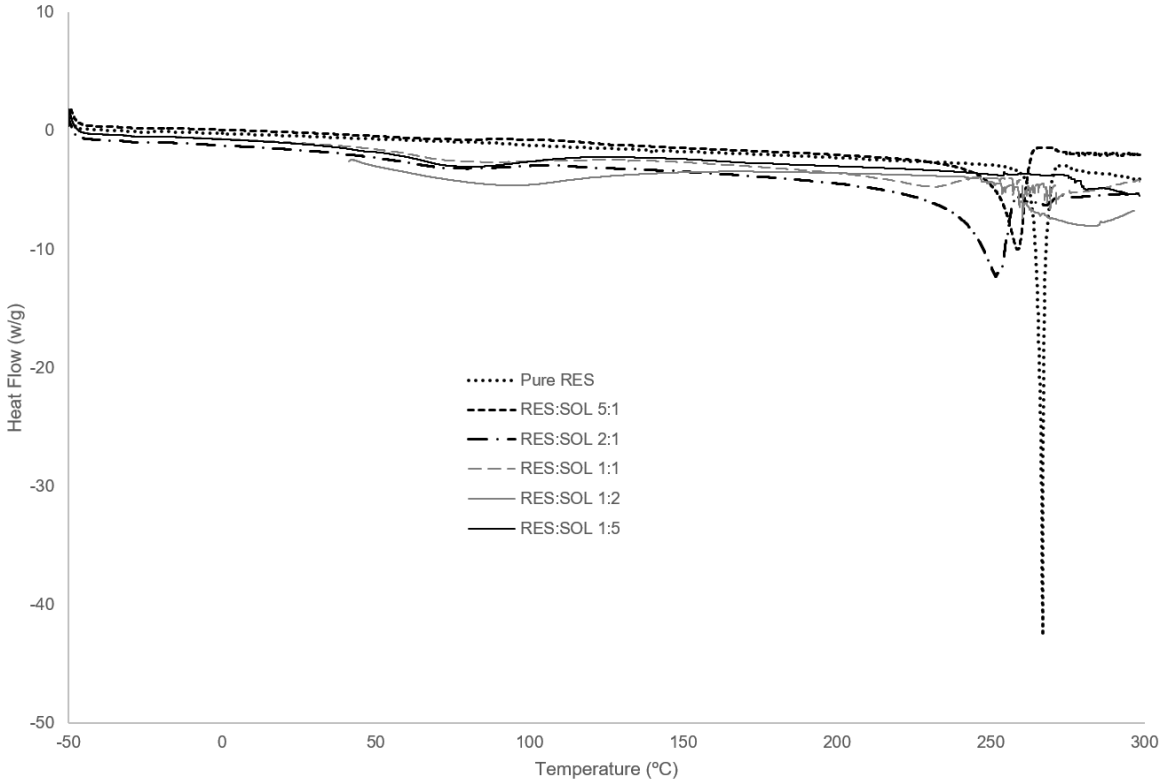

Figure 6-4 Thermograms of Resveratrol:Soluplus® at different ratios.

Table 6-1. Differential Scanning Calorimetry data of Resveratrol:Soluplus® formulations at different ratios.

Resveratrol:Soluplus® Ratio	Melting point (ºC)	Energy (J/g)	% of amorphisation
100:0	266.80	252.2	0
82:18	258.76	195.1	22.6
66.6:33.3	251.74	96.91	61.6
50:50	228.59	27.66	89.0
33.3:66.6	No peak	Not applicable	100
18:82	No peak	Not applicable	100

6.3.5. Third generation solid dispersions

Third-generation solid dispersions were manufactured using Resveratrol:Soluplus® at a ratio of 1:2, where two surfactants were included at 5 and 15%. The selected surfactants were poloxamer 407 and Gelucire. Poloxamer 407 was selected because in the screening phase it was the carrier that presented the higher solubility enhancement for Resveratrol.

Gelucire was selected due to its solid state at room temperature and the similar potential as poloxamer 407.

Formulations were evaluated for solubility, dissolution, DSC, permeability and drug release at pH 1.2 and 6.8.

6.3.5.1. Solubility

The inclusion of both surfactants in the third-generation amorphous solid dispersion significantly improved the Resveratrol solubility in around 2-fold over the solid dispersions without surfactants and more than 8 fold over pure Resveratrol (Figure 6.5).

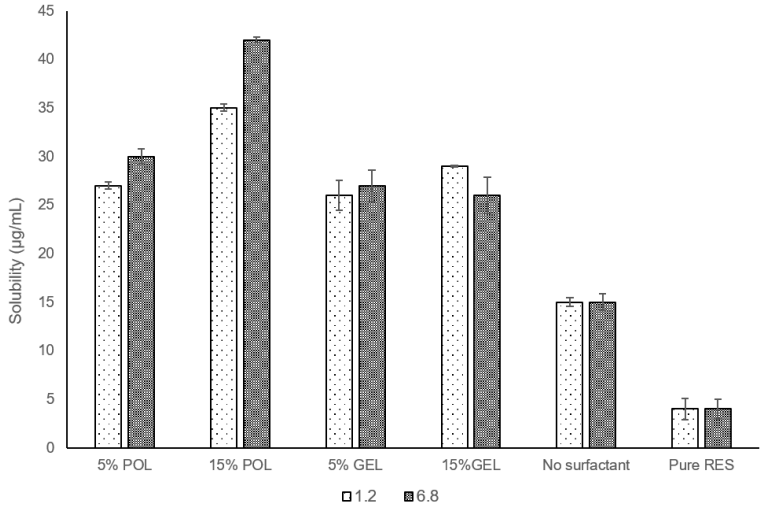

Figure 6-5 Solubility of pure Resveratrol and Resveratrol solid dispersions after 2h at pH 1.2 and 6.8. Pure RES= crystalline RES; POL 5% and 15% = solid dispersion composed by RES:Soluplus® (1:2) and poloxamer 407 at 5% and 15% respectively; GEL 5% and 15% = solid dispersion composed by RES:Soluplus® (1:2) and Gelucire at 5% and 15% respectively. No surfactant= solid dispersion composed by RES:Soluplus® (1:2).

All third-generation solid dispersion presented a significantly ($P< 0.05$) higher solubility than pure Resveratrol and second-generation solid dispersions for both pHs. At 5% concentration there was no significant difference between carriers but at 15%, poloxamer 407 presented a significantly higher solubility ($P<0.0.5$) than Gelucire for both pHs. No significant differences were observed between the two tested concentrations of Gelucire, nonetheless for poloxamer 407 when this surfactant was at 15%, the solubility of the formulation was significantly higher than of the 5% concentration for both values of pH.

Dissolution

Drug release was generally independent of the pH and reached a plateau after 30 minutes. Under simulated gastric pH conditions (Figure 6.6.A), solid dispersions showed a faster dissolution rate and stabilized in a plateau above the crystalline Resveratrol. All solid dispersions presented a very similar dissolution profile and rates, except formulation containing poloxamer 407 at 15% that presented a faster and higher dissolution profile. No precipitation (reduction in the dissolution) was observed for solid dispersions showing that those were able to maintain Resveratrol in a supersaturated state for at least 10 h under acidic conditions.

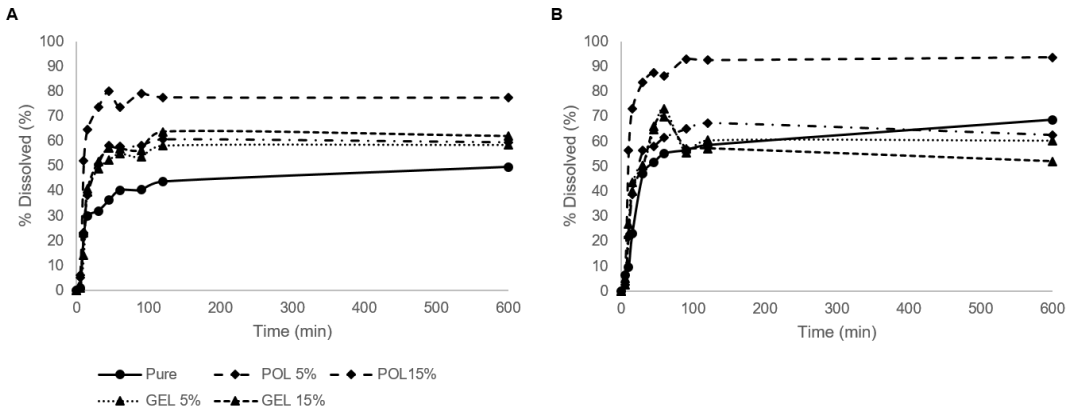

Figure 6-6 Dissolution of Resveratrol and Resveratrol third-generation solid dispersions after 10h at pH 1.2 (A) and at pH 6.8 (B). Pure RES= crystalline RES; POL 5% and 15% = solid dispersion composed by RES:Soluplus® (1:2) and poloxamer 407 at 5% and 15% respectively; GEL 5% and 15% = solid dispersion composed by RES:Soluplus® (1:2) and Gelucire at 5% and 15% respectively.

At pH 6.8, the formulations (Figure 6.6.B) showed a fast dissolution profile that reaches a plateau around 60 minutes. Formulation containing Gelucire presented a decrease in the dissolution values between 60 and 90 minutes suggesting that drug (Resveratrol) has crystalized. These was not observed for formulations containing poloxamer. Formulation containing poloxamer at 15% presented the faster and higher dissolution profile. All other solid dispersion formulation presented dissolution values close to the pure Resveratrol which was more evident above 1h of dissolution.

The analysis of these dissolution profiles suggested that a fast release in the stomach may occur and drug may be maintained in solution through the gastrointestinal tract (Figure 6.6.A and B), particularly the formulations containing poloxamer 407.

Dissolution profiles were subject of release kinetics analysis (Table 6.2) showing that a non-linear release process was observed for all profiles at both pHs since Korsmeyer-Peppas model was the best fit. Data suggest that non-fick diffusion balanced with erosion are the predominant drug release mechanisms [334].

Table 6-2. Drug release kinetics for dissolution profiles up to 60 minutes.

pH 1.2						
Model	Parameter	Pure RES	POL 5%	POL 15%	GEL 5%	GEL 15%
Zero order	K	0.626	0.986	1.233	0.966	0.984
	R^2	0.724	0.815	0.657	0.785	0.775
Higuchi	K	5.647	8.706	11.506	8.444	8.739
	R^2	0.853	0.919	0.826	0.866	0.884
Korsmeyer-Peppas	K	6.060	7.107	16.563	5.376	7.081
	R^2	0.925	0.958	0.916	0.931	0.939
	n	0.475	0.538	0.409	0.594	0.539
pH 6.8						
Zero order	K	0.993	1.064	1.355	1.185	1.202
	R^2	0.904	0.812	0.640	0.878	0.886
Higuchi	K	8.333	9.321	12.705	10.209	10.268
	R^2	0.920	0.902	0.813	0.943	0.935
Korsmeyer-Peppas	K	3.180	6.467	18.674	6.660	5.422
	R^2	0.969	0.949	0.910	0.973	0.970
	n	0.720	0.575	0.404	0.594	0.642

Pure RES= crystalline RES; POL 5% and 15% = solid dispersion composed by RES:Soluplus® (1:2) and poloxamer 407 at 5% and 15% respectively; GEL 5% and 15% = solid dispersion composed by RES:Soluplus® (1:2) and Gelucire at 5% and 15% respectively.

6.3.5.2. Differential Scanning Calorimetry

DSC experiments showed that the endothermic peak associated to the melting of Resveratrol was not presented in all solid dispersions evaluated at this stage. This data confirmed that all formulations presented Resveratrol in a fully amorphous state (Figure 6.7). Moreover, from DSC data it was possible to conclude that in all tested formulations, Resveratrol was completely miscible with the remaining excipients which was in line with the observed in the previous development stage for the formulation composed by Res:Soluplus® (1:2). The inclusion of poloxamer 407 and Gelucire within 5 to 15% of total formulation weight did not affect the Resveratrol miscibility remaining in an amorphous state.

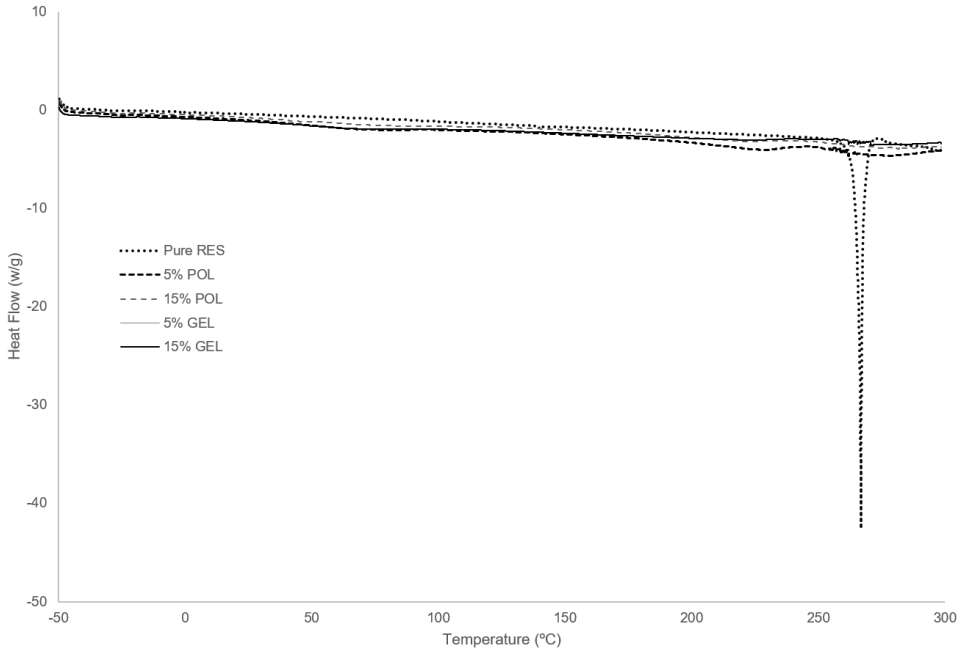

Figure 6-7 Thermograms of pure Resveratrol and Resveratrol third-generation solid dispersions containing poloxamer and Gelucire. Pure RES= crystalline RES; 5% and 15% poloxamer 407 = third-generation solid dispersions composed by RES:Soluplus® (1:2) and poloxamer 407 at 5% and 15% respectively; 5% and 15% Gelucire = Third-generation solid dispersions composed by RES:Soluplus® (1:2) and Gelucire at 5% and 15% respectively.

6.3.6. Permeability studies

Permeability studies were conducted on a Caco-2 cell monolayer model from apical to basal (A-B) and from basal to apical side (B-A) (Figure 6.8.A and B respectively).

The fraction of Resveratrol recovered in the sum of apical, cellular and basolateral compartments after adding second and third-generation solid dispersions into the apical side was below 50% in all tests, suggesting that Resveratrol metabolisation/ degradation was very intense and occurred rapidly. Control formulation, which was a second-generation solid dispersion composed by Resveratrol:Soluplus® (1:2) presented a Resveratrol recovery of 14%, and formulations with Gelucire and poloxamer 407 of 31% and 26% respectively, suggesting that these formulations may be able to reduce metabolisation and/or degradation of Resveratrol. Moreover, from all the recovered fractions, the permeated fraction corresponded to 79% in the control formulation, 72% in formulation containing Gelucire and 81% in formulation containing poloxamer 407, suggesting that the latter formulation was the least influenced by efflux mechanisms.

When Resveratrol was applied in the basal compartment the P_{app} was generally maintained for all formulations (Table 6.3). The permeability kinetics of all formulations was

comparable to the observed with the second-generation solid dispersion. All formulations showed a slow, but constant, permeation rate. This was significantly higher for formulations containing surfactants when compared to second-generation formulation. Between third-generation solid dispersions no statistical differences were observed.

The total fractions recovered when formulations were applied in the basolateral compartment were similar for second-generation solid dispersion (21%) and for formulation containing poloxamer 407 (30%) but much higher for formulation containing Gelucire ® (54%).

The fraction recovered in the donor compartment was almost neglected for the second-generation solid dispersion (control group).This data associated to the fact that P_{app} was only marginally affected when this formulation was applied in the basolateral compartment indicates that an efflux mechanism may be involved, as described by Shirasaka *et al* [336]. In the case of third-generation solid dispersions the fraction recovered in the donor compartment was below 50%, suggesting that efflux mechanisms of Resveratrol were blocked by these formulations.

TEER values of all formulations were maintained over the study, indicating that the monolayers remained intact until the end of the experiment and in this way, the permeability results really reflect the drug transport across the cell monolayers.

Table 6-3. P_{app} of all formulations of Resveratrol apical to basal and basal to apical applications (n=3, mean ± standard deviation).

Formulation	P_{app} (Apical-Basal) (cm/s)	P_{app} (Basal-Apical) (cm/s)	Ratio (A-B/B-A)
RES:Sol (1:2)	$4.2 \times 10^{-6} \pm 8.0 \times 10^{-7}$	$5.9 \times 10^{-6} \pm 8.1 \times 10^{-7}$	0.70
RES:Sol (1:2) GEL 15%	$8.8 \times 10^{-6} \pm 1.2 \times 10^{-6}$	$10.0 \times 10^{-6} \pm 2.5 \times 10^{-6}$	0.88
RES:Sol (1:2) POL 15%	$8.2 \times 10^{-6} \pm 1.9 \times 10^{-6}$	$7.7 \times 10^{-6} \pm 1.5 \times 10^{-6}$	1.07

RES – Resveratrol; Sol – Soluplus ®; POL – poloxamer; GEL – Gelucire® ; (A-B/BA) – Apical to Basal/ Basal to Apical

Permeability on Caco-2 cells showed that the inclusion of both surfactants increased drug permeability, which can be justified by the capacity that both have to inhibit P-gp [52]. Additionally, poloxamer 407 inhibits MRP2 transporters [337], which are known to be used as efflux mechanisms for Resveratrol [338]. In previous reports [338, 339], pure Resveratrol presented a tendency to accumulate in enterocytes, fact that was not observed in the presented data, particularly for formulations containing Gelucire® and poloxamer 407 further corroborating the potential efflux mechanism inhibition by these formulations.

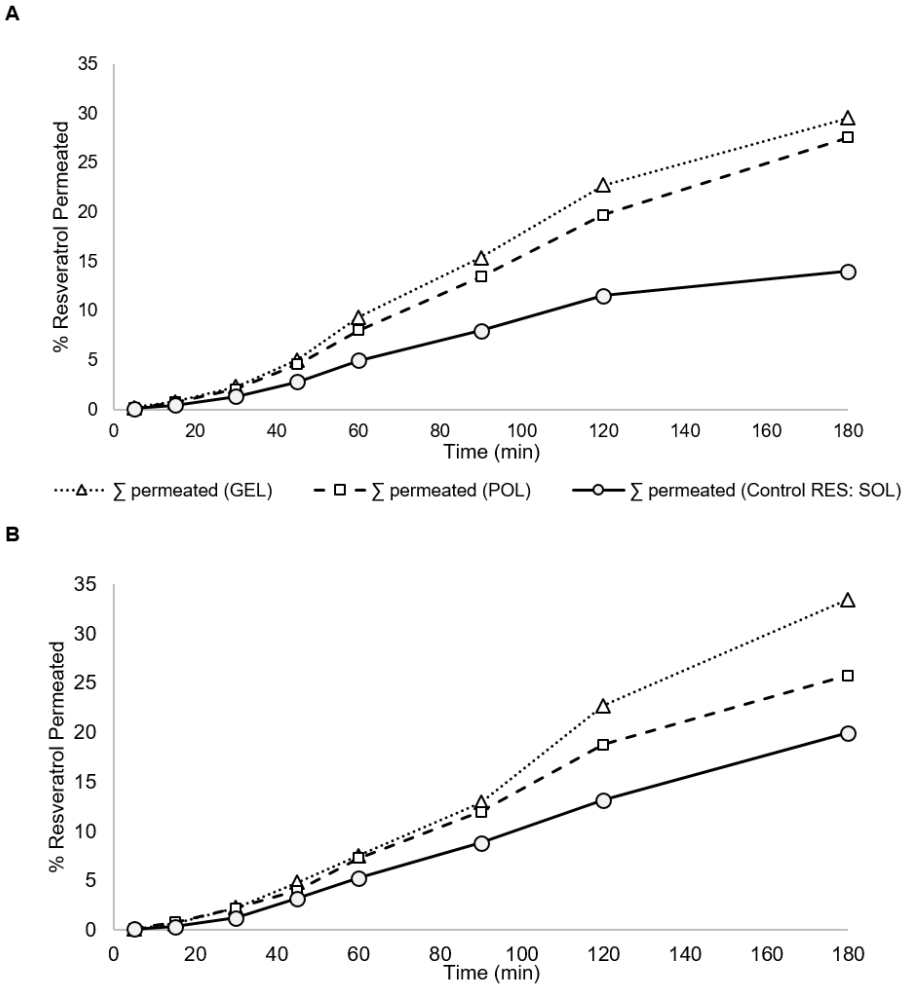

Figure 6-8 Caco-2 permeability data from Apical to Basal (A) and from Basal to Apical (B).SD RES:Sol = solid dispersion composed by RES:Soluplus® (1:2); SD RES:SOL:GEL = solid dispersion composed by RES:Soluplus® (1:2) and Gelucire at 15%; SD RES:SOL:POL = solid dispersion composed by RES:Soluplus® (1:2) and poloxamer 407 at 15%.

Both surfactants increased the Resveratrol fraction recovered in permeability studies indicating that were able to reduce metabolism, which was more evident for formulation containing poloxamer 407. Moreover, the later formulation was the one showing lower impact of Apical to Basal/ Basal to Apical ratio (A-B/B-A) proving that was the most effective in reducing efflux mechanisms. Therefore, solid dispersions composed by Resveratrol:Soluplus® (1:2) and Resveratrol:Soluplus® (1:2) POL 15% were prepared in a larger scale and more extensible characterized.

6.3.7. Pharmacokinetics batches characterisation

Batches used in pharmacokinetics studies were also characterized regarding assay, SEM with particle size and polymorphism by XRPD as observed in Table 6.4 and figures 6.9 and 6.10.

Table 6-4. Characterisation of formulations subjected to pharmacokinetic studies. Particle size determination correspond to a cumulative measurement of 21841 and 6568 particles of RES:Sol (1:2) and RES:Sol (1:2) POL 15%, respectively.

Formulation	Assay (%)	D_{10}(µm)	D_{50} (µm)	D_{90} (µm)
RES:Sol (1:2)	92.8	15	49	105
RES:Sol (1:2) POL 15%	101.2	51	138	308

RES – Resveratrol; Sol – Soluplus ®; POL – poloxamer 407

Assay results were acceptable for both formulations (Table 6.4), but particle size was much higher than expected, particularly for formulation containing poloxamer 407. The formulation containing poloxamer presented a particularly large particle size that should be associated to the manufacturing process (solvent evaporation by rotavapor) and not to composition. The relevant difference in particle size distribution may impact the pharmacokinetics profile by reducing Resveratrol absorption.

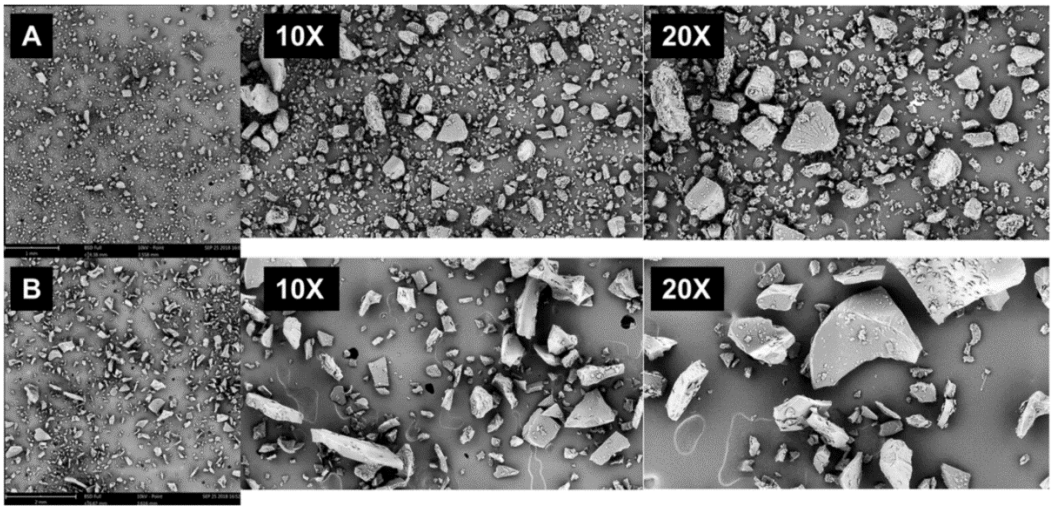

Figure 6-9 SEM images of Resveratrol solid dispersions. A (RES:SOL (1:2)) and B (RES:SOL (1:2) POL 15%) correspond to a preparation overview composed by a superimposition of 144 and 100 images, respectively. 10X and 20X correspond to a ten and twenty-fold digital magnification of a representative area of the original image, respectively. RES:SOL (1:2) = solid dispersion composed by RES:Soluplus® (1:2); RES:SOL (1:2) POL 15% = solid dispersion composed by RES:Soluplus® (1:2) and poloxamer 407 at 15%.

Both presented Resveratrol in a fully amorphous status based on SEM (Figure 6.9), XRPD (Figure 6.10) and DSC data (Figure 6.7).

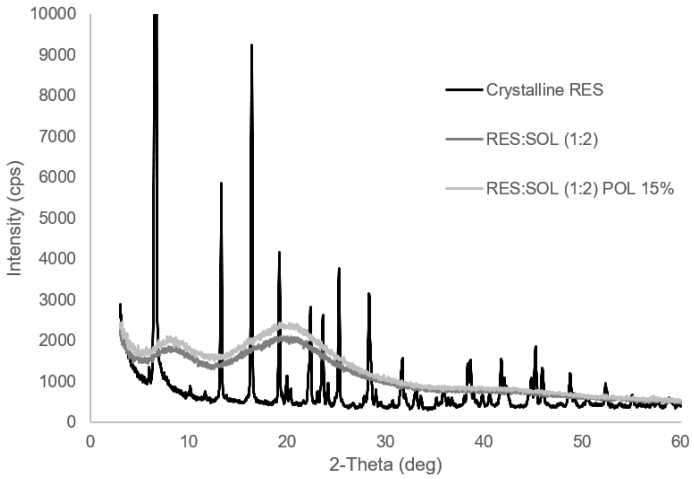

Figure 6-10 XRPD of Resveratrol and Resveratrol solid dispersions. Crystalline RES = crystalline RES; RES:SOL (1:2) = solid dispersion composed by RES:Soluplus® (1:2); RES:SOL (1:2) POL 15% = solid dispersion composed by RES:Soluplus® (1:2) and poloxamer 407 at 15%.

6.3.8. Pharmacokinetics studies

The pharmacokinetic parameters derived from Resveratrol after the oral administration of Resveratrol (100mg/kg) to rats using two different formulations are depicted in Table 6.5 and Figure 6.11. The third-generation solid dispersion containing Resveratrol:Soluplus® (1:2) with poloxamer at 15% reached maximal concentration at first timepoint (0.5 h) with a maximum plasma concentration (C_{max}) of 134 ± 78 and an AUC of 279 ± 54ng.h/mL. In the control formulation, which was a solid dispersion composed by Resveratrol:Soluplus® (1:2), a maximum plasma concentration (C_{max}) of 45.6 ± 50.0 ng/mL within 0.5 h was reached before falling back to low levels over the next 7 h. The area under the curve (AUC_{0-t}) obtained for this formulation was 162 ± 44 ng.h/mL.

Table 6-5. Pharmacokinetics parameters of all formulations.

Formulation	C_{max} (ng/mL)	T_{max}(h)	AUC_{0-t} (ng.h/mL)
RES:SOL (1:2)	46 ± 50	0.5	162 ± 44
RES:SOL (1:2) POL15%	134 ± 78	0.5	279 ± 54*

RES – Resveratrol; SOL – Soluplus®; POL – poloxamer 407; * Statistically significant ($p<0.05$).

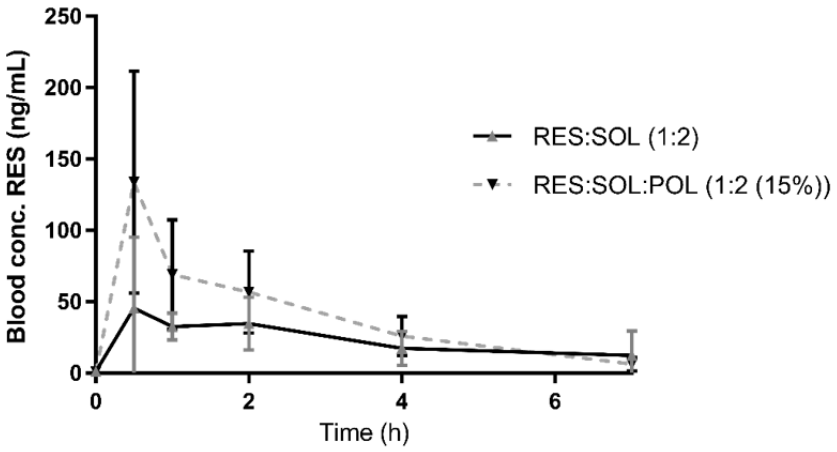

Figure 6-11 Pharmacokinetic profile of Resveratrol after oral administration in rats formulated as second and third generation solid dispersions.

In the present pharmacokinetics studies, Resveratrol solid dispersion only with Soluplus® (control) showed a secondary peak in its pharmacokinetic profile, thus suggesting entero-hepatic recirculation as observed and described by Marier *et al* [340]. This was not observed when poloxamer 407 was included to the formulation suggesting that it may reduce this phenomenon.

The observed C_{max} for the control formulation (Resveratrol:Soluplus® 1:2) was very similar to the observed by Branton and Snehasis in male Sprague Dawley rats [341] using the same dose of pure Resveratrol. However, AUC_{0-t} was 1.5-fold higher in present study suggesting that the supersaturate sate of Resveratrol in the solid dispersion extended the absorption period but not the rate which is in line with an absence of interference with efflux mechanisms. Curiously, both solid dispersions presented lower PK parameters than pure Resveratrol reported in a previous study [342]. This may be attributed to its larger particle size which was 2 to 5 fold higher when compared to pure Resveratrol. These large particles may have been responsible for the slow but continuous permeability over time in Caco-2 cells model. *In vivo*, this slow release may have prevented a burst effect, and consequent large amount of Resveratrol in absorption window able to completely saturate degradation and efflux mechanism. However, even in the absence of this burst effect the presence of poloxamer 407 was able to improve at least 2-fold C_{max} and AUC over the formulation without poloxamer, even presenting a much larger particle size and clearly indicating that poloxamer 407 was able to modulate intestinal metabolism and or efflux mechanisms.

This pharmacokinetics data corroborated the *in vitro* data, namely a relevant increase of exposure in the formulation containing poloxamer 407, confirming that this excipient was able to increase Resveratrol exposure which may be by inhibiting transporters

and/or metabolism over the improvement achieved by the solubility increase. This increase can be considered even more relevant considering the fact that particle size distribution of formulation containing poloxamer 407 were approximately 3-fold higher for D10, D50 and D90 descriptors when compared to the solid dispersion without surfactant.

6.4. Conclusions

Resveratrol solid dispersions can rationally be developed and are an important tool in the translation of Resveratrol into clinical use. The developed formulations presented Resveratrol in a stable amorphous state which was critical to increase drug solubility/ dissolution maintaining it in an oversaturated condition for the longest period of time possible [343].

The proposed development process allowed the selection of several formulations that presented Resveratrol in an amorphous state and enhanced its solubility several folds. From these, Soluplus® was selected as carrier. Additionally, two surfactants, poloxamer 407 and Gelucire, at two concentrations (5% and 15%) were assessed aiming to maximize drug solubilisation and reducing drug metabolism and efflux mechanisms [94, 137-139]. Poloxamer 407 at 15% presented a significantly higher dissolution rate and solubility than Gelucire but, both surfactants reduced efflux mechanisms and metabolisation in permeability studies on Caco-2 cells monolayer model which is in contradiction to the previously reported for poloxamer [94].

Amorphous solid dispersion composed by Resveratrol:Soluplus® (1:2) and Resveratrol:Soluplus® (1:2) with 15% poloxamer 407 were tested *in vivo*. A fast absorption was observed for both formulations. However, the inclusion of poloxamer 407 in a low concentration (15%) resulted in an increase in C_{max} and AUC of around 2-fold that could be due to a reduction in metabolisation and efflux mechanisms as supported by the Caco-2 cell permeability data [94]. Thus, these findings reveal extreme importance to support the biological impact of formulations components. Additionally, poloxamer 407 showed to be effective in reducing efflux mechanisms and Resveratrol intestinal metabolisation.

The use of third-generation solid dispersion can be very relevant to enhance the bioavailability of drugs, such as Resveratrol, that present low bioavailability due to poor solubility associated to intestinal metabolism and efflux mechanisms.

As future perspectives, this third-generation solid dispersion, produced at laboratorial scale should be scaled up by using, spray drying, freeze drying or hot-melt extrusion. Scale-up solid dispersion can then be combined with further excipient to be converted into oral tablet.

H. Development of a Self-Emulsifying Drug Delivery System of Resveratrol

This chapter was based on the following publications:

Teófilo Vasconcelos, Sara Marques, Bruno Sarmento. Measuring the emulsification dynamics and stability of self-emulsifying drug delivery systems. European Journal of Pharmaceutics and Biopharmaceutics 123: 1-8, 2018

Teófilo Vasconcelos, Francisca Araújo, Carlos Lopes, Ana Loureiro, José das Neves, Sara Marques, Bruno Sarmento. Multicomponent self-nano emulsifying delivery systems of Resveratrol with enhanced pharmacokinetics profile. European Journal of Pharmaceutical Sciences 137: 105011, 2019

7. Measuring the emulsification dynamics and stability of self-emulsifying drug delivery systems

7.1. Introduction

In the last two decades the pharmaceutical industry faced a shift in its development strategy due to the advent of computerized systems and the correspondent molecular design. This transformation led to the development of more potent and specific drugs, but also to drugs more challenging from the druggable space. These new drugs are particularly very poorly soluble and as a consequence present poor bioavailability [52, 74]. The pharmaceutical industry reacted to these new challenges by developing new drug delivery systems able to improve the observed inconsistent exposure and to maximize drug bioavailability. Among these strategies, amorphous solid dispersion and lipid formulations are the most promising. From the later, self-emulsifying drug delivery systems (SEDDS) are one of the most likely technologies [7, 344].

SEDDS are one of the most promising technologies in the drug delivery field, particularly for solubility and bioavailability enhancement [344]. SEDDSs are isotropic and thermodynamically stable solutions consisting of oil, surfactant, co-surfactant and drug mixtures that spontaneously form oil-in-water (O/W) emulsions when mixed with water under gentle stirring [345]. These drug delivery systems are, thus, lipid formulations, and, according to Pouton, classified in four classes depending on its composition, ranging from formulations composed by (I) pure lipid compounds, (II) lipids with low hydrophilic-lipophilic balance (HLB) generally used to form water in oil emulsions, (III) lipids with high HLB used to form oil in water emulsions and the last class (IV) is mainly hydrophilic components such as co-solvents [7].The principles of these systems assume that in contact with aqueous liquids these lipid formulations are able to emulsify and form stable nano or microemulsions containing drugs [346, 347] by using the motility of stomach and intestine for *in vivo* self-emulsification. SEEDS, particularly the ones belonging to class III, are able to generate stable emulsions in the presence of water vehicles. Self-emulsification occurs when the entropy change that favors dispersion is greater than the energy required to increase the surface area of the dispersion [348, 349]. These emulsions have a droplet size ranging from few nanometers to several micrometers. An adequate selection of excipients is crucial for the development of a successful SEDDS affecting the type of emulsion, dispersibility and stability after dispersion [346, 350, 351].

SEDDS able to form stable self-nano-emulsifying drug delivery systems (SNEDDS) or self-micro-emulsifying drug delivery systems (SMEDDS) present advantageous over the ones forming larger and generally unstable emulsion (Type I and II described by Pouton). This happens because the small droplets size allows a higher contact surface of drug with intestinal mucosa, improving its absorption [351-353]. Additionally, depending on the lipid composition and droplet size these particles can be absorbed by Peyer patches improving exposure and avoiding first hepatic passage effect [52, 347, 350, 352]. Droplet size and droplet stability after dispersion are, thus, key elements in the formulation development of SEDDS [7, 354-357].

The current methodology to evaluate SEDDS properties consists in the particle size measurement of the dispersions by dynamic light scattering (DLS) [355, 356, 358-361], photon correlation spectroscopy (PCS) [362] or, in a less extension, by laser diffraction (LD) [345]. Moreover, formulation stability is highly empirical based on visual observation [354, 356] or indirectly by the zeta potential [360]. These data were considered to be a proof of a successful self-emulsification process [363, 364].

In this work it is presented for the first time a process to observe (measure) the self-emulsification process allowing an online measurement of droplet size. Additionally, it is proposed a strategy to predict formulation stability based on droplet size stability when subject of physical stress conditions. Resveratrol, which is natural product that is under research due to its anti-cancer and anti-inflammatory properties, is also assessed as a blood sugar-lowering agent and a cardioprotective, was used as drug model in this study [365]. Resveratrol presents very low oral bioavailability (< 5%) due to its extremely low solubility, associated to high intestinal metabolisation and being substrate of efflux mechanism[366]. These factors make it an excellent model drug for bioavailability enhancement strategies of Biopharmaceutical classification system (BCS) class II and IV drugs.

7.2. Materials and methods

7.2.1. Reagents

Transcutol® was a gift from Gatefossé, France. Imwitor® 742 was a gift from Oxi-Med, Spain. Tween® 80 was acquired from Croda, Spain. Resveratrol was a gift from BIAL, Portugal. Purified water was obtained by a milliQ purification system.

7.2.2. Preparation of emulsions

In order to study a wide variety self-emulsifying processes, excipients of three different structural classes were selected with three HLB values (ranging from 4 to 15). Seven different formulations were studied (Table 7.1). Three formulations corresponded to single excipients, two were self-micro-emulsifying and another two self-nano-emulsifying drug delivery systems. Resveratrol was included into the formulations with different loadings, corresponding to the maximum solubility values of Resveratrol in each formulation (previously determined). Loading of formulations was 226 mg/mL, 19 mg/mL, 48 mg/mL, 168 mg/mL, 144 mg/mL, 47 mg/mL and 140 mg/mL, respectively (Table 7.1).

7.2.3. Characterisation of emulsions

7.2.3.1. Dispersibility

All formulations were assessed visually for spontaneous emulsification. SEEDS were diluted in distilled water at the ratio of 1:200 (v/v) under magnetic stirring at room temperature as described by Williams *et al* [356]. The type of dispersion was assessed based on Singh *et al* classification [354] where dispersions were classified in five grades based on time to disperse and aspect after dispersion. Grade I emulsions were formed in less than 1 minute and were of clear bluish appearance, in opposition, grade V emulsions were formed in more than 3 minutes and presented minimal emulsification and large oil droplets on surface.

7.2.3.2. Robustness to dilution of SEDDS

Robustness to dilution was studied by diluting SEDDS 5 and 200 times with purified water. The diluted SEDDS were stored for 24 h and observed for presence of phase separation or drug precipitation as proposed by Williams *et al* [356].

7.2.3.3. Emulsification process and droplet size measurement

The emulsification process was observed and measured using a Mastersizer® 2000 from Malvern (Worcestershire, United Kingdom). Briefly, 150 mL of purified water were added to the measurement compartment, then around 100 to 500 µL of SEDDS was added from which provided an obscuration of the detector (obscuration) between 3 to 25 % in line with the recommended by the equipment manufacturer for a good measurement. Dispersion

conditions in the system were set as 1750 rpm (50% of equipment capacity) and no ultrasounds.

A continuous particle size measurement (every 10 seconds) during 240 seconds was performed to allow the measurement of the self-emulsification process. The stable particle size (after 240 seconds) was considered as the droplet size after dispersion. Particle diameter corresponding to cumulative $D_{10\,(10\%)}$, $D_{50\,(50\%)}$, $D_{90\,(90\%)}$, specific surface area (SSA) which is the measurement of the area of per mass unit (m^2/kg), obscuration (of detector) and Span (representing the width of the distribution) were retrieved from the analysis and subject of investigation. Residuals were used to confirm the accuracy of the analysis.

7.2.3.4. Physical stability of SEDDS after emulsification

Physical stability of SEDDS after emulsification was evaluated by submitting the preparation described in previous section to 3500 rpm and 100 % ultrasounds capacity for 240 seconds followed by a period of stabilisation as described in previous section (1750 rpm and no ultrasounds). Particle size was continuously measured (every 10 seconds) during this process as described in the previous section.

7.2.3.5. Loading impact

The loading impact in the emulsification and physical stability of SEDDS after emulsification was evaluated by comparing the behavior of emulsions with Resveratrol and formulations without Resveratrol, submitted to the same conditions described in the two previous sections.

7.2.4. Statistical analysis

Triplicates of formulations were statistically analysed in Microsoft® Excel® 2016 MSO. T-student tests were performed within pairs of experiments using a two-tail test with two-sample equal variance. Pairs were considered statically different with p values below 0.05.

7.3. Results and discussion

The current state of the art in the development of SEDDS presents several limitations, particularly regarding the understanding of emulsification process and physical stability of formulations after emulsification. This has been highly supported on a visual observation and empirical rationales. The use of an analytical measurement of the

emulsification process with multiparameter being retrieved and subject of analysis removed the subjectivity from the emulsification process characterisation and provided a better understanding of this critical process for SEDDS. Moreover, the possibility to predict the physical stability of SEDDS after emulsification under stress conditions contribute for a more rationale formulation selection.

7.3.1. Dispersibility and physical stability

All formulations formed a micro-emulsion when diluted 1:5 with purified water. Moreover, when diluted 1:200 with purified water formulations I, III, VI and VII rapidly formed (< 1 min) a nano-emulsion, having a clear or bluish appearance and 24 hours later did not show phase separation. In the case of formulations II and V a slightly less clear nano-emulsion with a bluish white appearance was also rapidly formed (< 1 min). However, formulation IV rapidly (< 1 min) formed a milky micro-emulsion and showed a slight phase separation 24h later, which was not observed after 4 hours.

Accordingly to Singh *et al* [354] a formulation with the behaviour of formulations I to III and V to VII will remain as nano-emulsion when dispersed in gastrointestinal tract, while formulation IV is still recommend for SEDDS formulation. Moreover, all formulations except formulation IV were considered as physically stable after dispersion [367]. Formulation IV was also stable for at least 4h after dispersion, which was a positive indicator of its stability.

7.3.2. Droplet size and specific surface area

The droplet size measured after 240 seconds of dispersibility was considered as droplet size. The 240 seconds were selected because a plateau (stabilisation) in the droplet size was achieved at this time. The lowest droplet size was achieved for formulations VII (D_{50} = 167 nm) and VI (D_{50} = 362 nm) which were real nano-emulsion. All the other formulations were micro-emulsion: IV (D_{50} = 15.8 µm) and I (D_{50} = 24.5 µm) followed by formulation V (D_{50} = 47.2 µm) and II (D_{50} = 50.3 µm). Formulation III presented the largest particles (D_{50} = 83.6 µm) (Table 7.1). However, these values apparently contradict the visually observed (previous section) for formulations I-III and V. These differences between both experiments could be attributed to dilution and stirring speed variations.

Table 7-1. Droplet size measurements in a Mastersizer® 2000 (Malvern, Worcestershire, United Kingdom) after 240 seconds (loaded particles). T.: Transcutol®. I. 742: Imwitor® 742. T.80: Tween® 80. HLB: Hydrophilic-Lipophilic Balance. *: estimated.

Formulation	T. (%)	I. 742 (%)	T. 80 (%)	HLB	Loading (mg/mL)	D_{10} (µm)	D_{50} (µm)	D_{90} (µm)
I	100			4	226	7.20±1.40	24.5±12.9	45.3±16.9
II		100		4	19	4.60 ±1.70	50.3±9.7	129.9±41.0
III			100	15	48	37.50±20.30	83.6±25.9	140.4±44.2
IV	45	45	10	5.1 *	168	3.60±3.20	15.8±10.4	55.1±23.6
V	33.3	33.3	33.3	7.6 *	144	10.30±3.70	47.2±29.8	121.2±83.8
VI	12.5	75	12.5	5.4*	47	0.10±0.01	0.4±0.04	1.2±0.03
VII	25	25	50	9.5 *	140	0.08±0.10	0.2±0.02	16..5±16.0

Despite formulation III, all other formulations presented a relatively low variability in D_{10} and D_{50} values after 240 seconds, indicating that the emulsification process generally occurred similarly. The D_{90} measurements presented a higher variability, which may suggest that the largest particles were dependent on the microenvironmental conditions. An exception to this high variability was formulation VI, which after 240 seconds presented a very low variability in 3 droplet size parameters.

Traditionally, droplet size of lipid based formulations of SEDDS is determined by DLS after an equilibrium period of 30 min [356]. However, this approach presents some limitations starting with the particle size range of the DLS technique that is from 0.3 nm to 2 µm [368], which means that this technique could not detect all micro droplets in opposition to the laser diffraction that can measure particles from 20 nm to 2 mm [369, 370] underestimating the small nano size droplets. Moreover, the 30 minutes equilibrium period recommend for DLS is very long compared to the proposed one of 240 seconds (4 minutes).

The SSA is a measurement of the area of particles exposed to the dispersion medium. Translating this to an *in vivo* process, the higher the SSA (more and smaller particles), the highest exposure of particles to the intestinal walls, the higher is lipid digestion and, consequently, the higher absorption potential and lower inter-individual variability will occur [371]. Moreover, the SSA is a measure of all the droplets population. Formulations VI and VII presented the highest SSA which was expected due its nanoscale droplet size when compared to the other formulations. Among the micro-emulsions, formulation IV presented

the highest SSA, followed by formulations V, II, I with similar values and III presented the lower SSA (Figure 7.1). Furthermore, these data supported the droplet size measurements and its reliability since nano-scale emulsions presented a much higher SSA over the micro-scale ones. Formulation III presented the smallest Span, probably because it presented tightest droplets distribution but with the largest size, however all the other formulations presented a similar Span value (Figure 7.1). These data indicated that span value was independent of the droplet size scale and type of emulsion (nano Vs micro) but is a relevant tool to compare the width of the droplet size population.

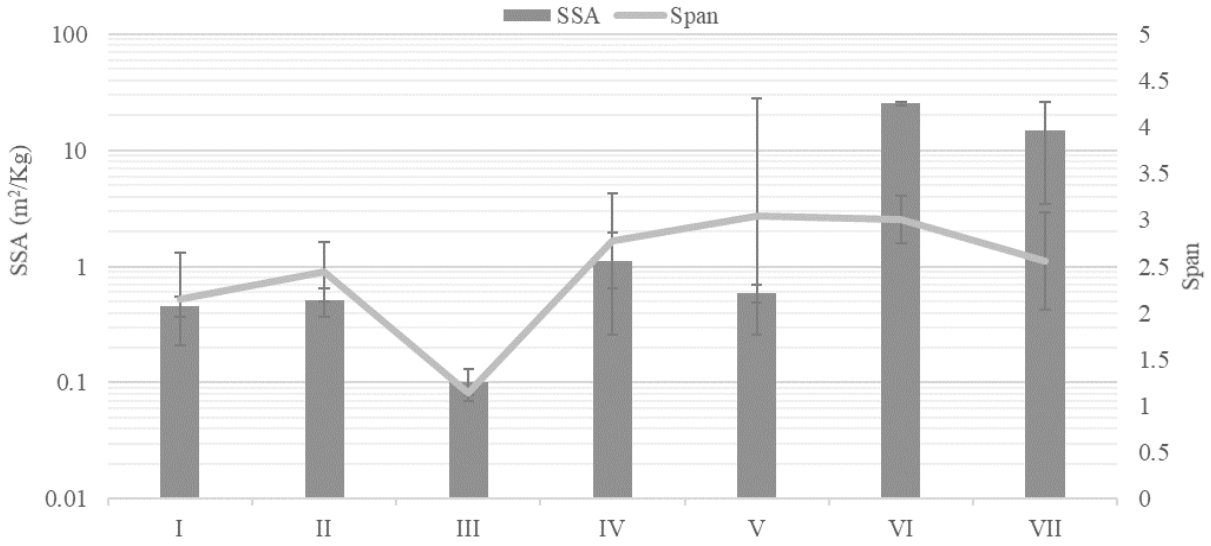

Figure 7-1 Specific surface area and span measured after 240 seconds (n = 3, mean ± SD).

The DLS droplet size determinations are generally reported as droplet size (average) and Polydispersity Index (PdI), which is a descriptive of the distribution width [355, 356, 371-373]. Average droplet size is equivalent to D_{50} and PdI is equivalent to Span provided by laser diffraction analysis. With the proposed analytical procedure, it was possible to have a clear picture of the droplet size distribution by having D_{10} and D_{90} and particularly the SSA detection, which corresponded to the measurement of whole droplet size distribution.

7.3.3. Emulsification process

The emulsification process and its dynamics were depicted in Figure 7.2 regarding the droplet size of the seven different formulations composed by a single component (I, II, III) or the mixture of them forming micro-emulsions (IV and V) or nano-emulsions (VI and VII.

In general, the use of laser diffraction allows the measurement and surveillance of the emulsification process. This process consisted, for most of the developed formulations,

in a fast (30 seconds) formation of very large droplets that then divided in smaller droplets until stabilisation (Figure 7.2). Generally, the stabilisation process firstly impacted the D_{10} followed by D_{50} and later D_{90}. A particular case of this type of emulsification was presented by formulation VI which almost instantaneously formed droplets of nano size that were not further divided. On the contrary, formulations IV and VII were exceptions of this process, which presented a much slower droplet size increase, formed smaller particles, followed by a slow droplet size decrease that kept occurring over a long time.

The formulations were dropped in the test equipment as a large droplet that then emulsified in smaller droplets. The observed process was aligned with the emulsification principles where the emulsified droplet size is considered to be the result of the droplet breakup and the droplet coalescence competition processes [374]. Particularly in SEEDS, emulsification requires very little input energy, which was provided by the stirring force resulting in a destabilisation of local interfacial regions through contraction. Thus, for emulsification to occur, interfacial structure should not have resistance to surface shearing, which could be achieved by using surfactants [375]. As the formulation interfacial tension decreased, droplet breakup occurred and formed smaller droplets. At the same time, the emulsion stability became very low, due to fast coalescence, which favoured the occurrence of larger droplets. For most of the formulations studied, in the first moments of emulsification, coalescence mechanism was preponderant as showed by the large droplet size [374]. This was followed by a period that droplet breakup become the most relevant mechanism until a balance was reached. However, formulation III presented very unstable droplet formation and droplet size reduction. Since formulation III was composed by Tween® 80, this phenomenon could be attributed to a dissolution/ emulsification process of this surfactant.

It is proposed that emulsification process of SEDDS consisted in converting large droplets into small droplets that reach stable D_{10} followed by a stabilisation in the D_{50} value and only later the D_{90} value stabilized. Moreover, fast and slow emulsifiers occurred in both micro and nano-emulsions similarly. Composition of SEDDS impacted the droplet structure, but also its viscosity which contributed for the behaviour as slow or fast emulsifiers.

Furthermore, these data suggested that the emulsification process was not a continuing process where droplet size was continuously reducing. Instead each formulation presented a relatively stable droplet size distribution and the variation was the time and mode to reach those droplet sizes.

The proposed mechanism of large droplets division into small droplets could be corroborated by the increase of obscuration and SSA over time (Figure 7.3) which was particularly evident for micro-emulsion and less for nano-emulsions. Obscuration and SSA

also proved that stabilisation in the formed particles occurred quickly, which supported the results for the particle size.

The droplet size dispersion (Span) increased rapidly and greatly in particularly for formulations I, II, V and VII that were followed by stabilisation (Figure 7.3). Formulation VI reached a span stabilisation extremely fast (10-20 seconds) and kept this value almost constant, this is an indicator that it quickly reached and kept a stable droplet size distribution over time.

Considering the obtained data, SEDDS emulsification could be categorized in 2 types: fast or slow emulsifying. The fast emulsifying SEDDS were characterized by quickly forming very large droplets that then were rapidly divided into small and stable droplets. On the other side, slow emulsifying was characterized by not so large droplets formation in the initial phase that then were slowly divided or fragmented into smaller droplets. This mechanism was observed for both micro and nano-emulsions.

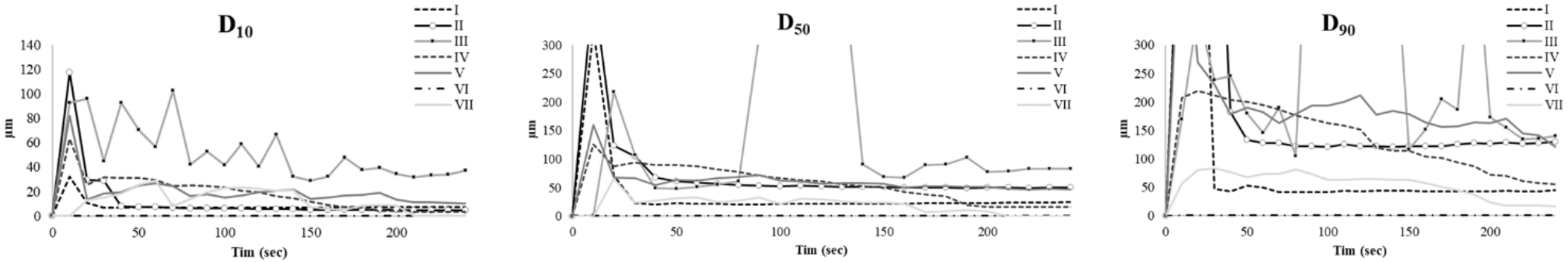

Figure 7-2 Droplet size measurements (D_{10}, D_{50}, D_{90}) over 240 seconds (n = 3).

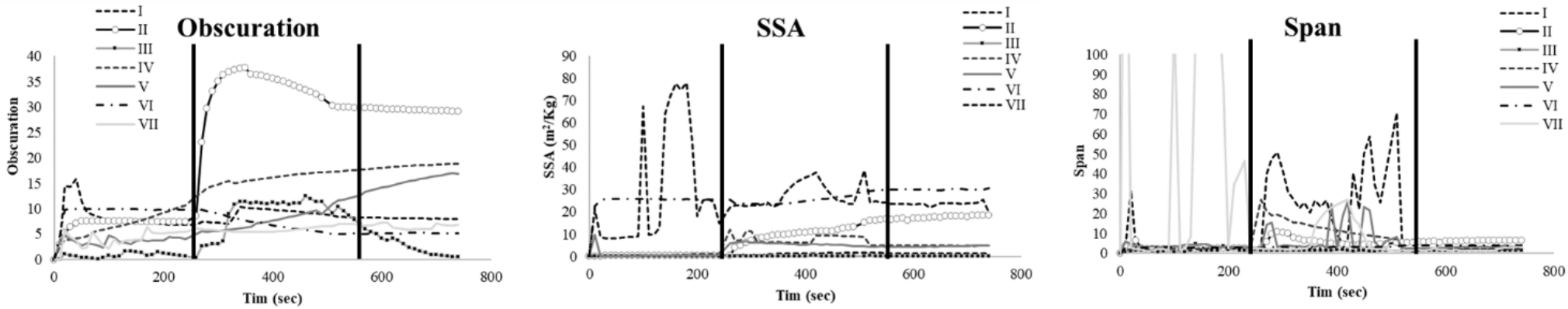

Figure 7-3 Obscuration, Span and SSA over stabilisation phase, stress phase and resting phase (n=3).

7.3.4. Physical stability of SEDDS after emulsification

After emulsification, the stress conditions that formulations were subjected, 3500 rpm and ultrasound at maximum capacity during 240 seconds, were followed by an additional resting period of 240 seconds. The behavior of emulsions was monitored for D_{10}, D_{50}, D_{90}, SSA, obscuration and Span every 10 seconds.

During the stress phase formulations behaved in two different ways (Figure 7.4): decreasing of general droplet size with major prominence in D_{90} was observed in formulations II, IV and VII (only D90 decreased), which was expected, since droplet size of an emulsion can be affected by the shear force [376, 377]. Alternatively, erratic droplet size increase in D_{90} was observed in formulations I and V with decrease in D_{10} and D_{50}, Formulation VI showed only a small increase of D10 and D50 during stress phase. Formulation III was not significantly affected by the stress conditions and resting phase.

On resting phase, formulations I, V and VI returned to their original droplet size, and even presented statistically (except formulation VI) lower D_{10}. However, formulation II during stress and resting phase showed a continuous decrease in droplet size which was at the end of the process statically smaller ($P< 0.05$) in all three parameters (D_{10}, D_{50} and D_{90}). By the contrary, formulations IV and III were not affected by the resting process (Figure 7.4). This data suggested that droplet size could be affected in some formulations, such as formulation I and V, by the emulsification conditions, such as agitation, but after standard conditions establishment the droplet size was able to revert to its original properties. Additionally, other formulations were only minimally affected by the emulsification conditions. Thus, it can be suggested that droplet size is mostly affected by the composition than by the emulsification conditions and that micro-emulsions are mostly affected by stress conditions than nano-emulsions that were only minimally affected.

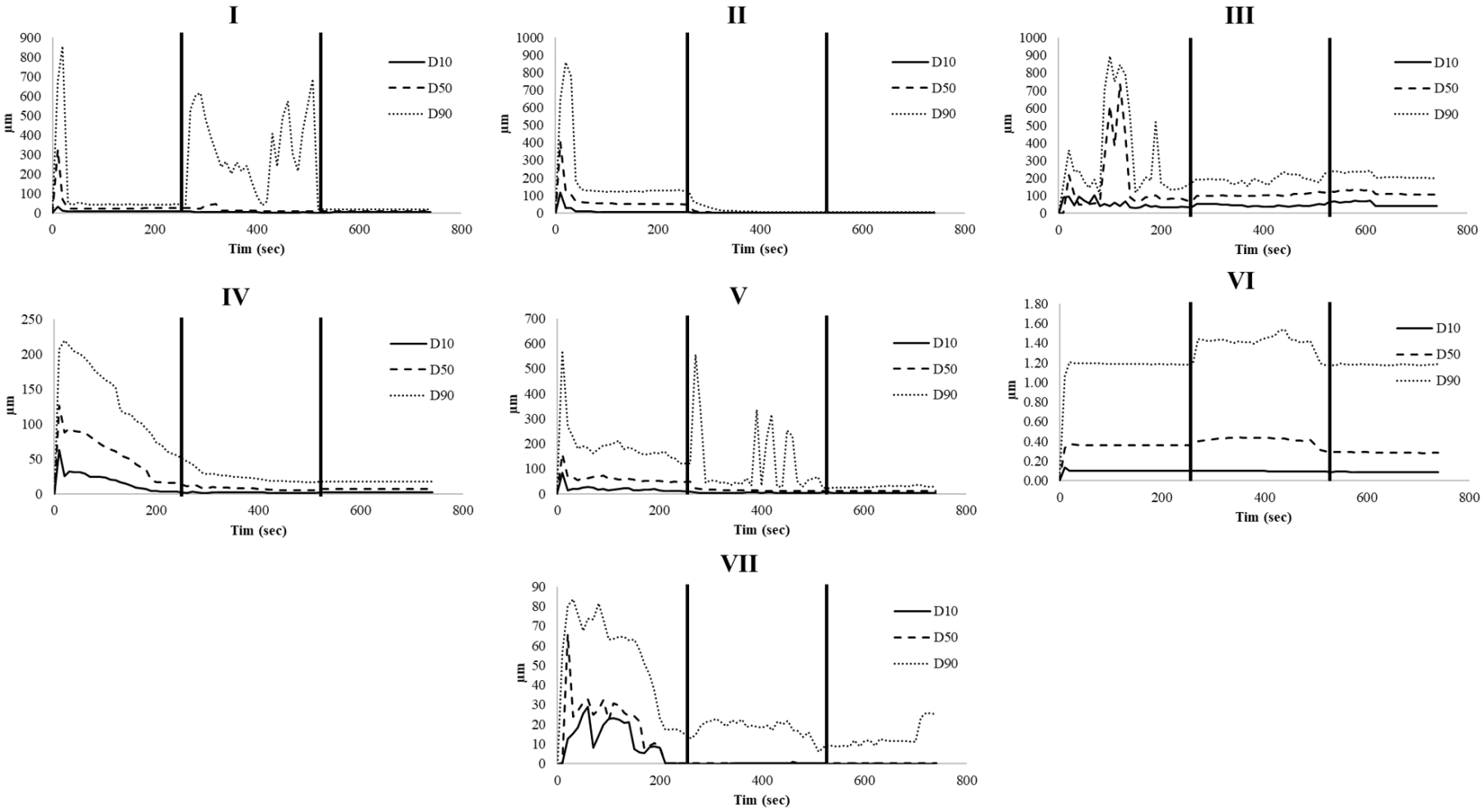

Figure 7-4 Droplet size measurement (D_{10}, D_{50}, and D_{90}) over dispersion (first segment), stress (second segment) and resting periods (third segment) (n = 3).

During stress phase, the shear forces increased and it was expected that droplet breakup became dominant over coalescent resulting in an increase of the number of droplets [374, 377]. However, the way that it would occur, the extension and the resting process was unpredictable.

Again, this phenomenon was more evident for micro-emulsions than for nano-emulsions, corroborating the previously observed for particle size. Therefore, obscuration, span and SSA were only minimally affected by stress and resting conditions applied to nano-emulsions. Regarding, micro-emulsions, formulation II during the stress phase registered a fast and steep increase in the number of particles (obscuration) followed by a slight decrease and stabilisation, which was maintained until the end of the study (Figure 7.3). The new droplets formation during the stress phase was accompanied with a decrease in the width of the particle size distribution (Span) resulting in a fast and sustained increase in the SSA. This supported the observed in Figure 7.4 that during stress phase a relevant droplet size reduction was observed particularly for D_{90} where the large droplets were fragmented in several smaller droplets.

On the other hand, formulation IV and V showed a slow formation of new particles during stress phase that was maintained during the resting phase (Figure 7.3). For formulation IV, this was associated to a slight narrowing of the droplet size distribution (Span), which was more evident for D_{90}, over the entire study resulting in a slight and slow increase in the SSA. On the contrary, an erratic increase in the droplet size distribution was observed during the stress phase for formulation V that was narrowed and stabilized as soon as stress conditions disappeared. This event leaded to a rapid increase in the SSA in the beginning of the stress phase followed by stabilisation.

Formulations I, and III showed a delayed fast but not very high increase in the droplet number during stress conditions followed by a stabilisation that was maintained during the resting phase for formulation I and decreased for formulation III. The behaviour of the latter formulation was associated to a slender increase in the SSA but not on the droplet size distribution which was maintained almost constant during the entire process. The decrease on the obscuration after the stress phase could be due to a combination of enlargement of the droplets size and solubilisation. Regarding formulation I the increase in droplets number was associated to a widening of the droplets size distribution only during the stress phase, which returned to their stabilisation values after removal of stress conditions. The SSA increased during the stress phase and was maintained almost constant until the end of the study.

Traditionally, the SEEDS droplet size stability consists in the measurement of the PdI, which is a dimensionless measure of the width of the particle size distribution [373]. This determination is performed 30 minutes after emulsification and consequently does not provide any type of information about the emulsification dynamics. Therefore, its correlation with SEDDS stability is limited. The proposed procedure on the other hand permits an almost online visualisation of the emulsification process. Moreover, as observed for Span alone, it provided limited information. However, the measurement of Span associated to SSA and obscuration, all together provided a clear picture of the formulation and equivalent Span values were achieved for very different formulations (ex. micro-emulsions VS nano-emulsions).

Depending on formulation components, the emulsification process can be reversibly or irreversibly affected by extreme stress conditions or not be affected by it. The later were considered to be the most desirable formulations as will be less prone to inter-individual variability due to different gastrointestinal mechanical conditions.

These data suggest that formulations composed by high lipophilic compounds (II) require more mechanical energy to emulsify into very small droplets, since the droplet size (reduction) and the SSA (increase) were significantly affected by the stress conditions. Nevertheless, after emulsification these are relatively stable, which can be included in the group of irreversibly affected by stress conditions. High lipid formulations showed a larger droplet size particularly because there was lack of surfactants to be present in the border of the emulsion droplets to reduce the interfacial energy as well as providing a mechanical barrier to coalescence as previously reported by Kang *et al* [355].

In the opposite, emulsions composed by water soluble components (I) or surfactants with very high HLB (III) or multi components (IV - VII) were less affected by the stress conditions and when were affected the effects were reversible. The major impact of stress conditions in these formulations consisted in an acceleration of the larger particle's fragmentation process into smaller and stable ones, reflected in particularly the decrease of D_{90} and not in the other parameters. This was also aligned with the reported by Kang *et al* that with increasing the surfactant and co-surfactant content the particle size decreased [355].

7.3.5. Resveratrol loading effect

The presence or absence of Resveratrol in the formulations was evaluated by submitting the non-loaded formulations to the same cycles of emulsification, stress and stabilisation (Figure 7.5).

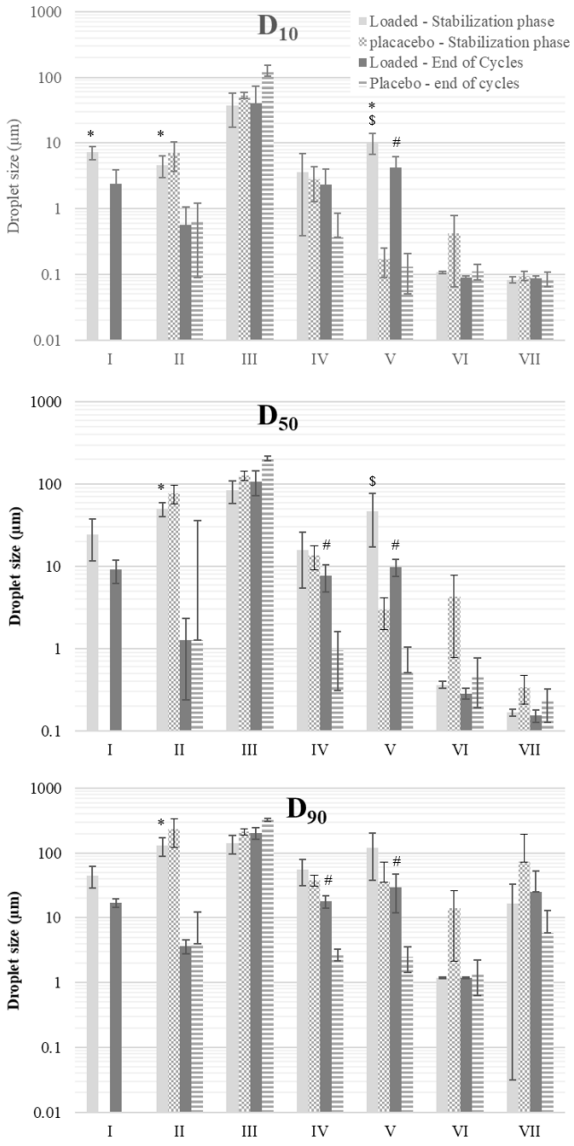

Figure 7-5 Droplet size at different stages with and without Resveratrol (n=3, mean ± SD). *Statistically different end of cycle vs stabilisation phase on loaded particles; # statistically different at the end of cycle loaded vs not loaded; $ statistically different at the end of stabilisation loaded vs not loaded (P<0.05).

The presence of Resveratrol showed minimal impact in the droplet size of formulation II and III, due to the low loading of Resveratrol on these formulations (2 and 5 % respectively). Similar results for low loading were reported by Kang [355] *et al* and Shah [378] *et al* using different drugs. When nano-emulsions were formed, loading level showed no impact in the droplet size (formulations VI and VII). Surprisingly, all of these formulations, the droplet size was higher (D_{10}, D_{50} and D_{90}) for non-loaded particles and was more evident after emulsification phase than at the end of the stress cycle study. This reinforce that the

entire cycle measurement provided relevant information impossible to obtain by a simple means droplet size and PdI measurement (Figure 7.5).

As non-loaded, formulation I was not able to emulsify, it solubilized and consequently presented an obscurity close to zero and thus no droplet size determinations were possible. At same time, this formulation was the one with the highest loading, around 23%, and since loaded particles were able to generate reproducible determinations it can be speculated that Resveratrol contributed to the emulsification process and stabilisation of droplets, preventing solubilisation.

Micro-emulsions formulations (IV, V) with high loading (around 15%) presented larger droplets in loaded particles as previously observed by other authors [355, 378].

Formulation IV, that emulsified equally with or without the presence of Resveratrol, after a stress cycle, non-loaded formulations droplet size significantly reduced (D_{50} and D_{90}) which did not occur in the loaded particles. In fact, this was a tendency in most of non-loaded formulations, maintaining or exacerbating the differences between loaded and non-loaded, like in case of formulation V that after these cycles was statically different in all three measurements. These data suggested that the presence of Resveratrol in these formulations prevented their droplet division and consequent droplet size reduction. When low loading levels were used or the systems were able to generate nano-emulsions, loading did not affect the droplet size. Moreover, it appeared to promote smaller droplet sizes in some case.

Generally, high loading levels, in a composition dependent manner impacted the droplet size. Droplet size of high loaded droplets was always smaller after stress cycles than after emulsification phase at least in D_{90}, in opposition to low loading levels that generally were less affect by the stress conditions.

7.4. Conclusion

Self-emulsifying delivery systems are an important tool to improve drug bioavailability of BCS class II and IV drugs, particularly for those with high lipidic solubility. However, its emulsification was a key process to ensure an adequate performance of these advanced drug delivery systems and therefore an adequate selection of the formulation is crucial. In this manuscript, it was shown that laser diffraction was a technique able to measure the emulsification process for micro and nano-emulsions providing important information of the drug delivery systems, far beyond its droplet size. Additionally, it was proposed a process to evaluate the stability of emulsified formulations to mechanical stress by evaluating droplet size, Span, obscuration and SSA allowing the selection of the most robust formulations that

will be less prone to suffer from *in vivo* intra or inter individual variabilities, such has peristaltic movements.

The use of a continuous measurement and multiparameter evaluation showed to be worth to understand the emulsification process and emulsion stability, allowing the differentiation of SEDDS during these phases. Using this process, it was possible to classify SEDDS regarding its emulsification process as slow or fast emulsifiers, which was not possible to determine with current characterisation processes. Data was generated using Resveratrol as model of poor water-soluble drug with several bioavailability issues and could be translated for another drug with similar bioavailability problems. Additionally, it was possible to observe that SEDDS with different compositions behave differently in the presence of a mechanical stress followed by a resting phase. All this information regarding emulsification dynamics and droplet stability to mechanical stress conditions could only be possible by using a continuous measurement of multiparameter against the current state of the art that uses a single point static analysis of two parameters. The present manuscript defined a new state of the art in SEEDS emulsification characterisation and droplet stability.

Formulations able to form nano-emulsion or with low loadings were less affected by mechanical stress. In particular cases, drug content appears to contribute to the droplet stabilisation promoting its smaller droplet size.

A desirable SEDDS formulation should be able to form a stable nano-emulsion with a small span value and very high specific surface area.

8. Multicomponent self nano emulsifying delivery systems of Resveratrol with enhanced pharmacokinetics profile

8.1. Introduction

Resveratrol (3,5,4'-trihydroxy-trans-stilbene) is currently being developed by several companies and in academia as an anti-cancer [379, 380], an anti-inflammatory [381-383], a blood sugar-lowering agent [384], anti-microbial compound [385, 386], or a cardioprotective agent [32, 387, 388]. It also present potential to be used in the management of neurodegenerative central nervous system diseases such as Parkinson's disease [389] and Alzheimer's disease [25, 390, 391]. Resveratrol has shown multiple pharmacological activity and it has been speculated that it can activate Sirtuin 1, an enzyme that deacetylates proteins involved in cellular regulation [392, 393]. It also activates peroxisome proliferator-activated receptor-gamma coactivator (PGC-1α) and improves mitochondrial activity [394]. It further possesses antioxidant and anti-angiogenic properties [395] and can directly inhibit cardiac fibroblasts [396]. Resveratrol interacts with several other enzymes, such as aromatase [34, 397] and gamma-glutamylcysteine ligase, which could contribute to the various pharmacological claims being advocated for this natural compound.

Despite all potential and data gathered from pre-clinical models, clinical evidence supporting the usefulness of Resveratrol is limited and, in many cases, ambiguous [39, 40, 398-401]. This is primarily attributed to the pharmacokinetic properties of Resveratrol, which has poor oral bioavailability (less than 5% of the oral dose is detected in plasma), mainly due to its poor water solubility and fast metabolism [39, 40]. Therefore, there is a compelling need to improve the oral bioavailability of Resveratrol in order to fully attest the potential of this multifaceted drug. Several technological approaches may be helpful in achieving this purpose. The use of amorphous solid dispersions and lipid formulations (such as self-emulsifying drug delivery systems (SEDDS)) are among the most promising approaches being currently tested in the pharmaceutical industry [52, 402]. SEDDSs are isotropic and thermodynamically stable solutions consisting of mixtures of oil, surfactant, co-surfactant and drug(s), and that spontaneously form oil-in-water (O/W) emulsions when mixed with water under gentle stirring [345]. Depending on composition, these lipid-based formulations can even self-emulsify and form stable nano or micro-emulsions [7, 347] under the influence of the motility observed at the stomach and intestine. SEDDS that are able to form stable self nano emulsifying drug delivery systems (SNEDDS) or self-micro emulsifying drug delivery systems (SMEDDS) may be particularly beneficial when compared to those forming

larger and commonly unstable emulsions. The small droplet size provides higher contact surface between drugs in the inner oil phase of the emulsion and the intestinal mucosa, thus enhancing absorption [351-353]. Moreover, and depending on the lipid components properties and droplet size of the emulsions, drugs can be absorbed via Peyer patches, which enables increasing systemic exposure and circumventing the hepatic first-pass effect [52, 347, 353].

Several studies explored SEDDs for the delivery of Resveratrol but only a few presented pharmacokinetics studies. For example, Chen *et al* [403] developed an ethyl oleate/Tween 80/PEG 400 (35:40:25, w/w/w) SMEDDS and showed that this strategy allowed improving the native antioxidant activity of Resveratrol using a cell-based model. In another study, Seljak *et al* [404] developed a castor oil/Capmul® MCM/Kolliphor® EL/Kolliphor® RH (1:1:1:1) SMEDDS formulation that presented a reduction in pre-systemic metabolism when tested using *in vitro* and *ex vivo* intestinal models. A Capryol® 90, Cremophor® EL, and Tween® 20 (60:35:5) SNEDD formulation was further developed by Yen *et al* [405], and shown able to improve blood glycemia and reduce fatigue in rats following exercise. These effects were, presumably, due to improved bioavailability. Finally, Balata *et al* [406] developed a SNEDDS formulation comprising olive oil, Tween® 80, and propylene glycol (20.0:26.7:53.3) and showed that such strategy allowed reaching significantly higher hypoglycemic and hypolipidemic effects in diabetic-induced rats as compared to unprocessed Resveratrol. Again, improved oral bioavailability was assumed for animals treated with SNEDDS. In this work, we developed and optimized a Resveratrol SEDDS presenting improved pharmacokinetics, namely C_{max}, with potential in increasing its brain bioavailability [407].

8.2. Materials and methods

8.2.1. Reagents

Transcutol® (Trans), Labrasol® (Lab), Lauroglycol® 90 (Lau), Labrafac® WL1349, Labrafil® M2125, Peceol®, Gelucire® 44/14 and Capryol® PGMC (Cap) were a gift from Gatefossé, France. Imwitor® 742 (Imw), Softigen® 767, Softigen® 701, Miglyol® 810, Miglyol® 829 and Miglyol® 840 were a gift from Oxi-Med®, Spain. Kollisolv® MCT 70, Kollisolv® P124, Kollisolv® PEG400, Kolliphor® TPGS, Kolliphor® EL, Kolliphor® HS15 and Kolliphor® RH40 were a gift from BASF (BTC-Europe), Spain. Tween® 80 (T80) was acquired from Croda, Spain. Resveratrol was purchased from Abatra Technology, China. Acetonitrile was obtained from Sigma-Aldrich, Germany.

Culture flasks and Transwell® plates were purchased from Corning Inc., USA. Dulbecco's Modified Eagle medium (DMEM), L-glutamine, non-essential amino acids (NEAA), penicillin (10,000 IU/mL), streptomycin (10 mg/mL) and trypsin-EDTA were purchased from HyClone, USA. Hank's balanced salt solution (HBBS) and heat inactivated foetal bovine serum (FBS) were purchased from Life Technologies Gibco, USA.

Purified water was obtained in-house using a milliQ purification system. All other materials were of analytical grade or equivalent.

8.2.2. High-throughput screening of Resveratrol solubility

Resveratrol solubility was accessed in Trans, Lab, Lau, Labrafac® WL1349, Labrafil® M2125, Peceol®, Gelucire® 44/14, Cap, Imw, Softigen® 767, Softigen® 701, Miglyol® 810, Miglyol® 829, Miglyol® 840, Kollisolv® MCT 70, Kollisolv® P124, Kollisolv® PEG400, Kolliphor® TPGS, Kolliphor® EL, Kolliphor® HS15, Kolliphor® RH40 and T80 that have a hydrophilic-lipophilic balance (HLB) values in the range of 1-18 (values for each excipient are present in Table 8.1). Briefly, an excess amount (10-150 mg) of Resveratrol was added to a two milliliters High Performance Liquid Chromatography (HPLC) vial. One milliliter of each of the above excipients was added to a vial and the preparations were stirred for two hours at room temperature (15-25 ºC). Each preparation was prepared in triplicate. The solubility in purified water was also accessed as control. After two hours, the suspensions were filtered through 0.45 µm filters (Pall Corporation, USA) and assayed by HPLC-UV.

8.2.3. Preparation of emulsions

Two sets of ternary qualitative compositions, Lauroglycol® 90/Labrasol®/Capryol® PGMC (Lau/Lab/Cap) and Tween®80/Transcutol®/Imwitor 742 (T80/Trans/Imw), were explored. In each, excipients of three different structural classes were selected with HLB values ranging from one to fifteen. Formulations were prepared ranging each component from 0% to 100%, as depicted in Fig. 8.1. Resveratrol was included into the formulations with different loadings, corresponding to the maximum solubility values previously determined. For permeability and pharmacokinetics studies, formulations were prepared at 100 mg/mL loading. Manufacturing process of formulations was adapted from Yen *et al* [405].

8.2.4. Characterisation of emulsions

8.2.4.1. Dispersibility

All formulations were assessed visually for spontaneous emulsification. SEDDS were diluted in distilled water, under magnetic stirring and at room temperature, in a ratio of 1:200 (v/v), as described by Williams *et al* [356]. The type of dispersion was assessed based on the classification of Singh *et al* [354] with some modifications. Dispersions were classified in four grades, based on time to disperse and appearance after dispersion: Tindal (grade I) as emulsions formed in less than 1 min and with clear bluish appearance; Nano-emulsions as formulations forming slightly less clear emulsion and having a bluish to white appearance (grade II); micro-emulsions as bright white formulations (similar to milk in appearance; grade III); and real solutions as formulations presenting a single liquid phase (grade IV).

8.2.4.2. Robustness to dilution of SEDDS

Robustness of SEDDS to dilution was studied by diluting 200-times with purified water. The diluted SEDDS were stored for 48 h under stirring and observed for additional presence of phase separation or drug precipitation as proposed by Williams *et al* [356].

8.2.4.3. Loading impact

The loading impact in the physical stability of SEDDS after emulsification was evaluated by comparing the behaviour of emulsions with and without Resveratrol when submitted to the same conditions described in the two previous sections.

8.2.4.4. Droplet size measurement

Droplet size was measured as cumulative percentile values of 10, 50 and 90% of droplets (D_{10}, D_{50} and D_{90}) and specific surface area (SSA) of SEDDS containing Resveratrol after emulsification using a Mastersizer® 2000 from Malvern (Worcestershire, United Kingdom) according to the method described by our group in a previous work [402].

8.2.4.5. Emulsification process and physical stability of SEDDS after emulsification

In selected formulations, the emulsification process and physical stability of SEDDS after emulsification were observed and measured using a Mastersizer® 2000 from Malvern

(Worcestershire, United Kingdom) according the method described by our group in a previous work [402].

8.2.5. Permeability studies

Permeability experiments were performed on a Caco-2 cell monolayer model [335]. The Caco-2 (C2BBe1) cell line was obtained from the American Type Culture Collection (ATCC, Manassas, VA, USA) and used at passages 64-66. Cells grew in culture flasks in DMEM supplemented with 10% (v/v) FBS, 1.0% (v/v) L-glutamine, 1.0% (v/v) NEAA, and 1.0% (v/v) antibiotic mixture (final concentration of 100 U/mL penicillin and 100 U/mL streptomycin). Cells were sub-cultured once a week using 0.25% Trypsin-EDTA to detach the cells from the flasks and seeded at a density of 5 x 10^5 cells per 75 cm^2 flask. The culture medium was replaced every other day. Cells were maintained at 37 °C, 5% CO_2 and 95% relative humidity. For permeability experiments, Caco-2 cells were seeded in 6-Transwell® cell culture inserts at a density of 10^5 cells/cm^2, and were allowed to grow and differentiate for 21 days with medium replacement every other day. After that time, medium was carefully removed from the apical and basolateral compartments and the inserts were gently washed twice with PBS (pH 7.4, 37 ºC). Then, 1.5 and 2.5 mL of HBSS was added to the apical and basolateral part of the Transwell®, respectively, and allowed to equilibrate for 30 min inside the incubator. Afterwards, the media from the apical compartment was removed and 1.5 mL of free Resveratrol at 50 µg/mL in HBSS was added. The formulations were placed directly in the apical compartment without removing the medium. Plates were placed inside an orbital shaking incubator (IKA®KS 4000 IC, IKA, Staufen, Germany) at 100 rpm and 37 ºC. Aliquots (200 µL) were withdrawn from the basolateral chamber at pre-determined times (5, 15, 30, 45, 60, 90, 120, and 180 min) and immediately replaced with HBSS. At the end, an aliquot from the apical compartment was collected [335]. Tests were performed in triplicate and an insert without the addition of sample was used as control. Before, during, and at the end of the permeability experiments, the Transepithelial Electrical Resistance (TEER) was measured using an EVOM2® epithelial voltammeter with chopstick electrodes (World Precision Instruments, Sarasota, FL, USA) in order to monitor the formation, confluence, and integrity of the cell monolayers. Experiments were performed in triplicate. The concentration of Resveratrol in the samples was determined by HPLC-UV analysis. The drug apparent permeability (P_{app}) was calculated using the following Equation (Eq. 1):

$$P_{app} = [(dQ/dt) \times V]/(A \times C_0) \qquad \text{(Eq. 1)}$$

Where P_{app} is the apparent permeability (cm/s); dQ/dt (μM/s) is the flux across the monolayer obtained from the angular coefficient of the curve of the amount of drug transported versus time; V (cm^3) is the acceptor chamber volume, which in this case corresponds to 2.5 cm^3 (basolateral chamber); A (cm^2) is the insert membrane growth area (equal to 4.67 cm^2 for a 6-well plate); and C_0 (μM) is the initial concentration in the apical compartment [335].

After sample collection at the last time point (180 min), Caco-2 cell monolayers were washed with PBS and then lysed with Triton® X-100 in order to extract Resveratrol. Cell-associated drug levels were measured by HPLC-UV.

8.2.6. Pharmacokinetic studies

Seven-weeks old male Wistar rats (150-250 grams) were purchased from Charles River Laboratories (France) and housed upon reception in cages containing wood litter, with free access to pellet chow diet (2014 Harlan) and tap water. Animals were maintained in a 12-hour light/dark cycle and in a controlled ambient temperature of 22 ± 2ºC and relative humidity of 50 ± 20%. Rats were randomly divided into three groups with five animals each, and received either Resveratrol suspension (group 1), Lau/Lab/Cap emulsion (group 2) or T80/Trans/Imw emulsion (group 3). Administrations were performed by single oral gavage at a volume of 4.0 mL/kg. Hydroxypropyl methylcellulose solution (0.25%, *w/v*) was used as vehicle. All animal procedures followed the guidelines from Directive 2010/63/EU of the European Parliament on the protection of animals used for scientific purposes and the Portuguese law on animal welfare (Decreto-Lei 113/2013). Resveratrol was administered at a dose of 100 mg/kg. Blood samples of approximately 150 μL were collected from the tail vein before oral gavage and at 0.5, 1, 2, 4 and 7 h post-administration, and were assayed for Resveratrol by LC-MS/MS. The C_{max}, T_{max} and area under the curve (AUC_{0-t}) over seven hours were calculated for each group using GraphPad Prism (GraphPad Software Inc., USA) [405, 408].

8.2.7. Chromatographic conditions

8.2.7.1. HPLC – UV

Quantification of Resveratrol in samples from the solubility assay and permeability studies was conducted using a Waters HPLC system and data was processed with Empower3® Software (Waters Corporation, Milford, MA, USA). The stationary phase consisted of a Waters Symmetry Shield RP18 column (3.5μm, 100×4.6 mm) at 30 ºC. The

mobile phase consisted of water and acetonitrile (65:35, v/v) in isocratic mode and at a flow rate of 1.0 mL/min. The run time was set to 10 min, while the injection volumes were 10 µL for assay and solubility determinations and 50 µL for permeability studies. Detection by UV was fixed at 307 nm. Analytical method was validated according the applicable ICH guidelines.

8.2.7.2. LC – MS/MS

Quantification of Resveratrol in plasma was conducted using a LC-MS/MS TQ G6470A from Agilent (USA), and data was acquired with MassHunter workstation data acquisition version B.08.00 and analysed with MassHunter workstation software for quantitative analysis version B.07.01. The stationary phase consisted of a Waters CORTECS T3 column (2.7µm, 100×2.1 mm) at 40°C. The mobile phases consisted of (A) 0.1% (v/v) formic acid in water and (B) 0.1% formic acid (v/v) in acetonitrile using the following gradient: 0 min - 80% of A and 20% of B; 0.5 min - 80% of A and 20% of B; 4.0 min - 50% of A and 50% of B; 4.1 min - 80% of A and 20% of B. Flow rate was 0.3 mL/min throughout the full run (6 min), while the injection volume was 2 µL and the autosampler was kept at 4 °C. The samples were injected into the detector using the Agilent Jetstream electrospray ionization in negative mode polarity. The multiple reaction monitoring pair was *m/z* 227.3→143.1 for Resveratrol with a collision energy of 26 V; and *m/z* 271.3→119.1 for naringenin (ISTD) with a collision energy of 25 V. The fragmentation used was 140 V. The analytical method was validated according to applicable ICH guidelines.

8.2.8. Statistical analysis

For solubility determinations, triplicates of formulations were statistically analysed in Microsoft® Excel® 2016 MSO. Student's *t*-test was used within pairs of experiments using a two-tail test with two-sample equal variance. For pharmacokinetics, Student's *t*-test for pairs of samples and one-way analysis of variance for all tests (ANOVA) with unpaired and Bonferroni post-hoc test (GraphPadPrism, GraphPad software Inc., CA, USA) were used to analyse the data, respectively. In all cases, $p < 0.05$ was considered has denoting significance.

8.3. Results and discussion

8.3.1. High-throughput screening of Resveratrol solubility

The solubility of Resveratrol in 22 lipid solvents was screened and the results are presented in Table 8.1.

Table 8-1. Resveratrol solubility in excipients generally used for SEDDS. Results are presented as mean ± SD (*n*=3). (*) denotes a statistically significant difference from control ($p < 0.05$).

Excipient	HLB	Solubility (mg/mL)
Purified water (control)		0.003 ± 0.002
Labrafac® WL1349	1	0.605 ± 0.058*
Peceol®	1	4.257 ± 0.013*
Miglyol® 810	N/A	0.606 ± 0.069*
Kollisolv® MCT 70	1	1.025 ± 0.070*
Miglyol® 840	N/A	0.975 ± 0.086*
Miglyol® 829	N/A	1.364 ± 0.136*
Lauroglycol® 90	3	6.362 ± 0.686*
Imwitor® 742	4	9.014 ± 0.488*
Labrafil® M2125	5	5.778 ± 0.163*
Capryol® PGMC	6	12.460 ± 1.654*
Gelucire® 44/14 (5%)	12	3.787 ± 0.184*
Labrasol®	13	83.754 ± 10.168*/#
Kolliphor® TPGS	13	4.921 ± 0.331*
Kolliphor® EL	13	22.957 ± 2.296*/#
Kollisolv® P124	15	39.514 ± 11.806*
Kolliphor® RH40	15	30.410 ± 13.748*/#
Kolliphor® HS15	15	30.433 ± 0.170*/#
Tween® 80	15	4.346 ± 0.113*
Softigen® 767	18	5.696 ± 0.734*
Transcutol®	N/A	107.478 ± 9.085*/#
Kollisolv® PEG400	N/A	0.151 ± 0.033*
Softigen® 701	N/A	22.535 ± 2.172*

N/A – not available; (#) saturation of Transcutol®, Labrasol®, Kolliphor® EL, RH40 and HS15 was not achieved.

Resveratrol presented aqueous solubility of 3.0 µg/mL with significant enhancement by all tested vehicles, in particular Labrasol®, Trascutol®, Kolliphor® EL, RH40 and HS15, and Kollisolv® P124 (Table 8.1). Furthermore, some of these solvents improved solubility by more than 4000-fold, with the least effective, Kollisolv® PEG400, still showing an improvement of 50-fold.

Based on these data, two sets of three excipients were considered for the formulation of SEDDS. One excipient with HLB above ten and another below six were selected for each set. The third component was selected from co-solvents and/or excipients with HLB in the range of 6-10. Therefore, set 1 was compose of Lau/Lab/Cap and set 2 by T80/Trans/Imw.

8.3.2. Loading

The maximum drug loading achieved for each formulation is depicted in Figure 8.1. In the Lau/Lab/Cap formulations (24 formulations) the loading levels increased with Labrasol content and, consequently, with the increase in the HLB of the ternary formulation (Figure 8.2). The lowest loading achieved was of 22 mg/mL with the formulation containing 100% Lau and the highest with formulation of 25/65/10 of Lau/Lab/Cap respectively. In this last case, a loading values of 146 mg/mL was achieved.

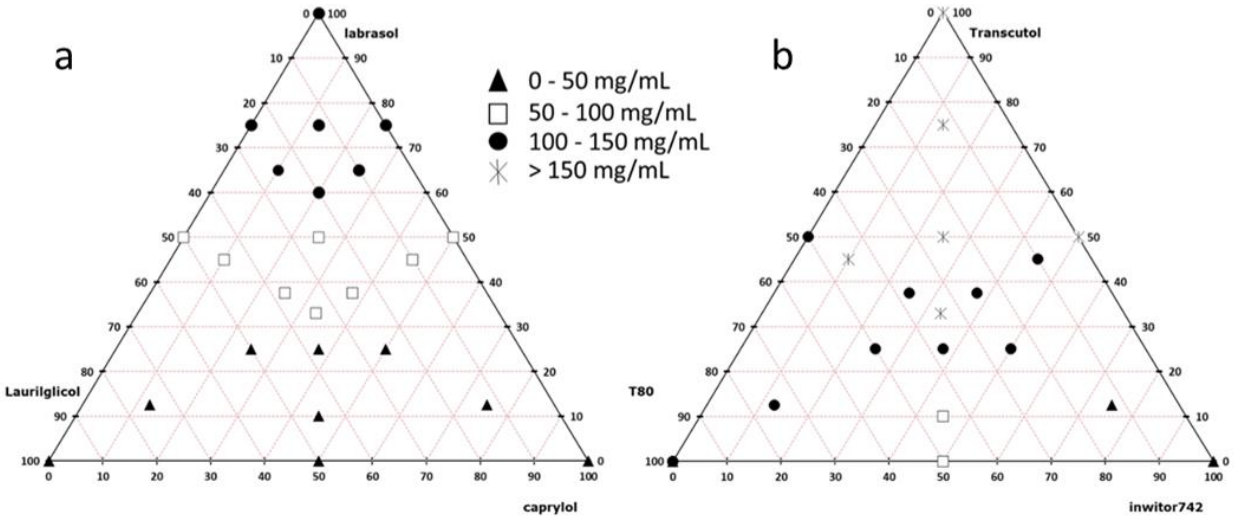

Figure 8-1 Resveratrol loading in two sets of ternary qualitative compositions of Lau/Lab/Cap (a) and T80/Trans/Imw (b). Loading values are reported as: ▲ loading values below 50 mg/mL; □ loading values between 50 and 100 mg/mL; ● loading values between 100 and 150 mg/mL; * loading values above 150 mg/mL.

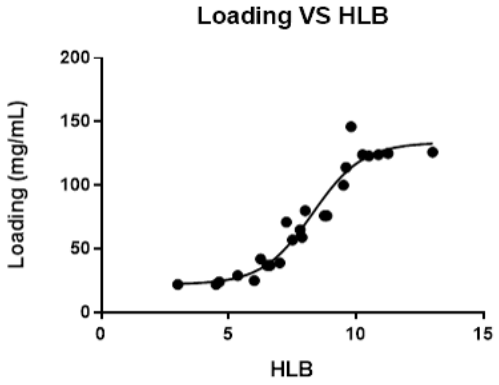

Figure 8-2 Effect HLB in Resveratrol loading in Lau/Lab/Cap formulations. HLB values of the formulation increased the loading in a sigmoidal manner.

Conversely, loadings of ternary formulations composed of T80/Trans/Imw (19 formulations) were generally higher than the ones observed for the previous formulations. The maximum loading was 226 mg/mL, as observed for the 100% Trans formulation, followed by the formulations composed of 12.5/75/12.5 and 33/33/33 of T80/Trans/Imw, with values of 190 and 168 mg/mL, respectively. The correlation between HLB and solubility was not assessed since Trans is a solvent and does not possess a HLB value. Nevertheless, the increase in Trans and Imw contents resulted in increased and decreased solubility, respectively, in a non-linear mode.

8.3.3. Dispersibility and robustness to dilution

8.3.3.1. Lauroglycol® 90/ Labrasol®/ Capryol®

All the twenty-four formulations prepared according to this ternary composition, and without Resveratrol, formed a nano-emulsion when diluted at a ratio of 1:200 in purified water (Figure 8.3A). Resveratrol addition did not alter the formulations visual appearance for most of the formulations (Figure 8.3B). After 48h, some of those formulations were present as micro-emulsion with two liquid phases (Figures 8.3C and 8.3D) and a small number of formulations were kept as stable nano-emulsion. The dispersibility behavior after 48h was similar in the presence or absence of Resveratrol for most of the formulations. However, formulations with high Resveratrol loading showed some precipitation after 48h.

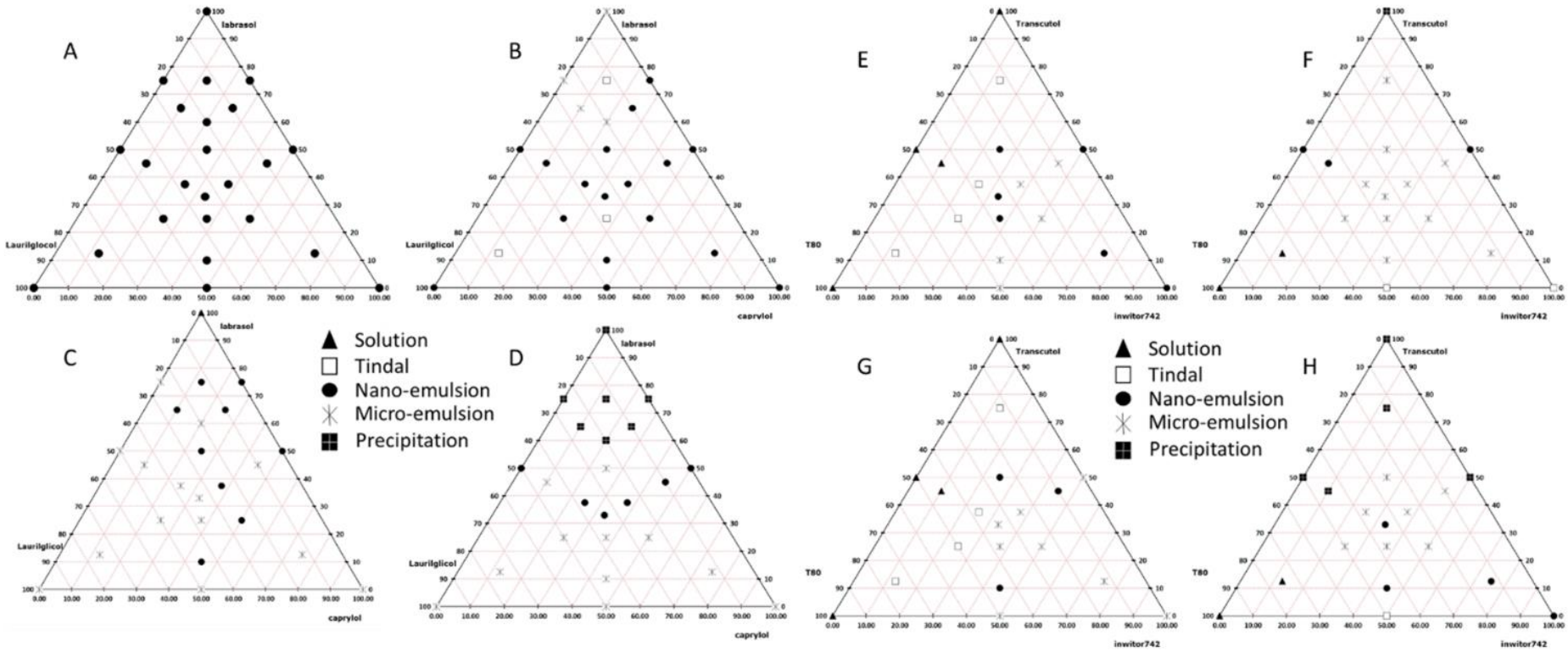

Figure 8-3 Dispersibility and robustness to dilution of two ternary compositions: Lau/Lab/Cap formulations dispersibility and robustness to dilution without (A, C) and with (B, D) Resveratrol, respectively; and T80/Trans/Imw formulations dispersibility and robustness to dilution without (E, G) and with (F, H) Resveratrol, respectively. Dispersibility (A, B, E and F) was classified in four grades, based on time to disperse and appearance after dispersion. Formulations were categorized as: (i) Solutions if forming a single liquid phase; (ii) Tindal if forming an emulsion in less than 1 min and featured clear bluish appearance; (iii) Nano-emulsions if forming slightly less clear emulsion having a bluish white appearance; and (iv) Micro-emulsions if forming bright white emulsion (similar to milk in appearance). Robustness to dilution (C, D, G, and H) included an additional classification, precipitation, when crystalline material was precipitated.

8.3.3.2. Tween® 80/ Transcutol®/ Imwitor® 742

Nineteen formulations were prepared based on these three components. Among these, formulations without Resveratrol and presenting a high content of Trans or its association with T80 formed clear solutions after dispersion (Figure 8.3E). However, Imw increment resulted in the formation of emulsions with larger droplet size based on a visual observation as described by Singh *et al* [354]. Most of the formulations dispersed as micro-emulsion when Resveratrol was included (Figure 8.3F). Formulations with T80 at a level above or equal to 75% dispersed as solutions, while the formulation with 100% Trans precipitated, most likely due to its very high drug loading level.

At 48h after dispersions (Figure 8.3G and F), most of the formulations without Resveratrol presented the same initial appearance. Most of the loaded formulations showed a similar behavior, even if an increased number of formulations presented signs of precipitation (Figure 8.3F).

8.3.4. Droplet size and SSA

The droplet size of the formulation was considered as the one measured after 240 seconds of dispersion. Also, SSA was retrieved in the same analysis at the same time point. Resveratrol powder used to prepare these formulations showed a particle size of D_{10} of 9.7 µm, D_{50} of 24.2 µm and a D_{90} of 52.2 µm and a SSA of 0.324 m^2/Kg.

8.3.4.1. Lauroglycol® 90/ Labrasol®/ Capryol®

The average droplet size (D_{50}) of the twenty-four Lau/Lab/Cap formulations ranged from close to 200 nm to above 34 µm (Figure 8.4A). Nevertheless, most of the formulations dispersed as nano-emulsions (D_{50} < 500 nm) or small droplet micro-emulsions (D_{50} < 5µm). Generally, droplet size decreased when the three components were present and with the increase of Lab content. The same was observed for D_{90} (Figure 8.4B), which was for most of the formulations below 10 µm.

SSA values for most formulations were in the range of 20-40 m^2/Kg (Figure 8.4C), reflecting that the whole droplet population was composed by small droplets. This was a considerable improvement compared to the pure Resveratrol powder. Only the formulations composed of Lau/Lab/Cap (50/0/50) showed SSA comparable to the powder.

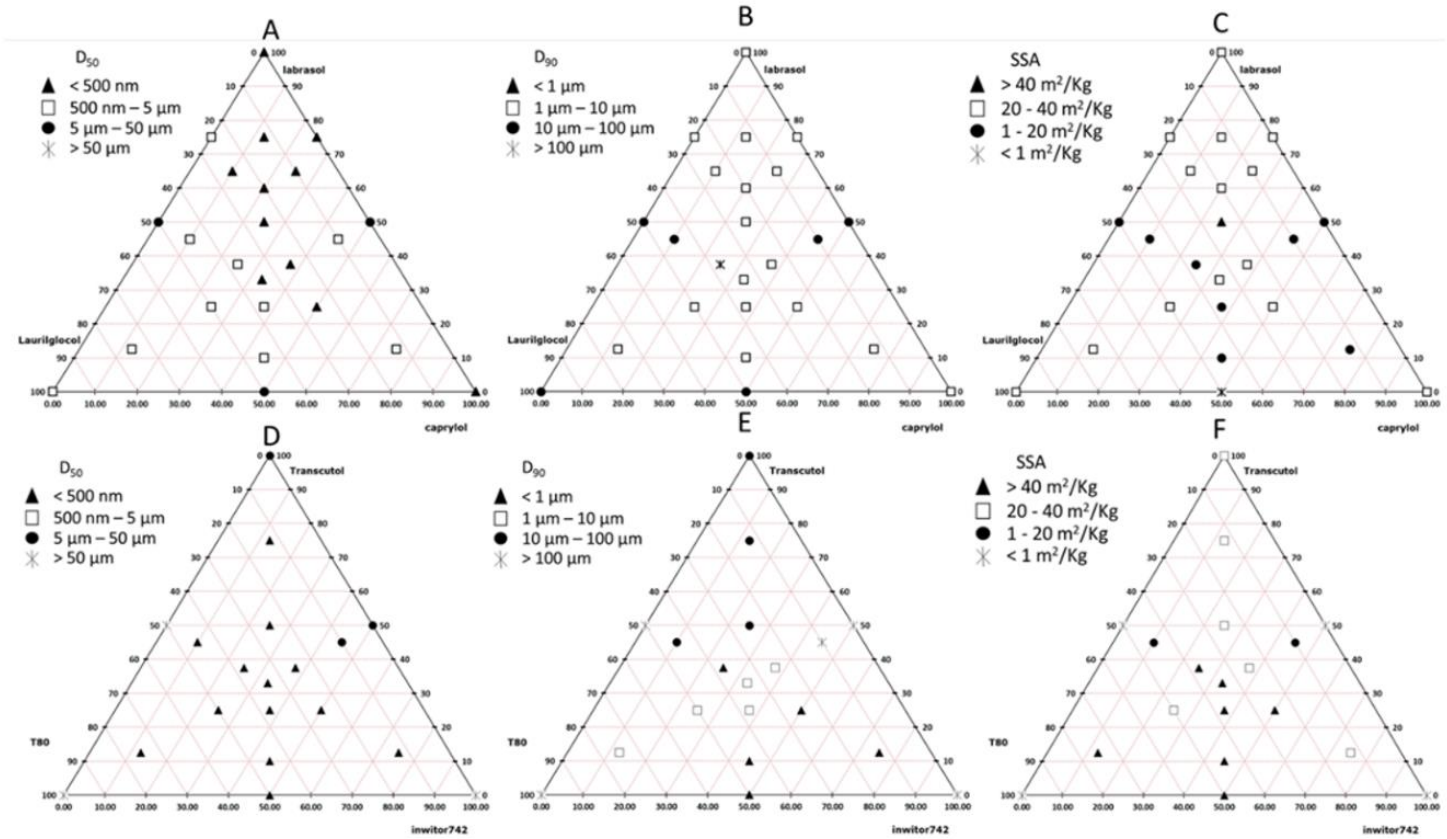

Figure 8-4 Droplet characteristics (D_{50}, D_{90} and SSA) for formulations Lau/Lab/Cap (A, B and C) and formulations T80/Trans/Imw (D, E and F). Droplet size of emulsified formulations was classified for D_{50} (A and D) in four classes: < 500 nm; 500 nm to 5 µm; 5 µm to 50 µm; and > 50 µm. With regards to D_{90} (B and E) classes were: < 1µm; 1µm to 10 µm; 10 µm to 100 µm; and > 100 µm. SSA was also evaluated (C and F) and formulations were grouped in the following classes: < 1 m^2/Kg; 1 m^2/Kg to 20m^2/Kg; 20 m^2/Kg to 40 m^2/Kg; and > 40 m^2/Kg.Tween® 80/ Transcutol®/ Imwitor® 742

The nineteen formulations composed of T80/Trans/Imw presented smaller droplet size than formulations with Lau/Lab/Cap (Figure 8.4), validating the qualitative observations of the dispersibility studies.

Average droplet size (D_{50}) and D_{90} ranged from around 100 nm to over 100 µm and 200 nm to over 200 µm, respectively, revealing that composition played an important role in the droplet size (Figure 8.4D) of SEDDS. Despite the large range of droplet size values, most of the formulations emulsified as nano-emulsions (D_{50} < 500 nm).

Overall, smaller droplet size was achieved when the three components were present in the formulation. Among these, a content in Trans above or equal to 50% presented a negative impact in the droplet size by forming larger droplets, which was more evident at D_{90} (Figure 8.4E).

Furthermore, most of the formulations presented above 100-fold increase in SSA over Resveratrol powder (Figure 8.4F).

8.3.5. Selection of formulations

Formulations were ranked based on their dispersibility, robustness to dilution, loading, droplet size (D50) and SSA. Each of those parameters were classified from one to four based on their performance and the total score was depicted in Figure 8.5.

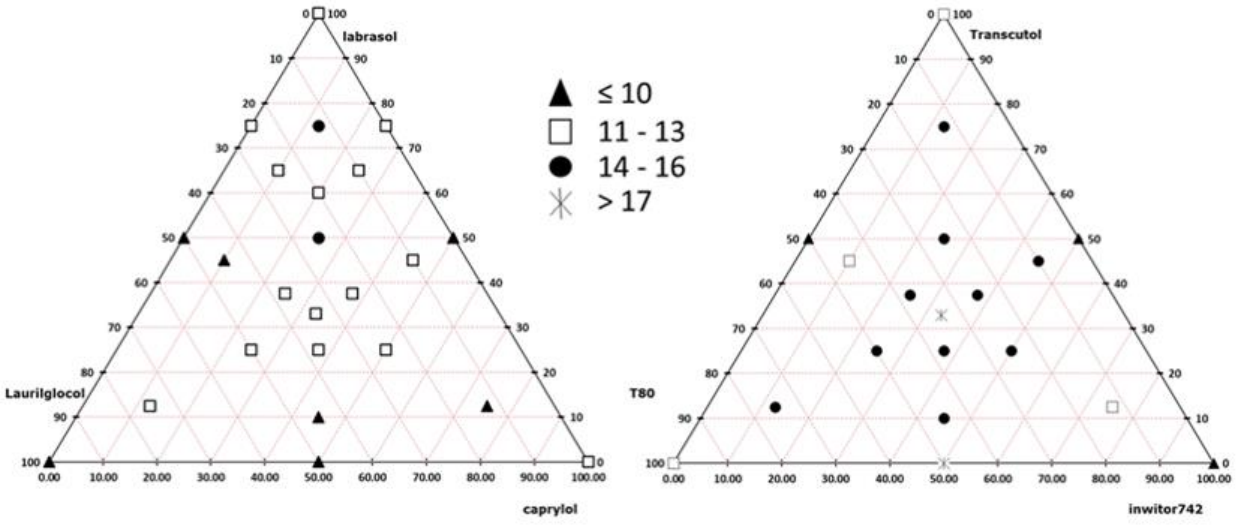

Figure 8-5 Formulations ranking accordingly to dispersibility, robustness to dilution, loading, droplet size (D_{50}) and SSA. Higher values denote better performance of the formulation.

Formulations for each set of ternary mixtures were ranked in four different classes. In the case of Lau/Lab/Cap, formulations composed of 12.5/75/12.5 and 25/50/25 were the best performers. The one compose of 12.5/75/12.5 was selected for further studies due to its higher loading. In the case of T80/Trans/Imw, formulations with 50/0/50 and 33/33/33 were the top ranked. Again, the formulation composed of 33/33/33 was selected based on its higher loading.

Both selected formulations presented a solubility increase over pure drug (>3000 folds) that was higher than previously described by Bolko *et al* that developed a formulation composed of castor oil, Capmul® MCM and Cremophor® EL/RH40/RH 60 that showed only 25-fold increase [409].

8.3.6. Dispersion characterisation of selected formulations

One batch of each of the previously selected formulations was prepared at a dose of 100 mg/mL and subjected to emulsification characterisation according to the methodology previously described by our group [402].

Formulation T80/Trans/Imw was a typical fast emulsifier, forming a nano-emulsion in less than one minute that was stable under mild stress conditions. Moreover, when high stress conditions were applied, droplet size increased most probably due to foam formation since this effect was only observed on the last third period of the high stress conditions period. During the resting phase, droplet size returned to its stable nano-emulsion form after a certain period. Additionally, D_{10}, D_{50} and D_{90} were equally affected during emulsification, stress and resting phases (Figure 8.6). Conversely, Lau/Lab/Cap was classified as a moderately slow emulsifier that after forming a stable nano-emulsion showed a sustained decrease in droplet size when subjected to high stress condition. However, this effect was not reverted during resting phase.

SSA in both selected formulations denoted the same described behavior ascertained by dynamic droplet size analysis. Values increased over time and phase in formulation Lau/Lab/Cap and varied between phases in formulation T80/Trans/Imw. However, at the end of dispersion and resting phases the formulation T80/Trans/Imw presented higher SSA than formulation Lau/Lab/Cap.

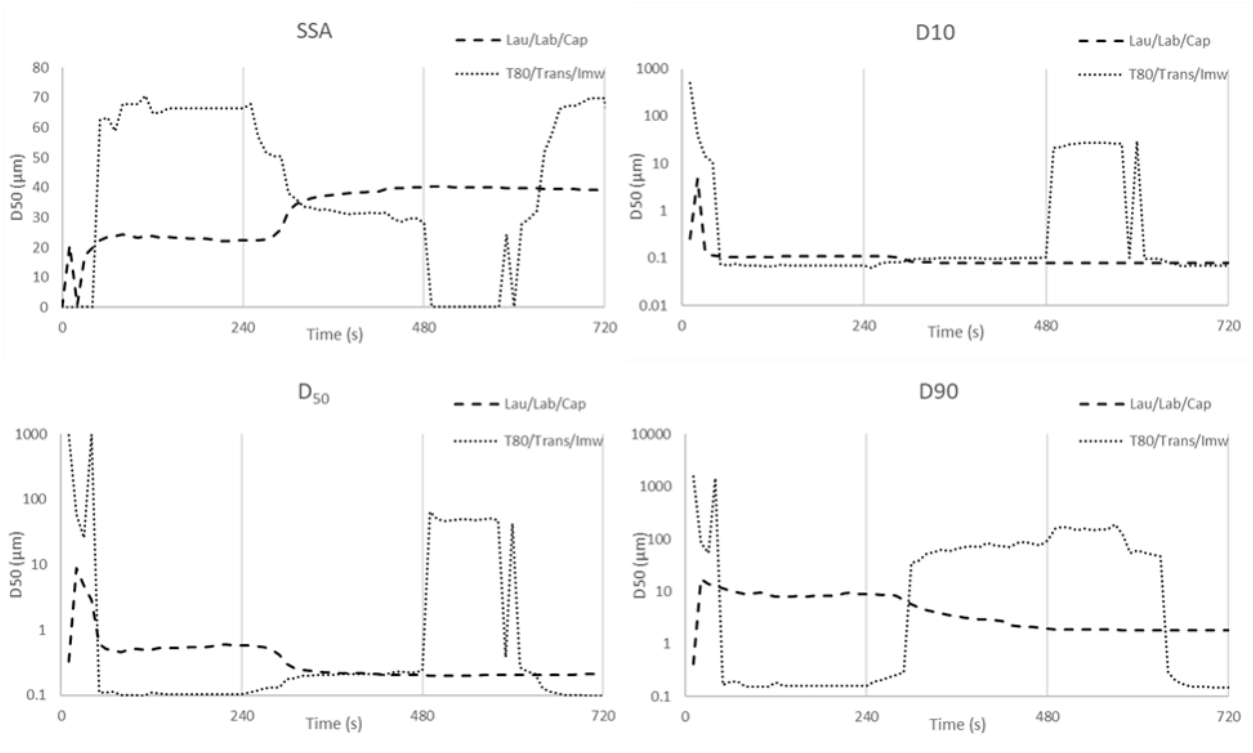

Figure 8-6 Dispersion characterization of selected Lau/Lab/Cap and T80/Trans/Imw formulations. Formulations were characterised for dispersion. The first segment of 240 seconds represented a standard self-emulsifying process. In second segment (240s to 480s) formulations were submitted to very high physical stress. In last segment (480s -720s), formulations were allowed to rest.

8.3.7. Permeability studies

Permeability studies were conducted from apical to basal (A-B) and from basal to apical side (B-A) (Figures 8.7 and 8.8, respectively) using the Caco-2 cell monolayer model. The combined amount of Resveratrol recovered from apical, cellular and basolateral compartments after adding formulations and free Resveratrol into the apical side was below 50%, suggesting that Resveratrol metabolisation/degradation was very intense and occurred rapidly. This effect is in line with previous reports [338, 410], which noted a reduction in Resveratrol transport at longer times points of incubation (more than one hour). Sulfation and, to a minor extent, glucuronidation are the major metabolisation pathways of Resveratrol in Caco-2 cells [338]. Control formulation presented a Resveratrol recovery of 10%, Lau/Lab/Cap SEDDS of 18% (p<0.05) and T80/Trans/Imw of 21% (p<0.05), suggesting that these formulations may be able to reduce metabolisation and/or degradation of Resveratrol. Moreover, from all the recovered fractions, the permeated fraction

corresponded to 76% in the control formulation, 78% in the T80/Trans/Imw formulation and 92% in the Lau/Lab/Cap formulation, suggesting that Lau/Lab/Cap formulation was the least influenced by efflux mechanisms.

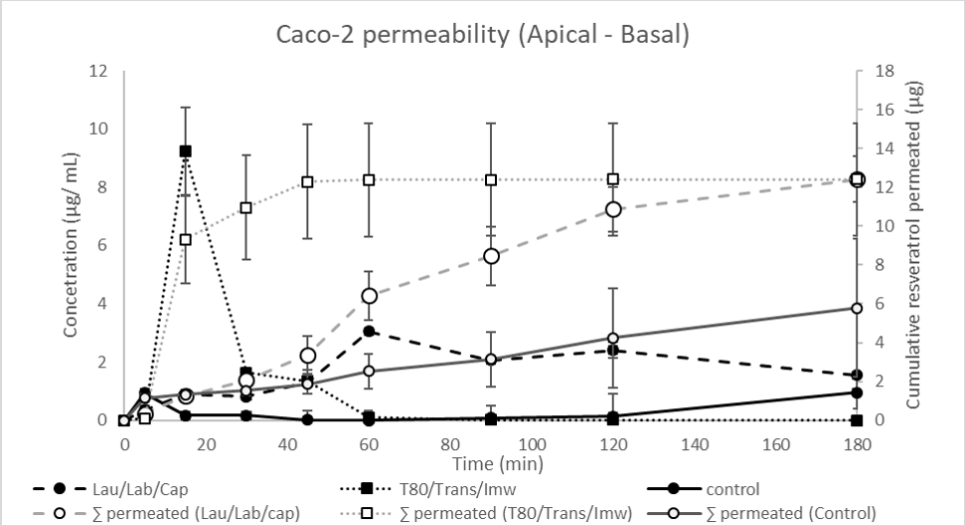

Figure 8-7 Permeability of Resveratrol across Caco-2 cell monolayers from the apical to the basal compartments (A), and from the basal to the apical compartments (B). Results are presented as mean ± SD (*n*=3). Cumulative Resveratrol permeated over time is also presented as mean values. (#) and (%) denote that formulations Lau/Lab/Cap and T80/Trans/Imw are significantly different from control, respectively (*p*<0.05). ($) denotes that formulation T80/Trans/Imw is significantly different from Lau/Lab/Cap (*p*<0.05).

When Resveratrol was applied in the basal compartment, the P_{app} value was significantly reduced for all formulations (Table 8.2), which is in line with the described by Kaldas *et al* [338] and Seljak *et al* [404]. The permeability kinetics of all formulations was comparable to the one observed when free Resveratrol was placed in the apical compartment. In the case of the control, slow but steady permeation was observed in opposition to T80/Trans/Imw formulation that showed a fast and intense permeation, reaching maximum permeability at 15 min. One hour after the start of the experiment, permeability reached a plateau. However, Lau/Lab/Cap formulation appeared to promote sustained permeability, which was higher than the control formulation. These data can be justified by the fast emulsifying characteristics of T80/Trans/Imw and slow emulsifying properties of Lau/Lab/Cap.

The fractions recovered when Resveratrol was applied in the basolateral compartment were similar for SEDDS and two-fold higher than for control group. The fractions recovered in the donor compartment were the most representative in control formulation (83%) and T80/Trans/Imw (82%), showing an increase of around 4-fold and

indicating that drug was not permeating or was being subject to efflux mechanisms. In the case of Lau/Lab/Cap, the fraction recovered in the donor compartment was only 16%. Nevertheless, this was a ten-fold increase over the fraction determined when it was applied in the apical compartment. This data associated to the fact that the P_{app} value was much lower when Resveratrol was applied in the basolateral compartment suggests that efflux mechanisms may be involved, as described by Shirasaka *et al* [336], namely via Multidrug Resistance-associated Protein type 3 (MRP3) and P-glycoprotein (P-gp) [338, 404]. Overall, it is speculated that formulation Lau/Lab/Cap may have inhibited efflux mechanisms as observed by Seljak *et al* by using 20% each of Capmul® MCM and castor oil; 30% each of Kolliphor® EL and Kolliphor® RH40 [404].

TEER values of control, Lau/Lab/Cap and T80/Trans/Imw formulations in the last time point were 86%, 104% and 83% of initial values in the apical to basolateral study and 76%, 118% and 84%, respectively in the basolateral to apical study. These data support that cell monolayers remained intact until the end of the experiment and in this way, the permeability results reflect drug transport across a membrane-like barrier.

Table 8-2. Values of P_{app} for Resveratrol when tested from apical to basal or basal to apical compartments. (*) and (#) denote significant differences as compared to control or between SEDDS formulations, respectively (p<0.05).

Formulation	P_{app}* (Apical-Basal) (cm/s)	P_{app}* (Basal-Apical) (cm/s)	Ratio (A-B/B-A)
Control	2.3 x10^{-6}	96 x10^{-6}	2.4
Lau/Lab/Cap	4.9 x10^{-6*}	1.3 x$10^{-6*/\#}$	3.7
T80/Trans/Imw	4.9 x10^{-6*}	56 x10^{-6}	8.8

8.3.8. Pharmacokinetics studies

The pharmacokinetics data after the oral administration of Resveratrol (100mg/kg) to rats using three different formulations are depicted in Table 8.3 and Figure 8.8. In the control formulation, Resveratrol reached a maximum plasmatic concentration (C_{max}) of 202 ± 114 ng/mL within 2 h before falling back to residual levels over the next 7 h. The area under the curve (AUC_{0-t}) obtained for Resveratrol was 827.2 ± 233 ng.h/mL. Both Lau/Lab/Cap and T80/Trans/Imw formulations reached maximal drug concentrations earlier than in the control group, namely within 30 min. This suggests that Resveratrol is promptly absorbed when formulated in developed SEDDS. This can be justified by the liquid state and small droplet

size of these formulations. The Lau/Lab/Cap formulation further showed higher rate of absorption with a C_{max} value that was approximately 2-fold higher than that of the control formulation. However, Resveratrol exposure (AUC_{0-t}) was similar to the control group. The obtained C_{max} value for the T80/Trans/Imw formulation was similar to the control but the AUC_{0-t} was approximately two-fold lower, thus suggesting that Resveratrol formulated in T80/Trans/Imw is absorbed to a lower extent. Still, there is also the possibility that, due to its fast emulsifying properties and small droplet size (100 nm), the T80/Trans/Imw formulation leads to very fast absorption of Resveratrol (in less than 30 minutes). In such case, the actual C_{max} may have been observed earlier than the first time point considered in this study.

Table 8-3. Pharmacokinetic parameters of all formulations. Results are presented as mean ± SD (*n*=5). (*) denote significant differences as compared to control (*p*<0.05).

Formulation	C_{max} (ng/mL)	T_{max}(h)	AUC_{0-t} (ng*h/mL)
Control	202 ± 114	2.0	827 ± 233
Lau/Lab/Cap	405 ± 140	0.5 *	832 ± 194
T80/Trans/Imw	199 ± 137	0.5 *	425 ±118

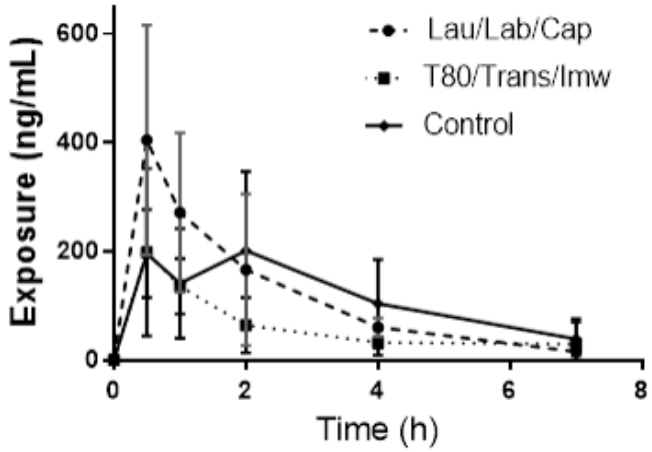

Figure 8-8 Pharmacokinetics profiles of Resveratrol after oral administration of control, Lau/Lab/Cap and T80/Trans/Imw formulations. Data presented as mean ± SD (*n*=5).

Batches used in pharmacokinetics studies were also characterized regarding assay and droplet/particle size (Table 8.4). Droplet size values were in line with those obtained in the development phase and their distribution can be observed in Fig. 8.9.

Table 8-4. Physical-chemical characterization of all formulations. Particle size measurements were performed in triplicate. (*) and (#) denote significant differences as compared to control or between SEDDS formulations, respectively (p<0.05).

Formulation	Assay (%)	D_{10}(µm)	D_{50} (µm)	D_{90} (µm)
Control	99.5	9.870	26.455	60.844
Lau/Lab/Cap	96.2	0.111*	0.578*	8.817*
T80/Trans/Imw	93.7	0.071*	0.104 */#	0.157 */#

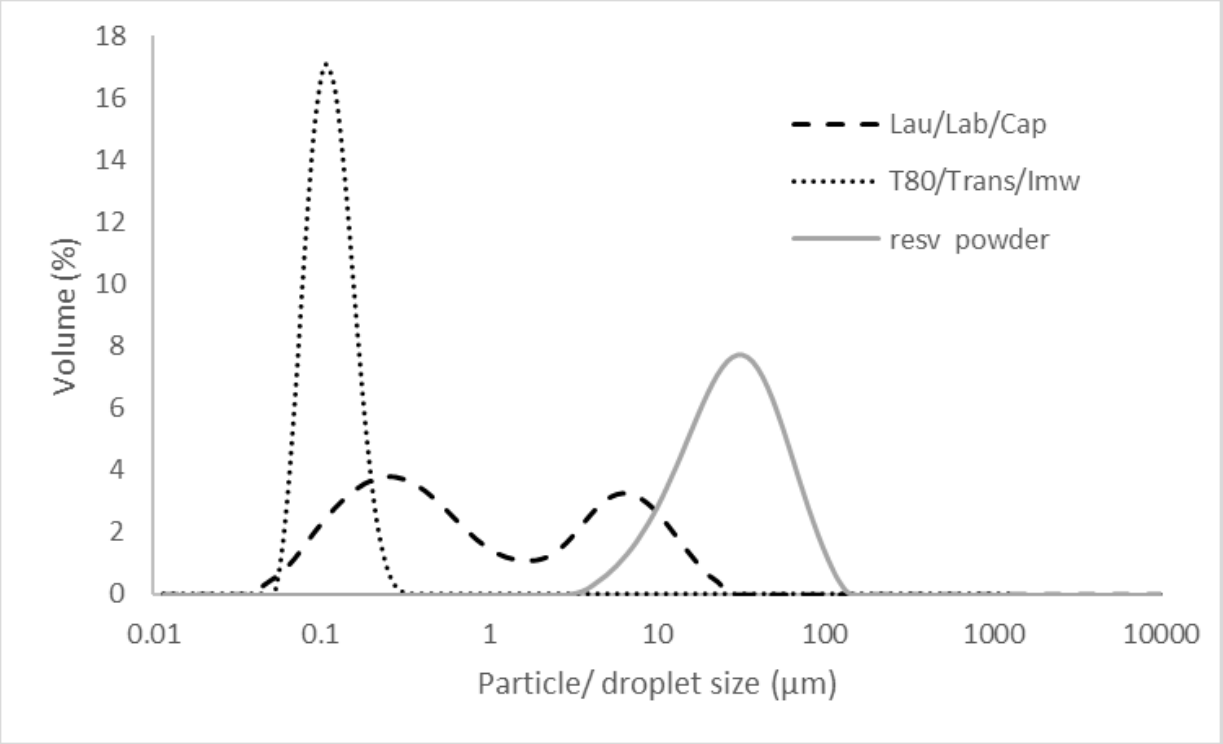

Figure 8-9 Pharmacokinetics profiles of Resveratrol after oral administration of control, Lau/Lab/Cap and T80/Trans/Imw formulations. Data presented as mean ± SD (n=5).

It is well established [7] that SEDDS should be able to quickly emulsify and keep a stable emulsion with small droplet size. In this study, the quantitative composition of Lau/Lab/Cap and T80/Trans/Imw ternary formulations was shown to highly impact the emulsification process, droplet size, emulsion stability and loading. The proposed development process allowed the selection of two candidate formulations with high drug loading capacity (over 100 mg/mL of Resveratrol) and that quickly disperse in water, forming nano-emulsions. These high drug loading, small droplet sized formulations were expected to provide higher and faster absorption due to the high SSA of contact between Resveratrol

incorporated into the formulation and permeation surface [411]. Caco-2 cell monolayer permeability studies were successful in demonstrating that both SEDDS formulations were able to increase the amount of drug permeation, as well as – possibly – reduce the amount of drug metabolized or subject to efflux, thus confirming our hypothesis. Reduction in drug metabolisation and inhibition of efflux mechanisms by proposed SEDDS need further confirmation but could potentially be attributed to formulation components that have possibly inhibited degradation mechanisms. T80 [52] and Lab [412] were previously described as reducing intestinal drug metabolisation. Moreover, the small droplet size could also allow the permeation of intact droplets through paracellular or transcellular mechanisms and, therefore, avoid degradation mechanisms [346, 413]. The small droplet size and the efflux mechanisms inhibition were also recognized to be responsible for the observed increase in permeability.

The T80/Trans/Imw formulation presenting more than 90% of droplets with a size below 160 nm showed high and fast permeability. After 15 minutes, more than 70% of the total Resveratrol permeation occurred. T80 is known to be BCRP (Breast Cancer Resistance Protein) and MRP inhibitor, Imw a P-gp inhibitor, and Trans a MRP inhibitor [52]. Therefore, the small droplet size as well as the high efflux inhibition of this formulation could justify the fast and intense permeability that then could have been followed by degradation/metabolisation since Resveratrol was no longer detected after 60 min.

Since the formulation composed of Lau/Lab/Cap presented larger droplet size than the one featuring T80/Trans/Imw, permeation through paracellular mechanisms may have been harder and consequently a slower and lesser intense permeability over time was observed. However, at the end of permeability studies, both Lau/Lab/Cap and T80/Trans/Imw formulations exhibited similar levels of Resveratrol permeated, which were around two-fold higher than values observed with the control formulation. Moreover, since the Lau/Lab/Cap formulation was significantly less affected by the basal-apical versus apical-basal permeability it may be assumed that efflux mechanisms could have been affected [338, 404]. It should be highlighted that Resveratrol in the control formulation was already in solution and in the presence of a permeation enhancer (DMSO). Furthermore, the Lau/Lab/Cap formulation may have also contributed to a reduction in metabolisation/degradation. Regarding its individual components, Lab is the only excipient known to be able to inhibit glucuronidation [412] and P-gp efflux mechanisms [120] and it represented 75% of the formulation.

In the pharmacokinetics studies, Resveratrol suspension (control) showed a secondary peak in its pharmacokinetic profile, thus suggesting entero-hepatic recirculation as observed and described by Marier *et al* [340]. The observed AUC_{0-t} and C_{max} for the

control group was eight and four times higher than that observed by Branton and Snehasis in male Sprague Dawley rats [341] using the same dose. The AUC_{0-t} value obtained in our study was similar to the ones observed by Zhou *et al* [412] when using 10 mg/kg (10 fold lower) in male Wistar rats, and Yen *et al* [405] when using 50 mg/kg in male Sprague Dawley rats. These data suggest that Resveratrol exposure is highly dependent on species and group of animals. Therefore, comparison between different studies should be made with caution. Moreover, our control group provided a relatively higher exposure than previously described studies which could have further contributed to the relative lower differences observed when comparing to data from SEDDS formulations.

The pharmacokinetic profile following administration of SEDDS formulations did not show any secondary peaks, suggesting that entero-hepatic recirculation may have not occurred, thus consequently affecting in a negative way the total exposure to Resveratrol. Based on the available pharmacokinetics profile where T_{max} was the first timepoint (0.5h) studied, associated to the permeability studies and droplet size, it can be speculated that the actual C_{max} of SEDDS formulations, particularly for the T80/Trans/Imw formulation, was not observed and therefore total exposure could have been underestimated. Nevertheless, a two-fold increase in C_{max} was still observed for Lau/Lab/Cap formulation, which can be a relevant advantage particularly for CNS therapeutic indications, such as Parkinson and Alzheimer diseases that require a blood brain barrier permeability (BBB), where an increase in C_{max} may improve brain exposure [407].

8.4. Conclusions

In this work, SEDDS were rationally developed with the intention of increasing the oral bioavailability of Resveratrol and potentially contribute to its long time sought translation into clinical use.

I. General Discussion and Conclusions

Resveratrol is a natural nonflavonoid polyphenol found in numerous plant species, particularly in grapes, blueberries, and peanuts [414]. Resveratrol consists of two aromatic rings that are connected through a methylenic bridge. It occurs as two geometrical isomers: trans-Resveratrol and the cis form. Trans-Resveratrol presents the greater stability and biological activity and the second is less active. Cis-Resveratrol is formed by isomerisation of the trans-form following the breakdown of the Resveratrol due to the action of UV light or under high pH conditions [415].

While several studies reported that Resveratrol possesses health beneficial effects, it displays uncommon pharmacokinetic characteristics that limit its use. Resveratrol presents poor water solubility, is extensively metabolized and rapidly eliminated displaying consequently a poor bioavailability [410, 416]. After oral administration, in the intestine, Resveratrol undergoes a presystemic metabolism through glucuronidation and sulfate conjugation of the phenolic groups and hydrogenation of the aliphatic double bond. The remaining fraction is absorbed at the intestinal level by passive diffusion or by membrane transporters [417]. In circulation, Resveratrol mainly occurs associated to albumin and lipoproteins and undergoes Phase II metabolism in the liver [418]. In addition, Resveratrol metabolites undergo enterohepatic recirculation, which allows its deconjugation in the small intestine and reabsorption [340].

Considering the challenges presented above, the current thesis intended to develop a drug delivery system able to improve Resveratrol bioavailability. Two different strategies were explored in parallel: third generation solid dispersion and SEDDS. Both strategies started by a high-throughput screening of Resveratrol solubility in a large number of excipients. Resveratrol solubility was accessed in twenty-two lipidic excipients with hydrophilic-lipophilic balance (HLB) value ranging from 1 to 18 and used in SEDDS, and in fourteen excipients (carriers), from the major groups of hydrophilic carriers with potential to be used in solid dispersions. The later was not assessed directly in the carriers due to its solid state, alternatively water solutions containing 5% of each carrier were used.

Generally, Resveratrol solubility was significantly enhanced in the presence of carriers and SEDDS excipients tested. This was particularly evident for Labrasol®, Transcutol®, Kolliphor® EL, RH40 and HS15, as SEDDS excipients examples, and Soluplus® and T80, as carriers which showed an enhancement higher than 2000 folds. In the opposite side, Kollisolv® PEG400, although showed an improvement of 50-fold, was the less effective excipient used in SEDDS and Eudragit RLPO and both HPMCASs were the only carriers that did not significantly improved Resveratrol solubility under tested conditions.

From the above a series of carriers and SEDDS excipients were selected for further studies in each development streaming.

In the third-generation solid dispersion approach, a total of forty-five solid dispersions using nine different carriers with five Resveratrol to polymer ratios were prepared to select a carrier to be used to amorphize Resveratrol. The carrier selection was based on FTIR and solubility data. From FTIR data, Resveratrol OH stretching peak positions (lower peak position corresponds to stronger hydrogen bonding) in Resveratrol: polymer dispersions together with carbonyl region provided evidence for the formation of hydrogen bonds between polymers and Resveratrol. Additionally, some pi interactions between Resveratrol aromatic rings were present for some excipients. This evidence was in line with the previously described for Resveratrol drug delivery by Wegiel *et al* [419] that was able to predict amorphous loading level of Resveratrol based on FTIR interactions and by Aloisio *et al* [420] that reported changes corresponding to the vibration of the aromatic ring of Resveratrol (1509 cm-1) and the signal of the O-H bond vibration as the most evident changes in FTIR data. The solubility data from the forty-five solid dispersions indicate that carrier type as well as Resveratrol:carrier ratio were crucial for Resveratrol amorphisation. Therefore, Soluplus®, which presented the highest Resveratrol solubility improvement during screening, demonstrated molecular interaction observed by FTIR and a significant but small improvement in solubility when solid dispersions were prepared by solvent cast, was selected as carrier. The optimum Resveratrol: Soluplus® ratio was defined based on DSC data as 1:2. This was the highest Resveratrol loading formulation showing Resveratrol fully amorphous. Poloxamer 407 and Gelucire®, which are surfactant with some potential to influence efflux transport and intestinal metabolism [52], were explored at 5% and 15% to generate a third-generation solid dispersion.

In parallel, two sets of three excipients were selected to be formulated as SEDDS, based on the solubility screening data. One excipient with HLB above 10 and another below 6 were selected for each set. The third component was selected from co-solvents and/or excipients with HLB 6-10. Therefore, set 1 was composed by Lau/Lab/Cap and set 2 by T80/Trans/Imw. These two sets of SEDDS compositions, in a total of forty-three formulations, were further characterised regarding loading, which ranged from 22 to 226 mg/mL. Dispersibility studies revealed solutions, micro and nano-emulsions, tindal and precipitated formulations that presented droplet size (D50) ranging from 100 nm to above 100 µm and with a SSA lower 1 m^2/Kg to more than 40 m^2/Kg. Generally, formulations composed by T80/Trans/Imw presented smaller droplet size than formulations with Lau/Lab/Cap. Formulations were ranked based on their dispersibility, robustness to dilution, loading, droplet size (D50) and SSA. In each set of formulations, two formulations were

ranked in a higher class. Thus, Lau/Lab/Cap formulations composed by 12.5/75/12.5 and 25/50/25 were the best performers. From these the one composed by 12.5/75/12.5 was selected for further studies due to its higher loading. In case of T80/Trans/Imw, formulations with 50/0/50 and 33/33/33 were the top ranked. Equally to the previous group, formulation composed by 33/33/33 was selected based on its higher loading. Selected formulations from solid dispersion and SEDDS approaches were subjected to permeability studies. Combined results are presented in Table 9.1.

Table 8-1. P_{app} of all formulations of Resveratrol apical to basal and basal to apical applications.

Formulation	$P_{app\ (Apical\text{-}Basal)}$ (cm/s)	$P_{app\ (Basal\text{-}Apical)}$ (cm/s)	Ratio (A-B/B-A)
RES	2.3×10^{-06}	9.6×10^{-07}	2.4
Lau/Lab/Cap	4.9×10^{-06}	1.3×10^{-06}	3.7
T80/Trans/Imw	4.9×10^{-06}	5.6×10^{-07}	8.8
RES:Sol (1:2)	4.2×10^{-6}	5.9×10^{-6}	0.70
RES:Sol (1:2) GEL 15%	8.8×10^{-6}	10.0×10^{-6}	0.88
RES:Sol (1:2) POL 15%	8.2×10^{-6}	7.7×10^{-6}	1.07

RES – Resveratrol; Lau/Lab/cap - Lauroglycol® 90/ Labrasol®/ Capryol® (12.5/75/12.5); T80/Trans/Imw - Tween® 80/ Transcutol®/ Imwitor® 742 (33/33/33); Sol – Soluplus ®; POL – poloxamer 407; GEL – Gelucire®; (A-B/B-A) – Apical to Basal/ Basal to Apical

SEDDS formulations and second-generation solid dispersion (RES:Sol (1:2)) presented a 2-fold increase in permeability over pure Resveratrol. Both third generation solid dispersions showed a 2-fold increase in permeability over SEDDS and second-generation solid dispersion and 4-fold over pure Resveratrol. Permeability of all solid dispersions was minimally affected by its application in basolateral side, but SEDDS and pure Resveratrol were highly affected. These data suggest that solid dispersion may be more effective in inhibiting efflux mechanisms or that the extra dissolution step in this formulation display a more sustained Resveratrol concentration in the test medium than solution, as observed by Das *et al* [421] in an animal study.

The permeability kinetics was also different among formulations. T80/Trans/Imw formulation showed a fast and intense permeation with a maximum permeability at 15 min

and after sixty minutes no more permeability was observed. Differently, free Resveratrol, Lau/Lab/Cap formulation and the three solid dispersion formulations showed a slow, but constant, permeation over time.

The fraction of Resveratrol recovered in the sum of apical, cellular and basolateral compartments after adding formulation and free Resveratrol into the apical side was generally below 50%, suggesting that Resveratrol metabolisation/ degradation was very intense and occurred rapidly. Pure Resveratrol presented a recovery of 10%, Lau/Lab/Cap SEDDS of 18%, T80/Trans/Imw and Resveratrol:Soluplus® (1:2) solid dispersion of 21%, RES:Sol (1:2) POL solid dispersion of 30 % and RES:Sol (1:2) GEL solid dispersion of 54%. These data suggest that all formulations may be able to reduce Resveratrol metabolisation and/or degradation. Solid dispersions appear to have lower metabolisation which can be related to its components properties but also by the fact that in these formulations drug release is occurring at the same time of permeability and the formulation can act as a reservoir, which can potentiate and extend over time the permeability and consequently, (artificially) reducing drug degradation. This data is in line with the previously described by Maier *et al* [339], that concluded by inhibiting Resveratrol biotransformation, a significant increase of its permeability in Caco-2 cells was observed.

Altogether, four formulation, two SEDDS and two solid dispersions, plus pure Resveratrol (micronized) as control were tested *in vivo* for pharmacokinetic profile. All test formulations presented a T_{max} at 0.5h and since T_{max} was the first time point and due to the nature of the formulations, a real T_{max} may have occurred earlier than 30 minutes, as observed by Chang *et al* [422]. Micronized Resveratrol presented a T_{max} of 2 hours and a secondary peak corresponding to entero-hepatic recirculation as observed and described by Marier *et al* [340] and Das *et al* [421]. All study formulations did not show secondary peaks, meaning that no entero-hepatic recirculation occurred.

When comparing all studies, SEDDS Lau/Lab/Cap and T80/Trans/Imw that were able to quickly emulsify and keep a stable emulsion with a small droplet size showed a high and faster absorption due to a very high SSA of contact between the formulation and permeation surface [411]. Moreover, the metabolic reduction could be speculated and attributed to T80 [52] and/ or Lab [412]. Formulation T80/Trans/Imw that presented more than 90% of droplets with a size below 160 nm showed high and fast permeability in Caco-2 cells and therefore a real C_{max} could not have been seen in rat PK and consequently no advantage over micronized Resveratrol was observed. Formulation composed by Lau/Lab/Cap presented larger droplet size than T80/Trans/Imw and therefore permeation through paracellular mechanisms was harder and consequently a slower and lesser intense permeability over time was observed in Caco-2 cells. Due to this slower absorption, it can

be speculated that a real T_{max} was observed, which was 2-fold higher C_{max} when compared to micronized Resveratrol, but not AUC, which is in line with the described by Das *et al* [421] that increased C_{max} but not AUC when used a solution versus Resveratrol suspension.

Nevertheless, a two-fold increase in C_{max} was still observed for Lau/Lab/Cap formulation, which can be a relevant advantage particularly for central nervous system therapeutic indications, such as Parkinson and Alzheimer diseases that require a blood brain barrier permeability, where an increase in C_{max} may improve brain exposure [407].

Curiously, both solid dispersions presented higher permeability in Caco-2 cells studies than SEDDS and micronized Resveratrol but lower PK parameters than these formulations. This may be attributed to its larger particle size which was 2 to 5-fold higher when compared to micronized Resveratrol. This large particle may have been the responsible for the slow but continuous permeability over time in Caco-2 cells model. *In vivo*, this slow release may have prevented a burst effect, and consequent large amount of Resveratrol in absorption window able to saturate degradation and efflux mechanism. Maier *et al* [339] concluded that efflux and/ or degradation mechanisms were either inhibited or saturated at 200 µM Resveratrol in Caco-2 cells, however, Das *et al* [421] concluded that this metabolic saturation is unlikely to be achievable at *in vivo* level at a dose of 50 mg/kg. This data is corroborated by the nonlinear pharmacokinetics observed by the previous study [421] between 15 and 50 mg/kg and Kapetanovic *et al* [423] between 50 and 150 mg/ kg. Therefore, slowing down Resveratrol release may facilitate a metabolic pathway. However, even in the absence of this burst effect the presence of poloxamer 407 was able to improve at least 2-fold C_{max} and AUC over the formulation without poloxamer, even presenting a much larger particle size and clearly indicating that poloxamer 407 is able to modulate intestinal metabolism and or efflux mechanisms.

All data indicate that is possible to improve Resveratrol bioavailability by increasing it solubility but mostly by reducing its metabolism and efflux mechanisms. In this thesis, SEDDS presented higher bioavailability than third generation solid dispersion and therefore are suggested as a better strategy to improve Resveratrol bioavailability. Additionally, depending on the indication it may be possible to increase C_{max} or AUC by “playing” with particle/droplet size and components ability to interfere with efflux and metabolism mechanisms.

One additional achievement of this thesis was the development of an analytical process able to observe the self-emulsification process occurring in SEDDS. The use of a continuous measurement and multiparameter evaluation showed to be a strong tool to understand the emulsification process and emulsion stability, allowing the differentiation of

SEDDS during these phases. Additionally, it was proposed to classify SEDDS regarding its emulsification process as slow or fast emulsifiers.

9. Future Perspectives

As future perspectives regarding the developed third-generation solid dispersion, it can be further optimised to present a faster release able to allow a burst effect that can inhibit efflux transport and metabolism mechanisms. Additionally, stability studies should be performed to understand long term behaviour of current formulation, particularly regarding its solid state and consequent release profile. Currently, this formulation is produced at laboratorial scale by rotavapor and should be scaled up by using, spray drying, freeze drying or hot-melt extrusion. The scale up process by using freeze drying or spray drying can also contribute to achieve a faster release profile. Scale-up solid dispersion can then be combined with further excipient to be converted into oral tablet.

Regarding self-emulsifying drug delivery strategy, further optimisation can be conducted aiming to sustain the pharmacokinetic profile of current formulation. Additionally, stability studies should be performed to understand its long-term stability particularity chemical stability. This formulation can be further, scaled-up in order to develop a softgel as final dosage form.

Resveratrol still is a very promising compound for multiple potential indications and therefore should be focus of adequate attention from Drug Delivery Sciences.

J. References

1. Youn YS, Jung JY, Oh SH, Yoo SD, Lee KC. Improved intestinal delivery of salmon calcitonin by Lys18-amine specific PEGylation: stability, permeability, pharmacokinetic behavior and *in vivo* hypocalcemic efficacy. Journal of Controlled Release 2006; 114:334-42.
2. Sugawara M, Kadomura S, He X, Takekuma Y, Kohri N, Miyazaki K. The use of an *in vitro* dissolution and absorption system to evaluate oral absorption of two weak bases in pH-independent controlled-release formulations. European Journal of Pharmaceutical Sciences 2005; 26:1-8.
3. Ikegami K, Tagawa K, Osawa T. Bioavailability and *in vivo* release behavior of controlled-release multiple-unit theophylline dosage forms in beagle dogs, cynomolgus monkeys, and göttingen minipigs. Journal of Pharmaceutical Sciences 2006; 95:1888-95.
4. Charman SA, Charman WN. Oral modified-release delivery systems. In: Rathbone MJ, Hadgraft J, Roberts M, editors. Modified-Release Drug Delivery Technology USA: Marcel Dekker; 2003, p. 1-10.
5. van Drooge DJ, Hinrichs WLJ, Visser MR, Frijlink HW. Characterization of the molecular distribution of drugs in glassy solid dispersions at the nano-meter scale, using differential scanning calorimetry and gravimetric water vapour sorption techniques. International Journal of Pharmaceutics 2006; 310:220-9.
6. Vippagunta SR, Wang Z, Hornung S, Krill SL. Factors affecting the formation of eutectic solid dispersions and their dissolution behavior. Journal of Pharmaceutical Sciences 2007; 96:294-304.
7. Pouton CW. Formulation of poorly water-soluble drugs for oral administration: physicochemical and physiological issues and the lipid formulation classification system. European Journal of Pharmaceutical Sciences 2006; 29:278-87.
8. Bogdanova S, Pajeva I, Nikolova P, Tsakovska I, Müller B. Interactions of poly(vinylpyrrolidone) with ibuprofen and naproxen: experimental and modeling studies. Pharmaceutical Research 2005; 22:806-15.
9. Streubel A, Siepmann J, Bodmeier R. Drug delivery to the upper small intestine window using gastroretentive technologies. Current Opinion in Pharmacology 2006; 6:501-8.
10. Desai J, Alexander K, Riga A. Characterization of polymeric dispersions of dimenhydrinate in ethyl cellulose for controlled release. International Journal of Pharmaceutics 2006; 308:115-23.
11. Silva P, Sureda A, Tur JA, Andreoletti P, Cherkaoui-Malki M, Latruffe N. How efficient is Resveratrol as an antioxidant of the mediterranean diet, towards alterations during the aging process? Free Radical Research 2019; 53:1101-12.
12. Xia N, Daiber A, Förstermann U, Li H. Antioxidant effects of Resveratrol in the cardiovascular system. British Journal of Pharmacology 2017; 174:1633-46.
13. Rauf A, Imran M, Butt MS, Nadeem M, Peters DG, Mubarak MS. Resveratrol as an anti-cancer agent: a review. Critical Reviews in Food Science and Nutrition 2018; 58:1428-47.
14. Ko JH, Sethi G, Um JY, Shanmugam MK, Arfuso F, Kumar AP, Bishayee A, Ahn KS. The role of Resveratrol in cancer therapy. International Journal of Molecular Sciences 2017; 18.

15. de Sá Coutinho D, Pacheco MT, Frozza RL, Bernardi A. Anti-inflammatory effects of Resveratrol: mechanistic insights. International Journal of Molecular Sciences 2018; 19.

16. Lançon A, Frazzi R, Latruffe N. Anti-Oxidant, Anti-inflammatory and anti-angiogenic properties of Resveratrol in ocular diseases. Molecules 2016; 21:304.

17. Bonnefont-Rousselot D. Resveratrol and cardiovascular diseases. Nutrients 2016; 8.

18. Vestergaard M, Ingmer H. Antibacterial and antifungal properties of Resveratrol. International Journal of Antimicrobial Agents 2019; 53:716-23.

19. Bostanghadiri N, Pormohammad A, Chirani AS, Pouriran R, Erfanimanesh S, Hashemi A. Comprehensive review on the antimicrobial potency of the plant polyphenol Resveratrol. Biomedicine & Pharmacotherapy 2017; 95:1588-95.

20. Li YR, Li S, Lin CC. Effect of Resveratrol and pterostilbene on aging and longevity. Biofactors 2018; 44:69-82.

21. Klimova B, Novotny M, Kuca K. Anti-aging drugs - prospect of longer life? Current Medicinal Chemistry 2018; 25:1946-53.

22. Kulashekar M, Stom SM, Peuler JD. Resveratrol's potential in the adjunctive management of cardiovascular disease, obesity, diabetes, Alzheimer disease, and cancer. Journal of the American Osteopathic Association 2018; 118:596-605.

23. Öztürk E, Arslan AKK, Yerer MB, Bishayee A. Resveratrol and diabetes: a critical review of clinical studies. Biomedicine & Pharmacotherapy 2017; 95:230-4.

24. Kim OY, Chung JY, Song J. Effect of Resveratrol on adipokines and myokines involved in fat browning: perspectives in healthy weight against obesity. Pharmacological Research 2019; 148:104411.

25. Gomes BAQ, Silva JPB, Romeiro CFR, Dos Santos SM, Rodrigues CA, Gonçalves PR, Sakai JT, Mendes PFS, Varela ELP, Monteiro MC. Neuroprotective mechanisms of Resveratrol in Alzheimer's disease: role of SIRT1. Oxidative Medicine and Cellular Longevity 2018; 2018:8152373.

26. Amro MS, Teoh SL, Norzana AG, Srijit D. The potential role of herbal products in the treatment of Parkinson's disease. Clinical Therapeutics 2018; 169:e23-e33.

27. Lai F, Schlich M, Pireddu R, Fadda AM, Sinico C. Nanocrystals as effective delivery systems of poorly water-soluble natural molecules. Current Medicinal Chemistry 2019; 26:4657-80.

28. Machado ND, Fernández MA, Díaz DD. Recent strategies in Resveratrol delivery systems. Chempluschem 2019; 84:951-73.

29. Alcaín FJ, Villalba JM. Sirtuin activators. Expert Opinion on Therapeutic Patents 2009; 19:403-14.

30. Lagouge M, Argmann C, Gerhart-Hines Z, Meziane H, Lerin C, Daussin F, Messadeq N, Milne J, Lambert P, Elliott P, Geny B, Laakso M, Puigserver P, Auwerx J. Resveratrol improves mitochondrial function and protects against metabolic disease by activating SIRT1 and PGC-1alpha. Cell 2006; 127:1109-22.

31. Macmillan-Crow LA, Cruthirds DL. Invited review: manganese superoxide dismutase in disease. Free Radical Research 2001; 34:325-36.

32. Hung L-M, Chen J-K, Huang S-S, Lee R-S, Su M-J. Cardioprotective effect of Resveratrol, a natural antioxidant derived from grapes. Cardiovascular Research 2000; 47:549-55.

33. Olson ER, Naugle JE, Zhang X, Bomser JA, Meszaros JG. Inhibition of cardiac fibroblast proliferation and myofibroblast differentiation by Resveratrol. American Journal of Physiology-Heart and Circulatory Physiology 2005; 288:H1131-8.

34. Wang Y, Lee KW, Chan FL, Chen S, Leung LK. The red wine polyphenol Resveratrol displays bilevel inhibition on aromatase in breast cancer cells. Toxicological Sciences 2006; 92:71-7.

35. Kode A, Rajendrasozhan S, Caito S, Yang SR, Megson IL, Rahman I. Resveratrol induces glutathione synthesis by activation of Nrf2 and protects against cigarette smoke-mediated oxidative stress in human lung epithelial cells. American Journal of Physiology - Lung Cellular and Molecular Physiology 2008; 294:L478-88.

36. Malaguarnera L. Influence of Resveratrol on the Immune Response. Nutrients 2019; 11.

37. Gliemann L, Schmidt JF, Olesen J, Bienso RS, Peronard SL, Grandjean SU, Mortensen SP, Nyberg M, Bangsbo J, Pilegaard H, Hellsten Y. Resveratrol blunts the positive effects of exercise training on cardiovascular health in aged men. The Journal of Physiology 2013; 591:5047-59.

38. Athar M, Back JH, Tang X, Kim KH, Kopelovich L, Bickers DR, Kim AL. Resveratrol: a review of preclinical studies for human cancer prevention. Toxicology and Applied Pharmacology 2007; 224:274-83.

39. la Porte C, Voduc N, Zhang G, Seguin I, Tardiff D, Singhal N, Cameron DW. Steady-state pharmacokinetics and tolerability of trans-Resveratrol 2000 mg twice daily with food, quercetin and alcohol (ethanol) in healthy human subjects. Clinical Pharmacokinetics 2010; 49:449-54.

40. Boocock DJ, Faust GES, Patel KR, Schinas AM, Brown VA, Ducharme MP, Booth TD, Crowell JA, Perloff M, Gescher AJ, Steward WP, Brenner DE. Phase I dose escalation pharmacokinetic study in healthy volunteers of Resveratrol, a potential cancer chemopreventive agent. Cancer Epidemiology Biomarkers & Prevention 2007; 16:1246-52.

41. Tanaka N, Imai K, Okimoto K, Ueda S, Tokunaga Y, Ibuki R, Higaki K, Kimura T. Development of novel sustained-release system, disintegration-controlled matrix tablet (DCMT) with solid dispersion granules of nilvadipine (II): *in vivo* evaluation. Journal of Controlled Release 2006; 112:51-6.

42. Ohara T, Kitamura S, Kitagawa T, Terada K. Dissolution mechanism of poorly water-soluble drug from extended release solid dispersion system with ethylcellulose and hydroxypropylmethylcellulose. International Journal of Pharmaceutics 2005; 302:95-102.

43. Leuner C, Dressman J. Improving drug solubility for oral delivery using solid dispersions. European Journal of Pharmaceutics and Biopharmaceutics 2000; 50:47-60.

44. Majerik V, Charbit G, Badens E, Horvath G, Szokonya L, Bosc N, Teillaud E. Bioavailability enhancement of an active substance by supercritical antisolvent precipitation. The Journal of Supercritical Fluids 2007; 40:101-10.

45. Prabhu S, Ortega M, Ma C. Novel lipid-based formulations enhancing the *in vitro* dissolution and permeability characteristics of a poorly water-soluble model drug, piroxicam. International Journal of Pharmaceutics 2005; 301:209-16.

46. Craig DQ. The mechanisms of drug release from solid dispersions in water-soluble polymers. International Journal of Pharmaceutics 2002; 231:131-44.

47. Karavas E, Ktistis G, Xenakis A, Georgarakis E. Effect of hydrogen bonding interactions on the release mechanism of felodipine from nanodispersions with polyvinylpyrrolidone. European Journal of Pharmaceutics and Biopharmaceutics 2006; 63:103-14.

48. Muhrer G, Meier U, Fusaro F, Albano S, Mazzotti M. Use of compressed gas precipitation to enhance the dissolution behavior of a poorly water-soluble drug: generation of drug microparticles and drug-polymer solid dispersions. International Journal of Pharmaceutics 2006; 308:69-83.

49. Serajuddin AT. Solid dispersion of poorly water-soluble drugs: early promises, subsequent problems, and recent breakthroughs. Journal of Pharmaceutical Sciences 1999; 88:1058-66.

50. Rasenack N, Muller BW. Micron-size drug particles: common and novel micronization techniques. Pharmaceutical Development and Technology 2004; 9:1-13.

51. Gursoy RN, Benita S. Self-emulsifying drug delivery systems (SEDDS) for improved oral delivery of lipophilic drugs. Biomedicine & Pharmacotherapy 2004; 58:173-82.

52. Vasconcelos T, Marques S, Sarmento B. The biopharmaceutical classification system of excipients. Therapeutic Delivery 2017; 8:65-78.

53. Vasconcelos T, Sarmento B, Costa P. Solid dispersions as strategy to improve oral bioavailability of poor water soluble drugs. Drug Discovery Today 2007; 12:1068-75.

54. Shah NH, Carvajal MT, Patel CI, Infeld MH, Malick AW. Self-emulsifying drug delivery systems (SEDDS) with polyglycolyzed glycerides for improving *in vitro* dissolution and oral absorption of lipophilic drugs. International Journal of Pharmaceutics 1994; 106:15-23.

55. Gentilli M, Mazoit JX, Bouaziz H, Fletcher D, Casper RF, Benhamou D, Savouret JF. Resveratrol decreases hyperalgesia induced by carrageenan in the rat hind paw. Life Sciences 2001; 68:1317-21.

56. Deng J-Y, Hsieh P-S, Huang J-P, Lu L-S, Hung L-M. Activation of estrogen receptor is crucial for Resveratrol-stimulating muscular glucose uptake via both insulin-dependent and-independent pathways. Diabetes 2008; 57:1814-23.

57. Stef G, Csiszar A, Lerea K, Ungvari Z, Veress G. Resveratrol inhibits aggregation of platelets from high-risk cardiac patients with aspirin resistance. Journal of Cardiovascular Pharmacology 2006; 48:1-5.

58. EMA. 2015. ICH guideline Q8 (R2) on pharmaceutical development.

59. EMA. 2007. Guideline on excipients in the dossier for application for marketing authorisation of a medicinal product. EMEA/CHMP/QWP/396951/2006 ed.

60. Chaudhari SP, Patil PS. Pharmaceutical Excipients: a review. International Journal of Advances in Pharmacy, Biology and Chemistry 2012; 1:21-34.

61. Zhang W, Li Y, Zou P, Wu M, Zhang Z, Zhang T. The effects of pharmaceutical excipients on gastrointestinal tract metabolic enzymes and transporters-an update. AAPS Journal 2016; 18:830-43.

62. Peng Soh JL, Liew CV, Sia Heng PW. Impact of excipient variability on drug product processing and performance. Current Pharmaceutical Design 2015; 21:5890-9.

63. Rowe RC, Sheskey PJ, Quinn ME. Handbook of pharmaceutical excipients. 6th Edition; 2009.

64. Mwesigwa E, Basit AW. An investigation into moisture barrier film coating efficacy and its relevance to drug stability in solid dosage forms. International Journal of Pharmaceutics 2016; 497:70-7.

65. Patel P, Dave A, Vasava A. Formulation and characterization of sustained release dosage form of moisture sensitive drug. International Journal of Pharmaceutical Investigation 2015; 5:92-100.

66. Joshi S, Petereit HU. Film coatings for taste masking and moisture protection. International Journal of Pharmaceutics 2013; 457:395-406.

67. Czarnocka JK, Alhnan MA. Gastro-resistant characteristics of GRAS-grade enteric coatings for pharmaceutical and nutraceutical products. International Journal of Pharmaceutics 2015; 486:167-74.

68. Raffin RP, Colomé LM, Hoffmeister CR, Colombo P, Rossi A, Sonvico F, Natalini CC, Pohlmann AR, Costa TD, Guterres SS. Pharmacokinetics evaluation of soft agglomerates for prompt delivery of enteric pantoprazole-loaded microparticles. European Journal of Pharmaceutics and Biopharmaceutics 2010; 74:275-80.

69. Lainé AL, Price D, Davis J, Roberts D, Hudson R, Back K, Bungay P, Flanagan N. Enhanced oral delivery of celecoxib via the development of a supersaturable amorphous formulation utilising mesoporous silica and co-loaded HPMCAS. International Journal of Pharmaceutics 2016; 512:118-25.

70. Yue H, Nicholson SJ, Young JD, Hsieh D, Ketner RJ, Hall RG, Sackett J, Banks EC, Castoro JA, Randazzo ME. Development of a control strategy for benzene impurity in HPMCAS-stabilized spray-dried dispersion drug products using a science-based and risk-based approach. Pharmaceutical Research 2015; 32:2636-48.

71. Dave VS, Saoji SD, Raut NA, Haware RV. Excipient variability and its impact on dosage form functionality. Journal of Pharmaceutical Sciences 2015; 104:906-15.

72. Lipinski CA, Lombardo F, Dominy BW, Feeney PJ. Experimental and computational approaches to estimate solubility and permeability in drug discovery and development settings. Advanced Drug Delivery Reviews 1997; 23:3-25.

73. Lipinski CA. Rule of five in 2015 and beyond: target and ligand structural limitations, ligand chemistry structure and drug discovery project decisions. Advanced Drug Delivery Reviews 2016; 101:34-41.

74. Vasconcelos T, Marques S, das Neves J, Sarmento B. Amorphous solid dispersions: rational selection of a manufacturing process. Advanced Drug Delivery Reviews 2016; 100:85-101.

75. Loftsson T. Excipient pharmacokinetics and profiling. International Journal of Pharmaceutics 2015; 480:48-54.

76. Hanna J, Bian J, Hogan WR. An accurate and precise representation of drug ingredients. Journal of Biomedical Semantics 2016; 7:7.

77. Engel A, Oswald S, Siegmund W, Keiser M. Pharmaceutical excipients influence the function of human uptake transporting proteins. Molecular Pharmaceutics 2012; 9:2577-81.

78. Ren X, Mao X, Si L, Cao L, Xiong H, Qiu J, Schimmer AD, Li G. Pharmaceutical excipients inhibit cytochrome P450 activity in cell free systems and after systemic administration. European Journal of Pharmaceutics and Biopharmaceutics 2008; 70:279-88.

79. Pang KS. Modeling of intestinal drug absorption: roles of transporters and metabolic enzymes (for the Gillette Review Series). Drug Metabolism and Disposition 2003; 31:1507-19.

80. Paine MF, Khalighi M, Fisher JM, Shen DD, Kunze KL, Marsh CL, Perkins JD, Thummel KE. Characterization of interintestinal and intraintestinal variations in human CYP3A-dependent metabolism. Journal of Pharmacology and Experimental Therapeutics 1997; 283:1552-62.

81. Estudante M, Morais JG, Soveral G, Benet LZ. Intestinal drug transporters: an overview. Advanced Drug Delivery Reviews 2013; 65:1340-56.

82. Shugarts S, Benet LZ. The role of transporters in the pharmacokinetics of orally administered drugs. Pharmaceutical Research 2009; 26:2039-54.

83. Mottino AD, Hoffman T, Jennes L, Vore M. Expression and localization of multidrug resistant protein mrp2 in rat small intestine. Journal of Pharmacology and Experimental Therapeutics 2000; 293:717-23.

84. Goole J, Lindley DJ, Roth W, Carl SM, Amighi K, Kauffmann JM, Knipp GT. The effects of excipients on transporter mediated absorption. International Journal of Pharmaceutics 2010; 393:17-31.

85. Weinheimer M, Fricker G, Burhenne J, Mylius P, Schubert R. The application of P-gp inhibiting phospholipids as novel oral bioavailability enhancers - an *in vitro* and *in vivo* comparison. European Journal of Pharmaceutical Sciences 2017; 108:13-22.

86. Yang X, Liu K. P-gp inhibition-based strategies for modulating pharmacokinetics of anticancer drugs: an update. Current Drug Metabolism 2016; 17:806-26.

87. Hosea NA, Guengerich FP. Oxidation of nonionic detergents by cytochrome P450 enzymes. Archives of Biochemistry and Biophysics 1998; 353:365-73.

88. Tompkins L, Lynch C, Haidar S, Polli J, Wang H. Effects of commonly used excipients on the expression of CYP3A4 in colon and liver cells. Pharmaceutical Research 2010; 27:1703-12.

89. Ren X, Mao X, Cao L, Xue K, Si L, Qiu J, Schimmer AD, Li G. Nonionic surfactants are strong inhibitors of cytochrome P450 3A biotransformation activity *in vitro* and *in vivo*. European Journal of Pharmaceutical Sciences 2009; 36:401-11.

90. Bravo González RC, Huwyler J, Boess F, Walter I, Bittner B. *In vitro* investigation on the impact of the surface-active excipients Cremophor EL, Tween 80 and Solutol HS 15 on the metabolism of midazolam. Biopharmaceutics & Drug Disposition 2004; 25:37-49.

91. Schulze JD, Waddington WA, Eli PJ, Parsons GE, Coffin MD, Basit AW. Concentration-dependent effects of polyethylene glycol 400 on gastrointestinal transit and drug absorption. Pharmaceutical Research 2003; 20:1984-8.

92. Johnson BM, Charman WN, Porter CJ. An *in vitro* examination of the impact of polyethylene glycol 400, Pluronic P85, and vitamin E d-alpha-tocopheryl polyethylene glycol 1000 succinate on P-glycoprotein efflux and enterocyte-based metabolism in excised rat intestine. AAPS PharmSci 2002; 4:E40.

93. Mudra DR, Borchardt RT. Absorption barriers in the rat intestinal mucosa. 3: effects of polyethoxylated solubilizing agents on drug permeation and metabolism. Journal of Pharmaceutical Sciences 2010; 99:1016-27.

94. Guan Y, Huang J, Zuo L, Xu J, Si L, Qiu J, Li G. Effect of pluronic P123 and F127 block copolymer on P-glycoprotein transport and CYP3A metabolism. Archives of Pharmacal Research 2011; 34:1719-28.

95. Christiansen A, Backensfeld T, Denner K, Weitschies W. Effects of non-ionic surfactants on cytochrome P450-mediated metabolism *in vitro*. European Journal of Pharmaceutics and Biopharmaceutics 2011; 78:166-72.

96. Rao Z, Si L, Guan Y, Pan H, Qiu J, Li G. Inhibitive effect of cremophor RH40 or Tween 80-based self-microemulsiflying drug delivery system on cytochrome P450 3A enzymes in murine hepatocytes. Journal of Huazhong University of Science and Technology - Medical Science 2010; 30:562-8.

97. Martin P, Giardiello M, McDonald TO, Rannard SP, Owen A. Mediation of *in vitro* cytochrome p450 activity by common pharmaceutical excipients. Molecular Pharmaceutics 2013; 10:2739-48.

98. Huang J, Si L, Jiang L, Fan Z, Qiu J, Li G. Effect of pluronic F68 block copolymer on P-glycoprotein transport and CYP3A4 metabolism. International Journal of Pharmaceutics 2008; 356:351-3.

99. Zhu S, Huang R, Hong M, Jiang Y, Hu Z, Liu C, Pei Y. Effects of polyoxyethylene (40) stearate on the activity of P-glycoprotein and cytochrome P450. European Journal of Pharmaceutical Sciences 2009; 37:573-80.

100. Iqbal J, Sakloetsakun D, Bernkop-Schnürch A. Thiomers: inhibition of cytochrome P450 activity. European Journal of Pharmaceutics and Biopharmaceutics 2011; 78:361-5.

101. Ishikawa M, Yoshii H, Furuta T. Interaction of modified cyclodextrins with cytochrome P-450. Bioscience, Biotechnology, and Biochemistry 2005; 69:246-8.

102. Takeshita A, Igarashi-Migitaka J, Nishiyama K, Takahashi H, Takeuchi Y, Koibuchi N. Acetyl tributyl citrate, the most widely used phthalate substitute plasticizer, induces cytochrome p450 3a through steroid and xenobiotic receptor. Toxicological Sciences 2011; 123:460-70.

103. Wang HJ, Hsiong CH, Ho ST, Lin MJ, Shih TY, Huang PW, Hu OY. Commonly used excipients modulate UDP-glucuronosyltransferase 2b7 activity to improve nalbuphine oral bioavailability in humans. Pharmaceutical Research 2014; 31:1676-88.

104. Xiao L, Yi T, Chen M, Lam CW, Zhou H. A new mechanism for increasing the oral bioavailability of scutellarin with Cremophor EL: activation of MRP3 with concurrent inhibition of MRP2 and BCRP. European Journal of Pharmaceutical Sciences 2016; 93:456-67.

105. Akhtar N, Ahad A, Khar RK, Jaggi M, Aqil M, Iqbal Z, Ahmad FJ, Talegaonkar S. The emerging role of P-glycoprotein inhibitors in drug delivery: a patent review. Expert Opinion on Therapeutic Patents 2011; 21:561-76.

106. Al-Mohizea AM. Influence of intestinal efflux pumps on the absorption and transport of furosemide. Saudi Pharmaceutical Journal 2010; 18:97-101.

107. Bromberg L, Alakhov V. Effects of polyether-modified poly(acrylic acid) microgels on doxorubicin transport in human intestinal epithelial Caco-2 cell layers. Journal of Controlled Release 2003; 88:11-22.

108. Choi YA, Yoon YH, Choi K, Kwon M, Goo SH, Cha JS, Choi MK, Lee HS, Song IS. Enhanced oral bioavailability of morin administered in mixed micelle formulation with PluronicF127 and Tween80 in rats. Biological and Pharmaceutical Bulletin 2015; 38:208-17.

109. Kiss L, Hellinger É, Pilbat AM, Kittel Á, Török Z, Füredi A, Szakács G, Veszelka S, Sipos P, Ózsvári B, Puskás LG, Vastag M, Szabó-Révész P, Deli MA. Sucrose esters increase drug penetration, but do not inhibit p-glycoprotein in Caco-2 intestinal epithelial cells. Journal of Pharmaceutical Sciences 2014; 103:3107-19.

110. Collnot EM, Baldes C, Wempe MF, Kappl R, Hüttermann J, Hyatt JA, Edgar KJ, Schaefer UF, Lehr CM. Mechanism of inhibition of P-glycoprotein mediated efflux by

vitamin E TPGS: influence on ATPase activity and membrane fluidity. Molecular Pharmaceutics 2007; 4:465-74.

111. Huang LM, Zhao JH, Wang GC, Zhou JP. [Recent advance in the mechanism study of polymeric inhibitors of P-glycoprotein]. Yao xue xue bao = Acta pharmaceutica Sinica 2010; 45:1224-31.

112. Shah D, Paruchury S, Matta M, Chowan G, Subramanian M, Saxena A, Soars MG, Herbst J, Haskell R, Marathe P, Mandlekar S. A systematic evaluation of solubility enhancing excipients to enable the generation of permeability data for poorly soluble compounds in Caco-2 model. Drug Metabolism Letters 2014; 8:109-18.

113. Yamagata T, Kusuhara H, Morishita M, Takayama K, Benameur H, Sugiyama Y. Effect of excipients on breast cancer resistance protein substrate uptake activity. Journal of Controlled Release 2007; 124:1-5.

114. Aller SG, Yu J, Ward A, Weng Y, Chittaboina S, Zhuo R, Harrell PM, Trinh YT, Zhang Q, Urbatsch IL, Chang G. Structure of P-glycoprotein reveals a molecular basis for poly-specific drug binding. Science 2009; 323:1718-22.

115. Tayrouz Y, Ding R, Burhenne J, Riedel KD, Weiss J, Hoppe-Tichy T, Haefeli WE, Mikus G. Pharmacokinetic and pharmaceutic interaction between digoxin and Cremophor RH40. Clinical Pharmacology & Therapeutics 2003; 73:397-405.

116. Katneni K, Charman SA, Porter CJ. Impact of cremophor-EL and polysorbate-80 on digoxin permeability across rat jejunum: delineation of thermodynamic and transporter related events using the reciprocal permeability approach. Journal of Pharmaceutical Sciences 2007; 96:280-93.

117. Regev R, Katzir H, Yeheskely-Hayon D, Eytan GD. Modulation of P-glycoprotein-mediated multidrug resistance by acceleration of passive drug permeation across the plasma membrane. The FEBS Journal 2007; 274:6204-14.

118. Tomaru A, Takeda-Morishita M, Maeda K, Banba H, Takayama K, Kumagai Y, Kusuhara H, Sugiyama Y. Effects of Cremophor EL on the absorption of orally administered saquinavir and fexofenadine in healthy subjects. Drug Metabolism and Pharmacokinetics 2015; 30:221-6.

119. Hanke U, May K, Rozehnal V, Nagel S, Siegmund W, Weitschies W. Commonly used nonionic surfactants interact differently with the human efflux transporters ABCB1 (p-glycoprotein) and ABCC2 (MRP2). European Journal of Pharmaceutics and Biopharmaceutics 2010; 76:260-8.

120. Ma L, Wei Y, Zhou Y, Ma X, Wu X. Effects of pluronic F68 and Labrasol on the intestinal absorption and pharmacokinetics of rifampicin in rats. Archives of Pharmacal Research 2011; 34:1939-43.

121. Rege BD, Kao JP, Polli JE. Effects of nonionic surfactants on membrane transporters in Caco-2 cell monolayers. European Journal of Pharmaceutical Sciences 2002; 16:237-46.

122. Li M, Si L, Pan H, Rabba AK, Yan F, Qiu J, Li G. Excipients enhance intestinal absorption of ganciclovir by P-gp inhibition: assessed *in vitro* by everted gut sac and in situ by improved intestinal perfusion. International Journal of Pharmaceutics 2011; 403:37-45.

123. Li GF, Tan YF, Guo D, Wang L. [Effect of Tween-80 on the permeability of rhodamine 123, a P-gp substrate across rat intestinal membranes *in vitro*]. Nan Fang Yi Ke Da Xue Xue Bao 2008; 28:579-81.

124. Shaik N, Giri N, Elmquist WF. Investigation of the micellar effect of pluronic P85 on P-glycoprotein inhibition: cell accumulation and equilibrium dialysis studies. Journal of Pharmaceutical Sciences 2009; 98:4170-90.

125. Batrakova EV, Li S, Li Y, Alakhov VY, Kabanov AV. Effect of pluronic P85 on ATPase activity of drug efflux transporters. Pharmaceutical Research 2004; 21:2226-33.

126. Krylova OO, Pohl P. Ionophoric activity of pluronic block copolymers. Biochemistry 2004; 43:3696-703.

127. Yu H, Hu YQ, Ip FC, Zuo Z, Han YF, Ip NY. Intestinal transport of bis(12)-hupyridone in Caco-2 cells and its improved permeability by the surfactant Brij-35. Biopharmaceutics & Drug Disposition 2011; 32:140-50.

128. Cornaire G, Woodley J, Hermann P, Cloarec A, Arellano C, Houin G. Impact of excipients on the absorption of P-glycoprotein substrates *in vitro* and *in vivo*. International Journal of Pharmaceutics 2004; 278:119-31.

129. Sachs-Barrable K, Thamboo A, Lee SD, Wasan KM. Lipid excipients Peceol and Gelucire 44/14 decrease P-glycoprotein mediated efflux of rhodamine 123 partially due to modifying P-glycoprotein protein expression within Caco-2 cells. Journal of Pharmacy and Pharmaceutical Sciences 2007; 10:319-31.

130. Parsa A, Saadati R, Abbasian Z, Azad Aramaki S, Dadashzadeh S. Enhanced permeability of etoposide across everted sacs of rat small intestine by vitamin E-TPGS. Iranian Journal of Pharmaceutical Research 2013; 12:37-46.

131. Dintaman JM, Silverman JA. Inhibition of P-glycoprotein by D-alpha-tocopheryl polyethylene glycol 1000 succinate (TPGS). Pharmaceutical Research 1999; 16:1550-6.

132. Bogman K, Zysset Y, Degen L, Hopfgartner G, Gutmann H, Alsenz J, Drewe J. P-glycoprotein and surfactants: effect on intestinal talinolol absorption. Clinical Pharmacology & Therapeutics 2005; 77:24-32.

133. Ashiru-Oredope DA, Patel N, Forbes B, Patel R, Basit AW. The effect of polyoxyethylene polymers on the transport of ranitidine in Caco-2 cell monolayers. International Journal of Pharmaceutics 2011; 409:164-8.

134. Collnot EM, Baldes C, Schaefer UF, Edgar KJ, Wempe MF, Lehr CM. Vitamin E TPGS P-glycoprotein inhibition mechanism: influence on conformational flexibility, intracellular ATP levels, and role of time and site of access. Molecular Pharmaceutics 2010; 7:642-51.

135. Simon S, Schubert R. Inhibitory effect of phospholipids on P-glycoprotein: cellular studies in Caco-2, MDCKII mdr1 and MDCKII wildtype cells and P-gp ATPase activity measurements. Biochimica et Biophysica Acta 2012; 1821:1211-23.

136. Barta CA, Sachs-Barrable K, Feng F, Wasan KM. Effects of monoglycerides on P-glycoprotein: modulation of the activity and expression in Caco-2 cell monolayers. Molecular Pharmaceutics 2008; 5:863-75.

137. Li L, Yi T, Lam CW. Inhibition of human efflux transporter ABCC2 (MRP2) by self-emulsifying drug delivery system: influences of concentration and combination of excipients. Journal of Pharmacy and Pharmaceutical Sciences 2014; 17:447-60.

138. Li L, Yi T, Lam CW. Interactions between human multidrug resistance related protein (MRP2; ABCC2) and excipients commonly used in self-emulsifying drug delivery systems (SEDDS). International Journal of Pharmaceutics 2013; 447:192-8.

139. Legen I, Kracun M, Salobir M, Kerc J. The evaluation of some pharmaceutically acceptable excipients as permeation enhancers for amoxicillin. International Journal of Pharmaceutics 2006; 308:84-9.

140. Bu P, Narayanan S, Dalrymple D, Cheng X, Serajuddin AT. Cytotoxicity assessment of lipid-based self-emulsifying drug delivery system with Caco-2 cell model: Cremophor EL as the surfactant. European Journal of Pharmaceutical Sciences 2016; 91:162-71.

141. Dimitrijevic D, Shaw AJ, Florence AT. Effects of some non-ionic surfactants on transepithelial permeability in Caco-2 cells. Journal of Pharmacy and Pharmacology 2000; 52:157-62.

142. Ujhelyi Z, Fenyvesi F, Váradi J, Fehér P, Kiss T, Veszelka S, Deli M, Vecsernyés M, Bácskay I. Evaluation of cytotoxicity of surfactants used in self-micro emulsifying drug delivery systems and their effects on paracellular transport in Caco-2 cell monolayer. European Journal of Pharmaceutical Sciences 2012; 47:564-73.

143. Amidon GL, Lennernäs H, Shah VP, Crison JR. A theoretical basis for a biopharmaceutic drug classification: the correlation of *in vitro* drug product dissolution and *in vivo* bioavailability. Pharmaceutical Research 1995; 12:413-20.

144. FDA. 2015. Waiver of i*n vivo* bioavailability and bioequivalence studies for immediate-release solid oral dosage forms based on a biopharmaceutics classification system.

145. EMA. 2010. Guideline on the investigation of bioequivalence

146. Ku MS. Use of the biopharmaceutical classification system in early drug development. AAPS Journal 2008; 10:208-12.

147. Benet LZ, Broccatelli F, Oprea TI. BDDCS applied to over 900 drugs. AAPS Journal 2011; 13:519-47.

148. Borhani DW, Shaw DE. The future of molecular dynamics simulations in drug discovery. Journal of Computer-Aided Molecular Design 2012; 26:15-26.

149. Marshall GR. Computer-Aided Drug Design. Annual Review of Pharmacology and Toxicology 1987; 27:193-213.

150. Kawakami K. Current status of amorphous formulation and other special dosage forms as formulations for early clinical phases. Journal of Pharmaceutical Sciences 2009; 98:2875-85.

151. Ku MS, Dulin W. A biopharmaceutical classification-based Right-First-Time formulation approach to reduce human pharmacokinetic variability and project cycle time from First-In-Human to clinical Proof-Of-Concept. Pharmaceutical Development and Technology 2012; 17:285-302.

152. Giacomini KM, Huang SM, Tweedie DJ, Benet LZ, Brouwer KL, Chu X, Dahlin A, Evers R, Fischer V, Hillgren KM, Hoffmaster KA, Ishikawa T, Keppler D, Kim RB, Lee CA, Niemi M, Polli JW, Sugiyama Y, Swaan PW, Ware JA, Wright SH, Yee SW, Zamek-Gliszczynski MJ, Zhang L. Membrane transporters in drug development. Nature Reviews Drug Discovery 2010; 9:215-36.

153. Cutler L, Howes C, Deeks NJ, Buck TL, Jeffrey P. Development of a P-glycoprotein knockout model in rodents to define species differences in its functional effect at the blood-brain barrier. Journal of Pharmaceutical Sciences 2006; 95:1944-53.

154. Seo JH, Park JB, Choi WK, Park S, Sung YJ, Oh E, Bae SK. Improved oral absorption of cilostazol via sulfonate salt formation with mesylate and besylate. Drug Design, Development and Therapy 2015; 9:3961-8.

155. Novozhilov YV, Dorogov MV, Blumina MV, Smirnov AV, Krasavin M. An improved kilogram-scale preparation of atorvastatin calcium. Chemistry Central Journal 2015; 9:7.

156. Sarkar A, Rohani S. Molecular salts and co-crystals of mirtazapine with promising physicochemical properties. Journal of Pharmaceutical and Biomedical Analysis 2015; 110:93-9.

157. Serrano DR, Gallagher KH, Healy AM. Emerging nanonisation technologies: tailoring crystalline versus amorphous nanomaterials. Current Topics in Medicinal Chemistry 2015; 15:2327-40.

158. Zhang ZH, Zhang Q, Zhang QQ, Chen C, He MY, Chen Q, Song GQ, Xuan XP, Huang XF. From a binary salt to salt co-crystals of antibacterial agent lomefloxacin with improved solubility and bioavailability. Acta Crystallographica Section B: Structural Science, Crystal Engineering and Materials 2015; 71:437-46.

159. Chadha R, Bhandari S, Khullar S, Mandal SK, Jain DV. Characterization and evaluation of multi-component crystals of hydrochlorothiazide. Pharmaceutical Research 2014; 31:2479-89.

160. Weuts I, Kempen D, Verreck G, Peeters J, Brewster M, Blaton N, Van den Mooter G. Salt formation in solid dispersions consisting of polyacrylic acid as a carrier and three basic model compounds resulting in very high glass transition temperatures and constant dissolution properties upon storage. European Journal of Pharmaceutical Sciences 2005; 25:387-93.

161. Seefeldt K, Miller J, Alvarez-Núñez F, Rodríguez-Hornedo N. Crystallization pathways and kinetics of carbamazepine–nicotinamide cocrystals from the amorphous state by in situ thermomicroscopy, spectroscopy, and calorimetry studies. Journal of Pharmaceutical Sciences 2007; 96:1147-58.

162. Dimopoulou M, Mourouti CS, Vertzoni M, Symillides M, Reppas C. *In-vitro* evaluation of performance of solid immediate release dosage forms of weak bases in upper gastrointestinal lumen: experience with miconazole and clopidogrel salts. Journal of Pharmacy and Pharmacology 2016; 68:579-87.

163. Terebetski JL, Cummings JJ, Fauty SE, Michniak-Kohn B. Combined use of crystalline sodium salt and polymeric precipitation inhibitors to improve pharmacokinetic profile of ibuprofen through supersaturation. AAPS PharmSciTech 2014; 15:1334-44.

164. Sai Gouthami K, Kumar D, Thipparaboina R, Chavan RB, Shastri NR. Can crystal engineering be as beneficial as micronisation and overcome its pitfalls? A case study with cilostazol. International Journal of Pharmaceutics 2015; 491:26-34.

165. Bhakay A, Merwade M, Bilgili E, Dave RN. Novel aspects of wet milling for the production of microsuspensions and nanosuspensions of poorly water-soluble drugs. Drug Development and Industrial Pharmacy 2011; 37:963-76.

166. Gupta S, Kesarla R, Omri A. Formulation strategies to improve the bioavailability of poorly absorbed drugs with special emphasis on self-emulsifying systems. ISRN Pharmaceutics 2013; 2013:848043.

167. Laitinen R, Löbmann K, Strachan CJ, Grohganz H, Rades T. Emerging trends in the stabilization of amorphous drugs. International Journal of Pharmaceutics 2013; 453:65-79.

168. Karolewicz B, Górniak A, Owczarek A, Nartowski K, Zurawska-Płaksej E, Pluta J. Solid dispersion in pharmaceutical technology. Part II. The methods of analysis of solid dispersions and examples of their application. Polimery w Medycynie 2012; 42:97-107.

169. Lee EH. A practical guide to pharmaceutical polymorph screening & selection. Asian Journal of Pharmaceutical Sciences 2014; 9:163-75.

170. Murshedkar T. 2002. Effect of crystalline to amorphous conversions on solubility of cefuroxime axetil: University of Rhode Island.

171. Tawa M, Almarsson O, Remenar J. 2005. Pharmaceutical salts of zafirlukast. Google Patents.

172. Pastrano G, Ghaly E. Physicochemical characterization of spray dried formulation containing amorphous drug. International Journal of Pharmacy and Pharmaceutical Sciences 2012; 4:563-70.

173. Talaczyńska A, Lewandowska K, Jelińska A, Garbacki P, Podborska A, Zalewski P, Oszczapowicz I, Sikora A, Kozak M, Cielecka-Piontek J. Application of vibrational spectroscopy supported by theoretical calculations in identification of amorphous and crystalline forms of cefuroxime axetil. The Scientific World Journal 2015; 2015:921049.

174. Jelińska A, Dudzińska I, Zajac M, Oszczpowicz I. The stability of the amorphous form of cefuroxime axetil in solid state. Journal of Pharmaceutical and Biomedical Analysis 2006; 41:1075-81.

175. Guo Y, Byrn SR, Zografi G. Physical characteristics and chemical degradation of amorphous quinapril hydrochloride. Journal of Pharmaceutical Sciences 2000; 89:128-43.

176. Stanisz B. The Stability of quinapril hydrochloride - A mixture of amorphous and crystalline forms (QHCl-AC) - In solid state. Acta Poloniae Pharmaceutica 2003; 60:443-50.

177. Urbanetz NA. Stabilization of solid dispersions of nimodipine and polyethylene glycol 2000. European Journal of Pharmaceutical Sciences 2006; 28:67-76.

178. Tanaka N, Imai K, Okimoto K, Ueda S, Tokunaga Y, Ohike A, Ibuki R, Higaki K, Kimura T. Development of novel sustained-release system, disintegration-controlled matrix tablet (DCMT) with solid dispersion granules of nilvadipine. Journal of Controlled Release 2005; 108:386-95.

179. Vilhelmsen T, Eliasen H, Schfer T. Effect of a melt agglomeration process on agglomerates containing solid dispersions. International Journal of Pharmaceutics 2005; 303:132-42.

180. Karata A, Yksel N, Baykara T. Improved solubility and dissolution rate of piroxicam using gelucire 44/14 and labrasol. Il Farmaco 2005; 60:777-82.

181. Damian F, Blaton N, Naesens L, Balzarini J, Kinget R, Augustijns P, Van den Mooter G. Physicochemical characterization of solid dispersions of the antiviral agent UC-781 with polyethylene glycol 6000 and Gelucire 44/14. European Journal of Pharmaceutical Sciences 2000; 10:311-22.

182. Vasconcelos T, Barrocas P, Lima R, Soares-da-Silva P. Development of an opicapone third generation solid dispersion; 2013; in AAPS Annual Meeting; San Antonio, USA.

183. He Y, Ho C. Amorphous solid dispersions: utilization and challenges in drug discovery and development. Journal of Pharmaceutical Sciences 2015; 104:3237-58.

184. Nielsen LH, Rades T, Müllertz A. Stabilisation of amorphous furosemide increases the oral drug bioavailability in rats. International Journal of Pharmaceutics 2015; 490:334-40.

185. Vo CL, Park C, Lee BJ. Current trends and future perspectives of solid dispersions containing poorly water-soluble drugs. European Journal of Pharmaceutics and Biopharmaceutics 2013; 85:799-813.

186. Huang Y, Dai W-G. Fundamental aspects of solid dispersion technology for poorly soluble drugs. Acta Pharmaceutica Sinica B 2014; 4:18-25.

187. Lin Y, Cogdill RP, Wildfong PL. Informatic calibration of a materials properties database for predictive assessment of mechanically activated disordering potential for small molecule organic solids. Journal of Pharmaceutical Sciences 2009; 98:2696-708.

188. Sóti PL, Bocz K, Pataki H, Eke Z, Farkas A, Verreck G, Kiss É, Fekete P, Vigh T, Wagner I, Nagy ZK, Marosi G. Comparison of spray drying, electroblowing and electrospinning for preparation of Eudragit E and itraconazole solid dispersions. International Journal of Pharmaceutics 2015; 494:23-30.

189. Passerini N, Calogerà G, Albertini B, Rodriguez L. Melt granulation of pharmaceutical powders: a comparison of high-shear mixer and fluidised bed processes. International Journal of Pharmaceutics 2010; 391:177-86.

190. Homayouni A, Sadeghi F, Nokhodchi A, Varshosaz J, Afrasiabi Garekani H. Preparation and characterization of celecoxib dispersions in soluplus(®): comparison of spray drying and conventional methods. Iranian Journal of Pharmaceutical Research 2015; 14:35-50.

191. Potter C, Tian Y, Walker G, McCoy C, Hornsby P, Donnelly C, Jones DS, Andrews GP. Novel supercritical carbon dioxide impregnation technique for the production of amorphous solid drug dispersions: a comparison to hot melt extrusion. Molecular Pharmaceutics 2015; 12:1377-90.

192. Won D-H, Kim M-S, Lee S, Park J-S, Hwang S-J. Improved physicochemical characteristics of felodipine solid dispersion particles by supercritical anti-solvent precipitation process. International Journal of Pharmaceutics 2005; 301:199-208.

193. Dhirendra K, Lewis S, Udupa N, Atin K. Solid dispersions: a review. Pakistan Journal of Pharmaceutical Sciences 2009; 22:234-46.

194. Taylor LS, Zografi G. Spectroscopic characterization of interactions between PVP and indomethacin in amorphous molecular dispersions. Pharmaceutical Research 1997; 14:1691-8.

195. Repka MA, Shah S, Lu J, Maddineni S, Morott J, Patwardhan K, Mohammed NN. Melt extrusion: process to product. Expert Opinion on Drug Delivery 2012; 9:105-25.

196. Paudel A, Worku ZA, Meeus J, Guns S, Van den Mooter G. Manufacturing of solid dispersions of poorly water soluble drugs by spray drying: formulation and process considerations. International Journal of Pharmaceutics 2013; 453:253-84.

197. Patil H, Tiwari RV, Repka MA. Hot-melt extrusion: from theory to application in pharmaceutical formulation. AAPS PharmSciTech 2016; 17:20-42.

198. Ha ES, Baek IH, Cho W, Hwang SJ, Kim MS. Preparation and evaluation of solid dispersion of atorvastatin calcium with Soluplus® by spray drying technique. Chemical & Pharmaceutical Bulletin (Tokyo) 2014; 62:545-51.

199. Xie T, Taylor L. Dissolution performance of high drug loading celecoxib amorphous solid dispersions formulated with polymer combinations. Pharmaceutical Research 2015:1-12.

200. Fong SYK, Ibisogly A, Bauer-Brandl A. Solubility enhancement of BCS Class II drug by solid phospholipid dispersions: spray drying versus freeze-drying. International Journal of Pharmaceutics 2015; 496:382-91.

201. Park JH, Choi HK. Enhancement of solubility and dissolution of cilostazol by solid dispersion technique. Archives of Pharmacal Research 2015; 38:1336-44.

202. Kim YH, Kim DW, Kwon MS, Cho KH, Kim JO, Yong CS, Choi H-G. Clopidogrel napadisilate monohydrate loaded surface-modified solid dispersion: physicochemical characterization and *in vivo* evaluation. Biological and Pharmaceutical Bulletin 2015; 38:1033-40.

203. Lim SM, Pang ZW, Tan HY, Shaikh M, Adinarayana G, Garg S. Enhancement of docetaxel solubility using binary and ternary solid dispersion systems. Drug Development and Industrial Pharmacy 2015:1-9.

204. Sanganwar GP, Gupta RB. Dissolution-rate enhancement of fenofibrate by adsorption onto silica using supercritical carbon dioxide. International Journal of Pharmaceutics 2008; 360:213-8.

205. Pestieau A, Krier F, Lebrun P, Brouwers A, Streel B, Evrard B. Optimization of a PGSS (particles from gas saturated solutions) process for a fenofibrate lipid-based solid dispersion formulation. International Journal of Pharmaceutics 2015; 485:295-305.

206. Yoshihashi Y, Iijima H, Yonemochi E, Terada K. Estimation of physical stability of amorphous solid dispersion using differential scanning calorimetry. Journal of Thermal Analysis and Calorimetry 2006; 85:689-92.

207. Censi R, Gigliobianco M, Dubbini A, Malaj L, Di Martino P. New nanometric solid dispersions of Glibenclamide in Neusilin® UFL2. AAPS PharmSciTech 2015:1-9.

208. Higashi K, Hayashi H, Yamamoto K, Moribe K. The effect of drug and Eudragit® S 100 miscibility in solid dispersions on the drug and polymer dissolution rate. International Journal of Pharmaceutics 2015; 494:9-16.

209. Tabbakhian M, Hasanzadeh F, Tavakoli N, Jamshidian Z. Dissolution enhancement of glibenclamide by solid dispersion: solvent evaporation versus a supercritical fluid-based solvent -antisolvent technique. Research in Pharmaceutical Sciences 2014; 9:337-50.

210. Sui X, Wei W, Yang L, Zu Y, Zhao C, Zhang L, Yang F, Zhang Z. Preparation, characterization and *in vivo* assessment of the bioavailability of glycyrrhizic acid microparticles by supercritical anti-solvent process. International Journal of Pharmaceutics 2012; 423:471-9.

211. Purohit HS, Taylor LS. Miscibility of itraconazole–hydroxypropyl methylcellulose blends: insights with high resolution analytical methodologies. Molecular Pharmaceutics 2015; 12:4542-53.

212. Yin X, Daintree LS, Ding S, Ledger DM, Wang B, Zhao W, Qi J, Wu W, Han J. Itraconazole solid dispersion prepared by a supercritical fluid technique: preparation, *in vitro* characterization, and bioavailability in beagle dogs. Drug Design, Development and Therapy 2015; 9:2801-10.

213. Ha E-S, Kim J-S, Baek I-h, Yoo J-W, Jung Y, Moon HR, Kim M-S. Development of megestrol acetate solid dispersion nanoparticles for enhanced oral delivery by using a supercritical antisolvent process. Drug Design, Development and Therapy 2015; 9:4269-77.

214. Singh A, De Bisschop C, Schut H, Van Humbeeck J, Van Den Mooter G. Compression effects on the phase behaviour of miconazole–poly (1-vinylpyrrolidone-co-vinyl acetate) solid dispersions—role of pressure, dwell time, and preparation method. Journal of Pharmaceutical Sciences 2015; 104:3366-76.

215. Keratichewanun S, Yoshihashi Y, Sutanthavibul N, Terada K, Chatchawalsaisin J. An investigation of nifedipine miscibility in solid dispersions using Raman spectroscopy. Pharmaceutical Research 2015; 32:2458-73.

216. Falconer JR, Wen J, Zargar-Shoshtari S, Chen JJ, Mohammed F, Chan J, Alany RG. The effects of supercritical carbon dioxide processing on progesterone dispersion systems: a multivariate study. AAPS PharmSciTech 2012; 13:1255-65.

217. Li Y, Yang DJ, Chen SL, Chen SB, Chan AS. Process parameters and morphology in puerarin, phospholipids and their complex microparticles generation by supercritical antisolvent precipitation. International Journal of Pharmaceutics 2008; 359:35-45.

218. Vasconcelos T, Marques S, Sarmento B. Development of a Resveratrol solid dispersion with soluplus®; 2015; in 2nd Annual Meeting & Exposition of the Controlled Release Society; Edinburgh, Scotland.

219. Ahuja N, Katare OP, Singh B. Studies on dissolution enhancement and mathematical modeling of drug release of a poorly water-soluble drug using water-soluble carriers. European Journal of Pharmaceutics and Biopharmaceutics 2007; 65:26-38.

220. Craye G, Löbmann K, Grohganz H, Rades T, Laitinen R. Characterization of amorphous and co-amorphous simvastatin formulations prepared by spray drying. Molecules 2015; 20:19784.

221. Cho Y, Ha E-S, Baek I-H, Kim M-S, Cho C-W, Hwang S-J. Enhanced supersaturation and oral absorption of sirolimus using an amorphous solid dispersion based on Eudragit® E. Molecules 2015; 20:9496.

222. Wlodarski K, Sawicki W, Kozyra A, Tajber L. Physical stability of solid dispersions with respect to thermodynamic solubility of tadalafil in PVP-VA. European Journal of Pharmaceutics and Biopharmaceutics 2015; 96:237-46.

223. Wlodarski K, Sawicki W, Haber K, Knapik J, Wojnarowska Z, Paluch M, Lepek P, Hawelek L, Tajber L. Physicochemical properties of tadalafil solid dispersions - Impact of polymer on the apparent solubility and dissolution rate of tadalafil. European Journal of Pharmaceutics and Biopharmaceutics 2015; 94:106-15.

224. Kim MS, Baek IH. Fabrication and evaluation of valsartan-polymer- surfactant composite nanoparticles by using the supercritical antisolvent process. International Journal of Nanomedicine 2014; 9:5167-76.

225. Yoshida VM, Balcão VM, Vila MM, Oliveira Júnior JM, Aranha N, Chaud MV, Gremião MP. Zidovudine-poly(L-lactic acid) solid dispersions with improved intestinal permeability prepared by supercritical antisolvent process. Journal of Pharmaceutical Sciences 2015; 104:1691-700.

226. Milne M, Liebenberg W, Aucamp M. The Stabilization of Amorphous Zopiclone in an Amorphous Solid Dispersion. AAPS PharmSciTech 2015; 16:1190-202.

227. Lloyd GR, Craig DQ, Smith A. A calorimetric investigation into the interaction between paracetamol and polyethlene glycol 4000 in physical mixes and solid dispersions. European Journal of Pharmaceutics and Biopharmaceutics 1999; 48:59-65.

228. Engers D, Teng J, Jimenez-Novoa J, Gent P, Hossack S, Campbell C, Thomson J, Ivanisevic I, Templeton A, Byrn S, Newman A. A solid-state approach to enable early development compounds: selection and animal bioavailability studies of an itraconazole amorphous solid dispersion. Journal of Pharmaceutical Sciences 2010; 99:3901-22.

229. Shanbhag A, Rabel S, Nauka E, Casadevall G, Shivanand P, Eichenbaum G, Mansky P. Method for screening of solid dispersion formulations of low-solubility compounds--miniaturization and automation of solvent casting and dissolution testing. International Journal of Pharmaceutics 2008; 351:209-18.

230. Sinha S, Ali M, Baboota S, Ahuja A, Kumar A, Ali J. Solid dispersion as an approach for bioavailability enhancement of poorly water-soluble drug Ritonavir. AAPS PharmSciTech 2010; 11:518-27.

231. Gangurde AB, Kundaikar HS, Javeer SD, Jaiswar DR, Degani MS, Amin PD. Enhanced solubility and dissolution of curcumin by a hydrophilic polymer solid dispersion and its *in silico* molecular modeling studies. Journal of Drug Delivery Science and Technology 2015; 29:226-37.

232. Drooge DJv, Braeckmans K, Hinrichs WLJ, Remaut K, Smedt SCD, Frijlink HW. Characterization of the mode of incorporation of lipophilic compounds in solid dispersions at the nanoscale using fluorescence resonance energy transfer (FRET). Macromolecular Rapid Communications 2006; 27:1149-55.

233. Teagarden DL, Baker DS. Practical aspects of lyophilization using non-aqueous co-solvent systems. European Journal of Pharmaceutical Sciences 2002; 15:115-33.

234. Pasquali I, Bettini R, Giordano F. Supercritical fluid technologies: an innovative approach for manipulating the solid-state of pharmaceuticals. Advanced Drug Delivery Reviews 2008; 60:399-410.

235. Srinarong P, de Waard H, Frijlink HW, Hinrichs WL. Improved dissolution behavior of lipophilic drugs by solid dispersions: the production process as starting point for formulation considerations. Expert Opinion on Drug Delivery 2011; 8:1121-40.

236. Fattahi A, Karimi-Sabet J, Keshavarz A, Golzary A, Rafiee-Tehrani M, Dorkoosh FA. Preparation and characterization of simvastatin nanoparticles using rapid expansion of supercritical solution (RESS) with trifluoromethane. The Journal of Supercritical Fluids 2016; 107:469-78.

237. Girotra P, Singh SK, Nagpal K. Supercritical fluid technology: a promising approach in pharmaceutical research. Pharmaceutical Development and Technology 2013; 18:22-38.

238. Mishima K, Honjo M, Sharmin T, Ito S, Kawakami R, Kato T, Misumi M, Suetsugu T, Orii H, Kawano H, Irie K, Sano K, Harada T, Ouchi M. Gas-saturated solution process to obtain microcomposite particles of alpha lipoic acid/hydrogenated colza oil in supercritical carbon dioxide. Pharmaceutical Development and Technology 2015:1-12.

239. Jiang Q, Li Y, Fu Q, Geng Y, Zhao J, Ma P, Zhang T. *In-vitro* and *in-vivo* study of amorphous spironolactone prepared by adsorption method using supercritical CO_2. Drug Development and Industrial Pharmacy 2015; 41:201-6.

240. Kim MS, Jin SJ, Kim JS, Park HJ, Song HS, Neubert RH, Hwang SJ. Preparation, characterization and *in vivo* evaluation of amorphous atorvastatin calcium nanoparticles using supercritical antisolvent (SAS) process. European Journal of Pharmaceutics and Biopharmaceutics 2008; 69:454-65.

241. Gong K, Viboonkiat R, Rehman IU, Buckton G, Darr JA. Formation and characterization of porous indomethacin-PVP coprecipitates prepared using solvent-free supercritical fluid processing. Journal of Pharmaceutical Sciences 2005; 94:2583-90.

242. Park J, Park HJ, Cho W, Cha KH, Kang YS, Hwang SJ. Preparation and pharmaceutical characterization of amorphous cefdinir using spray-drying and SAS-process. International Journal of Pharmaceutics 2010; 396:239-45.

243. Lee S, Nam K, Kim MS, Jun SW, Park JS, Woo JS, Hwang SJ. Preparation and characterization of solid dispersions of itraconazole by using aerosol solvent extraction system for improvement in drug solubility and bioavailability. Archives of Pharmacal Research 2005; 28:866-74.

244. Kikic I, Alessi P, Eva F, Moneghini M, Perissutti B. Supercritical antisolvent precipitation of atenolol: the influence of the organic solvent and of the processing approach. The Journal of Supercritical Fluids 2006; 38:434-41.

245. Hanna M, York P; 1995. Method and apparatus for the formation of particles. Google Patents.

246. Tres F, Coombes S, Phillips A, Hughes L, Wren S, Aylott J, Burley J. Investigating the dissolution performance of amorphous solid dispersions using magnetic resonance imaging and proton NMR. Molecules 2015; 20:16404.

247. Chan S-Y, Qi S, Craig DQM. An investigation into the influence of drug–polymer interactions on the miscibility, processability and structure of polyvinylpyrrolidone-based hot melt extrusion formulations. International Journal of Pharmaceutics 2015; 496:95-106.

248. Huang S, O'Donnell KP, Keen JM, Rickard MA, McGinity JW, Williams RO. A new extrudable form of hypromellose: Affinisol™ HPMC HME. AAPS PharmSciTech 2016;17:106-19.

249. De Jaeghere W, De Beer T, Van Bocxlaer J, Remon JP, Vervaet C. Hot-melt extrusion of polyvinyl alcohol for oral immediate release applications. International Journal of Pharmaceutics 2015; 492:1-9.

250. Shergill M, Patel M, Khan S, Bashir A, McConville C. Development and characterisation of sustained release solid dispersion oral tablets containing the poorly water soluble drug disulfiram. International Journal of Pharmaceutics 2016; 497:3-11.

251. Koh PT, Chuah JN, Talekar M, Gorajana A, Garg S. Formulation development and dissolution rate enhancement of Efavirenz by solid dispersion systems. Indian Journal of Pharmaceutical Sciences 2013; 75:291-301.

252. Alhijjaj M, Bouman J, Wellner N, Belton P, Qi S. Creating drug solubilization compartments via phase separation in multicomponent buccal patches prepared by direct hot melt extrusion–injection molding. Molecular Pharmaceutics 2015; 12:4349-62.

253. Feng X, Vo A, Patil H, Tiwari RV, Alshetaili AS, Pimparade MB, Repka MA. The effects of polymer carrier, hot melt extrusion process and downstream processing parameters on the moisture sorption properties of amorphous solid dispersions. Journal of Pharmacy and Pharmacology 2015; 68:692-704.

254. Maniruzzaman M, Nair A, Scoutaris N, Bradley MSA, Snowden MJ, Douroumis D. One-step continuous extrusion process for the manufacturing of solid dispersions. International Journal of Pharmaceutics 2015; 496:42-51.

255. Yuan X, Xiang T-X, Anderson BD, Munson EJ. Hydrogen bonding interactions in amorphous indomethacin and its amorphous solid dispersions with poly(vinylpyrrolidone) and poly(vinylpyrrolidone-co-vinyl acetate) studied using 13C solid-state NMR. Molecular Pharmaceutics 2015; 12:4518-28.

256. Lee JY, Kang WS, Piao J, Yoon IS, Kim DD, Cho HJ. Soluplus®/TPGS-based solid dispersions prepared by hot-melt extrusion equipped with twin-screw systems for enhancing oral bioavailability of valsartan. Drug Design, Development and Therapy 2015; 9:2745-56.

257. Shalaev EY, Lu Q, Shalaeva M, Zografi G. Acid-catalyzed inversion of sucrose in the amorphous state at very low levels of residual water. Pharmaceutical Research 2000; 17:366-70.

258. Vasconcelos T, Costa P. Development of a rapid dissolving Ibuprofen solid dispersion; 2007; in PSWC – 7 Pharmaceutical Sciences World Conference; Amsterdam, Netherlands.

259. Sekiguchi K, Obi N, Ueda Y. Studies on absorption of eutectic mixture. II. Absorption of fused conglomerates of chloramphenicol and urea in rabbits. Chemical & Pharmaceutical Bulletin (Tokyo) 1964; 12:134-44.

260. Pokharkar VB, Mandpe LP, Padamwar MN, Ambike AA, Mahadik KR, Paradkar A. Development, characterization and stabilization of amorphous form of a low Tg drug. Powder Technology 2006; 167:20-5.

261. Chiou WL, Riegelman S. Preparation and dissolution characteristics of several fast-release solid dispersions of griseofulvin. Journal of Pharmaceutical Sciences 1969; 58:1505-10.

262. Timko RJ, Lordi NG. Thermal characterization of citric acid solid dispersions with benzoic acid and phenobarbital. Journal of Pharmaceutical Sciences 1979; 68:601-5.

263. Nagapudi A, Jona J. 2008 Amorphous active pharmaceutical ingredients in preclinical studies: preparation, characterization, and formulation. Current Bioactive Compounds: 213-24.

264. Vippagunta SR, Wang Z, Hornung S, Krill SL. Factors affecting the formation of eutectic solid dispersions and their dissolution behavior. Journal of Pharmaceutical Sciences 2006; 96:294-304.

265. Gunawan L, Johari GP, Shanker RM. Structural relaxation of acetaminophen glass. Pharmaceutical Research 2006; 23:967-79.

266. Stanković M, Frijlink HW, Hinrichs WL. Polymeric formulations for drug release prepared by hot melt extrusion: application and characterization. Drug Discovery Today 2015; 20:812-23.

267. Nakamichi K, Nakano T, Yasuura H, Izumi S, Kawashima Y. The role of the kneading paddle and the effects of screw revolution speed and water content on the preparation of solid dispersions using a twin-screw extruder. International Journal of Pharmaceutics 2002; 241:203-11.

268. Breitenbach J, Lewis J. Two concepts, one technology: controlled release and solid dispersion with meltrex In: Rathbone MJ, Hadgraft J, Roberts MS, editors. Modified-release drug delivery technology, New York: Marcel Dekker; 2003, p. 125 - 34.

269. Loxley A. Devices and implants prepared using hot melt extrusion. In: Repka MA, Langley N, DiNunzio J, editors. Melt extrusion, New York, USA: Springer; 2013, p. 281-98.

270. Thybo P, Hovgaard L, Lindeløv J, Brask A, Andersen S. Scaling up the spray drying process from pilot to production scale using an atomized droplet size criterion. Pharmaceutical Research 2008; 25:1610-20.

271. Dobry DE, Settell DM, Baumann JM, Ray RJ, Graham LJ, Beyerinck RA. A model-based methodology for spray-drying process development. Journal of Pharmaceutical Innovation 2009; 4:133-42.

272. Paudel A, Loyson Y, Van den Mooter G. An investigation into the effect of spray drying temperature and atomizing conditions on miscibility, physical stability, and performance of naproxen-PVP K 25 solid dispersions. Journal of Pharmaceutical Sciences 2013; 102:1249-67.

273. Gu B, Linehan B, Tseng YC. Optimization of the Büchi B-90 spray drying process using central composite design for preparation of solid dispersions. International Journal of Pharmaceutics 2015; 491:208-17.

274. Tee LH, Luqman Chuah A, Pin KY, Abdull Rashih A, Yusof YA. Optimization of spray drying process parameters of Piper betle L. (Sirih) leaves extract coated with maltodextrin. Journal of Chemical and Pharmaceutical Research 2012; 4:1833-41.

275. Patel AS, Soni T, Thakkar V, Gandhi T. Effects of spray drying conditions on the physicochemical properties of the Tramadol-Hcl microparticles containing Eudragit® RS and RL. Journal of Pharmacy and Bioallied Sciences 2012; 4:S50-S3.

276. ICH. Impurities: guideline for residual solvents Q3C(R5); 2011.

277. Patel BB, Patel JK, Chakraborty S, Shukla D. Revealing facts behind spray dried solid dispersion technology used for solubility enhancement. Saudi Pharmaceutical Journal 2015; 23:352-65.

278. Al-Obaidi H, Ke P, Brocchini S, Buckton G. Characterization and stability of ternary solid dispersions with PVP and PHPMA. International Journal of Pharmaceutics 2011; 419:20-7.

279. Bain DF, Munday DL, Smith A. Solvent influence on spray-dried biodegradable microspheres. Journal of Microencapsulation 1999; 16:453-74.

280. Paluch KJ, Tajber L, Amaro MI, Corrigan OI, Healy AM. Impact of process variables on the micromeritic and physicochemical properties of spray-dried microparticles--Part II. Physicochemical characterisation of spray-dried materials. Journal of Pharmacy and Pharmacology 2012; 64:1583-91.

281. Ní Ógáin O, Tajber L, Corrigan OI, Healy AM. Spray drying from organic solvents to prepare nanoporous/nanoparticulate microparticles of protein: excipient composites designed for oral inhalation. Journal of Pharmacy and Pharmacology 2012; 64:1275-90.

282. Jung JY, Yoo SD, Lee SH, Kim KH, Yoon DS, Lee KH. Enhanced solubility and dissolution rate of itraconazole by a solid dispersion technique. International Journal of Pharmaceutics 1999; 187:209-18.

283. Dixit M, Kini AG, Kulkarni PK. Preparation and characterization of microparticles of piroxicam by spray drying and spray chilling methods. Research in Pharmaceutical Sciences 2010; 5:89-97.

284. Yang ZY, Le Y, Hu TT, Shen Z, Chen JF, Yun J. Production of ultrafine sumatriptan succinate particles for pulmonary delivery. Pharmaceutical Research 2008; 25:2012-8.

285. Paidi SK, Jena SK, Ahuja BK, Devasari N, Suresh S. Preparation, *in-vitro* and *in-vivo* evaluation of spray-dried ternary solid dispersion of biopharmaceutics classification system class II model drug. Journal of Pharmacy and Pharmacology 2015; 67:616-29.

286. Wang FJ, Wang CH. Effects of fabrication conditions on the characteristics of etanidazole spray-dried microspheres. Journal of Microencapsulation 2002; 19:495-510.

287. Sass A, Lee G. Evaluation of some water-miscible organic solvents for spray-drying enzymes and carbohydrates. Drug Development and Industrial Pharmacy 2014; 40:749-57.

288. Morgen M, Bloom C, Beyerinck R, Bello A, Song W, Wilkinson K, Steenwyk R, Shamblin S. Polymeric nanoparticles for increased oral bioavailability and rapid

absorption using celecoxib as a model of a low-solubility, high-permeability drug. Pharmaceutical Research 2012; 29:427-40.

289. Ghebremeskel AN, Vemavarapu C, Lodaya M. Use of surfactants as plasticizers in preparing solid dispersions of poorly soluble API: selection of polymer–surfactant combinations using solubility parameters and testing the processability. International Journal of Pharmaceutics 2007; 328:119-29.

290. Chen J, Ormes JD, Higgins JD, Taylor LS. Impact of surfactants on the crystallization of aqueous suspensions of celecoxib amorphous solid dispersion spray dried particles. Molecular Pharmaceutics 2015; 12:533-41.

291. Marasini N, Tran TH, Poudel BK, Cho HJ, Choi YK, Chi SC, Choi HG, Yong CS, Kim JO. Fabrication and evaluation of pH-modulated solid dispersion for telmisartan by spray-drying technique. International Journal of Pharmaceutics 2013; 441:424-32.

292. Janssens S, de Armas HN, Roberts CJ, Van den Mooter G. Characterization of ternary solid dispersions of itraconazole, PEG 6000, and HPMC 2910 E5. Journal of Pharmaceutical Sciences 2008; 97:2110-20.

293. Li X, Jiang C, Pan L, Zhang H, Hu L, Li T, Yang X. Effects of preparing techniques and aging on dissolution behavior of the solid dispersions of NF/Soluplus/Kollidon SR: identification and classification by a combined analysis by FT-IR spectroscopy and computational approaches. Drug Development and Industrial Pharmacy 2015; 41:2-14.

294. Van Goor FF, Alargova RG, Alcacio TE, Arekar SG, Johnston SC, Kadiyala IN, Keshavarz-Shokri A, Krawiec M, Lee EC, Medek A. 2015. Pharmaceutical compositions and administrations thereof. Google Patents.

295. Bittorf KJ, Gaspar F, Katstra JP. 2009. Fluidized spray drying. Google Patents.

296. Kiekens FRI, Voorspoels JFM, Baert LEC. 2007. Process for preparing spray dried formulations of tmc125. Google Patents.

297. Kulthe VV, Chaudhari PD, Aboul-Enein HY. Freeze-dried amorphous dispersions for solubility enhancement of thermosensitive API having low molecular lipophilicity. Drug Research 2014; 64:493-8.

298. Abdelwahed W, Degobert G, Stainmesse S, Fessi H. Freeze-drying of nanoparticles: formulation, process and storage considerations. Advanced Drug Delivery Reviews 2006; 58:1688-713.

299. Seo A, Holm P, Kristensen HG, Schaefer T. The preparation of agglomerates containing solid dispersions of diazepam by melt agglomeration in a high shear mixer. International Journal of Pharmaceutics 2003; 259:161-71.

300. Aleksić I, Duriš J, Ilić I, Ibrić S, Parojčić J, Srčič S. *In silico* modeling of *in situ* fluidized bed melt granulation. International Journal of Pharmaceutics 2014; 466:21-30.

301. Shanmugam S. Granulation techniques and technologies: recent progresses. Bioimpacts 2015; 5:55-63.

302. Passerini N, Albertini B, González-Rodríguez ML, Cavallari C, Rodriguez L. Preparation and characterisation of ibuprofen-poloxamer 188 granules obtained by melt granulation. European Journal of Pharmaceutical Sciences 2002; 15:71-8.

303. Gupta MK, Goldman D, Bogner RH, Tseng YC. Enhanced drug dissolution and bulk properties of solid dispersions granulated with a surface adsorbent. Pharmaceutical Development and Technology 2001; 6:563-72.

304. Kowalski J, Kalb O, Joshi YM, Serajuddin AT. Application of melt granulation technology to enhance stability of a moisture sensitive immediate-release drug product. International Journal of Pharmaceutics 2009; 381:56-61.

305. Rosenberg J, Reinhold U, Liepold B, Berndl G, Breitenbach J, Alani L, Ghosh S. 2005. Solid pharmaceutical dosage form. Google Patents.

306. Crowley MM, Zhang F, Repka MA, Thumma S, Upadhye SB, Battu SK, McGinity JW, Martin C. Pharmaceutical applications of hot-melt extrusion: part I. Drug Development and Industrial Pharmacy 2007; 33:909-26.

307. Wilson M, Williams MA, Jones DS, Andrews GP. Hot-melt extrusion technology and pharmaceutical application. Therapeutic Delivery 2012; 3:787-97.

308. Breitenbach J. Melt extrusion: from process to drug delivery technology. European Journal of Pharmaceutics and Biopharmaceutics 2002; 54:107-17.

309. Van Melkebeke B, Vervaet C, Remon JP. Validation of a continuous granulation process using a twin-screw extruder. International Journal of Pharmaceutics 2008; 356:224-30.

310. Alshahrani SM, Morott JT, Alshetaili AS, Tiwari RV, Majumdar S, Repka MA. Influence of degassing on hot-melt extrusion process. European Journal of Pharmaceutical Sciences 2015; 80:43-52.

311. Morott JT, Pimparade M, Park JB, Worley CP, Majumdar S, Lian Z, Pinto E, Bi Y, Durig T, Repka MA. The effects of screw configuration and polymeric carriers on hot-melt extruded taste-masked formulations incorporated into orally disintegrating tablets. Journal of Pharmaceutical Sciences 2015; 104:124-34.

312. Brown C, DiNunzio J, Eglesia M, Forster S, Lamm M, Lowinger M, Marsac P, McKelvey C, Meyer R, Schenck L, Terife G, Troup G, Smith-Goettler B, Starbuck C. Hot-melt extrusion for solid dispersions: composition and design considerations. In: Shah N, Sandhu H, Choi DS, Chokshi H, Malick AW, editors. Amorphous solid dispersions, USA: Springer New York; 2014, p. 197-230.

313. Sakai T, Thommes M. Investigation into mixing capability and solid dispersion preparation using the DSM Xplore Pharma Micro Extruder. Journal of Pharmacy and Pharmacology 2014; 66:218-31.

314. Sotthivirat S, McKelvey C, Moser J, Rege B, Xu W, Zhang D. Development of amorphous solid dispersion formulations of a poorly water-soluble drug, MK-0364. International Journal of Pharmaceutics 2013; 452:73-81.

315. Yang Z, Nollenberger K, Albers J, Craig D, Qi S. Microstructure of an immiscible polymer blend and its stabilization effect on amorphous solid dispersions. Molecular Pharmaceutics 2013; 10:2767-80.

316. Liu X, Lu M, Guo Z, Huang L, Feng X, Wu C. Improving the chemical stability of amorphous solid dispersion with cocrystal technique by hot melt extrusion. Pharmaceutical Research 2012; 29:806-17.

317. Sakurai A, Sakai T, Sako K, Maitani Y. Polymer combination increased both physical stability and oral absorption of solid dispersions containing a low glass transition temperature drug: physicochemical characterization and *in vivo* study. Chemical & Pharmaceutical Bulletin (Tokyo) 2012; 60:459-64.

318. Alshehri SM, Park JB, Alsulays BB, Tiwari RV, Almutairy B, Alshetaili AS, Morott J, Shah S, Kulkarni V, Majumdar S, Martin ST, Mishra S, Wang L, Repka MA. Mefenamic acid taste-masked oral disintegrating tablets with enhanced solubility via molecular interaction produced by hot melt extrusion technology. Journal of Drug Delivery Science and Technology 2015; 27:18-27.

319. Agrawal AM, Dudhedia MS, Patel AD, Raikes MS. Characterization and performance assessment of solid dispersions prepared by hot melt extrusion and spray drying process. International Journal of Pharmaceutics 2013; 457:71-81.

320. Lang B, Liu S, McGinity JW, Williams RO. Effect of hydrophilic additives on the dissolution and pharmacokinetic properties of itraconazole-enteric polymer hot-melt extruded amorphous solid dispersions. Drug Development and Industrial Pharmacy 2015:1-17.

321. Fule R, Amin P. Development and evaluation of lafutidine solid dispersion via hot melt extrusion: investigating drug-polymer miscibility with advanced characterisation. Asian Journal of Pharmaceutical Sciences 2014; 9:92-106.

322. Djuris J, Ioannis N, Ibric S, Djuric Z, Kachrimanis K. Effect of composition in the development of carbamazepine hot-melt extruded solid dispersions by application of mixture experimental design. Journal of Pharmacy and Pharmacology 2014; 66:232-43.

323. Wang W, Kang Q, Liu N, Zhang Q, Zhang Y, Li H, Zhao B, Chen Y, Lan Y, Ma Q, Wu Q. Enhanced dissolution rate and oral bioavailability of Ginkgo biloba extract by preparing solid dispersion via hot-melt extrusion. Fitoterapia 2015; 102:189-97.

324. Ghebremeskel AN, Vemavarapu C, Lodaya M. Use of surfactants as plasticizers in preparing solid dispersions of poorly soluble API: stability testing of selected solid dispersions. Pharmaceutical Research 2006; 23:1928-36.

325. Verreck G, Decorte A, Heymans K, Adriaensen J, Cleeren D, Jacobs A, Liu D, Tomasko D, Arien A, Peeters J, Rombaut P, Van den Mooter G, Brewster ME. The effect of pressurized carbon dioxide as a temporary plasticizer and foaming agent on the hot stage extrusion process and extrudate properties of solid dispersions of itraconazole with PVP-VA 64. European Journal of Pharmaceutical Sciences 2005; 26:349-58.

326. Verreck G, Decorte A, Heymans K, Adriaensen J, Liu D, Tomasko DL, Arien A, Peeters J, Rombaut P, Van den Mooter G, Brewster ME. The effect of supercritical CO_2 as a reversible plasticizer and foaming agent on the hot stage extrusion of itraconazole with EC 20 cps. The Journal of Supercritical Fluids 2007; 40:153-62.

327. Joshi Y, Kowalski J, Lakshman JP, Royce AE, Tong WQ, Vasanthavada M; 2011. Formulation. Google Patents.

328. Fang LY, Harris D, Krishna G, Moton AE, Prestipino RC, Steinman M, Wan J, Waskin HA; 2015. Oral pharmaceutical compositions in a solid dispersion comprising preferably posaconazole and HPMCAs. Google Patents.

329. Miller JM, Morris JB, Sever NE, Schmitt EA, GAO PX, Shi Y, Gao Y, Liepold B, MOOSMANN A, Pauli M. 2015. Solid antiviral dosage forms. Google Patents.

330. Surwase SA, Itkonen L, Aaltonen J, Saville D, Rades T, Peltonen L, Strachan CJ. Polymer incorporation method affects the physical stability of amorphous indomethacin in aqueous suspension. European Journal of Pharmaceutics and Biopharmaceutics 2015; 96:32-43.

331. Knopp MM, Olesen NE, Holm P, Langguth P, Holm R, Rades T. Influence of polymer molecular weight on drug–polymer solubility: a comparison between experimentally determined solubility in PVP and prediction derived from solubility in monomer. Journal of Pharmaceutical Sciences 2015; 104:2905-12.

332. Forster A, Hempenstall J, Tucker I, Rades T. Selection of excipients for melt extrusion with two poorly water-soluble drugs by solubility parameter calculation and thermal analysis. International Journal of Pharmaceutics 2001; 226:147-61.

333. Weiskirchen S, Weiskirchen R. Resveratrol: how much wine do you have to drink to stay healthy? Advances in Nutrition (Bethesda, Md) 2016; 7:706-18.

334. Costa P, Sousa Lobo JM. Modeling and comparison of dissolution profiles. European Journal of Pharmaceutical Sciences 2001; 13:123-33.

335. Antunes F, Andrade F, Araújo F, Ferreira D, Sarmento B. Establishment of a triple co-culture *in vitro* cell models to study intestinal absorption of peptide drugs. European Journal of Pharmaceutics and Biopharmaceutics 2013; 83:427-35.

336. Shirasaka Y, Sakane T, Yamashita S. Effect of P-glycoprotein expression levels on the concentration-dependent permeability of drugs to the cell membrane. Journal of Pharmaceutical Sciences 2008; 97:553-65.

337. Pollard J, Rajabi-Siahboomi A, Badhan RKS, Mohammed AR, Perrie Y. High-throughput screening of excipients with a biological effect: a kinetic study on the effects of surfactants on efflux-mediated transport. Journal of Pharmacy and Pharmacology 2019; 71:889-97.

338. Kaldas MI, Walle UK, Walle T. Resveratrol transport and metabolism by human intestinal Caco-2 cells. Journal of Pharmacy and Pharmacology 2003; 55:307-12.

339. Maier-Salamon A, Hagenauer B, Wirth M, Gabor F, Szekeres T, Jäger W. Increased transport of Resveratrol across monolayers of the human intestinal Caco-2 cells is mediated by inhibition and saturation of metabolites. Pharmaceutical Research 2006; 23:2107-15.

340. Marier J-F, Vachon P, Gritsas A, Zhang J, Moreau J-P, Ducharme MP. Metabolism and disposition of Resveratrol in rats: extent of absorption, glucuronidation, and enterohepatic recirculation evidenced by a linked-rat model. Journal of Pharmacology and Experimental Therapeutics 2002; 302:369-73.

341. Branton A, Snehasis J. The influence of energy of consciousness healing treatment on low bioavailable Resveratrol in male Sprague Dawley rats. International Journal of Clinical and Developmental Anatomy 2017; 3:9-15.

342. Vasconcelos T, Araujo F, Lopes C, Loureiro A, das Neves J, Marques S, Sarmento B. Multicomponent self nano emulsifying delivery systems of Resveratrol with enhanced pharmacokinetics profile. European Journal of Pharmaceutical Sciences 2019; 137:105011.

343. Brouwers J, Brewster ME, Augustijns P. Supersaturating drug delivery systems: the answer to solubility-limited oral bioavailability? Journal of Pharmaceutical Sciences 2009; 98:2549-72.

344. Karwal R, Garg T, Rath G, Markandeywar TS. Current trends in self-emulsifying drug delivery systems (SEDDSs) to enhance the bioavailability of poorly water-soluble drugs. Critical Reviews in Therapeutic Drug Carrier Systems 2016; 33:1-39.

345. Nipun TS, Ashraful Islam SM. SEDDS of gliclazide: preparation and characterization by *in-vitro*, *ex-vivo* and *in-vivo* techniques. Saudi Pharmaceutical Journal : SPJ 2014; 22:343-8.

346. Rahman MA, Hussain A, Hussain MS, Mirza MA, Iqbal Z. Role of excipients in successful development of self-emulsifying/microemulsifying drug delivery system (SEDDS/SMEDDS). Drug Development and Industrial Pharmacy 2013; 39:1-19.

347. Singh B, Beg S, Khurana RK, Sandhu PS, Kaur R, Katare OP. Recent advances in self-emulsifying drug delivery systems (SEDDS). Critical Reviews in Therapeutic Drug Carrier Systems 2014; 31:121-85.

348. Kohli K, Chopra S, Dhar D, Arora S, Khar RK. Self-emulsifying drug delivery systems: an approach to enhance oral bioavailability. Drug Discovery Today 2010; 15:958-65.

349. Reiss H. Entropy-induced dispersion of bulk liquids. Journal of Colloid and Interface Science 1975; 53:61-70.

350. Bahloul B, Lassoued MA, Sfar S. A novel approach for the development and optimization of self emulsifying drug delivery system using HLB and response surface methodology: application to fenofibrate encapsulation. International Journal of Pharmaceutics 2014; 466:341-8.

351. Cherniakov I, Domb AJ, Hoffman A. Self-nano-emulsifying drug delivery systems: an update of the biopharmaceutical aspects. Expert Opinion on Drug Delivery 2015; 12:1121-33.

352. Cho H-Y, Choi J-H, Oh I-J, Lee Y-B. Self-emulsifying drug delivery system for enhancing bioavailability and lymphatic delivery of Tacrolimus. Journal of Nanoscience and Nanotechnology 2015; 15:1831-41.

353. Dokania S, Joshi AK. Self-microemulsifying drug delivery system (SMEDDS) – challenges and road ahead. Drug Delivery 2015; 22:675-90.

354. Singh AK, Chaurasiya A, Awasthi A, Mishra G, Asati D, Khar RK, Mukherjee R. Oral bioavailability enhancement of exemestane from self-microemulsifying drug delivery system (SMEDDS). AAPS PharmSciTech 2009; 10:906-16.

355. Kang BK, Lee JS, Chon SK, Jeong SY, Yuk SH, Khang G, Lee HB, Cho SH. Development of self-microemulsifying drug delivery systems (SMEDDS) for oral bioavailability enhancement of simvastatin in beagle dogs. International Journal of Pharmaceutics 2004; 274:65-73.

356. Williams HD, Sassene P, Kleberg K, Bakala-N'Goma J-C, Calderone M, Jannin V, Igonin A, Partheil A, Marchaud D, Jule E, Vertommen J, Maio M, Blundell R, Benameur H, Carrière F, Müllertz A, Porter CJH, Pouton CW. Toward the establishment of standardized *in vitro* tests for lipid-based formulations, Part 1: method parameterization and comparison of *in vitro* digestion profiles across a range of representative formulations. Journal of Pharmaceutical Sciences 2012; 101:3360-80.

357. Williams HD, Sassene P, Kleberg K, Calderone M, Igonin A, Jule E, Vertommen J, Blundell R, Benameur H, Müllertz A, Pouton CW, Porter CJH. Toward the establishment of standardized *in vitro* tests for lipid-based formulations, part 3: understanding supersaturation versus precipitation potential during the *in vitro* digestion of type I, II, IIIA, IIIB and IV lipid-based formulations. Pharmaceutical Research 2013; 30:3059-76.

358. Kollner S, Nardin I, Markt R, Griesser J, Prufert F, Bernkop-Schnurch A. Self-emulsifying drug delivery systems: design of a novel vaginal delivery system for curcumin. European Journal of Pharmaceutics and Biopharmaceutics 2017; 115:268-75.

359. Chang LC, Kang JJ, Gau CS. The evolution and challenges for the international harmonization of the regulation of pharmaceutical excipients in Taiwan. Regulatory Toxicology and Pharmacology 2015; 73:947-52.

360. Kalam MA, Raish M, Ahmed A, Alkharfy KM, Mohsin K, Alshamsan A, Al-Jenoobi FI, Al-Mohizea AM, Shakeel F. Oral bioavailability enhancement and hepatoprotective effects of thymoquinone by self-nanoemulsifying drug delivery system. Materials Science & Engineering C, Materials for Biological Applications 2017; 76:319-29.

361. Williams HD, Sassene P, Kleberg K, Calderone M, Igonin A, Jule E, Vertommen J, Blundell R, Benameur H, Müllertz A, Porter CJH, Pouton CW. Toward the establishment of standardized *in vitro* tests for lipid-based formulations, part 4:

proposing a new lipid formulation performance classification system. Journal of Pharmaceutical Sciences 2014; 103:2441-55.

362. Krstic M, Popovic M, Dobricic V, Ibric S. Influence of solid drug delivery system formulation on poorly water-soluble drug dissolution and permeability. Molecules 2015; 20:14684-98.

363. Bahloul B, Lassoued MA, Seguin J, Lai-Kuen R, Dhotel H, Sfar S, Mignet N. Self-emulsifying drug delivery system developed by the HLB-RSM approach: characterization by transmission electron microscopy and pharmacokinetic study. International Journal of Pharmaceutics 2015; 487:56-63.

364. Chintalapudi R, Murthy TEGK, Lakshmi KR, Manohar GG. Formulation, optimization, and evaluation of self-emulsifying drug delivery systems of nevirapine. International Journal of Pharmaceutical Investigation 2015; 5:205-13.

365. Diaz-Gerevini GT, Repossi G, Dain A, Tarres MC, Das UN, Eynard AR. Beneficial action of Resveratrol: how and why? Nutrition 32:174-8.

366. Neves AR, Lucio M, Lima JLC, Reis S. Resveratrol in medicinal chemistry: a critical review of its pharmacokinetics, drug-delivery, and membrane interactions. Current Medicinal Chemistry 2012; 19:1663-81.

367. Beg S, Swain S, Singh HP, Patra CN, Rao MB. Development, optimization, and characterization of solid self-nanoemulsifying drug delivery systems of valsartan using porous carriers. AAPS PharmSciTech 2012; 13:1416-27.

368. https://www.malvern.com/en/support/product-support/zetasizer-range. 11 July 2017.

369. https://www.malvern.com/en/support/product-support/mastersizer-range. 11 July 2017.

370. Levoguer C. 2012. Introducing the Malvern particle characterization toolkit: how to choose the right particle characterization toll for my needs. Malvern.

371. Kollipara S, Gandhi RK. Pharmacokinetic aspects and *in vitro-in vivo* correlation potential for lipid-based formulations. Acta Pharmaceutica Sinica B 2014; 4:333-49.

372. Williams HD, Anby MU, Sassene P, Kleberg K, Bakala-N'Goma J-C, Calderone M, Jannin V, Igonin A, Partheil A, Marchaud D, Jule E, Vertommen J, Maio M, Blundell R, Benameur H, Carrière F, Müllertz A, Pouton CW, Porter CJH. Toward the establishment of standardized *in vitro* tests for lipid-based formulations. 2: the effect of bile salt concentration and drug loading on the performance of type I, II, IIIA, IIIB, and IV formulations during *in vitro* digestion. Molecular Pharmaceutics 2012; 9:3286-300.

373. Chen LC, Chen YC, Su CY, Wong WP, Sheu MT, Ho HO. Development and characterization of lecithin-based self-assembling mixed polymeric micellar (saMPMs) drug delivery systems for curcumin. Scientific Reports 2016; 6:37122.

374. Salager J-L, Márquez L, Mira I, Peña A, Tyrode E, Zambrano NB. Principles of emulsion formulation engineering. In: Mittal KL, Shah DO, editors. Adsorption and aggregation of surfactants in solution, New York: Marcel Dekker, Inc.; 2002, p. 501-23.

375. Khedekar K, Mittal S. Self emulsifying drug delivery system: a review. International Journal of Pharmaceutical Sciences and Research 2013; 4:4494-507.

376. Dressman J, Schamp K, Beltz K, Alsenz J. Characterizing release from lipid-based formulations. Oral Lipid-Based Formulations: CRC Press; 2007, p. 241-55.

377. Sharma N, Madan P, Lin S. Effect of process and formulation variables on the preparation of parenteral paclitaxel-loaded biodegradable polymeric nanoparticles: a co-surfactant study. Asian Journal of Pharmaceutical Sciences 2016; 11:404-16.

378. Shah N, Phuapradit W, Zhang Y-E, Ahmed H, Malick A. Lipid-based isotropic solutions. Oral Lipid-Based Formulations: CRC Press; 2007, p. 129-48.

379. Cianciosi D, Varela-Lopez A, Forbes-Hernandez TY, Gasparrini M, Afrin S, Reboredo-Rodriguez P, Zhang J, Quiles JL, Nabavi SF, Battino M, Giampieri F. Targeting molecular pathways in cancer stem cells by natural bioactive compounds. Pharmacological Research 2018; 135:150-65.

380. Dei Cas M, Ghidoni R. Cancer prevention and therapy with polyphenols: sphingolipid-mediated mechanisms. Nutrients 2018; 10:940.

381. Koushki M, Dashatan NA, Meshkani R. Effect of Resveratrol supplementation on inflammatory markers: a systematic review and meta-analysis of randomized controlled trials. Clinical Therapeutics 2018; 40:1180-92.e5.

382. Lv C, Zhang Y, Shen L. Preliminary clinical effect evaluation of Resveratrol in adults with allergic rhinitis. International Archives of Allergy and Immunology 2018; 175:231-6.

383. Qi B, Shi C, Meng J, Xu S, Liu J. Resveratrol alleviates ethanol-induced neuroinflammation *in vivo* and *in vitro*: involvement of TLR2-MyD88-NF-κB pathway. The International Journal of Biochemistry & Cell Biology 2018; 103:56-64.

384. Khodabandehloo H, Seyyedebrahimi S, Esfahani EN, Razi F, Meshkani R. Resveratrol supplementation decreases blood glucose without changing the circulating CD14+CD16+ monocytes and inflammatory cytokines in patients with type 2 diabetes: a randomized, double-blind, placebo-controlled study. Nutrition Research 2018; 54:40-51.

385. Ma DSL, Tan LT-H, Chan K-G, Yap WH, Pusparajah P, Chuah L-H, Ming LC, Khan TM, Lee L-H, Goh B-H. Resveratrol—potential antibacterial agent against foodborne pathogens. Frontiers in Pharmacology 2018; 9:102.

386. Cannatelli A, Principato S, Colavecchio OL, Pallecchi L, Rossolini GM. Synergistic activity of colistin in combination with Resveratrol against colistin-resistant gram-negative pathogens. Frontiers in Microbiology 2018; 9:1808.

387. Hernandez-Cascales J. Resveratrol enhances the inotropic effect but inhibits the proarrhythmic effect of sympathomimetic agents in rat myocardium. PeerJ 2017; 5:e3113.

388. Arafa MH, Mohammad NS, Atteia HH, Abd-Elaziz HR. Protective effect of Resveratrol against doxorubicin-induced cardiac toxicity and fibrosis in male experimental rats. Journal of Physiology and Biochemistry 2014; 70:701-11.

389. Xia D, Sui R, Zhang Z. Administration of Resveratrol improved Parkinson's disease-like phenotype by suppressing apoptosis of neurons via modulating the MALAT1/miR-129/SNCA signaling pathway. Journal of Cellular Biochemistry 2019; 120:4942-51.

390. Andrade S, Ramalho MJ, Pereira MDC, Loureiro JA. Resveratrol brain delivery for neurological disorders prevention and treatment. Frontiers in Pharmacology 2018; 9:1261.

391. Drygalski K, Fereniec E, Koryciński K, Chomentowski A, Kiełczewska A, Odrzygóźdź C, Modzelewska B. Resveratrol and Alzheimer's disease. From molecular pathophysiology to clinical trials. Experimental Gerontology 2018; 113:36-47.

392. Maugeri A, Barchitta M, Mazzone MG, Giuliano F, Basile G, Agodi A. Resveratrol modulates SIRT1 and DNMT functions and restores LINE-1 methylation levels in ARPE-19 cells under oxidative stress and inflammation. International Journal of Molecular Sciences 2018; 19:2118.

393. Tsuchiya T, Endo A, Tsujikado K, Inukai T. Involvement of Resveratrol and w-3 polyunsaturated fatty acids on Sirtuin 1 gene expression in THP1 cells. The American Journal of the Medical Sciences 2017; 354:415-22.

394. Li J, Yu S, Ying J, Shi T, Wang P. Resveratrol prevents ROS-induced apoptosis in high glucose-treated retinal capillary endothelial cells via the activation of AMPK/Sirt1/PGC-1α pathway. Oxidative Medicine and Cellular Longevity 2017; 2017:7584691.

395. Montagnani Marelli M, Marzagalli M, Fontana F, Raimondi M, Moretti RM, Limonta P. Anticancer properties of tocotrienols: a review of cellular mechanisms and molecular targets. Journal of Cellular Physiology 2018; 0:1-18.

396. Wu H, Li G-N, Xie J, Li R, Chen Q-H, Chen J-Z, Wei Z-H, Kang L-N, Xu B. Resveratrol ameliorates myocardial fibrosis by inhibiting ROS/ERK/TGF-β/periostin pathway in STZ-induced diabetic mice. BMC Cardiovascular Disorders 2016; 16:5.

397. Sinha D, Sarkar N, Biswas J, Bishayee A. Resveratrol for breast cancer prevention and therapy: preclinical evidence and molecular mechanisms. Seminars in Cancer Biology 2016; 40-41:209-32.

398. Almeida L, Vaz-da-Silva M, Falcão A, Soares E, Costa R, Loureiro AI, Fernandes-Lopes C, Rocha J-F, Nunes T, Wright L, Soares-da-Silva P. Pharmacokinetic and safety profile of trans-Resveratrol in a rising multiple-dose study in healthy volunteers. Molecular Nutrition & Food Research 2009; 53:S7-S15.

399. Nunes T, Almeida L, Rocha J-F, Falcão A, Fernandes-Lopes C, Loureiro AI, Wright L, Vaz-da-Silva M, Soares-da-Silva P. Pharmacokinetics of trans-Resveratrol following repeated administration in healthy elderly and young subjects. The Journal of Clinical Pharmacology 2009; 49:1477-82.

400. Fontes-Ribeiro C, Macedo T, Nunes T, Neta C, Vasconcelos T, Cerdeira R, Lima R, Rocha J-F, Falcão A, Almeida L, Soares-da-Silva P. Dosage form proportionality and food effect of the final tablet formulation of eslicarbazepine acetate. Drugs in R & D 2008; 9:447-54.

401. Vaz-da-Silva M, Loureiro AI, Falcao A, Nunes T, Rocha JF, Fernandes-Lopes C, Soares E, Wright L, Almeida L, Soares-da-Silva P. Effect of food on the pharmacokinetic profile of trans-Resveratrol. International Journal of Clinical Pharmacology and Therapeutics 2008; 46:564-70.

402. Vasconcelos T, Marques S, Sarmento B. Measuring the emulsification dynamics and stability of self-emulsifying drug delivery systems. European Journal of Pharmaceutics and Biopharmaceutics 2018; 123:1-8.

403. Chen Y, Zhang H, Yang J, Sun H. Improved antioxidant capacity of optimization of a self-microemulsifying drug delivery system for Resveratrol. Molecules 2015; 20:21167-77.

404. Seljak KB, Berginc K, Trontelj J, Zvonar A, Kristl A, Gasperlin M. A self-microemulsifying drug delivery system to overcome intestinal Resveratrol toxicity and presystemic metabolism. Journal of Pharmaceutical Sciences 2014; 103:3491-500.

405. Yen C-C, Chang C-W, Hsu M-C, Wu Y-T. Self-nanoemulsifying drug delivery system for Resveratrol: enhanced oral bioavailability and reduced physical fatigue in rats. International Journal of Molecular Sciences 2017; 18:1853.

406. Balata GF, Essa EA, Shamardl HA, Zaidan SH, Abourehab MA. Self-emulsifying drug delivery systems as a tool to improve solubility and bioavailability of Resveratrol. Drug Design, Development and Therapy 2016; 10:117-28.

407. Warren KE. Beyond the blood:brain barrier: the importance of central nervous system (CNS) pharmacokinetics for the treatment of CNS tumors, including diffuse intrinsic pontine glioma. Frontiers in Oncology 2018; 8:239.

408. Singh G, Pai RS. *In vitro* and *in vivo* performance of supersaturable self-nanoemulsifying system of trans-Resveratrol. Artificial Cells, Nanomedicine, and Biotechnology 2016; 44:510-6.

409. Bolko K, Zvonar A, Gašperlin M. Mixed lipid phase SMEDDS as an innovative approach to enhance Resveratrol solubility. Drug Development and Industrial Pharmacy 2014; 40:102-9.

410. Wenzel E, Somoza V. Metabolism and bioavailability of trans-Resveratrol. Molecular Nutrition & Food Research 2005; 49:472-81.

411. Kollipara S, Gandhi RK. Pharmacokinetic aspects and *in vitro– in vivo* correlation potential for lipid-based formulations. Acta Pharmaceutica Sinica B 2014; 4:333-49.

412. Zhou J, Zhou M, Yang F-F, Liu C-Y, Pan R-L, Chang Q, Liu X-M, Liao Y-H. Involvement of the inhibition of intestinal glucuronidation in enhancing the oral bioavailability of Resveratrol by Labrasol containing nanoemulsions. Molecular Pharmaceutics 2015; 12:1084-95.

413. Pan R, Liu G, Li Y, Wei Y, Li S, Tao L. Size-dependent endocytosis and a dynamic-release model of nanoparticles. Nanoscale 2018; 10:8269-74.

414. Chimento A, De Amicis F, Sirianni R, Sinicropi MS, Puoci F, Casaburi I, Saturnino C, Pezzi V. Progress to improve oral bioavailability and beneficial effects of Resveratrol. International Journal of Molecular Sciences 2019; 20:1381.

415. Tokuşoglu O, Unal MK, Yemiş F. Determination of the phytoalexin Resveratrol (3,5,4'-trihydroxystilbene) in peanuts and pistachios by high-performance liquid chromatographic diode array (HPLC-DAD) and gas chromatography-mass spectrometry (GC-MS). J Agric Food Chem 2005; 53:5003-9.

416. Walle T, Hsieh F, DeLegge MH, Oatis JE, Jr., Walle UK. High absorption but very low bioavailability of oral Resveratrol in humans. Drug Metabolism and Disposition 2004; 32:1377-82.

417. Gambini J, Inglés M, Olaso G, Lopez-Grueso R, Bonet-Costa V, Gimeno-Mallench L, Mas-Bargues C, Abdelaziz KM, Gomez-Cabrera MC, Vina J, Borras C. Properties of Resveratrol: *in vitro* and *in vivo* studies about metabolism, bioavailability, and biological effects in animal models and humans. Oxidative Medicine and Cellular Longevity 2015; 2015:837042.

418. Delmas D, Aires V, Limagne E, Dutartre P, Mazue F, Ghiringhelli F, Latruffe N. Transport, stability, and biological activity of Resveratrol. Annals of the New York Academy of Sciences 2011; 1215:48-59.

419. Wegiel LA, Mauer LJ, Edgar KJ, Taylor LS. Crystallization of amorphous solid dispersions of Resveratrol during preparation and storage—impact of different polymers. Journal of Pharmaceutical Sciences 2013; 102:171-84.

420. Aloisio C, Bueno MS, Ponte MP, Paredes A, Palma SD, Longhi M. Development of solid self-emulsifying drug delivery systems (SEDDS) to improve the solubility of Resveratrol. Therapeutic Delivery 2019; 10:626-41.

421. Das S, Lin HS, Ho PC, Ng KY. The impact of aqueous solubility and dose on the pharmacokinetic profiles of Resveratrol. Pharmaceutical Research 2008; 25:2593-600.

422. Chang CW, Wong CY, Wu YT, Hsu MC. Development of a Solid Dispersion System for Improving the Oral Bioavailability of Resveratrol in Rats. European Journal of Drug Metabolism and Pharmacokinetics 2017; 42:239-49.

423. Kapetanovic IM, Muzzio M, Huang Z, Thompson TN, McCormick DL. Pharmacokinetics, oral bioavailability, and metabolic profile of Resveratrol and its dimethylether analog, pterostilbene, in rats. Cancer Chemotherapy and Pharmacology 2011; 68:593-601.

K. ANNEX

The following manuscripts were prepared during this Thesis and are presented per order of discretion in the Thesis.

Review

For reprint orders, please contact: reprints@futuremedicine.com

Therapeutic Delivery

The biopharmaceutical classification system of excipients

The increasing number of new chemical entities is bringing new challenges to the field of drug delivery. These drugs present bioavailability issues that are frequently associated with intestinal metabolism or efflux mechanisms. Some excipients, particularly surfactants, have demonstrated a capacity to interfere with these mechanisms, improving drug bioavailability. Consequently, these excipients can no longer be considered as inert and should be subject to special considerations from a regulatory perspective. In the present manuscript, the state-of-the-art research related to these abilities of excipients to interfere with intestinal metabolism and efflux mechanisms are presented and discussed. Here, a biopharmaceutical classification system of excipients is proposed for the first time as a tool in the development of new products and for regulatory purposes.

First draft submitted: 23 September 2016; Accepted for publication: 17 November 2016; Published online: 16 January 2017

Keywords: biopharmaceutical classification system of excipients (BCSE) • efflux transporters • efflux transporters inhibitors • intestinal metabolism inhibitors • permeability enhancers • P-gp

Teófilo Vasconcelos[1,2,3,4], Sara Marques[2,5] & Bruno Sarmento[*,3,4,6]

[1]BIAL-Portela & C[a], S.A. À Avenida da Siderugia Nacional, Trofa, Portugal

[2]Instituto de Ciências Biomédicas Abel Salazar, University of Porto, Porto, Portugal

[3]I3S – Instituto de Investigação e Inovação em Saúde, University of Porto, Porto, Portugal

[4]INEB – Instituto de Engenharia Biomédica, University of Porto, Porto, Portugal

[5]CIBIO/InBIO-UP – Research Centre in Biodiversity & Genetic Resources, University of Porto, Vairão, Portugal

[6]CESPU, Instituto de Investigação e Formação Avançada em Ciências e Tecnologias da Saúde & Instituto Universitário de Ciências da Saúde, Gandra, Portugal

*Author for correspondence: Bruno.sarmento@ineb.up.pt

Pharmaceutical excipients were traditionally defined as inert components used in medicine, crucial to guarantee an adequate quality, safety and efficacy of a drug [1–3]. They are substances other than the active drug which are included during the manufacturing process or are contained in a finished pharmaceutical dosage form [4]. Despite regarded as therapeutically inert, they are essential to transport the active drug to the location in the body where the drug is intended to exert its action [4,5]. In addition, pharmaceutical excipients are key elements to ensure an adequate processability or stabilization of the drug substance [1,2,5]. Considering this, a professional expert in pharmaceutical formulation could convert the most amazing drug substance in an ineffective medicine by altering and conjugating the pharmaceutical excipients present in the final dosage form. On the other hand, a drug substance with poor pharmacokinetic profile can be improved by an adequate selection of excipients. For example, a drug that undergoes degradation by oxidation or hydrolysis can have its stability improved by selecting excipients with reduction properties such as lactose [6], or moisture protection such as moisture sensitive film-coating [7–9], respectively; a drug that causes stomach irritation and therefore originating a high incidence of side effects can be improved by using a gastro-resistant coating system [10,11] or by being incorporated in a gastro-resistant matrix (e.g., containing hypromellose acetate succinate [12,13]). Thus, the role of excipients in the final dosage form is undeniable.

Excipient properties

Despite their widely pharmaceutical functions, chemical moiety or reactivity, physical state or source, pharmaceutical excipients

FUTURE SCIENCE part of fsg

were recognized as safe and without biological activity or interaction. Several excipients are able to modulate the drug performance by controlling the drug release, such as metacrylates, Carbopol® or hydroxypropyl methylcellulose matrices [2,14]. Others may improve the drug solubility resulting in higher bioavailability such as povidone or polyethylene glycols (PEGs). However, in any case, excipients are recognized as being able to interact with our biological systems [4,14]. In the last decade, new therapeutic challenges were overcome by using drugs that are outside the conventional drugable space driven by the Lipinski rule [15]. These valuable drugs are extremely challenging from the pharmaceutical perspective. Particularly because associated to their poor physical chemical properties for the oral route, such as high melting point and/or MW and/or high logP, are poor intrinsic permeable or present poor permeability due to efflux mechanisms or intestinal metabolization [15–17]. The combination of these factors result in an increased number of drugs belonging to class III and IV accordingly to the biopharmaceutical classification system (BCS) proposed by Amidon [4,17,18].

The pharmaceutical industry, in particular the industries associated to the development of new excipients, provided an assertive response to these new challenges developing new products that are able to support the establishment of new drug products. However, this effort led to the development of excipients that no longer can be considered as inert because they interfere and interact with our biological systems [18].

Biological mechanisms targeted by new excipients

The two major biological mechanisms used to protect our organisms from external xenobiotics are biotransformation and efflux pumps [4]. Among the metabolizing enzymes present in the small intestinal mucosa, the CYP450 are of particular importance, being responsible for the majority of phase I drug metabolism reactions [19–21]. From these, CYP3A and CYP2C are the most representative in the intestinal mucosa, in which, CYP3A4, CYP3A5 and CYP2C9 are the most representative in this order of relevance. Additionally CYP2J2 and CYP1A1 are also present in intestinal mucosa and are associated to inter-individual variability. The distribution of most CYP enzymes is not uniform along the human gastrointestinal tract. For instance, CYP3A shows a slightly lower level of expression at the duodenum followed by an increase at the jejunum, and then finally decreasing toward the ileum [22,23].

Efflux transporters are present in all human biological barriers, being the most important in intestine, liver, kidney and blood–brain barriers. This manuscript will only focus on the intestinal barrier where the most relevant efflux transporters include P-glycoprotein (P-gp), multidrug resistance proteins (MRPs), organic anion-transporting polypeptide (OATP) and breast cancer resistance protein (BCRP) [24,25]. These proteins located in the luminal side of the intestine walls, use ATP to actively pump drugs or xenobiotics back to the intestine. This mechanism is extremely important in drug resistance, resulting in poor bioavailability and drug–drug interaction. The efflux transporters distribution along the GI tract is not uniform. Both OATP and MRP2 have higher expression in the jejunum, but in the case of MRP2 jejunum predominance is followed by the duodenum and ileum, with very little expression in the colon [26,27]. The P-gp efflux pump expression increases from proximal to distal regions of the small intestine being higher at the jejunum and ileum. The BCRP maximum expression exists in the duodenum and decreases continuously down to the rectum, in which, the BCRP expression in the duodenum is comparable to P-gp [27].

Some excipients have shown the ability to interfere and inhibit these protective mechanisms [4]. This ability has been explored for enhancing the drug oral bioavailability in the drug delivery field [28,29]. The current state of the excipients that are able to influence these mechanisms is presented in the next sections.

Excipients able to interact with metabolic mechanisms

The excipients interaction with the metabolic mechanism in the intestine can occur by three different processes, namely direct inhibition (chemical) [30], regulation of mRNA expression (reduced or increased) [31] or regulation of protein expression (reduced or increased) [21,32]. Surfactants are the excipients that mostly interact with intestinal metabolism, as summarized in Table 1.

CYP3A inhibition

The Kolliphor® HS15 [33], Kolliphor® EL [32,33] Tween-20® [32], Tween-80® [33,34], PEG400 [35,36], Myrj® 52 [32] Poloxamer 188 [32] and Poloxamer 235 [35] showed *in vitro* ability to inhibit CYP3A, which was generally dose dependent [4]. This inhibition was further confirmed *in vivo* by an increase in bioavailability of midazolam, which is a CYP3A substrate in the presence of Kolliphor EL [33] and Tween-20® [32]. In opposite, Myrj 52 and Poloxamer 188 induced an *in vivo* reduction of midazolam AUC [32]. These excipients interact with CYP due to subtract competition [30], reduction in CYP3A protein expression as observed for Kolliphor® RH40 [34] or via enzymatic conformation change. In

Table 1. Properties of surfactants with interaction on intestinal metabolism.

Surfactant	Common name	Hydrophilic component	Lipid component	HLB
Kolliphor® HS15	Macrogol-15-hydroxystearate	15 molecules of ethylene oxide	Hydroxy stearate (mono and di esters)	14–16
Kolliphor® EL	PEG-35 castor oil	35 molecules of ethylene oxide	Glycerol triricinoleate	12–14
Kolliphor® RH40	PEG-40 hydrogenated castor oil	40–45 molecules of ethylene oxide	Hydrogenated Glycerol triricinoleate	14–16
Myrj® 52	PEG-40 stearate	40 molecules of ethylene oxide	Stearate	17
Brij® 30	Polyoxyl 4 lauryl ether	4 molecules of ethylene oxide	Lauryl (dodecyl)	10
Brij® 35	Polyoxyl 23 lauryl ether	23 molecules of ethylene oxide	Lauryl (dodecyl)	17
Tween-20®	Polyoxyethylene (20) sorbitan monolaurate	20 molecules of ethylene oxide	Sorbitan monolaurate	17
Tween-80®	Polyoxyethylene (20) sorbitan monooleate	20 molecules of ethylene oxide	Sorbitan monooleate	15
P181	Poloxamer 181	10% polyoxyethylene content	Polyoxypropylene molecular mass of 1800 g/mol	3
P188	Poloxamer 188	10% polyoxyethylene content	Polyoxypropylene molecular mass of 1800 g/mol	>24
P235	Poloxamer 235	50% polyoxyethylene content	Polyoxypropylene molecular mass of 2300 g/mol	Not available
P333	Poloxamer 333	30% polyoxyethylene content	Polyoxypropylene molecular mass of 3300 g/mol	7–12
P403	Poloxamer 403	30% polyoxyethylene content	Polyoxypropylene molecular mass of 4000 g/mol	7–12
P407	Poloxamer 407	70% polyoxyethylene content	Polyoxypropylene molecular mass of 4000 g/mol	18–23
Vitamin E TPGS	Vitamin E polyethylene glycol succinate	Polyethylene glycol 1000 succinate	Vitamin E	13
Labrasol®	Caprylocaproyl macrogol-8 glycerides	8 molecules of ethylene oxide	Caprylic/capric glycerides	12
Gelucire ® 44/12	Lauroyl macrogol-32 glycerides	32 molecules of ethylene oxide	Lauroyl glycerides	11

HLB: Hydrophilic–lipophilic balance; TPGS: Tocopherol polyethylene glycol succinate; PEG: Polyethylene glycol.

other studies, Poloxamers P403 and P407 [37], Kolliphor EL [36] and vitamin E TPGS [35,36] had little or no effect on intestinal cytochrome P4503A activity [37] in opposition to the previously stated. This data suggest that dose can be a relevant factor in the CYP inhibition.

CYP3A4 inhibition

The inhibition of specific CYP3A4 was observed *in vitro* for Kolliphor EL [38], Kolliphor RH40 [21,32,38,39], vitamin E TPGS [38], Tween-80 [38–40], Poloxamer 188 [40,41], Myrj 52 [42,43], Brij® 35 [43], thiomers [43], modified cyclodextrins [44] and sucrose laurate [38], in a dose dependent manner below the critical micellar concentration (CMC) [38]. From these, Tween-80 reduced the mRNA and protein expression of this metabolic mechanism [31]. Other excipients such as binders, fillers, solvents or co-solvents may also affect CYP3A activity. Thompkins *et al.* studied 19 common excipients and concluded that the polymers HPMC and croscarmellose sodium caused a moderate but statistically significant 1.8-fold and 2.4-fold increase in CYP3A4 mRNA expression, respectively [31]. Nevertheless, this was not translated into protein expression increase and the mRNA increase was marginal when compared with the positive control [31]. In the same study, the authors concluded that HPMC, pregelatinized starch and Tween-80 showed statistically significant effects over CYP3A4 in multiple cell lines studied.

Silicon dioxide, magnesium stearate and pregelatinized starch decreased CYP3A4 mRNA expression by more than 40, 70 and 65%, respectively [31]. However, dicalcium phosphate, HPMC, crospovidone, PEG3350, propylene glycol, citric acid and malic acid decreased the protein expression. The remaining excipients (lactose, cellulose microcrystalline, povidone, sodium starch glycolate, sodium lauryl sulfate and sucrose) showed no effect over this metabolism mechanism [31]. In another study, eight plasticizers were studied, acetyl tributyl citrate, tributyl citrate, acetyl triethyl citrate, triethyl citrate, diethyl phthalate, dibutyl phthalate, dibutyl sebacate and triacetin, in which all showed induction of CYP3A4. From these, acetyl tributyl citrate was the most potent *in vitro* with also *in vivo* confirmation. The demonstrated data suggested that this induction only occurred in the intestine and not in the liver [45].

CYP3A5 inhibition

The CYP3A5 has been *in vitro* inhibited by the following excipients, PEG1000, Tween-20, cetyltrimethylammonium bromide, Tween-80 and Poloxamer 188, through decreasing potency [40].

CYP2C9 inhibition

Christiansen *et al.* studied the *in vitro* inhibition of CYP2C9 caused by several excipients [38]. Results obtained by other researchers indicate that Kolliphor EL [38], Kolliphor RH40 [38], Myrj 52 [42] and Tween-80 [38] were the most powerful inhibitors followed by sucrose laurate [38]. Vitamin E TPGS was tenfold weaker than the most potent inhibitor. In another study using a screening kit, PEG1000 and Poloxamer 188 showed moderate inhibiting of CYP2C9 [40]. On the other hand, modified cyclodextrins enhanced CYP2C9 activity [44].

Glucuronidation

Excipients do not only limit their interaction with phase I metabolization, but can also interfere in the phase II path. This impact was recently assessed for glucuronidation. The reported data indicate that parabens (methyl and propyl) were able to almost completely inhibit glucuronidation. Surfactants also presented potential to inhibit this mechanism, with decreasing order: Tween-20 > Kolliphor EL > Kolliphor RH > PEG400 > Tween-80 > Kolliphor H15 [46].

Table 2 presents a summary of the excipients interaction with the metabolization systems.

Transporters interaction

As commonly accepted, drug transport mechanisms, in particular the efflux transport to the intestinal lumen, condition poor drug bioavailability [47]. In the last years, several reports suggested that some excipients are able to module and interact with this efflux mechanism [4,28,29,48,49]. Nevertheless, their mechanisms and specific transporter interaction is not yet clear.

Chelation of crucial micronutrients for an adequate enzymatic activity can be a possible mechanism to reduce the efflux transport mechanisms. Bromberg *et al.* demonstrated that polymers based on polymetacrylates were able to strongly bind bivalent cations such as zinc and calcium preventing their association to certain transporters, thereby inactivating them and enhancing doxorubicin permeability [27,50].

A transformation in the cell membrane implying an inactivation of the efflux pumps can be another mechanism of interaction between excipients and transporters mechanisms [24,28]. This type of interaction has been associated with surfactants that due to their amphiphilic structure are able to interact with lipids in the cell membrane and change both its physical and functional properties. Indeed, surfactants are able to alter the membrane fluidity, which can modify the orientation of the efflux pumps on its surface, preventing the substrate binding and/or activation of pump by co-factors [24,28]. In addition, surfactants have been found to enhance the absorption of compounds by both transcellular and paracellular routes through reduction of the membrane viscosity and increasing its elasticity [27,36,51,52].

Competitive inhibition of substrate binding and inhibition of efflux pump ATPase have also been proposed as possible mechanisms [35,53], as well as downregulation of the transporter, as observed for P-gp expression [54].

Among the pharmaceutical excipients surfactants, polymers and lipid compounds are the most frequently associated to inhibition of intestinal efflux transporters [27,55]. However, due to their unclear mechanism of action, most of the excipients are not specific of a single transporter [56].

P-gp inhibition

P-gp, also known as multidrug resistance protein (MDR1) or ATP-binding cassette sub-family B member 1 (ABCB1), is the most studied efflux mechanism in the GI tract [4]. This transporter is also widely presented in liver, kidney and blood-brain barrier [27]. P-gp is a 170 kDa transmembrane glycoprotein, which includes 10–15 kDa of N-terminal glycosylation. At intestinal level, P-gp is presented in the luminal side of the cell [57]. Substrate enters P-gp either from an opening within the membrane or from the cytoplasm. ATP binds at the cytoplasmic side of the protein. ATP hydrolysis moves the substrate into a position to be excreted from the cell [57].

Table 2. Excipients effect in cytochrome P450.

Excipient	CYP3A	CYP3A4	CYP3A5	CYP2C9	Glucuronidation
Kolliphor® HS15	+				+
Kolliphor® EL	+	+		+	+
Kolliphor® RH40		+		+	+
Tween-20®	+		+		+
Tween-80®	+	+	+	+	+
PEG400	+				+
PEG1000			+	+	
PEG3350	+				
Myrj® 52	±	+		+	
Brij® 35		+			
Poloxamer 188	±	+	+	+	
Poloxamer 235	+				
Poloxamer 403	–				
Poloxamer 407	–				
Vitamin E TPGS	–	+			
Thiomers		+			
Modified cyclodextrins		+		↑	
Sucrose laurate		+		+	
HPMC	+				
Croscarmelose sodium	+				
Sodium starch glycolate	+				
Silicon dioxide	+				
Magnesium stearate	+				
Dicalcium phosphate	+				
Crospovidone	+				
Propylene glycol	+				
Acetic acid	+				
Malic Acid	+				
Triacetin	↑				
Phtalates	↑				
Lactose	–				
Cellulose microcrystalline	–				
Povidone	–				
Sodium starch glycolate	–				
Sodium lauryl sulfate	–				
Sucrose	–				
Cetyltrimethylammonium bromide	+				

(+) inhibition; (–) no inhibition; (±) variable information (↑) enzymatic induction.
HPMC: Hydroxypropyl methylcellulose; TPGS: Tocopherol polyethylene glycol succinate.

Kolliphor RH [56,58], Kolliphor EL [28,36,59–62], Labrasol® [63], Tween-20 [60], Tween-80 [28,62,64–66], sucrose laurate [62] Span® 20 [56], Poloxamer 235 (P85) [27,67,68], Poloxamer 181 [60,69], Poloxamer 188 [41,63], Poloxamer 333 [62], Poloxamer 403 [37], Poloxamer 407 [37], Brij 35 [70], Myrj 52 [4,42], Softigen® 767 (PEG-6 Caprylic/Capric Glycerides) [71], PEG-15 Stearyl Ether (acconon E) [71] and Gelucire® 44/14 [72] were demonstrated to *in vitro* inhibit P-gp below or at their CMC concentration [56]. Generally, above the CMC concentration, surfactants tend to decrease their impact in P-gp due to drug entrapment into the formed micelles [39,67]. In a human study, Kolliphor EL was only effective below its CMC, suggesting that above CMC the drug may be entrapped into the micelles and was not able to be absorbed [61]. On the contrary, vitamin E TPGS is able to inhibit P-gp efflux above and below its CMC [36,56,62,73,74] enhancing the permeability of doxorubicin [74], vinblastine [74], paclitaxel [74], etoposide [73] and colchicine [74]. In an *in vivo* human study, it showed inhibition of P-gp at a concentration of 0.04% (w/v), resulting in an enhancement of talinolol AUC (0-infinity) and C_{max} at 40% and 100%, respectively [75].

The polymers PEG400 and PEG300 inhibit P-gp in a dose dependent manner, being PEG400 to be more potent [76].

The exact mechanism of action for the P-gp inhibition is unclear. An alteration in membrane fluidity was observed for vitamin E TPGS [53,64,77] which increased the membrane rigidity. On the other hand, Tween-80 [64], Kolliphor EL [64] and Poloxamer 235 [68] fluidized the membrane. Both changes resulted in a decrease in ATPase activity and in a P-gp inhibition. An interaction with one or both of the P-gp ATP nucleotide binding domain inhibition of ATPase activity of drug efflux proteins and intracellular ATP depletion was described for vitamin E TPGS [77], Myrj 52 [42] and Poloxamer 235 [68]. Poloxamer 181 on the other hand, which is a cationic surfactant was able to interfere with ionic flux in the plasma membrane and cause compensatory ATP consumption by Na^+/K^+-ATPase, thus decreasing the intracellular ATP concentration and inhibiting P-gp [69].

The surfactants effect on efflux mechanisms is structure and interaction dependent since the excipients from the same family of the ones presenting P-gp inhibition properties do not present the same capacity. For instance, Span 40, Span 80, Propylene glycol, triacetin and Ethyl oleate do not affect P-gp activity at levels below or at their CMC concentration [56]. Also, PEG200 [76] and PEG400 [73] at 5, 0.1 and 0.5% w/v also did not have P-gp effect. In other cases, excipients reported has P-gp inhibitors, such as Tween-80 [59], Poloxamer 188 (0.8%) [75] and Kolliphor RH40 [62] were shown to have negative results in some studies.

Phospholipids are another group of known P-gp inhibitors. The 1,2-dioctanoyl-sn-glycero-3-phosphocholine (8:0 PC) [28,78], 1,2-didecanoyl-sn-glycero-3-phosphocholine (10:0 PC) [28,78] and unsaturated docosahexaenoic acid residues (cis-22:6 PC) demonstrate strong inhibitory action. Their effects on membrane fluidity were not consistent with their P-gp inhibiting effects, and, therefore, suggested a more complex mode of action [28], such as direct P-gp inhibitors interacting with the transporter probably in their monomeric state, whereas a different, as yet unknown mechanism of action applied for cis-22:6 PC [78].

The monoglycerides 1-monoolein and 1-monostearin were not P-gp inhibitors at noncytotoxic concentrations but at higher concentrations P-gp inhibition was observed [79]. Caprylic/Capric Glycerides (Imwitor® 742) and Miglyol®, which are triglycerides showed P-gp inhibition, which was potent for Imwitor 742 [71].

MRP2 inhibition

MRP2, also known as ATP-binding cassette sub-family C member 2 is a transporter mainly expressed in the liver, kidney and intestine [4,80]. Surfactants and polymers, similarly for P-gp, have also demonstrated an influence on MRP2 transport. Kolliphor EL [47,62,80,81], vitamin E TPGS [62], Tween-80 [62], sodium lauryl sulfate (0.2 mg/ml) [82], Labrasol [81], Poloxamer 235 [68], Poloxamer 407 [80,81], PEG2000 [80,81], PEG400 [80,81], Trascutol® [80] and Kolliphor RH 40 [62,80,81] had previously demonstrated *in vitro* MRP2 inhibition. Other excipients as lipids have also been studied. Maisine® 35–1 (Glycerol monolinoleate) [80], Caprylic/capric triglyceride (Labrafac Lipophile® WL 1349) [81], Glyceryl caprylate (Capmul MCM) [81] and β-cyclodextrin [80] have some effect on MRP2.

Kolliphor RH 40 was more potent in inhibiting MRP2 than P-gp [62]. Tween-80 [62] and Poloxamer 235 [68] presented a lower potency in inhibiting MRP2 than P-gp. In the particular case of the Poloxamer 235, this was attributed to a considerably greater effect on the P-gp ATPase activity interaction when compared with the MRP2 ATPases [68]. On the other hand, Poloxamer 333 [62], Poloxamer 188 [80,82] and sucrose laurate [62] which are P-gp inhibitors, have no effect in MRP2 efflux mechanism. Other excipients showed variable results in inhibiting MRP2, for instance Kolliphor EL (0.2 mg/ml) [82], Poloxamer 407 [82] and Labrasol [80] also provided negative results.

Hanke *et al.* concluded that surfactants caused an alteration in ABCC2 mRNA or protein expression [62]. These findings indicate that the observed interactions are caused by specific inhibition of the transporter

activity [62]. Conformational changes of the transporter due to membrane fluidization and/or nonspecific steric interaction of the drug-binding sites were also speculated [68]. The effect of sodium lauryl sulfate on the active secretion of amoxicillin was mainly attributed to the reversible cellular ATP depletion [82]. Li *et al.* observed positive and negative interactions between excipients that alone are MRP2 inhibitors suggesting that an adequate selection and combination of these are crucial for an acceptable performance of the drug product [80].

BCRP inhibition

BCRP also known as ATP-binding cassette sub-family G member 2 (ABCG2) is present at the apical membrane of the intestine, in the blood–brain barrier among other tissues [4]. Surfactants, such as Kolliphor EL [47,56], Tween-20 [56], Poloxamer 235 [56], Span 20 [56] and Brij 30 [56] were found to inhibit the BCRP efflux mechanism. Some other compounds that are P-gp and MRP2 inhibitors and are not BCRP inhibitors include Kolliphor RH40 [56], Tween-80 [56], vitamin E TPGS [56], Myrj 52 [56] and Gelucire® 44/14 [56] which is a further evidence that structure specificity plays an important role in surfactant-mediated inhibition. Excipients such as Span 40, Span 80, propylene glycol, triacetin and ethyl oleate are not inhibitors of BCRP [56].

Excipients that are BCRP inhibitors have no significant effects on intracellular ATP levels of these transporters showing that ATP depletion is not their mechanism of action. In addition, it was demonstrated that the same excipient may have different mechanisms of action in different transporters such as BCRP and P-gp [56].

OATP inhibition

OATP is a membrane transport protein that mediates the transport of mainly organic anions across the cell membrane. Since these are uptake transporters and not efflux transporters, their inhibition may reduce the absorption of their substrate drugs [4]. The OATPs present in the intestine are OATP1A2, OATP1B3 and OATP12B1.

Very little information is available related to the inhibition of this transporter by excipients. Engel *et al.*, studied the effect of regular excipients in the inhibition of OATPs showing that Kolliphor HS15 and Kolliphor EL were the most potent inhibitors of all OATP transporters with the strongest effect on intestinal proteins [20]. PEG400 was a selective and potent modulator of only OATP1A2 [20].

Table 3 summarizes the effect of excipients on most relevant transporter mechanisms.

Data limitations on the excipients interaction with transporter & metabolism mechanisms

The current available information is rare and presents some limitations. One of the most important is the scarce number of *in vivo* studies and also, from these, the fact that almost none are from human. In fact, despite the talinolol case with TPGS [75], which is more than 10 years old, no other relevant human studies are available. This lack prevents an adequate translation of the *in vitro* data into clinical application.

Most of the studies used *in vitro* systems, particularly Caco-2 and modified Caco-2 monolayers. These models can be reliable, but caution must be taken when interpreting the data. Particularly, because excipients and formulation toxicities can artificially increase drug permeation by damaging and disrupting cell monolayers or killing the cells, consequently providing misleading results [83]. These effect has been demonstrated for some surfactants, which generally demonstrated concentration-dependent effects on reducing cell viability and consequently improved the drug permeability through the monolayer [83–85].

A large number of *in vitro* studies are currently available. However, some of these *in vitro* data are not translated into *in vivo* results, showing that some excipients that *in vitro* demonstrate positive results reveal negative results *in vivo* [32,71]. This fact suggests that additional physiological factors, such as intestinal liquid volume or endogenous amount of surfactants can impact the interaction of excipients with biological barriers.

Another current limitation on the accessible data is the study design of some *in vivo* studies. Some of these studies use ineffective doses [61] and/or high doses of surfactants [46,61]. These may result in both false positive and negative results, which in any case, will not be translationable into a daily use.

Despite these limitations, the potential of excipients to interact with our biological barriers is unquestionable and should be a subject of a deep scrutiny.

Regulatory perspective & BCS of excipients

More and more regulators have a huge concern about the risk associated to drug properties and its impact in safety efficacy and quality of the drug product. The BCS classification was an important tool in this work [86]. In fact, its translation into regulatory guidelines, such as '*Waiver of In Vivo Bioavailability and Bioequivalence Studies for Immediate-Release Solid Oral Dosage Forms Based on a Biopharmaceutics Classification System – FDA*' [87] and '*Guideline on the investigation of bioequivalence – EMA*' [88] is nothing more than the risk analysis of the drug substance properties. The concept of the BCS classification, despite it being 20 years

Table 3. Excipients effect on transporters.

Excipient	P-gp	MRP2	BCRP	OATP
Kolliphor® HS15				+
Kolliphor® EL	+	±	+	+
Kolliphor® RH40	±	+	–	
Tween-20®	+			
Tween-80®	±	+	+	
PEG400	+	+	–	+
PEG300	+			
PEG2000		+		
Myrj® 52	+		–	
Brij® 35	+			
Brij® 30			+	
Span® 20	+		+	
Span® 40	–		–	
Span® 80	–		–	
Poloxamer 181	+			
Poloxamer 188	±	–		
Poloxamer 235	+	+	+	
Poloxamer 333	+	–		
Poloxamer 403	+			
Poloxamer 407	+	±		
Vitamin E TPGS	+	+	–	
Sodium lauryl sulfate		+		
Transcutol®		+		
Sucrose laurate	+	–		
Labrasol®	+	±		
Gelucire® 44/14	+		–	
Stearyl ether	+			
Softigen® 767	+			
8:0 phosphocholine	+			
10:0 phosphocholine	+			
cis-22:6 phosphocholin	+			
Propylene glycol	–		–	
Ethyl oleate	–		–	
Triacetin	–		–	
Inwitor 742®	+			
Miglyol®	+			

(+) inhibition; (–) no inhibition; (±) variable information.
BCRP: Breast cancer resistance protein; MRP2: Multidrug resistance associated protein 2; OATP: Organic anion transporting polypeptide; P-gp: P-glycoprotein.

old, is extremely up to date based on recent ICH guidelines Q8/Q9/Q10 [1] which reinforce that the risk analysis and risk management of pharmaceutical products should start on its conception phase.

The risk associated to the drug substance regarding safety, quality and efficacy is well established and tightly controlled. However, for excipient, limited and scarce information and control is required. Nonetheless, based on the new classes of excipients and the recent studies [4,29,47,51], it is possible to conclude that the dogma related to the inertness of the excipients is a myth. As any myth, it is true until it is proven the opposite and at this stage it is possible to assume that this myth was busted. Current knowledge, particularly for drugs belonging to the BCS class III and IV and in some extension for drugs of BCS class II, excipients risk analysis and management is crucial and should be enforced. Guidelines refer that excipients are equivalent based on their action in the dosage form, however this should be extended for its *in vivo* interaction. For instance, the replacement of the surfactant Tween-80 for a similar excipient, even from chemical similar excipients, for example, Tween-20 may have a dramatic *in vivo* impact in a drug suffering of efflux by BCRP [56].

In here, it is proposed for the first time a new classification of excipients in four classes like drugs substances are. This would be the BCS of excipients (BCSE). The excipients are classified in their capacity to impact metabolization and efflux mechanisms. First class would include excipients with low risk of interference with intestinal metabolization and efflux mechanisms. Second class would include excipients that are able to interfere with intestinal metabolization without impact in the efflux mechanisms. Third class would include excipients with influence in the efflux mechanism and no impact in metabolism. The last and fourth class would include the most risky excipients, which have impact in both metabolization and efflux mechanisms. Figure 1 shows diagram of the BCSE.

BCSE class I present low risk of impact in drug safety and efficacy, and include excipients such as microcrystalline cellulose or lactose. The excipients included in this class can be replaced within technologically equivalent ones without major concerns.

BCSE class II and III excipients present a high risk, particularly when used with drugs that undergo intestinal metabolization or are efflux subtracts, respectively. Excipients known to belong to these classes are presented in Tables 2 and 3. These excipients should not be replaced by technologically similar ones without further studies. Any quali-quantitative change of these excipients in a formulation should consider using excipients from the same BCSE class. However, even within these ones, a large-scale bioequivalence study would be recommended in order to accommodate the inter-individual variability existent in the expression of metabolization and efflux mechanisms.

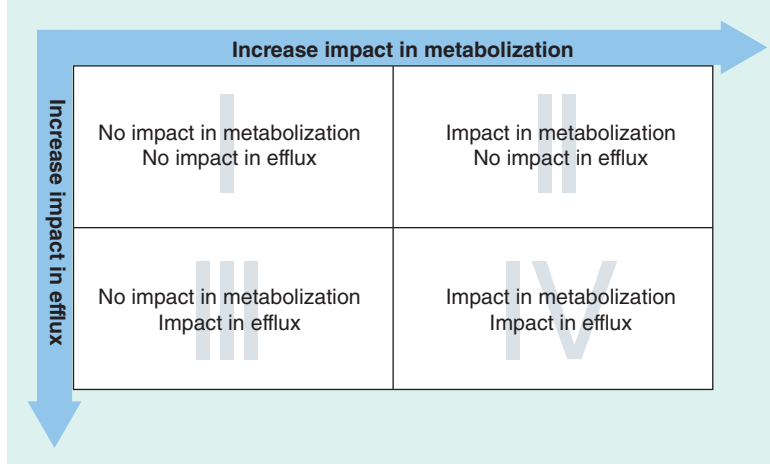

Figure 1. Biopharmaceutical classification system of excipients.

Like BCSE class II and III, the excipients belonging to the BCSE class IV are very critical because even a small change can have a dramatic impact in drug exposure and consequently efficacy and/or safety.

So far, there are no bio-inequivalence reports focused on the use of excipients. Despite being unexpected, the main reason for such absence of information, lays on the fact that negative results tend to not be published by scientific community. It is also not straightforward to demonstrate the *in vitro* or confirm the *in vivo* data. The later occurs because models are not specific and robust, being difficult to assure that a specific target was inhibited or interfered. Additionally, most of the reference drugs, stated as specific inhibitors are, in fact, acting simultaneously in multiple mechanisms, being impossible for the individualization of biological effects.

Excipients from BCSE classes II to IV are frequent key elements for the drug product performance due to their biopharmaceutical interaction and should not be avoided. However, waivers of products containing excipients from these classes and drug substances belonging to BCS class II–IV should be avoided.

At this stage, there is very limited information regarding the biopharmaceutical activity of excipients and it is highly probable that excipients can move from one to other class with the gathering of knowledge about them. Moreover, currently available data must be validated and translated into *in vivo* and clinical data. This is particularly important because negative results are generally not published, which would help to increase the number of excipients belonging to BCSE class I. Figure 2 presents a summary of the classification of the current state of the art and knowledge about the excipients.

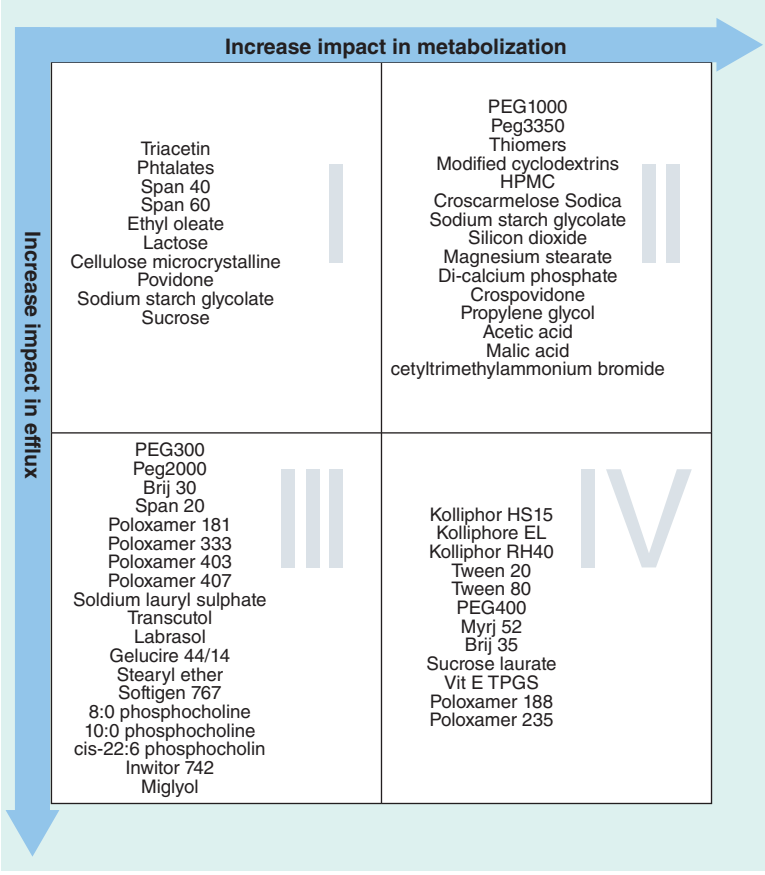

Figure 2. List of excipients included in each BCSE class.

Conclusion

Excipients are no longer considered as inert. Their ability to act as solubility enhancers is already widely known. The present manuscript showed its ability to act as permeability enhancers through intestinal inhibition of drug metabolism and efflux mechanisms.

A biopharmaceutical classification system of excipients was presented and considered as an important tool for drug development and regulatory analysis.

More and more reliable *in vitro* and *in vivo* data are required to strongly establish the BCSE.

Future perspective

The use of excipients as oral bioavailability enhancers through inhibition of efflux mechanism and/or intestinal metabolization enhancers is currently one of the hot topics in the pharmaceutical field. However, very limited information is available at this time related to these properties of the excipients. Moreover, the current *in vitro* methods are not robust and it is difficult to make sure that a specific target was inhibited or interfered. Most of the reference drugs, stated as specific inhibitors are, in fact, acting simultaneously in multiple mechanisms.

In the next years, new excipients, specifically designed to inhibit precise targets such as P-gp, BCRP or CYP3A4 will be developed by industry, being expected a raise on the number of compounds in

Executive summary

Biological mechanisms targeted by new excipients

- The two major biological mechanisms used to protect our organism from external xenobiotics are biotransformation and efflux.
- Among the metabolizing enzymes the cytochrome P450 (CYPs) are of particular importance, being responsible for the majority of phase I drug metabolism reactions. From these, CYP3A and CYP2C are the most representative in the intestinal mucosa.
- The most relevant efflux transporters expressed in the intestine include P-glycoprotein, multidrug resistance associated protein 2 and breast cancer resistance protein.
- The distribution of most CYP enzymes and efflux mechanisms is not uniform along the human GI tract.

Excipients able to interact with metabolic mechanisms

- Surfactants are the excipients in most studies regarding intestinal metabolism interaction.
- Excipients interact with CYP due to subtract completion, reduction in CYP3A protein expression or via enzymatic conformation change.

Transporters interaction

- Chelation of crucial micronutrients for an adequate enzymatic activity can be a possible mechanism to reduce efflux transport mechanisms.
- Surfactants are able to alter the membrane fluidity which can modify the orientation of the efflux pumps on its surface, preventing the substrate binding, and/or activation of pump by co-factors.
- Surfactants, polymers and lipid compounds are the ones more frequently associated to transporters interaction.

Regulatory perspective and biopharmaceutical classification system of excipients

- A biopharmaceutical classification system of excipients (BCSE) was presented.
- BCSE classified the excipients based on its ability to interfere with intestinal efflux and metabolization mechanisms.
- BCSE is a useful tool for risk management during drug product development.
- BCSE can be an adequate instrument for regulatory authorities.

BCSE classes II–IV. More and more information will be gathered related to the currently available excipients, increasing particularly the number of excipients in BCSE class I.

Moreover, new, reliable and robust *in vitro* methods will be developed or optimized for specific transporters or metabolizers. A significant increase in *in vivo* data, including data gathered from human studies, is expected to be generated in the upcoming years, which will allow to have a much better picture of the excipients' ability to interfere with biological barriers. Finally, regulatory authorities will increase its control and implement specific controls over excipients from BCSE classes II–IV.

The BCSE classification will be an important tool in the pharmaceutical development field. However, a risk analysis based on BCSE classification and its association to specific drugs or drug classes must be done to strengthen the application of this classification.

Financial & competing interests disclosure

S Marques gratefully acknowledges Fundação para a Ciência e a Tecnologia (FCT), Portugal for financial support (grant SFRH/BPD/75905/2011). This work was financed by FEDER – Fundo Europeu de Desenvolvimento Regional funds through the COMPETE 2020 – Operacional Programme for Competitiveness and Internationalisation (POCI), Portugal 2020, and by Portuguese funds through FCT/Ministério da Ciência, Tecnologia e Inovação in the framework of the project "Institute for Research and Innovation in Health Sciences" (POCI-01–0145-FEDER-007274). No writing assistance was utilized in the production of this manuscript.

References

Papers of special note have been highlighted as:
• of interest; •• of considerable interest

1 EMA. ICH guideline Q8 (R2) on pharmaceutical development. (2015). www.ich.org/fileadmin/Public_Web_Site/ICH_Products/Guidelines/Quality/Q8_R1/Step4/Q8_R2_Guideline.pdf

2 EMA. Guideline on excipients in the dossier for application for marketing authorisation of a medicinal product. (2007). www.ema.europa.eu/docs/en_GB/document_library/Scientific_guideline/2009/09/WC500003382.pdf

3 Chaudhari SP, Patil PS. Pharmaceutical excipients: a review. *Internat. J. Adv. Pharm. Biol. Chem.* 1(1), 21–34 (2012).

• **Review of excipients impact on the intestinal metabolism and transporters.**

4 Zhang W, Li Y, Zou P, Wu M, Zhang Z, Zhang T. The effects of pharmaceutical excipients on gastrointestinal tract metabolic enzymes and transporters-an update. *AAPS J.* 18(4), 830–843 (2016).

5 Peng Soh JL, Liew CV, Sia Heng PW. Impact of excipient variability on drug product processing and performance. *Curr. Pharm. Des.* 21(40), 5890–5899 (2015).

6 Rowe RC, Sheskey PJ, Quinn ME. *Handbook of Pharmaceutical Excipients.* Pharmaceutical Press and American Pharmacists association. London, UK (2009).

7 Mwesigwa E, Basit AW. An investigation into moisture barrier film coating efficacy and its relevance to drug stability in solid dosage forms. *Int. J. Pharm.* 497(1–2), 70–77 (2016).

8 Patel P, Dave A, Vasava A. Formulation and characterization of sustained release dosage form of moisture sensitive drug. *Int. J. Pharm. Investig.* 5(2), 92–100 (2015).

9 Joshi S, Petereit HU. Film coatings for taste masking and moisture protection. *Int. J. Pharm.* 457(2), 395–406 (2013).

10 Czarnocka JK, Alhnan MA. Gastro-resistant characteristics of GRAS-grade enteric coatings for pharmaceutical and nutraceutical products. *Int. J. Pharm.* 486(1–2), 167–174 (2015).

11 Raffin RP, Colomé LM, Hoffmeister CR *et al.* Pharmacokinetics evaluation of soft agglomerates for prompt delivery of enteric pantoprazole-loaded microparticles. *Eur. J. Pharm. Biopharm.* 74(2), 275–280 (2010).

12 Lainé AL, Price D, Davis J *et al.* Enhanced oral delivery of celecoxib via the development of a supersaturable amorphous formulation utilising mesoporous silica and co-loaded HPMCAS. *Int. J. Pharm.* 512(1), 118–125 (2016).

13 Yue H, Nicholson SJ, Young JD *et al.* Development of a control strategy for benzene impurity in HPMCAS-stabilized spray-dried dispersion drug products using a science-based and risk-based approach. *Pharm. Res.* 32(8), 2636–2648 (2015).

14 Dave VS, Saoji SD, Raut NA, Haware RV. Excipient variability and its impact on dosage form functionality. *J. Pharm. Sci.* 104(3), 906–915 (2015).

15 Lipinski CA, Lombardo F, Dominy BW, Feeney PJ. Experimental and computational approaches to estimate solubility and permeability in drug discovery and development settings. *Adv. Drug Deliv. Rev.* 23(1–3), 3–25 (1997).

16 Lipinski CA. Rule of five in 2015 and beyond: target and ligand structural limitations, ligand chemistry structure and drug discovery project decisions. *Adv. Drug. Deliv. Rev.* 101, 34–41 (2016).

17 Vasconcelos T, Marques S, das Neves J, Sarmento B. Amorphous solid dispersions: rational selection of a manufacturing process. *Adv. Drug. Deliv. Rev.* 100, 85–101 (2016).

18 Loftsson T. Excipient pharmacokinetics and profiling. *Int. J. Pharm.* 480(1–2), 48–54 (2015).

19 Hanna J, Bian J, Hogan WR. An accurate and precise representation of drug ingredients. *J. Biomed. Semantics* 7, 7 (2016).

20 Engel A, Oswald S, Siegmund W, Keiser M. Pharmaceutical excipients influence the function of human uptake transporting proteins. *Mol. Pharm.* 9(9), 2577–2581 (2012).

21 Ren X, Mao X, Si L *et al.* Pharmaceutical excipients inhibit cytochrome P450 activity in cell free systems and after systemic administration. *Eur. J. Pharm. Biopharm.* 70(1), 279–288 (2008).

22 Pang KS. Modeling of intestinal drug absorption: roles of transporters and metabolic enzymes (for the Gillette review series). *Drug Metab. Dispos.* 31(12), 1507–1519 (2003).

• **Review of excipients impact on the intestinal transporters.**

23 Paine MF, Khalighi M, Fisher JM *et al.* Characterization of interintestinal and intraintestinal variations in human CYP3A-dependent metabolism. *J. Pharmacol. Exp. Ther.* 283(3), 1552–1562 (1997).

• **Review of excipients impact on the intestinal metabolism mechanisms.**

24 Estudante M, Morais JG, Soveral G, Benet LZ. Intestinal drug transporters: an overview. *Adv. Drug Deliv. Rev.* 65(10), 1340–1356 (2013).

25 Shugarts S, Benet LZ. The role of transporters in the pharmacokinetics of orally administered drugs. *Pharm. Res.* 26(9), 2039–2054 (2009).

26 Mottino AD, Hoffman T, Jennes L, Vore M. Expression and localization of multidrug resistant protein mrp2 in rat small intestine. *J. Pharmacol. Exp. Ther.* 293(3), 717–723 (2000).

27 Goole J, Lindley DJ, Roth W *et al.* The effects of excipients on transporter mediated absorption. *Int. J. Pharm.* 393(1–2), 17–31 (2010).

28 Weinheimer M, Fricker G, Burhenne J, Mylius P, Schubert R. The application of P-gp inhibiting phospholipids as novel oral bioavailability enhancers – an *in vitro* and *in vivo* comparison. *Eur. J. Pharm. Sci.* doi:10.1016/j.ejps.2016.08.055 (2016) (Epub ahead of print).

29 Yang X, Liu K. P-gp inhibition-based strategies for modulating pharmacokinetics of anticancer drugs: an update. *Curr. Drug. Metab.* (2016).

•• **Gives an overview on the mechanisms to improve bioavailability through excipients modulation of efflux mechanisms.**

30 Hosea NA, Guengerich FP. Oxidation of nonionic detergents by cytochrome P450 enzymes. *Arch. Biochem. Biophys.* 353(2), 365–373 (1998).

31 Tompkins L, Lynch C, Haidar S, Polli J, Wang H. Effects of commonly used excipients on the expression of CYP3A4 in colon and liver cells. *Pharm. Res.* 27(8), 1703–1712 (2010).

32 Ren X, Mao X, Cao L *et al.* Nonionic surfactants are strong inhibitors of cytochrome P450 3A biotransformation activity *in vitro* and *in vivo*. *Eur. J. Pharm. Sci.* 36(4–5), 401–411 (2009).

33 Bravo González RC, Huwyler J, Boess F, Walter I, Bittner B. *In vitro* investigation on the impact of the surface-active excipients Cremophor EL, Tween 80 and Solutol HS 15 on the metabolism of midazolam. *Biopharm. Drug Dispos.* 25(1), 37–49 (2004).

•• **One of the few studies evaluating the effect of well-known excipients in the intestinal metabolism mechanisms.**

34 Schulze JD, Waddington WA, Eli PJ, Parsons GE, Coffin MD, Basit AW. Concentration-dependent effects of polyethylene glycol 400 on gastrointestinal transit and drug absorption. *Pharm. Res.* 20(12), 1984–1988 (2003).

35 Johnson BM, Charman WN, Porter CJ. An *in vitro* examination of the impact of polyethylene glycol 400, Pluronic P85, and vitamin E d-alpha-tocopheryl polyethylene glycol 1000 succinate on P-glycoprotein efflux and enterocyte-based metabolism in excised rat intestine. *AAPS PharmSci.* 4(4), E40 (2002).

36 Mudra DR, Borchardt RT. Absorption barriers in the rat intestinal mucosa. 3: effects of polyethoxylated solubilizing agents on drug permeation and metabolism. *J. Pharm. Sci.* 99(2), 1016–1027 (2010).

37 Guan Y, Huang J, Zuo L *et al.* Effect of pluronic P123 and F127 block copolymer on P-glycoprotein transport and CYP3A metabolism. *Arch. Pharm. Res.* 34(10), 1719–1728 (2011).

38 Christiansen A, Backensfeld T, Denner K, Weitschies W. Effects of non-ionic surfactants on cytochrome P450-mediated metabolism *in vitro*. *Eur. J. Pharm. Biopharm.* 78(1), 166–172 (2011).

39 Rao Z, Si L, Guan Y, Pan H, Qiu J, Li G. Inhibitive effect of cremophor RH40 or tween 80-based self-microemulsiflying drug delivery system on cytochrome P450 3A enzymes in murine hepatocytes. *J. Huazhong. Univ. Sci. Technolog. Med. Sci.* 30(5), 562–568 (2010).

40 Martin P, Giardiello M, McDonald TO, Rannard SP, Owen A. Mediation of *in vitro* cytochrome p450 activity by common pharmaceutical excipients. *Mol. Pharm.* 10(7), 2739–2748 (2013).

41 Huang J, Si L, Jiang L, Fan Z, Qiu J, Li G. Effect of pluronic F68 block copolymer on P-glycoprotein transport and CYP3A4 metabolism. *Int. J. Pharm.* 356(1–2), 351–353 (2008).

42 Zhu S, Huang R, Hong M *et al.* Effects of polyoxyethylene (40) stearate on the activity of P-glycoprotein and cytochrome P450. *Eur. J. Pharm. Sci.* 37(5), 573–580 (2009).

43 Iqbal J, Sakloetsakun D, Bernkop-Schnürch A. Thiomers: inhibition of cytochrome P450 activity. *Eur. J. Pharm. Biopharm.* 78(3), 361–365 (2011).

44 Ishikawa M, Yoshii H, Furuta T. Interaction of modified cyclodextrins with cytochrome P-450. *Biosci. Biotechnol. Biochem.* 69(1), 246–248 (2005).

45 Takeshita A, Igarashi-Migitaka J, Nishiyama K, Takahashi H, Takeuchi Y, Koibuchi N. Acetyl tributyl citrate, the most widely used phthalate substitute plasticizer, induces cytochrome p450 3a through steroid and xenobiotic receptor. *Toxicol. Sci.* 123(2), 460–470 (2011).

46 Wang HJ, Hsiong CH, Ho ST *et al.* Commonly used excipients modulate UDP-glucuronosyltransferase 2b7 activity to improve nalbuphine oral bioavailability in humans. *Pharm. Res.* 31(7), 1676–1688 (2014).

47 Xiao L, Yi T, Chen M, Lam CW, Zhou H. A new mechanism for increasing the oral bioavailability of scutellarin with Cremophor EL: activation of MRP3 with concurrent inhibition of MRP2 and BCRP. *Eur. J. Pharm. Sci.* 93, 456–467 (2016).

48 Akhtar N, Ahad A, Khar RK *et al.* The emerging role of P-glycoprotein inhibitors in drug delivery: a patent review. *Expert Opin. Ther. Pat.* 21(4), 561–576 (2011).

49 Al-Mohizea AM. Influence of intestinal efflux pumps on the absorption and transport of furosemide. *Saudi. Pharm. J.* 18(2), 97–101 (2010).

50 Bromberg L, Alakhov V. Effects of polyether-modified poly(acrylic acid) microgels on doxorubicin transport in human intestinal epithelial Caco-2 cell layers. *J. Control Rel.* 88(1), 11–22 (2003).

51 Choi YA, Yoon YH, Choi K *et al.* Enhanced oral bioavailability of morin administered in mixed micelle formulation with PluronicF127 and Tween80 in rats. *Biol. Pharm. Bull.* 38(2), 208–217 (2015).

52 Kiss L, Hellinger É, Pilbat AM *et al.* Sucrose esters increase drug penetration, but do not inhibit p-glycoprotein in caco-2 intestinal epithelial cells. *J. Pharm. Sci.* 103(10), 3107–3119 (2014).

53 Collnot EM, Baldes C, Wempe MF *et al.* Mechanism of inhibition of P-glycoprotein mediated efflux by vitamin E TPGS: influence on ATPase activity and membrane fluidity. *Mol. Pharm.* 4(3), 465–474 (2007).

54 Huang LM, Zhao JH, Wang GC, Zhou JP. Recent advance in the mechanism study of polymeric inhibitors of P-glycoprotein. *Yao Xue Xue Bao* 45(10), 1224–1231 (2010).

55 Shah D, Paruchury S, Matta M *et al.* A systematic evaluation of solubility enhancing excipients to enable the generation of permeability data for poorly soluble compounds in Caco-2 model. *Drug Metab. Lett.* 8(2), 109–118 (2014).

56 Yamagata T, Kusuhara H, Morishita M, Takayama K, Benameur H, Sugiyama Y. Effect of excipients on breast cancer resistance protein substrate uptake activity. *J. Control Rel.* 124(1–2), 1–5 (2007).

•• **Gives an overview on the molecular mechanism that polymers use to inhibit P-glycoprotein.**

57 Aller SG, Yu J, Ward A *et al.* Structure of P-glycoprotein reveals a molecular basis for poly-specific drug binding. *Science* 323(5922), 1718–1722 (2009).

58 Tayrouz Y, Ding R, Burhenne J *et al.* Pharmacokinetic and pharmaceutic interaction between digoxin and Cremophor RH40. *Clin. Pharmacol. Ther.* 73(5), 397–405 (2003).

59 Katneni K, Charman SA, Porter CJ. Impact of cremophor-EL and polysorbate-80 on digoxin permeability across rat jejunum: delineation of thermodynamic and transporter related events using the reciprocal permeability approach. *J. Pharm. Sci.* 96(2), 280–293 (2007).

60 Regev R, Katzir H, Yeheskely-Hayon D, Eytan GD. Modulation of P-glycoprotein-mediated multidrug resistance by acceleration of passive drug permeation across the plasma membrane. *FEBS J.* 274(23), 6204–6214 (2007).

61 Tomaru A, Takeda-Morishita M, Maeda K *et al.* Effects of Cremophor EL on the absorption of orally administered saquinavir and fexofenadine in healthy subjects. *Drug Metab. Pharmacokinet.* 30(3), 221–226 (2015).

62 Hanke U, May K, Rozehnal V, Nagel S, Siegmund W, Weitschies W. Commonly used nonionic surfactants interact differently with the human efflux transporters ABCB1 (p-glycoprotein) and ABCC2 (MRP2). *Eur. J. Pharm. Biopharm.* 76(2), 260–268 (2010).

63 Ma L, Wei Y, Zhou Y, Ma X, Wu X. Effects of Pluronic F68 and Labrasol on the intestinal absorption and pharmacokinetics of rifampicin in rats. *Arch. Pharm. Res.* 34(11), 1939–1943 (2011).

64 Rege BD, Kao JP, Polli JE. Effects of nonionic surfactants on membrane transporters in Caco-2 cell monolayers. *Eur. J. Pharm. Sci.* 16(4–5), 237–246 (2002).

•• **Gives an overview on the surfactant's inhibition on P-glycoprotein and also multidrug resistance associated protein 2.**

65 Li M, Si L, Pan H *et al.* Excipients enhance intestinal absorption of ganciclovir by P-gp inhibition: assessed *in vitro* by everted gut sac and *in situ* by improved intestinal perfusion. *Int. J. Pharm.* 403(1–2), 37–45 (2011).

66 Li GF, Tan YF, Guo D, Wang L. Effect of Tween-80 on the permeability of rhodamine 123, a P-gp substrate across rat intestinal membranes *in vitro*. *Nan Fang Yi Ke Da Xue Xue Bao* 28(4), 579–581 (2008).

67 Shaik N, Giri N, Elmquist WF. Investigation of the micellar effect of pluronic P85 on P-glycoprotein inhibition: cell accumulation and equilibrium dialysis studies. *J. Pharm. Sci.* 98(11), 4170–4190 (2009).

68 Batrakova EV, Li S, Li Y, Alakhov VY, Kabanov AV. Effect of pluronic P85 on ATPase activity of drug efflux transporters. *Pharm. Res.* 21(12), 2226–2233 (2004).

69 Krylova OO, Pohl P. Ionophoric activity of pluronic block copolymers. *Biochemistry* 43(12), 3696–3703 (2004).

70 Yu H, Hu YQ, Ip FC, Zuo Z, Han YF, Ip NY. Intestinal transport of bis(12)-hupyridone in Caco-2 cells and its improved permeability by the surfactant Brij-35. *Biopharm. Drug Dispos.* 32(3), 140–150 (2011).

71 Cornaire G, Woodley J, Hermann P, Cloarec A, Arellano C, Houin G. Impact of excipients on the absorption of P-glycoprotein substrates *in vitro* and *in vivo*. *Int. J. Pharm.* 278(1), 119–131 (2004).

72 Sachs-Barrable K, Thamboo A, Lee SD, Wasan KM. Lipid excipients Peceol and Gelucire 44/14 decrease P-glycoprotein mediated efflux of rhodamine 123 partially due to modifying P-glycoprotein protein expression within Caco-2 cells. *J. Pharm. Pharm. Sci.* 10(3), 319–331 (2007).

73 Parsa A, Saadati R, Abbasian Z, Azad Aramaki S, Dadashzadeh S. Enhanced permeability of etoposide across everted sacs of rat small intestine by vitamin E-TPGS. *Iran J. Pharm. Res,* 12(Suppl.), 37–46 (2013).

74 Dintaman JM, Silverman JA. Inhibition of P-glycoprotein by D-alpha-tocopheryl polyethylene glycol 1000 succinate (TPGS). *Pharm. Res.* 16(10), 1550–1556 (1999).

75 Bogman K, Zysset Y, Degen L *et al.* P-glycoprotein and surfactants: effect on intestinal talinolol absorption. *Clin. Pharmacol. Ther.* 77(1), 24–32 (2005).

76 Ashiru-Oredope DA, Patel N, Forbes B, Patel R, Basit AW. The effect of polyoxyethylene polymers on the transport of ranitidine in Caco-2 cell monolayers. *Int. J. Pharm.* 409(1–2), 164–168 (2011).

77 Collnot EM, Baldes C, Schaefer UF, Edgar KJ, Wempe MF, Lehr CM. Vitamin E TPGS P-glycoprotein inhibition mechanism: influence on conformational flexibility, intracellular ATP levels, and role of time and site of access. *Mol. Pharm.* 7(3), 642–651 (2010).

78 Simon S, Schubert R. Inhibitory effect of phospholipids on P-glycoprotein: cellular studies in Caco-2, MDCKII mdr1 and MDCKII wildtype cells and P-gp ATPase activity measurements. *Biochim. Biophys. Acta.* 1821(9), 1211–1223 (2012).

79 Barta CA, Sachs-Barrable K, Feng F, Wasan KM. Effects of monoglycerides on P-glycoprotein: modulation of the activity and expression in Caco-2 cell monolayers. *Mol. Pharm.* 5(5), 863–875 (2008).

80 Li L, Yi T, Lam CW. Inhibition of human efflux transporter ABCC2 (MRP2) by self-emulsifying drug delivery system: influences of concentration and combination of excipients. *J. Pharm. Pharm. Sci.* 17(4), 447–460 (2014).

81 Li L, Yi T, Lam CW. Interactions between human multidrug resistance related protein (MRP2; ABCC2) and excipients commonly used in self-emulsifying drug delivery systems (SEDDS). *Int. J. Pharm.* 447(1–2), 192–198 (2013).

82 Legen I, Kracun M, Salobir M, Kerc J. The evaluation of some pharmaceutically acceptable excipients as permeation enhancers for amoxicillin. *Int. J. Pharm.* 308(1–2), 84–89 (2006).

83 Bu P, Narayanan S, Dalrymple D, Cheng X, Serajuddin AT. Cytotoxicity assessment of lipid-based self-emulsifying drug delivery system with Caco-2 cell model: cremophor EL as the surfactant. *Eur. J. Pharm. Sci.* 91, 162–171 (2016).

84 Dimitrijevic D, Shaw AJ, Florence AT. Effects of some non-ionic surfactants on transepithelial permeability in Caco-2 cells. *J. Pharm. Pharmacol.* 52(2), 157–162 (2000).

85 Ujhelyi Z, Fenyvesi F, Váradi J *et al.* Evaluation of cytotoxicity of surfactants used in self-micro emulsifying drug delivery systems and their effects on paracellular transport in Caco-2 cell monolayer. *Eur. J. Pharm. Sci.* 47(3), 564–573 (2012).

86 Amidon GL, Lennernäs H, Shah VP, Crison JR. A theoretical basis for a biopharmaceutic drug classification: the correlation of *in vitro* drug product dissolution and *in vivo* bioavailability. *Pharm. Res.* 12(3), 413–420 (1995).

87 FDA. Waiver of *in vivo* bioavailability and bioequivalence studies for immediate-release solid oral dosage forms based on a biopharmaceutics classification system. (2015). www.fda.gov/downloads/Drugs/Guidances/ucm070246.pdf

88 EMA. Guideline on the investigation of bioequivalence (Eds). (2010). www.ema.europa.eu/docs/en_GB/document_library/Scientific_guideline/2010/01/WC500070039.pdf

Advanced Drug Delivery Reviews 100 (2016) 85–101

Contents lists available at ScienceDirect

Advanced Drug Delivery Reviews

journal homepage: www.elsevier.com/locate/addr

Amorphous solid dispersions: Rational selection of a manufacturing process☆

Teófilo Vasconcelos [a,b,c,d], Sara Marques [e], José das Neves [c,d], Bruno Sarmento [c,d,f,*]

[a] BIAL-Portela & Cª, S.A., Avenida da Siderugia Nacional, 4745-457 Trofa, Portugal
[b] Instituto de Ciências Biomédicas Abel Salazar, University of Porto, Rua de Jorge Viterbo Ferreira, n° 228, 4050-313 Porto, Portugal
[c] I3S—Instituto de Investigação e Inovação em Saúde, Universidade do Porto, Rua do Campo Alegre, 823, 4150-180 Porto, Portugal
[d] INEB—Instituto de Engenharia Biomédica, Universidade do Porto, Rua do Campo Alegre, 823, 4150-180 Porto, Portugal
[e] CIBIO/InBIO-UP—Research Centre in Biodiversity and Genetic Resources, University of Porto, Rua Padre Armando Quintas, n° 7, 4485-661 Vairão, Portugal
[f] Instituto de Investigação e Formação Avançada em Ciências e Tecnologias da Saúde and Instituto Universitário de Ciências da Saúde, CESPU, Rua Central de Gandra 1317, 4585-116 Gandra, Portugal

ARTICLE INFO

Article history:
Received 15 October 2015
Received in revised form 21 December 2015
Accepted 19 January 2016
Available online 27 January 2016

Keywords:
Amorphous products
Solid dispersions
Solvent evaporation process
Melting process
Laboratorial scale
Industrial scale
Drug delivery

ABSTRACT

Amorphous products and particularly amorphous solid dispersions are currently one of the most exciting areas in the pharmaceutical field. This approach presents huge potential and advantageous features concerning the overall improvement of drug bioavailability.
Currently, different manufacturing processes are being developed to produce amorphous solid dispersions with suitable robustness and reproducibility, ranging from solvent evaporation to melting processes. In the present paper, laboratorial and industrial scale processes were reviewed, and guidelines for a rationale selection of manufacturing processes were proposed. This would ensure an adequate development (laboratorial scale) and production according to the good manufacturing practices (GMP) (industrial scale) of amorphous solid dispersions, with further implications on the process validations and drug development pipeline.

Contents

Abbreviations: ASES, Aerosol solvent extraction system; BCS, Biopharmaceutical classification system; DMSO, Dimethyl sulfoxide; DSC, Differential Scanning Calorimetry; EMA, European Medicines Agency; EU, European Union;; FDA, Food and Drug Administration; GAS, Gaseous antisolvent; GMP, Good manufacturing practices; HME, Hot melt extrusion; HPC, hydroxypropylcellulose; HPMC, Hydroxypropyl methylcellulose; HPMCAS, Hydroxypropyl methylcellulose acetate succinate; ICH, International Conference Harmonization; N.A., Not available.; PCA, Particles by compressed antisolvent; PEG, Polyethyleneglycol; PEO, Polyethylene oxide; PGSS, Particles from gas saturated solutions; PVOH, Polyvinyl alcohol; PVP, Povidone; PVP-VA, Povidone-vinyl acetate; RESS, Rapid expansion of a supercritical solution; SAS, Supercritical antisolvent; SCFs, Supercritical fluids; SEDS, Solution enhanced dispersion by supercritical fluids; SEM, Scanning Electron Microscopy; SLS, Sodium Lauryl Sulphate; TPGS, d-alpha Tocopheryl Polyethylene Glycol 1000 Succinate; XRPD, X-ray Powder Diffraction; US, United States of America.

☆ This review is part of the *Advanced Drug Delivery Reviews* theme issue on "Amorphous pharmaceutical solids".

* Corresponding author. Tel.: +351 226074900; fax: +351 226094567.
E-mail address: Bruno.sarmento@ineb.up.pt (B. Sarmento).

http://dx.doi.org/10.1016/j.addr.2016.01.012
0169-409X/

1. Introduction

The majority of drugs molecules developed by the pharmaceutical industry during the last decades of the 20th century were classified according to the biopharmaceutical classification system (BCS) as class I drugs [1,2]. This means that most of the drugs presented high permeability and high solubility. If a molecule failed to meet these criteria, it would most probably be discarded from the industry development pipeline due to concerns about low bioavailability and/or troublesome formulation process [1].

In the 1990s, with the advent of Computer Science and its application to the pharmaceutical field, a new paradigm was raised in the Pharmaceutical Industry regarding drug candidate selection, introducing target-modulation candidate selection [3–5]. This new tool provided the Pharmaceutical Industry with the ability to produce more potent and specific drugs. However, these more potent drugs generally present poor water solubility, and consequently, fit BCS classes II or IV [6,7]. This change in drug candidate properties brought new challenges since most of the new molecules resulted in poor *in vivo* dissolution and consequently poor and/or highly variable bioavailability [8]. Additionally, most of them present small absorption windows, generally located in the upper small intestine [6,9]. In addition, and emphasizing the current challenges faced by the Pharmaceutical Industry, several of these drugs present poor permeability or are substrates of efflux transporters [10,11].

The presented challenges forced the Pharmaceutical Industry to pursuit approaches to improve dug solubility, exploring chemical, physical or formulation approaches [6]. Chemical approaches comprise molecular modification of drug structure, such as the inclusion of polar groups, resulting in the formation of new chemical entities that may present different potency and pharmacokinetics [12]. Other examples of chemical approaches include the formation of salts [12–18] and co-crystals [19], but their application is very restricted. Salts are only feasible for weak acid or basic drugs and co-crystals generally do not sufficiently enhance *in vivo* drug solubility. Additionally, both salts and co-crystals tend to precipitate *in vivo* [20,21]. The basic principle behind all physical approaches is that increasing the contact surface area enhances solubility [15]. This is accomplished by particle size reduction, resulting in crystals in the micro- or nano-size range [22,23]. The feasibility and simplicity of this approach is adequate in some cases. However, tends to be inadequate for drugs presenting water solubility below 50 μm/mL [22]. Formulation approaches consist in the production of liquid systems based on lipid vehicles and/or surfactants [24–26], or solid formulations that generally resembles in using carrier(s) [15]. From the later, amorphous solid dispersions depict one of the most interesting approaches, since drug presents a reduced particle size, improved wettability, high porosity and enhanced solubility [6]. A wide range of manufacturing processes to obtain amorphous products are currently available and will be further explored in this review, as well as, a rational approach for the selection of the manufacturing process.

2. Amorphous products

Amorphous products are pharmaceutical materials characterized by its solid-state nature and lack of distinct intermolecular arrangement, without crystalline structure and, consequently, with poor thermodynamically stability [6,7]. In a standard crystalline structure, the solubility/dissolution process firstly needs to break the crystal structure in order to occur molecular dissolution. In the case of amorphous products, the first step is abbreviated and lower energy is required to promote dissolution [7,27]. Amorphous materials also present broad background signal patterns in X-ray Powder Diffraction (XRPD) analysis, absence of enthalpy energy related to melting processes, and irregular surface structures, among other typical thermal, microscopic and spectroscopic properties, such as dynamic mechanical properties, particle porosity or Infra-red spectrum, respectively [28].

Amorphous products may be classified in two types: (i) molecularly pure and (ii) solid dispersions. Main features of different amorphous products are presented in Table 1.

2.1. Molecularly pure amorphous products

Molecularly pure amorphous products are only composed by the pure drug, which due to the specific manufacturing process results in amorphous products. Generally, processes to obtain molecularly pure amorphous products require a fast solvent evaporation process. It can be achieved by using rotary evaporator evaporation, spray-drying or freeze-drying. Fast removal of the solvent prevents the formation of crystal structures and, thus, random amorphous materials are formed [29]. Traditionally, pure amorphous products are obtained in a laboratorial scale and are undesirable because they are difficult to scale up due to their high instability, a consequence of their high-energy state [29]. Hence, pure amorphous products are rapidly converted into crystalline structures [29,30]. Zafirlukast (Accolate®, Astra Zeneca) is one of the very few commercially available molecularly pure amorphous drugs. This amorphous neutral drug is known to convert to a monohydrate form in the presence of water, with decreased bioavailability compared to the amorphous form [31,32]. Another example is cefuroxime axetil (Ceftin®, GlaxoSmithKline) [33,34], an amorphous drug that crystallizes in the presence of water [30].

2.2. Amorphous solid dispersions

Amorphous solid dispersions can be defined as molecular mixtures of poor water soluble drugs with hydrophilic carriers, responsible for modulate drug release profile, and characterized by the reduction of drug particle size to a molecular level solubilizing or co-dissolving the drug in the soluble carriers. Overall, they provide better wettability and dispersibility as the drug is in its supersaturated state due to forced solubilisation in the hydrophilic carriers [6,35–40]. Solid dispersions can be classified as first, second or third generation [6]. Briefly, first generation originates crystalline solid dispersions where a molecule of a crystalline carrier replaces one drug molecule in its crystalline structure. Second generation originates amorphous solid dispersions and uses polymeric carriers. The third generation comprises amorphous solid dispersion composed by a combination of amorphous carriers and most preferably a combination of amorphous carriers and surfactants, presenting enhanced drug release, long term stability and higher bioavailability [6].

Table 1
Classification and characteristics of amorphous products.

Amorphous products/materials	Characteristics	Production	Advantages	Disadvantages
Molecularly pure	Chemically composed by the pure drug alone	Laboratorial scale (mainly)	Enhanced solubility	Difficult to scale up and solid state instability
Solid dispersions	Formulated products	Laboratorial and industrial scales	Solid state stability and enhanced solubility	Drug substance loading in the final formulation

Amorphous solid dispersions use specific carriers that amorphise the drug substance and stabilize it in the solid state [27,41,42]. These formulated amorphous products with adequate stability drawn increased interest, particularly over the last decade, resulting in an increase of marketed products using this technology as documented in Table 2.

Solid dispersions currently represent the most exciting research and development field related to pharmaceutical amorphous products. The increasing number of medicines under development and reaching the market [43,44] justifies that the remaining review will be focused on this topic.

3. Manufacturing of amorphous products

Two major distinct processes are used to manufacture amorphous materials: solvent evaporation and melting. Both have been shown useful at the laboratorial and industrial scales (production accordingly to the good manufacturing practices—GMP). Some mechanical processes, such as ball milling or grinding, are also able to induce some amorphisation [45]. However, degree and robustness of amorphisation are very low and, thus, of limited usefulness [6,45].

Solvent evaporation processes consist in solubilizing both drug substance and carrier(s) in common solvents or solvent mixture followed by solvent removal. Non-covalent molecular interactions between drug and carrier(s) during solvent removal are responsible for the formation of an amorphous product [6,46,47].

As for melting processes, these generally comprise solubilizing a drug in a molten of amorphous polymer(s). The molten product is further solidified by cooling originating an amorphous solid dispersion [6].

3.1. General advantages and disadvantages

Both solvent evaporation and melting processes have their own advantages and drawbacks that should be considered in order to select the most suitable manufacturing process. Noteworthy, different manufacturing processes may originate products with different properties [48,49]. Therefore, an adequate selection of the manufacturing process is crucial for the success of the product.

In solvent evaporation processes the thermal decomposition of drugs and/or carriers is preventable in most cases since organic solvent evaporation can be performed at low temperature [50]. Additionally, the wide availability of organic solvents allows to select a solvent or mixture of solvents able to solubilize both drug and carrier(s) [50]. However, organic solvents may be difficult to remove from the final product, which can be especially concerning when highly toxic solvents are required to be employed [24,51]. Moreover, it is also possible that slight alterations in the conditions used for solvent evaporation may lead to large changes in product performance [52].

Avoidance of organic solvent use is a major advantage of melting methods as it better assures product safety and compliance with quality control and environmental requirements [53]. High temperatures can induce drug degradation, being this the major drawback of melting processes. Furthermore, some drugs may decompose under melting, thus

Table 2
Examples of commercially available medicines using solid dispersion technologies.

Product name	Drug substance	Carrier	Preparation method	Year of approval
Cesamet™ (US)/Canemes®(Austria)	Nabilone	PVP	N.A.	1985 (FDA)
Sporanox®	Itraconazole	HPMC	Spray drying on sugar beads	1992
Prograf™	Tacrolimus	HPMC	Spray drying	1994 (FDA/MHRA)
Gris-PEG™	Griseofluvin	PEG	Melt extrusion	2000 (FDA)
Crestor®	Rosuvastatin	HPMC	Spray drying	2004 (EMA) 2002 (FDA)
Cymbalta®	Duloxetine	HPMCAS	N/A	2004 (EMA/FDA)
Kaletra®	Lopinavir/ritonavir	PVP-VA	Melt extrusion	2005 (FDA) 2001(EMA)
Eucreas® Galvumet™	Vildagliptin/Metformin HCL	HPC	Melt extrusion (metfotrmin)	2007 (EMA)
Intelence®	Etravirine	HPMC	Spray drying	2008 (EMA/FDA)
Modigraf®	Tacrolimus	HPMC	Spray drying	2009 (EMA)
Samsca®	Tolvaptan	N/A	Granulation	2009 (EMA/FDA)
Zotress™ (US) Certican®/Votubia® (EU)	Everolimus	HPMC	Spray drying	2010 (EMA/FDA)
Onmel™	Itraconazole	HPMC	Melt extrusion	2010 (FDA)
Fenoglide™	Fenofibrate	PEG/Polaxamer 188	Spray melt	2010 (FDA)
Novir®	Ritonavir	PVP-VA	Melt extrusion	2010 (FDA) 2009 (EMA)
Incivek™ (US)/Incivo ® (EU)	Telaprevir	HPMCAS	Spray drying	2011 (EMA/FDA)
Zelboraf®	Vemurafenib	HPMCAS	Co-precipitation	2012 (EMA) 2011 (FDA)
Kalydeco®	Ivacaftor	HPMCAS / SLS	Spray drying	2012 (EMA/FDA)
Noxafil®	Posaconazole	HPMCAS	Melt-extrusion	2014 (EMA) 2013 (FDA)
Viekira™ (US)/Viekirax® (EU)	Ombitasvir/Paritaprevir/Ritonavir	PVP-VA/TPGS	Melt extrusion	2014 (EMA/FDA)
Orkambi®	Lumacaftor/Ivacaftor	HPMCAS/SLS	Spray drying	2015 (EMA/FDA)

HPMC—hydroxypropyl methylcellulose; HPC—hydroxypropylcellulose; HPMCAS—hydroxypropyl methylcellulose acetate succinate; PEG—polyethylene glycol; PVP—povidone; PVP-VA—povidone-vinyl acetate (copovidone); SLS—Sodium Lauryl sulfate; TPGS—d-alpha Tocopheryl Polyethylene Glycol 1000 Succinate. N.A.—Not available; US—United States of America; EU—European Union; EMA—European Medicines Agency; FDA—Food and Drug Administration; MHRA—Medicines and Health Products Regulatory Agency.

Table 3
List and description of some recent studies employing solvent evaporation methods.

Drug	Carrier	Drug: Carrier(s) ratio	Technique	Solvent	Solid content in solution	Solvent evaporation temperature	Comment	Ref
Atorvastatin	Soluplus®	2:8	Spray drying (Sd 1000)	Methanol	1%	Inlet temp. 65–80 °C; Outlet temp 50–60 °C	FR: 2–3 mL/min AAP: 10 kPa DAFR: 0.60–0.70 m^3/min	[56]
Celecoxib	PVP: HPMC	N/A	Rotavapor	Methanol:DCM (1:1 *V*/V)	N/A	N/A	N/A	[57]
Celecoxib	PVP: HPMCAS	N/A	Rotavapor	Methanol:DCM (1:1 *V*/V)	N/A	N/A	N/A	[57]
Celecoxib	Phospholipoid E80 (PL): trehalose	1:10:16	Spray drying (Büchi B-90 Nano Spray Dryer)	Ethanol:water (8:2, *W*/W)	N/A	Inlet temp. 80 °C	FR: 12.5 mL/min DAFR: 140 L/min	[58]
Celecoxib	Phospholipoid E80 (PL): trehalose	1:10:16	Freeze drying (Christ Gamma 2–16 Lsc)	TBA:water (6:4 *V*/V)	N/A	0.1 mbar @ 25 °C/24 h; FB 0.01 mbar @ 25 °C/4 h	Frozen at −80 °C for 24 h/freeze dryer at −60 °C.	[58]
Cilostazol	Eudragit(®) L100: Eudragit(®) S100 (1:1)	1:5	Spray drying (B-290, Buchi)	Methanol	N/A	Inlet temp. 75 °C	FR: 1.5 mL/min DAFR: 538 L/h	[59]
Clopidogrel	Tween 80/HPMC	10: 2.5: 2.5	Spray drying (Buchi Mini Spray-Dryer B290)	Water	20 mg/mL	Inlet temp. 150 °C Outlet temp 75–85 °C	FR: 5 mL/min Aspirator 100%	[60]
Diazepam	PVP	N/A	Freeze-drying (Christ Lyophilizer, Type Alpha 2-4)	TBA:water (4:6 *V*/V)	N/A	0.220 mbar @ −35 °C /1 day FB 0.05 mbar@ 20 °C /1 day	Condenser temp. 53 °C	[61]
Dimenhydrinate	Ethyl cellulose	1:1; 1:3;1:5	Solvent cast	Ethanol	N/A	60 °C	N/A	[62]
Docetaxel	Soluplus®	1:10	Freeze-drying	N/A	N/A	N/A	N/A	[63]
Felodipine	PVP	1:9	Solvent cast	Ethanol	N/A	40 °C	N/A	[64]
Fenofibrate	Silica	1:3	SCF	CO_2	N/A	Temp. 50 °C Pressure: 2550 PSI	N/A	[65]
Fenofibrate	Gelucire1 50/13	22:88	SCF-PGSS (Separex®)	CO_2	Not applicable	Temp. 78 °C Pressure:80 bar	Fenofibrate was melted in Gelucire® 50/13	[66]
Flurbiprofen	PVP	N/A	Solvent cast	Ethanol	N/A	40 °C	N/A	[67]
Glibenclamide	Magnesium aluminometasilicate (Neusilin® UFL2)	1:2.5	Rotavapor	DCM	2%	35 °C	N/A	[68]
Glibenclamide	Eudragit® S100	1:1	Spray drying	Methanol:DCM (1:1 *V*/V)	50 mg/mL	Inlet temp 90 °C	SFR: 4 g/mL AAP: 0.05 MPa	[69]
Glibenclamide	PMC (50%-60%): PEG (34–40%): Poloxamer (6–10%)	1:10	SCF-SAS	Methylene chloride–ethanol (1:1) FB CO_2	0.10%	Pressure: 1500 to 3000 PSI	FR CO_2: 2 mL/min FR sol. 0.2 mL/min	[70]
Glycyrrhizic acid	Silica	N/A	SCF-SAS	Ethanol FB CO_2	10–40 mg/ml	Temp. 35–65 °C Pressure: 200–250 bar	FR CO_2: 10-20 ml/min FR sol. 4–10 mL/min	[71]
Itraconazole	HPMC	1:1	Solvent cast	Methanol:DCM (1:1 *V*/V)	1%	N/A	N/A	[72]
Itraconazole	HPMC	N/A	Rotavapor	Methanol:DCM	N/A	45 °C	N/A	[72]
Itraconazole	Eudragit® E	N/A	Spray drying (Pro-Cep-T 4 m8-Trix Spray Dryer)	Methanol:DCM (1:4 *V*/V)	2.40%	Inlet temp 70 °C	SFR: 150 mL/g DARF: 0.3 m^3/min	[46]
Itaconazole	HPMC/Polaxamer 407/L-Ascorbic Acid	4:4.5:0.5:1	SCF-SAS	Methanol/DCM (1:3 *V*/V) FB CO_2	7.50%	Temp. 50 °C Pressure: 95 bars	FR CO_2: 20 mL/min FR sol. 0.4 mL/min	[73]
Megestrol acetate	HPMC	1:2	SCF-SAS (Thar SAS200 equipment)	Methylene chloride:ethanol (45:55 *W*/W) FB CO_2	5%	Temp. 40 °C Pressure: 15 MPa	FR CO_2: 11 g/min FR sol. 1 mL/min	[74]
Megestrol acetate	HPMC/TPGS	1:2:0.5	SCF-SAS (Thar SAS200 equipment)	Methylene chloride:ethanol (45:55 *W*/W) FB CO_2	5%	Temp. 40 °C Pressure: 15 MPa	FR CO_2: 11 g/min FR sol. 1 mL/min	[74]
Miconazole	PVP-VA	2:8–4:6	Spray drying (Buchi Mini Spray-Dryer B191)	DCM	5%	Inlet temp 60 °C, Outlet temp 40 °C	FR:6.8 mL/min DARF: 0.56 m^3/min	[75]
Nifedipine	Soluplus®	3:7	Freeze-drying (FD-80)	TBA:methanol	10%	0 °C for 4 days	Quenched by liquid nitrogen	[76]
Nifedipine	Soluplus®	3:7	Rotavapor	Methanol	N/A	N/A	N/A	[76]
Phenytoin	Eudragit® S100	15:85	Spray drying	Acetone:methanol (50:50 *W*/W)	50 mg/mL	Inlet temp 90 °C	SFR: 4 g/mL AAP: 0.05 MPa	[69]
Progesterone	Gelucire 44/14	1:10	SCF-PGSS	CO_2	Not applicable	Temp. 60 °C Pressure:186 bar	Progesterone was melted in Gelucire® 44/14	[77]
Puerarin	Phospholipids PC70	1:1.2	SCF-GAS	Ethanol FB CO_2	20%	Temp. 38 °C Pressure:10 MPa	N/A	[78]

Table 3 (*continued*)

Drug	Carrier	Drug: Carrier(s) ratio	Technique	Solvent	Solid content in solution	Solvent evaporation temperature	Comment	Ref
Puerarin	Phospholipids PC70	1:1.2	SCF-SEDS	Ethanol FB CO_2	100 mg/ml	Temp. 35 °C Pressure:10 MPa	FR CO_2: 45 ml/min FR sol. 0.45 mL/min	[78]
Resveratrol	Soluplus®	1:1	Solvent cast	Ethanol	10%	60 °C	N/A	[79]
Rofecoxib	PVP	1:1; 1:3; 1:9	Solvent cast	Methanol:chloroform (2:1 *V*/V)	N/A	45 °C	N/A	[80]
Simvastatin–lysine (1:1 M)	SLS	1:0.5	Spray drying (Buchi Mini Spray-Dryer B191)	Water	N/A	Inlet temp 100 °C Outlet temp 45 °C	FR: 3.9 mL/min DARF: 600 L/h	[81]
Sirolimus	Eudragit® E: TPGS	1:8:1	Spray drying (Buchi Mini Spray-Dryer B191)	Ethanol:methylene chloride (55:45, *W*/W)	3%	Inlet temp 65–80 °C Outlet temp 45–55 °C	FR: 3–6 mL/min	[82]
Tadalafil	PVP-VA	1:9–2:8	Spray drying (Buchi Mini Spray-Dryer B290)	Acetone:water (9:1, *V*/V)	1%	Inlet temp 65 C Outlet temp 52 °C	FR: 7 ml/min aspirator 100%	[83]
Tadalafil	PVP-VA	1:1	Freeze-drying	Water:ACN (55:45)	0.40%	0.2 mbar @ 50 C/72 h	N/A	[84]
Tolbutamide	PVP	N/A	Solvent cast	Ethanol	N/A	40 °C	N/A	[67]
Valsartan	HPMC:Poloxamer 407	2:7:1	SCF-SAS (Thar SAS200 equipment)	DCM:ethanol (45:55 *W*/W) FB CO_2	50 mg/mL	Temp. 40 °C Pressure: 15 MPa	FR CO_2: 11 g/min FR sol. 1 mL/min	[85]
Zidovudine	Poly(L-Lactic Acid)	1:2	SCF-SAS	Ethanol:DCM (5:95) FB CO_2	15%	Temp. 45 °C Pressure:85 bar	FR CO_2: 3 ml/min FR sol. 0.75 mL/min	[86]
Zoplicone	PVP	1:1	Rotavapor FB freeze-drying	Methanol	0.5%	N/A/-72 °C/12 h	N/A	[87]

FR—Fed Rate; AAP—Atomization Air Pressure; DAFR—Drying Air Flow Rate; DCM—Dichloromethane; N/A—Not available; Temp.—temperature; FB—Followed By; TBA—tert-butyl Alcohol; SFR—Solution Feed Rate; Sol.—Solution; SCF-PGSS—super critical fluid–particles from gas-saturated suspension; SCF-SAS—super critical fluid–supercritical antisolvent; ACN—Acetonitrile.

limiting application [54]. Melting processes also require drug solubility/miscibility, which can be very difficult to achieve for some molecules [6,44,55].

4. Laboratorial scale

Laboratorial processes by either melting or solvent-evaporation are expected to be fast, cheap and require low material resources, especially drug substance. Laboratorial processes can be divided in micro-scale and mini-scale. Micro-scale processes are intended to produce a few micrograms of product and can generally be used for preliminary screening. These processes have limited robustness and poor reproducibility. Mini-scale processes can already generate a few to several hundred grams of product and are characterized for being more robust and reproducible.

4.1. Solvent evaporation

Laboratorial solvent evaporation processes can be divided in four major groups depending on solvent removal conditions: (i) high temperature and normal pressure, (ii) high temperature and negative pressure, (iii) freeze-drying, or (iv) supercritical fluids (SCFs). Table 3 presents some of the most recent applications of laboratorial solvent evaporation methods to prepare amorphous solid dispersions.

Solvent casting [79] is a basic laboratorial process of preparing solid dispersions and consists in dissolving the drug and the polymeric carrier(s) in the same solvent(s). The solution is then spread into a petri dish and allowed to evaporate under normal pressure at room temperature [88], in a hot plate [62] or in a low temperature oven followed by cooling in a desiccator [79] which have successfully been employed in the development of solid dispersions of paracetamol, dimenhydrinate and resveratrol respectively. Typically, the resulting films are pulverized and milled [79]. As an alternative, miniaturization can be achieved by replacing petri dishes with low volume glass vials [89,90]. This type of approaches presents the possibility of producing very small amounts of product and was used for preliminary screening of itraconazole and JNJ-25,894,934 (a new chemical entity from ALZA corporation) [89,90]. However, it can only be used for solvents with very low boiling temperature such as ethanol [64,67,79,91], chloroform [80,92] or a mixture of ethanol and dichloromethane [36]. Additionally, it may be difficult to ensure that the solvent is completely removed, which may affect data generated for solubility, permeability or bioavailability. An alternative involves the use of scalable laboratorial spray driers [46,56,59,93]. The solution of drug and polymer(s) is sprayed into a hot air stream that induces fast solvent evaporation and, consequently, the production of small homogenous solid particles composed by drug and carrier(s) in an amorphous state (see Section 5.1).

One of the most practical laboratorial processes used to produce solids dispersion involves the use of a rotary evaporator [40,94,95] which has recently used in the development of celecoxib [57,58], glibenclamide [68–70], itraconazole [46,72,73], nifedipine [76], zoplicone [87] (see Table 3 for details). This is used to remove the solvent(s) under vacuum, allowing a faster sample processing and/or the use of solvents with higher boiling point such as tetrahydrofuran, dimethyl formamide or dimethyl sulfoxide (DMSO) that could not be used in a solvent casting process. The final product is removed from the volumetric flask and can be further milled if desirable. An alternative approach involves solvent casting in a petri dish or vial followed by evaporation in a low pressure chamber or oven.

Freeze-drying or lyophilisation, recently employed in the development of celecoxib [57,58], diazepam [61], docetaxel [63], nifedipine [76], tadalafil [83,84] and zoplicone [87] (see Table 3 for details), comprises freezing a solution/suspension of drug and carrier(s) followed by reducing the surrounding pressure to allow water and solvents in the sample to undergo solid–gas transition [61,96]. In a freeze-drying process, drug and carrier(s) maintain their molecular dispersion structure observed upon dissolution [63,76,87]. Laboratorial freeze-driers are able to produce from a few milligrams up to some grams of lyophilised products. The use of organic solvents in freeze-drying is

very limited, but possible for instance with 2-methyl-2-propanol [97], tert-butanol [97], methanol, acetonitrile or water/DMSO mixtures [51].

The use of supercritical fluids (SCFs) is also possible in order to produce solid dispersions. Recent applications of SCFs in the manufacture of solid dispersions are depicted in Table 3. SCFs are gases that under certain pressure and temperature present simultaneously gaseous and liquid state properties [98,99]. Liquid properties are advantageous for solubilisation, while gaseous features favour drug and carrier(s) diffusion and solvent removal [98]. Almost all gases present SCFs properties under adequate conditions. However, only few can be used in the pharmaceutical field due to their adequate critical temperature. More than 98% of all applications have been developed using carbon dioxide [99]. Carbon dioxide presents low critical temperature (31.18 °C) and pressure (7.4 MPa), and is inexpensive, non-flammable, non-toxic, recyclable and environmentally friendly [70,73,98]. Another example of SCF used in the pharmaceutical field is trifluoromethane [100] which was recently used in the development of simvastatin nanoparticles. SCFs major disadvantages are the difficulty to completely remove organic solvents (when used) and to scale-up, as well as the price of the equipment [99].

Processes using SCFs can be divided in two main groups [98]. The first includes processes that use SCFs as solvents, such as rapid expansion of a supercritical solution (RESS). RESS consists of dissolving the drug and carrier(s) in a SCF that is then rapidly expanded by sudden decompression, typically by passing through an orifice at low pressure [101]. The product properties produced by this process depend on the pre-expansion conditions like temperature and pressure of the vessel and post-expansion conditions such as the nozzle temperature, geometry, size, distance and angle of impact against the surface of the jet stream [98]. RESS process is adequate for laboratory scale since it can be easily implemented, but very difficult to scale up. Another limitation is the required solubility of drug and carriers in the SCFs that for most of drugs is not feasible, thus limiting the application of this process [98,101]. Solid dispersions of fenofibrate have been produced by RESS and deposited over silica particles [65]. Solid dispersions of alpha lipoic acid [102] and spironolactone [103] have also recently been produced by RESS process.

A second group of processes encompasses the use of SCFs as antisolvents. Drug and carrier(s) are dissolved in an organic solvent that is removed by a SCF antisolvent. There are different techniques based on such principle, differing in the mixing procedure between the drug/carrier(s) solution and the SCF [98,101]. The organic solvent can be sprayed into a SCF in supercritical antisolvent (SAS) (Fig. 1) or particles by compressed antisolvent (PCA). Atorvastatin [104], megestrol acetate [74] and valsartan [85] amorphous nanoparticles have been produced by a SAS approach, and shown to present enhanced solubility and bioavailability. Indomethacin [105], cefdinir [106] and glycyrrhizic acid [71] solid dispersions have also been produced by this process and obtained particles shown to have homogenous particle size and improved solubility. Zidovudine-poly(L-lactic acid) particles were further shown to possess improved permeability using an *ex vivo* everted rat intestinal sac model [86]. A recent study demonstrated that glibenclamide solid dispersions prepared by SAS presented higher solubility than products obtained by equivalent solvent evaporation processes [70]. This was attributed to the effects of the solution and the supercritical carbon dioxide on enhanced plasticization of polymers, thus increasing diffusion of the drug into the polymer matrix.

In aerosol solvent extraction system (ASES), both organic solvent and SCF are sprayed at the same time by different nozzles into the chamber [107]. Itraconazole solid dispersions have been produced by ASES using HPMC as carrier [107]. Obtained amorphous nanoparticles (100–500 nm) showed enhanced solubility and bioavailability [107]. Solid dispersions of atenolol have also been produced using ASES [108]. Alternatively, the SCF can be added into the organic solvent, being gaseous antisolvent (GAS) technique one example of this approach [98]. Phenytoin solid dispersions have been produced GAS associated to PCA using PVP as carrier [91].

Recently, solid dispersions of fenofibrate and Gelucire® 50/13 have been manufactured by particles from gas saturated solutions (PGSS) [66]. In this process, the SCF saturates the organic solution that is then sprayed to form particles [66,77]. In another study, PGSS was employed to produce solid dispersions of progesterone [77]. Optimized conditions included high pressure and temperature, and longer processing, as well as a lower drug:carrier ratio.

A technique termed solution enhanced dispersion by supercritical fluids (SEDS) which uses a special nozzle was patented by Hanna and York and proposed to produce particulate products [109]. This nozzle allows the organic solvent and SCF to be atomized simultaneously. Puerarin microparticles were produced by SEDS using phospholipids as carriers [78]. These were shown to possess a higher degree of amorphisation when compared to particles produced by GAS.

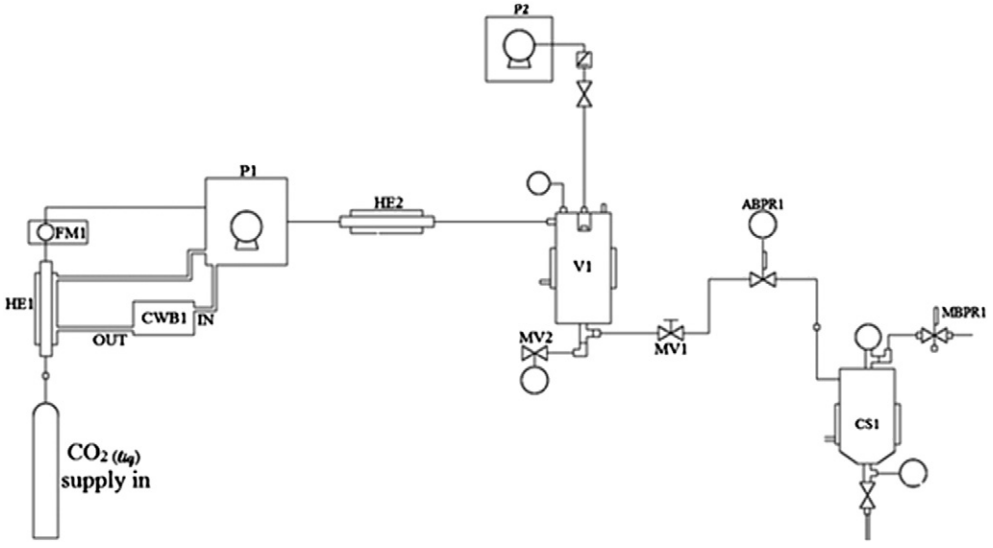

Fig. 1. Schematic representation of the SAS process. Republished with permission of John Wiley and Son, from [86], Copyright 2015; permission conveyed through Copyright Clearance Center, Inc.

Table 4
List of recent solid dispersions prepared by melting processes.

Drug	Carrier	Drug:carrier ratio	Technique	Temperature (°C)	Processing parameters	ref
Bicalutamide	PVP-VA	5:95	HME (TSE—Minilab II)	170	Screw speed: 150 rpm	[110]
Caffeine	PVP or PVP-VA	2:8	HME (TSE—Minilab II)	155	Screw speed: 100 rpm Residence time: 5 min	[111]
Carbamazepine	AFFINISOL™ HPMC	15:85/30:70	HME (TSE—Leistritz Nano-16)	120–180	Screw speed: 150–200 rpm Feed rate: 5 g/min Kneading elements: 2 (30° and 60°) Strand die: 3-mm Screw diameter: 16 mm	[112]
Carbamazepine	PVP-VA or Soluplus® or Eudragit® EPO	15:85/30:70	HME (TSE—Leistritz Nano-16)	120–180	Screw speed: 150–200 rpm Feed rate: 5 g/min Kneading elements: 2 (30° and 60°) Strand die: 3-mm Screw diameter: 16 mm	[112]
Celecoxib	PVOH:sorbitol (6:4)	15:85	HME (TSE—Prism Eurolab 16 Thermo)	140	Screw speed: 100 rpm Kneading elements: 3 Strand die: 3-mm Screw diameter: 16 mm	[113]
Disulfiram	Kolliphor® P 188 or Kolliphor® P 237	4:6	Melt quenching	80	Cooling at room temperature	[114]
Efavirenz	(PVP or PEG8000):Tween 80	1:10:1.1	Melt Quenching	80	Cooling at ice bath followed by 2 days in the freezer	[115]
Felodipine	PEG:PEO:Tween 80	10:36:27:27	HME (TSE—Minilab II)	65	Screw speed: 150–200 rpm Residence time: 5 min	[116]
Fenofibrate	Ethyl cellulose or hydroxypropyl cellulose or PEG	1:10	HME (TSE—Process 11 Thermo)	125, 140, 75	Screw speed: 100 rpm Feed rate: 10 g/min Screw diameter: 11 mm	[117]
Hydrochlorothiazide	PVOH:sorbitol (6:4)	15:85	HME (TSE—Prism Eurolab 16 Thermo)	140	Screw speed: 100 rpm Kneading elements: 3 Strand die: 3-mm Screw diameter: 16 mm	[113]
Indomethacin	Magnesium aluminometasilicate (MAS-Neusilin® US2)	2:8/4:6	HME (TSE)	180	Screw speed: 100 rpm Feed rate: 1 Kg/h Screw L/D ratio: 40:1	[118]
Indomethacin	PVP or PVP-VA	9:1–1:1	Cryomilling Followed By *In Situ* Melt Quenching	170	**Cryomilled** at 10 Hz, five cycles (2 min of milling and 2 min of cooling) **Melt quenching**: 170 °C/10 min Spinning at 4 khz Rapidly cooled to room temperature	[119]
Miconazole	PVP-VA	2:8	HME (TSE—MP19PC)	Zone 1: 25–40 Zone 2 and 3: 125	Screw speed: 300 rpm Kneading elements: Zone 1 (5 FP 30°, 4 FP 60°, 6 AP 90°) Zone 2 (3 RP 60°) Screw L/D ratio of 25/1	[75]
Paracetamol	PVP or PVP-VA	4:6	HME (TSE—Minilab II)	120	Screw speed: 100 rpm Residence time: 5 min	[111]
Valsartan	Soluplus®:TPGS	3:6:1	HME (TSE—STS-25HS)	80–100 (zone 1–6)	Screw speed: 150 rpm Feed rate: 28–30 g/min Extrusion pressure: 100 bars	[120]

HME—Hot Melt Extrusion;; TSE—Twin Screw Extruder; rpm—rotations per minute; min—minute; PVOH—Polyvinyl alcohol; PEO—Polyethylene Oxide; N.A.—Not Available; FPW—Forwarding Paddles; AP—Alternating Paddles; RP—Reversing Paddles; L/D—length/diameter.

4.2. Melting

Melting processes comprise heating a formulated sample followed by its cooling. The techniques employed to heat and cool are important variables of melting processes. Table 4 presents some of the most recent solid dispersions prepared by melting processes.

Laboratorial melting processes can be extremely simple. For example, a solid dispersion can be obtained by combining the formulation ingredients in a differential scanning calorimetry (DSC) pan and heating the sample until melting of all components, followed by natural or forced cooling [121]. Generally, less than 10 mg of product are obtained.

Moving up in scale, when both components present a low melting point, or when the drug substance has high solubility in the carrier(s), a melt- quenching approach can be used. Briefly, a water bath [122] or a hot plate [114] can be used to melt both components. Then the homogenous molten mass can be rapidly solidified by (i) placing it in a freezer [122], (ii) using an ice bath [123,124], (iii) placing it over a stainless steel surface as thin layer spreading followed by a cool air draft [125], (iv) spreading it on plates placed over dry ice [126], (v) immersing in liquid nitrogen or grinding the material in liquid nitrogen (cryo-grinding) [41,45,127], or (vi) pouring it into petri dishes placed at room temperature inside a desiccator [128,129]. After solidification, the mixture needs to be pulverized in order to facilitate handling [122]. These techniques can be used to produce up to several grams that then can be used to further physicochemical and technological characterization.

Hot melt extrusion (HME) has been explored as a scale-up procedure to produce solid dispersions by melting process. It consists in the

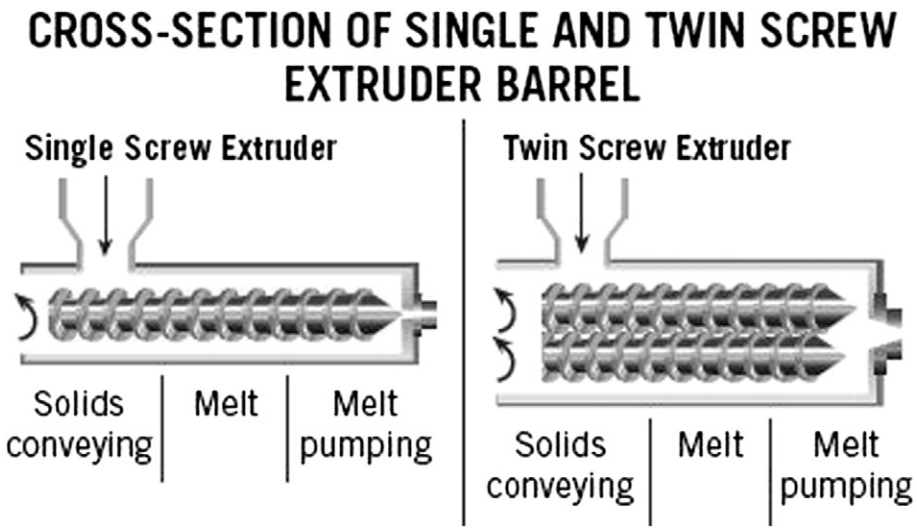

Fig. 2. Schematic of a single screw and twin-screw extruder. Reprinted from [133], with kind permission from Springer Science + Business Media (Copyright American Association of Pharmaceutical Scientists 2013).

extrusion at high rotation speed of the drug and carrier(s), previously mixed, at melting temperature for a small period. The resulting product is then collected after cooling at room temperature and milled into a powder or granule form [55,113,120,130]. A significant advance of HME has been the introduction of twin-screw melt extrusion as illustrated in Fig. 2 [120,131]. It consists in the use of a special twin screw extruder and the presence of two independent hoppers in which the temperature can vary over a broad range [132]. Currently several laboratory-scale equipment are available from different manufactures, such as Thermo Fisher Scientific, Brabender Technologies, Coperion GmbH or Leistritz Advanced Technologies Corp., which use this technology and can be used to produce from few grams of product to several Kilograms [53,55].

Advantages and description of hot melt extrusion will be further detailed below when industrial scale processes are discussed. Examples of laboratorial melt extrusion solid dispersion developments are depicted in Table 4.

Variations in preparation methods affect final product properties. Table 5 summarizes the differentiation among laboratorial methods regarding particle size reduction, particle porosity, wettability and process parameters such as yield and scalability.

5. Industrial scale

Industrial and, consequently, good manufacturing practices (GMP) compliant processes to manufacture solid dispersions are scarce. Mostly because the majority of the simple and easy laboratorial processes and equipment are difficult to scale up and fulfil GMP requirements, such as contact materials, reproducibility (automatization), and sanitation in addition to the most evident, such as the impossibility to perform installation/operational and performance qualification of these equipment. Additionally, processes need to be robust and reproducible, which again is hard to ensure for processes such as solvent cast evaporation or water bath melting process. At industrial scales, the production outputs vary from 1 kg batch size to several hundred kilograms.

5.1. Solvent evaporation

From an industrial point of view, the manufacture of solid dispersions by solvent evaporation is usually limited to a few specific cases. The types of solvent, drying conditions and therefore the rate of evaporation vary drastically among different processes. Overall, spray-drying and frezee-drying are the most representative of the solvent evaporation methods used in the industry for manufacturing solid dispersions.

The spray drying process is relatively easy to scale up from a laboratorial spray dryer to an industrial one (Fig. 3) [134,135]. Industrial spray dryers have a nominal drying gas rate ranging from 50 to 5000 kg/h which may result in a water evaporation capacity up to 400 kg/h. Product properties and perfomance depend on process parameters and formulation aspects [54]. Relevant pocess parameters include inlet temperature, feed rate humidity and flow rate of drying gas and atomization conditions [54,136,137]. The type and size of the spray nozzles highly contributes to the amorphous solid dispersions particles, in particularly to the particle size, but also texture and smoothness [134,135]. Additionally, the solid content may also affect the solution viscosity and consequently the drying process and the final product [135]. Formulation variables such as composition (drug, carrier, solvent) and solid content in the feed, solvent type, viscosity and surface tension of the drying solution are significant for product properties [54,137]. Table 6 presents

Table 5
Impact of laboratorial method in product properties. Subsequent operations such as milling were not considered.

Method	Particle size reduction	Particle porosity	Wettability*	Yield	Scalability
Solvent cast (different variations)	Poor (coarse product)	Poor	Poor	Poor	Poor
Rotavapor	Poor	Poor	Poor	Poor	Poor
Spray drying	High	Medium	High	Medium	Medium
Freeze drying	High	High	High	High	Medium
SCF	High	High	High	Medium	Poor
Melt-quenching (freeze/ice bath/room temp.)	Poor (coarse product)	Poor	Poor	Medium	Poor
Cryo-grinding	Poor	Poor	Poor	Medium	Poor
HME	Poor	Poor	Medium	High	High

* Wettability is more linked with composition of carriers than with manufacturing process.

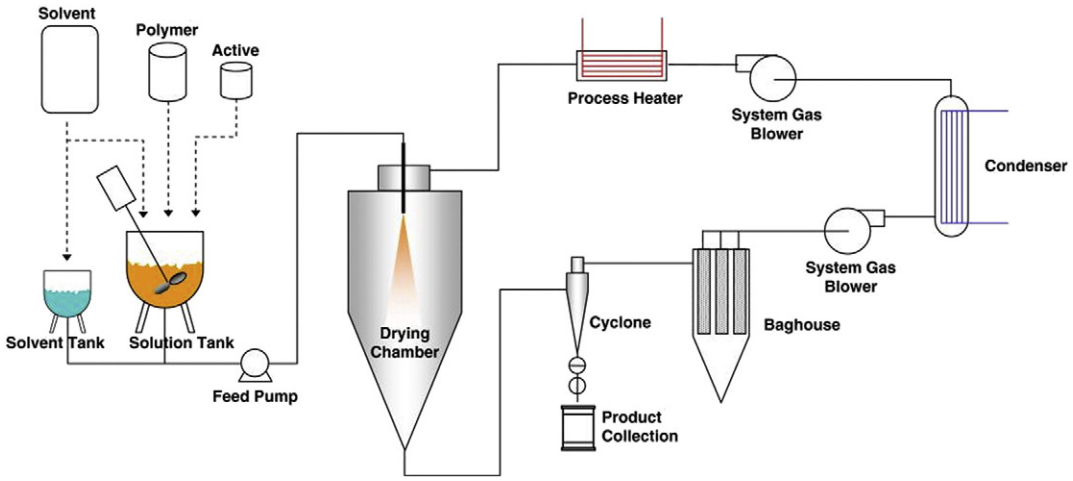

Fig. 3. Scheme of a spray drying process. Reprinted from [135], with kind permission from Springer Science + Business Media.

the impact of spray drying parameters in final product properties, such as particle size, porosity or smoothness.

The first challenge in developing an amorphous solid dispersion is finding an adequate solvent system. It must be able to solublize drug and carrier(s) to a large extension (idealy over 50 mg/mL) and produce a low viscosity solution [54]. Adittionally, from a GMP and industrial prespective solvent(s) should present low toxicitiy and high volatility, which is critical because residual solvents in final products must be within the acceptable values of the International Conference Harmonization (ICH) Q3C(R5) guideline [93,140]. This guideline defines three different classes of solvents, being Class 3 solvents preferable while the use of those in Classes 1 and 2 should be avoided or limited, respectively. Unfortunately, most of the times it is not possible to achieve an effective solvent system for the components of solid dispersions with solvents from Class 3, or these solvents do not present adequate properties for spray-drying. In these cases, Class II solvents may be justified. Typical examples of solvent used in pharmaceutical spray-drying processes are presented in Table 7 [141].

The carrier selection influences the final product properties, particularly amorphisation degree, physical and chemical stability and wettability. For instance, the inclusion of a surfactant as carriers, such as tween 80 [153,154], sodium lauryl sulfate [153,154], Poloxamer [153], Myrj® [153], sodium taurocholate [154] or Triton X100 [154], forming a third generation solid dispersion originates products with enhanced solubility, which may improve bioavailability [40]. Carriers used in the preparation of solid dispersions by spray drying are generally the same described in the melting methods. In these particular cases, polymers with high melting point or glass transition can be employed and are even preferred. Carriers such as Metacrilates [95,154,155], povidone and derivatives [156], PEG [157], HPMC [149,157], HPMCAS [137] and Soluplus® [48], which was originally developed for melt-extrusion, are frequently employed in the preparation of solid dispersions by spray drying. The interplay of formulation and process parameters is, thus, crucial to obtain a stable amorphous process and a smooth process [54,93,137]. A list of spray drying solid dispersions currently available in the market can be found in Tables 3, and 8 illustrates the details on processing parameters of some of the most recent products produced by this process.

Another industrial manufacturing process to obtain amorphous solid dispersions is freeze-drying, previously described in Section 4.1. Freeze-drying at industrial scale uses larger equipment capable to control both phases of the process (freeze and lyophilisation). This advantage over laboratorial equipment provides a higher robustness and reliability of the industrial scale. Additionally, freeze-drying has the advantage of promoting minimal stress (thermal) to the drug and presents minimal risk of phase separation [51]. The manufacture of solid dispersion by freeze-drying is limited to drugs with some water solubility or inorganic solvents miscible water [63,76,87,161]. Amorphous solid dispersions have been prepared using the carriers already presented for another processes [63,76,84,87,89,97]. At industrial scale, in order to obtain an adequate solid material after lyophilisation, a cryoprotective material may be required. Cryoprotectives are generally sugars such as: mannitol, glucose, sucrose, sorbitol, fructose, dextran, maltose or trehalose, among others [162]. The use of organic solvents at industrial scale s is more limited and it is recommended to be less than 10% [97].

5.2. Melting

Only two types of melting processes are available at an industrial scale. These are melt agglomeration and melt extrusion.

Melt agglomeration process use standard granulation equipment, like high shear mixers [37,163] as used for diazepam [163] or fluid bed driers [47,164] as used for paracetamol [164]. However, instead of a granulation liquid, a melted mass of drug and carrier(s) is added to the remaining excipients of the formulation [165]. This molten material acts as a granulation liquid, ensuring an adequate homogeneity and adsorption of the drug and carrier(s) on the remaining excipients that can then be further processed. This process allows a production from few kg to around 500 kg batch size. Carriers used in melt-agglomeration can be liquids, namely polyethylene glycol (PEG) 300 and caprylocaproyl

Table 6
Impact of spray drying parameters in product properties [138,139].

Parameter (Increase)	Particle size	Particle porosity	Product moisture	Particle smoothness	Assay	Powder yield
Inlet temperature	Increase	Decrease	Decrease	Decrease	Increase	Increase
Drying flow rate	Decrease	Increase	Decrease	Increase	Increase	Increase
Feed rate	Decrease	Decrease	Increase	Increase	Decrease	Decrease
Humidity	Increase	Increase	Increase	Decrease	Decrease	Increase
Spray nozzles (increase in droplet size)	Increase	Increase	Increase	Decrease	Decrease	Increase
Solid content in solution	Increase	Decrease	Decrease	Decrease	Increase	Increase
Solution viscosity or surface tension	Increase	Decrease	Increase	Decrease	Decrease	Increase

Table 7
Organic solvents commonly employed in spray drying.

Solvents	Boiling point (°C)	Dielectric constant	Solubility in water (g/100 g)	Density (g/ml)	ICH limit (ppm)
Acetone [142,143]	56.2	20.7	Miscible	1.049	Class 3
Chloroform [143]	61.7	4.81	0.795	1.498	60
Methanol [144,145]	64.6	32.6	Miscible	0.791	3000
Methylene chloride [146]	39.8	9.08	1.32	1.326	600
Isopropanol [147,148]	82.6	18.2	Miscible	0.786	Class 3
Ethanol [149]	78.5	24.6	Miscible	0.789	Class 3
Dichloromethane [143,150]	39.6	9.08	175	1.326	600
Dimethyl formamide [151]	153	36.7	Miscible	0.944	880
DMSO [151]	189	47	25.3	1.092	Class 3
Glycerin [141]	290	42.5	Miscible	1.261	–
Ethyl acetate [152]	77	6	8.7	0.895	Class 3
Butyl acetate [145]	126.1	5.07	0.68	0.882	Class 3
Water [144]	100	78.5	–	0.998	–
Tetrahydrofuran [148]	66	7.52	Miscible	0.889	720

macrogol-8 glycerides (Labrasol®), or solids presenting low melting/glass transition temperature, such as PEG 3000 [37], PEG 6000 [47], poloxamer 188 [37,166] or stearoyl polyoxyl-32 glycerides (Gelucire® 50/13) [163,167].

The avoidance of organic solvents and drying procedures are advantages of melt-agglomeration. Additionally, it can be helpful for water sensitive drugs [165,168]. The use of high temperatures, however, prevents its application to thermolabile drugs. The limited availability of suitable carriers for this process can also be seen as a limitation [165].

Hot melt extrusion (HME), and particularly the twin-screw melt extrusion with its highest representative being Meltrex™ from Soliqs, is one of the most employed industrial solid dispersion manufacturing process. In fact, the development and application of twin-screw melt extrusion should be considered one of the major driving forces for the wide dissemination of the solid dispersion concept (Fig. 4) [6,53,55] particularly after Kaletra® development [169]. Twin-screw presents several advantages over single screw versions and represent the current state of the art for melting processes. The use of two screws contributes to a reduced residence time of the drug in the extruder, allowing for continuous mass flow with enhanced mixing. Moreover, twin-screw extruders avoid drug and excipients thermal stress and feature self-cleaning of the screws [55,170]. The application of twin-screw technology to drugs susceptible to oxidation and hydrolysis is also possible by eliminating oxygen and moisture from the mixture [55,171,172]. It further presents easier material feeding and less tendency to over-heat [171]. The success is such that currently, almost all products developed by HME are in fact by HME using twin-screw extruders.

HME allows continuous processing, solvent-free and is easily scaled-up, since the same principle and design can be transposed to different scales [53]. The major difference between laboratorial and industrial equipment is the diameter of the screws. Screws, from laboratorial extruders can vary from 11 to 16 mm in diameter, while values for the industrial ones range from 16 to 50 mm [53,55]. The possibility of having continuous processing is highly advantageous in the pharmaceutical field because it allows huge versatility in manufacturing capability even with small extruders [173]. This process allows the industrial/GMP production of batch sizes ranging from few kg to tons.

The successful development of a solid dispersion by HME depends on composition and process parameters. Adequate selection of carriers and plasticizers is crucial. Apart from screw design, which is the most important variable, other parameters such as feed rate, temperature and rotation speed are crucial for defining the final product properties [55]. In a recent study, it was shown that the degassing process also enhanced the cross-sectional uniformity of the extruded material [174].The design of the equipment is highly versatile which allows the adaptation of processes to the desired results and to very different starting materials.

The reason for this versatility is the modular design comprising the screws and barrels [172]. Barrels can be flanged together or linked by internal tie rods. Screws are the most important part of the extruder. Their design distinguishes between processes that the extruder can or cannot fulfil and, therefore, define the quality and quantity of the extruded material [172,175]. The kneading paddle elements of the screws play an important role in changing the crystallinity and dissolution properties of solid dispersions (Fig. 5). Nakamichi *et al.* [131] showed that the physicochemical properties of the extruded material were significantly influenced by the operating conditions of the machine, namely by the revolution rate of screws and the amount of water added to the feed materials. The screw speed and feeding rate are related to shear stress, shear rate and mean residence time, which can affect the dissolution rate and stability of the final products [53]. Certain minimum temperatures are required in HME in order to reduce the torque needed to rotate the screw(s) and allow an efficient process [53]. Composition and process parameters of the most recent solid dispersions developed using melting extrusion processes are depicted in Table 4.

Carriers used in HME are generally polymers or waxes with low melting point or glass transition temperature that are used as solubilizers of the drug substance [171,175]. Commonly used carriers include PVP [157,175], povidone-vinyl acetate (PVP-VA) [157], copovidone [177–179], various grades of PEG [156,157], cellulose esters [175,180,181], cellulose acrylates [157], and poly-methacrylate derivatives [177,179,182]. Due to the specificities of this technology, the polymer industry has recently developed several polymers specifically for the HME, such as HPMC acetate succinate (HPMCAS) [49,178,183,184]

Table 8
Process parameters of some commercial spray drying solid dispersions.

Product	Orkambi®	Incivek™ (USA)/Incivo ® (EU)	Intelence®
Drug	Ivacaftor	Telaprevir	Etravirine
Carrier	HPMCAS: SLS	HPMCAS	HPMC
Drug:carrier(s) ratio	5:4.5:0.5	5:1	1:3
Technique	Spray drying	Spray drying	Spray drying
Solvent	Methanol	DCM	DCM:ethanol (9:1)
Equipment	N/A	Niro Size 4	SD12.5
Solid content in solution	10%	30%	5%
Inlet temperature (°C)	145	75	115
Outlet temperature (°C)	75	43	49
Aspiration	100%	N/A	N/A
Flow rate	35%	30%	1250 kg/h
Liquid flow rate	200 mL/h	150 kg/h	202 kg/h
Reference	US2015141459 [158]	WO2008080167 [159]	WO2007141308 [160]
Company	Vertex Pharma	Vertex Pharma	Tibotec

Fig. 4. Hot melt twin screw extruder (Image courtesy of Thermo Fisher Scientific Inc.)

and Soluplus® [177,180,185], as well as specific grades of HPMC (Affinisol®) [112]. Due to their individual properties, these carriers are frequently used in combination in order to achieve enhanced amorphisation, stability, dissolution or bioavailability [156,181].

HME processes are characterized by high shear stress. Therefore a plasticizer is frequently required to allow more efficient processing [55]. Additionally, the inclusion of these components can be explored in order to tailor drug release of final products. Vitamin E (tocopherol), D-alpha tocopheryl PEG 1000 succinate [120,184], poloxamers [185–187], Tween® [153,188], Myrj® [153] and low molecular weight PEGs [55,185] are examples of plasticizers that were shown able to improve product performance, namely concerning s dissolution and/or bioavailability. In a different approach, pressurized carbon dioxide injected during HME has been shown useful in reducing the temperature of various polymer melts in addition to acting as a foaming agent [189,190].

HME requires high energy input mainly due to the observed shear forces and temperatures used. This is an important drawback alongside the poor ability to process thermolabile compounds [53]. However, changes in the design of the equipment as well as the addition of plasticizers may contribute to reduce the processing temperatures and residence time and, thereby, avoid thermal degradation of drug substances during processing [55].

Currently there are several amorphous solid dispersions available in the market manufactured by this manufacturing process, such as Kaletra®; Novir®, Onmel™, Noxafil®, Gris-PEG™ and the recent Viekirax® (Europe)/Viekira™ (USA). Table 9 presents the composition and process parameters of some of these products.

6. Selection of a manufacturing process for amorphous products

Amorphous solid dispersions advantages over other solubility enhancement approaches are the presence of particles with reduced particle size, improved wettability, high porosity and the amorphous state. This later represents the major advantage of solid dispersions but also their major disadvantage. Amorphous products are thermodynamically instable and tend to crystallize during stability studies, storage, shipping or in vivo drug release. Therefore, an adequate solid dispersion should maintain its amorphous state from the manufacture moment until drug absorption [6,194,195]. Several factors contribute to drug crystallization, but most of them are related to drug mobility increase, induced by temperature, moisture or organic solvents presence. Consequently, an adequate manufacturing process and composition selection is crucial to meet the desired goals, namely obtaining a stable amorphous product with enhanced bioavailability [6,194–196]. A rational selection of the manufacturing process based on the physicochemical properties of the drug being formulated is possible and represents a key element in the product development.

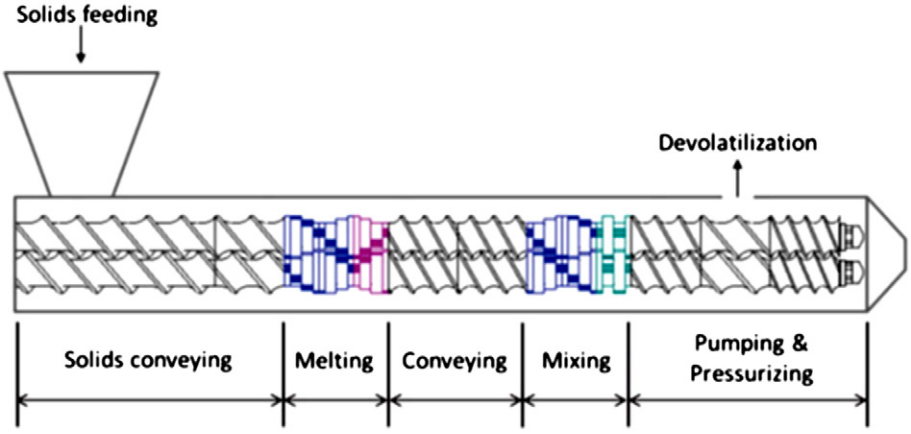

Fig. 5. Schematic representation of a twin-screw extruder and elementary steps. Reprinted from [176], with kind permission from Springer Science + Business Media (Copyright Controlled Release Society 2014).

Table 9
Process parameters of some commercial spray drying solid dispersions.

Product	Eucreas ®	Kaletra®	Noxafil®	Viekira™ (US)/Viekirax® (EU)
Drug	Vildagliptin/Metformin HCL (SD only Metformin)	Lopinavir/Ritonavir	Posaconazole	Ombitasvir/Paritaprevir/Ritonavir
Carrier	HPC	PVP-VA: Span20	HPMCAS	HPMCAS/TPGS/Propylene Glycol Monolaurate
Drug:carrier ratio	10:1	1:3.5:0.5	1:3	13:79:4:4
Equipment	Prism 16 Thermo	Leistritz Micro 18 Twin-Screw Extruder	Leistritz Micro 18 Twin-Screw Extruder	N/A
Temperature (°C)	170–185	120	120–135	160
Screw speed (rpm)	150	N/A	140	N/A
Feed rate	30–45 g/min	2.1 kg/h	4 kg/h	N/A
Reference	US2011/0045062 [191]	US20050084529 [169]	US20150150990 [192]	WO2015103490 [193]
Company	Novartis	Abbot	Merck	Abbvie

6.1. Laboratorial scale

At the laboratorial scale, the primary criteria for selecting the manufacturing process are based on drug properties such as thermal stability and melting point. Another important issue relates to equipment availability and the purpose of the study, for instance, if the work is still at a screening or optimization stage. When considering melting methods, the intention or not to scale up the process and the viscosity of the molten mass should be taken into account.

The properties of the organic solvents required to solubilize the drug and carrier(s) are the main factors to consider if selecting a solvent evaporation manufacturing process. Boiling point, solubility capacity

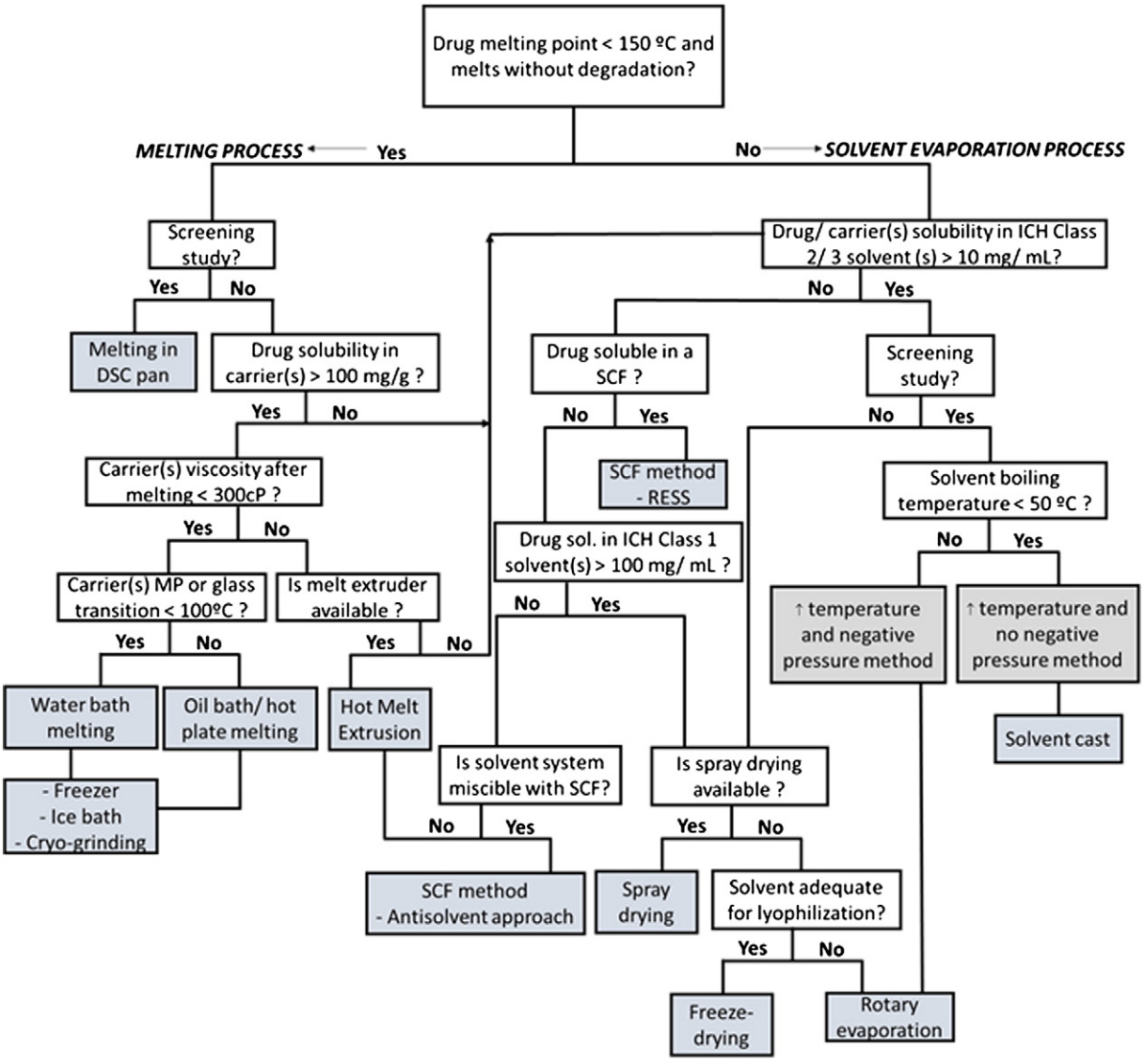

Fig. 6. Decision tree for selection of manufacturing process at the laboratorial scale. DSC—Differential scanning calorimetry; cP—CentiPoise; SCF—super critical fluid; MP—Melting point; Sol.—Solubility; ICH—International Conference Harmonization.

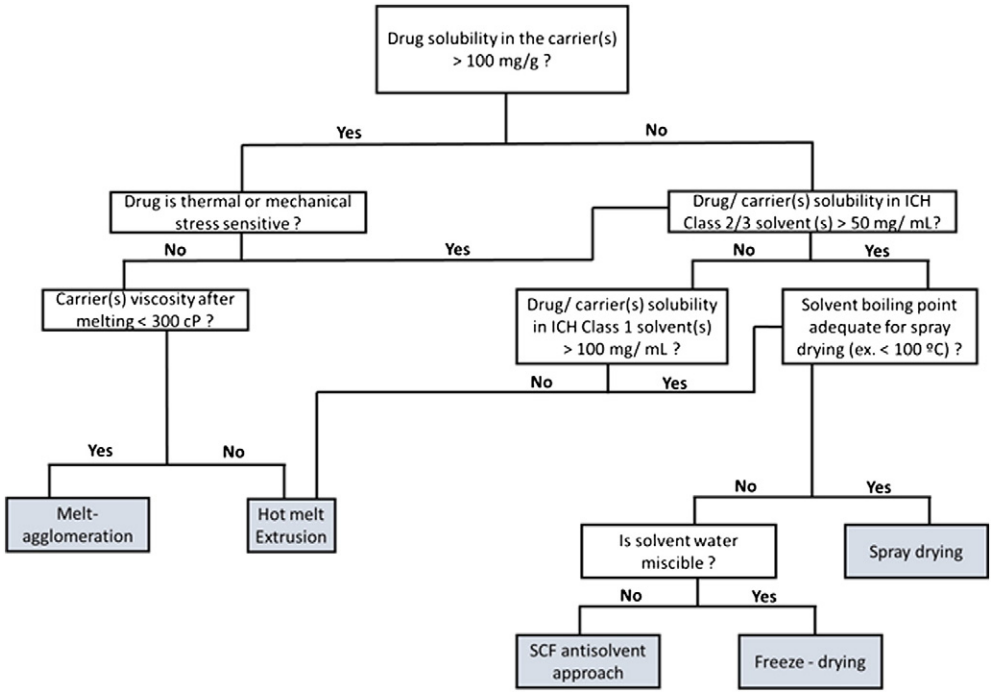

Fig. 7. Decision tree for selection of manufacturing process at the industrial scale. cP—CentiPoise; SCF—super critical fluid; ICH—International Conference Harmonization.

and solvent toxicity (classification) are of particular relevance. For instance, It is proposed that the drug/carrier solubility must be higher when ICH class 1 are required to be employed, due to its toxicity. Fig. 6 depicts a decision tree that can be used to select the most adequate manufacturing process at laboratorial scale.

6.2. Industrial scale

The industrial production of amorphous solid dispersions has limited options and is restricted to only a few manufacturing processes. At this scale, the main limitations will be equipment availability, as well as drug carrier solubility and thermal stability of the drug. HME is preferable among all melting processes. Alternatively, melt agglomeration can be used if the molten drug carrier mass presents low viscosity.

The selection rationale for solvent evaporation processes is based on solvent toxicity and solvent loading capacity that if very low will prevent an industrial effective process. Fig. 7 provides a decision tree for selecting the most adequate manufacturing process at the industrial scale. At this scale, additional considerations should be taken, such has process yield, batch size and particle properties. For instance, solvent evaporation processes generate smaller, rounder and porous particles than melting processes. However, increased porosity or presence of some residual solvents in the final product may induce drug crystallization by adsorbing environmental moisture and/or increasing drug mobility. In opposition, melting processes provide higher yields, and allow larger batch size than solvent evaporation processes.

7. Conclusions

Amorphous products, namely amorphous solid dispersions, are one of the most seething areas in the pharmaceutical field and, in particular, in the pharmaceutical industry. There is a current need to develop production processes at the laboratorial scale and scale these up to the industrial level in a reliable manner. In this review, the current state of the art of manufacturing processes used at laboratorial scale for development was presented. There is a wide range of different manufacturing processes, allowing the fitting of a suitable solution for all types of drugs. Industrial manufacturing processes were also described, particularly bearing in mind scalability of laboratorial methods previously used during development. Two decision trees for selecting available laboratorial and industrial scale manufacturing processes are also proposed. These tools could be used as guidance for an adequate development and industrialization of amorphous solid dispersions.

Acknowledgments

José das Neves and Sara Marques gratefully acknowledges Fundação para a Ciência e a Tecnologia (FCT), Portugal for financial support (grant SFRH/BPD/92934/2013 and grant SFRH/BPD/75905/2011, respectively). This work was financed by European Regional Development Fund (ERDF) through the Programa Operacional Factores de Competitividade—COMPETE, by Portuguese funds through FCT—Fundação para a Ciência e a Tecnologia in the framework of the project UID/BIM/04293/2013, via the PT2020 Partnership Agreement under the 4293 Unit I&D and co-financed by North Portugal Regional Operational Programme (ON.2—O Novo Norte) in the framework of project SAESCTN-PIIC&DT/2011, under the National Strategic Reference Framework (NSRF).

References

[1] M.S. Ku, Use of the biopharmaceutical classification system in early drug development, AAPS J. 10 (2008) 208–212.
[2] L.Z. Benet, F. Broccatelli, T.I. Oprea, BDDCS applied to over 900 drugs, AAPS J. 13 (2011) 519–547.
[3] D.W. Borhani, D.E. Shaw, The future of molecular dynamics simulations in drug discovery, J. Comput. Aided Mol. Des. 26 (2012) 15–26.
[4] G.R. Marshall, Computer-aided drug design, Annu. Rev. Pharmacol. Toxicol. 27 (1987) 193–213.
[5] K. Kawakami, Current status of amorphous formulation and other special dosage forms as formulations for early clinical phases, J. Pharm. Sci. 98 (2009) 2875–2885.
[6] T. Vasconcelos, B. Sarmento, P. Costa, Solid dispersions as strategy to improve oral bioavailability of poor water soluble drugs, Drug Discov. Today 12 (2007) 1068–1075.
[7] C. Leuner, J. Dressman, Improving drug solubility for oral delivery using solid dispersions, Eur. J. Pharm. Biopharm. 50 (2000) 47–60.
[8] M.S. Ku, W. Dulin, A biopharmaceutical classification-based right-first-time formulation approach to reduce human pharmacokinetic variability and project cycle time from first-In-human to clinical proof-of-concept, Pharm. Dev. Technol. 17 (2012) 285–302.

[9] A. Streubel, J. Siepmann, R. Bodmeier, Drug delivery to the upper small intestine window using gastroretentive technologies, Curr. Opin. Pharmacol. 6 (2006) 501–508.
[10] K.M. Giacomini, S.M. Huang, D.J. Tweedie, L.Z. Benet, K.L. Brouwer, X. Chu, A. Dahlin, R. Evers, V. Fischer, K.M. Hillgren, K.A. Hoffmaster, T. Ishikawa, D. Keppler, R.B. Kim, C.A. Lee, M. Niemi, J.W. Polli, Y. Sugiyama, P.W. Swaan, J.A. Ware, S.H. Wright, S.W. Yee, M.J. Zamek-Gliszczynski, L. Zhang, Membrane transporters in drug development, Nat. Rev. Drug Discov. 9 (2010) 215–236.
[11] L. Cutler, C. Howes, N.J. Deeks, T.L. Buck, P. Jeffrey, Development of a P-glycoprotein knockout model in rodents to define species differences in its functional effect at the blood–brain barrier, J. Pharm. Sci. 95 (2006) 1944–1953.
[12] J.H. Seo, J.B. Park, W.K. Choi, S. Park, Y.J. Sung, E. Oh, S.K. Bae, Improved oral absorption of cilostazol via sulfonate salt formation with mesylate and besylate, Drug Des. Devel. Ther. 9 (2015) 3961–3968.
[13] Y.V. Novozhilov, M.V. Dorogov, M.V. Blumina, A.V. Smirnov, M. Krasavin, An improved kilogram-scale preparation of atorvastatin calcium, Chem. Cent. J. 9 (2015) 7.
[14] A. Sarkar, S. Rohani, Molecular salts and co-crystals of mirtazapine with promising physicochemical properties, J. Pharm. Biomed. Anal. 110 (2015) 93–99.
[15] D.R. Serrano, K.H. Gallagher, A.M. Healy, Emerging nanonisation technologies: tailoring crystalline versus amorphous nanomaterials, Curr. Top. Med. Chem. 15 (2015) 2327–2340.
[16] Z.H. Zhang, Q. Zhang, Q.Q. Zhang, C. Chen, M.Y. He, Q. Chen, G.Q. Song, X.P. Xuan, X.F. Huang, From a binary salt to salt co-crystals of antibacterial agent lomefloxacin with improved solubility and bioavailability, Acta Crystallogr. Sect. B: Struct. Sci. Cryst. Eng. Mater. 71 (2015) 437–446.
[17] R. Chadha, S. Bhandari, S. Khullar, S.K. Mandal, D.V. Jain, Characterization and evaluation of multi-component crystals of hydrochlorothiazide, Pharm. Res. 31 (2014) 2479–2489.
[18] I. Weuts, D. Kempen, G. Verreck, J. Peeters, M. Brewster, N. Blaton, G. Van den Mooter, Salt formation in solid dispersions consisting of polyacrylic acid as a carrier and three basic model compounds resulting in very high glass transition temperatures and constant dissolution properties upon storage, Eur. J. Pharm. Sci. 25 (2005) 387–393.
[19] K. Seefeldt, J. Miller, F. Alvarez-Núñez, N. Rodríguez-Hornedo, Crystallization pathways and kinetics of carbamazepine–nicotinamide cocrystals from the amorphous state by in situ thermomicroscopy, spectroscopy, and calorimetry studies, J. Pharm. Sci. 96 (2007) 1147–1158.
[20] M. Dimopoulou, C.S. Mourouti, M. Vertzoni, M. Symillides, C. Reppas, In-vitro evaluation of performance of solid immediate release dosage forms of weak bases in upper gastrointestinal lumen: experience with miconazole and clopidogrel salts, J. Pharm. Pharmacol. (2015).
[21] J.L. Terebetski, J.J. Cummings, S.E. Fauty, B. Michniak-Kohn, Combined use of crystalline sodium salt and polymeric precipitation inhibitors to improve pharmacokinetic profile of ibuprofen through supersaturation, AAPS PharmSciTech 15 (2014) 1334–1344.
[22] K. Sai Gouthami, D. Kumar, R. Thipparaboina, R.B. Chavan, N.R. Shastri, Can crystal engineering be as beneficial as micronisation and overcome its pitfalls?: A case study with cilostazol, Int. J. Pharm. 491 (2015) 26–34.
[23] A. Bhakay, M. Merwade, E. Bilgili, R.N. Dave, Novel aspects of wet milling for the production of microsuspensions and nanosuspensions of poorly water-soluble drugs, Drug Dev. Ind. Pharm. 37 (2011) 963–976.
[24] C.W. Pouton, Formulation of poorly water-soluble drugs for oral administration: physicochemical and physiological issues and the lipid formulation classification system, Eur. J. Pharm. Sci. 29 (2006) 278–287.
[25] S. Prabhu, M. Ortega, C. Ma, Novel lipid-based formulations enhancing the in vitro dissolution and permeability characteristics of a poorly water-soluble model drug, piroxicam, Int. J. Pharm. 301 (2005) 209–216.
[26] S. Gupta, R. Kesarla, A. Omri, Formulation strategies to improve the bioavailability of poorly absorbed drugs with special emphasis on self-emulsifying systems, ISRN Pharm. 2013 (2013) 848043.
[27] R. Laitinen, K. Löbmann, C.J. Strachan, H. Grohganz, T. Rades, Emerging trends in the stabilization of amorphous drugs, Int. J. Pharm. 453 (2013) 65–79.
[28] B. Karolewicz, A. Górniak, A. Owczarek, K. Nartowski, E. Zurawska-Płaksej, J. Pluta, Solid dispersion in pharmaceutical technology. part II. the methods of analysis of solid dispersions and examples of their application, Polim. Med. 42 (2012) 97–107.
[29] E.H. Lee, A practical guide to pharmaceutical polymorph screening & selection, Asian J. Pharm. Sci. 9 (2014) 163–175.
[30] T. Murshedkar, Effect of Crystalline to Amorphous Conversions on Solubility of Cefuroxime Axetil, University of Rhode Island, 2002.
[31] M. Tawa, O. Almarsson, J. Remenar, Pharmaceutical Salts of Zafirlukast, Google Patents, 2005.
[32] G. Pastrano, E. Ghaly, Physicochemical characterization of spray dried formulation containing amorphous drug, Int. J. Pharm. Pharm. Sci. 4 (2012) 563–570.
[33] A. Talaczyńska, K. Lewandowska, A. Jelińska, P. Garbacki, A. Podborska, P. Zalewski, I. Oszczapowicz, A. Sikora, M. Kozak, J. Cielecka-Piontek, Application of vibrational spectroscopy supported by theoretical calculations in identification of amorphous and crystalline forms of cefuroxime axetil, Sci. World J. 2015 (2015) 921049.
[34] A. Jelińska, I. Dudzińska, M. Zajac, I. Oszczpowicz, The stability of the amorphous form of cefuroxime axetil in solid state, J. Pharm. Biomed. Anal. 41 (2006) 1075–1081.
[35] N.A. Urbanetz, Stabilization of solid dispersions of nimodipine and polyethylene glycol 2000, Eur. J. Pharm. Sci. 28 (2006) 67–76.
[36] N. Tanaka, K. Imai, K. Okimoto, S. Ueda, Y. Tokunaga, A. Ohike, R. Ibuki, K. Higaki, T. Kimura, Development of novel sustained-release system, disintegration-controlled matrix tablet (DCMT) with solid dispersion granules of nilvadipine, J. Control. Release 108 (2005) 386–395.
[37] T. Vilhelmsen, H. Eliasen, T. Schfer, Effect of a melt agglomeration process on agglomerates containing solid dispersions, Int. J. Pharm. 303 (2005) 132–142.
[38] A. Karata, N. Yksel, T. Baykara, Improved solubility and dissolution rate of piroxicam using gelucire 44/14 and labrasol, Farmaco 60 (2005) 777–782.
[39] F. Damian, N. Blaton, L. Naesens, J. Balzarini, R. Kinget, P. Augustijns, G. Van den Mooter, Physicochemical characterization of solid dispersions of the antiviral agent UC-781 with polyethylene glycol 6000 and gelucire 44/14, Eur. J. Pharm. Sci. 10 (2000) 311–322.
[40] T. Vasconcelos, P. Barrocas, R. Lima, P. Soares-da-Silva, Development of An Opicapone Third Generation Solid Dispersion, 2013 AAPS Annual MeetingSan Antonio, USA, 2013.
[41] Y. He, C. Ho, Amorphous solid dispersions: utilization and challenges in drug discovery and development, J. Pharm. Sci. 104 (2015) 3237–3258.
[42] L.H. Nielsen, T. Rades, A. Müllertz, Stabilisation of amorphous furosemide increases the oral drug bioavailability in rats, Int. J. Pharm. 490 (2015) 334–340.
[43] C.L. Vo, C. Park, B.J. Lee, Current trends and future perspectives of solid dispersions containing poorly water-soluble drugs, Eur. J. Pharm. Biopharm. 85 (2013) 799–813.
[44] Y. Huang, W.-G. Dai, Fundamental aspects of solid dispersion technology for poorly soluble drugs, APSB 4 (2014) 18–25.
[45] Y. Lin, R.P. Cogdill, P.L. Wildfong, Informatic calibration of a materials properties database for predictive assessment of mechanically activated disordering potential for small molecule organic solids, J. Pharm. Sci. 98 (2009) 2696–2708.
[46] P.L. Sóti, K. Bocz, H. Pataki, Z. Eke, A. Farkas, G. Verreck, É. Kiss, P. Fekete, T. Vigh, I. Wagner, Z.K. Nagy, G. Marosi, Comparison of spray drying, electroblowing and electrospinning for preparation of eudragit E and itraconazole solid dispersions, Int. J. Pharm. 494 (2015) 23–30.
[47] N. Passerini, G. Calogerà, B. Albertini, L. Rodriguez, Melt granulation of pharmaceutical powders: a comparison of high-shear mixer and fluidised bed processes, Int. J. Pharm. 391 (2010) 177–186.
[48] A. Homayouni, F. Sadeghi, A. Nokhodchi, J. Varshosaz, H. Afrasiabi Garekani, Preparation and characterization of celecoxib dispersions in Soluplus(®): comparison of spray drying and conventional methods, Iran J. Pharm. Res. 14 (2015) 35–50.
[49] C. Potter, Y. Tian, G. Walker, C. McCoy, P. Hornsby, C. Donnelly, D.S. Jones, G.P. Andrews, Novel supercritical carbon dioxide impregnation technique for the production of amorphous solid drug dispersions: a comparison to hot melt extrusion, Mol. Pharm. 12 (2015) 1377–1390.
[50] D.-H. Won, M.-S. Kim, S. Lee, J.-S. Park, S.-J. Hwang, Improved physicochemical characteristics of felodipine solid dispersion particles by supercritical anti-solvent precipitation process, Int. J. Pharm. 301 (2005) 199–208.
[51] K. Dhirendra, S. Lewis, N. Udupa, K. Atin, Solid dispersions: a review, Pak. J. Pharm. Sci. 22 (2009) 234–246.
[52] L.S. Taylor, G. Zografi, Spectroscopic characterization of interactions between PVP and indomethacin in amorphous molecular dispersions, Pharm. Res. 14 (1997) 1691–1698.
[53] M.A. Repka, S. Shah, J. Lu, S. Maddineni, J. Morott, K. Patwardhan, N.N. Mohammed, Melt extrusion: process to product, Expert Opin. Drug Deliv. 9 (2012) 105–125.
[54] A. Paudel, Z.A. Worku, J. Meeus, S. Guns, G. Van den Mooter, Manufacturing of solid dispersions of poorly water soluble drugs by spray drying: formulation and process considerations, Int. J. Pharm. 453 (2013) 253–284.
[55] H. Patil, R.V. Tiwari, M.A. Repka, Hot-melt extrusion: from theory to application in pharmaceutical formulation, AAPS PharmSciTech (2015).
[56] E.S. Ha, I.H. Baek, W. Cho, S.J. Hwang, M.S. Kim, Preparation and evaluation of solid dispersion of atorvastatin calcium with Soluplus® by spray drying technique, Chem. Pharm. Bull.(Tokyo) 62 (2014) 545–551.
[57] T. Xie, L. Taylor, Dissolution performance of high drug loading celecoxib amorphous solid dispersions formulated with polymer combinations, Pharm. Res. (2015) 1–12.
[58] S.Y.K. Fong, A. Ibisogly, A. Bauer-Brandl, Solubility enhancement of BCS class II drug by solid phospholipid dispersions: spray drying versus freeze-drying, Int. J. Pharm. 496 (2015) 382–391.
[59] J.H. Park, H.K. Choi, Enhancement of solubility and dissolution of cilostazol by solid dispersion technique, Arch. Pharm. Res. 38 (2015) 1336–1344.
[60] Y.H. Kim, D.W. Kim, M.S. Kwon, K.H. Cho, J.O. Kim, C.S. Yong, H.-G. Choi, Clopidogrel napadisilate monohydrate loaded surface-modified solid dispersion: physicochemical characterization and in vivo evaluation, Biol. Pharm. Bull. 38 (2015) 1033–1040.
[61] D.J. van Drooge, W.L.J. Hinrichs, M.R. Visser, H.W. Frijlink, Characterization of the molecular distribution of drugs in glassy solid dispersions at the nano-meter scale, using differential scanning calorimetry and gravimetric water vapour sorption techniques, Int. J. Pharm. 310 (2006) 220–229.
[62] J. Desai, K. Alexander, A. Riga, Characterization of polymeric dispersions of dimenhydrinate in ethyl cellulose for controlled release, Int. J. Pharm. 308 (2006) 115–123.
[63] S.M. Lim, Z.W. Pang, H.Y. Tan, M. Shaikh, G. Adinarayana, S. Garg, Enhancement of docetaxel solubility using binary and ternary solid dispersion systems, Drug Dev. Ind. Pharm. (2015) 1–9.
[64] E. Karavas, G. Ktistis, A. Xenakis, E. Georgarakis, Effect of hydrogen bonding interactions on the release mechanism of felodipine from nanodispersions with polyvinylpyrrolidone, Eur. J. Pharm. Biopharm. 63 (2006) 103–114.
[65] G.P. Sanganwar, R.B. Gupta, Dissolution-rate enhancement of fenofibrate by adsorption onto silica using supercritical carbon dioxide, Int. J. Pharm. 360 (2008) 213–218.
[66] A. Pestieau, F. Krier, P. Lebrun, A. Brouwers, B. Streel, B. Evrard, Optimization of a PGSS (particles from gas saturated solutions) process for a fenofibrate lipid-based solid dispersion formulation, Int. J. Pharm. 485 (2015) 295–305.

[67] Y. Yoshihashi, H. Iijima, E. Yonemochi, K. Terada, Estimation of physical stability of amorphous solid dispersion using differential scanning calorimetry, J. Therm. Anal. Calorim. 85 (2006) 689–692.
[68] R. Censi, M. Gigliobianco, A. Dubbini, L. Malaj, P. Di Martino, New nanometric solid dispersions of glibenclamide in Neusilin® UFL2, AAPS PharmSciTech (2015) 1–9.
[69] K. Higashi, H. Hayashi, K. Yamamoto, K. Moribe, The effect of drug and EUDRAGIT® S 100 miscibility in solid dispersions on the drug and polymer dissolution rate, Int. J. Pharm. 494 (2015) 9–16.
[70] M. Tabbakhian, F. Hasanzadeh, N. Tavakoli, Z. Jamshidian, Dissolution enhancement of glibenclamide by solid dispersion: solvent evaporation versus a supercritical fluid-based solvent–antisolvent technique, Res. Pharm. Sci. 9 (2014) 337–350.
[71] X. Sui, W. Wei, L. Yang, Y. Zu, C. Zhao, L. Zhang, F. Yang, Z. Zhang, Preparation, characterization and in vivo assessment of the bioavailability of glycyrrhizic acid microparticles by supercritical anti-solvent process, Int. J. Pharm. 423 (2012) 471–479.
[72] H.S. Purohit, L.S. Taylor, Miscibility of itraconazole–hydroxypropyl methylcellulose blends: insights with high resolution analytical methodologies, Mol. Pharm. 12 (2015) 4542–4553.
[73] X. Yin, L.S. Daintree, S. Ding, D.M. Ledger, B. Wang, W. Zhao, J. Qi, W. Wu, J. Han, Itraconazole solid dispersion prepared by a supercritical fluid technique: preparation, in vitro characterization, and bioavailability in beagle dogs, Drug Des. Devel. Ther. 9 (2015) 2801–2810.
[74] E.-S. Ha, J.-S. Kim, I.-h. Baek, J.-W. Yoo, Y. Jung, H.R. Moon, M.-S. Kim, Development of megestrol acetate solid dispersion nanoparticles for enhanced oral delivery by using a supercritical antisolvent process, Drug Des. Devel. Ther. 9 (2015) 4269–4277.
[75] A. Singh, C. De Bisschop, H. Schut, J. Van Humbeeck, G. Van Den Mooter, Compression effects on the phase behaviour of miconazole–poly (1-vinylpyrrolidone-co-vinyl acetate) solid dispersions—role of pressure, dwell time, and preparation method, J. Pharm. Sci. 104 (2015) 3366–3376.
[76] S. Keratichewanun, Y. Yoshihashi, N. Sutanthavibul, K. Terada, J. Chatchawalsaisin, An investigation of nifedipine miscibility in solid dispersions using Raman spectroscopy, Pharm. Res. 32 (2015) 2458–2473.
[77] J.R. Falconer, J. Wen, S. Zargar-Shoshtari, J.J. Chen, F. Mohammed, J. Chan, R.G. Alany, The effects of supercritical carbon dioxide processing on progesterone dispersion systems: a multivariate study, AAPS PharmSciTech 13 (2012) 1255–1265.
[78] Y. Li, D.J. Yang, S.L. Chen, S.B. Chen, A.S. Chan, Process parameters and morphology in puerarin, phospholipids and their complex microparticles generation by supercritical antisolvent precipitation, Int. J. Pharm. 359 (2008) 35–45.
[79] T. Vasconcelos, S. Marques, B. Sarmento, Development of a Resveratrol Solid Dispersion with Soluplus®, 2nd Annual Meeting & Exposition of the Controlled Release SocietyEdinburgh, Scotland, 2015.
[80] N. Ahuja, O.P. Katare, B. Singh, Studies on dissolution enhancement and mathematical modeling of drug release of a poorly water-soluble drug using water-soluble carriers, Eur. J. Pharm. Biopharm. 65 (2007) 26–38.
[81] G. Craye, K. Löbmann, H. Grohganz, T. Rades, R. Laitinen, Characterization of amorphous and co-amorphous simvastatin formulations prepared by spray drying, Molecules 20 (2015) 19784.
[82] Y. Cho, E.-S. Ha, I.-H. Baek, M.-S. Kim, C.-W. Cho, S.-J. Hwang, Enhanced supersaturation and oral absorption of sirolimus using an amorphous solid dispersion based on Eudragit® E, Molecules 20 (2015) 9496.
[83] K. Wlodarski, W. Sawicki, A. Kozyra, L. Tajber, Physical stability of solid dispersions with respect to thermodynamic solubility of tadalafil in PVP-VA, Eur. J. Pharm. Biopharm. 96 (2015) 237–246.
[84] K. Wlodarski, W. Sawicki, K. Haber, J. Knapik, Z. Wojnarowska, M. Paluch, P. Lepek, L. Hawelek, L. Tajber, Physicochemical properties of tadalafil solid dispersions—impact of polymer on the apparent solubility and dissolution rate of tadalafil, Eur. J. Pharm. Biopharm. 94 (2015) 106–115.
[85] M.S. Kim, I.H. Baek, Fabrication and evaluation of valsartan–polymer–surfactant composite nanoparticles by using the supercritical antisolvent process, Int. J. Nanomedicine 9 (2014) 5167–5176.
[86] V.M. Yoshida, V.M. Balcão, M.M. Vila, J.M. Oliveira Júnior, N. Aranha, M.V. Chaud, M.P. Gremião, Zidovudine-poly(L-lactic acid) solid dispersions with improved intestinal permeability prepared by supercritical antisolvent process, J. Pharm. Sci. 104 (2015) 1691–1700.
[87] M. Milne, W. Liebenberg, M. Aucamp, The stabilization of amorphous Zopiclone in an amorphous solid dispersion, AAPS PharmSciTech (2015).
[88] G.R. Lloyd, D.Q. Craig, A. Smith, A calorimetric investigation into the interaction between paracetamol and polyethlene glycol 4000 in physical mixes and solid dispersions, Eur. J. Pharm. Biopharm. 48 (1999) 59–65.
[89] D. Engers, J. Teng, J. Jimenez-Novoa, P. Gent, S. Hossack, C. Campbell, J. Thomson, I. Ivanisevic, A. Templeton, S. Byrn, A. Newman, A solid-state approach to enable early development compounds: selection and animal bioavailability studies of an itraconazole amorphous solid dispersion, J. Pharm. Sci. 99 (2010) 3901–3922.
[90] A. Shanbhag, S. Rabel, E. Nauka, G. Casadevall, P. Shivanand, G. Eichenbaum, P. Mansky, Method for screening of solid dispersion formulations of low-solubility compounds—miniaturization and automation of solvent casting and dissolution testing, Int. J. Pharm. 351 (2008) 209–218.
[91] G. Muhrer, U. Meier, F. Fusaro, S. Albano, M. Mazzotti, Use of compressed gas precipitation to enhance the dissolution behavior of a poorly water-soluble drug: generation of drug microparticles and drug–polymer solid dispersions, Int. J. Pharm. 308 (2006) 69–83.
[92] V. Majerik, G. Charbit, E. Badens, G. Horvath, L. Szokonya, N. Bosc, E. Teillaud, Bioavailability enhancement of an active substance by supercritical antisolvent precipitation, J. Supercrit. Fluids 40 (2007) 101–110.
[93] H. Yue, S.J. Nicholson, J.D. Young, D. Hsieh, R.J. Ketner, R.G. Hall, J. Sackett, E.C. Banks, J.A. Castoro, M.E. Randazzo, Development of a control strategy for benzene impurity in HPMCAS-stabilized spray-dried dispersion drug products using a science-based and risk-based approach, Pharm. Res. 32 (2015) 2636–2648.
[94] S. Sinha, M. Ali, S. Baboota, A. Ahuja, A. Kumar, J. Ali, Solid dispersion as an approach for bioavailability enhancement of poorly water-soluble drug ritonavir, AAPS PharmSciTech 11 (2010) 518–527.
[95] A.B. Gangurde, H.S. Kundaikar, S.D. Javeer, D.R. Jaiswar, M.S. Degani, P.D. Amin, Enhanced solubility and dissolution of curcumin by a hydrophilic polymer solid dispersion and its insilico molecular modeling studies, J. Drug Delivery Sci. Technol. 29 (2015) 226–237.
[96] D.J.v. Drooge, K. Braeckmans, W.L.J. Hinrichs, K. Remaut, S.C.D. Smedt, H.W. Frijlink, Characterization of the mode of incorporation of lipophilic compounds in solid dispersions at the nanoscale using fluorescence resonance energy transfer (FRET), Macromol. Rapid Commun. 27 (2006) 1149–1155.
[97] D.L. Teagarden, D.S. Baker, Practical aspects of lyophilization using non-aqueous co-solvent systems, Eur. J. Pharm. Sci. 15 (2002) 115–133.
[98] I. Pasquali, R. Bettini, F. Giordano, Supercritical fluid technologies: an innovative approach for manipulating the solid-state of pharmaceuticals, Adv. Drug Deliv. Rev. 60 (2008) 399–410.
[99] P. Srinarong, H. de Waard, H.W. Frijlink, W.L. Hinrichs, Improved dissolution behavior of lipophilic drugs by solid dispersions: the production process as starting point for formulation considerations, Expert Opin. Drug Deliv. 8 (2011) 1121–1140.
[100] A. Fattahi, J. Karimi-Sabet, A. Keshavarz, A. Golzary, M. Rafiee-Tehrani, F.A. Dorkoosh, Preparation and characterization of simvastatin nanoparticles using rapid expansion of supercritical solution (RESS) with trifluoromethane, J. Supercrit. Fluids 107 (2016) 469–478.
[101] P. Girotra, S.K. Singh, K. Nagpal, Supercritical fluid technology: a promising approach in pharmaceutical research, Pharm. Dev. Technol. 18 (2013) 22–38.
[102] K. Mishima, M. Honjo, T. Sharmin, S. Ito, R. Kawakami, T. Kato, M. Misumi, T. Suetsugu, H. Orii, H. Kawano, K. Irie, K. Sano, T. Harada, M. Ouchi, Gas-saturated solution process to obtain microcomposite particles of alpha lipoic acid/hydrogenated colza oil in supercritical carbon dioxide, Pharm. Dev. Technol. (2015) 1–12.
[103] Q. Jiang, Y. Li, Q. Fu, Y. Geng, J. Zhao, P. Ma, T. Zhang, In-vitro and in-vivo study of amorphous spironolactone prepared by adsorption method using supercritical CO2, Drug Dev. Ind. Pharm. 41 (2015) 201–206.
[104] M.S. Kim, S.J. Jin, J.S. Kim, H.J. Park, H.S. Song, R.H. Neubert, S.J. Hwang, Preparation, characterization and in vivo evaluation of amorphous atorvastatin calcium nanoparticles using supercritical antisolvent (SAS) process, Eur. J. Pharm. Biopharm. 69 (2008) 454–465.
[105] K. Gong, R. Viboonkiat, I.U. Rehman, G. Buckton, J.A. Darr, Formation and characterization of porous indomethacin-PVP coprecipitates prepared using solvent-free supercritical fluid processing, J. Pharm. Sci. 94 (2005) 2583–2590.
[106] J. Park, H.J. Park, W. Cho, K.H. Cha, Y.S. Kang, S.J. Hwang, Preparation and pharmaceutical characterization of amorphous cefdinir using spray-drying and SAS-process, Int. J. Pharm. 396 (2010) 239–245.
[107] S. Lee, K. Nam, M.S. Kim, S.W. Jun, J.S. Park, J.S. Woo, S.J. Hwang, Preparation and characterization of solid dispersions of itraconazole by using aerosol solvent extraction system for improvement in drug solubility and bioavailability, Arch. Pharm. Res. 28 (2005) 866–874.
[108] I. Kikic, P. Alessi, F. Eva, M. Moneghini, B. Perissutti, Supercritical antisolvent precipitation of atenolol: the influence of the organic solvent and of the processing approach, J. Supercrit. Fluids 38 (2006) 434–441.
[109] P.Y.M. Hanna, in: WO (Ed.), Method and Apparatus for the Formation of Particles, 1995.
[110] F. Tres, S. Coombes, A. Phillips, L. Hughes, S. Wren, J. Aylott, J. Burley, Investigating the dissolution performance of amorphous solid dispersions using magnetic resonance imaging and proton NMR, Molecules 20 (2015) 16404.
[111] S.-Y. Chan, S. Qi, D.Q.M. Craig, An investigation into the influence of drug–polymer interactions on the miscibility, processability and structure of polyvinylpyrrolidone-based hot melt extrusion formulations, Int. J. Pharm. 496 (2015) 95–106.
[112] S. Huang, K.P. O'Donnell, J.M. Keen, M.A. Rickard, J.W. McGinity, R.O. Williams, A new extrudable form of hypromellose: AFFINISOL™ HPMC HME, AAPS PharmSciTech (2015).
[113] W. De Jaeghere, T. De Beer, J. Van Bocxlaer, J.P. Remon, C. Vervaet, Hot-melt extrusion of polyvinyl alcohol for oral immediate release applications, Int. J. Pharm. 492 (2015) 1–9.
[114] M. Shergill, M. Patel, S. Khan, A. Bashir, C. McConville, Development and characterisation of sustained release solid dispersion oral tablets containing the poorly water soluble drug disulfiram, Int. J. Pharm. 497 (2016) 3–11.
[115] P.T. Koh, J.N. Chuah, M. Talekar, A. Gorajana, S. Garg, Formulation development and dissolution rate enhancement of efavirenz by solid dispersion systems, Indian J. Pharm. Sci. 75 (2013) 291–301.
[116] M. Alhijjaj, J. Bouman, N. Wellner, P. Belton, S. Qi, Creating drug solubilization compartments via phase separation in multicomponent buccal patches prepared by direct hot melt extrusion–injection molding, Mol. Pharm. 12 (2015) 4349–4362.
[117] X. Feng, A. Vo, H. Patil, R.V. Tiwari, A.S. Alshetaili, M.B. Pimparade, M.A. Repka, The effects of polymer carrier, hot melt extrusion process and downstream processing parameters on the moisture sorption properties of amorphous solid dispersions, J. Pharm. Pharmacol. (2015) (n/a-n/a).
[118] M. Maniruzzaman, A. Nair, N. Scoutaris, M.S.A. Bradley, M.J. Snowden, D. Douroumis, One-step continuous extrusion process for the manufacturing of solid dispersions, Int. J. Pharm. 496 (2015) 42–51.

[119] X. Yuan, T.-X. Xiang, B.D. Anderson, E.J. Munson, Hydrogen bonding interactions in amorphous indomethacin and its amorphous solid dispersions with poly(vinylpyrrolidone) and poly(vinylpyrrolidone-co-vinyl acetate) studied using 13C solid-state NMR, Mol. Pharm. 12 (2015) 4518–4528.
[120] J.Y. Lee, W.S. Kang, J. Piao, I.S. Yoon, D.D. Kim, H.J. Cho, Soluplus®/TPGS-based solid dispersions prepared by hot-melt extrusion equipped with twin-screw systems for enhancing oral bioavailability of valsartan, Drug Des. Devel. Ther. 9 (2015) 2745–2756.
[121] E.Y. Shalaev, Q. Lu, M. Shalaeva, G. Zografi, Acid-catalyzed inversion of sucrose in the amorphous state at very low levels of residual water, Pharm. Res. 17 (2000) 366–370.
[122] T. Vasconcelos, P. costa, Development of a rapid dissolving Ibuprofen solid dispersion, PSWC—7 Pharmaceutical Sciences World ConferenceAmsterdam, Netherlands, 2007.
[123] K. Sekiguchi, N. Obi, Y. Ueda, Studies on absorption of eutectic mixture. II. Absorption of fused conglomerates of chloramphenicol and urea in rabbits, Chem. Pharm. Bull.(Tokyo) 12 (1964) 134–144.
[124] V.B. Pokharkar, L.P. Mandpe, M.N. Padamwar, A.A. Ambike, K.R. Mahadik, A. Paradkar, Development, characterization and stabilization of amorphous form of a low Tg drug, Powder Technol. 167 (2006) 20–25.
[125] W.L. Chiou, S. Riegelman, Preparation and dissolution characteristics of several fast-release solid dispersions of griseofulvin, J. Pharm. Sci. 58 (1969) 1505–1510.
[126] R.J. Timko, N.G. Lordi, Thermal characterization of citric acid solid dispersions with benzoic acid and phenobarbital, J. Pharm. Sci. 68 (1979) 601–605.
[127] A. Nagapudi, J. Jona, Amorphous active pharmaceutical ingredients in preclinical studies: preparation, characterization, and formulation, Curr. Bioact. Compd. (2008) 213–224.
[128] S.R. Vippagunta, Z. Wang, S. Hornung, S.L. Krill, Factors affecting the formation of eutectic solid dispersions and their dissolution behavior, J. Pharm. Sci. 96 (2006) 294–304.
[129] L. Gunawan, G.P. Johari, R.M. Shanker, Structural relaxation of acetaminophen glass, Pharm. Res. 23 (2006) 967–979.
[130] M. Stanković, H.W. Frijlink, W.L. Hinrichs, Polymeric formulations for drug release prepared by hot melt extrusion: application and characterization, Drug Discov. Today 20 (2015) 812–823.
[131] K. Nakamichi, T. Nakano, H. Yasuura, S. Izumi, Y. Kawashima, The role of the kneading paddle and the effects of screw revolution speed and water content on the preparation of solid dispersions using a twin-screw extruder, Int. J. Pharm. 241 (2002) 203–211.
[132] J. Breitenbach, J. Lewis, Two concepts, one technology: controlled release and solid dispersion with meltrex, in: M.J. Rathbone, J. Hadgraft, M.S. Roberts (Eds.), Modified-Release Drug Delivery Technology, Marcel Dekker, New York 2003, pp. 125–134.
[133] A. Loxley, Devices and implants prepared using hot melt extrusion, in: M.A. Repka, N. Langley, J. DiNunzio (Eds.), Melt Extrusion, Springer, New York, USA 2013, pp. 281–298.
[134] P. Thybo, L. Hovgaard, J. Lindeløv, A. Brask, S. Andersen, Scaling up the spray drying process from pilot to production scale using an atomized droplet size criterion, Pharm. Res. 25 (2008) 1610–1620.
[135] D.E. Dobry, D.M. Settell, J.M. Baumann, R.J. Ray, L.J. Graham, R.A. Beyerinck, A model-based methodology for spray-drying process development, J. Pharm. Innov. 4 (2009) 133–142.
[136] A. Paudel, Y. Loyson, G. Van den Mooter, An investigation into the effect of spray drying temperature and atomizing conditions on miscibility, physical stability, and performance of naproxen-PVP K 25 solid dispersions, J. Pharm. Sci. 102 (2013) 1249–1267.
[137] B. Gu, B. Linehan, Y.C. Tseng, Optimization of the Büchi B-90 spray drying process using central composite design for preparation of solid dispersions, Int. J. Pharm. 491 (2015) 208–217.
[138] L.H. Tee, A. Luqman Chuah, K.Y. Pin, A. Abdull Rashih, Y.A. Yusof, Optimization of spray drying process parameters of *Piper betle* L. (Sirih) leaves extract coated with maltodextrin, J. Chem. Pharm. Res. 4 (2012) 1833–1841.
[139] A.S. Patel, T. Soni, V. Thakkar, T. Gandhi, Effects of spray drying conditions on the physicochemical properties of the tramadol-hcl microparticles containing Eudragit(®) RS and RL, J. Pharm. Bioallied Sci. 4 (2012) S50–S53.
[140] ICH, Impurities: guideline for residual solvents Q3C(R5), International Conference On Harmonisation Of Technical Requirements For Registration Of Pharmaceuticals For Human Use, 2011.
[141] B.B. Patel, J.K. Patel, S. Chakraborty, D. Shukla, Revealing facts behind spray dried solid dispersion technology used for solubility enhancement, Saudi Pharm. J. 23 (2015) 352–365.
[142] H. Al-Obaidi, P. Ke, S. Brocchini, G. Buckton, Characterization and stability of ternary solid dispersions with PVP and PHPMA, Int. J. Pharm. 419 (2011) 20–27.
[143] D.F. Bain, D.L. Munday, A. Smith, Solvent influence on spray-dried biodegradable microspheres, J. Microencapsul. 16 (1999) 453–474.
[144] K.J. Paluch, L. Tajber, M.I. Amaro, O.I. Corrigan, A.M. Healy, Impact of process variables on the micromeritic and physicochemical properties of spray-dried microparticles–part II. Physicochemical characterisation of spray-dried materials, J. Pharm. Pharmacol. 64 (2012) 1583–1591.
[145] O. Ní Ógáin, L. Tajber, O.I. Corrigan, A.M. Healy, Spray drying from organic solvents to prepare nanoporous/nanoparticulate microparticles of protein: excipient composites designed for oral inhalation, J. Pharm. Pharmacol. 64 (2012) 1275–1290.
[146] J.Y. Jung, S.D. Yoo, S.H. Lee, K.H. Kim, D.S. Yoon, K.H. Lee, Enhanced solubility and dissolution rate of itraconazole by a solid dispersion technique, Int. J. Pharm. 187 (1999) 209–218.
[147] M. Dixit, A.G. Kini, P.K. Kulkarni, Preparation and characterization of microparticles of piroxicam by spray drying and spray chilling methods, Res. Pharm. Sci. 5 (2010) 89–97.
[148] Z.Y. Yang, Y. Le, T.T. Hu, Z. Shen, J.F. Chen, J. Yun, Production of ultrafine sumatriptan succinate particles for pulmonary delivery, Pharm. Res. 25 (2008) 2012–2018.
[149] S.K. Paidi, S.K. Jena, B.K. Ahuja, N. Devasari, S. Suresh, Preparation, in-vitro and in-vivo evaluation of spray-dried ternary solid dispersion of biopharmaceutics classification system class II model drug, J. Pharm. Pharmacol. 67 (2015) 616–629.
[150] F.J. Wang, C.H. Wang, Effects of fabrication conditions on the characteristics of etanidazole spray-dried microspheres, J. Microencapsul. 19 (2002) 495–510.
[151] A. Sass, G. Lee, Evaluation of some water-miscible organic solvents for spray-drying enzymes and carbohydrates, Drug Dev. Ind. Pharm. 40 (2014) 749–757.
[152] M. Morgen, C. Bloom, R. Beyerinck, A. Bello, W. Song, K. Wilkinson, R. Steenwyk, S. Shamblin, Polymeric nanoparticles for increased oral bioavailability and rapid absorption using celecoxib as a model of a low-solubility, high-permeability drug, Pharm. Res. 29 (2012) 427–440.
[153] A.N. Ghebremeskel, C. Vemavarapu, M. Lodaya, Use of surfactants as plasticizers in preparing solid dispersions of poorly soluble API: selection of polymer–surfactant combinations using solubility parameters and testing the processability, Int. J. Pharm. 328 (2007) 119–129.
[154] J. Chen, J.D. Ormes, J.D. Higgins, L.S. Taylor, Impact of surfactants on the crystallization of aqueous suspensions of celecoxib amorphous solid dispersion spray dried particles, Mol. Pharm. 12 (2015) 533–541.
[155] N. Marasini, T.H. Tran, B.K. Poudel, H.J. Cho, Y.K. Choi, S.C. Chi, H.G. Choi, C.S. Yong, J.O. Kim, Fabrication and evaluation of pH-modulated solid dispersion for telmisartan by spray-drying technique, Int. J. Pharm. 441 (2013) 424–432.
[156] S. Janssens, H.N. de Armas, C.J. Roberts, G. Van den Mooter, Characterization of ternary solid dispersions of itraconazole, PEG 6000, and HPMC 2910 E5, J. Pharm. Sci. 97 (2008) 2110–2120.
[157] X. Li, C. Jiang, L. Pan, H. Zhang, L. Hu, T. Li, X. Yang, Effects of preparing techniques and aging on dissolution behavior of the solid dispersions of NF/soluplus/kollidon SR: identification and classification by a combined analysis by FT-IR spectroscopy and computational approaches, Drug Dev. Ind. Pharm. 41 (2015) 2–14.
[158] F.F. Van Goor, R.G. Alargova, T.E. Alcacio, S.G. Arekar, S.C. Johnston, I.N. Kadiyala, A. Keshavarz-Shokri, M. Krawiec, E.C. Lee, A. Medek, Pharmaceutical Compositions and Administrations thereof, Google Patents, 2015.
[159] K.J. Bittorf, F. Gaspar, J.P. Katstra, Fluidized Spray Drying, Google Patents, 2009.
[160] F.R.I. Kiekens, J.F.M. Voorspoels, L.E.C. Baert, Process for Preparing Spray Dried Formulations of tmc125, Google Patents, 2007.
[161] V.V. Kulthe, P.D. Chaudhari, H.Y. Aboul-Enein, Freeze-dried amorphous dispersions for solubility enhancement of thermosensitive API having low molecular lipophilicity, Drug. Res. (Stuttg) 64 (2014) 493–498.
[162] W. Abdelwahed, G. Degobert, S. Stainmesse, H. Fessi, Freeze-drying of nanoparticles: formulation, process and storage considerations, Adv. Drug Deliv. Rev. 58 (2006) 1688–1713.
[163] A. Seo, P. Holm, H.G. Kristensen, T. Schaefer, The preparation of agglomerates containing solid dispersions of diazepam by melt agglomeration in a high shear mixer, Int. J. Pharm. 259 (2003) 161–171.
[164] I. Aleksić, J. Duriš, I. Ilić, S. Ibrić, J. Parojčić, S. Srčič, In silico modeling of in situ fluidized bed melt granulation, Int. J. Pharm. 466 (2014) 21–30.
[165] S. Shanmugam, Granulation techniques and technologies: recent progresses, Bioimpacts 5 (2015) 55–63.
[166] N. Passerini, B. Albertini, M.L. González-Rodríguez, C. Cavallari, L. Rodriguez, Preparation and characterisation of ibuprofen-poloxamer 188 granules obtained by melt granulation, Eur. J. Pharm. Sci. 15 (2002) 71–78.
[167] M.K. Gupta, D. Goldman, R.H. Bogner, Y.C. Tseng, Enhanced drug dissolution and bulk properties of solid dispersions granulated with a surface adsorbent, Pharm. Dev. Technol. 6 (2001) 563–572.
[168] J. Kowalski, O. Kalb, Y.M. Joshi, A.T. Serajuddin, Application of melt granulation technology to enhance stability of a moisture sensitive immediate-release drug product, Int. J. Pharm. 381 (2009) 56–61.
[169] J. Rosenberg, U. Reinhold, B. Liepold, G. Berndl, J. Breitenbach, L. Alani, S. Ghosh, Solid Pharmaceutical Dosage Form, Google Patents, 2005.
[170] M.M. Crowley, F. Zhang, M.A. Repka, S. Thumma, S.B. Upadhye, S.K. Battu, J.W. McGinity, C. Martin, Pharmaceutical applications of hot-melt extrusion: part I, Drug Dev. Ind. Pharm. 33 (2007) 909–926.
[171] M. Wilson, M.A. Williams, D.S. Jones, G.P. Andrews, Hot-melt extrusion technology and pharmaceutical application, Ther. Deliv. 3 (2012) 787–797.
[172] J. Breitenbach, Melt extrusion: from process to drug delivery technology, Eur. J. Pharm. Biopharm. 54 (2002) 107–117.
[173] B. Van Melkebeke, C. Vervaet, J.P. Remon, Validation of a continuous granulation process using a twin-screw extruder, Int. J. Pharm. 356 (2008) 224–230.
[174] S.M. Alshahrani, J.T. Morott, A.S. Alshetaili, R.V. Tiwari, S. Majumdar, M.A. Repka, Influence of degassing on hot-melt extrusion process, Eur. J. Pharm. Sci. (2015).
[175] J.T. Morott, M. Pimparade, J.B. Park, C.P. Worley, S. Majumdar, Z. Lian, E. Pinto, Y. Bi, T. Durig, M.A. Repka, The effects of screw configuration and polymeric carriers on hot-melt extruded taste-masked formulations incorporated into orally disintegrating tablets, J. Pharm. Sci. 104 (2015) 124–134.
[176] C. Brown, J. DiNunzio, M. Eglesia, S. Forster, M. Lamm, M. Lowinger, P. Marsac, C. McKelvey, R. Meyer, L. Schenck, G. Terife, G. Troup, B. Smith-Goettler, C. Starbuck, Hot-melt extrusion for solid dispersions: composition and design considerations, in: N. Shah, H. Sandhu, D.S. Choi, H. Chokshi, A.W. Malick (Eds.), Amorphous Solid Dispersions, Springer, New York, USA 2014, pp. 197–230.
[177] T. Sakai, M. Thommes, Investigation into mixing capability and solid dispersion preparation using the DSM Xplore Pharma Micro Extruder, J. Pharm. Pharmacol. 66 (2014) 218–231.

[178] S. Sotthivirat, C. McKelvey, J. Moser, B. Rege, W. Xu, D. Zhang, Development of amorphous solid dispersion formulations of a poorly water-soluble drug, MK-0364, Int. J. Pharm. 452 (2013) 73–81.
[179] Z. Yang, K. Nollenberger, J. Albers, D. Craig, S. Qi, Microstructure of an immiscible polymer blend and its stabilization effect on amorphous solid dispersions, Mol. Pharm. 10 (2013) 2767–2780.
[180] X. Liu, M. Lu, Z. Guo, L. Huang, X. Feng, C. Wu, Improving the chemical stability of amorphous solid dispersion with cocrystal technique by hot melt extrusion, Pharm. Res. 29 (2012) 806–817.
[181] A. Sakurai, T. Sakai, K. Sako, Y. Maitani, Polymer combination increased both physical stability and oral absorption of solid dispersions containing a low glass transition temperature drug: physicochemical characterization and in vivo study, Chem. Pharm. Bull.(Tokyo) 60 (2012) 459–464.
[182] S.M. Alshehri, J.B. Park, B.B. Alsulays, R.V. Tiwari, B. Almutairy, A.S. Alshetaili, J. Morott, S. Shah, V. Kulkarni, S. Majumdar, S.T. Martin, S. Mishra, L. Wang, M.A. Repka, Mefenamic acid taste-masked oral disintegrating tablets with enhanced solubility via molecular interaction produced by hot melt extrusion technology, J. Drug Delivery Sci. Technol. 27 (2015) 18–27.
[183] A.M. Agrawal, M.S. Dudhedia, A.D. Patel, M.S. Raikes, Characterization and performance assessment of solid dispersions prepared by hot melt extrusion and spray drying process, Int. J. Pharm. 457 (2013) 71–81.
[184] B. Lang, S. Liu, J.W. McGinity, R.O. Williams, Effect of hydrophilic additives on the dissolution and pharmacokinetic properties of itraconazole-enteric polymer hot-melt extruded amorphous solid dispersions, Drug Dev. Ind. Pharm. (2015) 1–17.
[185] R. Fule, P. Amin, Development and evaluation of lafutidine solid dispersion via hot melt extrusion: investigating drug-polymer miscibility with advanced characterisation, Asian J. Pharm. Sci. 9 (2014) 92–106.
[186] J. Djuris, N. Ioannis, S. Ibric, Z. Djuric, K. Kachrimanis, Effect of composition in the development of carbamazepine hot-melt extruded solid dispersions by application of mixture experimental design, J. Pharm. Pharmacol. 66 (2014) 232–243.
[187] W. Wang, Q. Kang, N. Liu, Q. Zhang, Y. Zhang, H. Li, B. Zhao, Y. Chen, Y. Lan, Q. Ma, Q. Wu, Enhanced dissolution rate and oral bioavailability of *Ginkgo biloba* extract by preparing solid dispersion via hot-melt extrusion, Fitoterapia 102 (2015) 189–197.
[188] A.N. Ghebremeskel, C. Vemavarapu, M. Lodaya, Use of surfactants as plasticizers in preparing solid dispersions of poorly soluble API: stability testing of selected solid dispersions, Pharm. Res. 23 (2006) 1928–1936.
[189] G. Verreck, A. Decorte, K. Heymans, J. Adriaensen, D. Cleeren, A. Jacobs, D. Liu, D. Tomasko, A. Arien, J. Peeters, P. Rombaut, G. Van den Mooter, M.E. Brewster, The effect of pressurized carbon dioxide as a temporary plasticizer and foaming agent on the hot stage extrusion process and extrudate properties of solid dispersions of itraconazole with PVP-VA 64, Eur. J. Pharm. Sci. 26 (2005) 349–358.
[190] G. Verreck, A. Decorte, K. Heymans, J. Adriaensen, D. Liu, D.L. Tomasko, A. Arien, J. Peeters, P. Rombaut, G. Van den Mooter, M.E. Brewster, The effect of supercritical CO2 as a reversible plasticizer and foaming agent on the hot stage extrusion of itraconazole with EC 20 cps, J. Supercrit. Fluids 40 (2007) 153–162.
[191] Y. Joshi, J. Kowalski, J.P. Lakshman, A.E. Royce, W.Q. Tong, M. Vasanthavada, Formulation, Google Patents, 2011.
[192] L.Y. Fang, D. Harris, G. Krishna, A.E. Moton, R.C. Prestipino, M. Steinman, J. Wan, H.A. Waskin, Oral Pharmaceutical Compositions In A Solid Dispersion Comprising Preferably Posaconazole And HPMCAs, Google Patents, 2015.
[193] J.M. Miller, J.B. Morris, N.E. Sever, E.A. Schmitt, P.X. GAO, Y. Shi, Y. Gao, B. Liepold, A. MOOSMANN, M. Pauli, Solid Antiviral Dosage Forms, Google Patents, 2015.
[194] S.A. Surwase, L. Itkonen, J. Aaltonen, D. Saville, T. Rades, L. Peltonen, C.J. Strachan, Polymer incorporation method affects the physical stability of amorphous indomethacin in aqueous suspension, Eur. J. Pharm. Biopharm. 96 (2015) 32–43.
[195] M.M. Knopp, N.E. Olesen, P. Holm, P. Langguth, R. Holm, T. Rades, Influence of polymer molecular weight on drug–polymer solubility: a comparison between experimentally determined solubility in PVP and prediction derived from solubility in monomer, J. Pharm. Sci. 104 (2015) 2905–2912.
[196] A. Forster, J. Hempenstall, I. Tucker, T. Rades, Selection of excipients for melt extrusion with two poorly water-soluble drugs by solubility parameter calculation and thermal analysis, Int. J. Pharm. 226 (2001) 147–161.

International Journal of Pharmaceutics 595 (2021) 120245

Contents lists available at ScienceDirect

International Journal of Pharmaceutics

journal homepage: www.elsevier.com/locate/ijpharm

Third-generation solid dispersion combining Soluplus and poloxamer 407 enhances the oral bioavailability of resveratrol

Teófilo Vasconcelos [a,b,c,d], Fabíola Prezotti [e], Francisca Araújo [a], Carlos Lopes [a], Ana Loureiro [a], Sara Marques [b,f], Bruno Sarmento [c,d,g,*]

[a] BIAL-Portela & Cª, S.A., Avenida da Siderugia Nacional, 4745-457 Trofa, Portugal
[b] ICBAS - Instituto de Ciências Biomédicas Abel Salazar, University of Porto, Rua de Jorge Viterbo Ferreira, 228, 4050-313 Porto, Portugal
[c] INEB—Instituto de Engenharia Biomédica, Universidade do Porto, Rua Alfredo Allen, 208, 4200-135 Porto, Portugal
[d] i3S—Instituto de Investigação e Inovação em Saúde, Universidade do Porto, Rua Alfredo Allen, 208, 4200-135 Porto, Portugal
[e] Universidade Estadual Paulista, Faculdade de Ciências Farmacêuticas de Araraquara, Drugs and Pharmaceuticals, Brazil
[f] CIBIO/InBIO-UP—Research Centre in Biodiversity and Genetic Resources, University of Porto, Rua Padre Armando Quintas, 7, 4485-661 Vairão, Portugal
[g] CESPU - Instituto de Investigação e Formação Avançada em Ciências e Tecnologias da Saúde and Instituto Universitário de Ciências da Saúde, Rua Central de Gandra 1317, 4585-116, Gandra, Portugal

ARTICLE INFO

Keywords:
Solid dispersions
Bioavailability
Amorphous
Permeability enhancer
Metabolism inhibitor
Resveratrol

ABSTRACT

Resveratrol is a very promising anti-oxidant drug candidate with low oral bioavailability due to its intrinsic poor water solubility, intestinal efflux and metabolization mechanisms. Resveratrol solubility high-throughput screening with different carriers was performed showing an enhancement above 2000-fold with Soluplus® and Tween® 80. The former was selected as a carrier at the ratio of resveratrol: Soluplus® (1:2). Then, third-generation solid dispersions were developed with Gelucire® and poloxamer 407 at 5 and 15% to resveratrol: Soluplus® (1:2). All formulations enhanced solubility around 2-fold when compared to resveratrol: Soluplus® (1:2) solid dispersion. Caco-2 cells permeability studies showed that both surfactants increased drug permeability and the fraction recovered (2-fold) suggesting that these could reduce efflux mechanism and metabolism. Formulation with 15% poloxamer 407 demonstrated most promising results and was selected for further studies. In in vivo studies, resveratrol:Soluplus®: poloxamer 407 (1:2–15%) third generation solid dispersion presented an AUCo-t of 279 ± 54 ng.h/mL and a Cmax of 134 ± 78 ng/mL, 2.5 fold higher than solid dispersion without poloxamer 407. This work reports the development of third-generation solid dispersion that significantly improved resveratrol bioavailability. This was accomplished by an increased solubility and most probably by reducing intestinal efflux and metabolism mechanisms.

1. Introduction

Oral delivery is the simplest and easiest way to administer drugs (Sugawara et al., 2005; Youn et al., 2006). Therefore, most of the new chemical entities (NCE) under development are intended to be used as solid dosage forms that originate an effective and reproducible in vivo plasma concentration after oral administration (Charman and Charman, 2003; Ikegami et al., 2006). However, despite more potent, most of NCE are low water soluble drugs and/or poorly absorbed after oral administration (Charman and Charman, 2003; van Drooge et al., 2006) for which the use can be inhibited due to these drawbacks (Bogdanova et al., 2005; Pouton, 2006; Vippagunta et al., 2007). Moreover, most of this promising NCE, despite their high permeability, are only absorbed in the upper small intestine, presenting, therefore, a small absorption window (Streubel et al., 2006). Consequently, if these drugs are not completely released in this gastrointestinal area, they will present reduced oral bioavailability or at least high inter and intra-individual variability in bioavailability (Desai et al., 2006; Streubel et al., 2006).

Despite, a large variety of potential activities and data provided by animal models, the human clinical use of resveratrol is very limited and most of the clinical trials showed doubtful results (Athar et al., 2007; Gliemann et al., 2013). This is mainly attributed to the high doses required (>500 mg) and poor pharmacokinetic properties of resveratrol, since it presents very limited oral bioavailability (<5% of the oral dose reaches plasma), due to its poor water solubility and high metabolization (Boocock et al., 2007; la Porte et al., 2010).

* Corresponding author at: i3S—Instituto de Investigação e Inovação em Saúde, Universidade do Porto, Rua Alfredo Allen, 208, 4200-135 Porto, Portugal.
E-mail address: bruno.sarmento@ineb.up.pt (B. Sarmento).

https://doi.org/10.1016/j.ijpharm.2021.120245
Received 16 November 2020; Received in revised form 21 December 2020; Accepted 22 December 2020
Available online 21 January 2021
0378-5173/

Generally, solubility enhancement strategies based on formulation can be divided in particle size reduction techniques, liquid formulations or formulations using carriers.

The particle size reduction techniques such as milling or micronization are commonly used as approaches to improve solubility based on the increase of surface area (Craig, 2002; Pouton, 2006). These approaches present limited efficacy for compounds with a solubility below 0.1 mg/mL such as resveratrol, since the particle size reduction limit is around 2 to 5 μm which frequently is not enough to improve considerably the drug solubility or drug release in small intestine (Karavas et al., 2006; Muhrer et al., 2006; Pouton, 2006), and consequently to improve the bioavailability of these compounds (Karavas et al., 2006; Rasenack and Muller, 2004; Serajuddin, 1999). Moreover, the products obtained from these techniques generally present poor mechanical properties, such as low flow and high adhesion, and are extremely difficult to handle (Karavas et al., 2006; Muhrer et al., 2006) particularly in drug products with high dose, such as resveratrol. Finally, these techniques do not impact intestinal metabolism and/ or efflux and therefore have limited application in resveratrol.

In solid dispersion, drug is in its supersaturated state due to forced solubilisation in the carrier (Athar et al., 2007; Deng et al., 2008; Gentilli et al., 2001). It is characterized by the reduction of drug particle size to nearly a molecular level, by solubilizing or co-dissolving the drug in the water-soluble carrier, by providing better wettability and dispersibility and by forming amorphous products (Alcaín and Villalba, 2009; Stef et al., 2006). The use of excipients able to modulate intestinal metabolism and efflux mechanisms can be explored to improve the bioavailability of resveratrol (Vasconcelos et al., 2017). In the present work a third-generation solid dispersion was intended to be developed to improve resveratrol bioavailability over an equivalent second-generation solid dispersion.

2. Materials and methods

2.1. Reagents

Povidone, crospovidone, copovidone (COP) and sodium laurilsulfate were purchased from BASF (BTC-Europe), Spain. Soluplus®, PEG 6000, Kolliphor® P188 (poloxamer 188), Kolliphor® P 338 (poloxamer P338), Kolliphor® P 407 (poloxamer P407), were a gift from BASF (BTC-Europe), Spain. Hypromellose Acetate Succinate, low grade (HPMCAS-LG), Hypromellose Acetate Succinate, Medium grade (HPMCAS-MG) were a gift from Ashland, Spain. Copolymer of ethyl acrylate, methyl methacrylate and a low content of methacrylic acid ester with quaternary ammonium groups (Eudragit® RLPO) was acquired from Evonik, Germany. Polyoxyethylene (100) Stearate (Myrj 59P), Tween® 80 (T80) were acquired from Croda, Spain. Resveratrol was acquired to Abatra technology, China. Acetonitrile was obtained from Sigma Aldrich, Germany.

Culture flasks and Transwell® plates were purchased from Corning Inc., USA. Dulbecco's Modified Eagle medium (DMEM), L-glutamine, non-essential amino acids (NEAA), Penicillin (10000 IU/mL), Streptomycin (10 mg/mL) and trypsine-EDTA were purchased from HyClone, USA. Hank's balanced salt solution (HBBS) and heat inactivated fetal bovine serum (FBS) were purchased from Life Technologies Gibco, USA. Purified water was obtained by a milliQ purification system. All other materials were of analytical grade or equivalent.

2.2. High-throughput screening of resveratrol solubility

Resveratrol solubility was accessed in fourteen excipients (carriers), which were polymers selected from the major groups of hydrophilic carriers with potential to amorphize resveratrol. From Polyvinil derivates: povidone, crospovidone and COP were used. PEG6000, Soluplus® and Polyoxyethylene (100) Stearate (Myrj 59P) were selected from Polyethyleneglynol and derivates. From poloxamers, P 188, P 338 and P 407 were used. Hypromellose Acetate Succinate (low and medium grade) and copolymer of ethyl acrylate, methyl methacrylate and a low content of methacrylic acid ester with quaternary ammonium groups (Eudragit® RLPO) were evaluated. Finally, two surfactants were also tested, namely Tween 80 and sodium laurilsulfate.

Water solutions at 5% of each of the above excipients were prepared. In the particular case of HPMCAS that is not soluble in water pH (pH around 5.5), a phosphate buffer solution at pH 6.9 was prepared.

The resveratrol solubility was accessed in each of the above solutions. Briefly, an excess amount of resveratrol (15–25 mg) was added to a 2 mL HPLC vial. One millilitre of each of the above solutions was added to the vial and the preparations were magnet stirred for 2 h at room temperature 15–25 °C. Each preparation was prepared in triplicate. As a control, the solubility in purified water was accessed. After 2 h, the solutions were filtrated through a 0.45 μm filter and assayed by HPLC.

2.3. Preparation of resveratrol solid dispersions

The solid dispersions were prepared by the solvent cast method for the screening phase, selection of carrier and its content optimization. Briefly, approximately 0.6–1 g of resveratrol was dissolved in approximately 15 mL of ethanol under stirring at 40 °C. After resveratrol complete dissolution, the respective amount of polymer was dissolved in the previous solution under the same conditions. Then, after complete solubilisation, the obtained solution was spread into a Petri dish and dried at 65 °C during at least 18 h and until achieving a constant mass, meaning that no further ethanol was present in the formulation. The obtained films were removed from the Petri dish and pulverized in a mortar. For solubility, permeability and pharmacokinetic studies, solid dispersions were prepared by the same principle but using a rotavapor instead of a solvent cast process.

2.4. Selection of hydrophilic carrier and its content optimization

From the high throughput screening, several hydrophilic carriers were selected for further studies. Several solid dispersions with different resveratrol to polymer ratios were prepared for each selected polymer and accordingly to the following ratios: resveratrol:Polymer (5:1) - (83% resveratrol), resveratrol:Polymer (2:1) - (67% resveratrol), resveratrol:Polymer (1:1) - (50% resveratrol), resveratrol:Polymer (1:2) - (33% resveratrol) and resveratrol:Polymer (1:5) - (17% resveratrol).

2.5. Solid dispersions characterization

2.5.1. Fourier transform infrared

Attenuated total reflection ATR-FTIR spectra were obtained using a Bruker spectrophotometer (Tensor 27, Bruker, USA) equipped with a crystal diamond universal ATR sampling accessory. Before each measurement, the ATR crystal was carefully cleaned with ethanol. During the measurement, the sample was in contact with the universal diamond ATR top-plate. For each sample, the spectrum represented an average of 100 scans was recorded in the range of 4000–400 cm^{-1} with a 4 cm^{-1} resolution. Appearance, broadening or disappearance of absorption band(s) on the spectra of the solid dispersions in comparison with the individual spectrum of drug and polymeric carriers were used to determine possible interactions between pure resveratrol and polymers.

2.5.2. Water solubility

The solid dispersions solubility was accessed for each product after 24 h stirring. The 24 h timepoint was selected because it allowed the measurement of the thermodynamic solubility that also considers recrystallization events. Briefly, an excess amount of solid dispersion, corresponding to approximately 15–25 mg of resveratrol was added to a 2 mL HPLC vial. One milliliter of each polymer solution was added to the vial and the preparations were magnet stirred during 24 h at room temperature 15–25 °C. Each set of experiments was prepared in

triplicate (one from each solid dispersion batch with the same formula). As a control, the solubility of resveratrol in purified water was accessed.

2.5.3. Scanning electron microscopy

Optimized formulations were analysed by SEM. A Phenom Pro-X Electron microscope (PhenomWorld, Thermo Fisher Scientific, USA) equipped with a CeB6 electron source and backscatter electron detector was used to determine the morphology and particle size of the samples.

The powder was placed on the conductive adhesive tape. The holder for non-conductive samples was used. The excess of sample (loosely bound to the tape) was removed using compressed air.

2.5.4. X-Ray powder diffraction

Optimized formulations were analysed by XRPD. XRPD determinations were performed using a table-top diffractometer MiniFlex 600 (Rigaku, Japan) with a D/teX Ultra detector. In all measurements Cu Kα radiation (40 kV, 15 mA) was used.

2.5.5. Particle size measurement

Optimized formulations were analysed for particle size measurement. These were assessed as cumulative percentile of 10, 50 and 90% of particles (D10, D50 and D90) of solid dispersions containing resveratrol and measured using the SEM equipment described above. Particle morphology was assessed by Automated Image Mapping software and particle size determination was made by Particlemetric software.

2.5.6. Differential scanning calorimetry

A QA T2000 DSC was used for all the DSC studies performed on the drug, polymer and solid dispersions. Samples ranging from 5 to 10 mg were used and the results were normalized to the resveratrol content. The samples were placed in a 100 μL pan. The pans were covered with a lid and the lid is crimped into place. Thermograms were generated under inert atmosphere using a heating rate of 10 g/min from 0 to 300 °C.

2.5.7. Drug release profiles

Third-generation solid dispersions composed by resveratrol: carrier: surfactant were evaluated for drug release by micro-method. Briefly, an amount equivalent to 2 mg of resveratrol was added to a flask containing 4 mL of dissolution medium (pH 1.2 buffer or phosphate buffer pH 6.8). Drug release at pH 1.2 and 6.8 was evaluated and analysed by HPLC at different timepoints. In order to explain the drug release mechanism, three models were used, zero-order, Higuchi, and Korsmeyer-Peppas were explored (2001). The *in-vitro* release data up to 60 min were, fitted to them, and the best model that describes the drug release was selected based on the best fit expressed by the higher value of the determination coefficient (R2).

2.6. Permeability studies

Permeability experiments were performed on a Caco-2 cell monolayer model (Antunes et al., 2013). The Caco-2 (C2BBe1) cell line (passages 64–66) was obtained from the American Type Culture Collection (ATCC, Manassas, VA, USA). Cells grew in culture flasks in a complete medium consisting of DMEM supplemented with 10% (v/v) FBS, 1% (v/v) L-glutamine, 1% (v/v) NEAA, and 1% (v/v) antibiotic mixture (final concentration of 100 U/mL Penicillin and 100 U/mL Streptomycin). Cells were sub-cultured once a week using 0.25% Trypsin-EDTA (1x) to detach the cells from the flasks and seeded at a density of 0.5 × 106 cells per 75 cm2 flasks. The culture medium was replaced every other day. Cells were maintained at 37 °C, 5% CO2 and 95% relative humidity.

For the permeability experiments, 1×10^5 cells/cm2 of Caco-2 were seeded in 12-Transwell® cell culture inserts and were allowed to grow and differentiate for 21 days with medium replacement every other day. After that time, medium was carefully removed from the apical and basolateral compartments and the inserts were gently washed twice with phosphate buffered saline (PBS) (pH 7.4, 37 °C). Then, 1.5 and 2.5 mL of HBSS was added to the apical and basolateral part of the Transwell®, respectively, and allowed to equilibrate for 30 min inside the incubator. Afterwards, the media from the apical compartment was removed and 1.5 mL of free resveratrol at 50 μg/mL in HBSS was added. The formulations were placed directly in the apical compartment without removing the media. Plates were placed inside an orbital shaking incubator (IKA®KS 4000 IC, IKA, Staufen, Germany) at 100 rpm and 37 °C. Aliquots (200 μL) were withdrawn from the basolateral chamber at pre-determined times (5, 15, 30, 45, 60, 90, 120, and 180 min) and immediately replaced with HBSS. At the end, an aliquot from the apical compartment was collected (Antunes et al., 2013). Tests were performed in triplicate and an insert without the addition of sample was used as a control. Before, during, and at the end of the permeability experiments, the Transepithelial Electrical Resistance (TEER) was measured using an EVOM2® epithelial voltammeter with chopstick electrodes (World Precision Instruments, Sarasota, FL, USA) in order to monitor the formation, confluence, and integrity of the cell monolayers. Experiments were performed in triplicate. The concentration of resveratrol in the samples was determined by HPLC-UV analysis. The drug apparent permeability (Papp) was calculated from the following Eq. (X):

$$Papp = [(dQ/dt) \times V]/(A \times C0) \quad \text{(X)}$$

Where Papp is the apparent permeability (cm/s); dQ/dt (μM/s) is the flux across the monolayer obtained from the angular coefficient of the curve of the amount of drug transported versus time; V(cm^3) is the acceptor chamber volume, which in this case corresponds to 2.5 cm^3 (basolateral chamber); A(cm^2) is the insert membrane growth area (equal to 4.67 cm^2 for a 6 well plate); and C0 (μM) is the initial concentration in the apical compartment (Antunes et al., 2013).

2.7. Pharmacokinetic studies

For the pharmacokinetic studies, male, 7-weeks old Wistar rats, weighing 150–250 g, purchased from Charles River Laboratories (France), were housed in cages on wood litter with free access to pellet chow diet (2014 Harlan) and tap water. The animal houses were maintained in a 12-hour light/dark cycle (07.00 to 19.00 h) in a controlled ambient temperature of 22 ± 2 °C and relative humidity of 50 ± 20%. Rats were randomly divided into 2 groups, with 5 animals per group.

Administrations were performed by single intragastric bolus at a volume of 4 mL/kg. Hydroxypropyl Methylcellulose solution (0.25%, w/v) was used as vehicle. All animal procedures followed the guidelines from Directive 2010/63/EU of the European Parliament on the protection of animals used for scientific purposes and the Portuguese law on animal welfare (Decreto-Lei 113/2013). Resveratrol was orally administered at a dose of 100 mg/kg by gavage.

Approximately 150 μL of blood were collected at each time point from the tail vein. Samples were collected at pre-dose, 0.5, 1, 2, 4 and 7 h after administration and were assayed for resveratrol by Liquid Chromatography with tandem mass spectrometry (LC-MS/MS). The Cmax, Tmax and AUC0-t over 7 h were calculated for each group using GraphPad Prism, (GraphPad software Inc., CA, USA).

2.8. Chromatographic conditions

2.8.1. HPLC – UV**a

Resveratrol quantifications used in solubility assay and permeability studies were conducted using a Waters HPLC system and data was processed with Empower3®Software (Waters Corporation, Milford, MA, USA). The stationary phase consisted of a C18 reversed-phase column Waters Symmetry Shield RP18 (3.5 μm, 100 × 4.6 mm) at 30 °C. The mobile phase consisted of (A) water and (B) acetonitrile (65:35, v/v) in isocratic mode and a flow rate of 1 mL/min. The run time was set at 10

min, the injection volume used was 10 µL for assay and solubility determinations and 50 µL for permeability studies. Detection by UV was fixed at 307 nm. Analytical method was validated according the ICH guidelines.

2.8.2. LC – MS/MSxx

Resveratrol quantification used for exposure assessment were conducted in a LC-MS/MS TQ G6470A from Agilent, data was acquired with MassHunter workstation data acquisition version B.08.00 and analysed with MassHunter workstation software for quantitative analysis version B.07.01. The stationary phase consisted of a Waters CORTECS T3 column (2.7 µm, 100 × 2.1 mm) at 40 °C. The mobile phases consisted of (A) water 0.1% formic acid and (B) acetonitrile 0.1% formic acid using the following gradient: 0 min 80% of A and 20% of B; 0.5 min 80% of A and 20% of B; 4.0 min 50% of A and 50% of B; 4.1 min 80% of A and 20% of B at a flow rate of 0.3 mL/min. The run time was set at 6 min, the injection volume used was 2 µL and the autosampler was kept at 4 °C. The samples were injected into detector using the Agilent Jetstream electrospray ionization in negative mode polarity. The multiple reaction monitoring pair was m/z 227.3 → 143.1 for resveratrol with a collision energy of 26 V; and m/z 271.3 → 119.1 for Naringenin (ISTD) with a collision energy of 25 V. The fragmentation used was 140 V. The analytical method was validated according the ICH guidelines.

2.9. Statistical analysis

For solubility determinations, triplicates of formulations were statistically analysed in Microsoft® Excel® 2016 MSO. Student's *t*-test was used within pairs of experiments using a two-tail test with two-sample equal variance. Pairs were considered statically different with p values below 0.05. For Pharmacokinetics, Student's *t*-test for pairs of samples and one-way analysis of variance for all tests (ANOVA) with unpaired and Bonferroni post-hoc test (GraphPadPrism, GraphPad software Inc., CA, USA) were used to analyse the data, respectively. The level of significance was set at probabilities of $p < 0.05$.

3. Results

3.1. High-throughput screening of resveratrol solubility

Resveratrol solubility was assessed in water base solution containing 5% of carrier after two hours of stirring at room temperature. Fourteen carriers were screen and solubility data are depicted on Fig. 1. Pure resveratrol showed a solubility of 2 µg/mL in water after 2 h of stirring. Most of the tested carriers significantly enhanced the solubility of resveratrol. Particularly Soluplus® and T80, which showed an enhancement higher than 2000 folds. Then, poloxamer P407, Myrj 59P and Povidone increased solubility more than 500-fold. Eudragit RLPO and both HPMCASs were the only carriers that did not significantly improved resveratrol solubility under the tested conditions.

3.2. Solid dispersions characterization - FTIR data

FTIR spectrums were generated with the solid dispersions manufactured by solvent cast and using single carriers in different ratios in relation to resveratrol.

3.2.1. HPMCAS**a*

Generally, the number of resveratrol characteristic bands (Fig. 2.A and .B) decreased or presented slight shifts with the increase of the carrier content. Most of these changes were related to alcohol and aromatic functions of resveratrol, which may indicate some hydrogen bonds between resveratrol and HPMCAS through the alcohol function and some pi interactions between resveratrol aromatic rings, probably with the saccharide ring of HPMCAS. Additionally, is also observed a decrease in the intensity of resveratrol characteristic peaks over the expected by the dilution factor, which is more evident for formulations with a content of polymer of at least 50%. No major differences were observed between grades of HPMCAS.

3.2.2. PEG and derivates

Due to its chemical structure PEG6000 presented (Fig. 2.C) as most relevant bands the bands related to C-H and –CH at wave lengths 2882 cm^{-1} and around 1400 cm^{-1}, respectively, and the band related to the ether C-O stretching at wavelength 1096 cm^{-1}. The alcohol functional group was almost neglected in the PEG600 spectra determined. The evaluation of the solid dispersion preparations suggested some interactions between PEG6000 ether group and resveratrol alcohol group.

Generally, from Fig. 2.D, the number of resveratrol characteristic bands decreased or presented slight shifts with the increase of the carrier content. Most of these alterations were related to resveratrol alcohol and aromatic functions, which may indicate some hydrogen bonds between resveratrol and Soluplus® through resveratrol alcohol function and Soluplus® alcohol or ketone groups. Additionally, some pi interactions

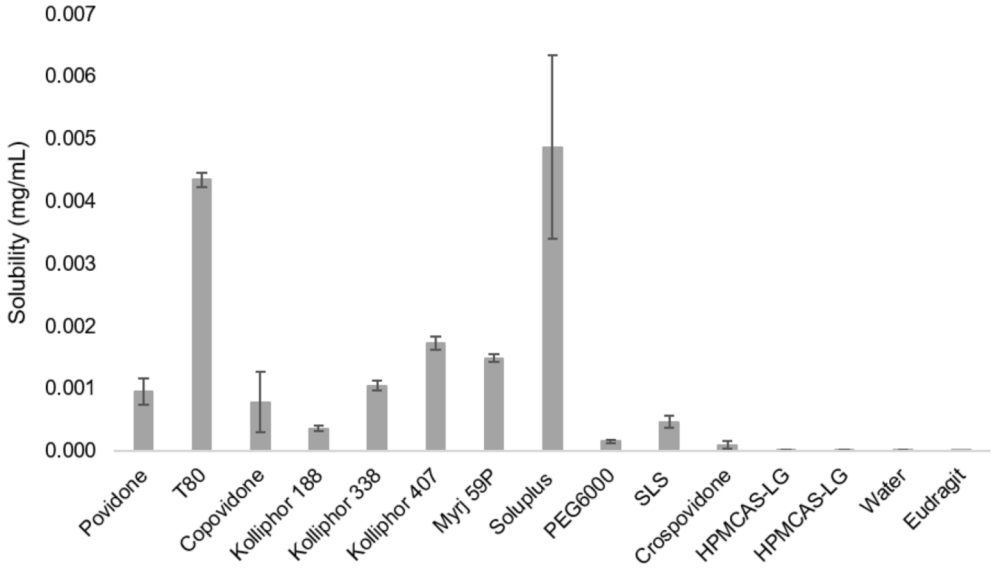

Fig. 1. Solubility of resveratrol in solutions containing five percent of each of the described carriers. (*) carriers that were significantly different from control (purified water).

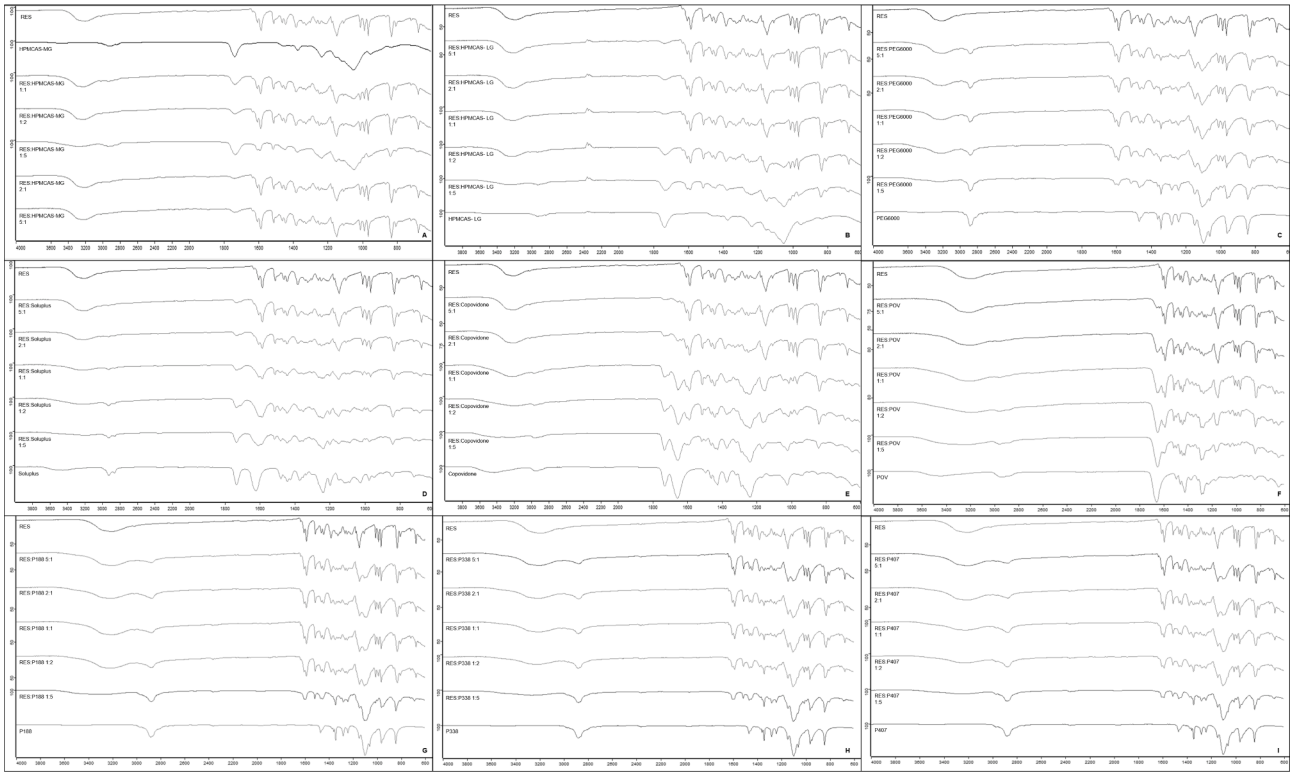

Fig. 2. Spectra of solid dispersions prepared with HPMCAS-MG (2.A), HPMCAS-LG (2.B), PEG6000 (2.C), Soluplus® (2.D), Copovidone (COP) (2.E), Povidone (2.F), Kolliphor® P 188 (2.G), Kolliphor® P 338 (2.H), Kolliphor® P 407 (2.I).

between resveratrol aromatic rings, probably with the oxygen of Soluplus® ester groups may have occurred. Also, generally it was observed a decrease in the intensity of characteristic resveratrol peaks in the solid dispersion over the expected dilution factor, which was more evident for formulations with a content of polymer higher than 50%.

3.2.3. *Polyvinil derivates*

The COP is a vinylpyrrolidone and vinyl acetate copolymer and therefore presented a strong band at wavelength 1655 cm^{-1} from the amide group and other at 1730 cm^{-1} and 1237 cm^{-1} from the acetate group (Fig. 2.E). The intensity of resveratrol bands decreased or disappeared with the polymer increase in the solid dispersions. This was above the expected by the dilution factor, which may indicate some interactions between resveratrol and COP that is corroborated by the same effect in the COP specific bands.

The Povidone is a vinylpyrrolidone polymer and therefore presented a strong band at around wavelength 1650 cm^{-1} from the amide group (Fig. 2.F). The resveratrol bands disappeared with the polymer increase in the solid dispersions. This was over the expected by the dilution factor, which may indicate some interactions between resveratrol and Povidone that is corroborated by the same effect in the Povidone specific bands.

3.2.4. *Poloxamers*

Poloxamers are non-ionic triblock copolymers composed of a central hydrophobic chain of polyoxypropylene (poly(propylene oxide)) flanked by two hydrophilic chains of polyoxyethylene (poly(ethylene oxide)). Thus, FTIR spectra was composed mainly by ether and alkane functional groups, which can be observed C-H and –CH bands at wavelengths 2881 cm^{-1} and around 1342 cm^{-1}, respectively and the band related to the ether C-O stretching at wavelength 1097 cm^{-1}. The alcohol functional group was almost neglected in the obtained spectra (Fig. 2.G, H, I). The evaluation of the solid dispersions suggested some interactions between poloxamers ether group and resveratrol alcohol or aromatic groups.

The poloxamers FTIR spectra were compared based on the poloxamer type (data not shown). Thus, generally the obtained spectra were very similar. Nevertheless, some considerations should be taken, in the cases that resveratrol was at a ratio of 1:1 and 2:1 to poloxamers, the resveratrol bands were more evident when poloxamer 188 was used, which may suggest a lower amorphization capacity of this polymer at these ratios.

3.3. *Solubility data*

Solubility data were generated with the solid dispersions manufactured by solvent cast method and using single carriers in different ratios in relation to resveratrol.

Resveratrol presented a water solubility of around 5.6 μg/ mL after 24 h of stirring at room temperature.

3.3.1. *HPMCAS**a*

Generally, the resveratrol preparation in solid dispersions using povidone derivates as carriers improved the resveratrol solubility in all the drug: carrier ratios tested (Fig. 3.A).

The observed improvements were generally at least 10-fold going up to 30 fold. No significant differences were observed between the two grades of HPMCAS tested within the same drug: carrier ratio. Nevertheless, HPMCAS-LG presented higher solubility values in almost all ratios which may be explained by the higher viscosity of MG grade that may slowdown the drug release. HPMCAS-MG generally presented lower standard deviations than HPMCAS-LG.

In the case of HPMCAS-MG the increase in carrier content did not presented an increase in the solubility as theoretically expected. In fact, the solubility was very similar within all ratios tested, which can be explained by the high incorporation capacity of this grade, showing that a small amount is required to obtain the optimum improvement. It may also indicate that a lower content is required for a complete resveratrol

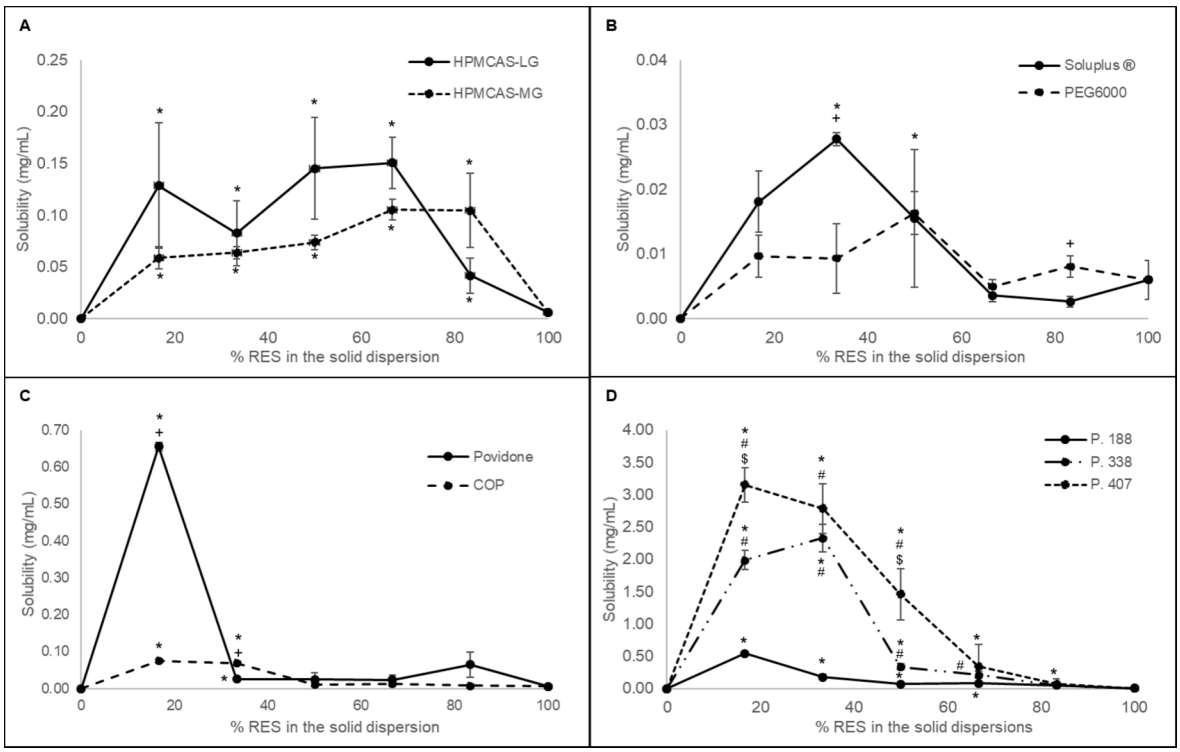

Fig. 3. Solubility, after 24 h of resveratrol solid dispersions prepared at different drug: carrier ratios – RES:HPMCAS (A); RES: PEG / Soluplus® (B); RES: Povidone (C); RES: Poloxamer (D). (*) significantly different from control (pure RES – 100%), (+) significantly different from the solid dispersion at the same drug: carrier ratio with the different carriers, (#) significantly different from the solid dispersion at the same drug: carrier ratio of P188, ($) significantly different from the solid dispersion at the same drug: carrier ratio of P338.

amorphization. In the case of HPMCAS-LG was observed that the formulation containing the highest drug content presented a lower solubility than all the other ratios. This may corroborate the data obtained with the HPMCAS-MG, since, this LG grade theoretically presents lower carrier capacity, it may require a higher amount to generate the fully amorphizations and consequently maximum increase in solubility. Additionally, this (83% resveratrol) was the only ratio where the MG present a higher solubility than the LG.

As conclusion, the HPMCAS appeared to be good carriers for resveratrol, which may require a small amount of carrier to achieve a complete amorphization. Despite, independently of the grade, the medium grade presented a higher amorphization capacity for very low ratios. After achieving a complete amorphization, the viscosity of the grade appeared to have an important role in the solubility obtained, lower viscosity (LG) resulted in higher solubility probably due to a faster release.

3.3.2. PEG and derivate

The resveratrol preparation in solid dispersions using Soluplus® and PEG6000 as carriers improved resveratrol solubility in drug: carrier ratios when the carrier was at least 50% (Fig. 3.B). The observed improvement was generally small, between 2 and 5 folds. Only one formulation (ratio) of each carrier was significantly higher than pure resveratrol, this was mainly due to high variability between replicates (High RSD).

As conclusion, PEG and the tested derivate, Soluplus®, despite presenting very good solubility improvement in the screening study, did not present such a good solubility when formulated as solid dispersions. This may indicate that the solid structure formed by these compounds presented lower release capacity that can be attribute to its high internal cohesiveness. Suggesting that these compounds may require the inclusion of a surfactant to promote the rupture of the internal structure.

3.3.3. Polyvinyl derivates

Generally, the resveratrol preparation in solid dispersions using povidone derivates as carriers improved the resveratrol solubility in all the drug: carrier ratios tested (Fig. 3.C). The observed improvement ranged from 2 to 10 folds with COP and between 4 and 100 folds with povidone. The improvements were statistically significant when both carriers were at a level of at least 67%. Moreover, from this value it was also possible to observe a significant difference between both polymers. Resveratrol solubility in povidone formulations was significantly higher than COP when carrier was at 83% and in COP was significantly higher than in povidone when the carrier content was 67%.

In the particular case of povidone, only when carrier was 67% of formulation a significant increase in resveratrol solubility was observed and was only around 5-fold increase, but, when the carrier was 83%, resveratrol solubility increased massively (more than 100 folds).

Regarding COP, when the solid dispersions contained<50% of carrier, none or minimal (2 folds) improvements in the solubility was observed. When the carrier was above this level a tenfold increase was observed, suggesting that only under these conditions a full amorphization was achieved. Resveratrol solubility increased with the increase in carrier content. This was common to both carriers (Povidone and COP), particularly when povidone was used at a level of 83%, with up to 100-fold solubility increase.

3.3.4. Poloxamers

Generally, resveratrol preparations in solid dispersions using poloxamers as carriers highly improved resveratrol solubility (Fig. 3.D). The observed improvement ranged from 10 to 600 folds. Generally, the solubility increased with the polyoxypropylene molecular mass of the carrier and with the carrier content in the solid dispersion.

Poloxamer 188 was the carrier that presented the lower solubility increase, which ranged from 10 to around 200 folds increasing with the increase in polymer content. When poloxamer was in the solid

dispersion at least at a level of 33% the solubility was significantly higher than pure resveratrol.

Poloxamer 338 was able to increase resveratrol solubility with the increment of carrier content in the solid dispersion ranging from 40 to around 500 folds. Formulations containing poloxamer 338 presented the highest solubility when its content in the solid dispersion was 67%. When poloxamer 338 was in the solid dispersion at least at a level of 33% the solubility was significantly higher than pure resveratrol and when it was equal or higher than 50% it was significantly higher than the solubility obtained with poloxamer 188.

The poloxamer 407, was the poloxamer that presented the highest solubility enhancement, which was observed in all drug: carrier ratios. The solubility increased with the increase of carrier content in the solid dispersion ranging from 60 to more than 600 folds presenting the highest solubility when its content in the solid dispersion was 83%. When poloxamer 407 was in the solid dispersion at least at a level of 17%, the solubility was significantly higher than pure resveratrol and when it was equal or higher than 50% it was significantly higher than the solubility obtained with poloxamer 188. Moreover, at the ratios where carrier was at 83% and 50% the solubility was also significantly higher than when poloxamer 338 was used.

Thus, poloxamers used as carriers promoted a solubility increase with the increase in carries content, this may be explained by the amorphization of resveratrol in combination with the surfactant properties of poloxamers. Poloxamer 407 presented the highest improvements. Unfortunately, all solid dispersions with poloxamers presented poor technological properties, such as lack of complete solidification, they look like a grass material. Nevertheless, these data suggest that the use of poloxamers in the resveratrol solid dispersions may be extremely beneficial, however their content must be at a low level.

3.4. Carrier selection

Generally, it was considered that from the screening data several carriers showed promising solubility data. Miscibility between carriers and resveratrol was demonstrated by FTIR for solid dispersions prepared by solvent cast. Here, solubility results lower than expected were observed. Therefore, Soluplus®, which presented the highest resveratrol solubility improvement during screening, demonstrated molecular interaction observed by FTIR and a significant but small improvement in solubility when solid dispersions were prepared by solvent cast. Thus, this carrier was selected as carrier for further studies, because of its potential observed on the screening solubility and FTIR data, which can be potentiated by the inclusion of a surfactant that was expected to improve solubility and dissolution data in addition to the potential to reduce intestinal metabolism and efflux mechanisms of resveratrol.

3.4.1. Differential scanning calorimetry

Thermograms of resveratrol: Soluplus® at different ratios, were obtained. Resveratrol thermogram present a sharp endothermic peak at 266.8 °C corresponding to its melting with an energy of 252.2 J/g. In DSC data (Fig. 4 and Table 1), when resveratrol is present at a level higher or equal than 50% an endothermic peak related to resveratrol melting point was observed around 260 °C. However, a decreased in intensity and shifted to an earlier melting point was observed with the increase of Soluplus®. When resveratrol was below 50% in the formulation no endothermic peak related to resveratrol was observed. This data corroborates solubility data previously described, meaning that a ratio above 1:1 between resveratrol and Soluplus® is required to achieve a fully amorphous solid dispersion. Based on solubility, FTIR and DSC data a ratio of resveratrol:Soluplus® (1:2) was selected for further studies.

Table 1
Differential Scanning Calorimetry data of resveratrol:Soluplus® formulations at different ratios.

Resveratrol:Soluplus® Ratio	Melting point (°C)	Energy (J/g)	% of amorphization
100:0	266.80	252.2	0
82:18	258.76	195.1	22.6
66.6:33.3	251.74	96.91	61.6
50:50	228.59	27.66	89.0
33.3:66.6	No peak	Not applicable	100
18:82	No peak	Not applicable	100

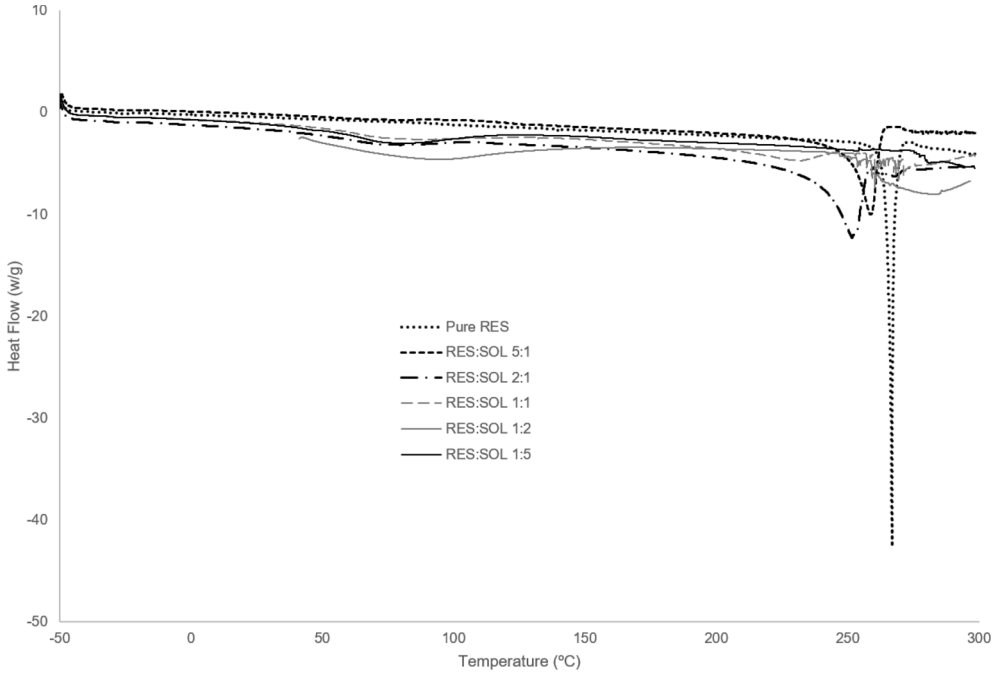

Fig. 4. Thermograms of resveratrol:Soluplus® at different ratios.

3.5. Third-generation solid dispersions

Third-generation solid dispersions were manufactured using resveratrol:Soluplus® at a ratio of 1:2, where two surfactants were included at 5 and 15%. The selected surfactants were poloxamer 407 and Gelucire. Poloxamer 407 was selected because in the screening phase it was the carrier that presented the higher solubility enhancement for resveratrol. Gelucire was selected due to its solid state at room temperature and the similar potential as poloxamer 407.

Formulations were evaluated for solubility, dissolution, DSC, permeability and drug release at pH 1.2 and 6.8.

3.5.1. Solubility

The inclusion of both surfactants in the third-generation amorphous solid dispersion significantly improved the resveratrol solubility in around 2-fold over the solid dispersions without surfactants and more than 8 fold over pure resveratrol (Fig. 5).

All third-generation solid dispersion presented a significantly ($P < 0.05$) higher solubility than pure resveratrol and second-generation solid dispersions for both pHs. At 5% concentration there was no significant difference between carriers but at 15%, poloxamer 407 presented a significantly higher solubility ($P < 0.0.5$) than Gelucire for both pHs. No significant differences were observed between the two tested concentrations of Gelucire, nonetheless for poloxamer 407 when this surfactant was at 15%, the solubility of the formulation was significantly higher than of the 5% concentration for both values of pH.

3.5.2. Dissolution

Drug release was generally independent of the pH and reached a plateau after 30 min. Under simulated gastric pH conditions (Fig. 6.A), solid dispersions showed a faster dissolution rate and stabilized in a plateau above the crystalline resveratrol. All solid dispersions presented a very similar dissolution profile and rates, except formulation containing poloxamer 407 at 15% that presented a faster and higher dissolution profile. No precipitation (reduction in the dissolution) was observed for solid dispersions showing that those were able to maintain resveratrol in a supersaturated state for at least 10 h under acidic conditions.

At pH 6.8, the formulations (Fig. 6.B) showed a fast dissolution profile that reaches a plateau around 60 min. Formulation containing Gelucire presented a decrease in the dissolution values between 60 and 90 min suggesting that drug (resveratrol) has crystalized. These was not observed for formulations containing poloxamer. Formulation containing poloxamer at 15% presented the faster and higher dissolution profile. All other solid dispersion formulation presented dissolution values close to the pure resveratrol which was more evident above 1 h of dissolution.

The analysis of these dissolution profiles suggested that a fast release in the stomach may occur and drug may be maintained in solution through the gastrointestinal tract (Fig. 6.A and B), particularly the formulations containing poloxamer 407.

Dissolution profiles were subject of release kinetics analysis (Table 2) showing that a non-linear release process was observed for all profiles at both pHs since Korsmeyer-Peppas model was the best fit. Data suggest that non-fick diffusion balanced with erosion are the predominant drug release mechanisms (Costa and Sousa Lobo, 2001).

3.5.3. Differential Scanning Calorimetry

DSC experiments showed that the endothermic peak associated to the melting of resveratrol was not presented in all solid dispersions evaluated at this stage. This data confirmed that all formulations presented resveratrol in a fully amorphous state (Fig. 7). Moreover, from DSC data it was possible to conclude that in all tested formulations, resveratrol was completely miscible with the remaining excipients which was in line with the observed in the previous development stage for the formulation composed by Res:Soluplus® (1:2). The inclusion of poloxamer 407 and Gelucire within 5 to 15% of total formulation weight did not affect the resveratrol miscibility remaining in an amorphous state.

3.6. Permeability studies

Permeability studies were conducted on a Caco-2 cell monolayer model from apical to basal (A-B) and from basal to apical side (B-A) (Fig. 8.A and B respectively).

The fraction of resveratrol recovered in the sum of apical, cellular

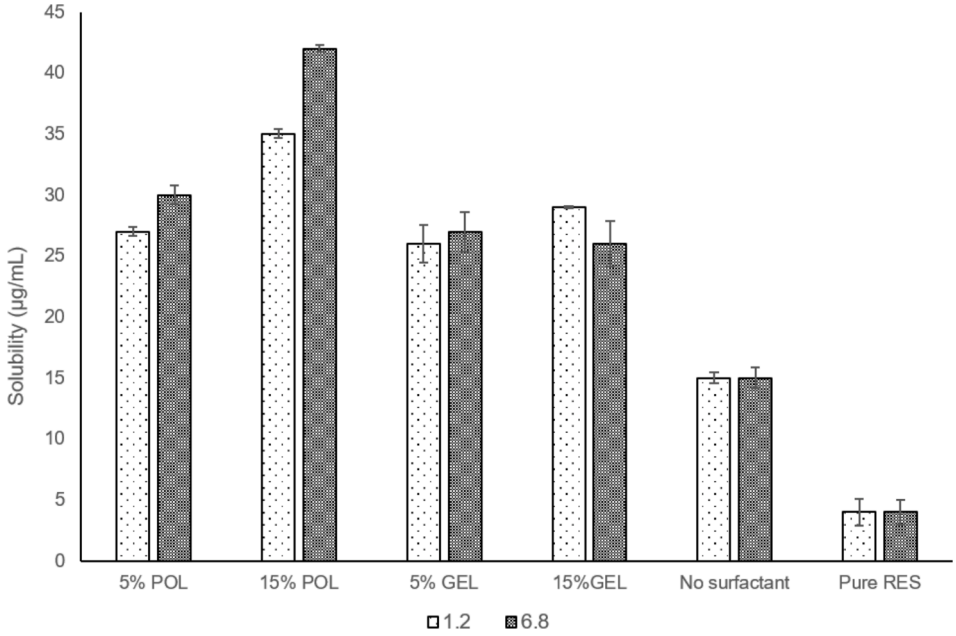

Fig. 5. Solubility of pure resveratrol and resveratrol solid dispersions after 2 h at pH 1.2 and 6.8. Pure RES = crystalline RES; POL 5% and 15% = solid dispersion composed by RES:Soluplus® (1:2) and poloxamer 407 at 5% and 15% respectively; GEL 5% and 15% = solid dispersion composed by RES:Soluplus® (1:2) and Gelucire at 5% and 15% respectively. No surfactant = solid dispersion composed by RES:Soluplus® (1:2).

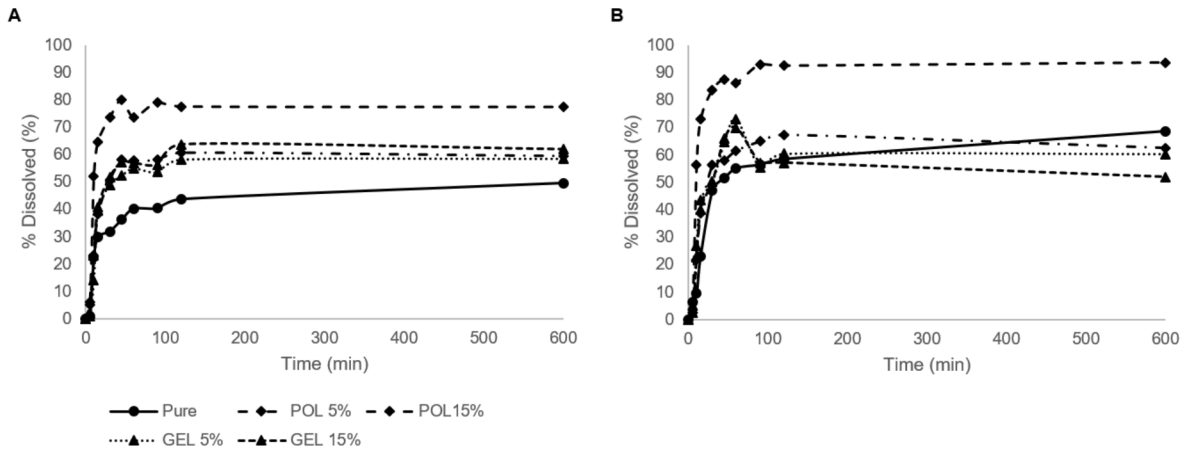

Fig. 6. Dissolution of resveratrol and resveratrol third-generation solid dispersions after 10 h at pH 1.2 (A) and at pH 6.8 (B). Pure RES = crystalline RES; POL 5% and 15% = solid dispersion composed by RES:Soluplus® (1:2) and poloxamer 407 at 5% and 15% respectively; GEL 5% and 15% = solid dispersion composed by RES:Soluplus® (1:2) and Gelucire at 5% and 15% respectively.

Table 2
Drug release kinetics for dissolution profiles up to 60 min.

Model	Parameter	Pure RES	POL 5%	POL 15%	GEL 5%	GEL 15%
pH 1.2						
Zero order	K	0.626	0.986	1.233	0.966	0.984
	R^2	0.724	0.815	0.657	0.785	0.775
Higuchi	K	5.647	8.706	11.506	8.444	8.739
	R^2	0.853	0.919	0.826	0.866	0.884
Korsmeyer-Peppas	K	6.060	7.107	16.563	5.376	7.081
	R^2	0.925	0.958	0.916	0.931	0.939
	n	0.475	0.538	0.409	0.594	0.539
pH 6.8						
Zero order	K	0.993	1.064	1.355	1.185	1.202
	R^2	0.904	0.812	0.640	0.878	0.886
Higuchi	K	8.333	9.321	12.705	10.209	10.268
	R^2	0.920	0.902	0.813	0.943	0.935
Korsmeyer-Peppas	K	3.180	6.467	18.674	6.660	5.422
	R^2	0.969	0.949	0.910	0.973	0.970
	n	0.720	0.575	0.404	0.594	0.642

Pure RES = crystalline RES; POL 5% and 15% = solid dispersion composed by RES:Soluplus® (1:2) and poloxamer 407 at 5% and 15% respectively; GEL 5% and 15% = solid dispersion composed by RES:Soluplus® (1:2) and Gelucire at 5% and 15% respectively.

and basolateral compartments after adding second and third-generation solid dispersions into the apical side was below 50% in all tests, suggesting that resveratrol metabolization/ degradation was very intense and occurred rapidly. Control formulation, which was a second-generation solid dispersion composed by resveratrol:Soluplus® (1:2) presented a resveratrol recovery of 14%, and formulations with Gelucire and poloxamer 407 of 31% and 26% respectively, suggesting that these formulations may be able to reduce metabolization and/or degradation of resveratrol. Moreover, from all the recovered fractions, the permeated fraction corresponded to 79% in the control formulation, 72% in formulation containing Gelucire and 81% in formulation containing poloxamer 407, suggesting that the latter formulation was the least influenced by efflux mechanisms.

When resveratrol was applied in the basal compartment the P_{app} was generally maintained for all formulations (Table 3). The permeability kinetics of all formulations was comparable to the observed with the second-generation solid dispersion. All formulations showed a slow, but constant, permeation rate. This was significantly higher for formulations containing surfactants when compared to second-generation formulation. Between third-generation solid dispersions no statistical differences were observed.

The total fractions recovered when formulations were applied in the basolateral compartment were similar for second-generation solid dispersion (21%) and for formulation containing poloxamer 407 (30%) but much higher for formulation containing Gelucire ® (54%).

The fraction recovered in the donor compartment was almost neglected for the second-generation solid dispersion (control group). This data associated to the fact that P_{app} was only marginally affected when this formulation was applied in the basolateral compartment indicates that an efflux mechanism may be involved, as described by Shirasaka et al. (2008). In the case of third-generation solid dispersions the fraction recovered in the donor compartment was below 50%, suggesting that efflux mechanisms of resveratrol were blocked by these formulations.

TEER values of all formulations were maintained over the study, indicating that the monolayers remained intact until the end of the experiment and in this way, the permeability results really reflect the drug transport across the cell monolayers.

Permeability on Caco-2 cells showed that the inclusion of both surfactants increased drug permeability, which can be justified by the capacity that both have to inhibit P-gp (Vasconcelos et al., 2017). Additionally, poloxamer 407 inhibits MRP2 transporters (Pollard et al., 2019), which are known to be used as efflux mechanisms for resveratrol (Kaldas et al., 2003). In previous reports (Kaldas et al., 2003; Maier-Salamon et al., 2006), pure resveratrol presented a tendency to accumulate in enterocytes, fact that was not observed in the presented data, particularly for formulations containing Gelucire® and poloxamer 407 further corroborating the potential efflux mechanism inhibition by these formulations.

Both surfactants increased the resveratrol fraction recovered in permeability studies indicating that were able to reduce metabolism, which was more evident for formulation containing poloxamer 407. Moreover, the later formulation was the one showing lower impact of Apical to Basal/ Basal to Apical ratio (A-B/B-A) proving that was the most effective in reducing efflux mechanisms. Therefore, solid dispersions composed by resveratrol:Soluplus® (1:2) and resveratrol:Soluplus® (1:2) POL 15% were prepared in a larger scale and more extensible characterized.

3.7. Pharmacokinetics batches characterization

Batches used in pharmacokinetics studies were also characterized regarding assay, particle size and polymorphism by XRPD as observed in Table 4 and Figs. 9 and 10.

Assay results were acceptable for both formulations (Table 4), but particle size was much higher than expected, particularly for

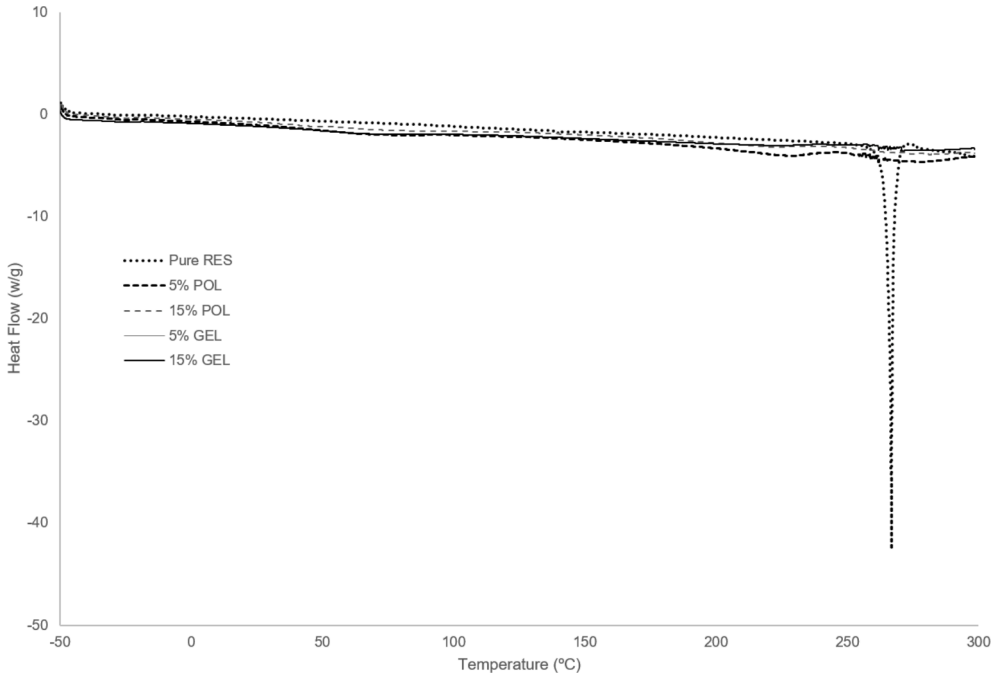

Fig. 7. Thermograms of pure resveratrol and resveratrol third-generation solid dispersions containing poloxamer and Gelucire. Pure RES = crystalline RES; 5% and 15% poloxamer 407 = third-generation solid dispersions composed by RES:Soluplus® (1:2) and poloxamer 407 at 5% and 15% respectively; 5% and 15% Gelucire = Third-generation solid dispersions composed by RES:Soluplus® (1:2) and Gelucire at 5% and 15% respectively.

formulation containing poloxamer 407. The formulation containing poloxamer presented a particularly large particle size that should be associated to the manufacturing process (solvent evaporation by rotavapor) and not to composition. The relevant difference in particle size distribution may impact the pharmacokinetics profile by reducing resveratrol absorption.

Both presented resveratrol in a fully amorphous status based on XRPD (Fig. 10), SEM (Fig. 9) and DSC data (Fig. 7).

3.8. Pharmacokinetics studies

The pharmacokinetic parameters derived from resveratrol after the oral administration of resveratrol (100 mg/kg) to rats using two different formulations are depicted in Table 5 and Fig. 11. The third-generation solid dispersion containing resveratrol:Soluplus®(1:2) with poloxamer at 15% reached maximal concentration at first timepoint (0.5 h) with a maximum plasma concentration (C_{max}) of 134 ± 78 and an AUC of 279 ± 54 ng.h/ml. In the control formulation, which was a solid dispersion composed by resveratrol:Soluplus® (1:2), a maximum plasma concentration (C_{max}) of 45.6 ± 50.0 ng/mL within 0.5 h was reached before falling back to low levels over the next 7 h. The area under the curve (AUC_{0-t}) obtained for this formulation was 162 ± 44 ng.h/ml.

In the present pharmacokinetics studies, resveratrol solid dispersion only with Soluplus® (control) showed a secondary peak in its pharmacokinetic profile, thus suggesting entero-hepatic recirculation as observed and described by Marier et al. (2002). This was not observed when poloxamer 407 was included to the formulation suggesting that it may reduce this phenomenon.

The observed C_{max} for the control formulation (resveratrol:Soluplus® 1:2) was very similar to the observed by Branton and Snehasis in male Sprague Dawley rats (2017) using the same dose of pure resveratrol. However, AUC_{0-t} was 1.5 fold higher in present study suggesting that the supersaturate sate of resveratrol in the solid dispersion extended the absorption period but not the rate which is in line with an absence of interference with efflux mechanisms. Curiously, both solid dispersions presented lower PK parameters than pure resveratrol reported in a previous study (Vasconcelos et al., 2019). This may be attributed to its larger particle size which was 2 to 5-fold higher when compared to pure resveratrol. These large particles may have been responsible for the slow but continuous permeability over time in Caco-2 cells model. *In vivo*, this slow release may have prevented a burst effect, and consequent large amount of resveratrol in absorption window able to completely saturate degradation and efflux mechanism. However, even in the absence of this burst effect the presence of poloxamer 407 was able to improve at least 2-fold C_{max} and AUC over the formulation without poloxamer, even presenting a much larger particle size and clearly indicating that poloxamer 407 was able to modulate intestinal metabolism and or efflux mechanisms.

This pharmacokinetics data corroborated the *in vitro* data, namely a relevant increase of exposure in the formulation containing poloxamer 407, confirming that this excipient was able to increase resveratrol exposure which may be by inhibiting transporters and/or metabolism over the improvement achieved by the solubility increase. This increase can be considered even more relevant considering the fact that particle size distribution of formulation containing poloxamer 407 were approximately 3-fold higher for D10, D50 and D90 descriptors when compared to the solid dispersion without surfactant.

4. Conclusions

Resveratrol solid dispersions can rationally be developed and are an important tool in the translation of resveratrol into clinical use. The developed formulations presented resveratrol in a stable amorphous state which was critical to increase drug solubility/ dissolution maintaining it in an oversaturated condition for the longest period of time possible (Brouwers et al., 2009).

The proposed development process allowed the selection of several formulations that presented resveratrol in an amorphous state and enhanced its solubility several folds. From these, Soluplus® was selected as carrier. Additionally, two surfactants, poloxamer 407 and Gelucire, at two concentrations (5% and 15%) were assessed aiming to maximize drug solubilisation and reducing drug metabolism and efflux mechanisms (Guan et al., 2011; Legen et al., 2006; Li et al., 2013, 2014). Poloxamer 407 at 15% presented a significantly higher dissolution rate

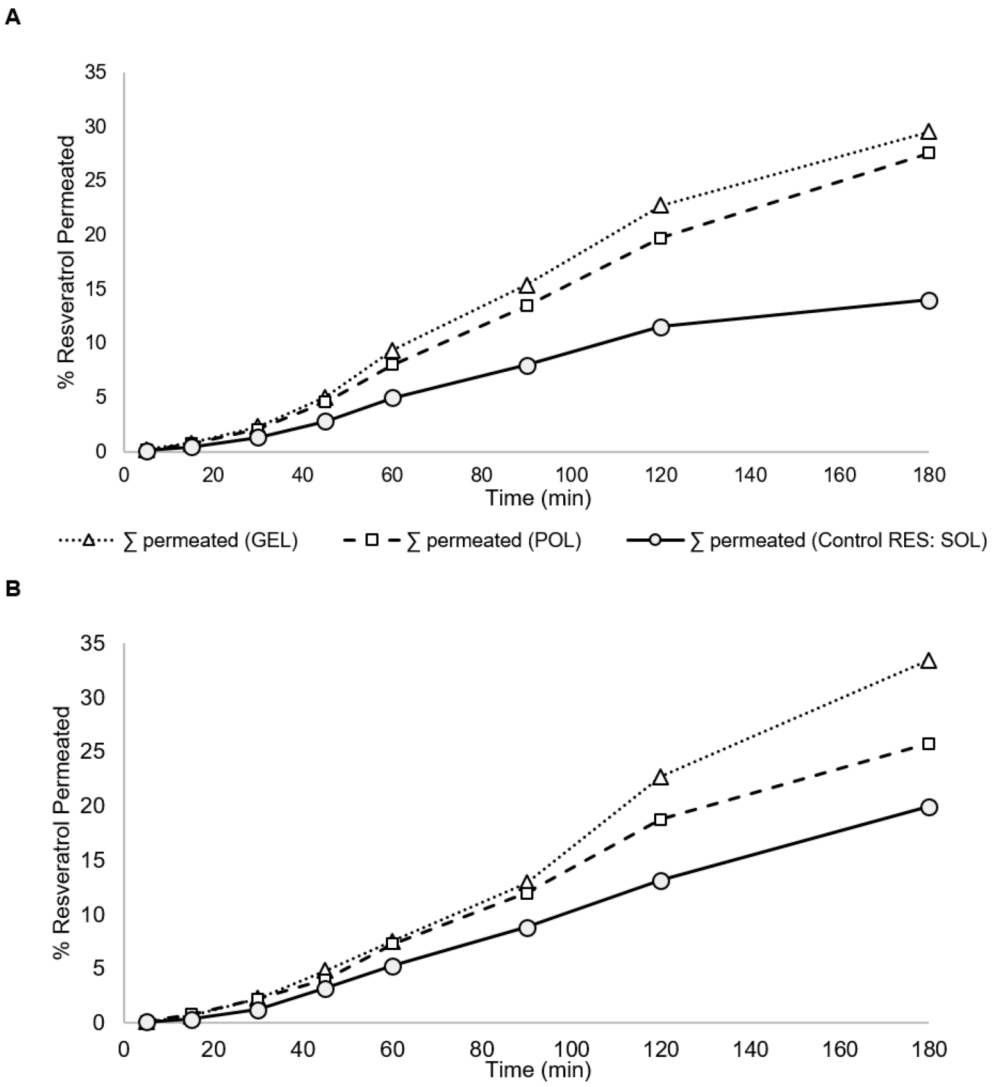

Fig. 8. Caco-2 permeability data from Apical to Basal (A) and from Basal to Apical (B). SD RES:Sol = solid dispersion composed by RES:Soluplus® (1:2); SD RES:SOL: GEL = solid dispersion composed by RES:Soluplus® (1:2) and Gelucire at 15%; SD RES:SOL:POL = solid dispersion composed by RES:Soluplus® (1:2) and poloxamer 407 at 15%.

Table 3
P_{app} of all formulations of resveratrol apical to basal and basal to apical applications (n = 3, mean ± standard deviation).

Formulation	$P_{app\ (Apical\text{-}Basal)}$ (cm/s)	$P_{app\ (Basal\text{-}Apical)}$ (cm/s)	Ratio (A-B/ B-A)
RES:Sol (1:2)	$4.2 \times 10^{-6} \pm 0.8 \times 10^{-6}$	$5.9 \times 10^{-6} \pm 0.8 \times 10^{-6}$	0.70
RES:Sol (1:2) GEL 15%	$8.8 \times 10^{-6} \pm 1.2 \times 10^{-6}$	$10.0 \times 10^{-6} \pm 2.5 \times 10^{-6}$	0.88
RES:Sol (1:2) POL 15%	$8.2 \times 10^{-6} \pm 1.9 \times 10^{-6}$	$7.7 \times 10^{-6} \pm 1.5 \times 10^{-6}$	1.07

RES – resveratrol; Sol – Soluplus ®; POL – poloxamer; GEL – Gelucire®; (A-B/B-A) – Apical to Basal/ Basal to Apical.

Table 4
Characterization of formulations subjected to pharmacokinetic studies. Particle size determination correspond to a cumulative measurement of 21,841 and 6568 particles of RES:Sol (1:2) and RES:Sol (1:2) POL 15%, respectively.

Formulation	Assay (%)	D_{10}(μm)	D_{50} (μm)	D_{90} (μm)
RES:Sol (1:2)	92.8	15	49	105
RES:Sol (1:2) POL 15%	101.2	51	138	308

RES – resveratrol; Sol – Soluplus ®; POL – poloxamer 407.

and solubility than Gelucire but, both surfactants reduced efflux mechanisms and metabolization in permeability studies on Caco-2 cells monolayer model which is in contradiction to the previously reported for poloxamer (Guan et al., 2011).

Amorphous solid dispersion composed by resveratrol:Soluplus® (1:2) and resveratrol:Soluplus® (1:2) with 15% poloxamer 407 were tested in vivo. A fast absorption was observed for both formulations. However, the inclusion of poloxamer 407 in a low concentration (15%) resulted in an increase in C_{max} and AUC of around 2-fold that could be due to a reduction in metabolization and efflux mechanisms as supported by the Caco-2 cell permeability data (Guan et al., 2011). Thus, these findings reveal extreme importance to support the biological impact of formulations components. Additionally, poloxamer 407 showed to be effective in reducing efflux mechanisms and resveratrol intestinal metabolization.

The use of third-generation solid dispersion can be very relevant to enhance the bioavailability of drugs, such as resveratrol, that present low bioavailability due to poor solubility associated to intestinal metabolism and efflux mechanisms.

As future perspectives, this third-generation solid dispersion,

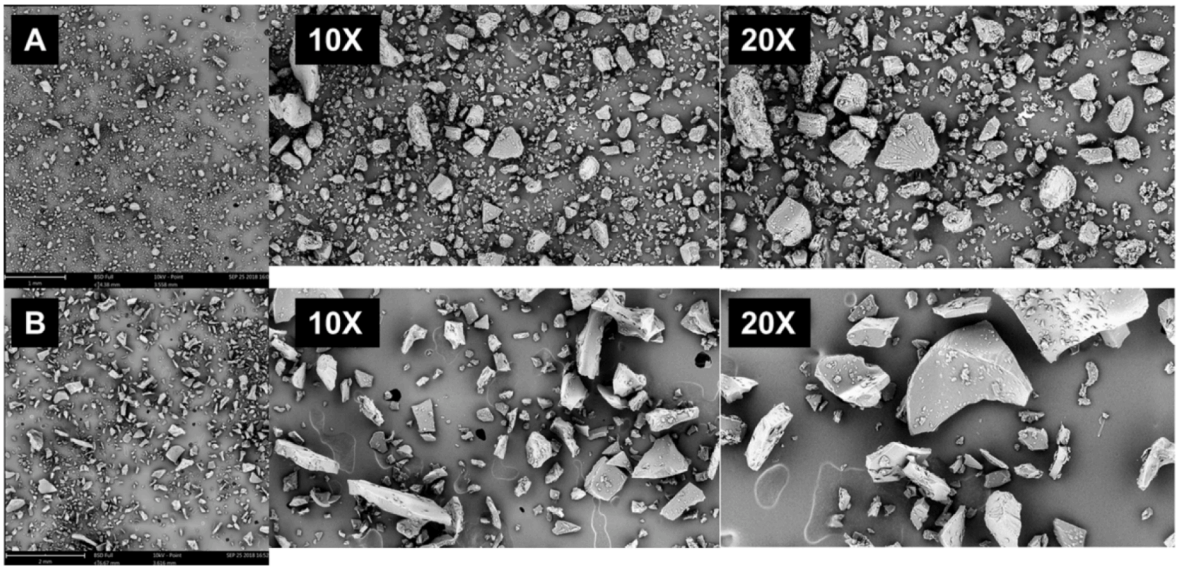

Fig 9. SEM images of resveratrol solid dispersions. A (RES:SOL (1:2)) and B (RES:SOL (1:2) POL 15%) correspond to a preparation overview composed by a superimposition of 144 and 100 images, respectively. 10X and 20X correspond to a ten and twenty-fold digital magnification of a representative area of the original image, respectively. RES:SOL (1:2) = solid dispersion composed by RES:Soluplus® (1:2); RES:SOL (1:2) POL 15% = solid dispersion composed by RES:Soluplus® (1:2) and poloxamer 407 at 15%.

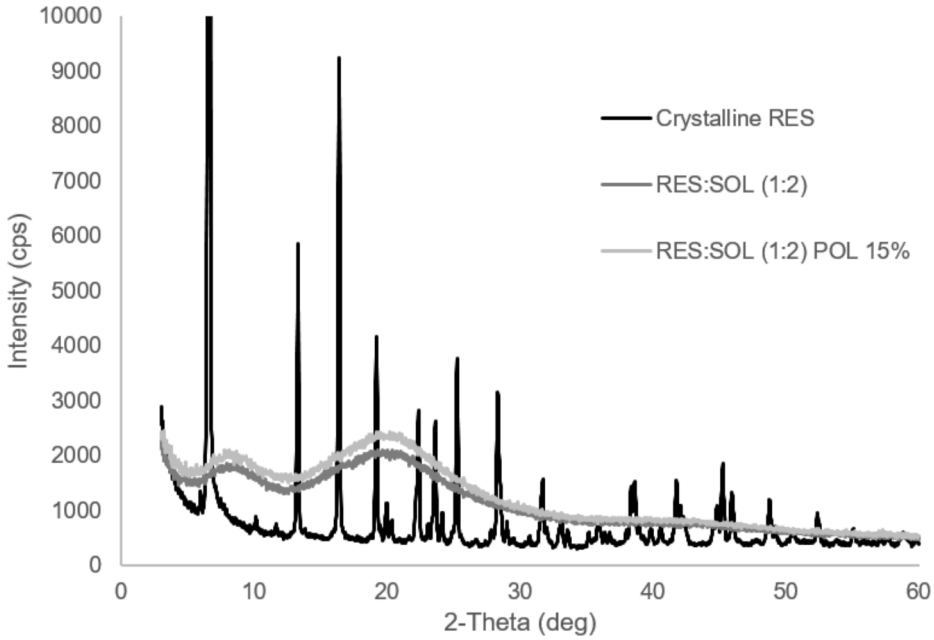

Fig 10. XRPD of resveratrol and resveratrol solid dispersions. Crystalline RES = crystalline RES; RES:SOL (1:2) = solid dispersion composed by RES:Soluplus® (1:2); RES:SOL (1:2) POL 15% = solid dispersion composed by RES:Soluplus® (1:2) and poloxamer 407 at 15%.

Table 5
Pharmacokinetics parameters of all formulations.

Formulation	C_{max} (ng/mL)	T_{max}(h)	$AUC_{0\text{-}t}$ (ng.h/mL)
RES:SOL (1:2)	46 ± 50	0.5	162 ± 44
RES:SOL (1:2) POL15%	134 ± 78	0.5	279 ± 54*

RES – resveratrol; SOL – Soluplus®; POL – poloxamer 407; * Statistically significant ($p < 0.05$).

produced at laboratorial scale should be scaled up by using spray drying, freeze drying or hot-melt extrusion. Scale-up solid dispersion can then be combined with further excipient to be converted into oral tablet.

CRediT authorship contribution statement

Teófilo Vasconcelos: Conceptualization, Methodology, Formal analysis, Investigation, Writing - original draft, Project administration. **Fabíola Prezotti:** Methodology, Investigation. **Francisca Araújo:** Methodology, Investigation. **Carlos Lopes:** Methodology, Investigation. **Ana Loureiro:** Methodology, Investigation. **Sara Marques:** Conceptualization, Formal analysis, Writing - review & editing, Supervision. **Bruno Sarmento:** Conceptualization, Formal analysis, Resources, Writing - review & editing, Supervision.

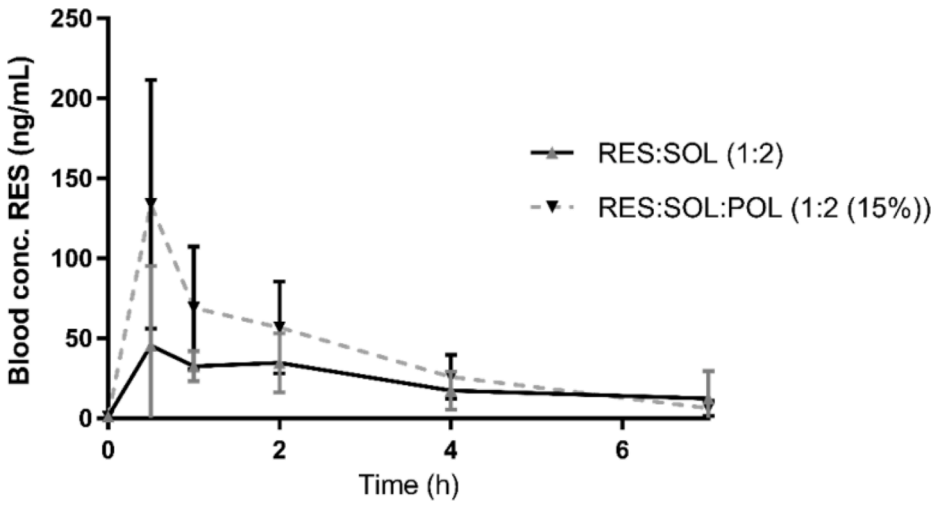

Fig. 11. Pharmacokinetic profile of resveratrol after oral administration in rats formulated as second and third generation solid dispersions.

Declaration of Competing Interest

The authors declare that they have no known competing financial interests or personal relationships that could have appeared to influence the work reported in this paper.

Acknowledgements

This work was financed by FEDER - Fundo Europeu de Desenvolvimento Regional, and by Portuguese funds through FCT - Fundação para a Ciência e a Tecnologia/ Ministério da Ciência, Tecnologia e Ensino Superior in the framework of the project "Institute for Research and Innovation in Health Sciences" UID/BIM/04293/2019 and NETDIAMOND (POCI-01-0145-FEDER-016385).

References

Alcaín, F.J., Villalba, J.M., 2009. Sirtuin activators. Expert Opin. Ther. Pat. 19, 403–414.
Antunes, F., Andrade, F., Araújo, F., Ferreira, D., Sarmento, B., 2013. Establishment of a triple co-culture *in vitro* cell models to study intestinal absorption of peptide drugs. Eur. J. Pharm. Biopharm. 83, 427–435.
Athar, M., Back, J.H., Tang, X., Kim, K.H., Kopelovich, L., Bickers, D.R., Kim, A.L., 2007. Resveratrol: a review of preclinical studies for human cancer prevention. Toxicol. Appl. Pharmacol. 224, 274–283.
Bogdanova, S., Pajeva, I., Nikolova, P., Tsakovska, I., Müller, B., 2005. Interactions of poly(vinylpyrrolidone) with ibuprofen and naproxen: experimental and modeling studies. Pharm Res 22, 806–815.
Boocock, D.J., Faust, G.E.S., Patel, K.R., Schinas, A.M., Brown, V.A., Ducharme, M.P., Booth, T.D., Crowell, J.A., Perloff, M., Gescher, A.J., Steward, W.P., Brenner, D.E., 2007. Phase I dose escalation pharmacokinetic study in healthy volunteers of resveratrol, a potential cancer chemopreventive agent. Cancer Epidemiol. Biomark. Prev. 16, 1246–1252.
Branton, A., Snehasis, J., 2017. The influence of energy of consciousness healing treatment on low bioavailable resveratrol in male Sprague Dawley rats. Int. J. Clin. Develop. Anatomy 3, 9–15.
Brouwers, J., Brewster, M.E., Augustijns, P., 2009. Supersaturating drug delivery systems: The answer to solubility-limited oral bioavailability? J. Pharm. Sci. 98, 2549–2572.
Charman, S.A., Charman, W.N., 2003. Oral modified-release delivery systems. In: Rathbone, M.J., Hadgraft, J., Roberts, M. (Eds.), Modified-Release Drug Delivery Technology, 1 ed. Marcel Dekker, USA, pp. 1–10.
Costa, P., Sousa Lobo, J.M., 2001. Modeling and comparison of dissolution profiles. Eur. J. Pharm. Sci. 13, 123–133.
Craig, D.Q., 2002. The mechanisms of drug release from solid dispersions in water-soluble polymers. Int. J. Pharm. 231, 131–144.
Deng, J.-Y., Hsieh, P.-S., Huang, J.-P., Lu, L.-S., Hung, L.-M., 2008. Activation of estrogen receptor is crucial for resveratrol-stimulating muscular glucose uptake via both insulin-dependent and-independent pathways. Diabetes 57, 1814–1823.
Desai, J., Alexander, K., Riga, A., 2006. Characterization of polymeric dispersions of dimenhydrinate in ethyl cellulose for controlled release. Int. J. Pharm. 308, 115–123.
Gentilli, M., Mazoit, J.X., Bouaziz, H., Fletcher, D., Casper, R.F., Benhamou, D., Savouret, J.F., 2001. Resveratrol decreases hyperalgesia induced by carrageenan in the rat hind paw. Life Sci. 68, 1317–1321.
Gliemann, L., Schmidt, J.F., Olesen, J., Bienso, R.S., Peronard, S.L., Grandjean, S.U., Mortensen, S.P., Nyberg, M., Bangsbo, J., Pilegaard, H., Hellsten, Y., 2013. Resveratrol blunts the positive effects of exercise training on cardiovascular health in aged men. J. Physiol. 591, 5047–5059.
Guan, Y., Huang, J., Zuo, L., Xu, J., Si, L., Qiu, J., Li, G., 2011. Effect of pluronic P123 and F127 block copolymer on P-glycoprotein transport and CYP3A metabolism. Arch. Pharmacal. Res. 34, 1719–1728.
Ikegami, K., Tagawa, K., Osawa, T., 2006. Bioavailability and in vivo release behavior of controlled-release multiple-unit theophylline dosage forms in beagle dogs, cynomolgus monkeys, and göttingen minipigs. J. Pharm. Sci. 95, 1888–1895.
Kaldas, M.I., Walle, U.K., Walle, T., 2003. Resveratrol transport and metabolism by human intestinal Caco-2 cells. J. Pharm. Pharmacol. 55, 307–312.
Karavas, E., Ktistis, G., Xenakis, A., Georgarakis, E., 2006. Effect of hydrogen bonding interactions on the release mechanism of felodipine from nanodispersions with polyvinylpyrrolidone. Eur. J. Pharm. Biopharm. 63, 103–114.
la Porte, C., Voduc, N., Zhang, G., Seguin, I., Tardiff, D., Singhal, N., Cameron, D.W., 2010. Steady-State pharmacokinetics and tolerability of trans-resveratrol 2000 mg twice daily with food, quercetin and alcohol (ethanol) in healthy human subjects. Clin. Pharmacokinet. 49, 449–454.
Legen, I., Kracun, M., Salobir, M., Kerc, J., 2006. The evaluation of some pharmaceutically acceptable excipients as permeation enhancers for amoxicillin. Int. J. Pharm. 308, 84–89.
Li, L., Yi, T., Lam, C.W., 2013. Interactions between human multidrug resistance related protein (MRP2; ABCC2) and excipients commonly used in self-emulsifying drug delivery systems (SEDDS). Int. J. Pharm. 447, 192–198.
Li, L., Yi, T., Lam, C.W., 2014. Inhibition of human efflux transporter ABCC2 (MRP2) by self-emulsifying drug delivery system: influences of concentration and combination of excipients. J. Pharm. Pharmaceut. Sci. 17, 447–460.
Maier-Salamon, A., Hagenauer, B., Wirth, M., Gabor, F., Szekeres, T., Jäger, W., 2006. Increased transport of resveratrol across monolayers of the human intestinal Caco-2 cells is mediated by inhibition and saturation of metabolites. Pharm. Res. 23, 2107–2115.
Marier, J.-F., Vachon, P., Gritsas, A., Zhang, J., Moreau, J.-P., Ducharme, M.P., 2002. Metabolism and disposition of resveratrol in rats: extent of absorption, glucuronidation, and enterohepatic recirculation evidenced by a linked-rat model. J. Pharmacol. Exp. Ther. 302, 369–373.
Muhrer, G., Meier, U., Fusaro, F., Albano, S., Mazzotti, M., 2006. Use of compressed gas precipitation to enhance the dissolution behavior of a poorly water-soluble drug: Generation of drug microparticles and drug-polymer solid dispersions. Int. J. Pharm. 308, 69–83.
Pollard, J., Rajabi-Siahboomi, A., Badhan, R.K.S., Mohammed, A.R., Perrie, Y., 2019. High-throughput screening of excipients with a biological effect: a kinetic study on the effects of surfactants on efflux-mediated transport. J. Pharm. Pharmacol. 71, 889–897.
Pouton, C.W., 2006. Formulation of poorly water-soluble drugs for oral administration: Physicochemical and physiological issues and the lipid formulation classification system. Eur. J. Pharm. Sci. 29, 278–287.
Rasenack, N., Muller, B.W., 2004. Micron-size drug particles: common and novel micronization techniques. Pharm. Dev. Technol. 9, 1–13.
Serajuddin, A.T., 1999. Solid dispersion of poorly water-soluble drugs: early promises, subsequent problems, and recent breakthroughs. J. Pharm. Sci. 88, 1058–1066.
Shirasaka, Y., Sakane, T., Yamashita, S., 2008. Effect of P-glycoprotein expression levels on the concentration-dependent permeability of drugs to the cell membrane. J. Pharm. Sci. 97, 553–565.
Stef, G., Csiszar, A., Lerea, K., Ungvari, Z., Veress, G., 2006. Resveratrol inhibits aggregation of platelets from high-risk cardiac patients with aspirin resistance. J. Cardiovasc. Pharmacol. 48, 1–5.
Streubel, A., Siepmann, J., Bodmeier, R., 2006. Drug delivery to the upper small intestine window using gastroretentive technologies. Curr. Opin. Pharmacol. 6, 501–508.

Sugawara, M., Kadomura, S., He, X., Takekuma, Y., Kohri, N., Miyazaki, K., 2005. The use of an in vitro dissolution and absorption system to evaluate oral absorption of two weak bases in pH-independent controlled-release formulations. Eur. J. Pharm. Sci. 26, 1–8.

van Drooge, D.J., Hinrichs, W.L.J., Visser, M.R., Frijlink, H.W., 2006. Characterization of the molecular distribution of drugs in glassy solid dispersions at the nano-meter scale, using differential scanning calorimetry and gravimetric water vapour sorption techniques. Int. J. Pharm. 310, 220–229.

Vasconcelos, T., Araujo, F., Lopes, C., Loureiro, A., das Neves, J., Marques, S., Sarmento, B., 2019. Multicomponent self nano emulsifying delivery systems of resveratrol with enhanced pharmacokinetics profile. Eur. J. Pharm. Sci. 137, 105011.

Vasconcelos, T., Marques, S., Sarmento, B., 2017. The biopharmaceutical classification system of excipients. Therapeutic Deliv. 8, 65–78.

Vippagunta, S.R., Wang, Z., Hornung, S., Krill, S.L., 2007. Factors affecting the formation of eutectic solid dispersions and their dissolution behavior. J. Pharm. Sci. 96, 294–304.

Youn, Y.S., Jung, J.Y., Oh, S.H., Yoo, S.D., Lee, K.C., 2006. Improved intestinal delivery of salmon calcitonin by Lys18-amine specific PEGylation: stability, permeability, pharmacokinetic behavior and in vivo hypocalcemic efficacy. J. Control. Release 114, 334–342.

European Journal of Pharmaceutics and Biopharmaceutics 123 (2018) 1–8

Contents lists available at ScienceDirect

European Journal of Pharmaceutics and Biopharmaceutics

journal homepage: www.elsevier.com/locate/ejpb

Research paper

Measuring the emulsification dynamics and stability of self-emulsifying drug delivery systems

Teófilo Vasconcelos[a,b,c,d], Sara Marques[b,e], Bruno Sarmento[c,d,f,g,*]

[a] BIAL-Portela & Cª, S.A., Avenida da Siderugia Nacional, 4745-457 Trofa, Portugal
[b] ICBAS – Instituto de Ciências Biomédicas Abel Salazar, University of Porto, Rua de Jorge Viterbo Ferreira, 228, 4050-313 Porto, Portugal
[c] INEB – Instituto Nacional de Engenharia Biomédica, Universidade do Porto, Rua Alfredo Allen, 208, 4200-135 Porto, Portugal
[d] I3S – Instituto de Investigação e Inovação em Saúde, Universidade do Porto, Rua Alfredo Allen, 208, 4200-135 Porto, Portugal
[e] CIBIO/InBIO-UP – Research Centre in Biodiversity and Genetic Resources, University of Porto, Rua Padre Armando Quintas, 7, 4485-661 Vairão, Portugal
[f] CESPU – Instituto de Investigação e Formação Avançada em Ciências e Tecnologias da Saúde and Instituto Universitário de Ciências da Saúde, Rua Central de Gandra 1317, 4585-116 Gandra, Portugal
[g] School of Pharmacy, Queen's University Belfast, Medical Biology Centre, 97 Lisburn Road, Belfast BT9 7BL, UK

ARTICLE INFO

Keywords:
Self-emulsifying drug delivery systems
Laser diffraction
Emulsifying agents
Lipid-based drug delivery systems
Bioavailability

ABSTRACT

Self-emulsifying drug delivery systems (SEDDS) are one of the most promising technologies in the drug delivery field, particularly for addressing solubility and bioavailability issues of drugs. The development of these drug carriers excessively relies in visual observations and indirect determinations. The present manuscript intended to describe a method able to measure the emulsification of SEDDS, both micro and nano-emulsions, able to measure the droplet size and to evaluate the physical stability of these formulations. Additionally, a new process to evaluate the physical stability of SEDDS after emulsification was also proposed, based on a cycle of mechanical stress followed by a resting period. The use of a multiparameter continuous evaluation during the emulsification process and stability was of upmost value to understand SEDDS emulsification process. Based on this method, SEDDS were classified as fast and slow emulsifiers. Moreover, emulsification process and stabilization of emulsion was subject of several considerations regarding the composition of SEDDS as major factor that affects stability to physical stress and the use of multicomponent with different properties to develop a stable and robust SEDDS formulation. Drug loading level is herein suggested to impact droplets size of SEDDS after dispersion and SEDDS stability to stress conditions. The proposed protocol allows an online measurement of SEDDS droplet size during emulsification and a rationale selection of excipients based on its emulsification and stabilization performance.

1. Introduction

In the last two decades the pharmaceutical industry faced a shift in its development strategy due to the advent of computerized systems and the correspondent molecular design. This transformation led to the development of more potent and specific drugs, but also to drugs more challenging from the druggable space. These new drugs are particularly very poorly soluble and as a consequence present poor bioavailability [1,2]. The pharmaceutical industry reacted to these new challenges by developing new drug delivery systems able to improve the observed inconsistent exposure and to maximize drug bioavailability. Among these strategies, amorphous solid dispersion and lipid formulations are the most promising. From the later, self-emulsifying drug delivery systems (SEDDS) are one of the most likely technologies [3,4].

SEDDS are one of the most promising technologies in the drug delivery field, particularly for solubility and bioavailability enhancement [3]. SEDDSs are isotropic and thermodynamically stable solutions consisting of oil, surfactant, co-surfactant and drug mixtures that spontaneously form oil-in-water (O/W) emulsions when mixed with water under gentle stirring [5]. These drug delivery systems are, thus, lipid formulations, and, according to Pouton, classified in four classes depending on its composition, ranging from formulations composed by (I) pure lipid compounds, (II) lipids with low hydrophilic-lipophilic balance (HLB) generally used to form water in oil emulsions, (III) lipids

Abbreviations: SEDDS, self-emulsifying drug delivery systems; O/W, oil-in-water; HLB, hydrophilic-lipophilic balance; SNEDDS, self-nano-emulsifying drug delivery systems; SMEDDS, self-micro-emulsifying drug delivery systems; DLS, dynamic light scattering; PCS, photon correlation spectroscopy; LD, laser diffraction; SSA, specific surface area; PdI, polydispersity index; W/O, water-in-oil

* Corresponding author at: Rua Alfredo Allen 208, 4200-135 Porto, Portugal.
E-mail address: bruno.sarmento@ineb.up.pt (B. Sarmento).

https://doi.org/10.1016/j.ejpb.2017.11.003
Received 26 July 2017; Received in revised form 4 November 2017; Accepted 5 November 2017
Available online 10 November 2017
0939-6411/

with high HLB used to form oil in water emulsions and the last class (IV) is mainly hydrophilic components such as co-solvents [4]. The principles of these systems assume that in contact with aqueous liquids these lipid formulations are able to emulsify and form stable nano or microemulsions containing drugs [6,7] by using the motility of stomach and intestine for *in vivo* self-emulsification. SEEDS, particularly the ones belonging to class III, are able to generate stable emulsions in the presence of water vehicles. Self-emulsification occurs when the entropy change that favors dispersion is greater than the energy required to increase the surface area of the dispersion [8,9]. These emulsions have a droplet size ranging from few nanometers to several micrometers. An adequate selection of excipients is crucial for the development of a successful SEDDS affecting the type of emulsion, dispersibility and stability after dispersion [6,10,11].

SEDDS able to form stable self-nano-emulsifying drug delivery systems (SNEDDS) or self-micro-emulsifying drug delivery systems (SMEDDS) present advantageous over the ones forming larger and generally unstable emulsion (Type I and II described by Pouton). This happens because the small droplets size allows a higher contact surface of drug with intestinal mucosa, improving its absorption [11–13]. Additionally, depending on the lipid composition and droplet size these particles can be absorbed by Peyer patches improving exposure and avoiding first hepatic passage effect [2,7,10,12]. Droplet size and droplet stability after dispersion are, thus, key elements in the formulation development of SEDDS [4,14–17].

The current methodology to evaluate SEDDS properties consists in the particle size measurement of the dispersions by dynamic light scattering (DLS) [15,16,18–21], photon correlation spectroscopy (PCS) [22] or, in a less extension, by laser diffraction (LD) [5]. Moreover, formulation stability is highly empirical based on visual observation [14,16] or indirectly by the zeta potential [20]. These data were considered to be a proof of a successful self-emulsification process [23,24].

In this work it is presented for the first time a process to observe (measure) the self-emulsification process allowing an online measurement of droplet size. Additionally, it is proposed a strategy to predict formulation stability based on droplet size stability when subject of physical stress conditions. Resveratrol, which is natural product that is under research due to its anti-cancer and anti-inflammatory properties, is also assessed as a blood sugar-lowering agent and a cardioprotective, was used as drug model in this study [25]. Resveratrol presents very low oral bioavailability (< 5%) due to its extremely low solubility, associated to high intestinal metabolization and being substrate of efflux mechanism [26]. These factors make it an excellent model drug for bioavailability enhancement strategies of Biopharmaceutical classification system (BCS) class II and IV drugs.

2. Materials and methods

2.1. Reagents

Transcutol® was a gift from Gatefossé, France. Imwitor® 742 was a gift from Oxi-Med, Spain. Tween® 80 was acquired from Croda, Spain. Resveratrol was a gift from BIAL, Portugal. Purified water was obtained by a milliQ purification system.

2.2. Preparation of emulsions

In order to study a wide variety self-emulsifying processes, excipients of three different structural classes were selected with three HLB values (ranging from 4 to 15). Seven different formulations were studied (Table 1). Three formulations corresponded to single excipients, two were self-micro-emulsifying and another two self-nano-emulsifying drug delivery systems. Resveratrol was included into the formulations with different loadings, corresponding to the maximum solubility values of resveratrol in each formulation (previously determined). Loading of formulations was 226 mg/mL, 19 mg/mL, 48 mg/mL, 168 mg/mL 144 mg/mL, 47 mg/mL and 140 mg/mL, respectively (Table 1).

2.3. Characterization of emulsions

2.3.1. Dispersibility

All formulations were assessed visually for spontaneous emulsification. SEEDS were diluted in distilled water at the ratio of 1:200 (v/v) under magnetic stirring at room temperature as described by Williams et al. [16]. The type of dispersion was assessed based on Singh et al. classification [14] where dispersions were classified in five grades based on time to disperse and aspect after dispersion. Grade I emulsions were formed in less than 1 min and were of clear bluish appearance, in opposition, grade V emulsions were formed in more than 3 min and presented minimal emulsification and large oil droplets on surface.

2.3.2. Robustness to dilution of SEDDS

Robustness to dilution was studied by diluting SEDDS 5 and 200 times with purified water. The diluted SEDDS were stored for 24 h and observed for presence of phase separation or drug precipitation as proposed by Williams et al. [16].

2.3.3. Emulsification process and droplet size measurement

The emulsification process was observed and measured using a Mastersizer® 2000 from Malvern (Worcestershire, United Kingdom). Briefly, 150 mL of purified water were added to the measurement compartment, then around 100–500 μL of SEDDS was added from which provided an obscuration of the detector (obscuration) between 3 and 25% in line with the recommended by the equipment manufacturer for a good measurement. Dispersion conditions in the system were set as 1750 rpm (50% of equipment capacity) and no ultrasounds.

A continuous particle size measurement (every 10 s) during 240 s was performed to allow the measurement of the self-emulsification process. The stable particle size (after 240 s) was considered as the droplet size after dispersion. Particle diameter corresponding to cumulative $D_{10\ (10\%)}$, $D_{50\ (50\%)}$, $D_{90\ (90\%)}$, specific surface area (SSA) which is the measurement of the area of per mass unit (m^2/kg), obscuration (of detector) and Span (representing the width of the distribution) were retrieved from the analysis and subject of investigation. Residuals were used to confirm the accuracy of the analysis.

2.3.4. Physical stability of SEDDS after emulsification

Physical stability of SEDDS after emulsification was evaluated by submitting the preparation described in previous section to 3500 rpm and 100% ultrasounds capacity for 240 s followed by a period of stabilization as described in previous section (1750 rpm and no ultrasounds). Particle size was continuously measured (every 10 s) during this process as described in the previous section.

2.3.5. Loading impact

The loading impact in the emulsification and physical stability of SEDDS after emulsification was evaluated by comparing the behavior of emulsions with resveratrol and formulations without resveratrol, submitted to the same conditions described in the two previous sections.

2.4. Statistical analysis

Triplicates of formulations were statistically analyzed in Microsoft® Excel® 2016 MSO. T-student tests were performed within pairs of experiments using a two-tail test with two-sample equal variance. Pairs were considered statically different with p values below 0.05.

3. Results and discussion

The current state of the art in the development of SEDDS presents several limitations, particularly regarding the understanding of

Table 1
Droplet size measurements in a Mastersizer® 2000 (Malvern, Worcestershire, United Kingdom) after 240 s (loaded particles). T.: Transcutol®. I. 742: Imwitor® 742. T.80: Tween® 80. HLB: Hydrophilic-Lipophilic Balance. *: estimated.

Formulation	T. (%)	I. 742 (%)	T. 80 (%)	HLB	Loading (mg/mL)	D_{10} (μm)	D_{50} (μm)	D_{90} (μm)
I	100			4	226	7.2 ± 1.4	24.5 ± 12.9	45.3 ± 16.9
II		100		4	19	4.6 ± 1.7	50.3 ± 9.7	129.9 ± 41.0
III			100	15	48	37.5 ± 20.3	83.6 ± 25.9	140.4 ± 44.2
IV	45	45	10	5.1 *	168	3.6 ± 3.2	15.8 ± 10.4	55.1 ± 23.6
V	33.3	33.3	33.3	7.6 *	144	10.3 ± 3.7	47.2 ± 29.8	121.2 ± 83.8
VI	12.5	75	12.5	5.4*	47	0.1 ± 0.0	0.4 ± 0.1	1.2 ± 0.1
VII	25	25	50	9.5 *	140	0.1 ± 0.1	0.2 ± 0.0	16.5 ± 16.0

emulsification process and physical stability of formulations after emulsification. This has been highly supported on a visual observation and empirical rationales. The use of an analytical measurement of the emulsification process with multiparameter being retrieved and subject of analysis removed the subjectivity from the emulsification process characterization and provided a better understanding of this critical process for SEDDS. Moreover, the possibility to predict the physical stability of SEDDS after emulsification under stress conditions contribute for a more rationale formulation selection.

3.1. Dispersibility and physical stability

All formulations formed a micro-emulsion when diluted 1:5 with purified water. Moreover, when diluted 1:200 with purified water formulations I, III, VI and VII rapidly formed (< 1 min) a nano-emulsion, having a clear or bluish appearance and 24 h later did not show phase separation. In the case of formulations II and V a slightly less clear nano-emulsion with a bluish white appearance was also rapidly formed (< 1 min). However, formulation IV rapidly (< 1 min) formed a milky micro-emulsion and showed a slight phase separation 24 h later, which was not observed after 4 h.

Accordingly to Singh et al. [14] a formulation with the behavior of formulations I to III and V to VII will remain as nano-emulsion when dispersed in gastrointestinal tract, while formulation IV is still recommend for SEDDS formulation. Moreover, all formulations except formulation IV were considered as physically stable after dispersion [27]. Formulation IV was also stable for at least 4 h after dispersion, which was a positive indicator of its stability.

3.2. Droplet size and specific surface area

The droplet size measured after 240 s of dispersibility was considered as droplet size. The 240 s were selected because a plateau (stabilization) in the droplet size was achieved at this time. The lowest droplet size was achieved for formulations VII (D_{50} = 167 nm) and VI (D_{50} = 362 nm) which were real nano-emulsion. All the other formulations were micro-emulsion: IV (D_{50} = 15.8 μm) and I (D_{50} = 24.5 μm) followed by formulation V (D_{50} = 47.2 μm) and II (D_{50} = 50.3 μm). Formulation III presented the largest particles (D_{50} = 83.6 μm) (Table 1). However, these values apparently contradict the visually observed (previous section) for formulations I-III and V. These differences between both experiments could be attributed to dilution and stirring speed variations.

Despite formulation III, all other formulations presented a relatively low variability in D_{10} and D_{50} values after 240 s, indicating that the emulsification process generally occurred similarly. The D_{90} measurements presented a higher variability, which may suggest that the largest particles were dependent on the microenvironmental conditions. An exception to this high variability was formulation VI, which after 240 s presented a very low variability in 3 droplet size parameters.

Traditionally, droplet size of lipid based formulations of SEDDS is determined by DLS after an equilibrium period of 30 min [16]. However, this approach presents some limitations starting with the particle size range of the DLS technique that is from 0.3 nm to 2 μm [28], which means that this technique could not detect all micro droplets in opposition to the laser diffraction that can measure particles from 20 nm to 2 mm [29,30] underestimating the small nano size droplets. Moreover, the 30 min equilibrium period recommend for DLS is very long compared to the proposed one of 240 s (4 min).

The SSA is a measurement of the area of particles exposed to the dispersion medium. Translating this to an *in vivo* process, the higher the SSA (more and smaller particles), the highest exposure of particles to the intestinal walls, the higher is lipid digestion and, consequently, the higher absorption potential and lower inter-individual variability will occur [31]. Moreover, the SSA is a measure of all the droplets population. Formulations VI and VII presented the highest SSA which was expected due its nanoscale droplet size when compared to the other formulations. Among the micro-emulsions, formulation IV presented the highest SSA, followed by formulations V, II, I with similar values and III presented the lower SSA (Fig. 1). Furthermore, these data supported the droplet size measurements and its reliability since nano-scale emulsions presented a much higher SSA over the micro-scale ones. Formulation III presented the smallest Span, probably because it presented tightest droplets distribution but with the largest size, however

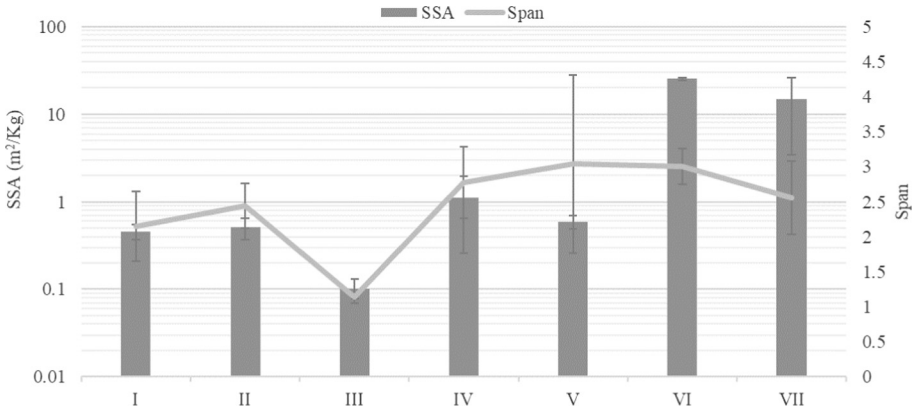

Fig. 1. Specific surface area and span measured after 240 s (n = 3, mean ± SD).

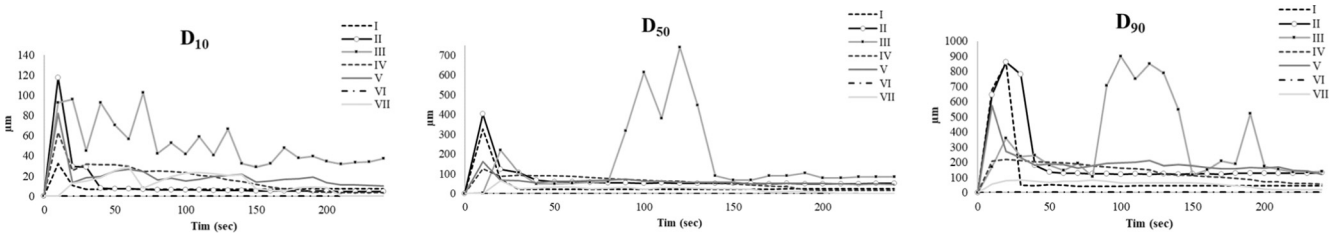

Fig. 2. Droplet size measurements (D_{10}, D_{50}, D_{90}) over 240 s (n = 3).

all the other formulations presented a similar Span value (Fig. 1). These data indicated that span value was independent of the droplet size scale and type of emulsion (nano Vs micro) but is a relevant tool to compare the width of the droplet size population.

The DLS droplet size determinations are generally reported as droplet size (average) and Polydispersity Index (PdI), which is a descriptive of the distribution width [15,16,31–33]. Average droplet size is equivalent to D_{50} and PdI is equivalent to Span provided by laser diffraction analysis. With the proposed analytical procedure, it was possible to have a clear picture of the droplet size distribution by having D_{10} and D_{90} and particularly the SSA detection, which corresponded to the measurement of whole droplet size distribution.

3.3. Emulsification process

The emulsification process and its dynamics were depicted in Fig. 2 regarding the droplet size of the seven different formulations composed by a single component (I, II, III) or the mixture of them forming micro-emulsions (IV and V) or nano-emulsions (VI and VII).

In general, the use of laser diffraction allows the measurement and surveillance of the emulsification process. This process consisted, for most of the developed formulations, in a fast (30 s) formation of very large droplets that then divided in smaller droplets until stabilization (Fig. 2). Generally, the stabilization process firstly impacted the D_{10} followed by D_{50} and later D_{90}. A particular case of this type of emulsification was presented by formulation VI which almost instantaneously formed droplets of nano size that were not further divided. On the contrary, formulations IV and VII were exceptions of this process, which presented a much slower droplet size increase, formed smaller particles, followed by a slow droplet size decrease that kept occurring over a long time.

The formulations were dropped in the test equipment as a large droplet that then emulsified in smaller droplets. The observed process was aligned with the emulsification principles where the emulsified droplet size is considered to be the result of the droplet breakup and the droplet coalescence competition processes [34]. Particularly in SEEDS, emulsification requires very little input energy, which was provided by the stirring force resulting in a destabilization of local interfacial regions through contraction. Thus, for emulsification to occur, interfacial structure should not have resistance to surface shearing, which could be achieved by using surfactants [35]. As the formulation interfacial tension decreased, droplet breakup occurred and formed smaller droplets. At the same time, the emulsion stability became very low, due to fast coalescence, which favored the occurrence of larger droplets. For most of the formulations studied, in the first moments of emulsification, coalescence mechanism was preponderant as showed by the large droplet size [34]. This was followed by a period that droplet breakup become the most relevant mechanism until a balance was reached. However, formulation III presented very unstable droplet formation and droplet size reduction. Since formulation III was composed by Tween® 80, this phenomenon could be attributed to a dissolution/emulsification process of this surfactant.

It is proposed that emulsification process of SEDDS consisted in converting large droplets into small droplets that reach stable D10 followed by a stabilization in the D_{50} value and only later the D_{90} value stabilized. Moreover, fast and slow emulsifiers occurred in both micro and nano-emulsions similarly. Composition of SEDDS impacted the droplet structure, but also its viscosity which contributed for the behavior as slow or fast emulsifiers.

Furthermore, these data suggested that the emulsification process was not a continuing process where droplet size was continuously reducing. Instead each formulation presented a relatively stable droplet size distribution and the variation was the time and mode to reach those droplet sizes.

The proposed mechanism of large droplets division into small droplets could be corroborated by the increase of obscuration and SSA over time (Fig. 3) which was particularly evident for micro-emulsion and less for nano-emulsions. Obscuration and SSA also proved that stabilization in the formed particles occurred quickly, which supported the results for the particle size.

The droplet size dispersion (Span) increased rapidly and greatly in particularly for formulations I, II, V and VII that were followed by stabilization (Fig. 3). Formulation VI reached a span stabilization extremely fast (10–20 s) and kept this value almost constant, this is an indicator that it quickly reached and kept a stable droplet size distribution over time.

Considering the obtained data, SEDDS emulsification could be categorized in 2 types: fast or slow emulsifying. The fast emulsifying SEDDS were characterized by quickly forming very large droplets that then were rapidly divided into small and stable droplets. On the other side, slow emulsifying were characterized by not so large droplets formation in the initial phase that then were slowly divided or fragmented into smaller droplets. This mechanism was observed for both micro and nano-emulsions.

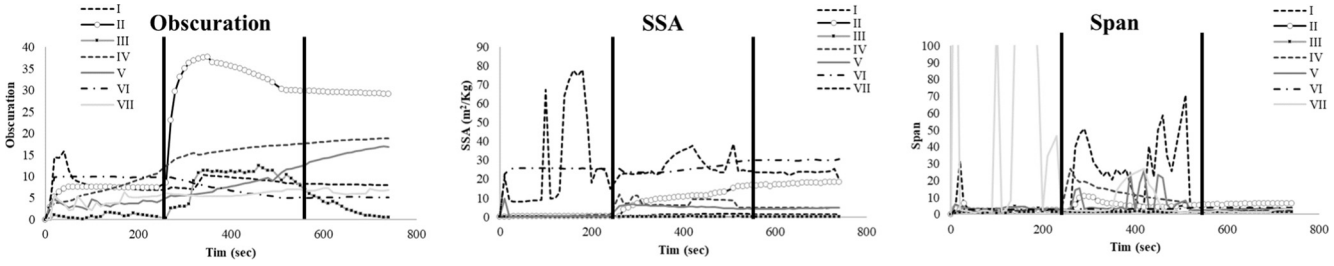

Fig. 3. Obscuration, span and SSA over stabilization phase, stress phase and resting phase (n = 3).

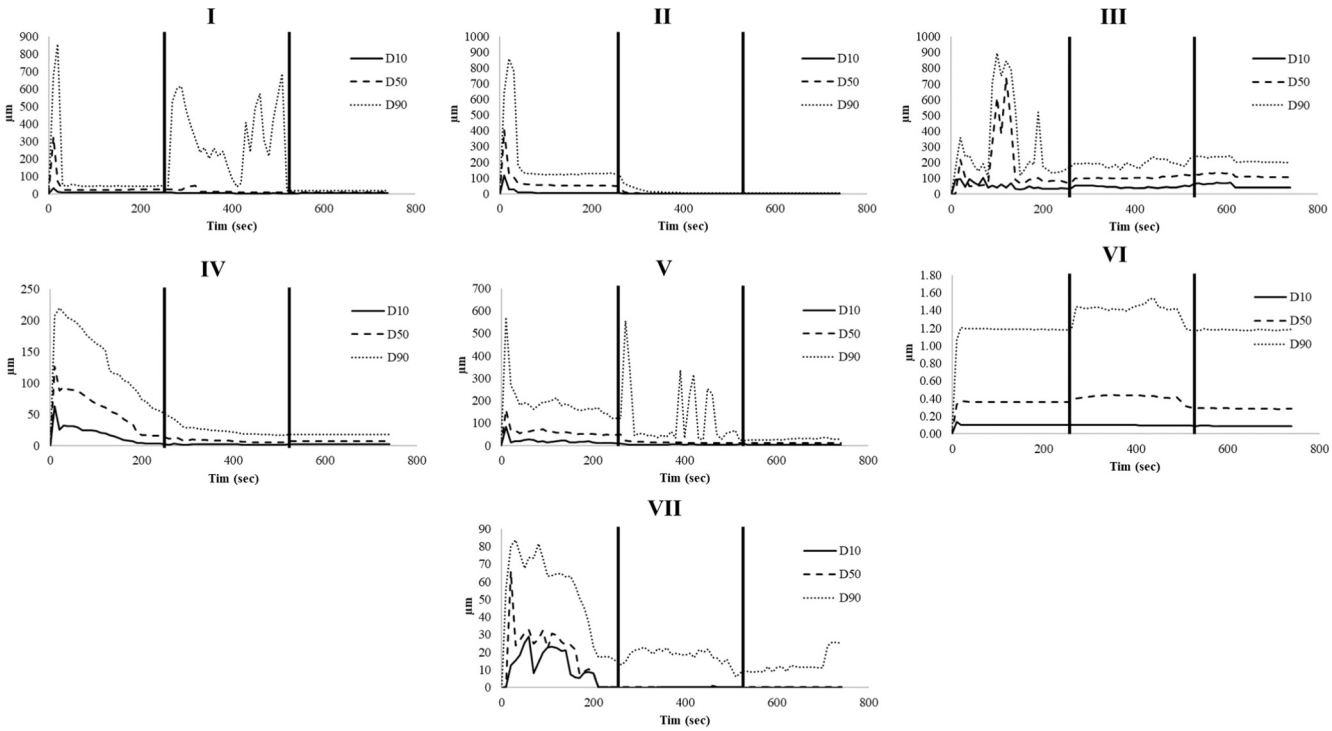

Fig. 4. Droplet size measurement (D_{10}, D_{50}, and D_{90}) over dispersion (first segment), stress (second segment) and resting periods (third segment) (n = 3).

3.4. Physical stability of SEDDS after emulsification

After emulsification, the stress conditions that formulations were subjected, 3500 rpm and ultrasound at maximum capacity during 240 s, were followed by an additional resting period of 240 s. The behavior of emulsions was monitored for D_{10}, D_{50}, D_{90}, SSA, obscuration and Span every 10 s.

During the stress phase formulations behaved in two different ways (Fig. 4): decreasing of general droplet size with major prominence in D_{90} was observed in formulations II, IV and VII (only D90 decreased), which was expected, since droplet size of an emulsion can be affected by the shear force [36,37]. Alternatively, erratic droplet size increase in D_{90} was observed in formulations I and V with decrease in D_{10} and D_{50}, Formulation VI showed only a small increase of D10 and D50 during stress phase. Formulation III was not significantly affected by the stress conditions and resting phase.

On resting phase formulations I, V and VI returned to their original droplet size, and even presented statistically (except formulation VI) lower D_{10}. However, formulation II during stress and resting phase showed a continuous decrease in droplet size which was at the end of the process statically smaller ($P < .05$) in all three parameters (D_{10}, D_{50} and D_{90}). By the contrary, formulations IV and III were not affected by the resting process (Fig. 4). This data suggested that droplet size could be affected in some formulations, such as formulation I and V, by the emulsification conditions, such as agitation, but after standard conditions establishment the droplet size was able to revert to its original properties. Additionally, other formulations were only minimally affected by the emulsification conditions. Thus, it can be suggested that droplet size is mostly affected by the composition than by the emulsification conditions and that micro-emulsions are mostly affected by stress conditions than nano-emulsions that were only minimally affected.

During stress phase, the shear forces increased and it was expected that droplet breakup became dominant over coalescent resulting in an increase of the number of droplets [34,37]. However, the way that it would occur, the extension and the resting process was unpredictable.

Again, this phenomenon was more evident for micro-emulsions than for nano-emulsions, corroborating the previously observed for particle size. Therefore, obscuration, span and SSA were only minimally affected by stress and resting conditions applied to nano-emulsions. Regarding, micro-emulsions, formulation II during the stress phase registered a fast and steep increase in the number of particles (obscuration) followed by a slight decrease and stabilization, which was maintained until the end of the study (Fig. 3). The new droplets formation during the stress phase was accompanied with a decrease in the width of the particle size distribution (Span) resulting in a fast and sustained increase in the SSA. This supported the observed in Fig. 4 that during stress phase a relevant droplet size reduction was observed particularly for D_{90} where the large droplets were fragmented in several smaller droplets.

On the other hand, formulation IV and V showed a slow formation of new particles during stress phase that was maintained during the resting phase (Fig. 3). For formulation IV, this was associated to a slight narrowing of the droplet size distribution (Span), which was more evident for D_{90}, over the entire study resulting in a slight and slow increase in the SSA. On the contrary, an erratic increase in the droplet size distribution was observed during the stress phase for formulation V that was narrowed and stabilized as soon as stress conditions disappeared. This event leaded to a rapid increase in the SSA in the beginning of the stress phase followed by stabilization.

Formulations I, and III showed a delayed fast but not very high increase in the droplet number during stress conditions followed by a stabilization that was maintained during the resting phase for formulation I and decreased for formulation III. The behavior of the latter formulation was associated to a slender increase in the SSA but not on the droplet size distribution which was maintained almost constant during the entire process. The decrease on the obscuration after the stress phase could be due to a combination of enlargement of the droplets size and solubilization. Regarding formulation I the increase in droplets number was associated to a widening of the droplets size distribution only during the stress phase, which returned to their stabilization values after removal of stress conditions. The SSA increased during the stress phase and was maintained almost constant until the end of the study.

Traditionally, the SEEDS droplet size stability consists in the measurement of the PdI, which is a dimensionless measure of the width of the particle size distribution [33]. This determination is performed 30 min after emulsification and consequently does not provide any type of information about the emulsification dynamics. Therefore, its correlation with SEDDS stability is limited. The proposed procedure on the other hand permits an almost online visualization of the emulsification process. Moreover, as observed for Span alone, it provided limited information. However, the measurement of Span associated to SSA and obscuration, all together provided a clear picture of the formulation and equivalent Span values were achieved for very different formulations (ex. micro-emulsions VS nano-emulsions).

Depending on formulation components, the emulsification process can be reversibly or irreversibly affected by extreme stress conditions or not be affected by it. The later were considered to be the most desirable formulations as will be less prone to inter-individual variability due to different gastrointestinal mechanical conditions.

These data suggest that formulations composed by high lipophilic compounds (II) require more mechanical energy to emulsify into very small droplets, since the droplet size (reduction) and the SSA (increase) were significantly affected by the stress conditions. Nevertheless, after emulsification these are relatively stable, which can be included in the group of irreversibly affected by stress conditions. High lipidic formulations showed a larger droplet size particularly because there was lack of surfactants to be present in the border of the emulsion droplets to reduce the interfacial energy as well as providing a mechanical barrier to coalescence as previously reported by Kang et al. [15].

In the opposite, emulsions composed by water soluble components (I) or surfactants with very high HLB (III) or multi components (IV - VII) were less affected by the stress conditions and when were affected the effects were reversible. The major impact of stress conditions in these formulations consisted in an acceleration of the larger particles fragmentation process into smaller and stable ones, reflected in particularly the decrease of D_{90} and not in the other parameters. This was also aligned with the reported by Kang et al. that with increasing the surfactant and co-surfactant content the particle size decreased [15].

3.5. Resveratrol loading effect

The presence or absence of resveratrol in the formulations was evaluated by submitting the non-loaded formulations to the same cycles of emulsification, stress and stabilization (Fig. 5).

The presence of resveratrol showed minimal impact in the droplet size of formulation II and III, due to the low loading of resveratrol on these formulations (2 and 5% respectively). Similar results for low loading were reported by Kang et al. [15] and Shah et al. [38] using different drugs. When nano-emulsions were formed, loading level showed no impact in the droplet size (formulations VI and VII). Surprisingly, all of these formulations droplet size was higher (D_{10}, D_{50} and D_{90}) for non-loaded particles and was more evident after emulsification phase than at the end of the stress cycle study. This reinforce that the entire cycle measurement provided relevant information impossible to obtain by a simple means droplet size and PdI measurement (Fig. 5).

As non-loaded, formulation I was not able to emulsify, it solubilized and consequently presented an obscurity close to zero and thus no droplet size determinations were possible. At same time, this formulation was the one with the highest loading, around 23%, and since loaded particles were able to generate reproducible determinations it can be speculated that resveratrol contributed to the emulsification process and stabilization of droplets, preventing solubilization.

Micro-emulsions formulations (IV, V) with high loading (around 15%) presented larger droplets in loaded particles as previously observed by other authors [15,38]. Formulation IV, that emulsified equally with or without the presence of resveratrol after a stress cycle, non-loaded formulations droplet size significantly reduced (D_{50} and D_{90}) which did not occur in the loaded particles. In fact, this was a tendency in most of non-loaded formulations, maintaining or exacerbating the differences between loaded and non-loaded, like in case of formulation V that after these cycles was statically different in all three measurements. These data suggested that the presence of resveratrol in this formulations prevented their droplet division and consequent droplet size reduction.

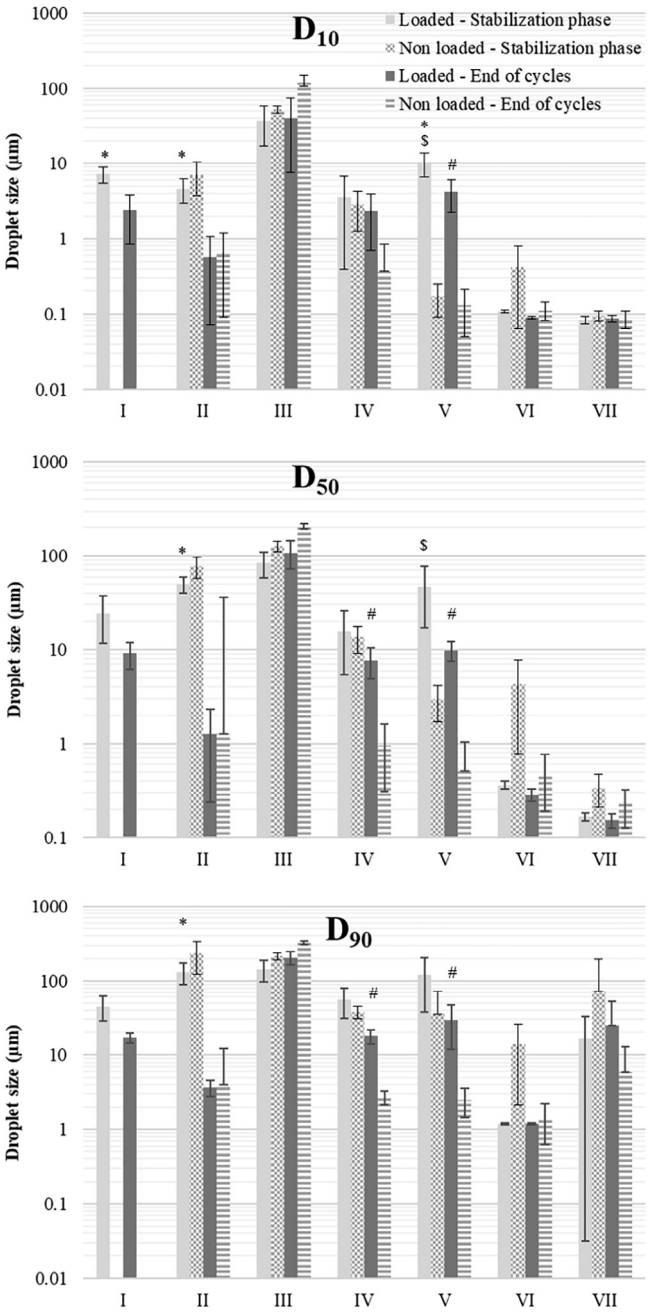

Fig. 5. Droplet size at different stages with and without resveratrol (n = 3, mean ± SD). *Statistically different end of cycle vs stabilization phase on loaded particles; # statistically different at the end of cycle loaded vs not loaded; $ statistically different at the end of stabilization loaded vs not loaded ($P < .05$).

When low loading levels were achieved or the system were able to generate nano-emulsions loading did not affect the droplet size. Moreover, it appeared to promote smaller droplet sizes in some case.

Generally, high loading levels, in a composition dependent manner impacted the droplet size. Droplet size of high loaded droplets was always smaller after stress cycles than after emulsification phase at least in D_{90}, in opposition to low loading levels that generally were less affect by the stress conditions.

4. Conclusion

Self-emulsifying delivery systems are an important tool to improve drug bioavailability of BCS class II and IV drugs, particularly for those with high lipidic solubility. However, its emulsification was a key process to ensure an adequate performance of these advanced drug delivery systems and therefore an adequate selection of the formulation is crucial. In this manuscript, it was shown that laser diffraction was a technique able to measure the emulsification process for micro and nano-emulsions providing important information of the drug delivery systems, far beyond its droplet size. Additionally, it was proposed a process to evaluate the stability of emulsified formulations to mechanical stress by evaluating droplet size, Span, obscuration and SSA allowing the selection of the most robust formulations that will be less prone to suffer from *in vivo* intra or inter individual variabilities, such has peristaltic movements.

The use of a continuous measurement and multiparameter evaluation showed to be worth to understand the emulsification process and emulsion stability, allowing the differentiation of SEDDS during these phases. Using this process, it was possible to classify SEDDS regarding its emulsification process as slow or fast emulsifiers, which was not possible to determine with current characterization processes. Data was generated using resveratrol as model of poor water-soluble drug with several bioavailability issues and could be translated for another drug with similar bioavailability problems. Additionally, it was possible to observe that SEDDS with different compositions behave differently in the presence of a mechanical stress followed by a resting phase. All this information regarding emulsification dynamics and droplet stability to mechanical stress conditions could only be possible by using a continuous measurement of multiparameter against the current state of the art that uses a single point static analysis of two parameters. The present manuscript defined a new state of the art in SEEDS emulsification characterization and droplet stability.

Formulations able to form nano-emulsion or with low loadings were less affected by mechanical stress. In particular cases, drug content appears to contribute to the droplet stabilization promoting its smaller droplet size.

A desirable SEDDS formulation should be able to form a stable nano-emulsion with a small span value and very high specific surface area.

Acknowledgements

This article is a result of the project NORTE-01-0145-FEDER-000012, supported by Norte Portugal Regional Operational Programme (NORTE 2020), under the PORTUGAL 2020 Partnership Agreement, through the European Regional Development Fund (ERDF). This work was also financed by FEDER – Fundo Europeu de Desenvolvimento Regional funds through the COMPETE 2020 – Operacional Programme for Competitiveness and Internationalisation (POCI), Portugal 2020, and by Portuguese funds through FCT – Fundação para a Ciência e a Tecnologia/Ministério da Ciência, Tecnologia e Ensino Superior in the framework of the project "Institute for Research and Innovation in Health Sciences" (POCI-01-0145-FEDER-007274) and NETDIAMOND (POCI-01-0145-FEDER-016385).

Sara Marques gratefully acknowledges Fundação para a Ciência e a Tecnologia (FCT), Portugal for financial support (grant SFRH/BPD/75905/2011).

Appendix A. Supplementary data

Supplementary data associated with this article can be found, in the online version, at http://dx.doi.org/10.1016/j.ejpb.2017.11.003.

References

[1] T. Vasconcelos, S. Marques, J. das Neves, B. Sarmento, Amorphous solid dispersions: rational selection of a manufacturing process, Adv. Drug Deliv. Rev 100 (2016) 85–101.
[2] T. Vasconcelos, S. Marques, B. Sarmento, The biopharmaceutical classification system of excipients, Ther. Deliv. 8 (2) (2017) 65–78.
[3] R. Karwal, T. Garg, G. Rath, T.S. Markandeywar, Current trends in self-emulsifying drug delivery systems (SEDDSs) to enhance the bioavailability of poorly water-soluble drugs, Crit. Rev. Ther. Drug Carrier Syst. 33 (1) (2016) 1–39.
[4] C.W. Pouton, Formulation of poorly water-soluble drugs for oral administration: physicochemical and physiological issues and the lipid formulation classification system, Eur. J. Pharm. Sci. 29 (3) (2006) 278–287.
[5] T.S. Nipun, S.M. Ashraful Islam, SEDDS of gliclazide: preparation and characterization by *in-vitro*, *ex-vivo* and *in-vivo* techniques, Saudi Pharm. J. 22 (4) (2014) 343–348.
[6] M.A. Rahman, A. Hussain, M.S. Hussain, M.A. Mirza, Z. Iqbal, Role of excipients in successful development of self-emulsifying/microemulsifying drug delivery system (SEDDS/SMEDDS), Drug Dev. Ind. Pharm. 39 (1) (2013) 1–19.
[7] B. Singh, S. Beg, R.K. Khurana, P.S. Sandhu, R. Kaur, O.P. Katare, Recent advances in self-emulsifying drug delivery systems (SEDDS), Crit. Rev. Ther. Drug Carrier Syst. 31 (2) (2014) 121–185.
[8] K. Kohli, S. Chopra, D. Dhar, S. Arora, R.K. Khar, Self-emulsifying drug delivery systems: an approach to enhance oral bioavailability, Drug Discov. Today 15 (21–22) (2010) 958–965.
[9] H. Reiss, Entropy-induced dispersion of bulk liquids, J. Colloid Interface Sci. 53 (1) (1975) 61–70.
[10] B. Bahloul, M.A. Lassoued, S. Sfar, A novel approach for the development and optimization of self emulsifying drug delivery system using HLB and response surface methodology: application to fenofibrate encapsulation, Int. J. Pharm. 466 (1) (2014) 341–348.
[11] I. Cherniakov, A.J. Domb, A. Hoffman, Self-nano-emulsifying drug delivery systems: an update of the biopharmaceutical aspects, Expert Opin. Drug Deliv. 12 (7) (2015) 1121–1133.
[12] H.-Y. Cho, J.-H. Choi, I.-J. Oh, Y.-B. Lee, Self-emulsifying drug delivery system for enhancing bioavailability and lymphatic delivery of Tacrolimus, J. Nanosci. Nanotechnol. 15 (2) (2015) 1831–1841.
[13] S. Dokania, A.K. Joshi, Self-microemulsifying drug delivery system (SMEDDS) – challenges and road ahead, Drug Deliv. 22 (6) (2015) 675–690.
[14] A.K. Singh, A. Chaurasiya, A. Awasthi, G. Mishra, D. Asati, R.K. Khar, R. Mukherjee, Oral bioavailability enhancement of exemestane from self-microemulsifying drug delivery system (SMEDDS), AAPS PharmSciTech. 10 (3) (2009) 906–916.
[15] B.K. Kang, J.S. Lee, S.K. Chon, S.Y. Jeong, S.H. Yuk, G. Khang, H.B. Lee, S.H. Cho, Development of self-microemulsifying drug delivery systems (SMEDDS) for oral bioavailability enhancement of simvastatin in beagle dogs, Int. J. Pharm. 274 (1–2) (2004) 65–73.
[16] H.D. Williams, P. Sassene, K. Kleberg, J.-C. Bakala-N'Goma, M. Calderone, V. Jannin, A. Igonin, A. Partheil, D. Marchaud, E. Jule, J. Vertommen, M. Maio, R. Blundell, H. Benameur, F. Carrière, A. Müllertz, C.J.H. Porter, C.W. Pouton, Toward the establishment of standardized *in vitro* tests for lipid-based formulations, part 1: method parameterization and comparison of *in vitro* digestion profiles across a range of representative formulations, J. Pharm. Sci. 101 (9) (2012) 3360–3380.
[17] H.D. Williams, P. Sassene, K. Kleberg, M. Calderone, A. Igonin, E. Jule, J. Vertommen, R. Blundell, H. Benameur, A. Müllertz, C.W. Pouton, C.J.H. Porter, Toward the establishment of standardized *in vitro* tests for lipid-based formulations, part 3: understanding supersaturation versus precipitation potential during the *in vitro* digestion of type I, II, IIIA, IIIB and IV lipid-based formulations, Pharm. Res. 30 (12) (2013) 3059–3076.
[18] S. Kollner, I. Nardin, R. Markt, J. Griesser, F. Prufert, A. Bernkop-Schnurch, Self-emulsifying drug delivery systems: design of a novel vaginal delivery system for curcumin, Eur. J. Pharm. Biopharm. 115 (2017) 268–275.
[19] L.C. Chang, J.J. Kang, C.S. Gau, The evolution and challenges for the international harmonization of the regulation of pharmaceutical excipients in Taiwan, Regul. Toxicol. Pharmacol. 73 (3) (2015) 947–952.
[20] M.A. Kalam, M. Raish, A. Ahmed, K.M. Alkharfy, K. Mohsin, A. Alshamsan, F.I. Al-Jenoobi, A.M. Al-Mohizea, F. Shakeel, Oral bioavailability enhancement and hepatoprotective effects of thymoquinone by self-nanoemulsifying drug delivery system, Mater. Sci. Eng. C. Mater. Biol. Appl. 76 (2017) 319–329.
[21] H.D. Williams, P. Sassene, K. Kleberg, M. Calderone, A. Igonin, E. Jule, J. Vertommen, R. Blundell, H. Benameur, A. Müllertz, C.J.H. Porter, C.W. Pouton, Toward the establishment of standardized *in vitro* tests for lipid-based formulations, part 4: proposing a new lipid formulation performance classification system, J. Pharm. Sci. 103 (8) (2014) 2441–2455.
[22] M. Krstic, M. Popovic, V. Dobricic, S. Ibric, Influence of solid drug delivery system formulation on poorly water-soluble drug dissolution and permeability, Molecules 20 (8) (2015) 14684–14698.
[23] B. Bahloul, M.A. Lassoued, J. Seguin, R. Lai-Kuen, H. Dhotel, S. Sfar, N. Mignet, Self-emulsifying drug delivery system developed by the HLB-RSM approach: characterization by transmission electron microscopy and pharmacokinetic study, Int. J. Pharm. 487 (1) (2015) 56–63.
[24] R. Chintalapudi, T.E.G.K. Murthy, K.R. Lakshmi, G.G. Manohar, Formulation, optimization, and evaluation of self-emulsifying drug delivery systems of nevirapine, Int. J. Pharm. Invest. 5 (4) (2015) 205–213.
[25] G.T. Diaz-Gerevini, G. Repossi, A. Dain, M.C. Tarres, U.N. Das, A.R. Eynard, Beneficial action of resveratrol: how and why? Nutrition 32 (2) 174–178.
[26] A.R. Neves, M. Lucio, J.L. Lima, S. Reis, Resveratrol in medicinal chemistry: a critical review of its pharmacokinetics, drug-delivery, and membrane interactions, Curr. Med. Chem. 19 (11) (2012) 1663–1681.
[27] S. Beg, S. Swain, H.P. Singh, C.N. Patra, M.B. Rao, Development, optimization, and

characterization of solid self-nanoemulsifying drug delivery systems of valsartan using porous carriers, AAPS PharmSciTech. 13 (4) (2012) 1416–1427.
[28] Malvern, i. Zetasizer range – Support. https://www.malvern.com/en/support/product-support/zetasizer-range (accessed 11 July 2017).
[29] Malvern, i. Mastersizer range – Support. https://www.malvern.com/en/support/product-support/mastersizer-range (accessed 11 July 2017).
[30] C. Levoguer, Introducing the Malvern particle characterization toolkit: how to choose the right particle characterization toll for my needs, Malvern (2012).
[31] S. Kollipara, R.K. Gandhi, Pharmacokinetic aspects and *in vitro-in vivo* correlation potential for lipid-based formulations, Acta Pharm. Sin. B 4 (5) (2014) 333–349.
[32] H.D. Williams, M.U. Anby, P. Sassene, K. Kleberg, J.-C. Bakala-N'Goma, M. Calderone, V. Jannin, A. Igonin, A. Partheil, D. Marchaud, E. Jule, J. Vertommen, M. Maio, R. Blundell, H. Benameur, F. Carrière, A. Müllertz, C.W. Pouton, C.J.H. Porter, Toward the establishment of standardized in vitro tests for lipid-based formulations. 2: the effect of bile salt concentration and drug loading on the performance of type I, II, IIIA, IIIB, and IV formulations during in vitro digestion, Mol. Pharm. 9 (11) (2012) 3286–3300.
[33] L.C. Chen, Y.C. Chen, C.Y. Su, W.P. Wong, M.T. Sheu, H.O. Ho, Development and characterization of lecithin-based self-assembling mixed polymeric micellar (saMPMs) drug delivery systems for curcumin, Sci. Rep. 6 (2016) 37122.
[34] J.-L. Salager, L. Márquez, I. Mira, A. Peña, E. Tyrode, N.B. Zambrano, Principles of emulsion formulation engineering, in: K.L. Mittal, D.O. Shah (Eds.), Adsorption and Aggregation of Surfactants in Solution, Marcel Dekker Inc, New York, 2002, pp. 501–523.
[35] K. Khedekar, S. Mittal, Self emulsifying drug delivery system: a review, Int. J. Pharm. Sci. Res. 4 (12) (2013) 4494–4507.
[36] J. Dressman, K. Schamp, K. Beltz, J. Alsenz, Characterizing release from lipid-based formulations, Oral Lipid-Based Formulations, CRC Press, 2007, pp. 241–255.
[37] N. Sharma, P. Madan, S. Lin, Effect of process and formulation variables on the preparation of parenteral paclitaxel-loaded biodegradable polymeric nanoparticles: a co-surfactant study, Asian J. Pharm. Sci. 11 (3) (2016) 404–416.
[38] N. Shah, W. Phuapradit, Y.-E. Zhang, H. Ahmed, A. Malick, Lipid-based isotropic solutions, Oral Lipid-Based Formulations, CRC Press, 2007, pp. 129–148.

European Journal of Pharmaceutical Sciences 137 (2019) 105011

Contents lists available at ScienceDirect

European Journal of Pharmaceutical Sciences

journal homepage: www.elsevier.com/locate/ejps

Multicomponent self nano emulsifying delivery systems of resveratrol with enhanced pharmacokinetics profile

Teófilo Vasconcelos[a,b,c,d], Francisca Araújo[a], Carlos Lopes[a], Ana Loureiro[a], José das Neves[c,d], Sara Marques[b,e], Bruno Sarmento[c,d,f,*]

[a] BIAL - Portela & Cª, S.A., Avenida da Siderugia Nacional, 4745-457 Trofa, Portugal
[b] ICBAS - Instituto de Ciências Biomédicas Abel Salazar, Universidade do Porto, Rua de Jorge Viterbo Ferreira, 228, 4050-313 Porto, Portugal
[c] INEB - Instituto de Engenharia Biomédica, Universidade do Porto, Rua Alfredo Allen, 208, 4200-135 Porto, Portugal
[d] i3S - Instituto de Investigação e Inovação em Saúde, Universidade do Porto, Rua Alfredo Allen, 208, 4200-135 Porto, Portugal
[e] CIBIO/InBIO-UP - Research Centre in Biodiversity and Genetic Resources, Universidade do Porto, Rua Padre Armando Quintas, 7, 4485-661 Vairão, Portugal
[f] CESPU - Instituto de Investigação e Formação Avançada em Ciências e Tecnologias da Saúde, Instituto Universitário de Ciências da Saúde, Rua Central de Gandra 1317, 4585-116 Gandra, Portugal

ARTICLE INFO

Keywords:
Bioavailability
Emulsifying agents
Lipid-based drug delivery systems
Nano-emulsion
Resveratrol
Self-emulsifying drug delivery systems

ABSTRACT

Resveratrol is a drug with high potential for clinical application based on experimental models. Though, resveratrol translation to clinical use has not been successful yet due to its poor pharmacokinetics, related to poor solubility and fast metabolism. The use of drug delivery systems, namely self-emulsifying drug delivery systems (SEDDS), may be a viable strategy to overcome the poor in vivo performance of resveratrol. In this work, a rational development of two different ternary SEDDS was conducted. Experimental data showed that quantitative variations on SEDDS composition impacted dispersion and robustness to dilution of SEDDS, as well as loading capacity and droplet size. Formulations composed of Lauroglycol® 90/Labrasol®/Capryol® PGMC (12.5/75.0/12.5) (Lau/Lab/Cap) and Tween® 80/Transcutol®/Imwitor® 742 (33.3/33.3/33.3) (T80/Trans/Imw) featured improved performance and were selected for further studies. T80/Trans/Imw formulation yield faster emulsification and originated smaller droplet size, with lower cumulative percentile of 90% of particles (D_{90}) (below 200 nm), as compared to the than Lau/Lab/Cap formulation. Higher resveratrol permeation rate was observed in Caco-2 cell monolayer permeability studies for both formulations as compared to the free drug. Reduction of the metabolization and/or efflux of resveratrol was also noticed in the case of SEDDs, as suggested by the increased recovery of total drug. Plasmatic drug concentrations in rats observed after oral gavage indicate that both formulations provided faster resveratrol absorption than free drug, resulting in shorter T_{max} values (30 min vs. 2 h). No statistically significant differences were observed for AUC_{0-t} values of both formulations and the free drug. Still, C_{max} for the Lau/Lab/Cap SEDDs formulation was 2-fold higher than for the free drug. These findings suggest that SEDDS can increase resveratrol solubility and reduce its metabolization, resulting in an overall improvement of its oral pharmacokinetics profile.

1. Introduction

Resveratrol (3,5,4′-trihydroxy-trans-stilbene) is currently being developed by several companies and in academia as an anti-cancer (Cianciosi et al., 2018; Dei Cas and Ghidoni, 2018), an anti-inflammatory (Koushki et al., 2018; Lv et al., 2018), a blood sugar-lowering agent (Khodabandehloo et al., 2018), anti-microbial compound (Cannatelli et al., 2018; Ma et al., 2018), or a cardioprotective agent (Hung et al., 2000; Arafa et al., 2014; Hernandez-Cascales, 2017). It also present potential to be used in the management of

Abbreviations: A-B, apical to basal; AUC, Area under the curve; B-A, basal to apical; Cap, Capryol® PGMC; C_{max}, maximum concentration; D $_{(10, 50 \text{ and } 90)}$, Cumulative percentile of 10, 50 and 90% of particles; HLB, Hydrophilic-lipophilic balance; HPLC, High Performance Liquid Chromatography; Imw, Imwitor® 742; Lab, Labrasol®; Lau, Lauroglycol® 90; P_{app}, drug apparent permeability; SEDDS, Self-emulsifying drug delivery systems; SMEDDS, Self micro emulsifying drug delivery systems; SNEDDS, Self nano emulsifying drug delivery systems; SSA, Specific surface area; T80, Tween® 80; TEER, Transepithelial Electrical Resistance; T_{max}, time of maximum concentration; Trans, Transcutol®

* Corresponding author at: Rua Alfredo Allen 208, 4200-135 Porto, Portugal.
E-mail address: bruno.sarmento@ineb.up.pt (B. Sarmento).

https://doi.org/10.1016/j.ejps.2019.105011
Received 20 September 2018; Received in revised form 25 March 2019; Accepted 15 July 2019
Available online 19 July 2019
0928-0987/

neurodegenerative central nervous system diseases such as Parkinson's disease (Xia et al., 2019) and Alzheimer's disease (Andrade et al., 2018; Drygalski et al., 2018; Gomes et al., 2018). Resveratrol has shown multiple pharmacological activity and it has been speculated that it can activate Sirtuin 1, an enzyme that deacetylates proteins involved in cellular regulation (Tsuchiya et al., 2017; Maugeri et al., 2018). It also activates peroxisome proliferator-activated receptor-gamma coactivator (PGC-1α) and improves mitochondrial activity (Li et al., 2017). It further possesses antioxidant and anti-angiogenic properties (Montagnani Marelli et al., 2018) and can directly inhibit cardiac fibroblasts (Wu et al., 2016). Resveratrol interacts with several other enzymes, such as aromatase (Wang et al., 2006; Sinha et al., 2016) and gamma-glutamylcysteine ligase, which could contribute to the various pharmacological claims being advocated for this natural compound.

Despite all potential and data gathered from pre-clinical models, clinical evidence supporting the usefulness of resveratrol is limited and, in many cases, ambiguous (Boocock et al., 2007; Fontes-Ribeiro et al., 2008; Vaz-da-Silva et al., 2008; Almeida et al., 2009; Nunes et al., 2009; la Porte et al., 2010). This is primarily attributed to the pharmacokinetic properties of resveratrol, which has poor oral bioavailability (< 5% of the oral dose is detected in plasma), mainly due to its poor water solubility and fast metabolism (Boocock et al., 2007; la Porte et al., 2010). Therefore, there is a compelling need to improve the oral bioavailability of resveratrol in order to fully attest the potential of this multifaceted drug. Several technological approaches may be helpful in achieving this purpose. The use of amorphous solid dispersions and lipid formulations (such as self-emulsifying drug delivery systems (SEDDS)) are among the most promising approaches being currently tested in the pharmaceutical industry (Vasconcelos et al., 2017; Vasconcelos et al., 2018). SEDDSs are isotropic and thermodynamically stable solutions consisting of mixtures of oil, surfactant, co-surfactant and drug(s), and that spontaneously form oil-in-water (O/W) emulsions when mixed with water under gentle stirring (Nipun and Ashraful Islam, 2014). Depending on composition, these lipid-based formulations can even self-emulsify and form stable nano or micro-emulsions (Pouton, 2006; Singh et al., 2014) under the influence of the motility observed at the stomach and intestine. SEDDS that are able to form stable self nano emulsifying drug delivery systems (SNEDDS) or self micro emulsifying drug delivery systems (SMEDDS) may be particularly beneficial when compared to those forming larger and commonly unstable emulsions. The small droplet size provides higher contact surface between drugs in the inner oil phase of the emulsion and the intestinal mucosa, thus enhancing absorption (Cherniakov et al., 2015; Cho et al., 2015; Dokania and Joshi, 2015). Moreover, and depending on the lipid components properties and droplet size of the emulsions, drugs can be absorbed via Peyer patches, which enables increasing systemic exposure and circumventing the hepatic first-pass effect (Singh et al., 2014; Dokania and Joshi, 2015; Vasconcelos et al., 2017).

Several studies explored SEDDs for the delivery of resveratrol but only a few presented pharmacokinetics studies. For example, Chen et al. (2015) developed an ethyl oleate/Tween 80/PEG 400 (35:40:25, *w/w/w*) SMEDDS and showed that this strategy allowed improving the native antioxidant activity of resveratrol using a cell-based model. In another study, Seljak et al. (Seljak et al., 2014) developed a castor oil/Capmul® MCM/Kolliphor® EL/Kolliphor® RH (1:1:1:1) SMEDDS formulation that presented a reduction in pre-systemic metabolism when tested using in vitro and ex vivo intestinal models. A Capryol® 90, Cremophor® EL, and Tween® 20 (60:35:5) SNEDD formulation was further developed by Yen et al. (Yen et al., 2017), and shown able to improve blood glycemia and reduce fatigue in rats following exercise. These effects were, presumably, due to improved bioavailability. Finally, Balata et al. (Balata et al., 2016) developed a SNEDDS formulation comprising olive oil, Tween® 80, and propylene glycol (20.0:26.7:53.3) and showed that such strategy allowed reaching significantly higher hypoglycemic and hypolipidemic effects in diabetic-induced rats as compared to unprocessed resveratrol. Again, improved oral bioavailability was assumed for animals treated with SNEDDS.

In this work, we developed and optimized a resveratrol SEDDS presenting improved pharmacokinetics, namely C_{max}, with potential in increasing its brain bioavailability (Warren, 2018).

2. Materials and methods

2.1. Reagents

Transcutol® (Trans), Labrasol® (Lab), Lauroglycol® 90 (Lau), Labrafac® WL1349, Labrafil® M2125, Peceol®, Gelucire® 44/14 and Capryol® PGMC (Cap) were a gift from Gatefossé, France. Imwitor® 742 (Imw), Softigen® 767, Softigen® 701, Miglyol® 810, Miglyol® 829 and Miglyol® 840 were a gift from Oxi-Med®, Spain. Kollisolv® MCT 70, Kollisolv® P124, Kollisolv® PEG400, Kolliphor® TPGS, Kolliphor® EL, Kolliphor® HS15 and Kolliphor® RH40 were a gift from BASF (BTC-Europe), Spain. Tween® 80 (T80) was acquired from Croda, Spain. Resveratrol was purchased from Abatra Technology, China. Acetonitrile was obtained from Sigma-Aldrich, Germany.

Culture flasks and Transwell® plates were purchased from Corning Inc., USA. Dulbecco's Modified Eagle medium (DMEM), L-glutamine, non-essential amino acids (NEAA), penicillin (10,000 IU/mL), streptomycin (10 mg/mL) and trypsin-EDTA were purchased from HyClone, USA. Hank's balanced salt solution (HBBS) and heat inactivated fetal bovine serum (FBS) were purchased from Life Technologies Gibco, USA.

Purified water was obtained in-house using a milliQ purification system. All other materials were of analytical grade or equivalent.

2.2. High-throughput screening of resveratrol solubility

Resveratrol solubility was accessed in Trans, Lab, Lau, Labrafac® WL1349, Labrafil® M2125, Peceol®, Gelucire® 44/14, Cap, Imw, Softigen® 767, Softigen® 701, Miglyol® 810, Miglyol® 829, Miglyol® 840, Kollisolv® MCT 70, Kollisolv® P124, Kollisolv® PEG400, Kolliphor® TPGS, Kolliphor® EL, Kolliphor® HS15, Kolliphor® RH40 and T80 that have a hydrophilic-lipophilic balance (HLB) values in the range of 1–18 (values for each excipient are present in Table 1). Briefly, an excess

Table 1
Resveratrol solubility in excipients generally used for SEDDS. Results are presented as mean ± SD ($n = 3$). (*) denotes a statistically significant difference from control ($p < 0.05$).

Excipient	HLB	Solubility (mg/mL)
Purified water (control)		0.003 ± 0.002
Labrafac® WL1349	1	0.605 ± 0.058*
Peceol®	1	4.257 ± 0.013*
Miglyol® 810	N/A	0.606 ± 0.069*
Kollisolv® MCT 70	1	1.025 ± 0.070*
Miglyol® 840	N/A	0.975 ± 0.086*
Miglyol® 829	N/A	1.364 ± 0.136*
Lauroglycol® 90	3	6.362 ± 0.686*
Imwitor® 742	4	9.014 ± 0.488*
Labrafil® M2125	5	5.778 ± 0.163*
Capryol® PGMC	6	12.460 ± 1.654*
Gelucire® 44/14 (5%)	12	3.787 ± 0.184*
Labrasol®	13	83.754 ± 10.168*/#
Kolliphor® TPGS	13	4.921 ± 0.331*
Kolliphor® EL	13	22.957 ± 2.296*/#
Kollisolv® P124	15	39.514 ± 11.806*
Kolliphor® RH40	15	30.410 ± 13.748*/#
Kolliphor® HS15	15	30.433 ± 0.170*/#
Tween® 80	15	4.346 ± 0.113*
Softigen® 767	18	5.696 ± 0.734*
Transcutol®	N/A	107.478 ± 9.085*/#
Kollisolv® PEG400	N/A	0.151 ± 0.033*
Softigen® 701	N/A	22.535 ± 2.172*

N/A – not available; (#) saturation of Transcutol®, Labrasol®, Kolliphor® EL, RH40 and HS15 was not achieved.

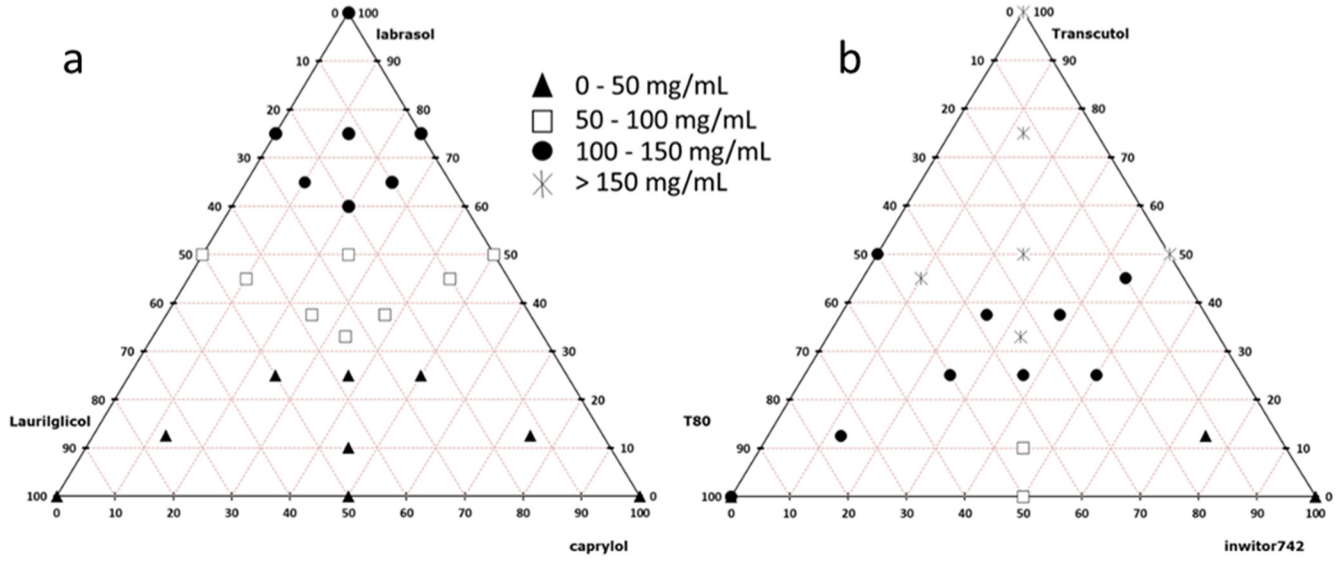

Fig. 1. Resveratrol loading in two sets of ternary qualitative compositions of Lau/Lab/Cap (**a**) and T80/Trans/Imw (**b**). Loading values were reported as: ▲ loading values below 50 mg/mL □ loading values between 50 and 100 mg/mL ● loading values between 100 and 150 mg/mL * loading values above 150 mg/mL.

amount (10–150 mg) of resveratrol was added to a two milliliters High Performance Liquid Chromatography (HPLC) vial. One milliliter of each of the above excipients was added to a vial and the preparations were stirred for 2 h at room temperature (15–25 °C). Each preparation was prepared in triplicate. The solubility in purified water was also accessed as control. After 2 h, the suspensions were filtered through 0.45 µm filters (Pall Corporation, USA) and assayed by HPLC-UV.

2.3. Preparation of emulsions

Two sets of ternary qualitative compositions, Lauroglycol® 90/Labrasol®/Capryol® PGMC (Lau/Lab/Cap) and Tween®80/Transcutol®/Imwitor 742 (T80/Trans/Imw), were explored. In each, excipients of three different structural classes were selected with HLB values ranging from one to fifteen. Formulations were prepared ranging each component from 0% to 100%, as depicted in Fig. 1. Resveratrol was included into the formulations with different loadings, corresponding to the maximum solubility values previously determined. For permeability and pharmacokinetics studies, formulations were prepared at 100 mg/mL loading. Manufacturing process of formulations was adapted from Yen et al. (Yen et al., 2017).

2.4. Characterization of emulsions

2.4.1. Dispersibility

All formulations were assessed visually for spontaneous emulsification. SEDDS were diluted in distilled water, under magnetic stirring and at room temperature, in a ratio of 1:200 (*v/v*), as described by Williams et al. (2012). The type of dispersion was assessed based on the classification of Singh et al. (Singh et al., 2009) with some modifications. Dispersions were classified in four grades, based on time to disperse and appearance after dispersion: Tindal (grade I) as emulsions formed in < 1 min and with clear bluish appearance; Nano-emulsions as formulations forming slightly less clear emulsion and having a bluish to white appearance (grade II); micro-emulsions as bright white formulations (similar to milk in appearance; grade III); and real solutions as formulations presenting a single liquid phase (grade IV).

2.4.2. Robustness to dilution of SEDDS

Robustness of SEDDS to dilution was studied by diluting 200-times with purified water. The diluted SEDDS were stored for 48 h under stirring and observed for additional presence of phase separation or drug precipitation as proposed by Williams et al. (2012).

2.4.3. Loading impact

The loading impact in the physical stability of SEDDS after emulsification was evaluated by comparing the behavior of emulsions with and without resveratrol when submitted to the same conditions described in the two previous sections.

2.4.4. Droplet size measurement

Droplet size was measured as cumulative percentile values of 10, 50 and 90% of droplets (D_{10}, D_{50} and D_{90}) and specific surface area (SSA) of SEDDS containing resveratrol after emulsification using a Mastersizer® 2000 from Malvern (Worcestershire, United Kingdom) according to the method described by our group in a previous work (Vasconcelos et al., 2018).

2.4.5. Emulsification process and physical stability of SEDDS after emulsification

In selected formulations, the emulsification process and physical stability of SEDDS after emulsification were observed and measured using a Mastersizer® 2000 from Malvern (Worcestershire, United Kingdom) according the method described by our group in a previous work (Vasconcelos et al., 2018).

2.5. Permeability studies

Permeability experiments were performed on a Caco-2 cell monolayer model (Antunes et al., 2013). The Caco-2 (C2BBe1) cell line was obtained from the American Type Culture Collection (ATCC, Manassas, VA, USA) and used at passages 64–66. Cells grew in culture flasks in DMEM supplemented with 10% (*v/v*) FBS, 1.0% (*v/v*) L-glutamine, 1.0% (*v/v*) NEAA, and 1.0% (*v/v*) antibiotic mixture (final concentration of 100 U/mL penicillin and 100 U/mL streptomycin). Cells were sub-cultured once a week using 0.25% Trypsin-EDTA to detach the cells from the flasks and seeded at a density of 5×10^5 cells per 75 cm^2 flask. The culture medium was replaced every other day. Cells were maintained at 37 °C, 5% CO_2 and 95% relative humidity. For permeability experiments, Caco-2 cells were seeded in 6-Transwell® cell culture inserts at a density of 10^5 cells/cm^2, and were allowed to grow and differentiate for 21 days with medium replacement every other day. After that time, medium was carefully removed from the apical and basolateral compartments and the inserts were gently washed twice with

PBS (pH 7.4, 37 °C). Then, 1.5 and 2.5 mL of HBSS was added to the apical and basolateral part of the Transwell®, respectively, and allowed to equilibrate for 30 min inside the incubator. Afterwards, the media from the apical compartment was removed and 1.5 mL of free resveratrol at 50 µg/mL in HBSS was added. The formulations were placed directly in the apical compartment without removing the medium. Plates were placed inside an orbital shaking incubator (IKA®KS 4000 IC, IKA, Staufen, Germany) at 100 rpm and 37 °C. Aliquots (200 µL) were withdrawn from the basolateral chamber at pre-determined times (5, 15, 30, 45, 60, 90, 120, and 180 min) and immediately replaced with HBSS. At the end, an aliquot from the apical compartment was collected (Antunes et al., 2013). Tests were performed in triplicate and an insert without the addition of sample was used as control. Before, during, and at the end of the permeability experiments, the Transepithelial Electrical Resistance (TEER) was measured using an EVOM2® epithelial voltammeter with chopstick electrodes (World Precision Instruments, Sarasota, FL, USA) in order to monitor the formation, confluence, and integrity of the cell monolayers. Experiments were performed in triplicate. The concentration of resveratrol in the samples was determined by HPLC-UV analysis. The drug apparent permeability (P_{app}) was calculated using the following Equation (Eq. (1)):

$$P_{app} = [(dQ/dt) \times V]/(A \times C_0) \quad (1)$$

where P_{app} is the apparent permeability (cm/s); dQ/dt (µM/s) is the flux across the monolayer obtained from the angular coefficient of the curve of the amount of drug transported versus time; V (cm^3) is the acceptor chamber volume, which in this case corresponds to 2.5 cm^3 (basolateral chamber); A (cm^2) is the insert membrane growth area (equal to 4.67 cm^2 for a 6-well plate); and C_0 (µM) is the initial concentration in the apical compartment (Antunes et al., 2013).

After sample collection at the last time point (180 min), Caco-2 cell monolayers were washed with PBS and then lysed with Triton® X-100 in order to extract resveratrol. Cell-associated drug levels were measured by HPLC-UV.

2.6. Pharmacokinetics studies

Seven-weeks old male Wistar rats (150–250 g) were purchased from Charles River Laboratories (France) and housed upon reception in cages containing wood litter, with free access to pellet chow diet (2014 Harlan) and tap water. Animals were maintained in a 12-hour light/dark cycle and in a controlled ambient temperature of 22 ± 2 °C and relative humidity of 50 ± 20%. Rats were randomly divided into three groups with five animals each, and received either resveratrol suspension (group 1), Lau/Lab/Cap emulsion (group 2) or T80/Trans/Imw emulsion (group 3). Administrations were performed by single oral gavage at a volume of 4.0 mL/kg. Hydroxypropyl methylcellulose solution (0.25%, *w/v*) was used as vehicle. All animal procedures followed the guidelines from Directive 2010/63/EU of the European Parliament on the protection of animals used for scientific purposes and the Portuguese law on animal welfare (Decreto-Lei 113/2013). Resveratrol was administered at a dose of 100 mg/kg. Blood samples of approximately 150 µL were collected from the tail vein before oral gavage and at 0.5, 1, 2, 4 and 7 h post-administration, and were assayed for resveratrol by LC-MS/MS. The C_{max}, T_{max} and area under the curve (AUC_{0-t}) over 7 h were calculated for each group using GraphPad Prism (GraphPad Software Inc., USA) (Singh and Pai, 2016; Yen et al., 2017).

2.7. Chromatographic conditions

2.7.1. HPLC-UV

Quantification of resveratrol in samples from the solubility assay and permeability studies was conducted using a Waters HPLC system and data was processed with Empower3® Software (Waters Corporation, Milford, MA, USA). The stationary phase consisted of a Waters Symmetry Shield RP18 column (3.5 µm, 100 × 4.6 mm) at 30 °C. The mobile phase consisted of water and acetonitrile (65:35, *v/v*) in isocratic mode and at a flow rate of 1.0 mL/min. The run time was set to 10 min, while the injection volumes were 10 µL for assay and solubility determinations and 50 µL for permeability studies. Detection by UV was fixed at 307 nm. Analytical method was validated according the applicable ICH guidelines.

2.7.2. LC-MS/MS

Quantification of resveratrol in plasma was conducted using a LC-MS/MS TQ G6470A from Agilent (USA), and data was acquired with MassHunter workstation data acquisition version B.08.00 and analyzed with MassHunter workstation software for quantitative analysis version B.07.01. The stationary phase consisted of a Waters CORTECS T3 column (2.7 µm, 100 × 2.1 mm) at 40 °C. The mobile phases consisted of (A) 0.1% (*v/v*) formic acid in water and (B) 0.1% formic acid (*v/v*) in acetonitrile using the following gradient: 0 min - 80% of A and 20% of B; 0.5 min - 80% of A and 20% of B; 4.0 min - 50% of A and 50% of B; 4.1 min - 80% of A and 20% of B. Flow rate was 0.3 mL/min throughout the full run (6 min), while the injection volume was 2 µL and the autosampler was kept at 4 °C. The samples were injected into the detector using the Agilent Jetstream electrospray ionization in negative mode polarity. The multiple reaction monitoring pair was m/z 227.3 → 143.1 for resveratrol with a collision energy of 26 V; and m/z 271.3 → 119.1 for naringenin (ISTD) with a collision energy of 25 V. The fragmentation used was 140 V. The analytical method was validated according to applicable ICH guidelines.

2.8. Statistical analysis

For solubility determinations, triplicates of formulations were statistically analyzed in Microsoft® Excel® 2016 MSO. Student's *t*-test was used within pairs of experiments using a two-tail test with two-sample equal variance. For pharmacokinetics, Student's *t*-test for pairs of samples and one-way analysis of variance for all tests (ANOVA) with unpaired and Bonferroni post-hoc test (GraphPadPrism, GraphPad software Inc., CA, USA) were used to analyze the data, respectively. In all cases, $p < 0.05$ was considered has denoting significance.

3. Results and discussion

3.1. High-throughput screening of resveratrol solubility

The solubility of resveratrol in 22 lipid solvents was screened and the results are presented in Table 1.

Resveratrol presented aqueous solubility of 3.0 µg/mL with significant enhancement by all tested vehicles, in particular Labrasol®, Trascutol®, Kolliphor® EL, RH40 and HS15, and Kollisolv® P124 (Table 1). Furthermore, some of these solvents improved solubility by > 4000-fold, with the least effective, Kollisolv® PEG400, still showing an improvement of 50-fold.

Based on these data, two sets of three excipients were considered for the formulation of SEDDS. One excipient with HLB above ten and another below six were selected for each set. The third component was selected from co-solvents and/or excipients with HLB in the range of 6–10. Therefore, set 1 was compose of Lau/Lab/Cap and set 2 by T80/Trans/Imw.

3.2. Loading

The maximum drug loading achieved for each formulation is depicted in Fig. 1. In the Lau/Lab/Cap formulations (24 formulations) the loading levels increased with Labrasol content and, consequently, with the increase in the HLB of the ternary formulation (Fig. 2). The lowest loading achieved was of 22 mg/mL with the formulation containing 100% Lau and the highest with formulation of 25/65/10 of Lau/Lab/Cap respectively. In this last case, a loading values of 146 mg/mL was

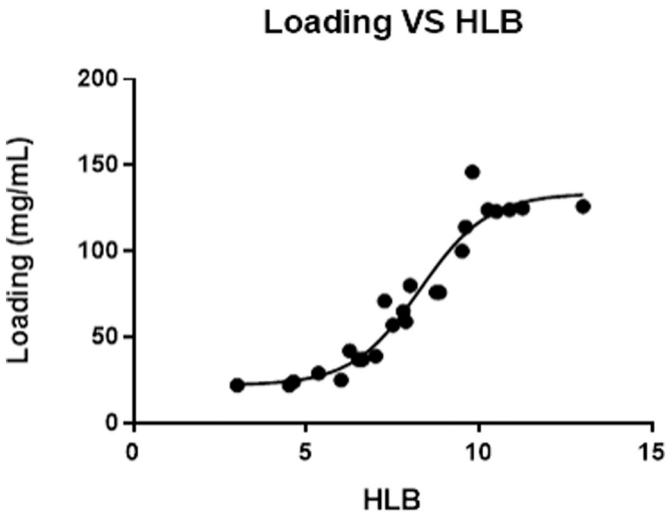

Fig. 2. Effect HLB in resveratrol loading in Lau/Lab/Cap formulations. HLB value of formulation increased the loading of formulations Lau/Lab/Cap in a sigmoidal manner.

achieved.

Conversely, loadings of ternary formulations composed of T80/Trans/Imw (19 formulations) were generally higher than the ones observed for the previous formulations. The maximum loading was 226 mg/mL, as observed for the 100% Trans formulation, followed by the formulations composed of 12.5/75/12.5 and 33/33/33 of T80/Trans/Imw, with values of 190 and 168 mg/mL, respectively. The correlation between HLB and solubility was not assessed since Trans is a solvent and does not possess a HLB value. Nevertheless, the increase in Trans and Imw contents resulted in increased and decreased solubility, respectively, in a non-linear mode.

3.3. Dispersibility and robustness to dilution

3.3.1. Lauroglycol® 90/Labrasol®/Capryol®

All the twenty-four formulations prepared according to this ternary composition, and without resveratrol, formed a nano-emulsion when diluted at a ratio of 1:200 in purified water (Fig. 3A). Resveratrol addition did not alter the formulations visual appearance for most of the formulations (Fig. 3B). After 48 h, some of those formulations were presented as micro-emulsion with two liquid phases (Fig. 3C and D) and a small number of formulations were kept as stable nano-emulsion. The dispersability behavior after 48 h was similar in the presence or absence of resveratrol for most of the formulutions. However, formulations with high resveratrol loading showed some precipitation after 48 h.

3.3.2. Tween® 80/Transcutol®/Imwitor® 742

Nineteen formulations were prepared based on these three components. Among these, formulations without resveratrol and presenting a high content of Trans or its association with T80 formed clear solutions after dispersion (Fig. 3E). However, Imw increment resulted in the formation of emulsions with larger droplet size based on a visual observation as described by Singh et al. (2009). Most of the formulations dispersed as micro-emulsion when resveratrol was included (Fig. 3F). Formulations with T80 at a level above or equal to 75% dispersed as solutions, while the formulation with 100% Trans precipitated, most likely due to its very high drug loading level.

At 48 h after dispersion (Fig. 3G and F), most of the formulations without resveratrol presented the same initial appearance. Most of the loaded formulations showed a similar behavior, even if an increased number of formulations presented signs of precipitation (Fig. 3F).

3.4. Droplet size and SSA

The droplet size of the formulation was considered as the one measured after 240 s of dispersion. Also, SSA was retrieved in the same analysis at the same time point. Resveratrol powder used to prepare these formulations showed a particle size of D_{10} of 9.7 µm, D_{50} of 24.2 µm and a D_{90} of 52.2 µm and a SSA of 0.324 m^2/kg.

3.4.1. Lauroglycol® 90/Labrasol®/Capryol®

The average droplet size (D_{50}) of the twenty-four Lau/Lab/Cap formulations ranged from close to 200 nm to above 34 µm (Fig. 4A). Nevertheless, most of the formulations dispersed as nano-emulsions (D_{50} < 500 nm) or small droplet micro-emulsions (D_{50} < 5 µm). Generally, droplet size decreased when the three components were present and with the increase of Lab content. The same was observed for D_{90} (Fig. 4B), which was for most of the formulations below 10 µm.

SSA values for most formulations were in the range of 20–40 m^2/kg (Fig. 4C), reflecting that the whole droplet population was composed by small droplets. This was a considerable improvement compared to the pure resveratrol powder. Only the formulations composed of Lau/Lab/Cap (50/0/50) showed SSA comparable to the powder.

3.4.2. Tween® 80/Transcutol®/Imwitor® 742

The nineteen formulations composed of T80/Trans/Imw presented smaller droplet size than formulations with Lau/Lab/Cap (Fig. 4), validating the qualitative observations of the dispersibility studies.

Average droplet size (D_{50}) and D_{90} ranged from around 100 nm to over 100 µm and 200 nm to over 200 µm, respectively, revealing that composition played an important role in the droplet size (Fig. 4D) of SEDDS. Despite the large range of droplet size values, most of the formulations emulsified as nano-emulsions (D_{50} < 500 nm).

Overall, smaller droplet size was achieved when the three components were present in the formulation. Among these, a content in Trans above or equal to 50% presented a negative impact in the droplet size by forming larger droplets, which was more evident at D_{90} (Fig. 4E).

Furthermore, most of the formulations presented above 100-fold increase in SSA over resveratrol powder (Fig. 4F).

3.5. Selection of formulations

Formulations were ranked based on their dispersibility, robustness to dilution, loading, droplet size (D50) and SSA. Each of those parameters were classified from one to four based on their performance and the total score was depicted in Fig. 5.

Formulations for each set of ternary mixtures were ranked in four different classes. In the case of Lau/Lab/Cap, formulations composed of 12.5/75/12.5 and 25/50/25 were the best performers. The one compose of 12.5/75/12.5 was selected for further studies due to its higher loading. In the case of T80/Trans/Imw, formulations with 50/0/50 and 33/33/33 were the top ranked. Again, the formulation composed of 33/33/33 was selected based on its higher loading.

Both selected formulations presented a solubility increase over pure drug (> 3000 folds) that was higher than previously described by Bolko et al. that developed a formulation composed of castor oil, Capmul® MCM and Cremophor® EL/RH40/RH60 that showed only 25-fold increase (Bolko et al., 2014).

3.6. Dispersion characterization of selected formulations

One batch of each of the previously selected formulations was prepared at a dose of 100 mg/mL and subjected to emulsification characterization according to the methodology previously described by our group (Vasconcelos et al., 2018).

Formulation T80/Trans/Imw was a typical fast emulsifier, forming a nano-emulsion in less than 1 min that was stable under mild stress conditions. Moreover, when high stress conditions were applied,

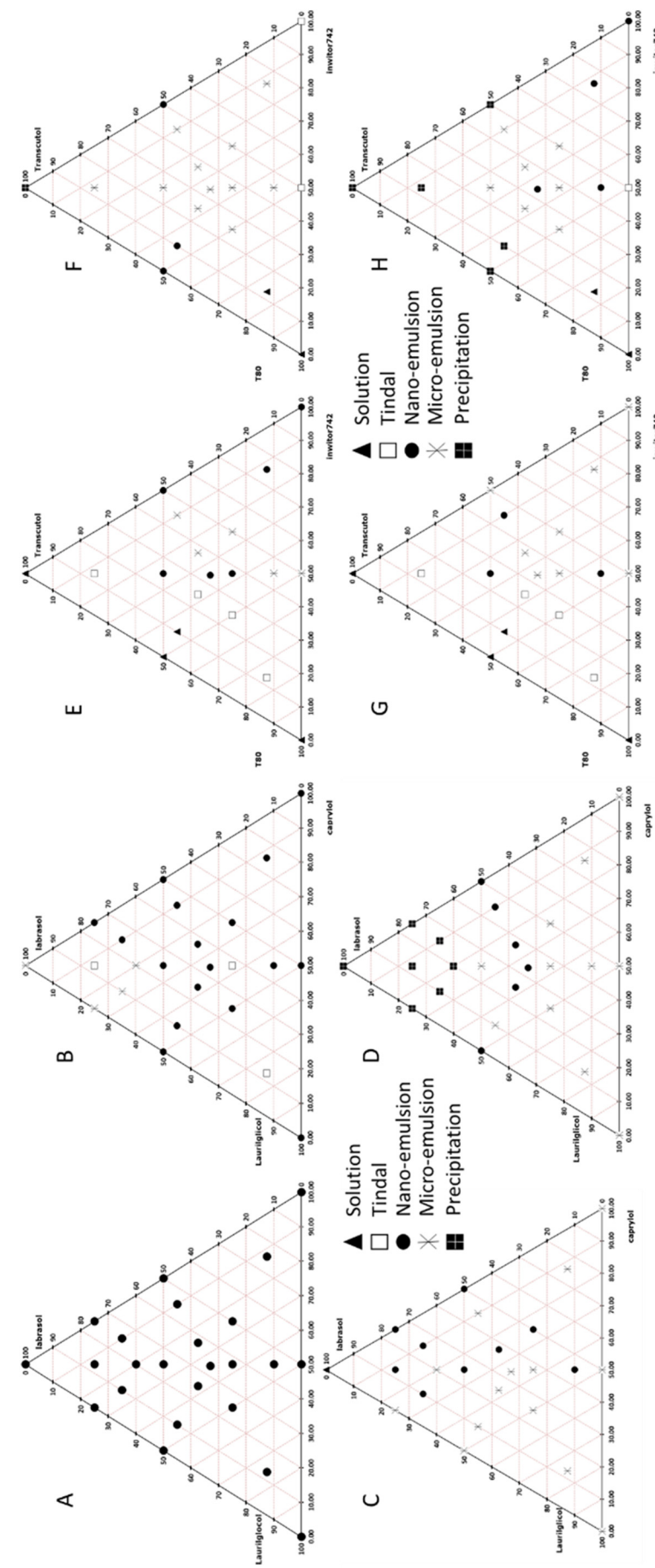

Fig. 3. Dispersibility and robustness to dilution of 2 ternary compositions. Lau/Lab/Cap formulations dispersibility and robustness to dilution without (A, C) and with (B, D) resveratrol, respectively. T80/Trans/Imw formulations dispersibility and robustness to dilution without (E, G) and with (F, H) resveratrol, respectively. Dispersibility (A, B E and F) was classified in four grades, based on time to disperse and aspect after dispersion. Solutions were categorized as formulations presenting a single liquid phase. Tindal as emulsions formed in < 1 min and with clear bluish appearance. Nano-emulsions as formulations forming, slightly less clear emulsion which had a bluish white appearance and micro-emulsions as bright white emulsion (similar to milk in appearance). Robustness to dilution (C, D, G, and H) included an additional classification, precipitation, when crystalline material was precipitated.

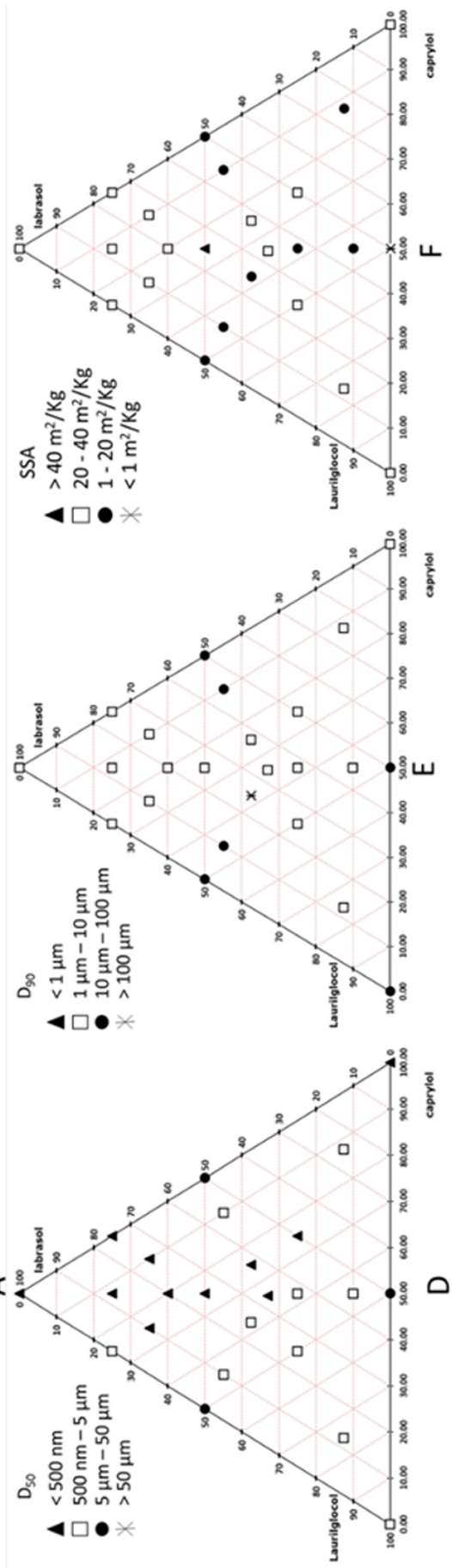

Fig. 4. Droplet characteristics D_{50}, D_{90} and SSA for formulations Lau/Lab/Cap (A, B and C) and formulations T80/Trans/Imw (D, E and F). Droplet size of emulsified formulations was classified for D_{50} (A and D) in four classes: < 500 nm; 500 nm to 5 µm; 5 µm to 50 µm and > 50 µm. With regards to D_{50} (B and E) classes were: < 1 µm; 1 µm to 10 µm; 10 µm to 100 µm and > 100 µm. SSA was also evaluated (C and F) formulations were grouped in the following classes: < 1 m^2/kg; 1 m^2/kg to 20m^2/kg; 20 m^2/kg to 40 m^2/kg and > 40 m^2/kg.

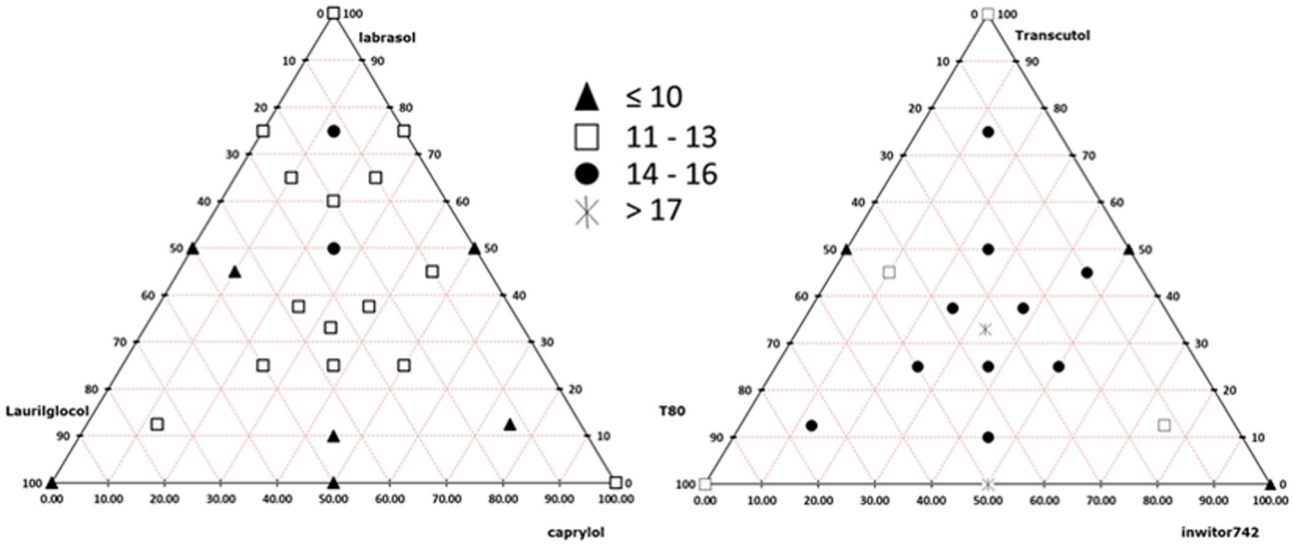

Fig. 5. Formulations ranking accordingly to dispersibility, robustness to dilution, loading, droplet size (D50) and SSA. A higher classification represented a better performance of to the formulation.

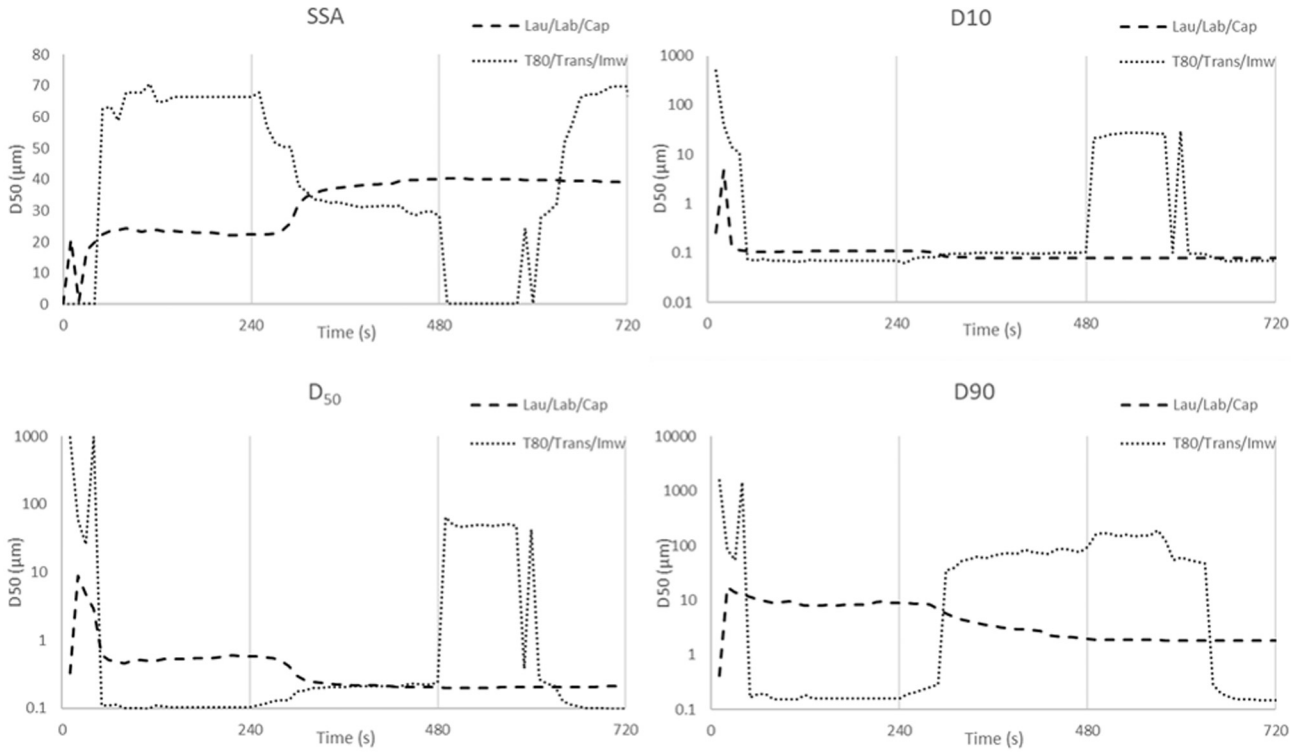

Fig. 6. Dispersion characterization of selected Lau/Lab/Cap and T80/Trans/Imw formulations. Formulations were characterized for dispersion. The first segment of 240 s represented a standard self-emulsifying process. In second segment (240 s to 480 s) formulations were submitted to very high physical stress. In last segment (480 s–720 s) formulations were allowed to rest.

droplet size increased most probably due to foam formation since this effect was only observed on the last third period of the high stress conditions period. During the resting phase, droplet size returned to its stable nano-emulsion form after a certain period. Additionally, D_{10}, D_{50} and D_{90} were equally affected during emulsification, stress and resting phases (Fig. 6). Conversely, Lau/Lab/Cap was classified as a moderately slow emulsifier that after forming a stable nano-emulsion showed a sustained decrease in droplet size when subjected to high stress condition. However, this effect was not reverted during resting phase.

SSA in both selected formulations denoted the same described behavior ascertained by dynamic droplet size analysis. Values increased over time and phase in formulation Lau/Lab/Cap and varied between phases in formulation T80/Trans/Imw. However, at the end of dispersion and resting phases the formulation T80/Trans/Imw presented higher SSA than formulation Lau/Lab/Cap.

3.7. Permeability studies

Permeability studies were conducted from apical to basal (A-B) and from basal to apical side (B-A) (Fig. 7A and B, respectively) using the Caco-2 cell monolayer model. The combined amount of resveratrol recovered from apical, cellular and basolateral compartments after

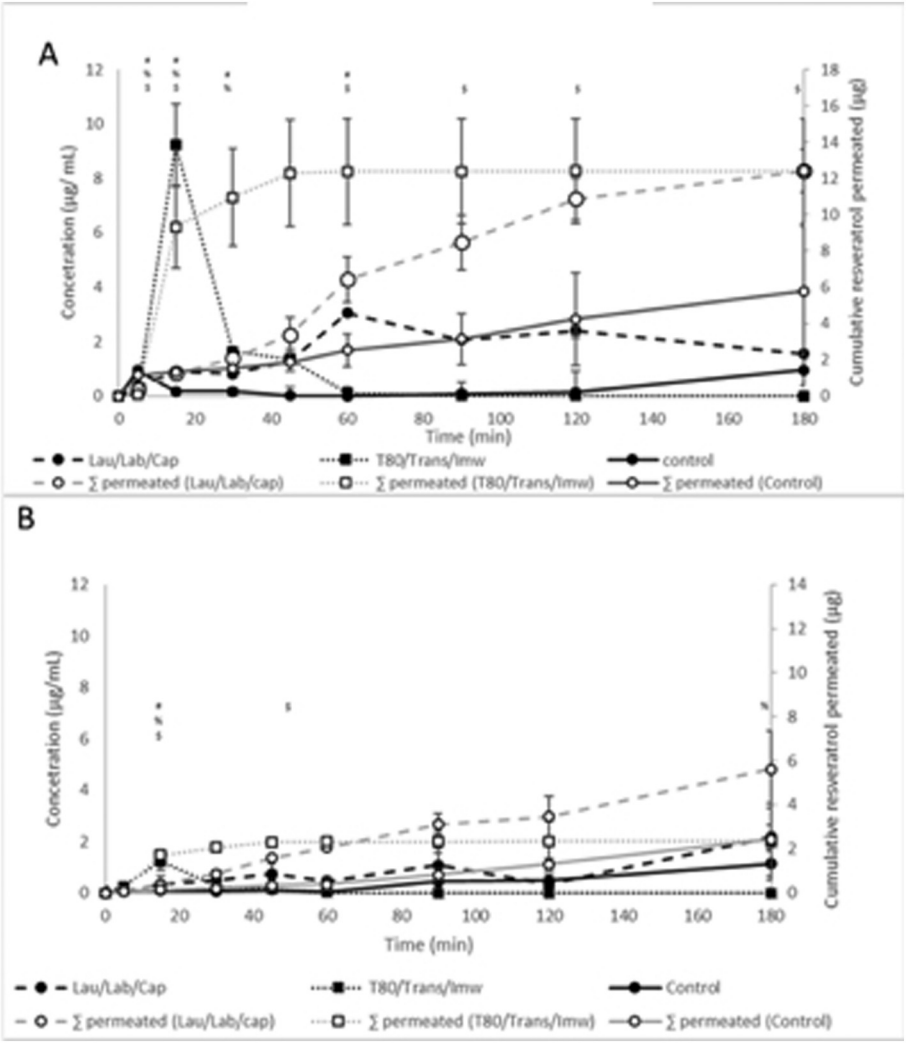

Fig. 7. Cumulative permeability of resveratrol in Caco-2 cells from apical to basal (A) and basal to apical (B) (average ± SD; $n = 3$) # and % – Formulations Lau/Lab/Cap and T80/Trans/Imw statistically different than control, respectively; $ – Formulation T80/Trans/Imw statistically different than Lau/Lab/Cap;

adding formulations and free resveratrol into the apical side was below 50%, suggesting that resveratrol metabolization/degradation was very intense and occurred rapidly. This effect is in line with previous reports (Kaldas et al., 2003) (Wenzel and Somoza, 2005), which noted a reduction in resveratrol transport at longer times points of incubation (more than 1 h). Sulfation and, to a minor extent, glucuronidation are the major metabolization pathways of resveratrol in Caco-2 cells (Kaldas et al., 2003). Control formulation presented a resveratrol recovery of 10%, Lau/Lab/Cap SEDDS of 18% ($p < 0.05$) and T80/Trans/Imw of 21% ($p < 0.05$), suggesting that these formulations may be able to reduce metabolization and/or degradation of resveratrol. Moreover, from all the recovered fractions, the permeated fraction corresponded to 76% in the control formulation, 78% in the T80/Trans/Imw formulation and 92% in the Lau/Lab/Cap formulation, suggesting that Lau/Lab/Cap formulation was the least influenced by efflux mechanisms.

When resveratrol was applied in the basal compartment, the P_{app} value was significantly reduced for all formulations (Table 2), which is in line with the described by Kaldas et al. (2003) and Seljak et al. (2014). The permeability kinetics of all formulations was comparable to the one observed when free resveratrol was placed in the apical compartment. In the case of the control, slow but steady permeation was observed in opposition to T80/Trans/Imw formulation that showed a fast and intense permeation, reaching maximum permeability at 15 min. One hour after the start of the experiment, permeability reached a plateau. However, Lau/Lab/Cap formulation appeared to promote sustained permeability, which was higher than the control formulation. These data can be justified by the fast emulsifying characteristics of T80/Trans/Imw and slow emulsifying properties of Lau/Lab/Cap.

Table 2
Values of P_{app} for resveratrol when tested from apical to basal or basal to apical compartments. (*) and (#) denote significant differences as compared to control or between SEDDS formulations, respectively ($p < 0.05$).

Formulation	$P_{app\ (Apical\text{-}Basal)}$ (cm/s)	$P_{app\ (Basal\text{-}Apical)}$ (cm/s)	Ratio (A-B/B-A)
Control	2.3×10^{-6}	96×10^{-6}	2.4
Lau/Lab/Cap	$4.9 \times 10^{-6*}$	$1.3 \times 10^{-6*/\#}$	3.7
T80/Trans/Imw	$4.9 \times 10^{-6*}$	56×10^{-6}	8.8

The fractions recovered when resveratrol was applied in the basolateral compartment were similar for SEDDS and two-fold higher than for control group. The fractions recovered in the donor compartment were the most representative in control formulation (83%) and T80/Trans/Imw (82%), showing an increase of around 4-fold and indicating that drug was not permeating or was being subject to efflux mechanisms. In the case of Lau/Lab/Cap, the fraction recovered in the donor

compartment was only 16%. Nevertheless, this was a ten-fold increase over the fraction determined when it was applied in the apical compartment. This data associated to the fact that the P_{app} value was much lower when resveratrol was applied in the basolateral compartment suggests that efflux mechanisms may be involved, as described by Shirasaka et al. (2008), namely via Multidrug Resistance-associated Protein type 3 (MRP3) and P-glycoprotein (P-gp) (Kaldas et al., 2003; Seljak et al., 2014). Overall, it is speculated that formulation Lau/Lab/Cap may have inhibited efflux mechanisms as observed by Seljak et al. by using 20% each of Capmul® MCM and castor oil; 30% each of Kolliphor® EL and Kolliphor® RH40 (Seljak et al., 2014).

TEER values of control, Lau/Lab/Cap and T80/Trans/Imw formulations in the last time point were 86%, 104% and 83% of initial values in the apical to basolateral study and 76%, 118% and 84%, respectively in the basolateral to apical study. These data support that cell monolayers remained intact until the end of the experiment and in this way, the permeability results reflect drug transport across a membrane-like barrier.

3.8. Pharmacokinetics studies

The pharmacokinetics data after the oral administration of resveratrol (100 mg/kg) to rats using three different formulations are depicted in Table 3 and Fig. 8. In the control formulation, resveratrol reached a maximum plasmatic concentration (C_{max}) of 202 ± 114 ng/mL within 2 h before falling back to residual levels over the next 7 h. The area under the curve (AUC_{0-t}) obtained for resveratrol was 827.2 ± 233 ng.h/ml. Both Lau/Lab/Cap and T80/Trans/Imw formulations reached maximal drug concentrations earlier than in the control group, namely within 30 min. This suggests that resveratrol is promptly absorbed when formulated in developed SEDDS. This can be justified by the liquid state and small droplet size of these formulations. The Lau/Lab/Cap formulation further showed higher rate of absorption with a C_{max} value that was approximately 2-fold higher than that of the control formulation. However, resveratrol exposure (AUC_{0-t}) was similar to the control group. The obtained C_{max} value for the T80/Trans/Imw formulation was similar to the control but the AUC_{0-t} was approximately two-fold lower, thus suggesting that resveratrol formulated in T80/Trans/Imw is absorbed to a lower extent. Still, there is also the possibility that, due to its fast emulsifying properties and small droplet size (100 nm), the T80/Trans/Imw formulation leads to very fast absorption of resveratrol (in < 30 min). In such case, the actual C_{max} may have been observed earlier than the first time point considered in this study.

Batches used in pharmacokinetics studies were also characterized regarding assay and droplet/particle size (Table 4). Droplet size values were in line with those obtained in the development phase and their distribution can be observed in Fig. 9.

It is well established (Pouton, 2006) that SEDDS should be able to quickly emulsify and keep a stable emulsion with small droplet size. In this study, the quantitative composition of Lau/Lab/Cap and T80/Trans/Imw ternary formulations was shown to highly impact the emulsification process, droplet size, emulsion stability and loading. The proposed development process allowed the selection of two candidate formulations with high drug loading capacity (over 100 mg/mL of resveratrol) and that quickly disperse in water, forming nano-emulsions. These high drug loading, small droplet sized formulations were expected to provide higher and faster absorption due to the high SSA of contact between resveratrol incorporated into the formulation and permeation surface (Kollipara and Gandhi, 2014). Caco-2 cell monolayer permeability studies were successful in demonstrating that both SEDDS formulations were able to increase the amount of drug permeation, as well as – possibly – reduce the amount of drug metabolized or subject to efflux, thus confirming our hypothesis. Reduction in drug metabolization and inhibition of efflux mechanisms by proposed SEDDS need further confirmation but could potentially be attributed to formulation components that have possibly inhibited degradation mechanisms. T80 (Vasconcelos et al., 2017) and Lab (Zhou et al., 2015) were previously described as reducing intestinal drug metabolization. Moreover, the small droplet size could also allow the permeation of intact droplets through paracellular or transcellular mechanisms and, therefore, avoid degradation mechanisms (Rahman et al., 2013; Pan et al., 2018). The small droplet size and the efflux mechanisms

Table 3
Pharmacokinetic parameters of all formulations. Results are presented as mean ± SD (n = 5). (*) denote significant differences as compared to control (p < 0.05).

Formulation	C_{max} (ng/mL)	T_{max}(h)	AUC_{0-t} (ng*h/mL)
Control	202 ± 114	2.0	827 ± 233
Lau/Lab/Cap	405 ± 140	0.5*	832 ± 194
T80/Trans/Imw	199 ± 137	0.5*	425 ± 118

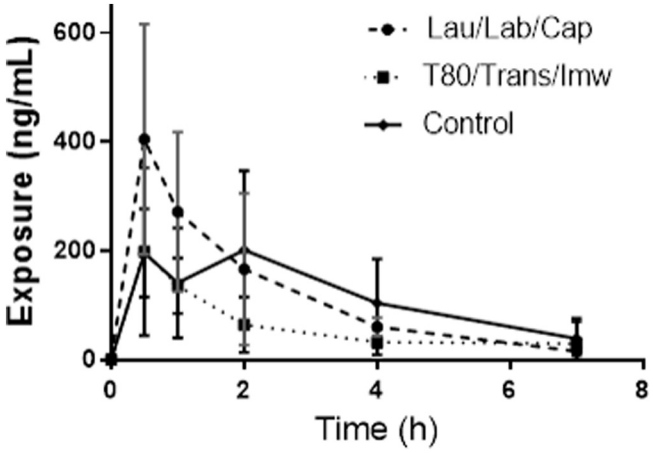

Fig. 8. Pharmacokinetics profile of control, Lau/Lab/Cap and T80/Trans/Imw formulations (average ± SD; n = 5).

Table 4
Physical-chemical characterization of all formulations. Particle size measurements were performed in triplicate. (*) and (#) denote significant differences as compared to control or between SEDDS formulations, respectively (p < 0.05).

Formulation	Assay (%)	D_{10}(μm)	D_{50} (μm)	D_{90} (μm)
Control	99.5	9.870	26.455	60.844
Lau/Lab/Cap	96.2	0.111*	0.578*	8.817*
T80/Trans/Imw	93.7	0.071*	0.104*/#	0.157*/#

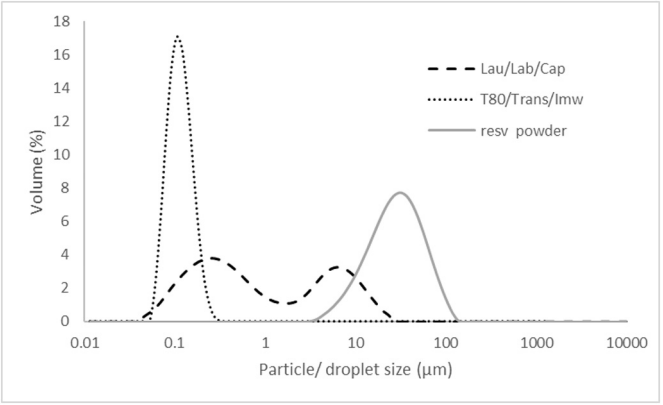

Fig. 9. Droplet/particle size distribution of batches used in the PK study.

inhibition were also recognized to be responsible for the observed increase in permeability.

The T80/Trans/Imw formulation presenting > 90% of droplets with a size below 160 nm showed high and fast permeability. After 15 min, > 70% of the total resveratrol permeation occurred. T80 is known to be BCRP (Breast Cancer Resistance Protein) and MRP inhibitor, Imw a P-gp inhibitor, and Trans a MRP inhibitor (Vasconcelos et al., 2017). Therefore, the small droplet size as well as the high efflux inhibition of this formulation could justify the fast and intense permeability that then could have been followed by degradation/metabolization since resveratrol was no longer detected after 60 min.

Since the formulation composed of Lau/Lab/Cap presented larger droplet size than the one featuring T80/Trans/Imw, permeation through paracellular mechanisms may have been harder and consequently a slower and lesser intense permeability over time was observed. However, at the end of permeability studies, both Lau/Lab/Cap and T80/Trans/Imw formulations exhibited similar levels of resveratrol permeated, which were around two-fold higher than values observed with the control formulation. Moreover, since the Lau/Lab/Cap formulation was significantly less affected by the basal-apical versus apical-basal permeability it may be assumed that efflux mechanisms could have been affected (Kaldas et al., 2003; Seljak et al., 2014). It should be highlighted that resveratrol in the control formulation was already in solution and in the presence of a permeation enhancer (DMSO). Furthermore, the Lau/Lab/Cap formulation may have also contributed to a reduction in metabolization/degradation. Regarding its individual components, Lab is the only excipient known to be able to inhibit glucuronidation (Zhou et al., 2015) and P-gp efflux mechanisms (Ma et al., 2011) and it represented 75% of the formulation.

In the pharmacokinetics studies, resveratrol suspension (control) showed a secondary peak in its pharmacokinetic profile, thus suggesting entero-hepatic recirculation as observed and described by Marier et al. (2002). The observed $AUC_{0\text{-}t}$ and C_{max} for the control group was eight and four times higher than that observed by Branton and Snehasis in male Sprague Dawley rats (2017) using the same dose. The $AUC_{0\text{-}t}$ value obtained in our study was similar to the ones observed by Zhou et al. (2015) when using 10 mg/kg (10 fold lower) in male Wistar rats, and Yen et al. (2017) when using 50 mg/kg in male Sprague Dawley rats. These data suggest that resveratrol exposure is highly dependent on species and group of animals. Therefore, comparison between different studies should be made with caution. Moreover, our control group provided a relatively higher exposure than previously described studies which could have further contributed to the relative lower differences observed when comparing to data from SEDDS formulations.

The pharmacokinetic profile following administration of SEDDS formulations did not show any secondary peaks, suggesting that entero-hepatic recirculation may have not occurred, thus consequently affecting in a negative way the total exposure to resveratrol. Based on the available pharmacokinetics profile where T_{max} was the first timepoint (0.5 h) studied, associated to the permeability studies and droplet size, it can be speculated that the actual C_{max} of SEDDS formulations, particularly for the T80/Trans/Imw formulation, was not observed and therefore total exposure could have been underestimated. Nevertheless, a two-fold increase in C_{max} was still observed for Lau/Lab/Cap formulation, which can be a relevant advantage particularly for CNS therapeutic indications, such as Parkinson's and Alzheimer's diseases that require a blood brain barrier permeability (BBB), where an increase in C_{max} may improve brain exposure (Warren, 2018).

4. Conclusions

In this work, SEDDS were rationally developed with the intention of increasing the oral bioavailability of resveratrol and potentially contribute to its long time sought translation into clinical use. The developed formulations presented high drug loadings and were able to self-emulsify as stable nano-emulsions. Additionally, fast and intense in vivo oral absorption was observed for formulation composed of Lau/Lab/Cap. The increase in C_{max} may have been associated to the reduction in metabolization and/or efflux mechanisms as suggested by Caco-2 cell permeability data. Overall, the hereby presented findings appear to support further development of the Lau/Lab/Cap-based SEDDS as a promising vehicle for improving the oral bioavailability of resveratrol.

Declaration of Competing Interest

The authors declare that they have no conflict of interest.

Acknowledgements

This article is a result of the project NORTE-01-0145-FEDER-000012, supported by Norte Portugal Regional Operational Programme (NORTE 2020), under the PORTUGAL 2020 Partnership Agreement, through the European Regional Development Fund (ERDF). This work was financed by FEDER - Fundo Europeu de Desenvolvimento Regional funds through the COMPETE 2020 - Operacional Programme for Competitiveness and Internationalisation (POCI), Portugal 2020, and by Portuguese funds through FCT - Fundação para a Ciência e a Tecnologia/Ministério da Ciência, Tecnologia e Ensino Superior in the framework of the project "Institute for Research and Innovation in Health Sciences" (POCI-01-0145-FEDER-007274) and NETDIAMOND (POCI-01-0145-FEDER-016385). Sara Marques gratefully acknowledges Fundação para a Ciência e a Tecnologia (FCT), Portugal for financial support (grant SFRH/BPD/75905/2011).

References

Almeida, L., Vaz-da-Silva, M., Falcão, A., Soares, E., Costa, R., Loureiro, A.I., Fernandes-Lopes, C., Rocha, J.-F., Nunes, T., Wright, L., Soares-da-Silva, P., 2009. Pharmacokinetic and safety profile of trans-resveratrol in a rising multiple-dose study in healthy volunteers. Mol. Nutr. Food Res. 53 (S1), S7–S15.

Andrade, S., Ramalho, M.J., Pereira, M.D.C., Loureiro, J.A., 2018. Resveratrol brain delivery for neurological disorders prevention and treatment. Front. Pharmacol. 9, 1261.

Antunes, F., Andrade, F., Araújo, F., Ferreira, D., Sarmento, B., 2013. Establishment of a triple co-culture *in vitro* cell models to study intestinal absorption of peptide drugs. Eur. J. Pharm. Biopharm. 83 (3), 427–435.

Arafa, M.H., Mohammad, N.S., Atteia, H.H., Abd-Elaziz, H.R., 2014. Protective effect of resveratrol against doxorubicin-induced cardiac toxicity and fibrosis in male experimental rats. J. Physiol. Biochem. 70 (3), 701–711.

Balata, G.F., Essa, E.A., Shamardl, H.A., Zaidan, S.H., Abourehab, M.A., 2016. Self-emulsifying drug delivery systems as a tool to improve solubility and bioavailability of resveratrol. Drug Des. Devel. Ther. 10, 117–128.

Bolko, K., Zvonar, A., Gašperlin, M., 2014. Mixed lipid phase SMEDDS as an innovative approach to enhance resveratrol solubility. Drug Dev. Ind. Pharm. 40 (1), 102–109.

Boocock, D.J., Faust, G.E.S., Patel, K.R., Schinas, A.M., Brown, V.A., Ducharme, M.P., Booth, T.D., Crowell, J.A., Perloff, M., Gescher, A.J., Steward, W.P., Brenner, D.E., 2007. Phase I dose escalation pharmacokinetic study in healthy volunteers of resveratrol, a potential cancer chemopreventive agent. Cancer Epidemiol. Biomark. Prev. 16 (6), 1246–1252.

Cannatelli, A., Principato, S., Colavecchio, O.L., Pallecchi, L., Rossolini, G.M., 2018. Synergistic activity of colistin in combination with resveratrol against colistin-resistant gram-negative pathogens. Front. Microbiol. 9, 1808.

Chen, Y., Zhang, H., Yang, J., Sun, H., 2015. Improved antioxidant capacity of optimization of a self-microemulsifying drug delivery system for resveratrol. Molecules 20 (12), 21167–21177.

Cherniakov, I., Domb, A.J., Hoffman, A., 2015. Self-nano-emulsifying drug delivery systems: an update of the biopharmaceutical aspects. Expert Opin. Drug Deliv. 12 (7), 1121–1133.

Cho, H.-Y., Choi, J.-H., Oh, I.-J., Lee, Y.-B., 2015. Self-emulsifying drug delivery system for enhancing bioavailability and lymphatic delivery of tacrolimus. J. Nanosci. Nanotechnol. 15 (2), 1831–1841.

Cianciosi, D., Varela-Lopez, A., Forbes-Hernandez, T.Y., Gasparrini, M., Afrin, S., Reboredo-Rodriguez, P., Zhang, J., Quiles, J.L., Nabavi, S.F., Battino, M., Giampieri, F., 2018. Targeting molecular pathways in cancer stem cells by natural bioactive compounds. Pharmacol. Res. 135, 150–165.

Dei Cas, M., Ghidoni, R., 2018. Cancer prevention and therapy with polyphenols: sphingolipid-mediated mechanisms. Nutrients 10 (7), 940.

Dokania, S., Joshi, A.K., 2015. Self-microemulsifying drug delivery system (SMEDDS) – challenges and road ahead. Drug Deliv. 22 (6), 675–690.

Drygalski, K., Fereniec, E., Koryciński, K., Chomentowski, A., Kiełczewska, A., Odrzygóźdź, C., Modzelewska, B., 2018. Resveratrol and Alzheimer's disease. From

molecular pathophysiology to clinical trials. Exp. Gerontol. 113, 36–47.
Fontes-Ribeiro, C., Macedo, T., Nunes, T., Neta, C., Vasconcelos, T., Cerdeira, R., Lima, R., Rocha, J.-F., Falcão, A., Almeida, L., Soares-da-Silva, P., 2008. Dosage form proportionality and food effect of the final tablet formulation of eslicarbazepine acetate. Drugs R&D 9 (6), 447–454.
Gomes, B.A.Q., Silva, J.P.B., Romeiro, C.F.R., Dos Santos, S.M., Rodrigues, C.A., Gonçalves, P.R., Sakai, J.T., Mendes, P.F.S., Varela, E.L.P., Monteiro, M.C., 2018. Neuroprotective mechanisms of resveratrol in Alzheimer's disease: role of SIRT1. Oxidative Med. Cell. Longev. 2018, 8152373.
Hernandez-Cascales, J., 2017. Resveratrol enhances the inotropic effect but inhibits the proarrhythmic effect of sympathomimetic agents in rat myocardium. PeerJ 5, e3113.
Hung, L.-M., Chen, J.-K., Huang, S.-S., Lee, R.-S., Su, M.-J., 2000. Cardioprotective effect of resveratrol, a natural antioxidant derived from grapes. Cardiovasc. Res. 47 (3), 549–555.
Kaldas, M.I., Walle, U.K., Walle, T., 2003. Resveratrol transport and metabolism by human intestinal Caco-2 cells. J. Pharm. Pharmacol. 55 (3), 307–312.
Khodabandehloo, H., Seyyedebrahimi, S., Esfahani, E.N., Razi, F., Meshkani, R., 2018. Resveratrol supplementation decreases blood glucose without changing the circulating CD14 + CD16 + monocytes and inflammatory cytokines in patients with type 2 diabetes: a randomized, double-blind, placebo-controlled study. Nutr. Res. 54, 40–51.
Kollipara, S., Gandhi, R.K., 2014. Pharmacokinetic aspects and *in vitro– in vivo* correlation potential for lipid-based formulations. Acta Pharm. Sin. B 4 (5), 333–349.
Koushki, M., Dashatan, N.A., Meshkani, R., 2018. Effect of resveratrol supplementation on inflammatory markers: a systematic review and meta-analysis of randomized controlled trials. Clin. Ther. 40 (7), 1180–1192.e1185.
la Porte, C., Voduc, N., Zhang, G., Seguin, I., Tardiff, D., Singhal, N., Cameron, D.W., 2010. Steady-state pharmacokinetics and tolerability of trans-resveratrol 2000mg twice daily with food, quercetin and alcohol (ethanol) in healthy human subjects. Clin. Pharmacokinet. 49 (7), 449–454.
Li, J., Yu, S., Ying, J., Shi, T., Wang, P., 2017. Resveratrol prevents ROS-induced apoptosis in high glucose-treated retinal capillary endothelial cells via the activation of AMPK/Sirt1/PGC-1α pathway. Oxidative Med. Cell. Longev. 2017, 7584691.
Lv, C., Zhang, Y., Shen, L., 2018. Preliminary clinical effect evaluation of resveratrol in adults with allergic rhinitis. Int. Arch. Allergy Immunol. 175 (4), 231–236.
Ma, L., Wei, Y., Zhou, Y., Ma, X., Wu, X., 2011. Effects of pluronic F68 and Labrasol on the intestinal absorption and pharmacokinetics of rifampicin in rats. Arch. Pharm. Res. 34 (11), 1939–1943.
Ma, D.S.L., Tan, L.T.-H., Chan, K.-G., Yap, W.H., Pusparajah, P., Chuah, L.-H., Ming, L.C., Khan, T.M., Lee, L.-H., Goh, B.-H., 2018. Resveratrol—potential antibacterial agent against foodborne pathogens. Front. Pharmacol. 9, 102.
Marier, J.-F., Vachon, P., Gritsas, A., Zhang, J., Moreau, J.-P., Ducharme, M.P., 2002. Metabolism and disposition of resveratrol in rats: extent of absorption, glucuronidation, and enterohepatic recirculation evidenced by a linked-rat model. J. Pharmacol. Exp. Ther. 302 (1), 369–373.
Maugeri, A., Barchitta, M., Mazzone, M.G., Giuliano, F., Basile, G., Agodi, A., 2018. Resveratrol modulates SIRT1 and DNMT functions and restores LINE-1 methylation levels in ARPE-19 cells under oxidative stress and inflammation. Int. J. Mol. Sci. 19 (7), 2118.
Montagnani Marelli, M., Marzagalli, M., Fontana, F., Raimondi, M., Moretti, R.M., Limonta, P., 2018. Anticancer properties of tocotrienols: a review of cellular mechanisms and molecular targets. J. Cell. Physiol. 0 (0), 1–18.
Nipun, T.S., Ashraful Islam, S.M., 2014. SEDDS of gliclazide: preparation and characterization by *in-vitro*, *ex-vivo* and *in-vivo* techniques. Saudi Pharma. J. 22 (4), 343–348.
Nunes, T., Almeida, L., Rocha, J.-F., Falcão, A., Fernandes-Lopes, C., Loureiro, A.I., Wright, L., Vaz-da-Silva, M., Soares-da-Silva, P., 2009. Pharmacokinetics of trans-resveratrol following repeated administration in healthy elderly and young subjects. J. Clin. Pharmacol. 49 (12), 1477–1482.
Pan, R., Liu, G., Li, Y., Wei, Y., Li, S., Tao, L., 2018. Size-dependent endocytosis and a dynamic-release model of nanoparticles. Nanoscale 10 (17), 8269–8274.
Pouton, C.W., 2006. Formulation of poorly water-soluble drugs for oral administration: physicochemical and physiological issues and the lipid formulation classification system. Eur. J. Pharm. Sci. 29 (3), 278–287.
Rahman, M.A., Hussain, A., Hussain, M.S., Mirza, M.A., Iqbal, Z., 2013. Role of excipients in successful development of self-emulsifying/microemulsifying drug delivery system (SEDDS/SMEDDS). Drug Dev. Ind. Pharm. 39 (1), 1–19.
Seljak, K.B., Berginc, K., Trontelj, J., Zvonar, A., Kristl, A., Gašperlin, M., 2014. A self-microemulsifying drug delivery system to overcome intestinal resveratrol toxicity and presystemic metabolism. J. Pharm. Sci. 103 (11), 3491–3500.
Shirasaka, Y., Sakane, T., Yamashita, S., 2008. Effect of P-glycoprotein expression levels on the concentration-dependent permeability of drugs to the cell membrane. J. Pharm. Sci. 97 (1), 553–565.
Singh, G., Pai, R.S., 2016. In vitro and in vivo performance of supersaturable self-nanoemulsifying system of trans-resveratrol. Artif. Cells Nanomed. Biotechnol. 44 (2), 510–516.
Singh, A.K., Chaurasiya, A., Awasthi, A., Mishra, G., Asati, D., Khar, R.K., Mukherjee, R., 2009. Oral bioavailability enhancement of exemestane from self-microemulsifying drug delivery system (SMEDDS). AAPS PharmSciTech 10 (3), 906–916.
Singh, B., Beg, S., Khurana, R.K., Sandhu, P.S., Kaur, R., Katare, O.P., 2014. Recent advances in self-emulsifying drug delivery systems (SEDDS). Crit. Rev. Ther. Drug Carrier Syst. 31 (2), 121–185.
Sinha, D., Sarkar, N., Biswas, J., Bishayee, A., 2016. Resveratrol for breast cancer prevention and therapy: preclinical evidence and molecular mechanisms. Semin. Cancer Biol. 40–41, 209–232.
Tsuchiya, T., Endo, A., Tsujikado, K., Inukai, T., 2017. Involvement of resveratrol and w-3 polyunsaturated fatty acids on Sirtuin 1 gene expression in THP1 cells. Am J Med Sci 354 (4), 415–422.
Vasconcelos, T., Marques, S., Sarmento, B., 2017. The biopharmaceutical classification system of excipients. Ther. Deliv. 8 (2), 65–78.
Vasconcelos, T., Marques, S., Sarmento, B., 2018. Measuring the emulsification dynamics and stability of self-emulsifying drug delivery systems. Eur. J. Pharm. Biopharm. 123, 1–8.
Vaz-da-Silva, M., Loureiro, A.I., Falcao, A., Nunes, T., Rocha, J.F., Fernandes-Lopes, C., Soares, E., Wright, L., Almeida, L., Soares-da-Silva, P., 2008. Effect of food on the pharmacokinetic profile of trans-resveratrol. Int. J. Clin. Pharmacol. Ther. 46 (11), 564–570.
Wang, Y., Lee, K.W., Chan, F.L., Chen, S., Leung, L.K., 2006. The red wine polyphenol resveratrol displays bilevel inhibition on aromatase in breast cancer cells. Toxicol. Sci. 92 (1), 71–77.
Warren, K.E., 2018. Beyond the blood:brain barrier: the importance of central nervous system (CNS) pharmacokinetics for the treatment of CNS tumors, including diffuse intrinsic pontine glioma. Front. Oncol. 8, 239.
Wenzel, E., Somoza, V., 2005. Metabolism and bioavailability of trans-resveratrol. Mol. Nutr. Food Res. 49 (5), 472–481.
Williams, H.D., Sassene, P., Kleberg, K., Bakala-N'Goma, J.-C., Calderone, M., Jannin, V., Igonin, A., Partheil, A., Marchaud, D., Jule, E., Vertommen, J., Maio, M., Blundell, R., Benameur, H., Carrière, F., Müllertz, A., Porter, C.J.H., Pouton, C.W., 2012. Toward the establishment of standardized *in vitro* tests for lipid-based formulations, part 1: method parameterization and comparison of *in vitro* digestion profiles across a range of representative formulations. J. Pharm. Sci. 101 (9), 3360–3380.
Wu, H., Li, G.-N., Xie, J., Li, R., Chen, Q.-H., Chen, J.-Z., Wei, Z.-H., Kang, L.-N., Xu, B., 2016. Resveratrol ameliorates myocardial fibrosis by inhibiting ROS/ERK/TGF-β/periostin pathway in STZ-induced diabetic mice. BMC Cardiovasc. Disord. 16, 5.
Xia, D., Sui, R., Zhang, Z., 2019. Administration of resveratrol improved Parkinson's disease-like phenotype by suppressing apoptosis of neurons via modulating the MALAT1/miR-129/SNCA signaling pathway. J. Cell. Biochem. 120 (4), 4942–4951.
Yen, C.C., Chang, C.W., Hsu, M.C., Wu, Y.T., 2017. Self-nanoemulsifying drug delivery system for resveratrol: enhanced oral bioavailability and reduced physical fatigue in rats. Int. J. Mol. Sci. 18 (9).
Zhou, J., Zhou, M., Yang, F.-F., Liu, C.-Y., Pan, R.-L., Chang, Q., Liu, X.-M., Liao, Y.-H., 2015. Involvement of the inhibition of intestinal glucuronidation in enhancing the oral bioavailability of resveratrol by Labrasol containing nanoemulsions. Mol. Pharm. 12 (4), 1084–1095.